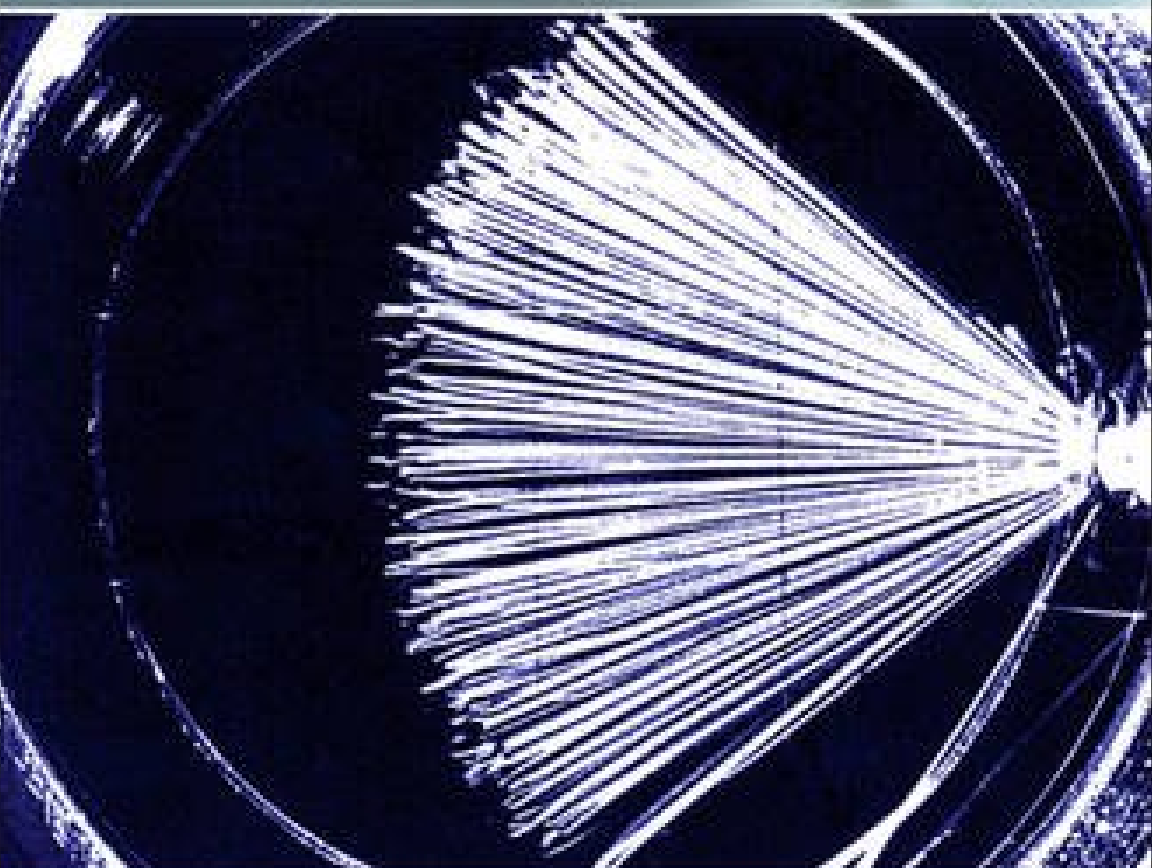




ELSEVIER INSIGHTS



NUCLEAR AND RADIOCHEMISTRY

JÓZSEF KÓNYA • NOÉMI M. NAGY

Nuclear and Radiochemistry

Nuclear and Radiochemistry

József Kónya and Noémi M. Nagy

*Isotope Laboratory, Department of Colloid and Environmental Chemistry
University of Debrecen
Debrecen, Hungary*



ELSEVIER

AMSTERDAM • BOSTON • HEIDELBERG • LONDON • NEW YORK • OXFORD
PARIS • SAN DIEGO • SAN FRANCISCO • SINGAPORE • SYDNEY • TOKYO

Elsevier
32 Jamestown Road, London NW1 7BY
225 Wyman Street, Waltham, MA 02451, USA

First edition 2012

Copyright © 2012 Elsevier Inc. All rights reserved

No part of this publication may be reproduced or transmitted in any form or by any means, electronic or mechanical, including photocopying, recording, or any information storage and retrieval system, without permission in writing from the publisher. Details on how to seek permission, further information about the Publisher's permissions policies and our arrangement with organizations such as the Copyright Clearance Center and the Copyright Licensing Agency, can be found at our website: www.elsevier.com/permissions

This book and the individual contributions contained in it are protected under copyright by the Publisher (other than as may be noted herein).

Notices

Knowledge and best practice in this field are constantly changing. As new research and experience broaden our understanding, changes in research methods, professional practices, or medical treatment may become necessary.

Practitioners and researchers must always rely on their own experience and knowledge in evaluating and using any information, methods, compounds, or experiments described herein. In using such information or methods they should be mindful of their own safety and the safety of others, including parties for whom they have a professional responsibility.

To the fullest extent of the law, neither the Publisher nor the authors, contributors, or editors, assume any liability for any injury and/or damage to persons or property as a matter of products liability, negligence or otherwise, or from any use or operation of any methods, products, instructions, or ideas contained in the material herein.

British Library Cataloguing-in-Publication Data

A catalogue record for this book is available from the British Library

Library of Congress Cataloging-in-Publication Data

A catalog record for this book is available from the Library of Congress

ISBN: 978-0-12-391430-9

For information on all Elsevier publications
visit our website at store.elsevier.com

This book has been manufactured using Print On Demand technology. Each copy is produced to order and is limited to black ink. The online version of this book will show color figures where appropriate.

Working together to grow
libraries in developing countries

www.elsevier.com | www.bookaid.org | www.sabre.org

ELSEVIER

BOOK AID
International

Sabre Foundation

Contents

| | |
|---|-------------|
| Preface | xiii |
| 1 Introduction | 1 |
| Further Reading | 11 |
| 2 Basic Concepts | 13 |
| 2.1 Atomic Nuclei | 13 |
| 2.1.1 Components of Nuclei | 13 |
| 2.2 Forces in the Nucleus | 15 |
| 2.3 Other Properties of Nuclei | 19 |
| 2.4 Elementary Particles | 20 |
| 2.5 Models of Nuclei | 21 |
| 2.5.1 The Liquid-Drop Model | 23 |
| 2.5.2 The Shell Model | 25 |
| 2.5.3 Unified and Collective Models | 25 |
| Further Reading | 25 |
| 3 Isotopes | 27 |
| 3.1 Isotopic Effects | 29 |
| 3.1.1 Physical Isotope Effects | 32 |
| 3.1.2 Spectroscopic Isotope Effects | 33 |
| 3.1.3 Phase Equilibrium Isotope Effects | 34 |
| 3.1.4 Isotope Effects in the Kinetics of Chemical Reactions | 34 |
| 3.1.5 The Isotope Effect in a Chemical Equilibrium | 38 |
| 3.1.6 Biological Isotope Effects | 39 |
| 3.2 Separation of Isotopes | 40 |
| 3.3 Isotope Composition in Nature | 41 |
| 3.4 Study of Geological Formations and Processes by Stable Isotope Ratios | 42 |
| 3.4.1 Study of the Temperature and Age of Geological Formations | 43 |
| 3.4.2 Study of the Hydrological Process by Measuring the Ratio of Oxygen and Hydrogen Isotopes | 44 |
| 3.4.3 Changes in the Isotope Ratio of Nitrogen | 45 |
| 3.4.4 Isotope Ratios of Carbon | 46 |
| 3.4.5 Stable Isotope Ratios in Ecological Studies | 47 |
| Further Reading | 47 |

| | | |
|----------|---|-----------|
| 4 | Radioactive Decay | 49 |
| 4.1 | Kinetics of Radioactive Decay | 49 |
| 4.1.1 | Statistics of Simple Radioactive Decay | 49 |
| 4.1.2 | Activity and Intensity | 51 |
| 4.1.3 | Decay of Independent (Mixed) Nuclei | 51 |
| 4.1.4 | Branching Decay | 52 |
| 4.1.5 | Kinetics of Successive Decay | 54 |
| 4.1.6 | Radioactive Equilibria | 57 |
| 4.2 | Radioactive Decay Series | 61 |
| 4.3 | Radioactive Dating | 61 |
| 4.3.1 | Radioactive Dating by Lead Isotope Ratios | 63 |
| 4.3.2 | Radioactive Dating by Helium Concentration | 65 |
| 4.3.3 | Radioactive Dating by Fission of Uranium | 66 |
| 4.3.4 | Radioactive Dating by Argon Concentration | 66 |
| 4.3.5 | Radioactive Dating by ^{87}Rb – ^{87}Sr , Parent–Daughter Pairs | 66 |
| 4.3.6 | Radiocarbon Dating | 67 |
| 4.4 | Mechanism of Radioactive Decay | 68 |
| 4.4.1 | Alpha Decay | 68 |
| 4.4.2 | Beta Decays | 74 |
| 4.4.3 | Electron Capture | 78 |
| 4.4.4 | Proton and Neutron Decay | 79 |
| 4.4.5 | Spontaneous Fission | 80 |
| 4.4.6 | Isomeric Transition (IT) | 80 |
| 4.4.7 | Exotic Decay | 82 |
| | Further Reading | 82 |
| 5 | Interaction of Radiation with Matter | 83 |
| 5.1 | Basic Concepts | 83 |
| 5.2 | Interaction of Alpha Particles with Matter | 85 |
| 5.2.1 | Energy Loss of Alpha Particles | 85 |
| 5.2.2 | Backscattering of Alpha Particles | 91 |
| 5.3 | Interaction of Beta Radiation with Matter | 94 |
| 5.3.1 | Interaction of Beta Particles with Orbital Electrons and the Nuclear Field | 96 |
| 5.3.2 | Cherenkov Radiation | 97 |
| 5.3.3 | Annihilation of Positrons | 98 |
| 5.3.4 | Absorption of Beta Radiation | 99 |
| 5.3.5 | Self-Absorption of Beta Radiation | 102 |
| 5.3.6 | Backscattering of Beta Radiation | 105 |
| 5.4 | Interaction of Gamma Radiation with Matter | 109 |
| 5.4.1 | Rayleigh Scattering | 111 |
| 5.4.2 | Thomson Scattering | 111 |
| 5.4.3 | Compton Scattering | 111 |
| 5.4.4 | The Photoelectric Effect | 113 |
| 5.4.5 | Pair Formation | 116 |

| | | |
|----------|--|------------|
| 5.4.6 | Total Absorption of Gamma Radiation | 116 |
| 5.4.7 | Resonance Absorption of Nuclei and the Mössbauer Effect | 117 |
| 5.5 | Interaction of Neutrons with Matter | 122 |
| 5.5.1 | Discovery of Neutrons | 123 |
| 5.5.2 | Production of Neutrons | 123 |
| 5.5.3 | Interaction of Neutrons with Matter | 125 |
| | Further Reading | 127 |
| 6 | Nuclear Reactions | 129 |
| 6.1 | Kinetics of Nuclear Reactions | 131 |
| 6.2 | Classification of Nuclear Reactions | 132 |
| 6.2.1 | Nuclear Reactions with Neutrons | 133 |
| 6.2.2 | Nuclear Reactions with Gamma Photons | 138 |
| 6.2.3 | Nuclear Reactions with Charged Particles | 138 |
| 6.2.4 | Thermonuclear Reactions | 141 |
| 6.2.5 | Nucleogenesis: The Production of Elements in the Universe | 142 |
| 6.2.6 | Production of Transuranium Elements | 147 |
| 6.3 | General Scheme of Radionuclide Production by Nuclear Reactions and Radioactive Decay | 150 |
| 6.4 | Chemical Effects of Nuclear Reactions | 150 |
| | Further Reading | 152 |
| 7 | Nuclear Energy Production | 153 |
| 7.1 | Nuclear Power Plants | 154 |
| 7.1.1 | The Main Parts of Nuclear Reactors | 156 |
| 7.1.2 | Natural Nuclear Reactors | 162 |
| 7.1.3 | The First Artificial Nuclear Reactor | 163 |
| 7.1.4 | Types of Nuclear Reactors | 163 |
| 7.1.5 | Environmental Impacts of Nuclear Reactors | 164 |
| 7.2 | Accidents in Nuclear Power Plants | 165 |
| 7.3 | Storage and Treatment of Spent Fuel and Other Radioactive Waste | 168 |
| 7.3.1 | Storage of Low- and Intermediate-Level Nuclear Waste | 171 |
| 7.3.2 | Treatment and Storage of High-Level Nuclear Waste | 171 |
| 7.4 | New Trends in Nuclear Energy Production | 173 |
| 7.4.1 | Improvement of the Fission in Nuclear Power Plants | 173 |
| 7.4.2 | Experiments with Fusion Energy Production | 174 |
| 7.5 | Nuclear Weapons | 175 |
| | Further Reading | 176 |
| 8 | Radioactive Tracer Methods | 177 |
| 8.1 | History of Radioactive Tracer Methods | 177 |
| 8.2 | Basic Concepts | 178 |
| 8.3 | Selection of Tracers | 183 |
| 8.4 | Position of the Labeling Atom in a Molecule | 187 |

| | | |
|--------|--|-----|
| 8.5 | General Methods for the Preparation of Radioactive Tracers | 190 |
| 8.5.1 | Tracers Received from Radioactive Decay Series | 191 |
| 8.5.2 | Artificial Radioactive Tracers | 194 |
| 8.6 | Radioactive Isotopes in Tracer Methods | 197 |
| 8.6.1 | Tritium | 198 |
| 8.6.2 | Carbon-14 | 199 |
| 8.6.3 | Isotopes Used in Medical PET | 200 |
| 8.6.4 | Sodium Isotopes | 200 |
| 8.6.5 | Magnesium-28 | 201 |
| 8.6.6 | Aluminum-28 | 201 |
| 8.6.7 | Phosphorus-32 (P-32) | 201 |
| 8.6.8 | Sulfur-35 (S-35) | 202 |
| 8.6.9 | Chlorine-36 | 202 |
| 8.6.10 | Potassium Isotopes | 202 |
| 8.6.11 | Calcium-45 | 202 |
| 8.6.12 | Chromium-51 (Cr-51) | 202 |
| 8.6.13 | Manganese-54 | 203 |
| 8.6.14 | Iron Isotopes | 203 |
| 8.6.15 | Cobalt-60 | 203 |
| 8.6.16 | Nickel-63 | 203 |
| 8.6.17 | Copper Isotopes | 203 |
| 8.6.18 | Zinc-65 | 204 |
| 8.6.19 | Gallium and Germanium Isotopes | 204 |
| 8.6.20 | Arsenic-76 (As-76) | 204 |
| 8.6.21 | Radioactive Isotopes of Selenium, Bromine, and Rare Earth Elements | 204 |
| 8.6.22 | Bromine Isotopes | 204 |
| 8.6.23 | Krypton-85 | 205 |
| 8.6.24 | Rubidium-86 | 205 |
| 8.6.25 | Strontium Isotopes | 205 |
| 8.6.26 | Yttrium-90 | 205 |
| 8.6.27 | Technetium-99m (Tc-99m) | 205 |
| 8.6.28 | Rutenium, Rhodium, and Palladium Isotopes | 206 |
| 8.6.29 | Silver Isotopes | 206 |
| 8.6.30 | Cadmium-115m | 206 |
| 8.6.31 | Indium Isotopes | 206 |
| 8.6.32 | Iodine Isotopes | 206 |
| 8.6.33 | Xenon Isotopes | 207 |
| 8.6.34 | Cesium Isotopes | 207 |
| 8.6.35 | Renium-186 | 207 |
| 8.6.36 | Iridium-192 | 207 |
| 8.6.37 | Gold-198 | 207 |
| 8.6.38 | Mercury-203 | 208 |
| 8.6.39 | Isotopes of Elements Heavier than Mercury | 208 |
| 8.6.40 | Transuranium Elements | 208 |

| | | |
|-----------|--|------------|
| 8.7 | The Main Steps of the Production of Unsealed Radioactive Preparations (Lajos Baranyai) | 208 |
| 8.7.1 | Unsealed Radioactive Preparations Using Reactor Irradiation | 209 |
| 8.7.2 | Unsealed Radioisotope Preparations Based on Cyclotron Irradiation | 222 |
| 8.7.3 | Quality Control of Unsealed Radioactive Preparations | 225 |
| 8.8 | Production of Encapsulated Radioactive Preparations (Sealed Sources) (Lajos Baranyai) | 225 |
| 8.8.1 | The Main Steps of the Production of Sealed Radioactive Sources | 226 |
| 8.8.2 | Quality Control of Sealed Radioactive Sources | 226 |
| 8.9 | Facilities, Equipment, and Tools Serving for Production of Radioactive Substances (Lajos Baranyai) | 226 |
| | Further Reading | 230 |
| 9 | Physicochemical Application of Radiotracer Methods | 233 |
| 9.1 | The Thermodynamic Concept of Classification (Distribution of Radioactive and Stable Isotopes) | 233 |
| 9.2 | Classification of Tracer Methods | 236 |
| 9.3 | Physicochemical Applications of Tracer Methods | 239 |
| 9.3.1 | Solubility Measurements | 239 |
| 9.3.2 | Measurements of the Rate of Migration, Diffusion, and Self-Diffusion | 240 |
| 9.3.3 | Isotope Exchange Reactions | 251 |
| 9.3.4 | Study of Interfacial Reactions | 265 |
| 9.3.5 | Coprecipitation | 268 |
| 9.3.6 | Tracer Techniques in Electrochemistry | 269 |
| | Further Reading | 270 |
| 10 | Radio- and Nuclear Analysis | 273 |
| 10.1 | Radioactive Isotopes as Tracers | 273 |
| 10.1.1 | The Measurement of Concentration Using Natural Radioactive Isotopes | 273 |
| 10.1.2 | Determination Yield of Separation Reactions by Radioactive Tracers | 274 |
| 10.1.3 | Solubility Measurements | 276 |
| 10.1.4 | Radiochromatography | 276 |
| 10.1.5 | Radiometric Titration | 276 |
| 10.1.6 | Isotope Dilution Methods | 279 |
| 10.2 | Radioanalytical Methods Using the Interaction of Radiation with Matter | 283 |
| 10.2.1 | Basic Concepts | 283 |
| 10.2.2 | Analytical Methods Using Irradiations with Neutrons | 286 |
| 10.2.3 | Irradiation with X-Ray and Gamma Photons | 302 |

| | | |
|-----------|---|------------|
| 10.2.4 | Irradiation with Electron and Beta Radiation | 309 |
| 10.2.5 | Irradiation with Charged Particles | 312 |
| | Further Reading | 317 |
| 11 | Industrial Application of Radioisotopes | 319 |
| 11.1 | Introduction | 319 |
| 11.2 | Tracer Investigations with Open Radioisotopes | 319 |
| 11.2.1 | The Principle, Types, and Sensitivity of the Radiotracer Technique | 320 |
| 11.2.2 | Unsealed Radionuclides Used for Labeling in Industrial Tracer Studies | 321 |
| 11.2.3 | Exploration of Leaks | 322 |
| 11.2.4 | Determination of Flow Rates | 324 |
| 11.2.5 | Measuring Volume and/or Mass of Large Quantities of Substances in Closed Equipment | 327 |
| 11.2.6 | Investigation of Homogeneity of Mixtures | 328 |
| 11.2.7 | Characterization of Material Flow and Determination of Chemical Engineering Parameters | 330 |
| 11.2.8 | Wear Studies | 337 |
| 11.2.9 | Groundwater Flow Studies | 338 |
| 11.3 | Absorption and Scattering Measurements with Sealed Radioactive Sources | 339 |
| 11.3.1 | Principle of the Measurements | 339 |
| 11.3.2 | Sealed Radioactive Sources Used for Measurement | 340 |
| 11.3.3 | Level Indication of Materials in Tanks | 340 |
| 11.3.4 | Material Thickness Determination | 341 |
| 11.3.5 | Material Density Determination | 344 |
| 11.3.6 | Moisture Content Determination | 345 |
| 11.3.7 | Industrial Radiography | 347 |
| 11.3.8 | Geological Borehole Logging with Nuclear Methods | 349 |
| | Further Reading | 350 |
| 12 | An Introduction to Nuclear Medicine | 351 |
| 12.1 | Fields of Nuclear Medicine | 352 |
| 12.1.1 | <i>In Vitro</i> Diagnostics | 352 |
| 12.1.2 | <i>In Vivo</i> Diagnostics | 352 |
| 12.1.3 | Therapy with Unsealed Radioactive Preparations | 353 |
| 12.2 | The Role and Aspects of Applying Radiotracers in Medicine | 353 |
| 12.2.1 | Comparison of Methods for <i>In Vitro</i> Measurement of Concentrations | 353 |
| 12.2.2 | Measurement of Tracers and Contrast Materials Inside the Organism by External Detectors | 353 |
| 12.2.3 | Production of Artificial Radionuclides | 354 |
| 12.2.4 | How Do You Choose Radiotracers for Medical Applications? | 354 |

- 12.2.5 Types of Electromagnetic Radiation
- 12.2.6 Most Common Radionuclides in Nuclear Medicine
- 12.3 In Vitro Diagnostics with Radioisotopes
 - 12.3.1 Basic Reaction of Immunoassays
 - 12.3.2 Immunometric ("Sandwich") Assay
- 12.4 Radionuclide Imaging
 - 12.4.1 Parts of a Gamma Camera
 - 12.4.2 Digital Gamma Cameras
 - 12.4.3 Methods for Emission Imaging
 - 12.4.4 Computer-Aided Processing of Nuclear Medical Images
- 12.5 Some Examples of Gamma Camera Imaging Procedures
 - 12.5.1 Thyroid Scintigraphy
 - 12.5.2 Tumor Imaging
 - 12.5.3 Myocardial Perfusion Scintigraphy
 - 12.5.4 SPECT Imaging of Epilepsy
- 12.6 Positron Emission Tomography
 - 12.6.1 The PET Camera
 - 12.6.2 ^{18}F -FDG PET Studies with PET/CT
 - 12.6.3 Research Studies Using PET
 - 12.6.4 Imaging Myocardial Metabolism
- Further Reading
- 13 Environmental Radioactivity
 - 13.1 Natural Radioactive Isotopes
 - 13.2 Radioactive Isotopes of Anthropogenic Origin
 - 13.3 Occurrence of Radioactive Isotopes in the Environment
 - 13.3.1 Radioactivity in the Atmosphere
 - 13.3.2 Radioactivity in the Hydrosphere
 - 13.3.3 Radioactivity in the Lithosphere
 - 13.3.4 Radioactive Isotopes in Living Organisms
 - 13.4 Biological Effects of Radiation
 - 13.4.1 Dose Units
 - 13.4.2 Mechanism of Biological Effects
 - 13.4.3 The Natural Background of Radiation
 - 13.4.4 Effects of Radiation on Living Organisms
- Further Reading

14 Detection and Measurement of Radioactivity

14.1 Gas-Filled Tubes

14.2 Scintillation Detectors

14.2.1 Scintillator Materials

14.2.2 Photomultipliers

14.3 Semiconductor Detectors

14.4 Electric Circuits Connected to Detectors

14.5 Track and Other Detectors

14.5.1 Cloud Chambers and Bubble Chambers

14.5.2 Autoradiography

14.5.3 Solid-State Detectors

14.5.4 Chemical Dosimeters

14.5.5 Detection of Neutrons by Nuclear Reactions

14.6 Absolute Measurement of Decomposition

14.7 Statistics of Radioactive Decay

14.7.1 Statistical Error of Radioactivity Measurement

14.7.2 Correction of Background Radioactivity

Further Reading

Preface

This book aims to provide the reader with a detailed description of the basic principles and applications of nuclear and radiochemistry. Its content is based on the authors' more than 50 and 25 years of experience, respectively, as professors of nuclear and radiochemistry at both the B.Sc. and M.Sc. levels in the Isotope Laboratory of the Department of Colloid and Environmental Chemistry at the University of Debrecen, Hungary.

Although the book contains all modern aspects of nuclear and radiochemistry, it still has a characteristic local flavor. Special attention is paid to the thermodynamics of radioisotope tracer methods and to the very diluted systems (carrier-free radioactive isotopes), to the principles of chemical processes with unsealed radioactive sources, and to the physical and mathematical aspects of radiochemistry. This approach originates from the first professor of the Isotope Laboratory, Lajos Imre, who himself was Otto Hahn's disciple and coworker.

The material is divided into 14 chapters. Chapters 1–6 discuss the basic concepts of nuclear and radiochemistry and Chapters 7–14 deal with the applications of radioactivity and nuclear processes. There are separate chapters dedicated to the main branches of modern radiochemistry: nuclear medicine and nuclear power plants, including the problems of the disposal of nuclear wastes. One chapter (Chapter 10) deals with nuclear analysis (both bulk and surface analyses), including the analytical methods based on the interactions of radiation with matter.

As mentioned previously, the authors have extensive experience in teaching nuclear and radiochemistry. Therefore, we have had the chance to work with many exceptional students and excellent colleagues. Many thanks for their contributions. We are grateful for their assistance in the improvement of our educational work and the useful discussions that helped to advance our understanding in this field.

We thank our colleagues who have contributed to this book, namely, Dr. Lajos Baranyai (Chapter 11 and Section 8.7) and Dr. József Varga (Chapter 12). Many thanks to Dr. Szabolcs Vass and Dr. József Kónya (a physician and an associate professor) for their assistance in the fields of neutron diffraction and the biological effects of radiation, respectively. Thanks also to those colleagues, namely, Prof. László Bartha, Prof. Dezső Beke, Dr. István Csige, Prof. Julius Csikai, Prof. Béla Kanyár, Dr. Anikó Kerkápoly, Dr. Zsófia Kertész, Dr. Péter Kovács-Pálffy, Dr. László Kövér, Prof. Ernő Kuzmann, Boglárka Makai, Katalin Nagy, Zoltán Nemes, Dr. Katalin Papp, Dr. Péter Raics, Dr. Zsolt Révay, Dr. László Szentmihályi, Dr. Edit Szilágyi, Dr. Nóra Vajda, who have provided excellent representative photographs, figures, data, and so on. Prof. Julius Csikai provided the beautiful photograph

on the book cover. Thanks to Zoltán Major for the improvement of the quality of the photograph.

We thank Dr. Klára Kónya for the critical reading of the manuscript and for her remarks and corrections.

The work is supported by the TÁMOP 4.2.1./B-09/1/KONV-2010-0007 project. The project is cofinanced by the European Union and the European Social Fund.

We recommend this book to students in chemistry, chemical engineering, environmental sciences, and specialists working with radiochemistry in industry, agriculture, geology, medicine, physics, analytics, and to those in other fields.

József Kónya and Noémi M. Nagy
December 2011, Debrecen (Hungary)

1 Introduction

From the dawn of natural sciences, scientists and philosophers have reflected on the nature of matter. In the end of the nineteenth century, the discoveries signed by Lavoisier, Dalton, and Avogadro (namely, the law of conservation of mass, the atomic theory, and the definition of a mole as a unit of the chemical quantity) led to a plausible model. This model was built on the principles of Dalton's atomic theory, which states that:

- all matter is composed of small particles called atoms,
- each element is composed of only one chemically distinct type of atom,
- that all atoms of an element are identical, with the same mass, size, and chemical behavior, and
- that atoms are tiny, indivisible, and indestructible particles.

In the same period, the basic laws of thermodynamics have been postulated. The first law of thermodynamics is an expression of the principle of conservation of energy.

This model of the matter has been challenged when it was discovered that the same element can have radioactive and stable forms (i.e., an element can have atoms of different mass). The discovery of the radioactivity is linked to Henri Becquerel's name and to the outcome of his experiments which were presented in 1896 at the conference of the French Academy and published in *Comptes Rendus e l'Académie des Sciences*.

Following his family tradition (his father and grandfather also studied fluorescence, and his father, Edmund Becquerel, studied the fluorescence of uranium salts), Becquerel examined the fluorescent properties of potassium uranyl sulfate [$\text{K}_2\text{UO}_2(\text{SO}_4)_2 \cdot 2\text{H}_2\text{O}$]. Since Wilhelm Röntgen's previous studies, it has been known that X-rays can be followed by phosphorescent light emitted by the wall of the X-ray tube, and Becquerel wanted to see if this process could be reversed, i.e., if phosphorescent light can produce X-rays. After exposing potassium uranyl sulfate to sunlight, he wrapped it in black paper, placed it on a photographic plate, and observed the "X-ray." He repeated the experiments with and without exposure to sunlight and obtained the same result: the blackening of the photographic plate. He has concluded that the blackening of the photographic plate was not caused by fluorescence induced by sunlight, but rather by an intrinsic property of the uranium salt. This property was first called Becquerel rays, and later it was termed

“radioactive radiation¹.” Becquerel also has observed that electroscope loses its charge under the effect of this radiation because the radiation induces charges in the air.

The same radiation was observed by Pierre Curie and Marie Curie, as well as G. Schmidt in Germany using thorium salts. They have found that the ores of uranium and thorium have more intense radiation than the pure salts: for example, pitchblende from Johanngeorgenstadt and Joachimstal has about five and four times more intense radiation, respectively, than black uranium oxide (U_3O_8). This more intense radiation originates from elements that were not present in the pure salts, which later were identified as the new radioactive elements polonium and radium, and which were separated from uranium ore in Joachimstal. The Curies presented the results at the French Academy in 1898 and published in *Comptes Rendus e l'Académie des Sciences*. As proposed by Marie Curie, the first new radioactive element, polonium, was named after her homeland of Poland. In the Curies' laboratory, radioactivity was detected by the ionization current produced by the radiation. In 1902, the Curies produced 100 mg of radium and determined the atomic mass, which they later corrected (226.5 g/mol). Marie Curie produced metallic radium by electrolysis of molten salts in 1910.

Rutherford has differentiated three types of radiation (alpha, beta, and gamma) by using absorption experiments in 1889. He also determined that the radiations had very high energy. In 1903, Rutherford and Soddy concluded that the radioactive elements are undergoing spontaneous transformation from one chemical atom into another and that the radioactive radiation was an accompaniment of these transitions. Radioactive elements were called radioelements. Since they were not known earlier, and therefore did not have names, some of them were named by adding letters to the name of the original (i.e., parent) element (e.g., UX, ThX). Others were given new names (such as radium, polonium, radium emanation-today radon).

The discovery of radium and polonium filled two empty places on the periodic table. Later studies, however, showed that some radioactive elements had the same chemical properties as known stable elements—they differed only in the amount of radioactivity. Therefore, they should be put in places in the periodic table that are already filled, which is impossible according to Dalton's atomic theory. For example, different types of thorium (thorium, UX1, iononium (Io), radioactinium, today Th-232, Th-234, Th-230, and Th-227, respectively) and radium (radium, mesothorium1, ThX, AcX, today Ra-226, Ra-228, Ra-224, or Ra-223, respectively) atoms have been recognized.

These experimental results presented serious contradictions to the Daltonian model of matter and the principle of the conservation of mass and energy. Einstein

¹ In 1867, Niepce de Saint-Victor showed that uranium salts emit radiations in the dark, but Becquerel rejected this saying that “Niepce could not have observed the radiation from uranium because the author used plates that were not sensitive enough.”

has solved part of these contradictions using the law of the equivalence of energy and mass:

$$E = mc^2 \quad (1.1)$$

where E is the energy of the system, m is the mass, and c means the velocity of light in a vacuum.

As the interpretation of the other part of the contradictions, Soddy defined the term “isotopes,” neglecting the postulate in Dalton’s theory on the identity of the atoms of an element. Accordingly, isotopes are atoms of the same element having different masses.

What kind of scientific and practical importance did these discoveries have? At first, they formed the basis of the modern atomic theory, resulting in the development of new fields and explaining some phenomena. For example, nucleogenesis, the formation of the elements in the universe, now can be explained based on the principles of natural sciences, attempting to give a philosophical significance of the “creation.”

From the beginning, the practical importance has been underestimated. In 1898, however, radium found its role in cancer therapy. In 1933 in the Royal Society meeting, Rutherford said that “any talk of atomic energy” was “moonshine.” Rutherford’s statement inspired Leo Szilárd to devise the principle of the nuclear chain reaction, which was experimentally discovered by Otto Hahn in 1938. The chain reaction of uranium fission led to the production of nuclear power plants, and, unfortunately, nuclear weapons as well. However, in the future, the production of cheap, safe atomic energy can play a significant role in supplying energy.

As the practical applications of radioactivity, tracer methods, activation analysis, nuclear medicine, and radiation therapy can be mentioned. As mentioned previously, radioactivity has been discovered to be a natural process. Therefore, it is not an artificial product as believed by many. The environmental radioactive isotopes can be classified into three groups:

1. The members of three natural decay series starting with ^{238}U , ^{235}U , and ^{232}Th isotopes. From an environmental point of view, the members with relatively long half-lives are important, for example, ^{226}Ra and its daughter elements, ^{222}Rn , ^{210}Pb , ^{210}Bi , ^{210}Po from the decay series of ^{238}U and ^{220}Rn from the thorium series.
2. Long-life nuclei produced during nucleogenesis, for example, ^{40}K , ^{50}V , ^{87}Rb , ^{113}Cd , ^{115}In , ^{123}Te , ^{138}La , ^{144}Nd , $^{147,148}\text{Sm}$, ^{152}Gd , ^{156}Dy , ^{174}Hf , ^{176}Lu , ^{186}Os , ^{187}Re , ^{190}Pt .
3. Natural radioactive isotopes continuously producing in the nuclear reactions of the atoms of air (nitrogen, oxygen, argon) with cosmic radiation, for example, ^3H , $^{7,10}\text{Be}$, ^{14}C , ^{22}Na , ^{26}Al , $^{32,33}\text{P}$, ^{35}S , ^{36}Cl , ^{39}Ar .

As previously discussed, many of these elements have naturally occurring radioactive isotopes.

The main stages of the history of nuclear science are summarized in [Table 1.1](#), including the Nobel prizes gained by the scientists working in this field. In addition, the chapters of this book related to the given stages are also listed.

Table 1.1 History of Nuclear Science

| Year | Discovery | Researcher(s)/country(ies) | Nobel Prize | In This Book |
|-------------|--|---|--------------------|----------------------------|
| 1895 | X-ray | W. Röntgen | 1901 | This chapter |
| 1896 | Radioactivity by the radiation of uranium salt | H. Becquerel | 1903 | This chapter |
| 1898 | Polonium and radium | P. and M. Curie | 1903 | This chapter |
| 1899 | Radioactivity is caused by the decomposition of atoms | J. Elster and H. Geitel | | This chapter |
| 1900 | Gamma radiation is considered as electromagnetic radiation | P. Villard and H. Becquerel, proved in 1914 by E. Rutherford and E. Andrade | | Section 4.6 in Chapter 4 |
| 1900 | Beta decay consists of electrons | H. Becquerel | | Section 4.2 in Chapter 4 |
| 1902 | Preparation of radium | P. and M. Curie, Debierne | 1911 | This chapter |
| 1903 | Alpha radiation consists of the ions of helium | E. Rutherford | 1908 | Section 4.1 in Chapter 4 |
| 1903 | Radon (radium emanation) | W. Ramsay and F. Soddy | 1904 | Section 4.2, Section 8.5.1 |
| 1898–1902 | Radiation has chemical and biological effects | P. Curie, A. Debierne, H. Becquerel, H. Danlos, and others | | Section 13.4 |
| 1896–1905 | Genetic relation of the radioelements | H. Becquerel, E. Rutherford, F. Soddy, B. Boltwood, and others | | Section 4.2 |
| 1905 | Equivalence of energy and mass | A. Einstein | | This chapter |
| 1907 | Therapeutic application of radium | T. Stenbeck | | Section 8.5.1 |
| 1909 | Alpha scattering experiments: discovery of nucleus | H. Geiger and E. Marsden | | Section 5.2.2 |
| 1909 | Terms of isotopes | F. Soddy | 1921 | Chapter 3 |

| | | | | |
|------|---|------------------------------|------|--|
| 1910 | Determination of atomic mass by deviation in electric and magnetic field | J.J. Thomson | | Section 3.1.1 |
| 1911 | Rutherford's atomic model | E. Rutherford | | Section 2.1.1, Section 5.2.2 |
| 1912 | Radioactive indication | G. Hevesy and F. Paneth | 1943 | Chapters 8–12 |
| 1912 | Cloud chamber | C.T. Wilson | 1927 | Section 14.5.1 |
| 1913 | Cosmic radiation | V.F. Hess | 1936 | Section 2.2, Section 13.4.3 |
| 1913 | Interpretation of the decay series by using isotopes | K. Fajans and F. Soddy | | Section 4.2 |
| 1913 | Separation of neon isotopes using the deviation in electric and magnetic field | F.W. Aston | 1922 | Section 3.1.1 |
| 1913 | Nucleus is surrounded by electrons moving on orbitals with well-determined energy | N. Bohr | 1922 | |
| 1913 | Determination of the size and charge of atomic nuclei | H. Geiger and E. Marsden | | Section 2.1.1, Section 5.2.2 |
| 1913 | Counter for radioactivity measurement | H. Geiger | | Section 14.1 |
| 1919 | The first nuclear reaction: ${}^4\text{He} + {}^{14}\text{N} \rightarrow {}^{17}\text{O} + {}^1\text{H}$ | E. Rutherford | | Chapter 6 |
| 1919 | Mass spectrometer | F.W. Aston | 1922 | Section 3.1.1 |
| 1921 | Isomer nuclei: ${}^{234\text{m}}\text{Pa}(\text{UX}_2) \rightarrow {}^{234}\text{Pa}(\text{UZ})$ | O. Hahn | | Section 4.4.6 |
| 1921 | Separation of isotopes by distillation | J.N. Brönsted and G. Hevesy | | Section 3.2 |
| 1923 | Inelastic scattering of gamma photons | A.H. Compton | 1927 | Section 5.4.3 |
| 1924 | Wave-particle duality of moving particles | L. De Broglie | | Section 4.4.1, Section 5.5.3, Section 6.1, Section 10.2.2.4 |
| 1924 | The radioactive tracer (Po) in biological research | A. Lacassagne and J.S. Lates | | Section 8.5.1 |
| 1925 | The exclusion principle | W. Pauli | 1945 | Section 2.3 |
| 1926 | Wave mechanics in quantum theory | E. Schrödinger | 1933 | Section 4.4.1 |

(Continued)

Table 1.1 (Continued)

| Year | Discovery | Researcher(s)/country(ies) | Nobel Prize | In This Book |
|-------------|---|--|--------------------|------------------------------|
| 1927 | Experimental confirmation of the wave-particle duality | C.J. Davisson, L.H. Germer, and G.P. Thomson | | Section 4.4.1 |
| 1927 | The uncertainty principle | W. Heisenberg | 1932 | Section 2.1.1 |
| 1928 | The Geiger–Müller counter | H. Geiger and W. Müller | | Section 14.1 |
| 1931 | A high-voltage generator for acceleration of ions | R.J. Van de Graaf | | Section 6.2.3 |
| 1932 | Cyclotron | E. Lawrence and M.S. Livingston | | Section 6.2.3, Section 8.5.2 |
| 1932 | Deuterium; isotope enrichment by evaporation of liquid hydrogen | H. Urey | 1934 | Chapter 3.2 |
| 1932 | Neutron | J. Chadwick | 1935 | Section 2.1, Section 5.5.3 |
| 1932 | Nucleus: protons + neutrons | W. Heisenberg | | Section 2.1 |
| 1932 | Positron | C.D. Andersson | 1936 | Section 4.2.2 |
| 1932 | Nuclear reactions with accelerated charged particles | J.D. Cockcroft and E.D.S. Walton | 1951 | Section 6.2.3 |
| 1933 | Isotopic effects in chemical reactions | H. Urey and D. Rittenberg | | Sections 3.1.4 and 3.1.5 |
| 1933 | Pair formation | I. Curie and F. Joliot-Curie | | Section 5.4.5 |
| 1933 | Magnetic momentum of proton | O. Stern | 1943 | Section 2.3 |
| 1931–1933 | Nuclear studies by improved cloud chamber | P.M.S. Blackett | 1948 | Section 14.5.1 |
| 1931–1937 | Symmetry principles of the nucleus | E.P. Wigner | 1963 | Section 2.3 |

| | | | | |
|-----------|--|---|------|---|
| 1934 | Annihilation | M. Thibaud and F. Joliot-Curie | | Section 5.3.3 |
| 1934 | Artificial radioactivity: ${}^4\text{He} + {}^{27}\text{Al} \rightarrow {}^{30}\text{P} + \text{n}$ | F. Joliot-Curie and I. Curie | 1935 | Chapter 6 |
| 1934 | Discovery of Cherenkov radiation | P.A. Cserenkov, I.M. Frank, and I.E. Tamm | 1958 | Section 5.3.2 |
| 1935 | Postulation of mesons | H. Yukawa | 1949 | Section 2.2 |
| 1935 | Semiempirical formula for the binding energy of nuclei | C.F. Weizsäcker | | Section 2.5.1 |
| 1935–1936 | Description of nuclear reactions with neutrons | E. Fermi | 1938 | Section 6.2.1 |
| 1936 | Neutron activation analysis (NAA) | G. Hevesy and H. Levi | | Section 10.2.2.1 |
| 1937 | Principle of Cherenkov radiation | P.A. Cserenkov, I.M. Frank, and I.E. Tamm | 1958 | Section 5.3.2 |
| 1937 | Technetium | G. Perrier and E. Segre | | |
| 1937 | μ -Mesons in cosmic radiation | S. Neddermeyer and C.D. Andersson | | Section 2.2 |
| 1938 | Theory of nuclear fusion in stars | H.A. Bethe and C.F. Weizsäcker | 1967 | Section 6.2.5 |
| 1938 | Fission of uranium using neutrons | O. Hahn and F. Strassman | 1944 | Section 6.2.1 |
| 1938 | Photomultiplier | Z. Bay | | Section 14.2.2 |
| 1930–1939 | Magnetic properties of nucleus | I.I. Rabi | 1944 | Section 2.3 |
| 1940 | First transuranium elements—neptunium and plutonium; chemistry of the transuranium elements; fission of plutonium-239 using neutrons | E.M. McMillan, G.T. Seaborg | 1951 | Section 6.2.6; the production of the additional transuranium elements are summarized in Table 6.3 |
| 1940 | Fission of ${}^{235}\text{U}$ by thermal neutrons; ${}^{232}\text{Th}$ and ${}^{238}\text{U}$ by fast neutrons produce two to three new neutrons and release a high amount of energy | | | Section 6.2.1 |
| 1942 | First nuclear reactor | E. Fermi and coworkers | | Section 7.1.3 |
| 1944 | Self-sustaining fission of uranium | Germany | | Section 7.1 |

(Continued)

Table 1.1 (Continued)

| Year | Discovery | Researcher(s)/country(ies) | Nobel Prize | In This Book |
|-------------|--|---|--------------------|---------------------|
| 1945 | Production of plutonium in kilograms. Application of nuclear weapons by the United States | Japan (Hiroshima, Nagasaki) | | Section 7.5 |
| 1946–1948 | Magnetic momentum of the nucleus | F. Bloch and E.M. Purcell | 1952 | Section 2.3 |
| 1949 | Radiocarbon dating | W. Libby | 1960 | Section 4.3.6 |
| 1950 | Shell model of nuclei | M.G. Mayer, O. Haxel, J.H.D. Jensen, and H.E. Suess | 1963 | Section 2.5.2 |
| 1951 | First breeder and energy production reactor | Argonne National Laboratory (Idaho, USA) | | Section 7.1 |
| 1951 | Positronium atom | M. Deutsch | | Section 5.3.3 |
| 1951 | Application of Co-60 in therapy of cancer | | | Chapter 12 |
| 1951 | Measurement of the time less than 10^{-6} s of the excited state in the nucleus by scintillation counter | | | |
| 1952 | Bubble chamber | D.A. Glaser | 1960 | Section 14.5.1 |
| 1952 | The first uncontrolled fusion reaction (hydrogen bomb) | United States | | Section 7.5 |
| 1952 | The first atomic bomb experiment by Great Britain | Australia | | Section 7.5 |
| 1953 | Collective motion of the nucleons in the nucleus | A.N. Bohr, B.R. Mattelson, and L.J. Rainwater | 1975 | Section 2.5.3 |

| | | | | |
|-----------|---|---|------|---------------------------------|
| 1953 | The first atomic bomb experiment by Soviet Union | Soviet Union | | Section 7.5 |
| 1953 | Establishment of European Organization of Nuclear Research (CERN) | Twelve countries | | |
| 1953–1955 | Unified nuclear model | A. Bohr, B.R. Mottelson, and S.G. Nilsson | | Section 2.5.3 |
| 1953–1960 | Electron scattering on the nucleus | R. Hofstadter | 1961 | Section 10.2.1 |
| 1953–1960 | Experimental detection of neutrinos | F. Reines | 1995 | Section 4.4.2 |
| 1954–1958 | Electron spectroscopy | K.M. Siegbahn | 1981 | Section 10.2.1 |
| 1955 | Nuclear-powered submarine (<i>Nautilus</i>) | | | |
| 1954–1956 | 5 MWe energy production reactor in Obninsk | Soviet Union | | Chapter 7 |
| 1955–1960 | Neutron spectroscopy and diffraction | B.N. Brockhouse C.G. Shull | 1994 | Section 5.5.3, Section 10.2.2.4 |
| 1956 | 45 MWe energy production reactor in Calder Hall | Great Britain | | Chapter 7 |
| 1956–1965 | Nucleogenesis: formation of elements in the universe | S. Chandrasekhar W.A. Fowler | 1983 | Section 6.2 |
| 1958 | Discovery of the Mössbauer effect | R. Mössbauer | 1961 | Section 5.4.7 |
| 1959 | Radioimmunoassay (RIA): determination of peptide hormones | R.S. Yalow | 1977 | Section 12.3.1 |
| 1959 | The first civilian nuclear-powered ship (the Lenin icebreaker) | Soviet Union | | |
| 1960 | The first atomic bomb experiment by France | Algeria | | Section 7.5 |
| 1960–1965 | Classification of elementary particles | M. Gell-Mann | 1969 | Section 2.4 |
| 1961 | Invention of ^{238}Pu -powered satellite (Transit-4A) | | | |
| 1961 | Semiconductor detectors | | | Section 14.3 |
| 1964 | The first atomic bomb experiment by China | China | | Section 7.5 |

(Continued)

Table 1.1 (Continued)

| Year | Discovery | Researcher(s)/country(ies) | Nobel Prize | In This Book |
|-------------|--|-----------------------------------|--------------------|---------------------|
| 1969 | Plasma with high density in Tokamak fusion reactor | Soviet Union | | Section 7.4 |
| 1974 | The first atomic bomb experiment by India | India | | Section 7.5 |
| 1974 | Discovery of ancient natural nuclear reactor in Oklo (Gabon) | French scientists | | Section 7.1.2 |
| 1976 | SI-compatible-dose units (gray and sievert) | IUPAC | | Section 13.4.1 |
| 1979 | Accident at the Three Mile Island nuclear power plant | PA, USA | | Section 7.2 |
| 1979? | The first atomic bomb experiment by Israel? | | | Section 7.5 |
| 1986 | Accident at the Chernobyl nuclear power plant | Chernobyl, Soviet Union | | Section 7.2 |
| 1998 | The first atomic bomb experiment by Pakistan | Pakistan | | Section 7.5 |
| 2006 | The first atomic bomb experiment by North Korea | North Korea | | Section 7.5 |
| 2011 | Accident at the Fukushima nuclear power plant | Fukushima, Japan | | Section 7.2 |

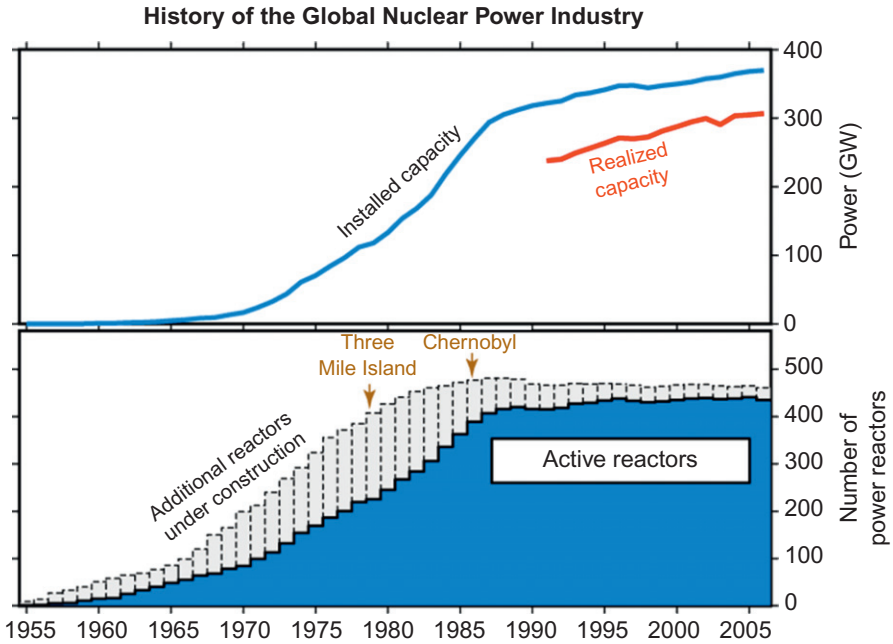


Figure 1.1 History of the use of nuclear power (top) and the number of active nuclear power plants (bottom).

Source: Free documentation from http://en.wikipedia.org/wiki/Nuclear_power.

In [Table 1.1](#), the time of the experimental nuclear explosions by different countries is also mentioned. The useful applications of nuclear energy can be indicated by the increase in the capacity and number of nuclear power plants, as shown in [Figure 1.1](#).

Further Reading

- Becquerel, H. (1896). Sur les Radiations Invisibles Emises par les Corps Phosphorescents. *Comptes Rendus Acad. Sci. Paris* 122:501–503.
- Curie, M. (1898). Rayons Émis par les Composes de l’Uranium et du Thorium. *Comptes Rendus Acad. Sci. Paris* 126:1101–1103.
- Curie, P. and Skłodowska-Curie, M. (1898). Sur une Nouvelle Substance Radioactive Contenu dans la Pechblende. *Comptes Rendus Acad. Sci. Paris* 127:175–178.
- Vroman, R., 2003. List of states with nuclear weapons. < http://en.wikipedia.org/wiki/List_of_states_with_nuclear_weapons.> (accessed 28.03.12.)
- Trelvis, 2002. Nuclear power. < http://en.wikipedia.org/wiki/Nuclear_power.> (accessed 28.03.12.).
- Atomarchive.com, 1998–2011. < <http://www.atomicarchive.com/Bios/Szilard.shtml>.> (accessed 28.03.12.)
- Hanh, O. (1962). *Vom Radiothor zur Uranspaltung*. Friedrich Vieweg & Sohn, Braunschweig.
- Haissinsky, M. (1964). *Nuclear Chemistry and its Applications*. Addison-Wesley, Reading, MA.
- Le Bon, G. (1912). *L’évolution de la matière*. Flammarion, Paris.
- Stein, W. (1958). *Kulturfahrplan*. F.A. Herbig Verlangbuchhandlung, Berlin.

2 Basic Concepts

2.1 Atomic Nuclei

2.1.1 Components of Nuclei

The atomic nuclei were discovered by the English physicist Ernest Rutherford on the basis of Ernest Mardsen's experiments (Figure 2.1). In their experiments, Mardsen and Hans Geiger studied the backscattering of alpha rays (which were known to be positively charged) from a gold plate and observed that a very small portion of these particles (about 1 in 100,000) were scattered back at an angle of 180° . Since the backscattering of the positive alpha particles is directed by electrostatic forces, this is possible only if a very high portion of the positive charge of the atom is concentrated in very little volume. This small component of the atom is the atomic nucleus. The backscattered portion of the alpha particles indicates that the radius of the nucleus is about 10^5 times smaller than the radius of the atom.

In addition to the positive charge, the mass of the atom is concentrated in the nucleus. The radius of the atomic nuclei (R) can be expressed approximately by Eq. (2.1):

$$R = R_0 \times A^{1/3} \quad (2.1)$$

where A is the mass number and R_0 is the radius of the nucleus of the hydrogen atom ($\sim 1.3 \times 10^{-15}$ m). As a consequence of Eq. (2.1), the density of any atomic nucleus is approximately the same ($\rho = 2 \times 10^{17}$ kg/m³), independent of the identity of the atoms. The mass of the nucleus is evenly distributed in the nucleus. This density then decreases quite abruptly to reach the density of the electron shell (which is very small—practically zero) at a distance of about 2.5×10^{-15} m from the nucleus. Similarly, the charge density surrounding the nucleus decreases over the same distance to reach the charge density of the electron shell, which is comparatively very small due to the relatively large size of the electron shell (about 10^{-10} m).

The alpha backscattering experiments proved that the atomic nuclei have mass, charge, and well-defined geometric size. At the time of the alpha backscattering experiments, not much was known about neutrons. It was conceptualized that in order to neutralize the positive charge of the protons, electrons must be present in the nucleus. This model is called J.J. Thomson's atomic model. According to this model, atomic

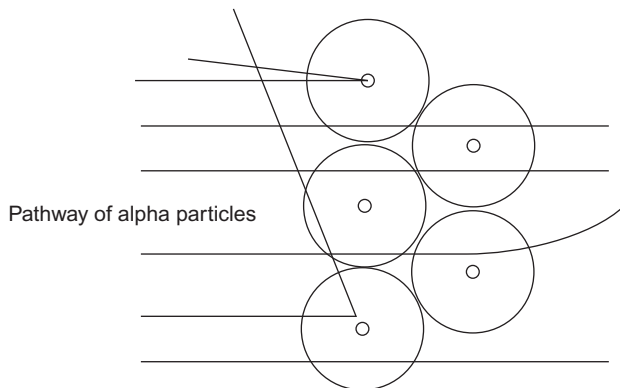


Figure 2.1 Backscattering of alpha particles.

nuclei should comprise protons and electrons. This model, however, can be disproved easily by the zero-point energy of the electron in the nucleus. Heisenberg's uncertainty principle says that

$$\Delta x \times \Delta v = \frac{h}{2\pi m} \quad (2.2)$$

where Δx and Δv are the uncertainty of the determination of the position and velocity, respectively; h is Planck's constant; and m is the mass of the particle. The radius of the nucleus (R) can be substituted for Δx in the equation; if $\Delta x > R$, then the electron is outside the nucleus. From Eq. (2.2), Δv , and from here the energy of the electron, can be expressed as follows:

$$\Delta v \approx \frac{h}{2\pi mR}, \quad E_{\text{kin}} = \frac{1}{2}mv^2 = \frac{h^2}{2mR^2} \quad (2.3)$$

These calculations for the nucleus show that the zero-point energy of the electron is two orders of magnitude greater than the binding energy of nucleons (7–8 MeV/nucleon). Thus, if the electrons were restricted in the nucleus, their energy would be so high that they would leave it instantly. So, it is clearly proved that electrons cannot be present in the nucleus. Subsequently, in 1920, Rutherford conceptualized that the nucleus contains neutral particles that explain the difference between the charge and the mass of the nucleus. These particles were called “neutrons,” and they were experimentally demonstrated by James Chadwick in 1932 (Section 5.5.1).

Atomic nuclei consist of protons and neutrons. The number of protons is the atomic number (Z), and the sum of the number of protons (Z) and neutrons (N) is the mass number (A). The particles composing the nuclei are called “nucleons.”

Table 2.1 The Masses of the Atomic Particles and Some Atoms Expressed in Different Units

| Particle/nucleus | kg | a.m.u. ^a | MeV ^b |
|--------------------|--------------------------|-----------------------|------------------|
| Proton (m_p) | 1.6726×10^{-27} | 1.0078 | 938.2 |
| Neutron (m_n) | 1.6749×10^{-27} | 1.0086 | 939.5 |
| Electron (m_e) | 9.1072×10^{-31} | 5.48×10^{-4} | 0.511 |
| ^1H | | 1.0078 | |
| ^2H | | 2.0140 | |
| ^4He | | 4.0026 | |
| ^{14}N | | 14.00307 | |
| ^{16}O | | 15.99491 | |
| ^{17}O | | 17.0045 | |
| ^{24}Mg | | 23.98504 | |
| ^{35}Cl | | 34.9688 | |
| ^{37}Cl | | 36.9775 | |
| ^{40}Ca | | 39.9626 | |
| ^{64}Zn | | 63.9295 | |
| ^{206}Pb | | 205.9745 | |

^aa.m.u., atomic mass unit.

^b1 a.m.u. = 931 MeV (million electron volts, [Section 2.2](#)).

2.2 Forces in the Nucleus

The mass of the charged particles (protons, nuclei, and electrons) can be determined by injecting them at a high speed into a magnetic field, where depending on their charge and mass, the path of particles deviates from a straight line. Neutrons, however, have no charges, so the mass of a neutron cannot be measured in this way; rather, its mass must be deduced. This can be achieved by the dissociation of the deuterium nucleus (one proton and one neutron) to a proton and neutron under the effect of gamma radiation.

The masses of free protons, neutrons, and electrons are listed in [Table 2.1](#). When comparing the mass of the nucleus of an atom to the total mass of the free protons and neutrons, we can see that the sum of the mass of the free nucleons is always greater than the mass of the corresponding nucleus in the atom.

This difference will be equal to the binding energy of the nucleus (ΔE). [Note that Einstein's formula for the equivalence of mass and energy (shown in Eq. (1.1)) can be used to calculate the binding energy.] When the binding energy of the nucleus is divided by the mass number, the binding energy per nucleon is obtained ($\Delta E/A$):

$$\frac{\Delta E}{A} = \frac{(M - Z \times m_p - N \times m_n - Z \times m_e)c^2}{A} \quad (2.4)$$

where M is the mass of the atom (not the nucleus!).

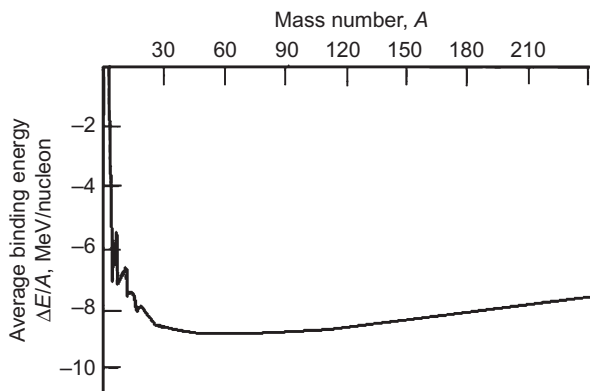


Figure 2.2 The binding energy per nucleon as a function of mass number.

The stability of a given nucleus can be characterized by the value of the binding energy per nucleon. The binding energy per nucleon as a function of atomic mass is shown in [Figure 2.2](#).

The characteristic binding energy per nucleon for the most stable nuclei is in the range of 7–9 MeV. The absolute value of the binding energy per nucleon—the mass number function shows a maximum of about mass numbers 50–60. This mass represents the elements of the iron group; thus, these elements are the most stable ones in the periodic table. The smallest nucleus, where the term of the binding energy per nucleon can be defined, is the deuterium, which has the smallest binding energy per nucleon (around 1.8 MeV).

The binding energy is usually expressed in millions of electron volts. One electron volt is the amount of energy gained by an electron (elementary charge, 1.6×10^{-19} C) when it is accelerated through an electric potential of 1 V. Transferring the electron volt to the SI unit of energy (joule), $1 \text{ eV} = 1.6 \times 10^{-19} \text{ C} \times 1 \text{ V} = 1.6 \times 10^{-19} \text{ J}$. For every 1 mol of electrons [found by multiplying by the Avogadro' number (6×10^{23} particles/mol)], about 10^5 J is obtained. The energy of an atomic mass unit (931 MeV), mentioned in [Table 2.1](#), is $\sim 10^{13}$ J. The binding energy per nucleon (7–9 MeV) is about 10^{11} J that is 10^8 kJ. Therefore, the binding energy of the nuclei is about 10^8 kJ/mol.

Now let's compare the binding energy of the nuclei to the energy of chemical bonds. The energy of primary (ionic, covalent) chemical bonds is a few hundred kJ/mol (an amount of electron volts). Thus, the difference is about six orders of magnitude: the binding energy of the nuclei is about a million times higher than the energy of the chemical reactions.

In 1935, Yukawa provided an interpretation of the nature of the forces in the atomic nuclei using quantum mechanics. He constructed a model similar to the one for electrostatic forces, where two charged particles interact through the electromagnetic field. In Yukawa's model, the so-called meson field should be substituted for the electromagnetic field. In the case of the meson field, the range of the interaction is very short (about 10^{-15} m), while the electromagnetic field has a much bigger range. The potential between two particles in the nuclei, known as the

Yukawa potential (U), can be expressed as a function of the distance of the two particles (r):

$$U = -g^2 \frac{\exp(r/R)}{r} \quad (2.5)$$

In Eq. (2.5), the potential is negative, indicating that the force is attractive. The constant g is a real number; it is equal to the coupling constant between the meson field and the field of the protons and neutrons. R is the range of the nuclear forces, expressed as follows:

$$R = \frac{h}{2\pi m_\pi c} \quad (2.6)$$

where h is Planck's constant, c is the velocity of light in a vacuum, and m_π is the rest mass of the meson. Assuming that the meson field range is about 10^{-15} m, Yukawa suggested that there must be a particle with a rest mass of about 200 times that of an electron. In fact, this particle was observed in the cosmic ray in 1948. It is called π -meson, and its rest mass is 273 times higher than the rest mass of the electron. The meson is a kind of elementary particle (as discussed in [Section 2.2](#)).

The total nuclear binding energy (ΔE) can be given approximately on the basis of nuclear forces, by the summation of the interaction energies of the nucleon pairs ($U_{r,kl}$) at the distance r :

$$\Delta E = -\frac{1}{2} \sum_k \sum_l U_{r,kl} \quad (2.7)$$

where ΔE is the total nuclear binding energy and k and l are the number of protons and neutrons, respectively. The protons and neutrons are considered to be identical. The factor $1/2$ is in Eq. (2.7) because of the two summations for protons and neutrons, so each nucleon appears twice. The total binding energy of the nucleus is proportional to the product of the number of protons and neutrons:

$$Z \times N = Z \times (A - Z) \quad (2.8)$$

The function of the total binding energy has a maximum of the atomic number expressed as follows:

$$\frac{d(AZ - Z^2)}{dZ} = 0 \quad (2.9)$$

From here

$$A = 2Z \quad (2.10)$$

In conclusion, those nuclei should be stable, such that the number of protons and neutrons are equal. This is indeed the case for light nuclei (e.g., ${}^4\text{He}$, ${}^{12}\text{C}$, ${}^{14}\text{N}$, ${}^{16}\text{O}$, ${}^{24}\text{Mg}$). However, for heavier nuclei, the number of protons increases, so the electrostatic repulsion of the positively charged protons increases. For this reason, extra neutrons are needed for stability. So Eq. (2.10) is modified as:

$$A \geq 2Z \quad (2.10a)$$

which means that the nuclei with high atomic numbers are stable at the ratio of neutron/proton = 1.4. The nuclei with medium atomic numbers have a ratio of neutron/proton between two values (1–1.4), i.e., the ideal neutron/proton ratio of the stable nuclei continuously changes in the periodic table (Figure 2.3).

The energy of the electrostatic repulsion can be calculated as follows:

$$E_c = \frac{3Z(Z-1) \times e^2}{5R_a} \quad (2.11)$$

where e is the elementary charge and R_a is the radius of the nucleus.

The nuclei are classified as isotope, isobar, isoton, or isodiaphere based on the number of nucleons (Table 2.2).

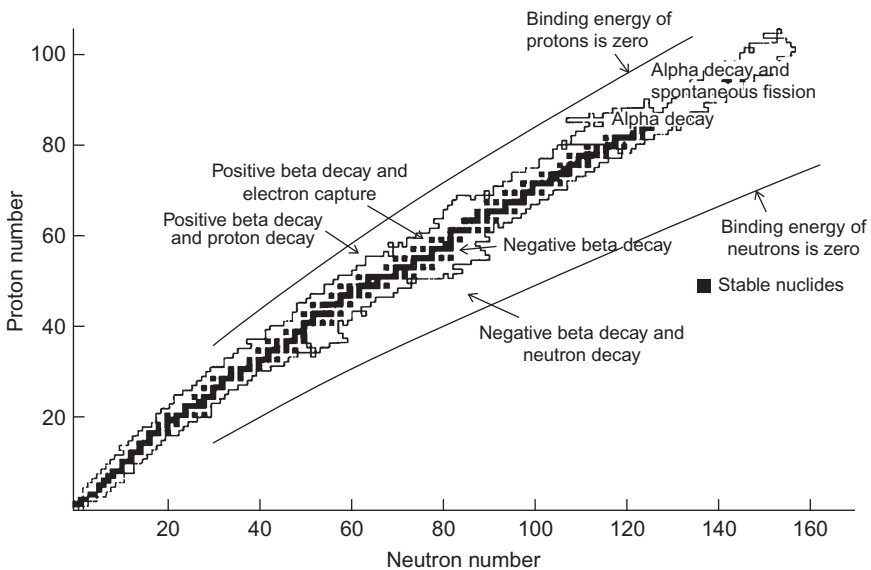


Figure 2.3 The stability of nuclei: atomic number as a function of the number of the neutrons.

Source: Conventional nuclear chart taken from Bes (1965) with permission from Elsevier.

2.3 Other Properties of Nuclei

The hyperfine structure observable in atomic spectra, including the interactions with nuclei, indicates that the nuclei have spin. The nuclear spin is a vector, and its absolute value is $\sqrt{I(I+1)}\frac{h}{2\pi}$, where I is the quantum number of the nuclear spin, simply called “nuclear spin.” Nuclei with even mass numbers have $I = 0, 1, 2, 3, \dots$, whereas nuclei with odd mass numbers have $I = \frac{1}{2}, \frac{3}{2}, \frac{5}{2}, \dots, \frac{11}{2}$. The nuclear spin is the sum of the spins of all protons and neutrons. In nuclear reactions, the conservation of spins also must occur.

Parity is related to the symmetry properties of nuclei. It expresses whether the wave function of a particle is even or odd (symmetrical or asymmetrical), depending on whether the wave function for the system changes sign when the spatial coordinates change their signs.

$$\text{Even parity: } \Psi(-x, -y, -z) = \Psi(x, y, z) \quad (2.12)$$

$$\text{Odd parity: } \Psi(-x, -y, -z) = -\Psi(x, y, z) \quad (2.13)$$

The conservation of parity also must occur for nuclear reactions.

The spin and the parity can be signed together: for nuclei with even parity, a + is written after the value of the spin, while for nuclei with odd parity, a – is written (e.g., $0+$ or $7/2-$).

The particles can be characterized by statistics describing the energies of single particles in a system comprising many identical particles, which has a close connection to the spin and parity of the particles. The particles with half-integral nuclear spin can be described using the Fermi–Dirac statistics. These particles obey the Pauli exclusion principle and have odd parity. These particles are called “fermions.” The particles with zero or integral spin and even parity can be described using the Bose–Einstein statistics. These particles are called “bosons.”

The movement of a charged particle causes magnetic momentum. The unit of measure for magnetic momentum is the Bohr magneton, which describes the magnetic momentum of an electron:

$$\mu_B = \frac{eh}{4\pi m_e} = 9.274 \times 10^{-24} \text{ J/T} \quad (2.14)$$

Table 2.2 Classification of Nuclei on the Basis of the Number of Nucleons

| Term | Z, Atomic Number | N, Number of Neutrons | A, Number of Nucleons | N–Z, Number of Extra Neutrons |
|-------------|------------------|-----------------------|-----------------------|-------------------------------|
| Isotope | Equal | Different | Different | |
| Isobar | Different | Different | Equal | |
| Isoton | Different | Equal | Different | |
| Isodiaphere | | | | Same |

For the nucleus, the mass of the proton can be substituted into Eq. (2.14) as follows:

$$\mu_N = \frac{eh}{4\pi m_p} = 5.050 \times 10^{-27} \text{ J/T} \quad (2.15)$$

where T is tesla. The quantity μ_N expresses the unit of nuclear magnetic momentum. The magnetic momentum of the different nuclei is in the range of $0-5\mu_N$. Surprisingly, the magnetic momentum of the proton is not equal to the value calculated from Eq. (2.15), but it is about 2.7926 times higher than the calculated value. Perhaps more surprising, the neutrons also have magnetic momentum, which is expressed by $-1.9135\mu_N$. This implies that the neutral neutron consists of smaller charged particles known as quarks, as discussed in Section 2.4. The negative sign of the magnetic momentum of the neutron indicates that the spin and magnetic momentums are in opposite directions.

Besides magnetic momentum, nuclei can have electric quadruple momentum too. The formation of quadruple momentum can be caused by the deviation of charge distribution from the spherical symmetry. Quadruple momentums have been determined for many nuclei by $I > 1/2$. Nuclei $I = 0$ or $1/2$ cannot have quadruple momentums.

In conclusion, the characteristic properties of nuclei are listed as follows:

1. Rest mass
2. Electric charge
3. Spin
4. Parity
5. Statistics
6. Magnetic momentum
7. Electric quadruple momentum (not all nuclei).

2.4 Elementary Particles

The main constituents of atoms are protons, neutrons, and electrons. After the revision of Dalton's atomic theory, these particles were considered to be elementary particles, the basic constituents of matter. Later, Yukawa recognized that the nucleons interact with each other through the meson field, and a new elementary particle, the meson, had to be postulated. Moreover, several different kinds of mesons with different rest masses and charges have been discovered. In addition, new elementary particles have been observed in different nuclear and cosmic processes. Today, more than 300 elementary particles are known (this fact raises the ironic question: How can something be called elementary if there are hundreds of them?).

The elementary particles can be classified on the basis of rest mass: light and heavy elementary particles are called leptons and hadrons, respectively. Hadrons can be divided into two groups: mesons (with medium rest mass) and baryons (with large rest mass). They are characterized similarly to the nuclei; as listed at

the end of [Section 2.3](#), they have rest mass, electric charge, spin, parity, statistics, magnetic moment, and electric quadruple moment. In addition, an important property of the elementary particle is the mean lifetime.

The heavy particles, hadrons, consist of more fundamental particles, which are called “quarks.” Particles are referred to as fundamental if they exhibit no inner structure. Quarks can be experimentally demonstrated, for example, by irradiating protons with 50 GeV electrons. The magnetic momentum of neutrons implies the presence of charged particles inside the neutron as well.

The physics of the elementary particles postulate six types and three families of quarks (up–down, charm–strange, top–bottom). Within the atomic nucleus, the up and down quarks are the most important. The rest mass of up and down quarks is about $1/3$ a.m.u. and their charge is $+2/3$ and $-1/3$, respectively. The proton consists of two up quarks and 1 down quark; the neutron contains one up quark and two down quarks. The sum of the rest masses of the three quarks gives 1 a.m.u. for both proton and neutron. In addition, the net charge of the nucleons ($+1$ for protons and 0 for neutrons) is the summation of the individual charges of the quarks. [Table 2.3](#) illustrates the important properties of some elementary particles. The particles with half-integral spin (fermions) are the fundamental constituents of matter; the particles with integral spin (bosons) are the exchange particles between quarks, which are similar to the exchange of photons in the electromagnetic force between two charged particles.

Interactions in the last column of [Table 2.3](#) can be ordered on the basis of their relative strength as follows:

| Interaction | Relative Strength |
|-----------------|-------------------|
| Strong | 1 |
| Electromagnetic | 10^{-2} |
| Weak | 10^{-14} |
| Gravitation | 10^{-39} |

The range of the interactions is inversely proportional to their relative strength. In nuclear processes, strong interactions are dominant. The range of strong interactions is about 10^{-15} m.

The antiparticles of all the particles listed in [Table 2.3](#) could and should exist. The electric charge of these antiparticles is the opposite of their corresponding particles. When the particle–antiparticle pairs interact with each other, they form other particles with lower or zero rest masses. As an example, the annihilation of positron and electron could be mentioned, which have a great practical importance (as discussed in [Section 5.3.3](#)).

2.5 Models of Nuclei

The structure of nuclei has been described by different models. At the moment, however, none of them alone explains all experimental observations. A useful review of 37 known models of the atomic nucleus is provided by Cook.

Table 2.3 Properties of Elementary (Fundamental) Particles

| Fermions: Spin 1/2 | | | | | | | | Bosons: Spin 1 | | | | |
|--------------------|------------|-----------------|--------|------------|------|---------------------|--------|-----------------------|----------|-------------------|---------|-----------------|
| Name | Sign | Rest Mass (MeV) | Charge | Name | Sign | Rest Mass (MeV) | Charge | Name | Sign | Rest Mass (MeV) | Charge | Interaction |
| Leptons | | | | Quarks | | | | | | | | |
| Electron | e | 0.511 | -1 | Up | u | 5.6 | +2/3 | Photon | γ | 0 | 0 | Electromagnetic |
| Electron neutrino | ν_e | 0 | 0 | Down | d | 9.9 | -1/3 | W-boson | W^\pm | 8.5×10^4 | ± 1 | Weak |
| Muon | μ^- | 105.8 | -1 | Charm | c | 1350 | +2/3 | Z ⁰ -boson | Z^0 | 9.5×10^4 | 0 | Strong |
| Muon neutrino | ν_μ | 0 | 0 | Strange | s | 199 | -1/3 | Gluon | g | 0 | 0 | |
| Tauon | τ^- | 1860 | -1 | Top | t | ca. 2×10^5 | +2/3 | Boson: Spin 2 | | | | |
| Tauon neutrino | ν_τ | 0 | 0 | Bottom | b | 5000 | -1/3 | Graviton | G | 0 | 0 | Gravitation |
| | | | | Heavy up | U | Existence | | | | | | |
| | | | | Heavy down | D | not proved | | | | | | |

The alpha model proposes the presence of alpha particles of great stability within the nuclei. This model has been suitable only for the interpretation of alpha decay.

2.5.1 The Liquid-Drop Model

The liquid-drop model is based on the constant density of nuclei, independent of the number and quality of nucleons. The phenomenon is analogous to a liquid drop in which the molecules are subjected to the same van der Waals forces, independent of the size of the drop.

According to the liquid-drop model, the nucleus can be imagined as a rather compact, spherical structure (similar to a liquid drop), the constituents of which are subjected to strong interactions acting in a very small range (about 10^{-15} m). Really, this is the nuclear force, the energy of which is approximately proportional to the mass number (A).

When the binding energy of a nucleus is calculated using this model, the nuclear energy has to be taken into account first. Let's suppose that the nuclear energy between two nucleons is U_0 . In the closest geometric packing of spheres, one nucleon has 12 neighbors (the coordination number is 12). It should mean $-12U_0$, the total energy for one nucleon; however, each nucleon is considered twice (nucleon pairs are investigated), so only $-12U_0/2 = -6U_0$ is the nuclear energy for one nucleon. For a nucleus with a mass number of A , the total nuclear energy is $-6U_0A$. This energy is shown as volume energy in [Figure 2.4](#).

Of course, the peripheral nucleons have only six neighbors, decreasing the nuclear energy. Considering the thickness of peripheral layer a , the volume of this layer is $4R^2\pi a$ (surface \times thickness). Since the volume of one nucleus is $4R^3\pi/3$ and the number of nucleons is A , the volume of one nucleon is $4R^3\pi/3A$. The number of nucleons in the peripheral layer can be obtained by dividing the volume of the layer with the volume of one nucleon: $3aA/R$. Therefore, the surface energy (E_s) of the nucleus can be expressed as:

$$E_s = 9 \frac{aAU_0}{R} \quad (2.16)$$

The nuclear energy corrected by the surface energy can also be seen in [Figure 2.4](#).

Since the protons repulse each other, the energy of repulsion has to be taken into account. The energy of the electrostatic repulsion can be expressed as in [Eq. \(2.11\)](#). So, the binding energy per nucleon has to be corrected with the electrostatic repulsion too ([Figure 2.4](#)):

$$\frac{\Delta E}{A} = -6U_0 + 9 \frac{a}{R} U_0 + \frac{3Z(Z-1)e^2}{5AR} \quad (2.17)$$

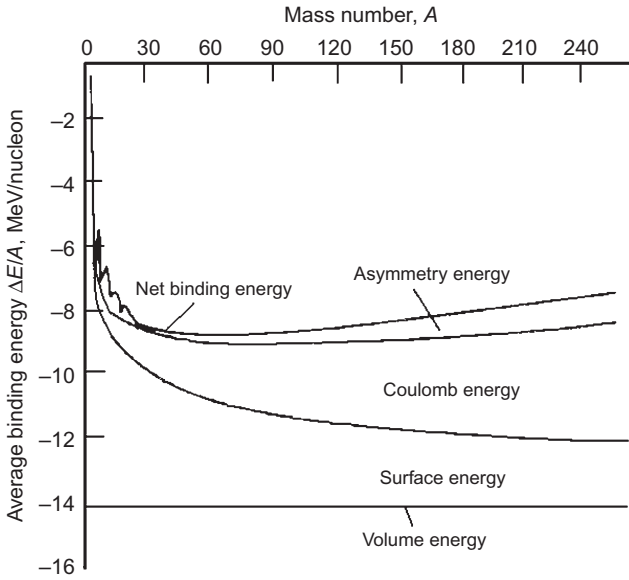


Figure 2.4 Factors influencing the binding energy by liquid drop.

The calculated binding energy per nucleon (Eq. (2.17)) is not accurately equal to the experimental value. The differences can be explained by two things. The first is that each value of A has a value of Z for which there is maximum stability (see Eqs. (2.10) and (2.10a)). When the ratio of the protons and neutrons is different from the maximum stability, a so-called asymmetry energy must also be taken into account because of the slightly different interaction energies of proton–proton, proton–neutron, and neutron–neutron pairs. The second is that the nuclei with even–even proton and neutron numbers are more stable than nuclei with odd–odd, even–odd, or odd–even nuclei. For even–odd and odd–even nuclei, this effect is taken to be zero, and for even–even nuclei, it is a negative number (increasing stability), whereas for odd–odd nuclei, it is a positive number (decreasing stability), and it will be discussed in Chapter 3.

The total semiempirical formula by Weizsäcker for the binding energy per nucleon is as follows:

$$\frac{\Delta E}{A} = -6U_0 + 9\frac{a}{R}U_0 + \frac{3}{5}\frac{Z(Z-1)e^2}{AR} + \frac{\varepsilon_4}{A} \pm \frac{\varepsilon_5}{A} \quad (2.18)$$

where

$$\frac{\varepsilon_4}{A} = \frac{\gamma}{A} \left(\frac{A}{2} - Z \right)^2 \quad (2.19)$$

and

$$\frac{\epsilon_5}{A} = \pm \alpha_5 A^{3/4} \quad (2.20)$$

and γ and α_5 are constants. As seen in [Figure 2.4](#), the binding energies calculated by Eq. (2.18) agree well with the experimental values.

2.5.2 The Shell Model

As seen in Section 2.5.1, the binding energy of nuclei can generally be expressed well by the liquid-drop model. However, this model cannot explain certain phenomena. For example, some nuclei with given mass numbers (2, 8, 20, 50, 82, 126, 184) are extremely stable. These numbers are called “magic numbers.” Also, a very small difference in the nuclei results in a very great difference in stability. For example, ^{210}Po and ^{212}Po isotopes differ in only two neutrons, but their half-lives are 138.37 days and 10^{-7} s, respectively, a fact that indicates very different stabilities.

These phenomena can be explained by the shell model of nuclei. This model postulates that, similar to electrons, nucleons are arranged in shells in the nucleus. The closed shells result in the most stability, and the magic numbers indicate filled shells. The stability is indicated by the mass of the nuclei: within the isobar nuclei, the nucleus with the lower mass is stable. The radioactive nuclei have unfilled shells.

According to the shell model, there should be some transuranium elements with relatively great stability and “long” half-lives.

2.5.3 Unified and Collective Models

Other models of nuclei take into consideration the different collective properties of nuclei: the nonspherical shape of some nuclei, especially in excited state, and vibrational and rotational levels of nuclei; and these models are used to explain the hyperfine structure of nuclear spectra. The two names, unified and collective models, are mostly used interchangeably since both represent collective effects. The unified model is a hybrid of the liquid-drop model and the shell model: the closed shells are treated as a liquid drop, and the outer, unclosed shell is treated separately, similar to the shell model. The collective model postulates a core and an extra core in the nucleus, and the core is treated again as a liquid drop.

Further Reading

Bès, D.R. (1965). Nuclear structure away from the region of β -stability. *Nucl. Instrum. Methods* 38:277–281.

Cook, N.D. (2006). *Models of the Atomic Nucleus*. Springer, Berlin, ISBN 3540285695.

-
- Choppin, G.R. and Rydberg, J. (1980). *Nuclear Chemistry, Theory and Applications*. Pergamon Press, Oxford.
- Friedlander, G., Kennedy, J.W., Macias, E.S. and Miller, J.M. (1981). *Nuclear and Radiochemistry*. Wiley, New York, NY.
- Haissinsky, M. (1964). *Nuclear Chemistry and its Applications*. Addison-Wesley, Reading, MA.
- Lieser, K.H. (1997). *Nuclear and Radiochemistry*. Wiley-VCH, Berlin.
- McKay, H.A.C. (1971). *Principles of Radiochemistry*. Butterworths, London.

3 Isotopes

The term “isotope” was coined by Soddy in 1910, who postulated that elements consist of atoms with the same number of protons but different numbers of neutrons.

If the ratio of the neutrons and protons is different from the optimal ratio associated with the stable state of an atom, the nucleus decomposes, emitting radiation. This process is known as “radioactive decay.” The rest mass of the initial, parent nucleus is greater than the total rest mass of the produced, daughter nucleus and the emitted particle(s). The difference in the masses can be accounted for as the energy of the emitted radiation or particles. The radioactive decay is always exothermal; the emitted energy, however, is usually not released in the form of thermal energy but rather as the energy of the emitted radiation and high-energy particles.

For understanding the radioactive decay, the isobar nuclei (i.e., nuclei that have the same mass number) is a good starting point. The isobars can have odd and even values. The binding energy per nucleon as a function of the mass number gives one parabola for the odd (Figure 3.1A) and two parabolas for the even isobar nuclei (Figure 3.1B–E). In the case of even isobars, the upper and lower parabolas refer to the binding energy of nuclei containing odd or even numbers of protons and neutrons, respectively (the fifth member in Eq. (2.18) can be positive or negative). Thus, the upper parabola is defined by nuclei with odd numbers of protons and neutrons (odd–odd) and the lower parabola by nuclei with even numbers of protons and neutrons (even–even).

In the case of odd isobars, one stable nucleus is at the minimum of the parabola (Figure 3.1A). For this nucleus, the ratio of protons and neutrons is optimal. On the left side of the parabola, the number of neutrons is too high, initiating a radioactive decay in which the number of the neutrons decreases and the number of the protons increases. This process is negative beta decay. On the right side of the parabola, the number of protons is too high, initiating a radioactive decay in which the number of the protons decreases and the number of the neutrons increases. This process is positive beta decay and/or electron capture.

For even isobars, the odd–odd parabolas contain one stable nucleus (Figure 3.1C), whereas the even–even parabolas have one (Figure 3.1B), two (Figure 3.1D), or three (Figure 3.1E) stable nuclei, depending on the relative position of the odd–odd and even–even parabolas. Similar to odd isobars, the nuclei

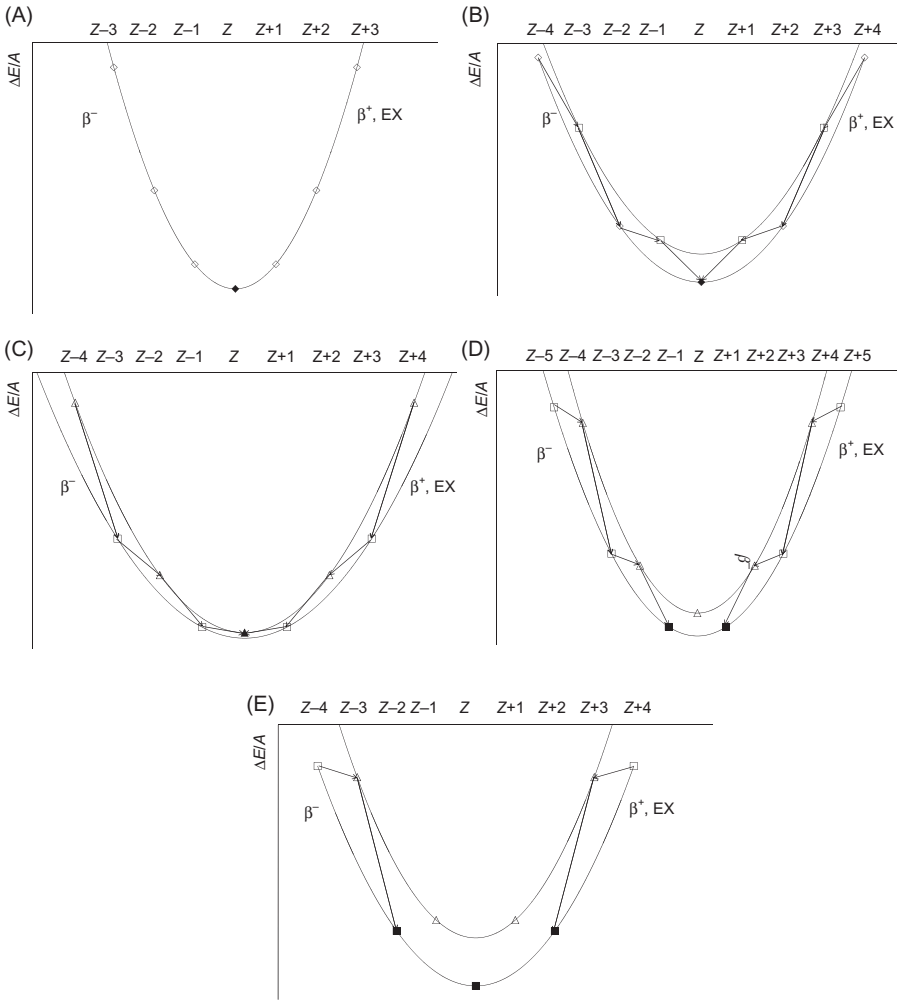


Figure 3.1 Isobar parabolas for odd (A) and even (B–E) mass numbers. Stable nuclei are signified with filled dots. For the even mass numbers, the upper parabola means the odd proton and neutron numbers, whereas the lower parabola refers to the even proton and neutron numbers.

on the sides of the parabolas decompose by negative and positive beta decays or electron capture; as a result of the decays, however, the nuclei go from the even–even parabola to the odd–odd parabola and vice versa. Since the odd–odd parabola is in the upper position, nuclei with odd numbers of protons and neutrons are stable only when they are located in the minimum of the upper parabola and the energy level of this minimum is below the energy level of adjacent even–even nuclei on the lower parabola (Figure 3.1C). This is only the case for four odd–odd light nuclei (^2H , ^6Li , ^{10}B , and ^{14}N).

Table 3.1 A Classification of Stable Nuclei

| Type | Number of Nuclei | Mass Number | Spin | Parity | Statistics |
|-----------|------------------|--------------------|--|--------|---------------|
| Even–even | 162 | $A = 2k$, even | 0 | Even | Bose–Einstein |
| Odd–odd | 4 | | 1,2,3,4... ... | Even | |
| Even–odd | 56 | $A = 2k + 1$, odd | $\frac{1}{2}, \frac{3}{2}, \frac{5}{2}, \dots$ | Odd | Fermi–Dirac |
| Odd–even | 52 | | | Odd | |

k means an integer.

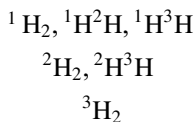
These occurrences of the stable nuclei are summarized by Mattauch’s rule, which states that odd isobars have one stable nucleus, whereas even isobars have two or more stable nuclei, and the atomic numbers of these latter items differ by two. Consequently, if two adjacent elements have nuclides of the same mass, then at least one of them must be radioactive. This rule provides an explanation, for example, why technetium (atomic number 43) does not have stable isotopes.

The parabolas show, too, that the number of radioactive nuclides is much more than that of stable nuclides. Today, we know of approximately 270 stable nuclides and 2000 radioactive nuclides, but the number of radioactive nuclides may reach about 6000. The stable nuclides are listed and classified in [Table 3.1](#).

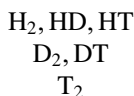
It can be stated that even–even nuclei are the most frequently stable. The most abundant nuclei of the Earth’s crust are even–even nuclei (^{16}O , ^{24}Mg , ^{28}Si , ^{40}Ca , ^{48}Ti , ^{56}Fe).

3.1 Isotopic Effects

Isotope atoms may have some different physical, chemical, geological, and biological properties. In addition, the isotopes are usually present not as free atoms, but in compounds, participating in chemical bonds. This means that there are isotope compounds or isotope molecules in which one atom (or perhaps more atoms) is substituted by another isotope. For example, the very simple hydrogen molecule represents six different isotope molecules, which can be written using two different symbolisms:

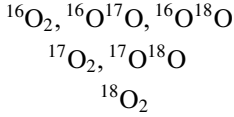


and



where D and T mean the isotope of hydrogen with mass number 2 and 3, namely, deuterium and tritium, respectively.

A similar situation exists for oxygen molecules, as follows:



The compound of these elements, water, may have 18 different isotope molecules. Of course, the relative amount of the isotope molecules is very different, determined by the natural abundance of the isotopes.

The thermodynamic properties of the substances can be characterized by the partition function, combining translation, rotation, vibration, and electron excitation. At a constant temperature, the translation energy of the isotope atoms or molecules is the same.

The rotation energy (E_r) of a diatomic molecule can be expressed by the Schrödinger equation for a rigid rotor:

$$\frac{\partial^2 \Psi}{\partial x^2} + \frac{\partial^2 \Psi}{\partial y^2} + \frac{\partial^2 \Psi}{\partial z^2} + \frac{8\pi^2 \mu}{h^2} E_r \Psi = 0 \quad (3.1)$$

The solution of Eq. (3.1) is:

$$E_r = \frac{1}{2} I \omega^2 = \frac{1}{2} \frac{L^2}{I} = J(J+1) \frac{h^3}{8\pi^2 c(I_x I_y I_z)} \quad (3.2)$$

where Ψ is the wave function, I is the moment of inertia, ω is the angular speed, L is the moment of impulse, and J is the rotation quantum number. The moment of inertia of a diatomic molecule is expressed as follows:

$$I = m_1 r_1^2 + m_2 r_2^2 = \mu r_0^2 \quad (3.3)$$

where r_1 and r_2 are the distance of the center of mass from the atoms with m_1 and m_2 mass and μ is the reduced mass, i.e.,

$$\mu = \frac{m_1 m_2}{m_1 + m_2} \quad (3.4)$$

The reduced mass can be very different for the isotope molecules, and this difference will affect the chemical properties. For example, the masses of the TH and D₂ molecules are very similar, but the reduced masses are rather different: 3/4 and 1 for TH and D₂, respectively.

The vibration energy of a diatomic molecule (E_v) can be expressed by the Schrödinger equation of a harmonic oscillator:

$$\frac{\partial^2 \Psi}{\partial x^2} + \frac{8\pi^2 \mu}{h^2} \left(E_v - \frac{1}{2} kx^2 \right) \Psi = 0 \quad (3.5)$$

where

$$E_v = \left(v + \frac{1}{2} \right) hc\omega \quad (3.6)$$

where ν is the vibration quantum number, ω can be defined as:

$$\omega = \frac{1}{2\pi c} \sqrt{\frac{k}{\mu}} \quad (3.7)$$

In this equation, k is a constant (a spring constant in classical physics), $x = r - r_e$, and r and r_e are the mean and the shortest distance between the two atoms, respectively.

When comparing the ratio of the vibration energies for two isotope molecules, look at the following equation:

$$\frac{E_{v1}}{E_{v2}} = \sqrt{\frac{\mu_2}{\mu_1}} \quad (3.8)$$

The electronic excitation can be characterized by the wave number (ν^*) of spectrum lines. It can be described by Moseley's law. For the hydrogen atom, it is:

$$\nu^* = \frac{2\pi^2 e^4}{h^3 c} \frac{M_a m_e}{M_a + m_e} \left(\frac{1}{n_1^2} - \frac{1}{n_2^2} \right) = Ry \left(\frac{1}{n_1^2} - \frac{1}{n_2^2} \right) \quad (3.9)$$

where M_a and m_e are the masses of the nucleus and the electron, n_1 and n_2 are the main quantum numbers of the electron shells involved in the excitation process, and Ry is the Rydberg constant. As seen, the reduced mass of the atom appears in Eq. (3.9), which may be different when the isotope is not the same because of the different masses of the nuclei.

All expressions of the rotation, vibration, and electronic excitation energies contain the reduced masses, which are different for isotope atoms and molecules. This difference in the reduced masses is responsible for the isotopic effects, namely, the different physical, chemical, and other properties of the isotopes and isotope molecules.

3.1.1 Physical Isotope Effects

At a given temperature, the thermal (kinetic) energy of ideal gases is the same, independent of the chemical identity of the gas. So, the kinetic energy (E_{kin}) of the different molecules of hydrogen isotopes (H,D,T) is:

$$E_{\text{kin}} = \frac{3}{2}RT = \frac{1}{2}m_{\text{H}}v_{\text{H}}^2 = \frac{1}{2}m_{\text{D}}v_{\text{D}}^2 = \frac{1}{2}m_{\text{T}}v_{\text{T}}^2 \quad (3.10)$$

Since the ratio of the masses of the isotopes is $m_{\text{H}}:m_{\text{D}}:m_{\text{T}} = 1:2:3$,

$$v_{\text{H}} : v_{\text{D}} : v_{\text{T}} = 1 : \frac{1}{\sqrt{2}} : \frac{1}{\sqrt{3}} \quad (3.11)$$

This difference in the velocity of the isotope molecules influences all the properties involving the movement of gases, for example, diffusion and viscosity.

In gas columns, such as the atmosphere, the isotopes separate because of their different masses. This separation can be calculated by the following barometric formula:

$$p_h = p_0 e^{-\frac{Mgh}{RT}} \quad (3.12)$$

where p_0 and p_h are the pressure at the level of a reference level (zero level) and at the height h , respectively, M is the molar mass of the gas, g is the gravitational constant, h is the height related to the reference level, R is the gas constant, and T is the temperature (in kelvin).

For two isotopes/isotope molecules with different mass numbers (M_1 and M_2):

$$\frac{p_2}{p_1} = \frac{p_{20}}{p_{10}} e^{-\frac{(M_2-M_1)gh}{RT}} \quad (3.13)$$

The partial pressures, of course, are proportional to the concentrations of the isotopes/isotope molecules.

A similar expression can be deduced for the centrifugation of the isotope molecules, substituting $g \times h$ with $(\omega r)^2$, where ω is the angular speed and r is the distance from the rotation axis:

$$\frac{p_2}{p_1} = \frac{p_{20}}{p_{10}} e^{-\frac{(M_2-M_1)(\omega r)^2}{RT}} \quad (3.14)$$

As seen in Eqs. (3.13) and (3.14), the degree of the isotope effects is determined by the difference of the masses. It means that these effects are observed for all isotopes, including heavy elements. Therefore, the centrifugation can be applied to the separation of isotopes of heavy elements, for example, ^{235}U and ^{238}U .

In electric and magnetic fields, the charged particles move along a curved path. The deviation from the initial direction is proportional to the specific charge of the moving particle.

In electric fields,

$$X = k \frac{E}{v^2} \frac{e}{m} \quad (3.15)$$

where X is the deviation, k is a constant, E is the strength of the electric field, v , e , and m are the speed, the charge, and the mass of the particle, and e/m is the specific charge (mass-to-charge ratio).

In magnetic fields,

$$Y = K_m \frac{H}{v} \frac{e}{m} \quad (3.16)$$

where Y is the deviation, K_m is a constant, and H is the strength of the magnetic field.

The specific charge of isotopes with different masses and the same charge is different; therefore, they move along differently curved paths in the same electric or magnetic field. The mass spectrometers utilize this process for determining the mass of particles. Isotopes can also be separated in macroscopic quantities using the deviation from the straight line in electric and magnetic fields.

3.1.2 Spectroscopic Isotope Effects

The different reduced mass of the molecules that contain isotope atoms may also have an effect on the optical spectra of the isotope molecules. The phenomenon is called the spectroscopic isotope effect, and it can be observed in both atomic and molecular spectra.

Light emission is the result of the change of the energy of a particle from a greater level (E') to a lower level (E''). In light absorption, the reversed process takes place. The energy levels mean rotation, vibration, and electron energies. The change in the rotation and vibration energies produces the molecular spectra, whereas the change of the electron energies gives the atomic spectra. As seen in [Section 3.1](#), all the rotation, vibration, and electron energies depend on the reduced mass of the molecule (Eqs. (3.2) and (3.6)) or the atom (Eq. (3.9)), so the spectra of the isotope molecules and atoms are different. For example, the reduced mass of the H^{35}Cl is $\mu = 0.9722$ and that of the H^{37}Cl molecule is $\mu = 0.9737$. As can be calculated by Eq. (3.8), the ratio of the vibration energies of the two molecules is 1.00076. This value is very close to 1, so the difference of the spectra can be observed only by very high resolution spectrometers.

The spectroscopic isotope effects can be observed in some atomic spectra too. However, the difference in the reduced masses of the isotope atoms is very small. As a result, only hydrogen–deuterium spectroscopic isotope effects can be detected easily. The wave number of the hydrogen isotopes can be calculated by Eq. (3.9).

The wave number of a H_{α} line is $15,233 \text{ cm}^{-1}$ and that of a D_{α} line is $15,237 \text{ cm}^{-1}$. The difference is 4 cm^{-1} , which can be observed by traditional spectrometers. As seen in Eq. (3.9), the reduced masses determine the Rydberg constant (R_y), the ratio of which for deuterium and hydrogen is:

$$\frac{R_y(D)}{R_y(H)} = \frac{M_D m_e}{M_D + m_e} \times \frac{M_H + m_e}{M_H m_e} = \frac{0.9997283}{0.9994568} = 1.0002717 \quad (3.17)$$

This value is about three times less than the ratio for the vibration energies of the HCl isotope molecules (1.00076). The natural isotope ratio of hydrogen to deuterium was determined on the spectral line intensities of hydrogen in 1939.

3.1.3 Phase Equilibrium Isotope Effects

The distribution of the isotope molecules is different in phases that are in thermodynamic equilibrium, including the liquid/gas, liquid/solid, and solid/gas phases. Similarly, the solubility of the isotope molecules is also different.

The isotope effects in the liquid/gas phases have been well studied. The effect can be characterized by the partial pressure of the isotope molecules:

$$\frac{p' - p}{p} = \frac{p'}{p} - 1 \approx \ln \frac{p'}{p} = \varepsilon \quad (3.18)$$

where p and p' are the partial pressure of the lighter and the heavier molecule, respectively, and ε is the relative partial pressure. The degree of the isotope effect is usually low: $\varepsilon \ll 1$. Of course, the different partial pressures result in different boiling points (Table 3.2).

Usually, the partial pressure of the lighter molecules is greater. If not, an inverse isotope effect exists. Among the molecules in Table 3.2, methane shows an inverse isotope effect.

A well-known isotope effect in the solid/liquid phase is the ice/water system. The boiling point of $^2\text{H}_2\text{O}$ and $^1\text{H}_2\text{O}$ is different. As a result, the deuterium content of the icy seas is greater than the average deuterium content of the oceans.

The adsorption of the isotope molecules can also be different, a fact that is used in adsorption chromatography to separate isotopes. As the pressure and temperature decrease, the isotope effects increase, resulting in increased separation factors.

The different solubility of the isotope molecules have mainly been studied during the dissolution of light and heavy water in organic solvents. The inorganic salts and some organic compounds dissolve differently in light and heavy water.

3.1.4 Isotope Effects in the Kinetics of Chemical Reactions

The reaction rate of the isotope molecules may be different. This effect is determined by the reaction mechanism, including thermodynamic properties of the transition state, so the kinetic isotope effects can be applied for the study of the mechanism of the chemical reactions.

Table 3.2 Relative Tension of Some Isotope Molecules

| | Relative Partial Pressure | |
|---|---------------------------|--------------------------|
| | At Triple Point | At Boiling Point (1 bar) |
| H ₂ (<i>ortho</i>)/HD | 3.61 | 1.81 |
| (NH ₃ /ND ₃) ^{1/3} | 1.080 | 1.036 |
| (H ₂ O/D ₂ O) ^{1/2} | 1.120 | 1.026 |
| CH ₄ /CH ₃ D | 1.0016 | 0.9965 |
| ³ He/ ⁴ He | 7.0 | |
| ²⁰ Ne/ ²² Ne | 1.043 | |
| ¹²⁸ Xe/ ¹³⁶ Xe | 1.006 | |
| ¹² CO/ ¹³ CO | 1.01 | |
| ¹⁴ NH ₃ / ¹⁵ NH ₃ | 1.0055 | 1.0025 |
| H ₂ ¹⁶ O/H ₂ ¹⁸ O | 1.01 | 1.0046 |
| ¹¹ BF ₃ / ¹⁰ BF ₃ | | ≈1.01 |

The kinetic effects are significant in the case of light elements since the mass of the isotopes of these elements has the greatest differences, resulting in relatively great differences in the rotation, vibration, and electron energies of the isotope molecules and the transition state. The reactions of the molecules containing different H, C, N, O, and S isotopes are important. Obviously, the reactions of such molecules are interesting mainly in organic chemistry.

The kinetic isotope effects can be classified as primary and secondary effects. In the primary effects, the bond that contains the isotope atoms breaks or forms in the rate-determining step. The primary kinetic isotope effects can be divided further in intermolecular and intramolecular effects. In the intermolecular effect, two molecules react with different rates. In the intramolecular effect, the equivalent sites within the same molecules show different rates because the sites have different isotopes.

A primary intermolecular isotope effect is as follows:



In Eqs. (3.19) and (3.20), two identical molecules (AX and AX') contain different isotopes of the same element (X and X'). When the reaction constants are different ($k_1 \neq k_2$), the reaction of the two isotope molecules (AX and AX') with the molecule BY shows a primary intermolecular isotope effect.

A primary intramolecular isotope effect can be observed in the following process:



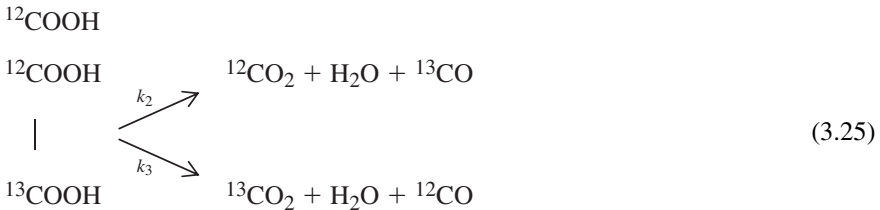
where k_3 and k_4 are the rate of the production of BX' and BX, respectively. An isotope effect occurs when $k_3 \neq k_4$.

In the secondary isotope effects, the isotope atom does not directly take part in the reaction. For example,



where $k_5 \neq k_6$.

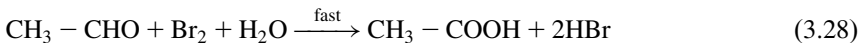
A primary isotope effect can be observed in the thermal decarboxilation of oxalic acid if one or both carbon atoms are substituted by the ^{13}C isotope:



An intramolecular isotope effect is found when k_2/k_3 , whereas intermolecular isotope effects can be observed in case of $k_1/(k_2 + k_3)$, k_1/k_4 , and $(k_2 + k_3)/k_4$, respectively.

As a secondary isotope effect, the reaction of carboxyl groups of malonic acid is mentioned when deuterium is substituted for the hydrogen bonded to the β -carbon atom. The maximum values of the kinetic isotope effects (shown in Table 3.3) are determined using the thermodynamic properties of the isotope molecules.

The study of the isotope effects can be used to elucidate the reaction mechanism, as the following example shows. The oxidation of alcohols to carboxylic acid by bromine is made up of two steps:

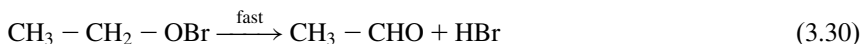
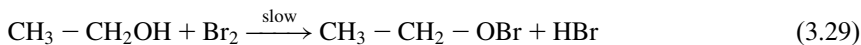


The rate-determining step is the oxidation of the alcohol, which results in the formation of aldehyde (Eq.(3.27)), a first-order reaction both for alcohol and

Table 3.3 Maximum Values of Isotope Effects in the Kinetics of Chemical Reactions

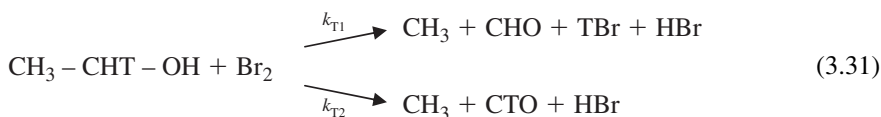
| Isotope Substitution | Bond | Ratio of Rate Constants | |
|--|------------------|-------------------------|-------|
| Maximum Primary Isotope Effects at 25°C | | | |
| H | D | 18 | |
| H | T | 60 | |
| ¹⁰ B | ¹¹ B | 1.3 | |
| ¹² C | ¹³ C | 1.25 | |
| ¹² C | ¹⁴ C | 1.5 | |
| ¹⁴ N | ¹⁵ N | 1.14 | |
| ¹⁶ O | ¹⁸ O | 1.19 | |
| ¹⁹ F | ¹⁸ F | 1.25 | |
| ³¹ P | ³² P | 1.02 | |
| ³² S | ³⁵ S | 1.05 | |
| Cl natural | ³⁸ Cl | 1.14 | |
| ¹²⁷ I | ¹³¹ I | 1.02 | |
| Maximum Secondary Isotope Effects at 25°C | | | |
| H | D | C–H | 1.74 |
| H | T | C–H | 2.20 |
| H | D | O–H | 2.02 |
| H | T | O–H | 2.74 |
| ¹² C | ¹³ C | C–C | 1.012 |
| ¹² C | ¹⁴ C | C–C | 1.023 |

bromine. There are two mechanistic possibilities. The first is that bromine reacts with the hydrogen in the hydroxide group and in a rate-determining step:



This support for this mechanism is that it resembles the fast reaction of alkyl hypochlorites. If this is the right mechanism, secondary isotope effects should be observed if the alcohol CH_2 group is labeled by an isotope of the hydrogen. In the case of H–T substitution, this mechanism can decrease the reaction rate by 2.2 times (Table 3.3).

The second possibility is that bromine reacts with the carbon atom of the alcohol CH_2 , which would result in a much higher (i.e., primary) isotope effect when substituting one of the hydrogen atoms of alcohol CH_2 by tritium. In this case, two types of aldehyde would form, an unlabeled and a labeled molecule:





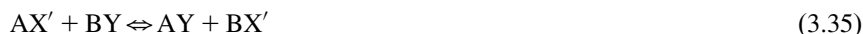
Because of the two product molecules of the labeled alcohol, the value of the isotope effect has to be calculated as:

$$\frac{2k_{\text{H}}}{k_{\text{T1}} + k_{\text{T2}}} = 8 \quad (3.33)$$

Thus, examining the relative rates, it can be determined if the reaction starts with the reaction of CH_2 and Br_2 , or if it proceeds via a hypobromite intermediare.

3.1.5 The Isotope Effect in a Chemical Equilibrium

The equilibrium constants of the reactions involving isotope molecules may also be different:



Both X and X' mean the isotopes of the same element. The equilibrium constants are as follows:

$$K = \frac{[\text{AY}][\text{BX}]}{[\text{AX}][\text{BY}]} \quad (3.36)$$

$$K' = \frac{[\text{AY}][\text{BX}']}{[\text{AX}'][\text{BY}]} \quad (3.37)$$

The ratio of the two equilibrium constants is:

$$\frac{K}{K'} = \bar{K} = \frac{[\text{BX}][\text{AX}']}{[\text{BX}'][\text{AX}]} \quad (3.38)$$

This ratio gives the equilibrium constant of the isotope exchange reaction:



When the equilibrium constant of the isotope exchange is equal to 1, there is no isotope effect—the distribution of the isotopes is the same in both compounds.

The equilibrium constants of some isotope exchange reactions are listed in [Table 3.4](#). The calculated values were obtained from the thermodynamic properties.

As seen in [Table 3.4](#), the equilibrium constants of isotope exchange reactions are close to 1 but frequently not equal to 1. These small differences from 1 have, however, a great theoretical and practical importance because they provide a way to separate isotopes and give important geological information (discussed further in [Section 3.4](#)).

Table 3.4 Equilibrium Constants of Some Isotope Exchange Reactions

| Isotope Exchange Reaction | Temperature (K) | Equilibrium Constant | |
|--|--------------------|----------------------|------------|
| | | Experimental | Calculated |
| $0.5\text{C}^{16}\text{O}_2 + \text{H}_2^{18}\text{O}_{\text{aq}} \rightleftharpoons 0.5\text{C}^{18}\text{O}_2 + \text{H}_2^{16}\text{O}_{\text{aq}}$ | 273 | 1.044 | 1.044 |
| $^{15}\text{NH}_3 + ^{14}\text{NH}_{3\text{aq}} \rightleftharpoons ^{15}\text{NH}_{3\text{aq}} + ^{14}\text{NH}_3$ | 298 | 1.026 | |
| $\text{H}^{12}\text{CN} + ^{13}\text{CN}_{\text{aq}}^- \rightleftharpoons \text{H}^{13}\text{CN} + ^{12}\text{CN}_{\text{aq}}^-$ | 295 | 1.026 | 1.030 |
| $\text{HC}^{14}\text{N} + \text{CN}_{\text{aq}}^- \rightleftharpoons \text{HC}^{15}\text{N} + \text{CN}_{\text{aq}}^-$ | 295 | 1 | 1.002 |
| $^{12}\text{CO}_3^{2-} + ^{13}\text{CO}_2 \rightleftharpoons ^{13}\text{CO}_3^{2-} + ^{12}\text{CO}_2$ | 273 | 1.017 | 1.016 |
| $\text{H}^{12}\text{CO}_3^- + ^{13}\text{CO}_2 \rightleftharpoons \text{H}^{13}\text{CO}_3^- + ^{12}\text{CO}_2$ | 298 | 1.014 | |
| $^{34}\text{SO}_2 + \text{H}^{32}\text{SO}_3^- \rightleftharpoons ^{32}\text{SO}_2 + \text{H}^{34}\text{SO}_3^-$ | 298 | 1.019 | |
| $^{36}\text{SO}_2 + \text{H}^{32}\text{SO}_3^- \rightleftharpoons ^{32}\text{SO}_2 + \text{H}^{36}\text{SO}_3^-$ | 298 | 1.043 | |
| $^7\text{Li}(\text{Hg}) + ^6\text{LiCl} \rightleftharpoons ^6\text{Li}(\text{Hg}) + ^7\text{LiCl}$ | 295 | 1.025 | |
| $\text{H}_2^{18}\text{O} + 1/3\text{C}^{16}\text{O}_3^{2-} \rightleftharpoons \text{H}_2^{16}\text{O} + 1/3\text{C}^{18}\text{O}_3^{2-}$ | 273 | 1.022 | |
| | 298 | 1.0176 | |
| $\text{H}_2^{18}\text{O} + 1/4\text{Si}^{16}\text{O}_4^{2-} \rightleftharpoons \text{H}_2^{16}\text{O} + 1/4\text{Si}^{18}\text{O}_4^{2-}$ | 273 | 1.0204 | |
| | 298 | 1.0157 | |
| $\text{H}_2^{18}\text{O} + 1/4\text{S}^{16}\text{O}_4^{2-} \rightleftharpoons \text{H}_2^{16}\text{O} + 1/4\text{S}^{18}\text{O}_4^{2-}$ | 288 | 1.03 | |
| | 413 | 1.014 | |
| $\text{H}_2^{18}\text{O} + 1/4\text{S}^{16}\text{O}_4^{3-} \rightleftharpoons \text{H}_2^{16}\text{O} + 1/4\text{S}^{18}\text{O}_4^{3-}$ | 273 | 1.0104 | |
| | 298 | 1.0037 | |

3.1.6 Biological Isotope Effects

Living organisms can react with the isotope molecules in different ways. As discussed in previous chapters, the cause of the physical and chemical isotope effects can be easily understood, but the biological effects are much more complicated. The most important isotope effects occur in the case of the isotope of hydrogen since the hydrogen bond plays a very important role in the secondary and tertiary structures of the proteins and nucleic acids. When substituting deuterium for hydrogen, the strength of the hydrogen bond increases, i.e., the cleavage of a deuterium bond requires more energy. This increase is similar to the differences in the partial pressure of water under the effect of hydrogen–deuterium substitution. Heavy water (D_2O) inhibits or can stop the proliferation of cells. The experience shows that living organism may die when the deuterium–hydrogen substitution happens quickly. However, when the deuterium–hydrogen substitution is slow, the living organisms can adapt to the heavy water. During the adaptation phase, cell destruction or cell proliferation may be observed. After the adaptation, the cells develop as usual.

Recently, there have been some reports claiming that drinking deuterium-free water has desirable physiological effects, such as reducing the risk of cancer. This effect may have been observed *in vitro*. However, because of the fast isotope exchange of deuterium and hydrogen in the environment (air, nutrients, etc.), deuterium concentration of the human body cannot be lowered in this manner.

3.2 Separation of Isotopes

Any of the above-mentioned isotope effects can be used to separate the isotopes. Distillation, gas diffusion, centrifugation, electromagnetic separation, electrolysis, and chemical isotope exchange are widely used methods for isotope separation. A newer, novel method of doing this is laser isotope separation (LIS).

The LIS technique was originally developed in the 1970s as a cost-effective, environmentally friendly way of supplying enriched uranium. The method is based on the fact that different isotopes of the same element absorb different wavelengths of laser light. Therefore, a laser can be precisely tuned to ionize only atoms of the desired isotope, which are then drawn to electrically charged collector plates.

The isotope separation is characterized by the separation factor. In a two-component system, the separation factor (α) is defined as:

$$\alpha = \frac{X_1(1 - X_0)}{(1 - X_1)X_0} = \frac{R_1}{R_0} \quad (3.40)$$

where X_0 and X_1 are the molar fraction of one of the isotopes before and after separation, respectively.

$$R_0 = \frac{X_0}{1 - X_0} \quad \text{and} \quad R_1 = \frac{X_1}{1 - X_1} \quad (3.41)$$

In addition, $1 - \alpha$ is called the enrichment factor.

Since the degree of the isotope effects is usually small, one separation step is frequently not enough to reach a high enough enrichment. In this case, a multistage process in cascade can be applied. The enrichment factor of a separation cascade (A) is proportional to the number of stages (n):

$$A = \alpha^n = \frac{R_1}{R_0} \quad (3.42)$$

By increasing n , the enrichment increases proportionally.

The enriched isotopes are used for the production of fuels and moderators of nuclear reactors and nuclear weapons, for analytical purposes (e.g., NMR, Mössbauer spectroscopy), and for the preparation of targets in the production of radioactive isotopes. In [Table 3.5](#), the most important enriched isotopes are listed. Beside enrichment, the depletion of the isotopes can be important for special applications. Depleted ^{64}Zn is used in nuclear industry. The addition of zinc to the cooling water inhibits the corrosion and the formation of ^{60}Co (discussed in Section 7.3) from the steel of the reactor, decreasing the workers' radiation exposure. Natural zinc contains 48% ^{64}Zn ; however, the gamma emitter ^{65}Zn isotope is produced by (n, γ) nuclear reaction of ^{64}Zn (discussed in Section 6.3). To avoid the production of ^{65}Zn , depleted ^{64}Zn (<1%) is produced by centrifugation and applied in nuclear reactors.

Table 3.5 Most Important Enriched (and Depleted) Isotopes

| Isotope | Separation Method | Application |
|-------------------------------------|--|--|
| ^2H | Electrolysis, fractionation, distillation, chemical exchange | Moderator in heavy water, nuclear reactors, nuclear weapons, NMR spectroscopy |
| ^6Li | Electrolysis of LiOH, transfer of lithium ions from an aqueous solution to a lithium amalgam | Production of tritium for nuclear weapons and fusion reactor experiments |
| ^{10}B | Distillation of BF_3 , exchange with distillation | Neutron absorber in nuclear reactors, neutron detection, boron cancer therapy |
| ^{13}C | Distillation of CO | Tracer studies, especially in organic chemistry, NMR spectroscopy |
| ^{15}N | Distillation of NO, exchange between $\text{NH}_{3(\text{g})}$ and NH_4^+ | Tracer studies |
| ^{18}O | Exchange between CO_2 and H_2O | Tracer studies, production of ^{18}F isotope for positron emission tomography (PET) |
| ^{20}Ne | Thermal diffusion | Tracer studies |
| ^{67}Zn , ^{68}Zn | Electromagnetic separation | Production of PET isotopes: |
| ^{112}Cd | | ^{67}Ga |
| ^{124}Xe | | ^{111}In |
| | | ^{123}I |
| | | Production of isotopes for radiation therapy: |
| ^{191}Ir | Electromagnetic separation | ^{192}Ir |
| ^{124}Xe | | ^{125}I |
| ^{186}W | | ^{188}Re |
| Depleted ^{46}Ti | | ^{46}Sc |
| ^{74}Se | Electromagnetic separation | Production of ^{75}Se for gamma cameras |
| depleted ^{64}Zn | Centrifugation | Corrosion inhibitor in the cooling water of nuclear reactors |
| ^{57}Fe | Electromagnetic separation | Mössbauer spectroscopy |
| ^{119}Sn | | |
| ^{235}U | Gas diffusion of UF_6 , electromagnetic separation, centrifugation of UF_6 , LIS | Nuclear reactors, nuclear weapons |

3.3 Isotope Composition in Nature

As a result of the isotope effects, isotopes are fractionated in nature. The amount of natural isotope fractionation, however, is usually smaller than would be expected from the isotope effects because the cyclic processes characteristic in nature tend to compensate for the fractionation caused by isotope effects. Only the isotope

Table 3.6 International Standard of Isotope Ratios

| Isotopes | Name of Standard | Notation of Standard | R_{standard} |
|----------------------------------|--|----------------------|-----------------------|
| D/ ¹ H | Vienna Standard Mean Ocean Water | VSMOW | 0.00015575 |
| ¹⁸ O/ ¹⁶ O | Vienna Standard Mean Ocean Water | VSMOW | 0.0020052 |
| ¹³ C/ ¹² C | Vienna Pee Dee Belemnite (carbonate rock) | VPDB | 0.0112372 |
| ¹⁵ N/ ¹⁴ N | Air (free of all anthropogenic impurities) | AIR | 0.003676 |
| ³⁴ S/ ³² S | Canyon Diablo Troilite (meteorite) | CDT | 0.045005 |

fractionation of the light elements can be easily observed. Thus, the heaviest element showing isotope separation in nature is germanium. Besides the isotope effects, the fractionation of the radioactive isotopes is also influenced by the radioactive decay.

The stable isotope concentrations of the substances are presented as the molar ratio of the heavy-to-light isotopes. Since this ratio is small, stable isotope abundances are usually presented relative to an international standard:

$$\delta = \left(\frac{R_{\text{sample}}}{R_{\text{standard}}} - 1 \right) \times 1000 \quad (3.43)$$

where δ is expressed in ‰. In Eq. (3.43), R_{sample} and R_{standard} are the ratio of heavy-to-light isotopes in the sample and the standard, respectively. For example, the value of δ for the stable isotopes of hydrogen is:

$$\delta = \left(\frac{(D/H)_{\text{sample}}}{(D/H)_{\text{standard}}} - 1 \right) \times 1000 \quad (3.44)$$

Traditionally, the isotope ratios of five elements (namely, hydrogen, carbon, nitrogen, oxygen, and sulfur) are used for practical, especially geochemical, purposes. The standard of the isotope ratios of these elements is summarized in Table 3.6. Standard materials are available from the International Atomic Energy Agency (IAEA) and the National Institute of Standards and Technology (NIST) to ensure accurate measurement and reporting of isotope ratios for unknown samples and to facilitate cross-lab comparability.

3.4 Study of Geological Formations and Processes by Stable Isotope Ratios

As mentioned previously, the isotope ratios of five elements, hydrogen, carbon, nitrogen, oxygen, and sulfur, are widely applied because

- they have small atomic mass, so their isotope effects are relatively high;
- they typically form covalent bonds. The strong covalent bond inhibits the equalizing effect of cyclic processes;

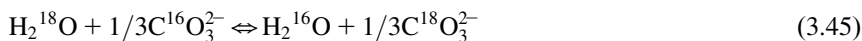
- they can form many compounds;
- the abundance of the heavier isotope is relatively high;
- the isotope ratios can be measured using the same technique.

The isotope ratios are routinely determined by mass spectrometers that have been improved especially for the measurements of isotope ratio, where the isotope ratios are measured in H_2 , CO_2 , N_2 , and SO_2 gases. In addition, other spectroscopic techniques, such as infrared spectroscopy, ion microprobe, diode laser spectroscopy, and hollow cathode spectroscopy, are used in some cases.

The ratios of the stable isotopes give information on changes of the composition of the Earth's mantle, climate (paleoclimatology), major extinction events, hydrological processes, and so on. In addition, stable isotope ratios can give useful tools for other disciplines connected to geological formations (archeology, criminology, environmental science, etc.). In addition, interesting information is obtained by studying the isotope ratios of other planets. For example, in the rocks from Mars and meteorites, the D/H ratio can be much higher than on the Earth (up to 4000%). This shows that the high portion of the light isotope, ^1H , evaporated from Mars. In the following sections, some example for the utilization of stable isotope ratios in geology and related disciplines will be shown.

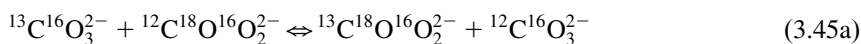
3.4.1 Study of the Temperature and Age of Geological Formations

During the slow formation of any other sedimentary rock from natural water, heterogeneous isotope exchange takes place between the oxygen in water and the surface layers of the rock. For example, in case of carbonate rock, the exchange can be described as:



The equilibrium constant of the reaction (3.45) depends on the temperature as postulated by the van't Hoff equation. This temperature dependence can be measured in laboratory conditions. Thus, the formation temperature of the rocks can be estimated, assuming that the oxygen isotopes inside particles that are more than $10\ \mu\text{m}$ in diameter do not exchange with the oxygen isotopes of water. Similarly, the temperature of the formation of sulfate, phosphate, and silicate rocks can be estimated. The disadvantage of this method is that the isotope ratio of ancient water is not known; it is usually estimated by modeling $\delta^{18}\text{O}$ gradients in marine sediment pore waters.

Another novel method for the determination of the formation temperature of carbonate rocks is based on the simultaneous measurement of $^{18}\text{O}/^{16}\text{O}$ and $^{13}\text{C}/^{12}\text{C}$ isotope ratios. Since a carbonate ion consists of one carbon and three oxygen atoms, it has 20 different versions depending on the isotope composition, and these versions are in chemical equilibrium with each other. The most abundant equilibrium is:



For the determination of the formation temperature, the quantity of $^{13}\text{C}^{18}\text{O}^{16}\text{O}_2^{2-}$ has to be measured, and the quantity of the other isotopologues can be considered constant. By digestion of the carbonate rock by phosphorous acid, the quantity of $^{13}\text{C}^{18}\text{O}^{16}\text{O}$ is proportional to the quantity of $^{13}\text{C}^{18}\text{O}^{16}\text{O}_2^{2-}$ therefore, the mass spectrometry of the CO_2 gives this value, and from there, the temperature of rock formation can be estimated.

The stable isotope ratios can give information on the age of rocks, too, assuming that the ratio of sulfur isotopes was the same at the time of the formation of the Earth. When the biological processes start, the biological isotope effects change the ratio of the sulfur isotopes: they become different in seawater and rocks. The ratio of $^{34}\text{S}/^{32}\text{S}$ increases in seawater and proportionally decreases in rocks. Since the biological activity started for about 700–800 million years ago, the ages of the geological samples from this period can be determined using $^{34}\text{S}/^{32}\text{S}$ isotope ratios.

3.4.2 Study of the Hydrological Process by Measuring the Ratio of Oxygen and Hydrogen Isotopes

In hydrogeology, the ratios of hydrogen and oxygen isotopes are frequently used. Hydrogen and oxygen are connected by covalent bonds; therefore, the ratios of $^{18}\text{O}/^{16}\text{O}$ and D/H are evaluated together. Since a portion of the subsurface water is originated from rainwater, the rate and degree of the accumulation of subsurface water can be determined using the isotope ratios. The IAEA measures the isotope ratios of rainwater monthly for some ten years. These measurements show the geographical distribution of the D/H and $^{18}\text{O}/^{16}\text{O}$ and the factors affecting the isotope ratios in water. In the following section, these factors and the related isotope effects are summarized. It is important to note that more than one isotope effect can influence the isotope ratios. The different partial pressure of the isotope molecules, for example, plays a role in all cases when evaporation takes place.

- The effect of height: the ratio of $^{18}\text{O}/^{16}\text{O}$ and D/H in the water vapor decreases with the height as postulated by the barometric formula (Eqs. (3.12) and (3.13)). The decrease of $\delta^{18}\text{O}$ and δD is about -0.12 to -0.5% /100 m and -1.5 to -4% /100 m, respectively.
- The effect of meridians is related to the centrifugation of the isotopes: the $\delta^{18}\text{O}$ and δD of the water vapor and rain decreases into the direction of the poles because of the decrease in the radius of the meridian (r in Eq. (3.14)).
- The continental effect: the diffusion rate of the lighter isotope molecules of the water vapor evaporated from the oceans is higher, so the ratios of $^{18}\text{O}/^{16}\text{O}$ and D/H decreases from the sea side to the inland area of the continents.
- The effect of temperature is associated with the change of the partial pressure of the isotope molecules, as shown in Eq. (3.18). When the temperature increases by 1°C , the $\delta^{18}\text{O}$ of water vapor increases by 0.5% . It results in several effects. Seasonal effects are observed: in winter, the $^{18}\text{O}/^{16}\text{O}$ and D/H ratios decrease. The difference of $^{18}\text{O}/^{16}\text{O}$ isotope ratios can reach 10% . The effect of temperature is shown in the isotope ratio of the rainwater, i.e., in Central Europe, warm, Mediterranean rainwater originating from the south usually contains more heavier isotopes than rainwater coming from the north.

- There is a linear relationship between the $\delta^{18}\text{O}$ and δD values. The function is called the Global Meteoric Water Line—GMWL:

$$\delta\text{D} = 8\delta^{18}\text{O} + \delta \quad (3.46)$$

The slope of the straight line is 8, while the intercept, which is the mean value of δ , is 10. $\delta^{18}\text{O} = 0$ represents the Standard Mean Ocean Water, in which the abundance (R_{standard}) of hydrogen isotopes is about 10 times lower than that of oxygen isotopes. It should be noted that the mean value (10) includes fairly high differences: in North America, this value is +6‰, while in Mediterranean areas, it is +22‰. The difference comes from the partial pressure of the isotope molecules. The slope of the GMWL, however, is independent of geographical location, except that when water evaporation is significant, the slope is in the range of 3–6. As before, this fact can be explained by the effect of the temperature: when the temperature increases, the heavier isotope molecules evaporate more quickly.

- At high temperatures, isotope exchanges can take place between water and rocks (Eq. (3.45)). This is a chemical isotope effect, which causes the increase of the $^{18}\text{O}/^{16}\text{O}$ ratio in water and simultaneously the decrease of this ratio in the rocks. Since the oxygen content of the rocks is much higher than the hydrogen content, the change of the hydrogen isotopes can be neglected.
- The isotope ratio allows for the possibility of finding the leakages in the aquifers. The δ values are additive, so they can be used to study the communication between the aquifers when the composition of water is very similar, but the isotope ratios are different. Because of the additive character of $\delta^{18}\text{O}$ and δD ratios, the degree of mixing, if any, can be calculated.

3.4.3 Changes in the Isotope Ratio of Nitrogen

The main source of nitrogen is the air; the $^{15}\text{N}/^{14}\text{N}$ isotope ratio of the air (free of anthropogenic pollutants) has been chosen as the standard (see Table 3.6 earlier in this chapter). In addition, the biosphere also contains a significant amount of nitrogen. Nitrogen is not frequently observed in the rocks because the nitrates usually dissolve in water. The nitrate in water, however, is toxic. The $\delta^{15}\text{N}$ value can give information on the origin of the polluting sources of nitrate, assuming that the nitrogen isotope ratios are different and that neither isotope exchanges nor chemical reactions take place between the different sources of nitrate.

The sources of nitrate can include the following:

- The nitrogen content of soils, including all nitrogen compounds. The characteristic value of $\delta^{15}\text{N}$ soils is in the range of +5‰ to +9‰.
- The nitrate content of the soil, $\delta^{15}\text{N}$ is +2‰ to +9‰. This value shows that the abundance of ^{15}N of the nitrate in soil can be lower than the mean value of $\delta^{15}\text{N}$.
- The fresh excrement of animals typically has $\delta^{15}\text{N}$ in the range of +1 and +6‰; however, for example, penguin excrement shows $\delta^{15}\text{N} \approx +8\%$. When aging, ammonia, with the

lighter isotope (^{14}N), evaporates because the partial pressure of ammonia containing the lighter isotope is higher. Therefore, $\delta^{15}\text{N}$ increases up to +10‰ to +23‰. In the soil of the rookeries, $\delta^{15}\text{N}$ is even higher, and in the soil of a penguin rookery, it can reach more than +30‰.

- Synthetic fertilizers have $\delta^{15}\text{N} = +2\text{‰}$ to $+7\text{‰}$. This value can be explained by the fact that the fertilizers are synthesized from air ($\delta^{15}\text{N} = 0$) and mineral nitrogen sources with much higher $\delta^{15}\text{N}$. In addition, the chemical isotope effects during the production (i.e., the contact catalytic synthesis of ammonia) can also influence the isotope ratio.
- When the nitrate content of the fertilizers (including organic and synthetic) by the evaporation of ammonia decreases by 20%, the $\delta^{15}\text{N}$ increases by 5‰. Since the nitrogen isotope ratios are different in the original organic and inorganic fertilizers, a given value of $\delta^{15}\text{N}$ can relate to different polluting sources. For example, in sandy soil, $\delta^{15}\text{N} = +4\text{‰}$ to $+5\text{‰}$ may show that the polluting source is synthetic fertilizer, while in clayey soil, the same value can mean that the pollution originates from organic fertilizer. Therefore, the nitrogen isotope ratio alone gives no definite information on the polluting sources.

The ratio of $^{15}\text{N}/^{14}\text{N}$ presents a characteristic distinction between herbivores and carnivores, as the ^{15}N isotope tends to be concentrated by 3–4‰ with each step of the food chain (terrestrial plants, with the exception of legumes, has the isotopic ratio 2–6‰ of N). Measuring the nitrogen isotope ratio in hair, for example, can give archeological information on alimentary habits.

3.4.4 Isotope Ratios of Carbon

Since carbon compounds are present in any sphere of the Earth (atmosphere, hydrosphere, lithosphere, or biosphere), the determination of the carbon isotope ratios obviously plays an important role in the study of the global carbon cycle. In addition, the isotope analysis of other planets provides important information. For example, the $\delta^{18}\text{O}$ is the same in the rocks of the upper parts of the Earth's crust and the Moon ($\delta^{18}\text{O} = 5.5 \pm 0.2\text{‰}$), proving that the Earth and Moon share the same origin.

An important question in the global carbon cycle is the carbon isotope ratio of the Earth's mantle. Because of the very high temperature, even isotope composition should be expected; however, there are significant differences in the isotope ratio of different minerals. Diamond and SiC mineral, for example, contain more ^{12}C isotopes than magmatic minerals.

Deviation from the mean carbon isotope ratios refers to the major extinction event. Since the $^{13}\text{C}/^{12}\text{C}$ ratio of the biomass is lower than that of the sedimentary carbonate rocks, the sediments forming during the extinction events from the biomass show lower $^{13}\text{C}/^{12}\text{C}$ ratio than the mean value of the carbonate rocks. The $^{13}\text{C}/^{12}\text{C}$ can continue to decrease via the release of methane-hydrate bound to the deep-sea sediments, which is due to bacterial activity that prefers the light carbon isotope. During global warming, the methane-hydrate releases as carbon dioxide, increasing the carbon dioxide content of the atmosphere. The industrial carbon dioxide emission also decreases the $^{13}\text{C}/^{12}\text{C}$ ratio because of the burning of fossil fuel. All the above processes are in fact the consequence of biological isotope effects.

3.4.5 Stable Isotope Ratios in Ecological Studies

The stable isotope ratios provide information on the presence and magnitude of important ecological processes. Many ecological processes produce characteristic isotope ratios. The stable isotope ratio value relative to known background values may indicate the presence or absence of such processes. The exact values of the isotope ratios make it possible to determine the magnitude of these processes, if any.

As mentioned previously, in the case of carbon isotope ratios, the climatic changes can influence the stable isotope ratios. In addition, the change of other environmental conditions can also affect the isotope ratios. Environmental changes can be studied using some substances (tree rings, hair, and ice cubes) that preserve a record of the isotope ratios for a long time.

The isotope ratios remain the same during the movement of different elements and compounds. As a result, the source of essential elements, resources, or pollutions is easily traced using isotope ratios. The isotope ratios can be very different depending on geographic location. This provides a way to trace the movement or origin of a substance or component in the landscape to continental scales. The origins of environmental pollutions can be identified in this way. For example, the origin of waste deposits by paint factories can be identified using the lead isotope ratios of the raw material. Lead has four stable isotopes: ^{204}Pb , ^{206}Pb , ^{207}Pb , and ^{208}Pb . ^{204}Pb is a primordial isotope, and the other ones are the final stable members of the radioactive decay series (as discussed in Section 4.2). Since the quantity of ^{204}Pb isotope remains constant and the quantity of ^{206}Pb , ^{207}Pb , and ^{208}Pb changes over time and depends on the uranium and thorium concentrations, the isotope composition of lead strongly depends on its origin, which can then easily be identified. As will be discussed in Section 4.3.1, the isotope ratios of lead can also be used to date rocks.

Further Reading

- Choppin, G.R. and Rydberg, J. (1980). *Nuclear Chemistry, Theory and Applications*. Pergamon Press, Oxford.
- Demény, A. (2004). *Stabilizotóp-geokémia (Stable isotope geochemistry)*. Magyar Kémiai Folyóirat 109–110:192–198.
- Friedlander, G., Kennedy, J.W., Macias, E.S. and Miller, J.M. (1981). *Nuclear and Radiochemistry*. John Wiley and Sons, New York, NY.
- Ghosh, P., Adkins, J., Affek, H., Balta, B., Guo, W., Schauble, E.A., et al. (2006). ^{13}C – ^{18}O bonds in carbonate minerals: a new kind of paleothermometer. *Geochim. Cosmochim. Acta* 70:1439–1456.
- Haisinsky, M. (1964). *Nuclear Chemistry and its Applications*. Addison-Wesley Publishing Company, Inc., Reading, MA.
- University of Wyoming, USA. <<http://www.uwyo.edu/sif/stable-isotopes/index.html>> (accessed 24.03.12.)
- Lieser, K.H. (1997). *Nuclear and Radiochemistry*. Wiley-VCH, Berlin.
- McKay, H.A.C. (1971). *Principles of Radiochemistry*. Butterworths, London.

4 Radioactive Decay

As mentioned earlier (Section 2.1.1), the stability of a nucleus (as characterized by the binding energy) is determined by the ratio of protons to neutrons (see Eq. (2.10)). The binding energy of isobar nuclei as a function of proton–neutron ratio forms a parabola or parabolas (see Figure 3.1), where those nuclei close to the minimum are stable while those farther away are undergoing radioactive decay in order to reach the optimal proton/neutron ratio. The radioactive decay is a random process for the individual nucleus so as to describe the kinetics of radioactive decay, a statistical approach has to be applied.

4.1 Kinetics of Radioactive Decay

4.1.1 Statistics of Simple Radioactive Decay

Let us consider that the probability of the decomposition of a radioactive nuclide in a Δt time interval is p :

$$p = \lambda \Delta t \quad (4.1)$$

where λ is a factor of proportionality. The probability of the process that the nuclide does not decompose in Δt is:

$$1 - p = 1 - \lambda \Delta t \quad (4.2)$$

The probability that the nuclide does not decompose in another second, third, or more Δt interval can also be defined by Eq. (4.2). The probability that the nuclide does not decompose in the $2 \times \Delta t$ interval is:

$$(1 - p)^2 = (1 - \lambda \Delta t)^2 \quad (4.3)$$

The probability that the nuclide does not decompose in $n \times \Delta t$ is:

$$(1 - p)^n = (1 - \lambda \Delta t)^n \quad (4.4)$$

Let us divide the total time of the observation (t) into n intervals:

$$\frac{t}{n} = \Delta t \quad (4.5)$$

Substituting Eq. (4.5) into Eq. (4.4), we obtain:

$$(1 - p)^n = \left(1 - \lambda \frac{t}{n}\right)^n \quad (4.6)$$

At $n \rightarrow \infty$:

$$\lim_{n \rightarrow \infty} (1 - p)^n = \lim_{n \rightarrow \infty} \left(1 - \lambda \frac{t}{n}\right)^n = e^{-\lambda t} \quad (4.7)$$

When the initial number of the radioactive nuclides is N_0 , the number of nuclides that do not undergo radioactive decomposing during t time (N) is:

$$N = N_0 e^{-\lambda t} \quad (4.8)$$

Equation (4.8) describes the kinetics of the simple radioactive decay, i.e., the radioactive decay law, where λ is the decay constant. The value of the decay constant characterizes the radionuclide; thus, it is independent of physical and chemical conditions (pressure, temperature, chemical environment, etc.).

As seen in Eq. (4.8), the radioactive decay has first-order kinetics, having all characteristics of first-order reactions. It has a well-defined half-life ($t_{1/2}$), i.e., the time needed to reduce the number of the radioactive nuclides to half:

$$\frac{N_0}{2} = N_0 e^{-\lambda t_{1/2}} \quad (4.9)$$

and from here,

$$\lambda = \frac{\ln 2}{t_{1/2}} \quad (4.10)$$

Half-life performance 7 and 10 times over gives the interval when the number of radionuclides decreases below 1% and 0.1% of the initial number, respectively.

The reciprocal of the decay constant (λ) is the average lifetime (τ) of the radionuclides, which is the time when the number of the radionuclides decreases by a factor of e (i.e., Euler's constant). This amount of time should be required for the decomposition of all radionuclides if the rate of decay remains constant.

$$\tau = \int_0^{\infty} \frac{t \lambda N}{N_0} dt = \int_0^{\infty} t \lambda e^{-\lambda t} dt = \lambda \left[\frac{e^{-\lambda t}}{\lambda^2} (-\lambda t - 1) \right]_0^{\infty} = \frac{1}{\lambda} \quad (4.11)$$

4.1.2 Activity and Intensity

Radioactivity (A , also known “absolute activity”) is defined as the number of decompositions in a unit time. Radioactivity is in proportion to the initial quantity of the radioactive nuclei:

$$A = -\frac{dN}{dt} = \lambda N = \lambda N_0 e^{-\lambda t} = A_0 e^{-\lambda t} \quad (4.12)$$

It is important to note that the activity–time function (Figure 4.12) is analogous to the number of the radioactive nuclei–time function (Eq. (4.8)).

The unit of radioactivity is the becquerel (Bq), which describes the number of decomposition/disintegrations that take place in 1 s (1 Bq = 1 dps = 1 disintegrations per second). An earlier unit of radioactivity was the curie (Ci), which is the number of decompositions in 1 g of radium in 1 s. The relation between the two activity units is 1 Ci = 3.7×10^{10} Bq. Besides these two, dpm (which means “disintegrations per minute”) is frequently used for practical purposes.

Radioactivity is usually measured not by identifying the radioactive nuclei but by counting the emitted particles. In theory, to achieve accurate activity measurement, all particles emitted in 4π spatial angles should be taken into consideration. In practical applications, however, it is more common that the radioactive intensity (I), a quantity proportional to the radioactivity, is measured. The proportionality factor is the measuring efficiency (k):

$$I = kA = k\lambda N \quad (4.13)$$

The intensity–time function, of course, is similar to the activity–time function (shown in Eq. (4.12)):

$$I = I_0 e^{-\lambda t} \quad (4.14)$$

Obviously, this relation is valid so long as the measuring efficiency (k) stays constant for all measurements.

The units of intensity are as follows:

- cpm means counted particles per minute,
- cps is counted particles per second.

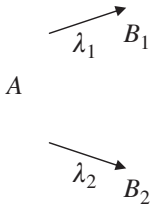
4.1.3 Decay of Independent (Mixed) Nuclei

There are cases when more than one radionuclide is present at the same time. The radioactivity, as well as the activity–time function, depends on all the radionuclides that are present. The identification of each nuclide requires the mathematical decomposition of the activity–time function into components. Then, the identification of the radionuclides present can be done on the basis of the type of decay, the energy, and the half-life of the emitted particles.

When the decays of the radioactive nuclei present are independent, the radioactivities of the mixed nuclides are the sum of the radioactivities of all nuclides. Consequently, the activity–time function cannot be described by the kinetic of the simple radioactive decay (Eq. (4.8)). This means that the radioactivity–time curve must be decomposed. In principle, the decomposition could be done easily by using computing techniques. However, since the functions have to be fitted to the experimental activity–time function, it has some limitations; for example, the activity/intensity and the half-life of the individual isotopes can be determined only by the decomposition of the activity/intensity–time function if there is at least one order of magnitude difference in the half-lives, and if the isotope mixture does contain only a limited number of different radioactive isotopes. If these conditions are not met, adding or neglecting additional nuclides does not improve the accuracy of the mathematical decomposition of the activity–time function.

4.1.4 Branching Decay

A radioactive decay is described as branching when one parent element decomposes to two daughter nuclides. This type of decay can be characterized by two decay constants and half-lives as follows:



where A is the parent nuclide, B_1 and B_2 are the daughter nuclides, and λ_1 and λ_2 are the decay constants for the production of B_1 and B_2 , respectively. Examples of such decay are the decomposition of the ^{212}Pb isotope into ^{212}Po and ^{212}Tl , the decay of ^{64}Cu isotope to ^{64}Zn and ^{64}Ni , and the disintegration of the ^{40}K isotope into ^{40}Ca and ^{40}Ar isotopes.

Since during branching decay, the quantity of the parent element decreases via two independent processes, the rate of decay of the parent element can be defined by the sum of the two decay constants:

$$-\frac{dN}{dt} = (\lambda_1 + \lambda_2)N \quad (4.15)$$

From here,

$$\frac{dN}{N} = -(\lambda_1 + \lambda_2)dt \quad (4.16)$$

By the integration of Eq. (4.16):

$$\ln N = -(\lambda_1 + \lambda_2)t + \text{constant} \quad (4.17)$$

Assuming that at $t = 0$, $N = N_0$:

$$N = N_0 e^{-(\lambda_1 + \lambda_2)t} \quad (4.18)$$

Equation (4.18) is similar to the kinetics of the simple radioactive decay (Eq. (4.8)), except that the sum of the individual constants is used as the decay constant. In those cases, when the daughter elements formed through different decay mechanisms or the energy of the emitted radiation is sufficiently different, the values of the decay constants can be determined separately. The proportion of the decay constants will determine the relative quantity of the daughter nuclides formed.

In most cases, however, both daughter elements are formed via beta decay, the spectra of which is continuous (see Section 4.4.2), and the decays are very difficult or impossible to separate. In this case, the ratio of the quantity of the daughter elements can be calculated as follows.

The sum of the quantities of the two daughter elements is equal to the quantity of the decomposed parent element at any time:

$$B_1 + B_2 = N_0 - N = N_0(1 - e^{-(\lambda_1 + \lambda_2)t}) \quad (4.19)$$

The rate of the formation of the daughter elements is:

$$\frac{dB_1}{dt} = \lambda_1 N = \lambda_1 N_0 e^{-(\lambda_1 + \lambda_2)t} \quad (4.20)$$

$$\frac{dB_2}{dt} = \lambda_2 N = \lambda_2 N_0 e^{-(\lambda_1 + \lambda_2)t} \quad (4.21)$$

By integrating Eqs. (4.20) and (4.21) from $t = 0$ to ∞ :

$$B_1 = \left[-\frac{\lambda_1}{\lambda_1 + \lambda_2} N_0 e^{-(\lambda_1 + \lambda_2)t} \right]_0^\infty \quad (4.22)$$

$$B_2 = \left[-\frac{\lambda_2}{\lambda_1 + \lambda_2} N_0 e^{-(\lambda_1 + \lambda_2)t} \right]_0^\infty \quad (4.23)$$

we obtain:

$$B_1 = \frac{\lambda_1}{\lambda_1 + \lambda_2} N_0 \quad (4.24)$$

$$B_2 = \frac{\lambda_2}{\lambda_1 + \lambda_2} N_0 \quad (4.25)$$

The ratio of Eqs. (4.24) and (4.25) is:

$$\frac{B_1}{B_2} = \frac{\lambda_1}{\lambda_2} \quad (4.26)$$

Therefore, in branching decay, the ratio of the quantities of the daughter elements is equal to the ratio of the decay constants. By determining the quantities of the daughter elements, the ratio of the decay constants can be calculated.

Equations (4.20) and (4.21) have been integrated from $t = 0$ to ∞ , but the same results are obtained by the integration over any time interval.

4.1.5 Kinetics of Successive Decay

When the daughter element of a parent element is also radioactive and decays further, we describe this as a successive decay series. It means that there are genetic relations between the radionuclides. There are some similar decay series in the products of uranium fission initiated by neutrons. For example, ^{90}Sr isotope decomposes by negative beta decay to ^{90}Y , which also decomposes by negative beta decay to stable ^{90}Zr . In this series, there are two successive decays; however, there are series with more than two successive decays. Three natural radioactive decay series where alpha and beta decays form long decay series are known. Their starting parent nuclides are ^{235}U , ^{238}U , and ^{232}Th isotopes, and the last, stable nuclides are different lead isotopes, namely, ^{207}Pb , ^{206}Pb , and ^{208}Pb . These natural radioactive decay series are shown in Figures 4.4–4.6.

For simplicity, the kinetics of the radioactive decay series are demonstrated for the two-member decay series (a parent nuclide and one radioactive daughter nuclide). The total radioactivity (A) is the sum of the radioactivities of the parent (A_1) and daughter (A_2) nuclides:

$$A = A_1 + A_2 \quad (4.27)$$

The kinetics of the radioactive decay of the parent nuclide can be described using the kinetics of the simple decay, as discussed previously:

$$A_1 = \lambda_1 N_1 = \lambda_1 N_0 e^{-\lambda_1 t} \quad (4.28)$$

The radioactivity of the daughter nuclides depends on two factors: it continuously forms from the parent nuclide and decays. Therefore, the quantity of the daughter nuclide is determined both by the rate of its formation and by its decay:

$$\frac{dN_2}{dt} = \lambda_1 N_1 - \lambda_2 N_2 \quad (4.29)$$

In Eqs. (4.28) and (4.29), N_1 and N_2 are the number of the parent and daughter nuclides, respectively; λ_1 and λ_2 are their decay constants.

For the solution of Eq. (4.29), the next substitutions are applied:

$$N_2 = u \times v \quad (4.30)$$

and

$$v = e^{-\lambda_2 t} \quad (4.31)$$

The total derivative with respect to t of the function in Eq. (4.30) is:

$$\frac{dN_2}{dt} = \frac{d(uv)}{dt} = uv' + u'v = -u\lambda_2 e^{-\lambda_2 t} + du e^{-\lambda_2 t} \quad (4.32)$$

From Eqs. (4.29) and (4.32):

$$-u\lambda_2 e^{-\lambda_2 t} + du e^{-\lambda_2 t} = \lambda_1 N_1 - \lambda_2 N_2 \quad (4.33)$$

By substituting Eqs. (4.28) and (4.30) into Eq. (4.33), we obtain:

$$-u\lambda_2 e^{-\lambda_2 t} + du e^{\lambda_2 t} + u\lambda_2 e^{-\lambda_2 t} - \lambda_1 N_{10} e^{-\lambda_1 t} = 0 \quad (4.34)$$

After mathematical simplification:

$$du e^{-\lambda_2 t} - \lambda_1 N_{10} e^{-\lambda_1 t} = 0 \quad (4.35)$$

The solution of Eq. (4.35) is:

$$\int du = \int \lambda_1 N_{10} e^{(\lambda_2 - \lambda_1)t} \quad (4.36)$$

$$u = \frac{\lambda_1}{\lambda_2 - \lambda_1} N_{10} e^{(\lambda_2 - \lambda_1)t} + C \quad (4.37)$$

where C is a constant. By substituting Eq. (4.37) into Eq. (4.30):

$$N_2 = \frac{\lambda_1}{\lambda_2 - \lambda_1} N_{10} e^{-\lambda_1 t} + C e^{-\lambda_2 t} \quad (4.38)$$

When at $t = 0$, $N_2 = N_{20}$, then from Eq. (4.38):

$$N_{20} = \frac{\lambda_1}{\lambda_2 - \lambda_1} N_{10} + C \quad (4.39)$$

By expressing C and substituting into Eq. (4.38), we obtain:

$$N_2 = \frac{\lambda_1}{\lambda_2 - \lambda_1} N_{10} e^{-\lambda_1 t} + \left(N_{20} - \frac{\lambda_1}{\lambda_2 - \lambda_1} N_{10} \right) e^{-\lambda_2 t} \quad (4.40)$$

After equivalent mathematical transformation:

$$N_2 = \frac{\lambda_1}{\lambda_2 - \lambda_1} N_{10} e^{-\lambda_1 t} [1 - e^{(\lambda_1 - \lambda_2)t}] + N_{20} e^{-\lambda_2 t} \quad (4.41)$$

or

$$N_2 = \frac{\lambda_1}{\lambda_2 - \lambda_1} N_{10} [e^{-\lambda_1 t} - e^{-\lambda_2 t}] + N_{20} e^{-\lambda_2 t} \quad (4.42)$$

Instead of the number of the radioactive nuclides, radioactivities can be written using $A_2 = N_2 \lambda_2$ and $A_1 = N_1 \lambda_1$:

$$A_2 = \frac{\lambda_2}{\lambda_2 - \lambda_1} A_{10} e^{-\lambda_1 t} [1 - e^{(\lambda_1 - \lambda_2)t}] + A_{20} e^{-\lambda_2 t} \quad (4.43)$$

This equation of the activity can be transformed directly to intensities only if the measuring efficiency for both the parent and daughter nuclides is the same. If not, intensity can be measured only after reaching radioactive equilibrium (see [Section 4.1.6](#)).

The first and second members in Eq. (4.41) express, respectively, the increase and decay of the quantity of the daughter nuclide compared to its quantity at $t = 0$. The maximum quantity of the daughter nuclide can be determined by the differentiation of Eq. (4.41): the quantity of the daughter nuclide is maximized when Eq. (4.41) has an extremum. For the sake of simplicity, suppose that, at $t = 0$, $N_2 = 0$:

$$\frac{dN_2}{dt} = -\frac{\lambda_1 \lambda_1}{\lambda_2 - \lambda_1} N_{10} e^{-\lambda_1 t} + \frac{\lambda_1 \lambda_2}{\lambda_2 - \lambda_1} N_{10} e^{-\lambda_2 t} = 0 \quad (4.44)$$

From here:

$$t_{\max} = \frac{1}{\lambda_1 - \lambda_2} \ln \frac{\lambda_1}{\lambda_2} \quad (4.45)$$

At $t = 0$, $N_2 \neq 0$, the equation has an additional member (which is not discussed here).

For radioactive decay series having more than two members, the formation and decay rates can be defined for the third to n th members, similar to Eq. (4.29):

$$\begin{aligned} \frac{dN_3}{dt} &= \lambda_2 N_2 - \lambda_3 N_3 \\ \frac{dN_n}{dt} &= \lambda_{n-1} N_{n-1} - \lambda_n N_n \end{aligned} \quad (4.46)$$

The solution of the rate equations can be given as follows:

$$N_n = \sum_{i=1}^n c_i^n e^{-\lambda_i t} \quad (4.47)$$

where

$$c_i^n = N_{10} \frac{\prod_{k=1}^{n-1} \lambda_k}{\prod_{\substack{k=1 \\ k \neq i}}^n (\lambda_k - \lambda_i)} \quad (4.48)$$

For three members:

$$N_3 = N_{10} \left[\frac{\lambda_1 \lambda_2 e^{-\lambda_1 t}}{(\lambda_2 - \lambda_1)(\lambda_3 - \lambda_1)} + \frac{\lambda_1 \lambda_2 e^{-\lambda_2 t}}{(\lambda_1 - \lambda_2)(\lambda_3 - \lambda_2)} + \frac{\lambda_1 \lambda_2 e^{-\lambda_3 t}}{(\lambda_1 - \lambda_3)(\lambda_2 - \lambda_3)} \right] \quad (4.49)$$

4.1.6 Radioactive Equilibria

The properties of the radioactive decay series depend on the ratio of the decay constants of the isotopes in genetic relations. Four different scenarios can occur:

1. $\lambda_1 < \lambda_2$: the parent nuclide decays more slowly than the daughter nuclide.
2. $\lambda_1 \ll \lambda_2$: the parent nuclide decays much more slowly than the daughter nuclide.
3. $\lambda_1 > \lambda_2$: the parent nuclide decays faster than the daughter nuclide.
4. $\lambda_1 \approx \lambda_2$: the decay rates are approximately the same.

Depending on the ratio of the decay constants, radioactive equilibria of the isotopes in genetic relations can (or cannot) be reached:

1. When the parent nuclide decays more slowly than the daughter nuclide ($\lambda_1 < \lambda_2$), the exponential function $e^{(\lambda_1 - \lambda_2)t}$ in Eq. (4.41) tends to become zero after a sufficient length of time. Supposing that no daughter nuclide is present at $t = 0$ (at $t = 0$, $N_2 = 0$), Eq. (4.41) becomes:

$$N_2 = \frac{\lambda_1}{\lambda_2 - \lambda_1} N_{10} e^{-\lambda_1 t} \quad (4.50)$$

that is,

$$N_2 = \frac{\lambda_1}{\lambda_2 - \lambda_1} N_1 \quad (4.51)$$

Expressing radioactivities, assuming that $N_2 = A_2/\lambda_2$ and $N_1 = A_1/\lambda_1$, we obtain:

$$A_2 = \frac{\lambda_2}{\lambda_2 - \lambda_1} A_1 \quad (4.52)$$

An equivalent mathematical transformation of Eq. (4.51) results in:

$$\frac{\lambda_1 N_1}{\lambda_2 N_2} = 1 - \frac{\lambda_1}{\lambda_2} \quad (4.53)$$

On the right side of Eq. (4.53), only constant values are present. This means that the right side itself is also constant. Since $\lambda_1 < \lambda_2$, its value is between 0 and 1. Consequently, the left side of Eq. (4.53) is also constant, which assumes that the ratio of the radioactivities of the parent and daughter nuclides is constant. This is a form of the radioactive equilibria of isotopes in genetic relation, called a transient or current equilibrium. In a transient equilibrium, the radioactivity of the daughter nuclide is always higher. In Figure 4.1, the radioactivities of the parent and daughter nuclides and the total activity are both plotted as a function of time.

As seen in Figure 4.1, the slope of the activity–time functions becomes the same (λ_1) after reaching the transient equilibrium, which means that the radioactivity of the daughter nuclide can be described by the decay constant (or the half-life) of the parent nuclide. The radioactivity can be measured correctly after reaching the transient equilibrium. The time needed to reach the transient equilibrium can be determined by the maximum quantity of the daughter nuclide (Eq. (4.45)) when $t = 0$, $N_2 = 0$; if not, an extended equation has to be used which is not discussed here.

2. When the parent nuclide decays much more slowly than the daughter nuclide, $\lambda_1 \ll \lambda_2$, and $t = 0$, $N_2 = 0$, Eq. (4.41) becomes:

$$N_2 = \frac{\lambda_1}{\lambda_2} N_{10} e^{-\lambda_1 t} [1 - e^{-\lambda_2 t}] \quad (4.54)$$

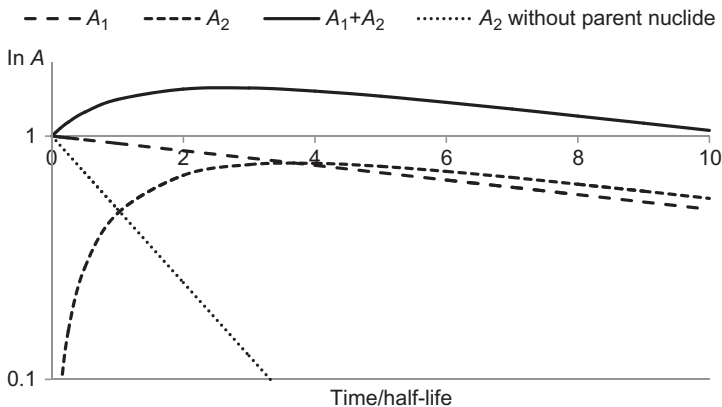


Figure 4.1 Transient equilibrium: activities of the parent nuclide (A_1), the daughter nuclide (A_2), the total activity ($A_1 + A_2$), and the activity of the daughter nuclide when not produced from the parent nuclide as a function of time. Time is expressed compared to the half-life of the daughter nuclide. The ratio of the half-life of parent nuclide:daughter nuclide is 10:1.

Since the parent nuclide decays very slowly (i.e., $e^{-\lambda_1 t} \approx 1$):

$$N_2 = \frac{\lambda_1}{\lambda_2} N_{10} [1 - e^{-\lambda_2 t}] \quad (4.55)$$

This is expressed in activities as follows:

$$A_2 = A_{10} [1 - e^{-\lambda_2 t}] \quad (4.56)$$

After about 10 half-lives of the daughter nuclide, $e^{-\lambda_2 t} \approx 0$; so, from Eq. (4.56), we obtain:

$$N_2 = \frac{\lambda_1}{\lambda_2} N_{10} \quad (4.57)$$

and from here,

$$N_2 \lambda_2 = N_{10} \lambda_1 \quad (4.58)$$

When the decay series composes more than two members, Eq. (4.58) applies to all members:

$$N_1 \lambda_1 = N_2 \lambda_2 = \dots = N_n \lambda_n = A_1 = A_2 = \dots = A_n \quad (4.59)$$

Equation (4.59) means that in equilibrium, the radioactivity of all nuclides is the same. This type of radioactive equilibria is called “secular equilibrium.” In Figure 4.2, the activities of the parent and daughter nuclides are plotted as a function of time under the conditions of the secular equilibrium.

In a secular equilibrium, the short or very long half-lives of the members can be determined if the quantity of the nuclides and the half-life or decay constant of one of the nuclides is known. For example, the second member in the decay series of ^{238}U is the ^{234}Th isotope. The half-lives are 24.1 days for ^{234}Th and 4.5×10^9 years for ^{238}U . The very long half-life of ^{238}U can be determined by the quantitative separation and activity measurement of ^{234}Th . The quantity of ^{238}U can be determined by any chemical analytical method (the chemical analysis and the activity measurements are independent methods). From these data, the half-life or the decay constant of ^{238}U can be calculated using Eq. (4.59) when ^{238}U and ^{234}Th are in secular equilibrium.

3. When $\lambda_1 > \lambda_2$, the parent nuclide decays faster than the daughter nuclide. This is important in the production of radioactive isotopes when the parent nuclide can be produced easily or a carrier-free daughter nuclide is required. Since the decay of the parent nuclide occurs faster, decomposition of the parent nuclide yields a pure daughter nuclide. The optimal conditions of the yield of the daughter nuclide (the time of the maximum activity) can be determined by Eq. (4.45). This time shows the time of the so-called ideal equilibrium, when the activities of the

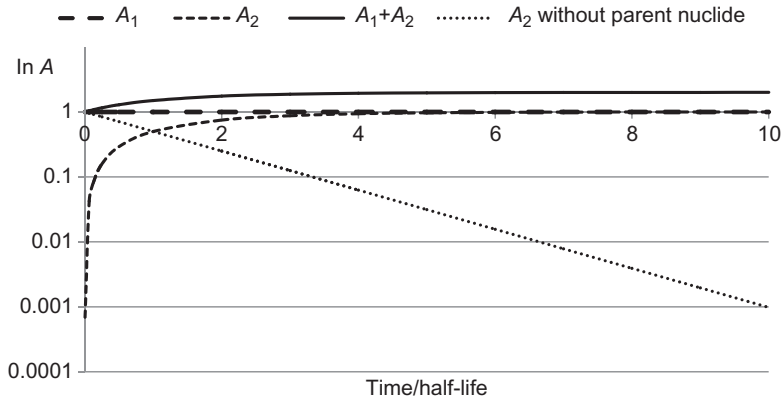


Figure 4.2 Secular equilibrium: activities of the parent nuclide (A_1), the daughter nuclide (A_2), the total activity ($A_1 + A_2$), and the activity of the daughter nuclide when not produced from the parent nuclide as a function of time. Time is expressed compared to the half-life of the daughter nuclide.

parent and daughter nuclides are the same. This means when the parent nuclide decays faster than the daughter nuclides, they are in equilibrium for one moment (at t_{\max} , $A_1 = A_2$). The kinetics of the decay of the daughter nuclide is described by Eqs. (4.41) and (4.42). In Figure 4.3, the activities of the parent and daughter nuclide are shown as a function of time.

As an example of the isotope production when $\lambda_1 > \lambda_2$, the production of ^{131}I from tellurium is mentioned:



4. When $\lambda_1 \approx \lambda_2$ (i.e., the decay rates of the parent and daughter nuclides are approximately the same), Eq. (4.41) cannot be solved because of the zero value of the denominator ($\lambda_2 - \lambda_1 \approx 0$). So, the limit of the function is expressed as follows:

$$\lim_{\lambda_1 \rightarrow \lambda_2} N_2 = \lambda t N_{10} e^{-\lambda t} = \lambda t N_1 \quad (4.61)$$

In Eq. (4.61), the decay constant has no index because equality is assumed. The quantity of the daughter nuclide depends on the quantity of the parent nuclide and the time:

$$N_2 = N_1 \lambda t \quad (4.62)$$

Among the decay products of ^{222}Rn , ^{214}Pb and ^{214}Bi have similar half-lives, 19.9 and 26.8 min, respectively. By measuring the half-lives, these two isotopes

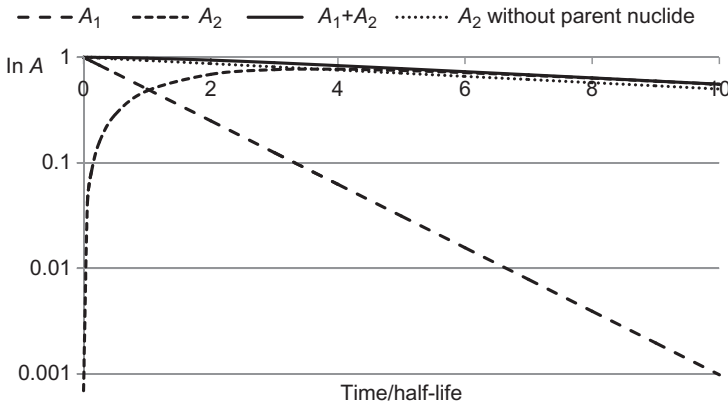


Figure 4.3 Activities of the parent nuclide (A_1), the daughter nuclide (A_2), the total activity ($A_1 + A_2$), and the activity of the daughter nuclide when not produced from the parent nuclide as a function of time. Time is expressed compared to the half-life of the parent nuclide. The ratio of the half-life of parent nuclide:daughter nuclide is 1:10.

cannot be separated. When they are present together, from the activity–time function, about 40 min is given for the half-life.

4.2 Radioactive Decay Series

There are three natural decay series that include the heavy elements, from thallium to uranium; their initial nuclides are ^{238}U , ^{235}U , and ^{232}Th isotopes, and via alpha and beta decays, they end up as lead isotopes (^{206}Pb , ^{207}Pb , and ^{208}Pb , respectively) (see [Figures 4.4–4.6](#)). The half-lives of the initial nuclides are about billion years, which is similar to the age of the Earth (as discussed in [Section 6.2.5](#)). The mass number of the members can be given as $4n$ in the thorium series, $4n + 2$ in the ^{238}U series, and $4n + 3$ in the ^{235}U series. The decay series characterized by $4n + 1$ starts with the ^{237}Np isotope, it can be produced artificially (see [Section 6.2.6](#)). Since the half-life of ^{237}Np is 2.2 million years, even if it was present at the time of the formation of the Earth, it has since decomposed.

4.3 Radioactive Dating

As discussed in [Section 3.4](#), stable isotope ratios can be applied for different geological, ecological, and environmental studies, including the dating of different geological formations and groundwater. Besides stable isotopes, radioactive

Figure 4.4 The main isotopes of the ^{238}U radioactive decay series.

| | |
|-----------------|-----------------------------|
| U-238 | |
| ↓ α | 4.5 × 10 ⁹ years |
| Th-234 | |
| ↓ α | 24.1 days |
| Pa-234 | |
| ↓ β | 1.2 min |
| U-234 | |
| ↓ α | 2.5 × 10 ⁵ years |
| Th-230 | |
| ↓ α | 8 × 10 ⁴ years |
| Ra-226 | |
| ↓ α | 1620 years |
| Rn-222 | |
| ↓ α | 3.825 days |
| Po-218 | |
| ↓ α | 3.05 min |
| Pb-214 | |
| ↓ β | 26.8 min |
| Bi-214 | |
| α ↙ ↘ β | 19.8 min |
| Tl-210 | Po-214 |
| 1.3 min β ↘ ↙ α | 1.6 × 10 ⁻⁴ s |
| Pb-210 | |
| ↓ β | 21.6 years |
| Bi-210 | |
| ↓ β | 5.013 days |
| Po-210 | |
| ↓ α | 138.4 days |
| Pb-206 | |

isotopes or the stable products of different radioactive decays can be used for dating. In these studies, the half-lives of the radioactive isotopes play an important role; the interval, which can be determined by any radioactive dating method, depends on the half-life of the applied radioactive decay. For example, the age of the Earth and the Earth's crust can be estimated by radioactive dating to be about 5 and 3.6 billion years, respectively. These determinations are based on the fact that the half-lives of different radioactive isotopes are in the range of the age of the Earth and the Earth's crust. In this chapter, the main methods of radioactive dating will be discussed.

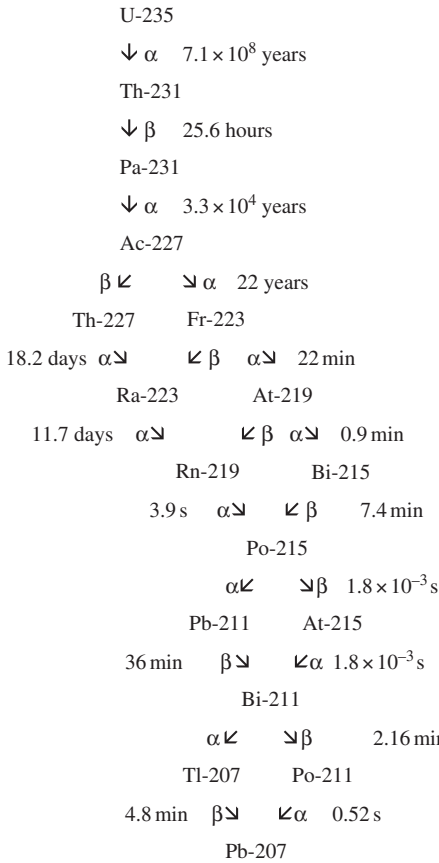


Figure 4.5 The main isotopes of the ^{235}U radioactive decay series.

4.3.1 Radioactive Dating by Lead Isotope Ratios

The age of rocks can be estimated by means of the radioactive decay series. Let us suppose that at the time of the rock formation, only the initial isotopes of the decay series had been produced, and the lead isotopes at the end of the decay series had been formed only from the initial uranium and thorium isotopes. As a result, the concentration of the lead isotopes (with 206, 207, and 208 mass numbers) in the rock is determined by the age. To derive the relationship between the ratio of the lead isotopes and the age of the rock, the ^{238}U decay series is used. According to the kinetics of the simple radioactive decay:

$$^{238}\text{N} = ^{238}\text{N}_0 e^{-\lambda_{238}t} \tag{4.63}$$

where ^{238}N and $^{238}\text{N}_0$ are the quantity of the ^{238}U isotope at the time of the measurement and at the time of the rock formation ($t = 0$), respectively, λ_{238} is the

| | |
|-----------------|-------------------------------|
| Th-232 | |
| ↓ α | 1.41 × 10 ¹⁰ years |
| Ra-228 | |
| ↓ β | 5.7 years |
| Ac-228 | |
| ↓ β | 6.13 hours |
| Th-228 | |
| ↓ α | 1.91 years |
| Ra-224 | |
| ↓ α | 3.64 days |
| Rn-220 | |
| ↓ α | 55 s |
| Po-216 | |
| ↓ α | 1.58 × 10 ⁻¹ s |
| Pb-212 | |
| ↓ β | 10.6 hours |
| Bi-212 | |
| α ↙ β ↘ | 0.6 min |
| Tl-208 | Po-212 |
| 3.1 min β ↘ ↙ α | 3 × 10 ⁻⁷ s |
| Pb-208 | |

Figure 4.6 The main isotopes of the ²³²Th radioactive decay series.

decay constant of ²³⁸U, and t is the age of the rock. As the quantity of ²³⁸U isotope decreases, the quantity of the stable nuclide (²⁰⁶N), the ²⁰⁶Pb isotope, increases:

$${}^{206}\text{N} = {}^{238}\text{N}_0 - {}^{238}\text{N} = {}^{238}\text{N}_0(1 - e^{-\lambda_{238}t}) \quad (4.64)$$

Equation (4.64), however, cannot be used directly because the quantity of the ²³⁸U at $t = 0$ is not known. This unknown quantity can be neglected if the ratio of the quantities of the first (²³⁸U) and last (²⁰⁶Pb) members of the decay series is expressed by dividing Eq. (4.64) by Eq. (4.63):

$$\frac{{}^{206}\text{N}}{{}^{238}\text{N}} = \frac{{}^{238}\text{N}_0(1 - e^{-\lambda_{238}t})}{{}^{238}\text{N}_0 e^{-\lambda_{238}t}} = \frac{1 - e^{-\lambda_{238}t}}{e^{-\lambda_{238}t}} = e^{\lambda_{238}t} - 1 \quad (4.65)$$

Similar equations can be described for the other decay series, namely, for the ratio of the ²⁰⁷Pb/²³⁵U and the ²⁰⁸Pb/²³²Th isotopes:

$$\frac{{}^{208}\text{N}}{{}^{232}\text{N}} = e^{\lambda_{232}t} - 1 \quad (4.66)$$

$$\frac{{}^{207}N}{{}^{235}N} = e^{\lambda_{235}t} - 1 \quad (4.67)$$

where the N s are the quantities of the isotopes (the mass numbers of which are signed in the upper indices), and the λ s are the decay constants.

By measuring these ratios, the age of the geological formations can be determined. However, the chemical behavior of uranium, thorium, and lead, as well as the intermediate members of the decay series, is different, so they may have been leached from the rock differently. So, in this form, Eq. (4.65) can be applied only when the loss of the members of the uranium or thorium decay series can be neglected. If not, the different leaching of the uranium and lead can be neglected if the ratio of the lead isotopes is taken into consideration. The ratio of the uranium isotopes in nature is ${}^{235}\text{U} : {}^{238}\text{U} = 1 : 139$, determined as follows:

$${}^{238}N = 139{}^{235}N \quad (4.68)$$

When Eq. (4.67) is divided by Eq. (4.65) and Eq. (4.68) is substituted, we obtain:

$$\frac{{}^{207}N}{{}^{206}N} = \frac{1}{139} \frac{(e^{\lambda_{235}t} - 1)}{(e^{\lambda_{238}t} - 1)} \quad (4.69)$$

As a conclusion, the age of rocks can be estimated by means of Eq. (4.69) from the ratio of lead isotopes determined by mass spectrometry since the decay constants are known and thus t can be calculated. The advantage of this method is that it gives the right results even if the lead has been leached from the rock because the leaching does not change the ratio of the lead isotopes.

With these dating methods, the quantity of ${}^{206}\text{Pb}$, ${}^{207}\text{Pb}$, and ${}^{208}\text{Pb}$ are measured by mass spectrometry. For more accurate measurements, these quantities are related to the quantity of the ${}^{204}\text{Pb}$ isotope as a reference nuclide, which is not radiogenic.

4.3.2 Radioactive Dating by Helium Concentration

As seen in Figures 4.4–4.6, there are alpha decays in all decay series. The numbers of alpha decays are eight, seven, or six in the series of ${}^{238}\text{U}$, ${}^{235}\text{U}$, and ${}^{232}\text{Th}$ isotopes, respectively. Since the alpha particles are the nuclei of helium, the quantity of the helium gas accumulated inside the rocks can be applied to estimate age. Of course, this method can give the right ages only if the helium gas has not escaped from the rock.

From 1 g of uranium or thorium, $1.195 \times 10^{-4} \text{ mm}^3$ or $2.9 \times 10^{-5} \text{ mm}^3$ of helium gas is formed in a year. Therefore, this method requires the accurate determination of small volumes of helium gas. For this purpose, the rock is dissolved in a mixture of $\text{H}_2\text{SO}_4 + \text{K}_2\text{S}_2\text{O}_8$ or in an acidic oxidizing solution containing CuCl_2 and KCl , avoiding the formation of hydrogen gas in significant volumes. The few hydrogen and nitrogen molecules that form are oxidized by palladium or barium

catalysts, respectively. The noble gases are separated by activated carbon in a chromatographic procedure performed at the temperature of liquid nitrogen. In this way, the quantity of helium can be determined with an accuracy of about $2 \times 10^{-7} \text{ cm}^3$.

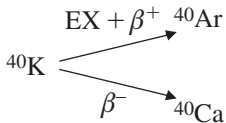
4.3.3 Radioactive Dating by Fission of Uranium

By spontaneous fission of uranium (discussed in Section 4.4.5), different xenon isotopes ($^{129}, ^{131}, ^{132}, ^{133}, ^{136}\text{Xe}$) are formed. The age of uranium-containing rocks or ores can be determined from the quantity of the xenon accumulated in the rocks.

Besides spontaneous fission, the neutrons coming from the cosmic ray also induce the fission of uranium in the silicates. The fission products destroy the silicate lattice. The fission tracks can be etched (e.g., by hydrogen fluoride) so that they can become visible through a microscope. The age can be estimated from the density of the fission tracks.

4.3.4 Radioactive Dating by Argon Concentration

The only source of ^{40}Ar isotopes is branching decay (discussed in Section 4.1.4) of ^{40}K isotopes:



If all the argon gas stays trapped in the rock, the age of a potassium-containing rock can be estimated from the argon concentration:

$${}_{\text{Ar-40}}N = {}_{\text{K-40}}N \frac{\lambda_{\text{EX}+\beta^+}}{\lambda_{\text{EX}+\beta^+} + \lambda_{\beta^-}} (e^{\lambda_{\text{EX}+\beta^+} + \lambda_{\beta^-} t} - 1) \quad (4.71)$$

where $\lambda_{\text{EX}+\beta^+}$ and $\lambda_{\text{EX}+\beta^+} + \lambda_{\beta^-}$ are the decay constants of ^{40}K for the production of ^{40}Ar and for the total decay, independent of the daughter nuclides, respectively. Since ^{40}Ca may form via other routes, the quantity of ^{40}Ca cannot be used for dating.

4.3.5 Radioactive Dating by ^{87}Rb – ^{87}Sr , Parent–Daughter Pairs

The ^{87}Rb isotope has a long half-life (4.88×10^{10} years). This isotope emits negative beta radiation (as discussed in Section 4.4.2), producing an ^{87}Sr isotope. Similarly to the ratio of $^{40}\text{K}/^{40}\text{Ar}$, the age of geological formations can be determined by the ratio of $^{87}\text{Rb}/^{87}\text{Sr}$. The problem with this approach, however, is that the source of an ^{87}Sr isotope is not the decay of ^{87}Rb alone; it was present at the time of the rock formation ($t = 0$). Thus, the quantity of ^{87}Sr (${}^{\text{Sr-87}}N$) can be expressed as:

$${}^{\text{Sr-87}}N = {}^{\text{Sr-87}}N_{t=0} + {}^{\text{Rb-87}}N(e^{\lambda_{\text{Rb-87}} t} - 1) \quad (4.72)$$

where ${}^{\text{Sr-87}}N_{t=0}$ is the quantity of Sr-87 at the time of the formation of the rock (at $t = 0$), ${}^{\text{Rb-87}}N$ is the quantity of Rb-87, $\lambda_{\text{Rb-87}}$ is the decay constant of Rb-87,

and t is the age of the rock. Since the initial quantity of the Sr-87 is not known, for dating purposes, it also has to be determined. This problem is solved by incorporating the quantity of Sr-86 into Eq. (4.72). Sr-86 is a stable isotope, the quantity of which does not change over time. By dividing Eq. (4.72) by the constant quantity of Sr-86 ($^{Sr-86}N$), we obtain:

$$\frac{^{Sr-87}N}{^{Sr-86}N} = \frac{^{Sr-87}N_{t=0}}{^{Sr-86}N} + \frac{^{Rb-87}N}{^{Sr-86}N} (e^{\lambda_{Rb-87}t} - 1) \quad (4.73)$$

When the quantities of Sr-86, Sr-87, and Rb-87 are determined in different rocks or minerals with the same genetics, and the ratio of $^{Sr-87}N/^{Sr-86}N$ is plotted as a function of $^{Rb-87}N/^{Sr-86}N$, a straight line is obtained. The slope of this straight line is $(e^{\lambda_{Rb-87}t} - 1)$, and the intercept is $^{Sr-87}N_{t=0}/^{Sr-86}N$, which shows the initial ratio of the strontium isotopes. The age can be determined from the slope of the straight line. The line is called an “isochron,” which means “similar age.” The method has been used to determine the age of igneous, metamorphic, and sedimentary rocks, and it is used frequently to date meteorites.

4.3.6 Radiocarbon Dating

Libby discovered that the radioactive isotope of carbon, ^{14}C isotope, is formed from the nitrogen that is present in air under the effect of neutrons from the cosmic ray. The nuclear reaction is $^{14}N(n,p)^{14}C$. (Nuclear reactions will be discussed in Chapter 6.) If the flux of the neutrons is assumed to be constant, the formation and subsequent decay of ^{14}C result in a constant concentration of ^{14}C . Since the living organisms continuously incorporate ^{14}C of the carbon dioxide in the air, the ^{14}C concentration of the living organism (i.e., the ratio of $^{14}C/^{12}C$) is the same. When the living organism dies, the continuous uptake of ^{14}C ends, and only the radioactive decay of ^{14}C continues. Thus, the concentration and the radioactivity of ^{14}C decrease. From the $^{14}C/^{12}C$ ratio, the time elapsed from the death of the living organism can be estimated. In radiocarbon dating, 5570 years is traditionally used as the half-life of ^{14}C (the actual half-life is 5736 years). This means that dating is feasible if the living organism lived between 250 and 35,000 years ago. The activity of ^{14}C in the carbon dioxide of the air and the living organisms is 16 dpm/g carbon. However, more accurate results can be obtained using modern mass spectrometry equipments to determine the $^{14}C/^{12}C$ isotope ratio.

An interesting application of the $^{14}C/^{12}C$ ratio of tooth enamel for the estimation of the age of individuals born after 1943 was published. Tooth enamel is formed at well-determined times of childhood and contains 0.4% carbon. After the formation, there is no exchange between the carbon in the enamel and the carbon dioxide in the air. Thus, the $^{14}C/^{12}C$ of the tooth enamel reflects the ratio in the air at the time of the enamel formation. The $^{14}C/^{12}C$ ratio in the air was nearly constant until 1955, when aboveground nuclear bomb tests raised it significantly. After the Limited Test Ban Treaty in 1963, atmospheric ^{14}C began to drop exponentially,

and it did not return to the level before 1955 until recently. Thus, if the $^{14}\text{C}/^{12}\text{C}$ ratio of the tooth enamel is determined, the time of the enamel formation, and from here the age of the individuals, can be estimated.

Besides radiocarbon, tritium is also formed of nitrogen in the air and neutrons in the nuclear reactions $^{14}\text{N}(\text{n},3\ ^4\text{He})\text{T}$ and $^{14}\text{N}(\text{n},\text{T})^{12}\text{C}$. Similar to ^{14}C , tritium isotopes can participate in continuous exchanges between the hydrogen in the air and living organisms. The half-life of tritium is 12.35 years, so it should be suitable for dating in the interval of 10–80 years (e.g., for the dating of wine in bottles). However, thermonuclear explosions in the atmosphere significantly increased the natural tritium concentration, so the dating on the basis of tritium concentration has become quite limited. Tritium activity can be used for the dating of glacier and polar ice in layers, however, because in these cases, the effect of the nuclear explosions is negligible.

4.4 Mechanism of Radioactive Decay

4.4.1 Alpha Decay

Alpha decay was discovered by Rutherford, who placed an isotope-emitting alpha radiation into a thin glass foil and put the foil into a glass vessel closed at the bottom with mercury. The alpha particles have great energy, so they can penetrate the foil into the glass vessel and transform to helium by reacting with two electrons. The gas, of course, shows helium spectrum under excitation. Helium gas, however, cannot penetrate the foil because of the low energy of the atoms, so helium cannot be detected outside the foil.

Alpha decay is characteristic for nuclei with great atomic and mass numbers. Thermodynamically, alpha decay can take place at $A > 150$, but it is only common at $A > 210$, except for samarium and neodymium, which have isotopes emitting alpha radiation. Alpha decay is possible when the mass decreases in Eq. (4.75).

Alpha particles consist of two protons and two neutrons. By emitting an alpha particle, the ratio of protons to neutrons changes and the atomic and mass number decreases by 2 or 4, respectively.



The alpha particle, consisting of two protons and two neutrons, is very stable because of the filled energy levels for protons and neutrons.

The energy of the alpha radiation is in the range of 4–9 MeV. The energy can be calculated from the difference of the rest masses between the parent nuclide and the daughter nuclide, the alpha particle, and the emitting electrons:

$$\Delta m = M_A - M_{A-4} - m_\alpha - 2m_e \quad (4.75)$$

where M_A , M_{A-4} , m_α , and m_e are the rest masses of the parent nuclide, daughter nuclide, alpha particle, and electron, respectively. Since 1 a.m.u. is equivalent to 931 MeV energy, the energy of the alpha particle can be expressed as:

$$\Delta E = 931 \text{ MeV} \times \Delta m \quad (4.76)$$

The energy of the alpha particle, however, is smaller than the value calculated by Eq. (4.76) because a portion of the energy recoils the daughter nuclide. The energy of the recoiling can be calculated on the basis of the law of conservation of linear momentum:

$$m_\alpha v_\alpha + Mv = 0 \quad (4.77)$$

where m_α and M are the masses of the alpha particle and the daughter nuclide, and v_α and v are the rates of the alpha particle and the daughter nuclide, respectively. The rate of the daughter nuclide is expressed from Eq. (4.77):

$$v = \frac{m_\alpha v_\alpha}{M} \quad (4.78)$$

The total energy emitted in alpha decay is the sum of the energies of the daughter nuclide and the alpha particle:

$$E = \frac{1}{2} Mv^2 + \frac{1}{2} m_\alpha v_\alpha^2 \quad (4.79)$$

By substituting Eq. (4.79) into Eq. (4.78), you get the following:

$$E = \frac{1}{2} M \frac{m_\alpha^2 v_\alpha^2}{M^2} + \frac{1}{2} m_\alpha v_\alpha^2 = \frac{1}{2} m_\alpha v_\alpha^2 \left(\frac{m_\alpha}{M} + 1 \right) \quad (4.80)$$

The energy of alpha radiation can be measured in a calorimeter, so the kinetics of the alpha decay can be studied by calorimetry.

In the case of alpha decay, the decay constants of alpha emitters (λ) in a decay series correlate to the radiation energy (E) and the range R of the alpha particles in air. This relation can be expressed by the Geiger–Nuttall rule:

$$\log \lambda = a + b \times \log R \quad (4.81)$$

$$\log \lambda = a' + b' \times \log E \quad (4.82)$$

where a , b , a' , and b' are constants in a decay series.

The $\log \lambda - \log E$ function for the alpha-emitting members of the ^{238}U decay series is shown in Figure 4.7.

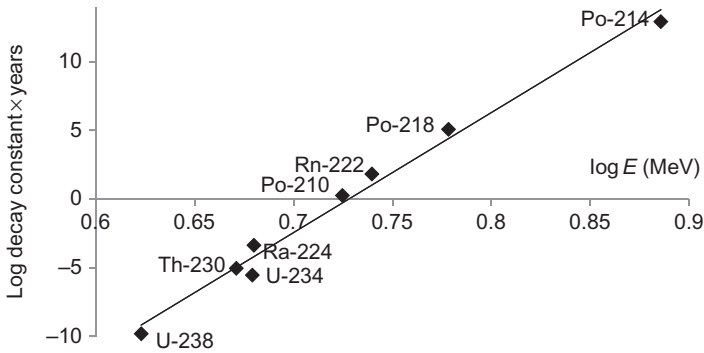


Figure 4.7 Log λ –log E function for the alpha-emitting members of the ^{238}U decay series, illustrating the Geiger–Nuttall rule.

The alpha particles have well-determined, discrete energies. An alpha emitter, however, can produce alpha particles with different energies. This phenomenon can be interpreted by the shell model of nuclei: after the decay, the nucleus is in an excited energy state. The energy of the alpha particles is lower than the value calculated from the differences of the rest masses (Eq. (4.75)), and the difference corresponds to the excitation energy of the nucleus. The excited nucleus may return to a lower excited state or ground state, emitting photons with a characteristic energy. These photons are called gamma photons (described in Section 4.4.6). Since the nucleus may return to the ground state via excited states, the emission of an alpha particle can be followed by more than one gamma photon. In the case of intermediate members of decay series, the energy of a small number of alpha particles may be greater than the value calculated from the differences of the rest masses if the parent nuclide has been in an excited state at the moment of the alpha emission.

In Figure 4.8, decay schemes of two alpha emitter nuclides (^{230}Th and ^{241}Am) are shown. Similar schemes are constructed for all radioactive nuclides. All important information on the nuclides (parent and daughter nuclides), the mechanism of the decay, and the half-life of the parent nuclide can be found. In addition, the ratio of the lines with different energy is given, and the spin and parity (+ or –) are also included.

Models describing the alpha decay postulate two stages of alpha emission: (1) the separation of the parent nuclide into the alpha particle and the daughter nuclide; (2) the penetration of the alpha particle through a potential barrier that is formed by the joint action of nuclear forces and a Coulomb (electrostatic) interaction of the alpha particle with the remaining portion of the nucleus (daughter nucleus; see Figure 4.9). The range of nuclear forces is very short (see Section 2.2), and at greater distances, the Coulomb interaction is determining. As seen previously, alpha particles have two positive charges. Since the daughter nucleus is also positive, the alpha particle and the daughter nucleus repulse each other. The energy

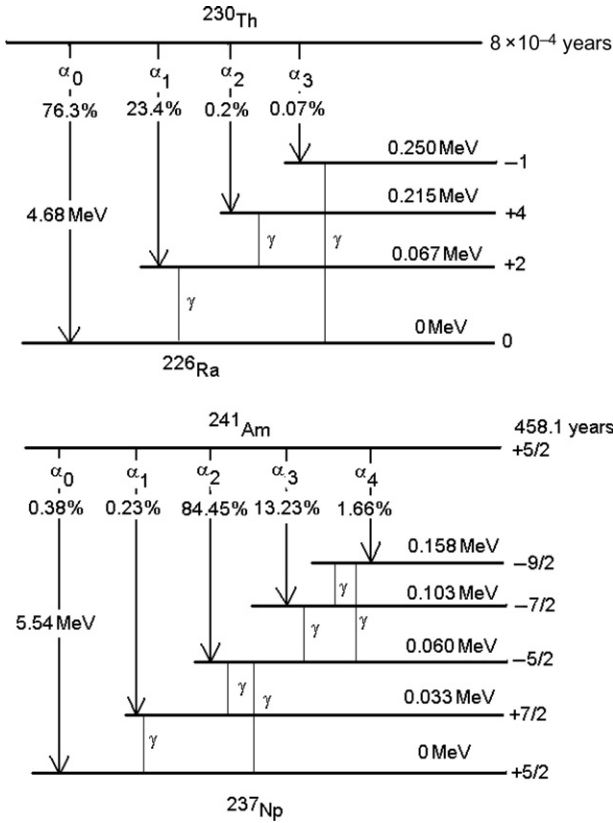


Figure 4.8 Decay scheme of alpha-emitting nuclides (^{230}Th and ^{241}Am).

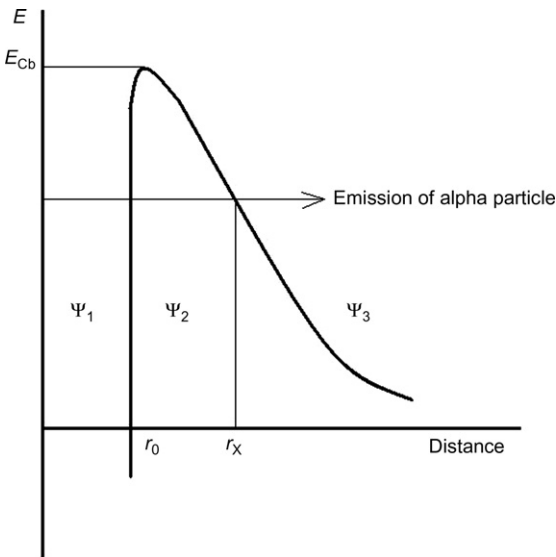


Figure 4.9 Potential barrier against alpha emission. The center of the nucleus is in the origin, Ψ are the wave function at the different spaces, E_{Cb} is the Coulomb repulsion energy, r_0 is the radius of the nucleus, r_x is the outer wall of the Coulomb barrier, and the emitted alpha particle is outside this barrier.

of the repulsion between the alpha particle and the daughter nuclide (the height of the potential barrier) is:

$$E_{Cb} = \frac{2Ze^2}{r_0} \quad (4.83)$$

where E_{Cb} is the height of the potential barrier, Z is the atomic number, and r_0 is the Coulomb radius. E_{Cb} can be determined experimentally in nuclear reactions with charged particles. It is about 20–25 MeV. The energy of the alpha radiation, however, is about 4–9 MeV. According to classical physics, the kinetic energy of the alpha particles is too low to penetrate the potential barrier. Therefore, alpha decay cannot be interpreted by classical physics. The problem of alpha decay can be solved by quantum physics, assuming the wave-particle dual nature. This means that each particle can be described by a wave function, an energy, a linear moment, and a direction of which is the same as those of the particle.

The total energy of the wave or the particle is:

$$E = h\nu \quad (4.84)$$

where ν is the frequency.

The moment of the wave function (g) is:

$$g = hk = h\frac{1}{\lambda} = \frac{h\nu}{c} \quad (4.85)$$

where λ is the wavelength of the alpha particle, its reciprocal (k) is the wave number, and c is the velocity of light in a vacuum.

The intensity of the wave is:

$$I = (\Psi)^2 \quad (4.86)$$

where Ψ is the probability amplitude of the wave function.

The kinetic energy of the particle at a place with U potential can be expressed by the difference between the total energy and the potential energy:

$$E_{kin} = E - U = \frac{1}{2}mv^2 = \frac{g^2}{2m} \quad (4.87)$$

From here,

$$g = \sqrt{2m(E - U)} = hk \quad (4.88)$$

The probability amplitude of the alpha particle is found as follows:

In the nucleus:

$$\Psi_1 = B_1 e^{2\pi i(k_1 r - \nu_1 t)} \quad (4.89)$$

At the place with U potential of the barrier:

$$\Psi_2 = B_2 e^{2\pi i(k_2 r - \nu_2 t)} \quad (4.90)$$

and over the barrier (outside the nucleus):

$$\Psi_3 = B_3 e^{2\pi i(k_3 r - \nu_3 t)} \quad (4.91)$$

As a consequence of Eq. (4.88), k is an imaginary number if the potential U is greater than the total energy of the particle (E). When the imaginary k is multiplied by $2\pi i$ as in the power, the power of Eq. (4.91) will be a real number. Therefore, the alpha particles can be present outside the nucleus.

The wave functions defined in Eqs. (4.89)–(4.91) can be summarized in the Schrödinger equation. An approximate solution of the Schrödinger equation for the alpha radiation is discussed here.

When the rate of the alpha particle in the nucleus is ν , the number of collisions on the potential barrier in 1 s is n_c :

$$n_c = \frac{\nu}{2r_0} \quad (4.92)$$

where r_0 is the radius inside the nucleus where the nuclear field is homogeneous. The number of hits can be given by means of the de Broglie wavelength (λ) of the particle:

$$\lambda = \frac{h}{mv} \approx 2r_0, \quad \text{from here } \nu = \frac{h}{2mr_0} \quad (4.93)$$

When substituting the rate (ν) into Eq. (4.92), we obtain:

$$n_c = \frac{h}{4mr_0^2} \quad (4.94)$$

The ratio of the probability amplitude of the alpha particle existing outside and inside the nucleus is:

$$\frac{|\Psi_3|^2}{|\Psi_1|^2} \quad (4.95)$$

The decay constant is given as the product of the number of collisions and the ratio of the probability amplitude as follows:

$$\lambda = \frac{h}{4mr_0^2} \frac{|\Psi_3|^2}{|\Psi_1|^2} \quad (4.96)$$

When substituting Eqs. (4.89) and (4.91) into Eq. (4.96) and integrating the Schrödinger equation from r_0 to r_x , we obtain:

$$\lambda = \frac{h}{4mr_0^2} \exp \left\{ -\frac{2\pi}{h} \int_{r_0}^{r_x} \sqrt{2m \frac{2(Z-2)[e]^2}{r} - E} \right\} dr \quad (4.97)$$

The approximate solution of Eq. (4.97) for heavy nuclei is:

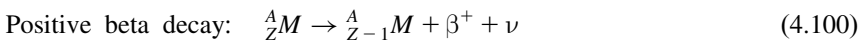
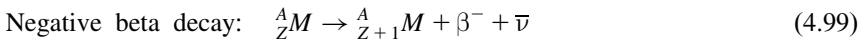
$$\log \lambda = 20.47 - 1.191 \times 10^9 \frac{Z-2}{v} \frac{1}{\sqrt{E}} + 4.084 \times 10^6 \sqrt{Z-2} \times \sqrt{r_0} \quad (4.98)$$

In this way, the decay constant (λ) is obtained in seconds. Equation (4.98) is formally similar to the Geiger–Nuttall rule.

The radius of the nucleus (r_0 in Eq. (4.98)) calculated from the decay constant is always smaller than the radius calculated from the alpha backscattering. For example, the radius of ^{238}U is 9.5×10^{-15} m calculated from the decay constant and 4×10^{-14} m from alpha backscattering. The differences originate in a different place than the location of the collision of the alpha particles: in the case of alpha decay, the alpha particles collide at the inner side of the potential barrier, while in the case of backscattering, alpha particles collide at the outer side of the potential barrier.

4.4.2 Beta Decays

Beta decays take place when the ratio of protons and neutrons is not optimal. Beta decays tend to allow the nucleus to approach the optimal proton/neutron ratio. When there are too many neutrons related to the protons, negative beta decay occurs; when there are too many protons related to the neutrons, positive beta decay takes place. As a result of beta decays, the mass number of the atoms remains the same, but the atomic number changes: the atomic number increases in the negative beta decay and decreases in the positive beta decay, respectively. Besides the beta particle, another particle is also emitted: antineutrino in the negative beta decay and neutrino in the positive beta decay.



In Eqs. (4.99) and (4.100), β^- and β^+ are the negative and positive beta particles, i.e., electrons and positrons. It is important to note that the term “beta particles” means only electrons (positive or negative) emitted from nuclei. Electrons emitted from the extranuclear shell are called “electrons” and designed by e^- .

Similar to alpha decay, the emitted energy of beta decays can be calculated from the rest masses of the parent and daughter nuclide plus the emitted particles:

$$\text{Negative beta decay: } E = ({}^A_Z M - {}^A_{Z+1} M) c^2 \quad (4.101)$$

$$\text{Positive beta decay: } E = ({}^A_Z M - {}^A_{Z-1} M - 2m_e) c^2 \quad (4.102)$$

The rest mass of the neutrino can be ignored because its rest mass is about 10,000 times lower (150 eV at most) than the rest mass of the electron (0.51 MeV). As seen in Eqs. (4.101) and (4.102), besides the differences between the rest masses of the parent and daughter nuclides, there are differences between the rest masses of two electrons since the increase of the atomic number in the negative beta decay requires the uptake of another electron, while the decrease of the atomic number in the positive beta decay causes the emission of another electron. This means that positive beta decay can take place only if the rest mass of the parent nuclide is at least two electron masses (1.02 MeV) heavier than the rest mass of the daughter nuclide.

Since the radioactive decay always releases energy (in the exothermic process), it takes place only if the rest mass of the parent nuclide is greater than the rest mass of the daughter nuclide + the emitted particle(s). (As mentioned previously, the rest mass of the neutrino can be ignored.) For negative beta decay, this can be expressed as:

$${}^A_Z M - Zm_e > {}^A_{Z+1} M - (Z+1)m_e + m_e \quad (4.103)$$

Similarly, for positive beta decay:

$${}^A_Z M - Zm_e > {}^A_{Z-1} M - (Z-1)m_e + m_e \quad (4.104)$$

The solution of Eqs. (4.103) and (4.104) is:

$${}^A_Z M > {}^A_{Z+1} M \quad (4.105)$$

$${}^A_Z M > {}^A_{Z-1} M + 2m_e \quad (4.106)$$

As seen in Eqs. (4.105) and (4.106), the differences in the rest masses give discrete values for the emitted energy. The spectrum of the beta radiation, however, is continuous (Figure 4.10), and the calculated energy is equal to the maximum energy. (The electrons with discrete energy are emitted from the electron shells.)

The continuous beta spectra can be interpreted by the two emitted particles, the beta particle and the neutrino. The energy of beta decay is divided into two parts: both beta particles and neutrinos have some energy. The emission of two particles explains the changes of the spin of the nucleus as a result of the decay: the spin of the nucleus changes by 1, the spin of both beta particle and neutrino is 1/2 (see Table 2.3).



Figure 4.10 General shape of beta spectra: the number of beta particles with a given energy ($N(E)$) versus beta energy (E).

The elementary process of the beta decay can be described as follows:

Negative beta decay:



Positive beta decay:



It is important to note that the processes in Eqs. (4.107) and (4.108) do not mean the free nucleons, but bound in the nucleus. Since the rest mass of the neutron is larger than the rest mass of the proton, the difference of masses in the process of Eq. (4.107) produces energy. The negative beta decay is obviously exothermic. In positive beta decay, however, a proton is transformed to a neutron. This requires energy because of the differences between the rest masses (1.3 MeV; see Table 2.1), which is provided by the decrease of the mass of the nucleus. In addition, the emission of the positron requires more 0.51 MeV energy, which is also to be provided by the decrease of the mass of the nucleus. The sum of the two energies is 1.8 MeV.

The neutrino emitted in the beta decays cannot be detected directly because it is neutral and its rest mass is very small. However, because of the conservation of linear momentum at beta decay, the momentum vectors (i.e., the pathways of the particles) of the daughter nuclide and the beta particle should be at an angle of 180° . However, as photographed in a cloud chamber in the beta decay of ${}^6\text{He}$ by Csikai and Szalay in 1957 (Figure 4.11), another particle (neutrino) has to be released during the decay as well.

The antineutrino can be detected using the following reaction:



Since the cross section of the reaction (4.109) is very low (as discussed in Chapter 6), the high flux of antineutrinos is required similar to those present in nuclear reactors. When an aqueous solution of CdCl_2 is placed into a nuclear

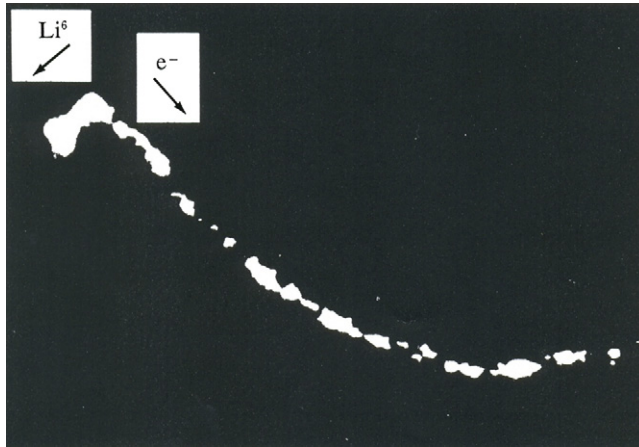


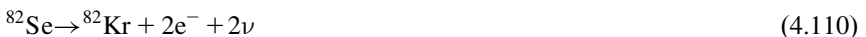
Figure 4.11 Cloud chamber photograph of the decay of ${}^6\text{He}$ to ${}^6\text{Li}$. The angle of the tracks of the ${}^6\text{Li}$ and the beta particle (e^-) is $<180^\circ$, proving the emission of a third particle, antineutrino.

Source: Reprinted from Csikai (1957), with kind permission of Società Italiana di Fisica.

reactor, antineutrinos react with the protons of water in the reaction (4.109). The two products, namely, the positive beta particle and the neutron, can be detected simultaneously in the following way. The positive beta particles and electrons are annihilated, and as a result, photons of 0.51 MeV are emitted (see Section 5.3.3). The neutrons are thermalized in a few microseconds and initiate the nuclear reaction ${}^{113}\text{Cd}(n,\gamma){}^{114}\text{Cd}$. The gamma photons emitted in this nuclear reaction of ${}^{113}\text{Cd}$ follow the emission of the photons with 0.51 MeV after a few microseconds. The two photons can be detected by coincidence measurements.

In beta decays, the nuclei usually emit one beta particle. However, two beta particles are emitted in a single process in some cases. This process is called double beta decay. Theoretically, two types of double beta decays can exist: in the first, two beta particles and two neutrinos are emitted [$\beta\beta(\nu\nu)$], in the other, only two beta particles (no neutrinos) are formed [$\beta\beta(0\nu)$]. In the first case, the two neutrinos annihilate each other; and in the second, the emitted neutrino is absorbed by another one.

Decay products of the double beta decay [$\beta\beta(\nu\nu)$] (by extraction of krypton and xenon from very old selenium and tellurium minerals) in geological samples were detected in 1950. Under laboratory conditions, double beta decay was observed in 1986 when the double beta decay of ${}^{82}\text{Se}$ was measured:



In the laboratory experiments, 1.1×10^{20} years was obtained for the half-life of the double beta decay of ${}^{82}\text{Se}$. This value is similar to the results obtained in geochemical measurements.

More than 60 naturally occurring isotopes are capable of undergoing double beta decay. Only 10 of them were observed to decay via the two-neutrino mode: ^{48}Ca , ^{76}Ge , ^{82}Se , ^{96}Zr , ^{100}Mo , ^{116}Cd , ^{128}Te , ^{130}Te , ^{150}Nd , and ^{238}U .

The neutrinoless double beta decay [$\beta\beta(0\nu)$] has not been demonstrated beyond any doubt.

4.4.3 Electron Capture

In this process, the nucleus captures an electron from an inner electron shell (K or L shell) resulting in the following transition:



The process is characterized as electron capture, EC decay, or EX decay. EC decay is energetically more desirable than positive beta decay since there is no beta particle emission in EC decay. The neutrinos formed in the electron capture are monoenergetic.

The electron capture is always followed by the emission of electromagnetic radiation because the orbital vacancy results in an excited electron state. When the vacancy in the K shell is filled with an electron from an outer, mainly L, shell, the difference between the K and L binding energies is emitted as characteristic X-ray radiation. It is emphasized here that the high-energy electromagnetic radiation is called “gamma radiation” if it is the result of nuclear transition, while if the source of the radiation is the transition of electrons between the extranuclear orbitals, it is called an “X-ray.”

Instead of X-ray radiation, the excitation energy can be transferred to another electron, which is then ejected from the atom. This second ejected electron is called an Auger electron. In this process, the produced nucleus has more than one positive charge, so it can react easily with other substances. The probability of the Auger effect decreases as the atomic number increases. As a result, the ratio of the gamma photons and the Auger electrons depends on the atomic number: for light elements, the Auger electrons are significant, while for heavy elements, the characteristic X-ray is dominant (Figure 4.12).

Furthermore, the electrons captured from the K and L shells, on their pathway toward the nucleus, lose their energy in the nuclear field. This process results in the emission of X-ray radiation called inner *Bremsstrahlung*, the spectrum of which is continuous. Thus, as a result of electron capture, both characteristic and continuous X-ray radiations are emitted.

The electron capture results in excited nuclei. This excitation energy may be lost through either the emission of gamma photons or the transition of the excitation energy to an electron on the atomic orbital (mainly a K electron) of the same atom, followed by an electron emission. The latter process is called “internal conversion,” and the emitted electrons are conversion electrons. The kinetic energy of the conversion electron is equal to the energy of the gamma quantum reduced by

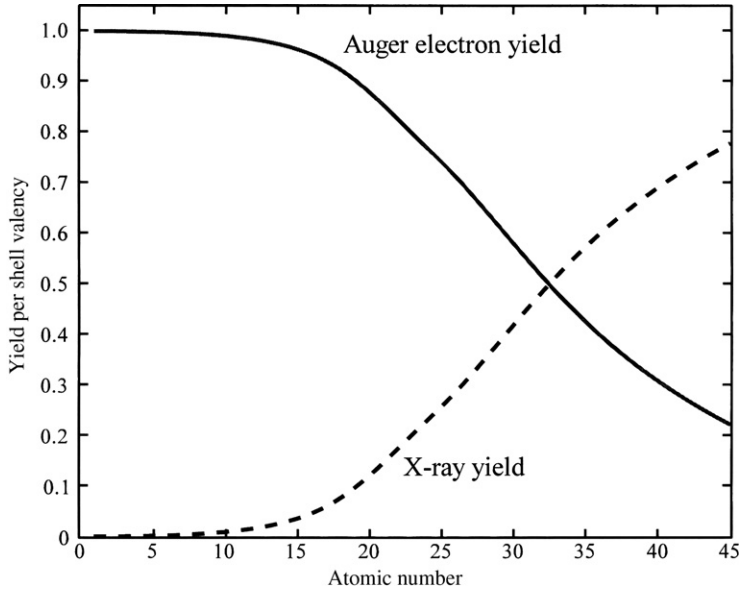
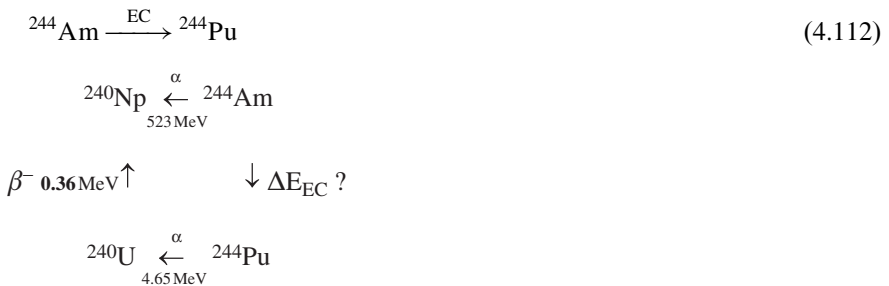


Figure 4.12 The relative yield of X-ray fluorescence photons and Auger electrons for the K shell. Similar curves can be constructed for the L and M transitions. Auger transitions (continuous curve) are more probable for lighter elements, while X-ray yield (dotted curve) becomes dominant at higher atomic numbers.

the binding energy of the electron. This means that the conversion electrons, similar to Auger electrons, have discrete energy.

In some cases, the energy of the electron capture can be measured by using the cyclic process, as shown by the following:



4.4.4 Proton and Neutron Decay

Proton decay can take place after positive beta radiation of the light elements, which is followed by proton emission. For example,



Neutron decay, or delayed neutron decay, may occur when a negative beta decay followed by neutron emission takes place. Neutron decay can be observed for the heavier nuclides too. For example,



Some fission products emit negative beta particles as well as neutrons, for example,



These isotopes are significant in the neutron flux of nuclear reactors, especially when the power is decreasing.

4.4.5 Spontaneous Fission

Similar to alpha decay, spontaneous fission takes place with heavy nuclides. The nucleus is split into two smaller nuclei, assuming that the sum of the mass of the daughter nuclides and the emitted neutrons, if any, is less than the mass of the parent nuclide. The energy of spontaneous fission can be calculated from the decrease of the mass:

$$E = 931 \text{ MeV} ({}^A_Z M - {}^{A_1}_{Z_1} M - {}^{A_2}_{Z_2} M - x m_n) \quad (4.117)$$

E has to be greater than zero, which is principally valid at about $A > 80$, as shown by the positive slope of Figure 2.2. However, spontaneous fission requires activation energy; therefore, it is characteristic of thorium and the heavier nuclides. Spontaneous fission was discovered by Petrzsak and Flerov in 1940, shortly after the discovery of neutron-induced fission by Otto Hahn (1939).



For spontaneous fission, the $\log \lambda$ versus Z^2/A function for the isotopes of a given element shows a maximum curve (Figure 4.13). The ratio Z^2/A is called the “fissionability parameter” because the liquid drop model (discussed in Section 2.5.1) predicts that the probability of fission should increase with this ratio. The composition of the fission products is similar for both spontaneous and neutron-induced fission (see Figure 6.4).

4.4.6 Isomeric Transition (IT)

As a result of radioactive decay, the nuclei of the daughter nuclides can be in an excited state. The excited nucleus may return to a lower excited state or ground state emitting photons with a characteristic energy. These photons are called

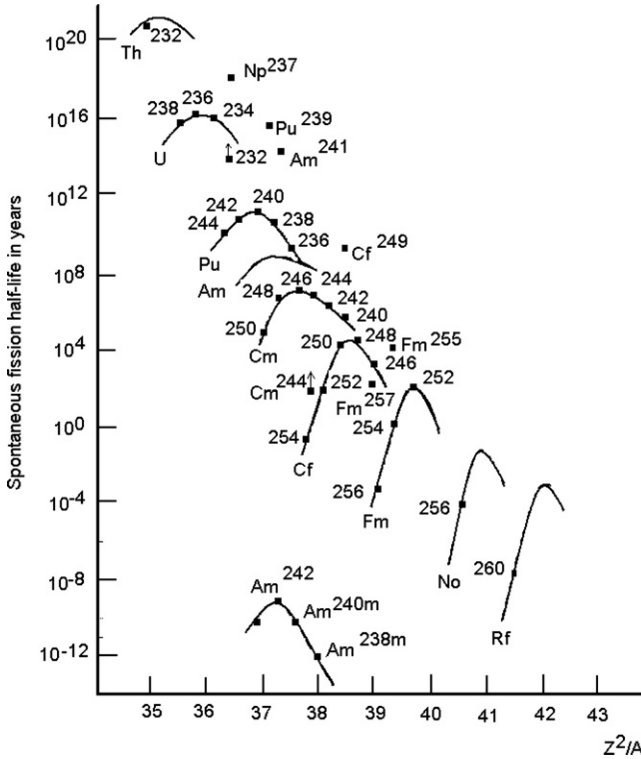


Figure 4.13 Log λ versus Z^2/A function for the spontaneous fission of isotopes of an element with an even mass number.

Source: Reprinted from Choppin and Rydberg (1980), with permission from Elsevier.

“gamma photons” or “gamma radiation.” Thus, gamma radiation is not independent; it always follows another radioactive decay process. The time between the original radioactive decay and the gamma photons can range from minutes to years. This process is called “isomeric transition”; the excited state of the nucleus is known as a “metastable state.” About 150 isomer pairs are known. An empirical relation between the mean lifetime (τ) and the radiation energy (E) has been found on the basis of the change in the spin (ΔJ):

$$\Delta J = 2 \log \tau = 4 - 5 \times \log E \tag{4.119}$$

$$\Delta J = 3 \log \tau = 17.5 - 7 \times \log E \tag{4.120}$$

$$\Delta J = 4 \log \tau = 27.7 - 9 \times \log E \tag{4.121}$$

In Eqs. (4.119)–(4.121), energy and mean lifetime are expressed in keV and seconds, respectively.

As an example of the isomer transition, let us discuss the ^{137}Cs isotope. ^{137}Cs itself is a beta emitter, while its daughter nuclide is ^{137m}Ba (m means the metastable, excited

state). The daughter nuclide, ^{137m}Ba , transforms into ^{137}Ba by emitting a gamma photon. The energy of the gamma photon is 662 keV. ^{137}Cs is frequently used to calibrate spectrometers; however, gamma photons are emitted by ^{137m}Ba , not directly by ^{137}Cs .

4.4.7 Exotic Decay

During exotic decay, the spontaneous emission of nuclei takes place. For example,



Exotic decays are very rare, so they are difficult to observe. In the case of the ^{223}Ra isotope, for example, the probability of the decay (4.123) is about 10^{11} times lower than the probability of the alpha decay. The emitted nuclei are very stable, having closed nucleon shells.

Further Reading

- Burshop, E.H.S. (1952). *The Auger Effect and Other Radiationless Transitions*. Cambridge University Press, Cambridge.
- Csikai, J. (1957). Photographic evidence for the existence of the neutrino. *Il nuove cimento* 5:1011–1012.
- Choppin, G.R. and Rydberg, J. (1980). *Nuclear Chemistry, Theory and Applications*. Pergamon Press, Oxford.
- Friedlander, G., Kennedy, J.W., Macias, E.S. and Miller, J.M. (1981). *Nuclear and Radiochemistry*. Wiley, New York, NY.
- Haissinsky, M. (1964). *Nuclear Chemistry and its Applications*. Addison-Wesley, Reading, MA.
- Kullerud, K. 2003. The Rb-Sr method of dating. <http://ansatte.uit.no/kku000/webgeology/webgeology_files/english/rbsr.html> (accessed 24.03.12.)
- National Nuclear Data Center, 2010. List of Adopted Double Beta ($\beta\beta$) Decay Values. <<http://www.nndc.bnl.gov/bbdecay/list.html>> (accessed 24.03.12.)
- Lagoutine, F., Ciursol, N. and Legrand, J. (1983). *Table de Radionucléides*. Commissariat à l'Energie Atomique, France.
- Lieser, K.H. (1997). *Nuclear and Radiochemistry*. Wiley-VCH, Berlin.
- McKay, H.A.C. (1971). *Principles of Radiochemistry*. Butterworths, London.
- Perkins, D.H. (2000). *Introduction to High Energy Physics*. 4th edition. Cambridge University Press, Cambridge.
- Spalding, K.L., Buchholz, B.A., Bergman, L.-E., Druid, H. and Frisé, J. (2005). Age written in teeth by nuclear tests. A legacy from above-ground testing provides a precise indicator of the year in which a person was born. *Nature* 437:15.

5 Interaction of Radiation with Matter

5.1 Basic Concepts

As discussed in Chapter 1, radioactivity was first detected when radiation interacted with material on photographic plates. Further studies of radioactivity have indicated that radiation may interact with matter in many other ways. The ionizing effect of radiation has been recognized very early. It has also been observed that the degree of the ionization strongly depends on the type of radiation. Rutherford called the radiation with the smallest range “alpha radiation,” the radiation with intermediate range “beta radiation,” and the radiation with the highest range “gamma radiation.” The radiation causes transitional or permanent physical and chemical changes in the molecules that interact with the radiation.

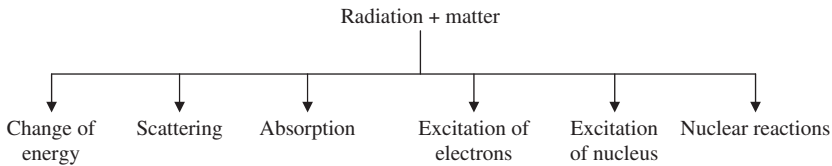
For the interpretation of these interactions, let us look at how energy transitions from radiation to matter and the ensuing changes. To do this, both particles (radiation) and their interactions with matter have to be classified. The particles can be classified on the basis of their characteristic properties, the charge and rest mass. Accordingly, there are charged and neutral particles, and heavy and light particles (Table 5.1).

As seen in Table 5.1, the particles, especially their rest mass, cover a large range, and as such, they can participate in various interactions depending on which part of a substance they interact with and on the mechanism type of the interaction. For example, the reaction of radiation with matter can involve the electron orbitals, the nuclear field, and the nucleus. The particles can partially or totally transfer their energy to matter, can be absorbed, or can be scattered elastically or nonelastically. Furthermore, as a consequence to the interaction, the matter undergoes excitation or ionization, or nuclear resonance or nuclear reactions can be induced. The interactions between radiation and matter may be strong, intermediate, or weak. All these possibilities are summarized in Figure 5.1.

In Figure 5.1, the first three branches show what can happen to the radiation, and the last three branches indicate the changes that they induce in matter. This classification also allows quantitative characterization of the changes that result from the interaction. The changes in the particles of radiation can be mathematically described, assuming that the number of interactions (ν) is proportional to the

Table 5.1 Classification of Particles

| Charged Particles | | Neutral Particles | |
|------------------------------|-----------|-------------------|----------|
| Heavy | Light | Heavy | Light |
| p | β^- | n | γ |
| D | Electron | | X-ray |
| T | β^+ | | ν |
| α | | | |
| Heavy ions without electrons | | | |

**Figure 5.1** Interaction of radiation with matter.

number of particles (n) introduced at a distance x into a substance with ρ atomic density:

$$\nu = \sigma(E)n\rho x \quad (5.1)$$

The cross section ($\sigma(E)$) is the probability of the interactions of the particle with the substance. The value of the cross section depends on the energy of the particle. Equation (5.1) is valid only if the thickness of the layer of the matter (ρx) is so thin that the energy of the particle does not change significantly during the transition through distance x , i.e., $\sigma(E)$ is constant.

The number of particles decreases when they transit through thickness dx of a substance:

$$\frac{dn}{dx} = -\sigma(E)n\rho \quad (5.2)$$

When at $x = 0$, $n = n_0$, the solution of Eq. (5.2) is:

$$n = n_0 e^{-\sigma(E)\rho x} \quad (5.3)$$

Equation (5.3) is the general equation of the absorption of radiation. A special form of this equation is known as the Lambert–Beer law, and it describes the absorption of light photons.

Table 5.2 Interactions of Alpha Particles with Matter

| Reacting Particles and Fields | Changes | |
|-------------------------------|--|---|
| | In Radiation | In Matter |
| Orbital electron | <i>Bremsstrahlung</i> , absorption | Excitation, ionization, chemical change |
| Nuclear field | Scattering, <i>Bremsstrahlung</i> , absorption | |
| Nucleus | Nuclear reaction | New nucleus, chemical change |

Source: Adapted from Kiss and Vértes (1979), with permission from Akadémiai Kiadó.

The number of particles left as a result of the interactions is expressed by:

$$n_0 - n = n_0[1 - \exp^{(-\sigma(E)\rho x)}] \quad (5.4)$$

The change that happens in the substance as a result of the interaction with radiation will be discussed in the sections dealing with the reactions induced by the different types of radiations [Sections 5.1–5.5](#). Also, the nuclear reactions will be discussed separately in Chapter 6.

5.2 Interaction of Alpha Particles with Matter

One of the most important heavy-charged particles is the alpha particle. As demonstrated by Rutherford, the alpha particle is the nucleus of a helium atom. The energy of alpha particles formed in alpha decay is in the range of 4–10 MeV.

Alpha particles can interact with orbital electrons, which leads to ionization or other chemical changes; with the nuclear field, where they can be scattered; or with the nucleus initiating nuclear reactions ([Table 5.2](#)).

5.2.1 Energy Loss of Alpha Particles

The alpha particles can transfer some of their energy and momentum to the orbital electrons, and their velocity decreases. The energy and momentum transfer can be understood as follows. Let us define a Cartesian coordinate system ([Figure 5.2](#)), the horizontal axis (x) of which coincides with the pathway of the alpha particle. In such a system, the electron that participates in the interaction is on the perpendicular axis (y), and the origin of the two axes is where the observation takes place.

During the journey from $-\infty$ to $+\infty$, the alpha particle transfers p momentum to the electron at distance b . Momentum is a vector with x - and y -components:

$$p_x = \int_{-\infty}^{+\infty} F_x dt \quad (5.5)$$

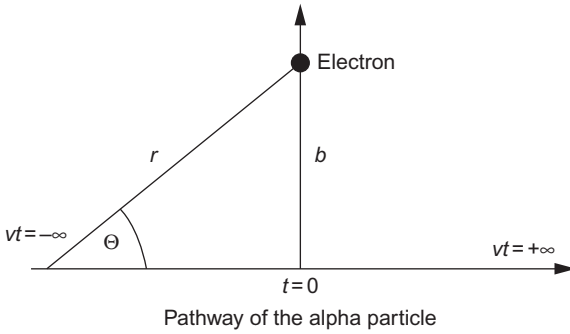


Figure 5.2 The pathway of the alpha particle next to the electron.

$$p_y = \int_{-\infty}^{+\infty} F_y dt \quad (5.6)$$

where F is the electrostatic force between the alpha particle and the electron in the directions of the x - and y -axis, respectively. The electrostatic force acting between two charged particles can be described by the Coulomb law:

$$F = \frac{Ze^2}{r^2} \quad (5.7)$$

$$F_x = \frac{Ze^2}{r^2} \cos \Theta \quad \text{and} \quad F_y = \frac{Ze^2}{r^2} \sin \Theta \quad (5.8)$$

Z means the charge of the alpha particle, $Z = 2$. As seen in [Figure 5.2](#):

$$r = \frac{b}{\sin \Theta} \quad (5.9)$$

By substituting Eq. (5.9) into Eq. (5.8), we obtain:

$$F_x = \frac{Ze^2}{b^2} \sin^2 \Theta \cos \Theta \quad \text{and} \quad F_y = \frac{Ze^2}{b^2} \sin^3 \Theta \quad (5.10)$$

The variable t of Eqs. (5.5) and (5.6) can be expressed by using an angle Θ :

$$\text{tg } \Theta = -\frac{b}{v_\alpha t} \quad (5.11)$$

$$t = -\frac{b}{v_\alpha} \text{ctg } \Theta \quad (5.12)$$

$$dt = \frac{b}{v_\alpha} \frac{1}{\sin^2 \Theta} d\Theta \quad (5.13)$$

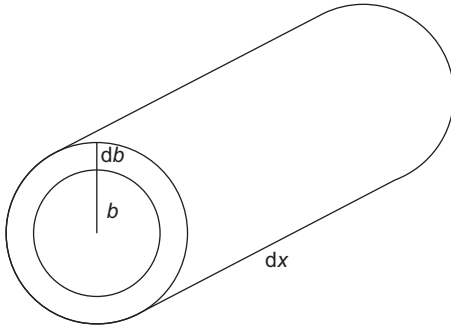


Figure 5.3 A cylinder shell surrounding the pathway of an alpha particle.

By substituting Eqs. (5.10) and (5.13) into Eqs. (5.5) and (5.6), we obtain the following:

$$p_x = \int_0^\pi \frac{Ze^2}{bv_\alpha} \cos \Theta \, d\Theta = \frac{Ze^2}{bv_\alpha} [-\sin \Theta]_0^\pi = 0 \quad (5.14)$$

$$p_y = \int_0^\pi \frac{Ze^2}{bv_\alpha} \sin \Theta \, d\Theta = \frac{Ze^2}{bv_\alpha} [\cos \Theta]_0^\pi = \frac{Ze^2}{bv_\alpha} (-1 - 1) = -\frac{2Ze^2}{bv_\alpha} \quad (5.15)$$

This means that the alpha particle transfers momentum to an electron as expressed by Eq. (5.15), and the electron moves in the y direction. The kinetic energy transferred to the electron (E_e) is:

$$E_e = \frac{p_y^2}{2m_e} = \frac{2Z^2e^4}{m_e b^2 v_\alpha^2} \quad (5.16)$$

where m_e is the rest mass of the electron.

Equation (5.16) gives the energy, which the alpha particle transfers to one electron. During its pathway, however, the alpha particle can interact with many electrons and can transfer energy to them. Therefore, the energies transferred to each electron have to be summed up. The moving alpha particle is surrounded by a cylindrical shell, the volume of which is $2\pi b \times db \times dx$ (Figure 5.3). If the number of atoms with the Z' atomic number in a unit volume is n , the total energy transferred to the electrons is:

$$-dE = E_e n Z' 2\pi b \, db \, dx = \frac{4\pi Z^2 e^4}{m_e v_\alpha^2} n Z' \frac{1}{b} \, db \, dx \quad (5.17)$$

$$-\frac{dE}{dx} = \frac{4\pi Z^2 e^4}{m_e v_\alpha^2} n Z' \int_{b_{\min}}^{b_{\max}} \frac{db}{b} \quad (5.18)$$

In Eq. (5.18), b_{\min} and b_{\max} are the minimal and maximal radius of the cylinder, inside which the alpha particle can interact with the electrons.

$$-\frac{dE}{dx} = \frac{4\pi Z^2 e^4 n}{m_e v_\alpha^2} Z' \ln \frac{b_{\max}}{b_{\min}} \quad (5.19)$$

The value of b_{\min} can be determined from the maximal energy transferred to the electron. This value can be calculated from the conservation of momentum (Eq. (5.20)) and energy (Eq. (5.21)):

$$m_\alpha v_\alpha = m_\alpha v'_\alpha + m_e v_e \quad (5.20)$$

$$\frac{m_\alpha v_\alpha^2}{2} = \frac{m_\alpha v'^2_\alpha}{2} + \frac{m_e v_e^2}{2} \quad (5.21)$$

The left and right sides of Eqs. (5.20) and (5.21) give the momentum and energy before and after the energy transfer, respectively. The rate of the electron (v_e) can be expressed by means of Eqs. (5.20) and (5.21):

$$v_e = \frac{2v_\alpha}{1 + \frac{m_e}{m_\alpha}} \approx 2v_\alpha \quad (5.22)$$

Since the mass of the electron is much smaller than the mass of the alpha particle, the denominator of Eq. (5.22) tends toward the value 1. The maximal energy transferred to the electron is:

$$E_{\max} = 2m_e v_\alpha^2 \quad (5.23)$$

By substituting Eq. (5.23) into Eq. (5.16), we obtain:

$$b_{\min} = \frac{Ze^2}{m_e v_\alpha^2} \quad (5.24)$$

The value of b_{\max} can be obtained from the distance where the electrostatic potential is a multiplied by the ionization and excitation potential (I):

$$b_{\max} = \frac{Ze^2}{aI} \quad (5.25)$$

By substituting Eqs. (5.24) and (5.25) into Eq. (5.19), the energy transferred in a unit pathway can be given as follows:

$$-\frac{dE}{dx} = \frac{4Z^2 e^4 \pi n}{m_e v_\alpha^2} Z' \ln \frac{m_e v_\alpha^2}{aI} \quad (5.26)$$

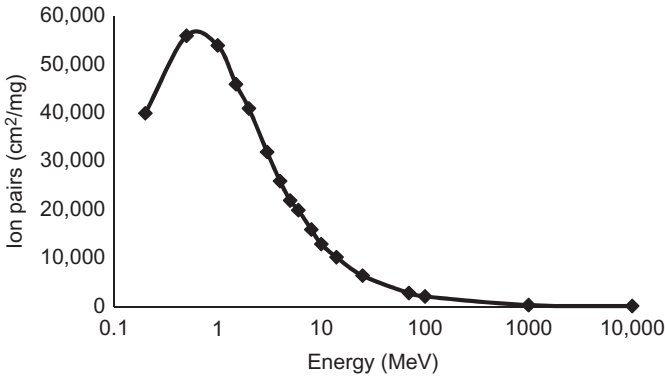


Figure 5.4 Specific ionization of alpha particles in air.

When the velocity of the electron is very high, the relativistic mass increase has to be taken into account. In this case, the Bethe-Bloch formula is obtained:

$$-\frac{dE}{dx} = \frac{4Z^2 e^4 \pi n}{m_e v_\alpha^2} Z' \left[\ln \frac{2m_e v_\alpha^2}{I} - \ln \left(1 - \frac{v^2}{c^2} \right) - \frac{v^2}{c^2} \right] \quad (5.27)$$

As seen in Eqs. (5.26) and (5.27), the energy transferred to the electrons is inversely proportional to the square of the velocity of the alpha particle (v_α^2); in other words, it is inversely proportional to the kinetic energy. Accordingly, we can observe the broadening of the tracks of the alpha particles in cloud chamber photographs due to the higher energy transfer at the later part of the pathway (Figure 5.7). The energy transfer ends when the alpha particle loses all its energy and transforms to a neutral helium atom as in Rutherford's experiment (discussed in Section 4.4.1). The ionization effect of the alpha particles of various energies is shown in Figure 5.4. At the same time as the ionization, the alpha particles take up electrons and lose their positive charge. The relative charge of the alpha particles as a function of the alpha energy is plotted in Figure 5.5. When the alpha particles lose their total energy, they lose their charge as well and produce neutral helium atoms.

During its passage through a substance, alpha particles lose energy until the energy becomes close to zero. The distance to this point is called the "particle range." The range (R) of the alpha radiation depends on the energy of the radiation and the composition of the matter. The range is usually expressed compared to the range in dry air (1 bar, 15°C) (R_0):

$$R = \frac{\rho_{\text{air}}}{\rho} \sqrt{\frac{A}{A_{\text{air}}}} R_0 \quad (5.28)$$

The range of alpha particles in air is several centimeters. In a more condensed medium, however, it is much lower: alpha radiation is absorbed by a sheet of paper or the dead, upper layer of the human skin.

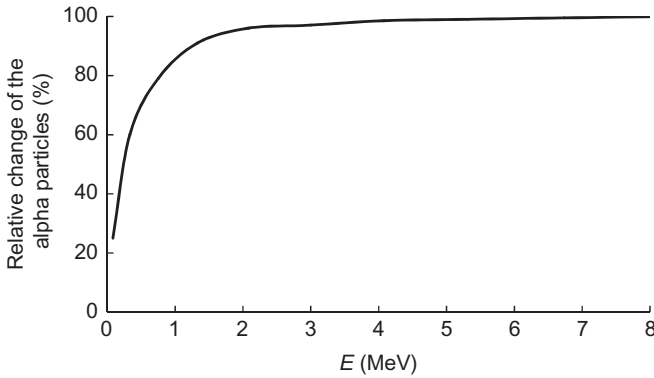


Figure 5.5 The relative charge of alpha particles as a function of alpha energy.

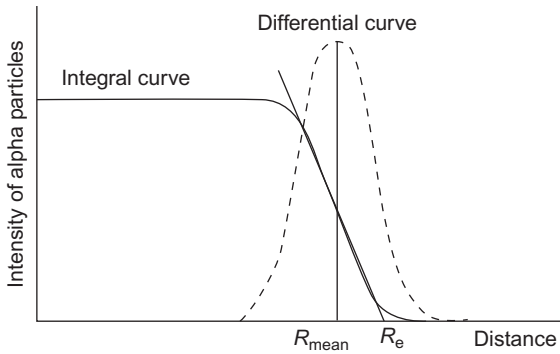


Figure 5.6 Determination of the range of alpha particles from the intensity–distance curve.

The stopping power of the alpha radiation is the energy loss per unit distance ($-dE/dx$), whose dimension is MeV/m. Since the stopping power relates to distance, it is called “linear stopping power.” If it is divided by the atomic density, the atomic stopping power is obtained, whose dimension is MeV \times m²/atom.

The relative stopping power (S) of the alpha radiation is the ratio of ranges in air and another medium:

$$S = \frac{R_0}{R} \quad (5.29)$$

The range of the alpha particles can be determined from the intensity–distance curve (Figure 5.6). The mean range (R_{mean}) is the point at which the number of alpha particles decreases into the half, i.e., the range at the inflexion point of the intensity–distance curve. The extrapolated range (R_e) is determined by the extrapolation of the decreasing branch of the intensity–distance curve.

The range and the linear pathway of the alpha particles can be seen in cloud chamber photographs (Figure 5.7).

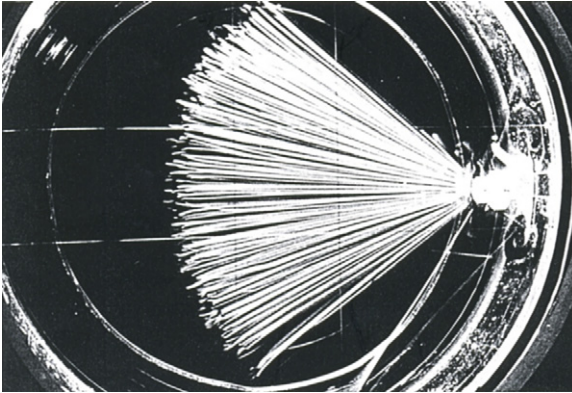


Figure 5.7 Cloud chamber photograph of the pathway of alpha particles. (Thanks to Prof. Julius Csikai, Department of Experimental Physics, University of Debrecen, Hungary, for the photograph.)

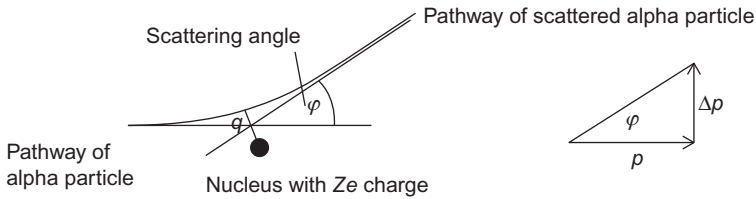


Figure 5.8 The pathway of an alpha particle next to a nucleus with Ze .

5.2.2 Backscattering of Alpha Particles

As discussed in Section 2.2.2, Geiger and Mardsen, led by Rutherford, studied the absorption of alpha radiation in thin gold foil (about 5×10^{-7} m thick). They observed that most of the alpha particles passed through the gold foil without being deflected. However, a very small number of alpha particles bounced back; i.e., they were deflected to 180° . Since the mass of the alpha particles is relatively great, the phenomenon was interpreted on the assumption that most of the space surrounding the atoms was empty; most of the alpha particles could pass through here. Only a few alpha particles were deflected at high angles. This is possible only if there is enormous repulsion between the alpha particles and the deflecting part of the atom. Since the alpha particles are positive, the enormous repulsion proves that the positive charge is found in a very small area of the atom. This means that the entire positive charge and mass are concentrated in this small area of the atom, which is called the nucleus.

When approaching a nucleus, the alpha particles follow a hyperbolic pathway with nucleus in one of the foci of the hyperbola (Figure 5.8). For the alpha particle, the conservation of both the energy and the momentum applies. Assuming that the Coulomb law is applicable at small distances ($<10^{-10}$ m):

$$\frac{1}{2}m_\alpha v_0^2 = \frac{1}{2}m_\alpha v^2 + \frac{Ze \times 2e}{q} \quad (5.30)$$

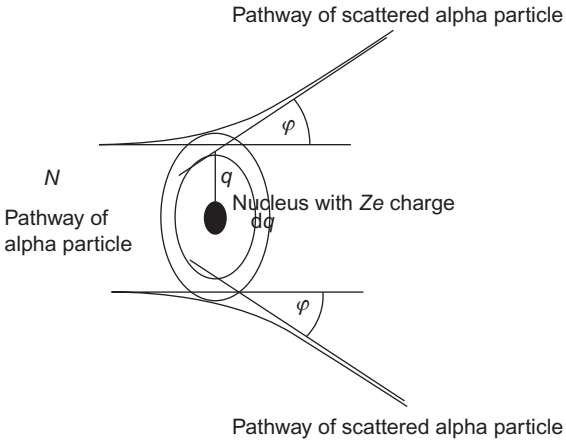


Figure 5.9 The scattering of an alpha beam with N flux on a nucleus with a Ze charge.

where m_α is the mass of the alpha particle, v_0 and v are the velocity of the alpha particle before and after the scattering, Ze is the charge of the nucleus, $2e$ is the charge of the alpha particle, and q is the distance of the nucleus from the original pathway of the alpha particle or, in other words, the collision parameter (Figure 5.8).

The angle of the deflection of the alpha particle is φ . As seen in Figure 5.8, the momentum of the original alpha particles and the change of momentum as a result of scattering can be expressed as:

$$\operatorname{tg} \varphi = \frac{\Delta p}{p} = \frac{F \Delta t}{p} = \frac{2Ze^2}{q^2} \frac{2q}{v_0} \frac{1}{p} = \frac{4Ze^2}{qv_0 p} \quad (5.31)$$

$\Delta p = F \Delta t$ has been discussed already in Eqs. (5.5) and (5.6) in Section 5.2.1. At small deflections (around 0 and π), $\operatorname{tg} \varphi \approx \operatorname{tg} \varphi/2$. From here:

$$\operatorname{tg} \frac{\varphi}{2} = \frac{4Ze^2}{qv_0 p} \quad (5.32)$$

When the flux of the irradiation alpha beam is N , the number of alpha particles deflected by one scattering atom is (Figure 5.9):

$$dN = 2\pi q dq N \quad (5.33)$$

The ratio of $dN/N = 2\pi q dq$ is called the “differential scattering cross section.” Assuming that the thickness of the scattering layer d , the number of the atoms in a unit volume n , and each alpha particle are scattered by only one nucleus:

$$dN_\varphi = nd2\pi q dq N \quad (5.34)$$

The ratio $dN_\varphi/N = nd2\pi q dq N$ is the macroscopic scattering cross section. By expressing q and dq by the angle φ and substituting into Eq. (5.34), after equivalent mathematical transformation, we obtain:

$$N_\varphi = \frac{NndZ^2e^4}{m_\alpha^2v_0^4} \frac{1}{\sin^4\frac{\varphi}{2}} \quad (5.35)$$

As seen in Eq. (5.35), the ratio of N_φ to N at a constant angle φ depends on the atomic number and the number of particles in a unit volume.

In addition to the number of deflected alpha particles at a given angle, the energy of the deflected alpha particles depends on the quality of the deflecting atoms:

$$E_\varphi = E_\alpha \left(\frac{\frac{4}{A} \cos \varphi + \sqrt{1 - \left(\frac{4}{A}\right)^2 \sin^2 \varphi}}{1 + \frac{4}{A}} \right)^2 \quad (5.36)$$

where E_φ and E_α are the energy of the deflected and the original alpha particles and A is the mass number.

One of the main results of the alpha backscattering studies was the experimental determination of the charge of the nuclei, which provides a confirmation about the position of the elements in the periodic table; that is, the atomic number is the number of positive charges. First, Rutherford determined the atomic number of gold, and later Chadwick measured the atomic number of copper, silver, and platinum in 1920.

The atomic number of hydrogen is 1, and its nucleus contains one positive charge, meaning that the nucleus of hydrogen is a proton. The determination of the charges in the nucleus of helium (which is 2) was also significant: the nuclei of helium are alpha particles.

The other important observation was that the alpha particles can get as close as 10^{-14} m to the center of the scattering atom; at this distance, only the Coulomb repulsion acts between the alpha particles and the center of the atoms. By substituting the momentum of the alpha particle, $p = m_\alpha \times v_0$, into Eq. (5.32), we obtain $\operatorname{tg}\frac{\varphi}{2} = \frac{4Ze^2}{qm_\alpha v_0^2}$.

From this expression, the distance of the closest approach (q) for the alpha particles at a given angle for the different elements can be determined. This value indicates the upper limit of the radius of the nuclei. Similar data for other elements are summarized in Table 5.3.

As seen in Table 5.3, the alpha scattering experiments show that the radius of the nuclei can be about 10^4 times smaller than the radius of the atoms ($\approx 10^{-10}$ m). The radius of the proton is about 1.3×10^{-15} m. Therefore, the alpha backscattering studies proved Rutherford's assumption that almost the entire positive charge and mass is concentrated on the small space of the atom, that is in the nucleus. The residual volume of the atoms is filled with electrons. Since electrons were found to be

Table 5.3 Radii of Several Nuclei on the Basis of the Alpha Backscattering Expression (Eq. 5.32)

| Atom | ²³⁸ U | ¹⁹⁷ Au | ¹⁰⁷ Ag | ⁶³ Cu | ¹⁹⁵ Pt |
|----------------------|------------------|-------------------|-------------------|------------------|-------------------|
| $r \times 10^{14}$ m | 4.0 | 3.1 | 2.0 | 1.2 | 3.0 |

even smaller than nucleons, this means that the atom consists of mostly empty space. This model of the atoms is the Rutherford model or planetary model, which became as the quantitative starting point for the term “chemical elements” in the twentieth century.

The alpha backscattering studies have analytical importance too. Equations (5.35) and (5.36) show that the number and energy of the scattered alpha particles at a given angle depend on the atomic (Z) number, mass number (A), and quantity of elements (n). This means that the deflection of the alpha particles can be applied to qualitative and quantitative analysis of surface layers. The thickness of the layer depends on the range of the alpha particles. The alpha backscattering spectra of an oxide layer produced on SiC are shown in Figure 5.10.

5.3 Interaction of Beta Radiation with Matter

The transformation of the nuclei and the electron orbitals may result in electron emission. As discussed in Section 4.4.2, the negative or positive particles (namely, electrons or positrons following the transformation of the nuclei) are called negative or positive beta radiation, respectively, and they have continuous spectra. The transformation of the atomic orbital can also produce electrons, as discussed in Section 4.4.3. These electrons, such as Auger and conversion electrons, have discrete energy. In addition, electromagnetic radiation can produce photo, Compton, and pair electrons, as discussed in Section 5.4.

The rest mass of the beta particle is 0.51 MeV, which is much less than the rest mass of the alpha particle. Therefore, at the same energy of the radiation, the velocity of the beta particle is much higher than that of the alpha particle. Because of the high velocity, the relative increase in the mass often has to be taken into account.

When beta radiation interacts with matter, the electrons in the matter may get excited or ionized, and the direction of the pathway of the beta particle may change as a result of elastic and inelastic collisions. In addition, the kinetic energy is partly or totally transmitted to the matter. When the beta particles interact with the nuclear field, *Bremsstrahlung* is emitted, which has a continuous spectrum. The inner *Bremsstrahlung* has been discussed in Section 4.4.3.

The beta particles can be scattered and absorbed, eventually losing all their energy (Table 5.4).

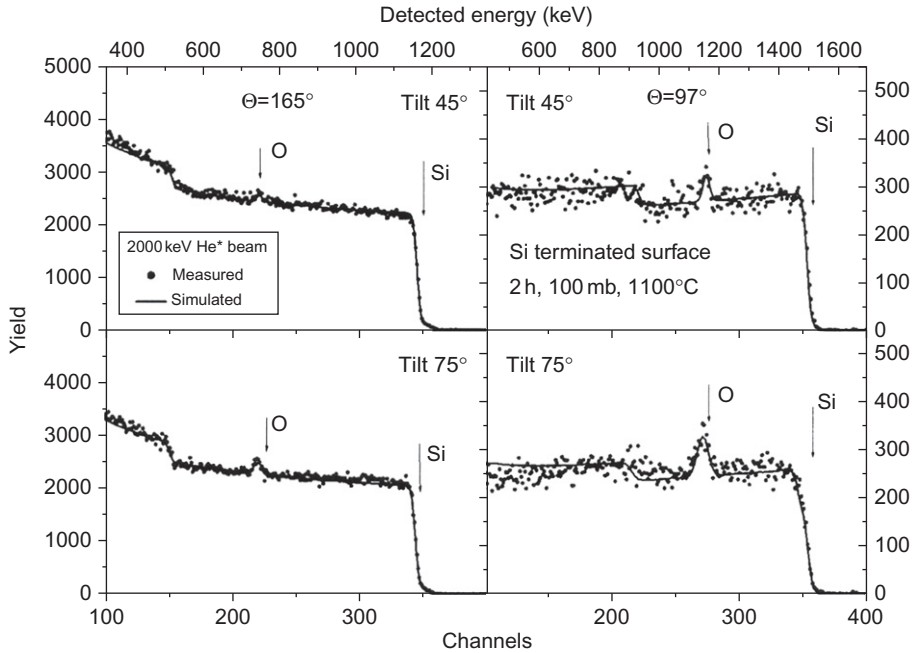


Figure 5.10 Measured and simulated RBS spectra taken on oxidized SiC at scattering angles of 165° and 97° . Each sample was measured at least at two different tilt angles. For the composition, Si:O ratio of 1:2 was determined for each sample. The arrows represent the surface positions of the elements. (Thanks to Dr. E. Szilágyi, KFKI Research Institute for Particle and Nuclear Physics, Budapest, Hungary, for the spectra.)

Source: Reprinted from Szilagy et al. (2008), with permission of the American Institute of Physics.

Table 5.4 Interaction of Beta Particles with Matter

| Reacting Particles and Fields | Changes | |
|-------------------------------|--|---|
| | In Radiation | In Matter |
| Orbital electron | <i>Bremsstrahlung</i> , scattering, absorption | Excitation, ionization, chemical change |
| Nuclear field | <i>Bremsstrahlung</i> , scattering, absorption | |
| Nucleus | No interaction | |

Source: Adapted from Kiss and Vértes (1979), with permission from Akadémiai Kiadó.

5.3.1 Interaction of Beta Particles with Orbital Electrons and the Nuclear Field

The transmitted energy of the beta particles to orbital electrons depends on the energy of the beta particle. The expressions describing the transmitted energy are different whether the velocity of the beta particle is below or above the velocity of light in a vacuum.

At $E_\beta < m_e c^2$ (E_β is the energy of the beta particle), the energy used up for ionization is:

$$-\left(\frac{dE}{dx}\right)_{\text{ion}} = \frac{4\pi e^4 n}{m_e v_\beta^2} Z' \ln \frac{1.66 m_e v_\beta^2}{2I} \quad (5.37)$$

Equation (5.37) is similar to Eq. (5.26), indicating that the ionization is similar for both alpha and beta particles. The numerical factors signify the differences in the size of the alpha and beta particles.

At $E_\beta > m_e c^2$, the energy used up for ionization is:

$$-\left(\frac{dE}{dx}\right)_{\text{ion}} = \frac{2\pi e^4 n}{m_e c^2} Z \ln \left(\frac{E^3}{2m_e c^2 I^2} + \frac{1}{8} \right) \quad (5.38)$$

Equation (5.38) takes into consideration the relative mass increase because of the high energy of the beta particle.

The decrease of the energy of the beta particles as a result of ionization is shown in Figure 5.11.

Some of the beta particles interact with the nuclear field, producing *Bremsstrahlung*. As discussed previously, *Bremsstrahlung* is a continuous X-ray. The energy of beta particles producing *Bremsstrahlung* can be expressed as:

$$-\left(\frac{dE}{dx}\right)_{\text{X-ray}} = \frac{4Z^2 e^2 n}{137 m_e^2 c^4} (E + m_e c^2) \left[\ln \frac{2(E + m_e c^2)}{m_e c^2} - \frac{1}{3} \right] \quad (5.39)$$

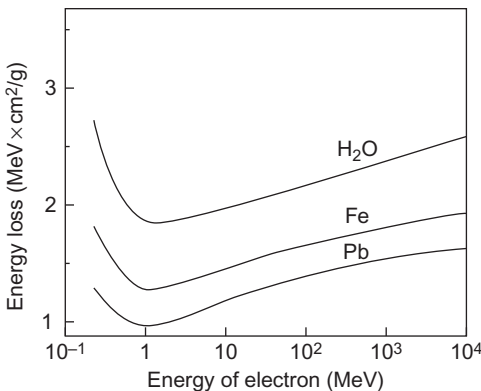


Figure 5.11 Specific energy loss of beta particles versus energy for different absorbers.

Source: Adapted from Kiss and Vértés (1979), with permission from Akadémiai Kiadó.

The total energy loss of the beta particle is the sum of the energies transmitted to orbital electrons (ionization) and producing *Bremsstrahlung* (X-rays):

$$\left(\frac{dE}{dx}\right)_{\text{tot}} = \left(\frac{dE}{dx}\right)_{\text{ion}} + \left(\frac{dE}{dx}\right)_{\text{X-ray}} \quad (5.40)$$

The ratio of the energies producing X-rays and ionization is expressed as follows:

$$\frac{\left(\frac{dE}{dx}\right)_{\text{X-ray}}}{\left(\frac{dE}{dx}\right)_{\text{ion}}} \approx \frac{EZ}{800} \quad (5.41)$$

where E is the energy of the beta particle, and Z is the atomic number of the absorber.

5.3.2 Cherenkov Radiation

Cherenkov radiation (also spelled Cerenkov or Čerenkov) is an electromagnetic radiation emitted when a beta particle passes through a dielectric medium at a speed greater than the velocity of light in that medium. It was discovered by Cherenkov in 1934, when he studied the radiation of radium salts in an aqueous solution. The experience was interpreted by I.M. Frank and I.E. Tamm. The gamma radiation of radium produces many secondary electrons with high energy (e.g., Compton electrons, discussed in [Section 5.4.3](#)), which pass through the medium (water) polarizing the molecules and arranging the dipoles. After passing the beta particle, the molecules rapidly revert to their ground state, emitting electromagnetic radiation. When the velocity of the beta particle (v) is greater than the velocity of light in the given medium ($v > cn$, where c is the velocity of light in vacuum, n is the refractive index of the medium), there is an angle (θ) where the waves of the electromagnetic radiation emitted at 0 and dt times interfere ([Figure 5.12](#)).

The angle of the interference is:

$$\cos \Theta = \frac{c}{nv} \quad (5.42)$$

For example, with water ($n = 1.337$):

$$\frac{c}{n} = \frac{3 \times 10^8}{1.337} \text{ m/s} \approx 2.2 \times 10^8 \text{ m/s} \quad (5.43)$$

This velocity is equal to 0.26 MeV. Therefore, to have Cherenkov radiation, the beta particles must have at least 0.26 MeV. In practice, however, to be observed easily, beta energies must be above ~ 0.5 MeV.

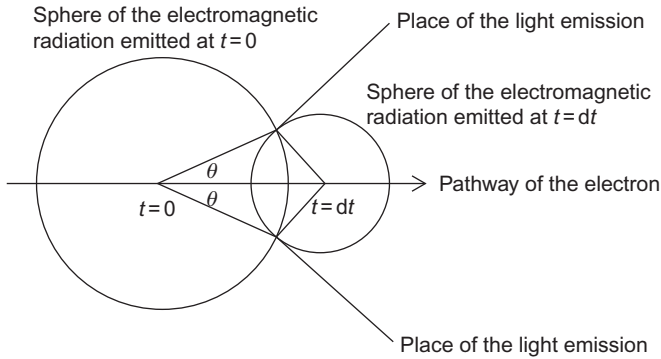


Figure 5.12 Formation of Cherenkov radiation.

The relation of the intensity ($I(\nu)$) and the frequency (f) of the Cherenkov radiation can be expressed as:

$$I(\nu) = \frac{2\pi e^2}{c^2} v \left[1 - \frac{c^2}{n^2 v^2} \right] f \quad (5.44)$$

The maximal intensity is:

$$I_{\max} = \frac{2\pi e^2}{c^2} \left[1 - \frac{1}{n^2} \right] f \quad (5.45)$$

This means that the intensity is proportional to the frequency; therefore, the Cherenkov radiation is blue.

This interaction of the beta radiation can be applied to the direct measurement of the beta radiation by light detectors, for example, by photo multipliers. Cherenkov light can be observed in the nuclear reactors.

5.3.3 Annihilation of Positrons

During β^+ -decay, positrons are emitted. The positron is the antiparticle of the electron, and therefore it is unstable. Its half time is the time of thermalization, which means that the time required for the velocity of the positron decreases to zero. It is about 10^{-10} s. If the positron encounters an electron in this interval, the two particles (electron and positron) transform to electromagnetic radiation, gamma photons. The process is called "annihilation." The rest mass of the positron (β^+ -particle) is 0.51 MeV, equal to the rest mass of the electron, so 2×0.51 MeV energy is emitted in the annihilation process. Usually, two gamma photons with 0.51 MeV energies are emitted at an angle of 180° . The probability of the formation of two photons is about 90%. (This process is applied in the PET (Section 12.6)). In about 10% of the annihilation process, only one photon with 1.02 MeV is formed.

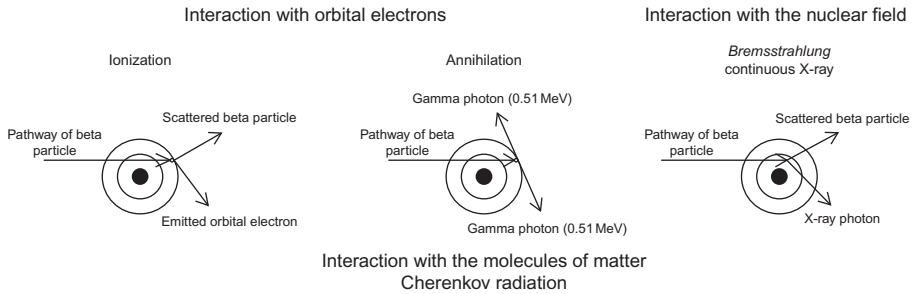


Figure 5.13 Summary of interaction of beta particles with matter.

In some cases, three photons are emitted, and the total energy of them is also 1.02 MeV. The positive beta decay can be detected easily through the detection of the gamma photons with 0.51 MeV.

It is interesting to mention here that before the total thermalization, the positron can interact with an electron, constructing a short-life light element, positronium, whose nucleus is the positron. Positronium can be treated as an atom with an atomic number of zero.

Positronium has two forms: *ortho*- and *para*-positronium, depending on the spins of the positron and electron. In *ortho*-positronium, the spins are parallel; the lifetime in a vacuum is 1.4×10^{-7} s. In *para*-positronium, the spins are antiparallel; the lifetime in a vacuum is 1.25×10^{-10} s. In other media, the chemical reactions (addition, substitution, oxidation, and reduction) decrease the lifetime; thus, the kinetics of chemical reactions can be studied by measuring the lifetime of positronium.

5.3.4 Absorption of Beta Radiation

As a result of the interactions of matter, beta particles can totally lose their energy and absorb into matter. This process is called “real absorption of the beta radiation.” However, during the transmission of beta particles through any substance, the intensity (I) of the beta radiation can also decrease as a result of other processes (e.g., by scattering). These processes have been discussed previously and summarized in Figure 5.13. Usually, all decreases in intensity are treated as absorption, regardless of the underlying cause of the decreases.

Quantitatively, the absorption of beta radiation can only be described with difficulty due to the continuous nature of the beta spectra. This means that the energy of beta particles when entering matter can range from zero to the maximum energy of the beta spectrum. Therefore, the expressions describing the beta absorption are usually empirical. It is interesting, however, that the empirical equation of beta absorption (Eq. (5.46)) is similar to the general equation of the absorption of radiation (Eq. (5.3)):

$$I = I_0 e^{-\mu(E)l} \quad (5.46)$$

where I_0 and I are the intensities of the beta radiation before and after the transmission through the matter, l is the thickness of the absorber, and $\mu(E)$ is the linear absorption coefficient; its dimension is reciprocal length (e.g., mm^{-1} , cm^{-1} , m^{-1}). The value of the linear absorption coefficient depends on both the energy of the radiation and the atomic number and density of the absorber. By introducing the mass absorption coefficient, it can be avoided to determine the linear absorption coefficient for all maximal beta energies and for all substances. For this purpose, the linear absorption coefficient in the exponent of Eq. (5.46) is divided and multiplied by the density of the absorber (ρ). Note that the density is the ratio of the mass and volume ($\rho = m/V = m/(l \times S)$):

$$I = I_0 e^{-\frac{\mu(E)}{\rho} \frac{m}{l \times S}} \quad (5.47)$$

where m and S are the mass and the surface area of the absorber, respectively. $\frac{\mu(E)}{\rho} = \mu$ is the mass absorption coefficient, and its dimension is surface area/mass. Since $l/l = 1$, the mass/surface area (m/S) remains in the exponent of Eq. (5.47). This quantity describes the mass of the absorber on a unit surface area; it is called "surface density" (d); its dimension is mass/surface area (e.g., mg/cm^2). This leads to:

$$I = I_0 e^{-\mu d} \quad (5.48)$$

The relation of the mass absorption coefficient and the maximum beta energy ($E_{\beta\text{max}}$) and the atomic number of the absorber (Z) can be approximated by empirical equations. When $Z < 13$:

$$\mu = \frac{35Z}{M_a E_{\beta\text{max}}^{1.14}} \quad (5.49)$$

When $Z > 13$:

$$\mu = \frac{7.7Z^{0.31}}{E_{\beta\text{max}}^{1.14}} \quad (5.50)$$

In Eq. (5.47), M_a is the relative atomic mass of the absorber. For compounds and mixtures, the mass absorption coefficient can be calculated by the mass absorption coefficients of the components, taking into consideration their mass ratio (w):

$$\mu = \sum_{i=1}^n w_i \mu_i \quad (5.51)$$

As seen in Eq. (5.48), the absorption of continuous beta radiation can be described by an exponential equation. However, the monoenergetic (> 0.2 MeV)

electron radiations (e.g., conversion electrons) show the linear absorption curve as a function of surface density. Below 0.2 MeV, the absorption curve of the monoenergetic electron deviates more or less from linearity.

To characterize the absorption of the beta radiation (exponential law, Eq. (5.48)), the half-thickness of the absorber ($d_{1/2}$) is defined. This is the thickness where the intensity of the beta radiation decreases by half:

$$d_{1/2} = \frac{\ln 2}{\mu} \quad (5.52)$$

As seen in Section 5.2.1, alpha radiation has a well-defined range (R). However, the range of beta radiation can be described only by empirical formulas at different maximal beta energies, such as:

$$R = \frac{1}{1.500} E_{\max}^{\frac{5}{3}}, \quad E_{\max} < 0.2 \text{ MeV} \quad (5.53)$$

$$R = 0.15 E_{\max} - 0.0028, \quad 0.03 < E_{\max} < 0.15 \text{ MeV} \quad (5.54)$$

$$R = 0.407 E_{\max}^{1.38}, \quad 0.15 < E_{\max} < 0.8 \text{ MeV} \quad (5.55)$$

$$R = 0.524 E_{\max} - 0.133, \quad E_{\max} > 0.8 \text{ MeV} \quad (5.56)$$

$$R = 0.571 E_{\max} - 0.161, \quad E_{\max} > 1 \text{ MeV} \quad (5.57)$$

In Eqs. (5.53)–(5.57), the dimensions of range and energy are g/cm^2 and MeV, respectively.

Cloud chamber photographs show the differences in the pathways of the beta and alpha particles (Figure 5.7 shows the alpha track, and Figure 5.14 shows the alpha and beta tracks). Since alpha particles are much heavier than beta particles/electrons, the pathway of alpha particles is linear. Beta particles, however, tend to deviate more or less, depending on their energy. The interaction of gamma radiation with matter will be discussed later (in Section 5.4); for now, just note that gamma radiation produces secondary electrons, the tracks of which will be shown in the later discussion.

In the presence of two or more beta emitters, Eq. (5.48) consists of several members:

$$I = I_{10} e^{-\mu_1 d} + I_{20} e^{-\mu_2 d} + \dots + I_{n0} e^{-\mu_n d} \quad (5.58)$$

This means that the absorption of each beta radiation has to be taken into account separately. The mass absorption coefficients and the range of some beta emitters as a function of maximal beta energy are plotted in Figure 5.15. These data are widely applied in the characterization of beta absorption and the planning of shielding against radiation. However, Eqs. (5.49) and (5.50) show that the mass

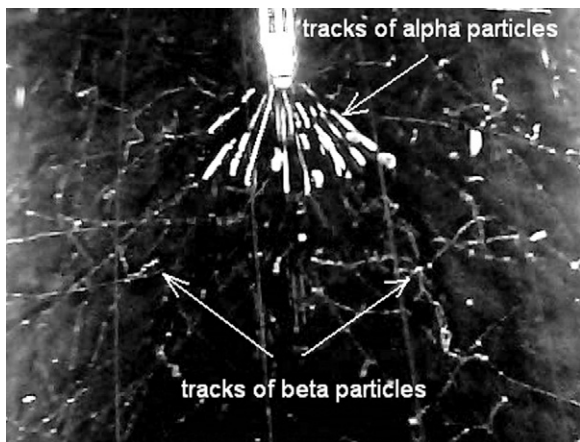


Figure 5.14 Cloud chamber photograph of the pathway of alpha and beta particles. (Thanks to Dr. Péter Raics, Department of Experimental Physics, University of Debrecen, Hungary, for the photograph.)

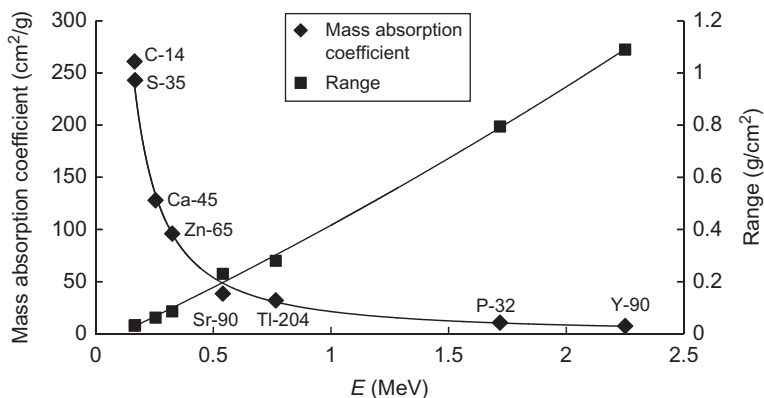


Figure 5.15 The mass absorption coefficients and ranges versus maximal beta energy.

absorption coefficients depend on the atomic number. Therefore, at $Z > 13$, the mass absorption coefficients calculated on the basis of Eq. (5.50) are about twice as high as the data in Figure 5.15. It should be noted, however, that the plan of shielding uses the principle of the so-called conservative estimation, which means that the plans consider the worst scenario. Therefore, the application of the lower mass absorption coefficient is permitted or even can be desirable.

5.3.5 Self-Absorption of Beta Radiation

In a sample containing the beta emitter, the beta particles can also be absorbed by the sample itself in a process called “self-absorption.” The precise and accurate measurement of the samples containing beta emitters requires taking into consideration the effect of self-absorption, except when the sample is “infinitely thin.” In every other case, the radioactive intensities measured for the same radioactivity

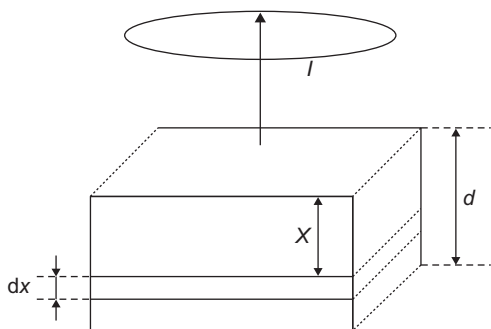


Figure 5.16 Study of self-absorption of beta radiation.

depend on the thickness of the sample, the quantity of the carrier (an excess of inactive atoms of the same elements in the same chemical state), or an inactive matrix (every other substance). In some cases, the molecule itself containing the radioactive isotope can absorb a part of the beta radiation. In solutions, the solvent can absorb the radiation to such a high degree that it becomes impossible to measure the activity. For this reason, beta emitters are usually measured in the solid phase. (It is important to note here that there is a special technique for the measurement of beta emitters, namely, the liquid scintillation technique, which utilizes this absorption. It will be discussed in Section 14.2.1.)

When the beta energy is low (so-called weak beta, e.g., ^{14}C , ^{35}S), the self-absorption is significant at thin layers. However, it cannot be ignored at high beta energies, either, especially when the sample is thick because of the presence of the inactive matrix. Depending on the quantity of inactive matrix, the measured intensity of the same radioactive substance can differ.

The effect of self-absorption can be corrected in two ways: the method of constant activities for high beta energies, and the method of constant specific activities for low beta energies. In the method of constant activities, the intensity is extrapolated for the infinitely thin layer, while in the method of constant specific activities, the intensity is measured at the so-called saturated thickness ($>10 \times d_{1/2}$). The two methods of the correction of self-absorption are discussed as follows.

In the method of constant activities, the total radioactivity of the sample is constant and the quantity of the matrix changes. The samples are arranged as shown in Figure 5.16.

The thickness of the sample is d (g cm^{-2}), and the total intensity of the radiation (the intensity without matrix) is I_0 . From here, the intensity of the radiation in a unit thickness is I_0/d . Consider a dx elementary thickness at a distance x from the upper surface of the sample; the intensity in this elementary thickness is $I_0 dx/d$. Passing through the distance x , the radiation is absorbed and the intensity decreases. The intensity reaching the upper surface (dI) is expressed by the radiation absorption law (Eq. (5.48)):

$$dI = \frac{I_0}{d} \exp(-\mu x) dx \quad (5.59)$$

where μ is the mass absorption coefficient.

By integrating Eq. (5.59) for the total thickness of the sample (d), we obtain the total intensity reaching the surface:

$$I = \frac{I_0}{\mu d} [1 - \exp(-\mu d)] \quad (5.60)$$

If the intensities of samples with constant radioactivity in different quantities of matrix are measured, the intensity decreases as the quantity of the matrix, i.e., the thickness of the samples increases. The I_0 can be obtained by extrapolating to zero thickness. It can be done graphically or by a parameter-estimating computer program from the I versus d function. The measurements can be done up to 1–2 half-thickness (Figure 5.17).

For thin layers (up to the 30% of the half-thickness), I_0 can be determined by the series expansion of Eq. (5.60):

$$I = I_0 \left(1 - \frac{1}{2} \mu d \right) \quad (5.61)$$

In the method of constant specific activities, the characteristic properties of self-absorption (mass absorption coefficient and half-thickness) can be determined as follows. Samples with different thickness are produced from a substance having the same specific activity. In this case, the intensity of a unit thickness is defined as I_0 (its dimension is intensity/surface density). The intensity reaching the surface decreases because of the absorption as described by the radiation absorption law (Eq. (5.48)): $I_0 \exp(-\mu d)$. The total intensity reaching the surface is:

$$I = \int_0^d I_0 \exp(-\mu x) dx = \frac{I_0}{\mu} [1 - \exp(-\mu d)] \quad (5.62)$$

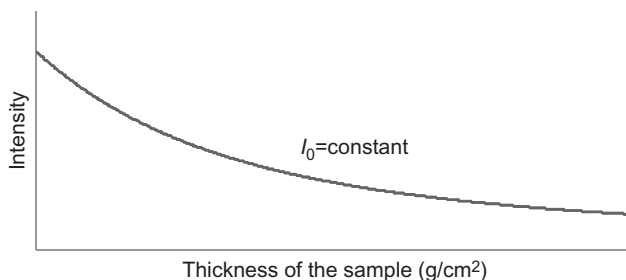


Figure 5.17 Intensity as a function of the thickness of a sample in cases of constant total activity.

Since

$$\frac{I_0}{\mu} = \text{constant} = I_\infty \quad (5.63)$$

from Eq. (5.62), we obtain the following:

$$I = I_\infty [1 - \exp(-\mu d)] \quad (5.64)$$

where I_∞ is the intensity at the saturation thickness. This is the maximal intensity, which does not increase even if the thickness increases. The intensity as a function of the thickness is shown in Figure 5.18.

In the method of constant specific activities, the half-thickness can be defined ($d_{1/2}$) as:

$$d_{1/2} = \frac{\ln 2}{\mu} \quad (5.65)$$

The half-thickness can be determined from Eq. (5.64) graphically or by a parameter-estimating computer program.

The method of constant specific activities can be used if the thickness is at least 7–10 times greater than the half-thickness. In this case, the specific intensities of the samples can be compared since they are proportional to the radioactivity.

5.3.6 Backscattering of Beta Radiation

The beta particles may scatter both on the orbital electrons and in the nuclear field. Since the beta particles are much lighter than the alpha particles, the degree of the scattering of the beta particles is much higher than that of the alpha particles, resulting in very important measuring and analytical consequences.

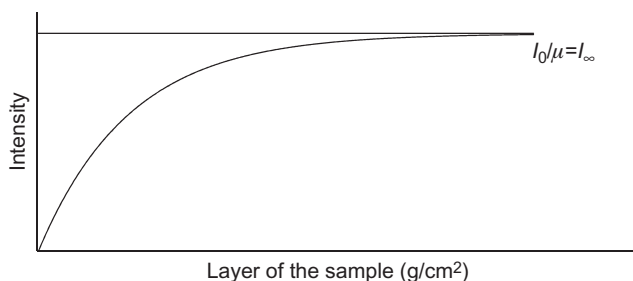


Figure 5.18 Intensity as a function of thickness in the method of constant specific activities.

The backscattering of the beta radiation as a function of the thickness of the scattering medium can be described as follows. Let us take a beta emitter on the bottom of a ring of lead-shielding, and a scattering medium with d thickness and arrange them as illustrated in Figure 5.19.

Then let us irradiate the surface area (F) of the medium with a beta radiation with I_0 intensity. Because of the absorption of the beta radiation, the intensity decreases when passed through a distance x , and the intensity reaching the dx unit thickness is:

$$dI_x = I_0 e^{-\mu x} \quad (5.66)$$

Let ν be the ratio of beta particles that are backscattered from the dx thickness:

$$\nu dI_x dx = \nu I_0 e^{-\mu x} dx \quad (5.67)$$

The backscattered beta particles are absorbed again when returned through the x thickness. Therefore, the intensity of the backscattered beta particles reaching the surface (F) can be expressed again by the absorption law. The energy of the backscattered beta particles may be lower than the energy of the original beta particles, so the values of the mass absorption coefficients may be different when the beta particles pass in (μ_{in}) or out (μ_{out}). In backscattering studies, the resultant effect of the two mass absorption coefficients is observed, so we can assume that $\mu_{in} + \mu_{out} = \mu_b$:

$$dI = \nu I_0 e^{-(\mu_{in} + \mu_{out})x} dx = \nu I_0 e^{-\mu_b x} dx \quad (5.68)$$

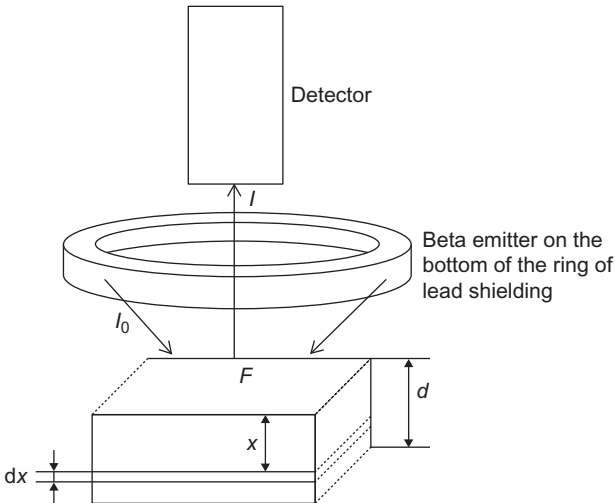


Figure 5.19 Study of backscattering of beta radiation.

The total backscattered intensity can be obtained by the integration of Eq. (5.68) for the total thickness (d):

$$I = \int_0^d dI = \frac{\nu}{\mu_b} I_0 [1 - e^{-\mu_b d}] \quad (5.69)$$

As seen from Eq. (5.69), the backscattered intensity tends to a limit as a function of the thickness. This limit for the infinite thickness of the sample is:

$$I_\infty = I_0 \frac{\nu}{\mu_b} \quad (5.70)$$

The backscattering of beta radiation can be characterized by the backscattering coefficient (Rf):

$$Rf = \frac{I_\infty}{I_0} \quad (5.71)$$

Rf can also be expressed in percent.

The energy of the backscattered beta particles is less than the energy of the original particles (Figure 5.20).

Similar to Eq. (5.65), the half-thickness of the backscattered beta radiation can be defined. The backscattered intensity of beta radiation of aluminum, zinc, and lead is shown in Figure 5.21 as a function of the half-thickness. As seen, the backscattered intensity depends on the atomic number of the scattering media.

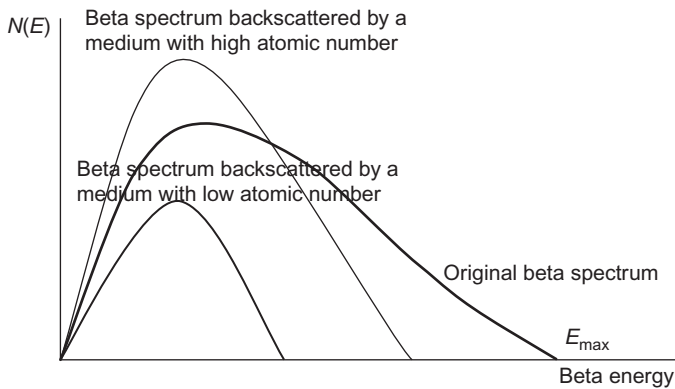


Figure 5.20 The energy of the backscattered beta particles for different scattering media.

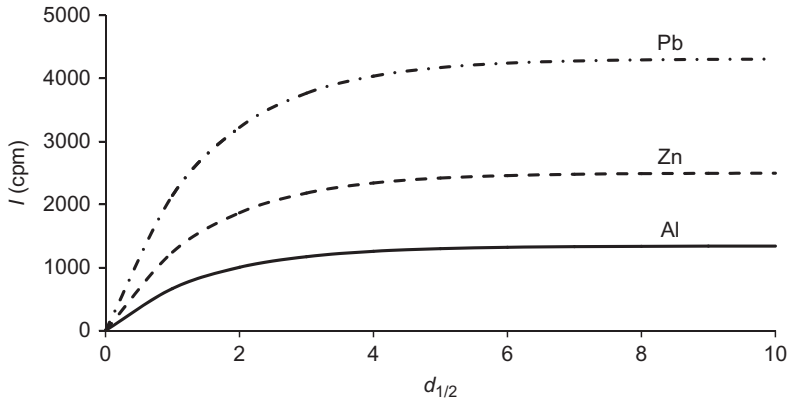


Figure 5.21 Backscattered intensity of beta radiation of aluminum, copper, and lead as a function of half-thickness.

Table 5.5 Constants of the Müller Formula for Backscattering of Beta Radiation

| Period | Z | a | b | R |
|--------|-------|---------|--------|-----------|
| II | 2–10 | 1.2311 | –2.157 | 0.3–10.2 |
| III | 10–18 | 0.96731 | 0.476 | 10.2–17.9 |
| IV | 18–36 | 0.68582 | 5.556 | 17.9–30.3 |
| V | 36–54 | 0.34988 | 17.664 | 30.3–36.6 |
| VI | 54–86 | 0.26225 | 22.396 | 36.6–45 |

Source: Adapted from Müller (1957), with permission from the American Chemical Society.

The values of Rf and the atomic number (Z) are in strict correlation. The backscattered intensity, or Rf versus Z function, cannot be calculated exactly; empirical correlations are usually applied. One of them is as follows:

$$I_{\infty\omega} = k_1 Z^{k_2} \quad (5.72)$$

where $I_{\infty\omega}$ is the scattered intensity at an angle, $k_1 = 0.0415 I_{\infty\omega}/2\pi$ and $k_2 = 2/3$.

Another Rf versus Z function is the so-called Müller formula:

$$R = aZ + b \quad (5.73)$$

where a and b are constants for the elements in a given period of the periodic table (Table 5.5). Hydrogen is a special element; it can be fitted into the system by a hypothetical atomic number, which is -7.434 . This can be explained by the fact that the ratio of nucleons to electrons is usually 2, while in the case of hydrogen, this ratio is only 1.

Equations (5.73) and (5.74) are also valid for compounds and mixtures if the mean atomic number is applied. The mean atomic number can be defined as:

$$\bar{Z} = \frac{\sum_{i=1}^n n_i A_i Z_i}{\sum_{i=1}^n n_i A_i} = \sum_{i=1}^n x_i Z_i \quad (5.74)$$

where Z_i is the atomic number of the constituents, n_i is the number of the atoms, A_i is the mass of the atoms, and x_i is the mass ratio of the i th atom in the compound or mixture.

Equations (5.73) and (5.74) can also be applied for solutions; the Rf versus x_i function is linear. Therefore, the Rf versus x_i function is suitable for the concentration measurement of solutions. In addition, by extrapolating the Rf versus x_i function to $x_i = 1$, the backscattering coefficient (Rf) of the pure solid substance is obtained.

In conclusion, the measurements of the backscattered intensities of beta radiation give information on:

1. The thickness of the scattering matter or the thickness of thin layers on a thick plate (Section 11.3.4).
2. The mean atomic number.
3. The concentration of solutions.

5.4 Interaction of Gamma Radiation with Matter

The gamma radiation (gamma photon) is very different from alpha and beta radiation. The most important difference is that it has no charge or mass. It forms during the transition of nucleons between the shells in the nuclei, and their energy is in a very broad range. As discussed previously, the gamma photons are always emitted from the nuclei, whereas the photons emitted by the inner electron orbitals are called "X-ray photons." However, both gamma and X-ray radiations are electromagnetic radiation, so their interactions with matter can be treated together.

The gamma and X-ray photons usually have intermediate interactions with matter. The interactions are summarized in Table 5.6 and Figure 5.22. The dominant type of the interaction is strongly affected by the energy of gamma photons. Depending on the energy, the gamma photos can interact with the orbital electrons, the nuclear field, and the nucleus. The cross section of the interactions (the absorption coefficient, in other words) also depends on the atomic number of the substance.

It is important to emphasize that one of the most important interactions is the scattering of the gamma photons. Depending on the energy, different scattering phenomena can be observed, namely, Rayleigh, Thompson, and Compton

Table 5.6 Interaction of gamma (X-ray) Radiation with Matter

| Reacting Particles and Fields | Absorption | Scattering | |
|-------------------------------|---|---|--|
| | | Elastic/Coherent | Inelastic/Incoherent |
| Orbital electron | Photoelectric effect $\sigma \sim Z^4$ | Rayleigh scattering $\sigma \sim Z^2$ Thomson scattering $\sigma \sim Z$ | Compton scattering $\sigma \sim Z$ |
| Nuclear field Nucleus | Pair formation $\sigma \sim Z^2$ Nuclear reaction with gamma photon (γ, n); (γ, p) $\sigma \sim Z$ Resonance absorption, Mössbauer effect | (γ, γ) nuclear reaction $\sigma \sim Z$ | (γ, γ') nuclear reaction |

Source: Adapted from Kiss and Vértes (1979), with permission from Akadémiai Kiadó.

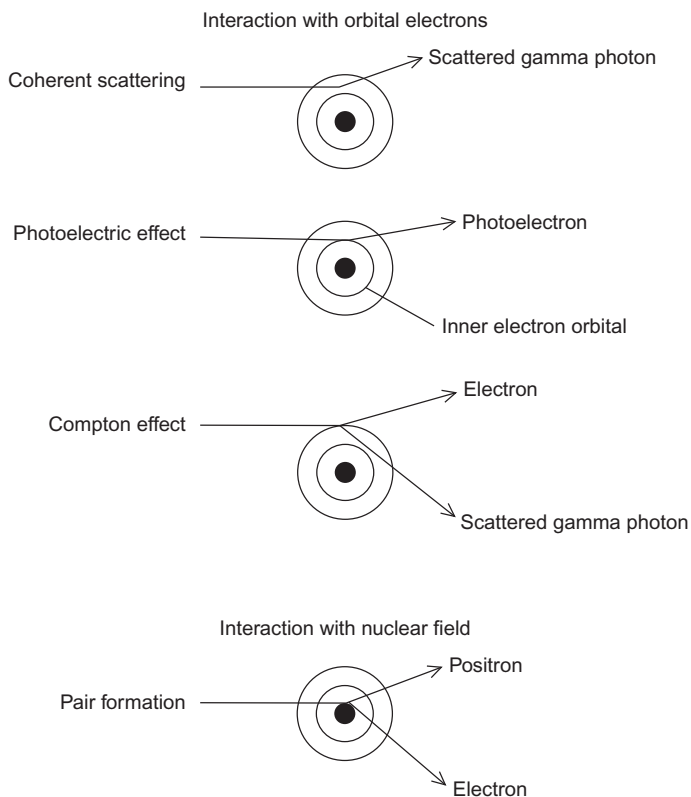


Figure 5.22 Interactions of gamma photons with the different constituents of matter.

Source: Reprinted from Choppin and Rydberg (1980), with permission from Elsevier.

scattering in the interaction with the orbital electrons, and the (γ, γ) and (γ, γ') nuclear reactions in the nuclei. In addition, gamma photons do not cause direct ionization; only the secondary electrons forming in the interactions of gamma radiation with matter can produce ions.

5.4.1 Rayleigh Scattering

At gamma energy below ~ 100 keV, the gamma photons are scattered on heavy elements (or their compounds) at small angles. The electromagnetic field of the gamma radiation polarizes the orbital electrons (i.e., induces dipoles), resulting in the emission of secondary radiation in the total space (in 4π spatial angle). The wavelength of the scattered radiation remains the same, i.e., the scattering is elastic or coherent.

5.4.2 Thomson Scattering

Thomson scattering can be observed in the case of both X-ray and gamma radiation. The wavelength of the scattered radiation does not change (elastic scattering). The phenomenon, similarly to Rayleigh scattering, has been interpreted by J.J. Thomson, using the classical theory of the scattering of electromagnetic radiation. The Rayleigh and Thomson scattering show differences in the cross section versus atomic number function (Table 5.6).

5.4.3 Compton Scattering

The classical theory of the scattering of electromagnetic radiation is valid only when $h\nu \ll mc^2$, i.e., at small energies. At higher energies, the wavelength of the scattered radiation changes: the frequency of gamma photons decreases, meaning that gamma energy is lost. This is called “inelastic” or “incoherent” scattering. This process was first studied by Compton.

The process is interpreted as follows. The gamma photons with $h\nu$ energy encounter an electron. By inelastic collision, part of their energy is transferred to the electron and the direction of the pathway of the gamma photon changes. The process can be described quantitatively by assuming a coordinate system, the x -axis of which is the direction of the pathway of the gamma photon; the y -axis is perpendicular to the x -axis. The electron is placed where the axes intersect, in the origin (Figure 5.23). The energy of the gamma photon before and after the collision with the electron is $h\nu$ or $h\nu'$. The energy of the electron before and after the collision is m_0c^2 and mc^2 , respectively. m_0 is the rest mass of the electron; m is the mass of the moving electron. Before the collision, the momentum of the gamma photon is $h\nu/c$ in the direction of the x -axis, and zero in the direction of the y -axis. The momentum of the electron before the collision is equal to zero in both directions of the coordinate system. After the collision, the electron gains momentum, which is $p_e \cos\varphi$ in the direction of the x -axis and $p_e \sin\varphi$ in the direction of the y -axis.

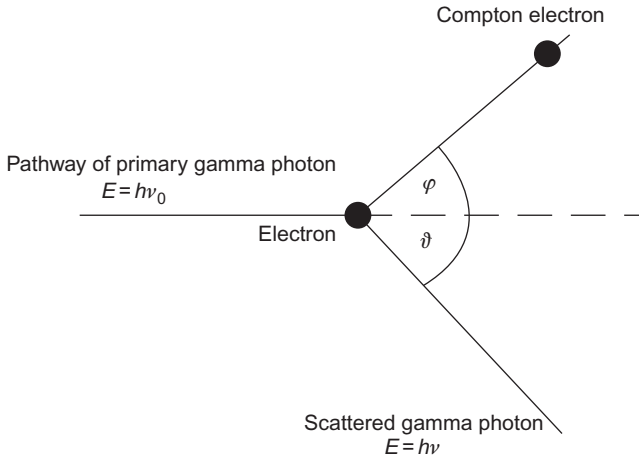


Figure 5.23 Compton scattering.

By applying the conservation of energies and momentums for the collision of the electron and the gamma photon, we can define the equations as follows:

$$h\nu_0 = h\nu + E_c \quad (5.75)$$

$$\frac{h\nu_0}{c} = \frac{h\nu}{c} \cos \vartheta + p_e \cos \varphi \quad (5.76)$$

$$0 = \frac{h\nu}{c} \sin \vartheta - p_e \sin \varphi \quad (5.77)$$

$$E_c = mc^2 - m_0c^2 \quad (5.78)$$

The relation between the rest mass of the electron and the mass of the moving electrons (m_0 and m) is:

$$m = \frac{m_0}{\sqrt{1 - \frac{v^2}{c^2}}} \quad (5.79)$$

where c is the velocity of light in a vacuum, and v is the velocity of the electron. By substituting Eq. (5.79) into Eq. (5.78), we obtain:

$$E_c = m_0c^2 \left(\frac{1}{\sqrt{1 - \frac{v^2}{c^2}}} - 1 \right) \quad (5.80)$$

The momentum of the electron (p_e) can be expressed as:

$$p_e = mv = \frac{m_0 v}{\sqrt{1 - \frac{v^2}{c^2}}} = \frac{m_0 c \frac{v}{c}}{\sqrt{1 - \frac{v^2}{c^2}}} \quad (5.81)$$

The momentum of the electron (p_e) can also be expressed from Eqs. (5.76) and (5.77):

$$p_e^2 = \left(\frac{h\nu_0}{c}\right)^2 + \left(\frac{h\nu}{c}\right)^2 - 2\left(\frac{h\nu_0}{c}\right)\left(\frac{h\nu}{c}\right)\cos\vartheta \quad (5.82)$$

In addition, p_e^2 can be obtained by means of Eqs. (5.78), (5.80), and (5.81), using $E = h\nu$. By equivalent mathematical transformation, we obtain the following:

$$\left(\frac{h\nu_0}{m_0 c^2}\right) + \left(\frac{h\nu}{m_0 c^2}\right) - 2\frac{h\nu_0 h\nu}{(m_0 c^2)^2} \cos\vartheta = \left(\frac{h\nu_0}{m_0 c^2} - \frac{h\nu}{m_0 c^2} + 1\right) - 1 \quad (5.83)$$

and

$$\nu_0 - \nu = \frac{h\nu_0 \nu}{m_0 c^2} (1 - \cos\vartheta) \quad (5.84)$$

By multiplying Eq. (5.84) by the Planck constant (h), we obtain the following:

$$h\nu_0 - h\nu = \frac{h\nu_0 h\nu}{m_0 c^2} (1 - \cos\vartheta) = E_0 - E = \frac{E_0 E}{0.51} (1 - \cos\vartheta) \quad (5.85)$$

In this equation, $m_0 c^2$ means the energy equivalent of the rest mass of the electron; i.e., 0.51 MeV.

The change of the energy of the primary gamma photon can be obtained using Eq. (5.85):

$$\Delta E = \frac{E_0^2 (1 - \cos\vartheta)}{E_0 (1 - \cos\vartheta) + 0.51} \quad (5.86)$$

As seen from Eq. (5.86), the energy of the photon as a result of Compton scattering depends on the energy of the primary photon ($h\nu_0$) and on the angle. The highest change of the gamma energy can be observed at 180° ; the energy does not change at 0° (no scattering). Compton scattering has an important effect on the gamma spectra (see Section 14.2.1 and Figure 14.5).

5.4.4 The Photoelectric Effect

The gamma photons can transfer energy to the orbital electrons. The electron is emitted as a photoelectron of a certain kinetic energy:

$$E_k = h\nu_0 - E_b \quad (5.87)$$

where E_k is the kinetic energy of the photoelectron, E_b is the binding energy of the electron, and $h\nu_0$ is the energy of the gamma photon before the interaction. Because of the great differences between the masses of the atom and the emitted electron, the energy of recoiling can be ignored in Eq. (5.87). The process is called the “photoelectric effect”; it can be observed when the energy of the gamma photon is similar to the binding energy of the electron. For this reason, high-energy gamma photons usually do not induce the photoelectric effect. The low-energy gamma photons have an energy that is closest to the binding energy of the K and L electrons, so the emission of photoelectrons from the K and L orbitals is the most likely.

The emission of the photoelectron results in the formation of an excited electron state because when one electron is missing from the inner shell of the atom, a vacancy is formed. This excited state can relax in two ways. One way is that an electron in outer orbitals moves into the inner orbital to fill the vacancy, emitting the excess energy between the orbitals as a characteristic X-ray photon. The wave number of the X-ray photon (ν^*) can be calculated by the Moseley law:

$$\nu^* = Ry(Z - 1)^2 \left(\frac{1}{n^2} - \frac{1}{m^2} \right) \quad (5.88)$$

where Ry is the Rydberg constant, Z is the atomic number, and n and m are the main quantum numbers of the electron orbitals. This process forms the basis of the X-ray fluorescence analysis.

The other way is the emission of low-energy Auger electrons (as discussed in Section 4.4.3). This process is called the Auger effect (Figure 5.24). For light elements, the emission of Auger electrons is the preferred result, while in the case of heavier elements, the emission of X-ray photons is more preferable. The two processes, the emission of X-ray photons and Auger electrons, continue until the atom reaches its ground-state energy. All the photoelectrons, Auger electrons, and X-ray photons intensively ionize the atoms of the absorber. This is a secondary ionization effect.

The cross section of the photoelectric effect (σ_f), or the absorption coefficient of the photoelectric effect (μ_f), can be given by a rude empirical formula:

$$\sigma_f = \text{constant} \frac{Z^{4.1}}{E_\gamma^3} \quad (5.89)$$

where E_γ is the energy of the gamma and X-ray photons. Equation (5.89) expresses the fact that the probability of the emission of photoelectrons increases as the atomic number increases and the energy of the gamma photons decreases.

The photoelectric effect produces photoelectrons, characteristic X-ray photons, and Auger electrons. The measurements of the energy and intensity of these radiations are used in different analytical techniques. The measurement of the photoelectrons gives information on the chemical environment of the atoms in a substance (high-resolution beta spectroscopy or photoelectron spectroscopy). The quality and

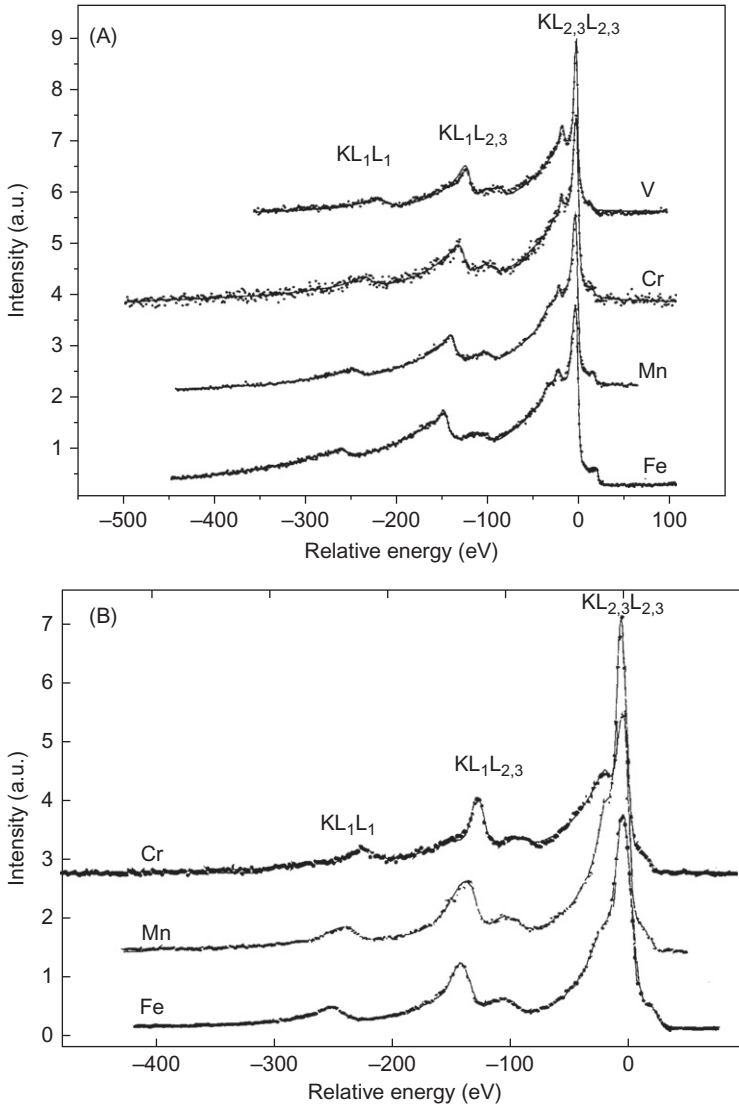


Figure 5.24 (A) Comparison of the measured photoexcited V, Cr, Mn, and Fe KLL Auger spectra. (B) Comparison of the Cr, Mn, and Fe KLL Auger spectra obtained following electron capture. The sign KLL means that the photoelectric effect produces the vacancy on the K shell, it is filled from the L shell, and the Auger electron also is emitted from the L shell. The indexes 1–3 mean the subshells of the L shell. (Thanks to Dr. László Kövér, Institute of Nuclear Research, Hungarian Academy of Sciences, Debrecen, Hungary, for the figure.)

Source: Reprinted from Némethy et al. (1996), with permission from Elsevier.

quantity of the elements of a substance can be determined by the measurement of the characteristic X-ray photons (X-ray fluorescence spectroscopy, as discussed in Section 10.2.3.1). Auger electron spectroscopy (AES) can be used for the analysis of surface layers.

5.4.5 Pair Formation

When the energy of the gamma photon ($h\nu$) is higher than the energy equivalent with the rest mass of two electrons ($2m_0c^2$), the gamma photon can transform into an electron and a positron when it passes the nuclear field. This process is called “pair formation,” the reverse process of annihilation (as discussed in Section 5.3.3). On the basis of the conservation of energy:

$$h\nu = m_0c^2 + E_{e^-} + m_0c^2 + E_{e^+} \quad (5.90)$$

where E_{e^-} and E_{e^+} are the kinetic energy of the electron and the positron, respectively.

The cross section of the pair formation can be described as:

$$\sigma_p = KZ^2f(E_\gamma) \quad (5.91)$$

where $f(E_\gamma)$ is a factor depending on the energy of the gamma radiation, Z is the atomic number of the interacting substance (absorber), and K is constant. As seen, the cross section of the pair formation increases as the gamma energy and the atomic number increase.

5.4.6 Total Absorption of Gamma Radiation

In the previous sections (Sections 5.4.1–5.4.5), the different interactions (namely, coherent and incoherent scattering), photoelectric effect, and pair formation of the gamma radiation have been discussed. As seen, the cross sections, or the absorption coefficients of all these interactions depends on the energy of gamma radiation and the atomic number of the absorber. The cross sections versus energy or atomic number functions are significantly different for the different processes. The total absorption of the gamma radiation is the sum of the different interactions, expressed by the cross sections:

$$\mu = \mu_{\text{Rayleigh}} + \mu_{\text{Thomson}} + \mu_{\text{photoelectric}} + \mu_{\text{Compton}} + \mu_{\text{pair}} \quad (5.92)$$

The absorption law (Eq. (5.3)) for the gamma radiation can be expressed as:

$$I = I_0 e^{-\mu x} \quad (5.93)$$

Equation (5.93) can be transformed to mass absorption coefficients, as is done in the case of beta radiation (see Section 5.3.4).

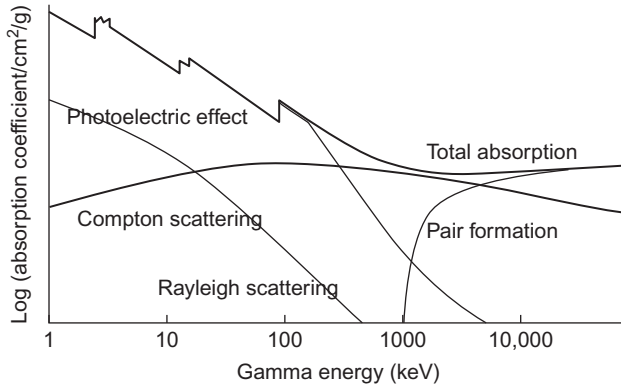


Figure 5.25 The scheme of the total absorption of gamma radiation as a function of gamma energy.

The scheme of the total absorption of gamma radiation as a function of the gamma energy is shown in [Figure 5.25](#).

As seen in [Figure 5.25](#), the mass absorption coefficients of the individual interactions show the range of gamma energy that is characteristic of the given interaction. The mass absorption coefficient of the total absorption (μ) as a function of gamma energy shows a minimum: the mass absorption coefficient decreases until the gamma energy exceeds 1.02 MeV; it is the start of the pair formation.

In [Figure 5.26](#), the mass absorption coefficient for different gamma energies as a function of the atomic number of the absorbers is shown.

5.4.7 Resonance Absorption of Nuclei and the Mössbauer Effect

As discussed in Chapter 2, the nucleons can be in different energy states in the nucleus (see the explanation of the shell model in Section 2.2.2). Therefore, the nucleons may be in excited states as a result of different nuclear processes. The excitation energy can produce the emission of a nucleon or radiation. The emission of a nucleon takes place in the nuclear reactions (Chapter 6), for example, in the (γ, n) nuclear reactions. As discussed in Section 4.4.6, the nuclei of the daughter nuclides can be in an excited state due to a radioactive decay. The excited nucleus may return to a lower excited state or ground state, emitting gamma photons with a characteristic energy.

The gamma photons can excite another nucleus. The cross section of this excitation process may be high when the energy of the gamma photon and the excitation energy of the nucleons are very close, for example, when the structure of the emitting and absorbing nuclei is similar, such as in the case of isobars, isotopes, or isoton nuclei. This process is called “nuclear resonance absorption.”

At first sight, the resonance absorption seems to be simple. However, the recoil of the nuclei during the emission and absorption reduces the energy of the gamma

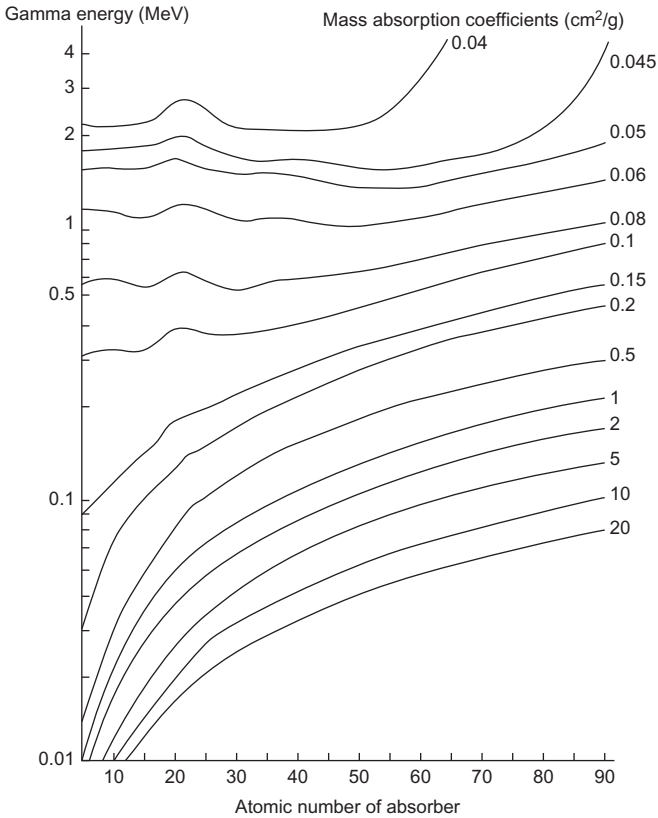


Figure 5.26 The mass absorption coefficient for different gamma energies as a function of the atomic number of the absorbers.

photons (E_0). The loss of energy (E_R) can be calculated using the principle of the conservation of momentum:

$$-Mv = \frac{E_0}{c} \quad (5.94)$$

where M is the mass of the nucleus, v is the velocity of the nucleus after the emission of the gamma photon, and c is the velocity of light in a vacuum. By expressing the velocity of the nucleus after the emission of gamma photon, we obtain:

$$v = -\frac{E_0}{Mc} \quad (5.95)$$

The kinetic energy of the recoiled nucleus can be given as:

$$E_R = \frac{1}{2}Mv^2 = \frac{E_0^2}{2Mc^2} \quad (5.96)$$

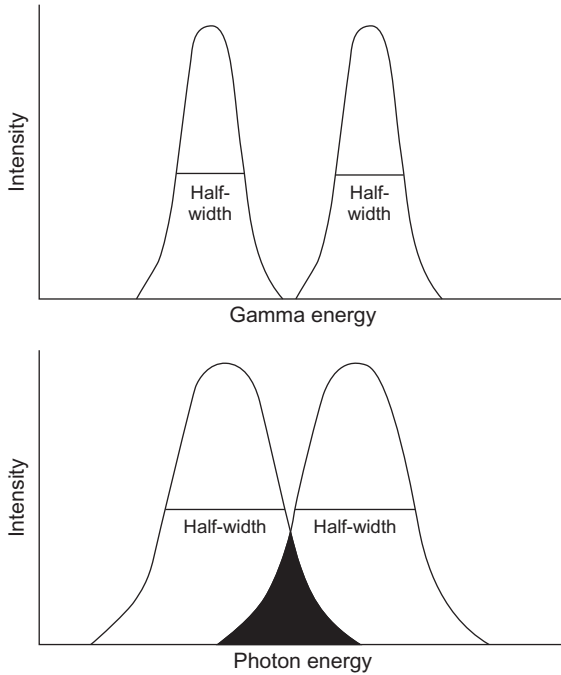


Figure 5.27 Overlapping of absorption (left) and emission (right) photons. (A) In the case of gamma radiations, the lines do not overlap because of the high energy of recoil. (B) The overlapping of the emission and absorption lines at electron transmissions (optical spectra).

Besides the energy loss at the emission, gamma photons lose energy again when absorbed in the nucleus of the absorber. Therefore, the energy of the gamma photon (E) after the absorption is:

$$E = E_0 - 2E_R \quad (5.97)$$

As a result of the recoils of the two nuclei, the gamma photon does not have enough energy to excite the nucleus of the absorber. However, resonance absorption can take place even if the gamma lines are so broad that the emission and absorption lines overlap (Figure 5.27).

The natural width of the lines (Γ) can be calculated by the Heisenberg uncertainty principle:

$$\Gamma\tau = \frac{h}{2\pi} \quad (5.98)$$

where τ is the lifetime of the excited state. In nuclear processes, this lifetime is about 10^{-9} – 10^{-7} s, so the natural line width is very small (Figure 5.27, A). Furthermore, the atoms that are emitting radiation have different velocities because of the thermal movement. So, the frequency of each emitted photons (ν) is shifted by the Doppler effect, depending on the velocity (v) of the atom relative to the observer:

$$\nu = \nu_0 \left(1 \pm \frac{v}{c}\right) \quad (5.99)$$

where ν_0 is the frequency of the gamma photons when there is no difference in the velocities. Therefore, there is still some possibility of resonance absorption. As the temperature increases, the line width and the probability of the resonance absorption increase.

^{191}Os isotope (half-life, 15 days) emits beta particles, producing an ^{191m}Ir isotope. This excited nuclide falls into its ground state (^{191}Ir) in 4.9 s, emitting gamma photons with 129 keV energy. Meantime, the nuclear spin decreases from $+5/2$ to $+3/2$. Mössbauer performed absorption experiments with this gamma radiation and iridium foil in 1958 and discovered the recoil-free resonance absorption of nuclei. Because he wanted to avoid resonance absorption, he did the experiments at very low temperatures. The unexpected result was that the resonance absorption increased enormously. At the first approximation, it is interpreted by the increased rigidity of the structure of the crystal lattice at low temperatures; i.e., the whole crystal can be considered to be a “recoiled atom.” So, the mass of the crystal can be substituted as M into Eqs. (5.95) and (5.96). As a result, the velocity and the energy of the recoiled atom will be negligible.

The recoil-free resonance absorption of nuclei can be used in the study of chemical states because the oxidation state and the chemical environment influence the energy state of the nucleus via the electrostatic interactions between the electrons and the nucleus. This change, called an “isomer shift” or a “chemical shift,” is by 7–8 orders of magnitude smaller than the characteristic energies of the nuclear processes. Therefore, a very small change of the very high energies has to be measured. The isomer shift is measured using the Doppler effect: the resonance absorption is created by the relative movement of the sample (absorber) and the gamma radiation source. The relative velocity of the sample and the radiation source corresponds to the degree of the isomer shift, and its dimension is measured in cm/s or mm/s (for example). This small velocity correlates with the small differences of the gamma energies caused by the different oxidation state or chemical environment of the Mössbauer nuclide in the absorber. The most important Mössbauer nuclides are ^{57}Fe , ^{119}Sn , ^{121}Sb , ^{151}Eu , ^{191}Ir , ^{195}Pt , ^{197}Au , and ^{237}Np .

The practical importance of the Mössbauer effect comes from the fact that one of the natural isotopes of iron, Fe-57 isotope, is a Mössbauer nuclide. The gamma radiation source is Co-57 (with a half-life of 9 months), the gamma radiation of 0.0144 MeV of which can excite the Fe-57 isotope. The decay scheme of Co-57 is shown in Figure 5.28.

The isomer shift of the different oxidation states of iron is illustrated in Figure 5.29 by the example of Fe(III) and Fe(II) fluorides. Figure 5.30 shows the Mössbauer spectrum of clay containing iron species.

As seen in Figure 5.29, the iron(III) in FeF_3 is in a symmetrical environment and the electron configuration is $3d^5$, indicating high spin and the presentation of a singlet. The chemical environment of iron(II) in FeF_2 is asymmetrical, with $3d^6$ configuration. The asymmetrical environment interacts with the electric quadrupole moment of the nucleus, resulting in the presentation of a doublet. At low temperatures, an inner magnetic field is formed, causing magnetic splitting (the Zeeman effect) with a sextet in the spectrum.

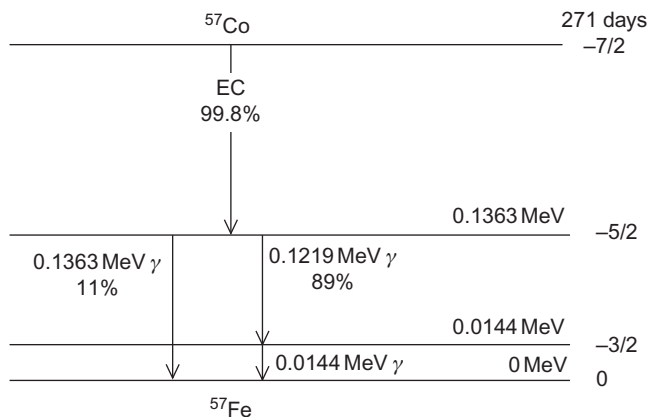


Figure 5.28 Decay scheme of Co-57.

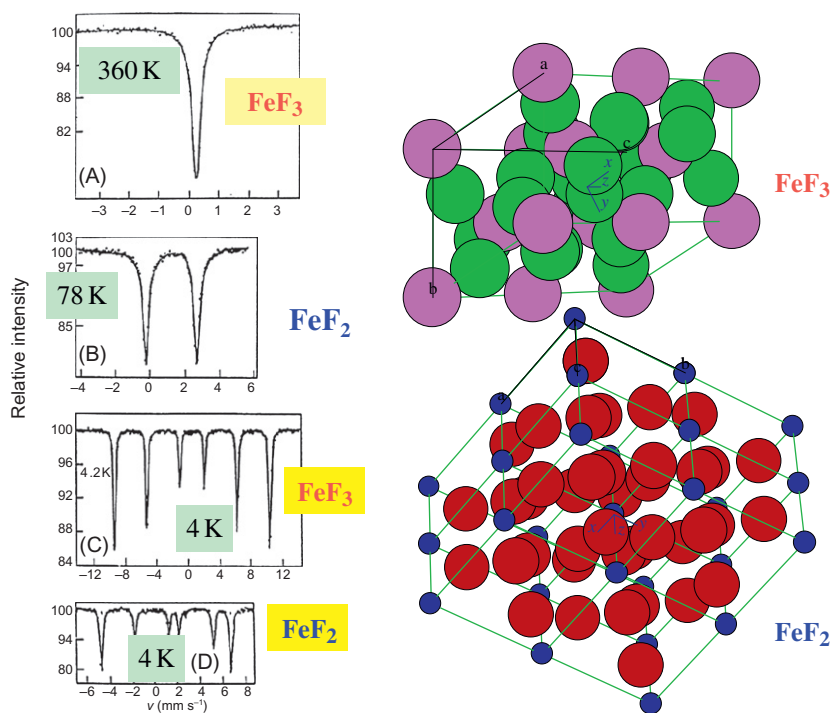


Figure 5.29 The Mössbauer spectrum of an iron(III) and iron(II) in fluorides spectrum. A: spectrum of iron(III) fluoride at 360 K; B: spectrum of iron(II) fluoride at 78 K; C: spectrum of iron(III) fluoride at 4.2 K; D: spectrum of iron(II) fluoride at 4 K. (Thanks to Prof. Ernő Kuzmann, Chemical Research Center, Budapest, Hungary, for the picture.)

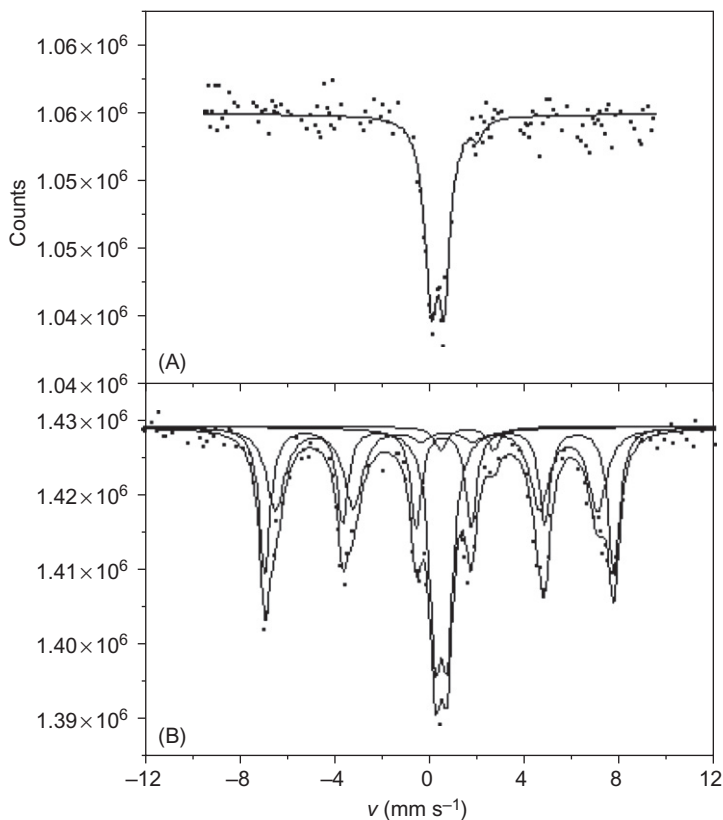


Figure 5.30 The Mössbauer spectrum of Bentonite clay at 74 K before (A) and after (B) treatment with FeCl_3 solved in acetones. (A) shows the +2 and +3 oxidation states of iron in Bentonite. The sextet in (B) refers to the formation of a magnetic phase.
Source: Reprinted from Komlósi et al. (2006), with permission from Springer.

Figure 5.30 illustrates the Mössbauer spectrum of bentonite clay at 74 K before (A) and after (B) treatment with FeCl_3 solved in acetones. Segment (A) shows the +2 and +3 oxidation states of iron in bentonite. The sextet in Figure 5.30B refers to the formation of a magnetic phase.

5.5 Interaction of Neutrons with Matter

As mentioned several times previously (Chapter 2), the neutrons are the basic particles of nuclei. They can be present as free neutrons as a result of neutron decay (see Section 4.4), but it is a very rare phenomenon. Neutrons, however, can be produced by nuclear reactions (Chapter 6) and can be widely used in different scientific and practical applications. Thus, in this chapter, the basic concepts of the interactions of neutrons with matter will be discussed.

5.5.1 Discovery of Neutrons

Since neutrons have no charge, detecting them is difficult. For this reason, neutrons were discovered relatively late, although Rutherford had postulated their existence in 1920.

In 1930, during the study of the energy levels of nuclei, Bothe and Becker irradiated beryllium with alpha particles and observed the emission of radiation with a very long range and high energy (5 MeV). Since the energy levels of nuclei were studied, the emitted radiation was supposed to be gamma radiation of beryllium. This experiment was repeated in 1932 by Irene Curie and Frederic Joliot-Curie; however, they detected the emitted radiation by other techniques and found that the energy of the radiation was much higher than what was given by Bothe and Becker. Similarly, Chadwick measured energy readings that were as high as 50 MeV. As a consequence, Chadwick stated that if the energy of the “gamma” radiation of the beryllium depends on the detection method, it cannot be “gamma” radiation, or at least another particle must be emitted besides gamma radiation. In addition, Chadwick postulated that the long-range radiation should consist of neutral particles that transfer energy only by colliding with nuclei. These particles were called “neutrons.”

Chadwick measured the rest masses of the neutrons by elastic collision with hydrogen and nitrogen nuclei and found that the ratio of the neutron to the hydrogen nucleus (proton) is about 1.1:1.

5.5.2 Production of Neutrons

Neutrons can be produced in different ways:

- In neutron sources.
- In neutron generators.
- In nuclear reactors.
- By nuclear spallation.

In neutron sources, neutrons are mostly produced by (α, n) nuclear reactions (as discussed in Section 6.2.3). The alpha particles are obtained from an alpha emitter radioactive isotope such as Ra-226, Pu-239, or Po-210. These isotopes are mixed with a light element (the binding energy of neutron is relatively low), mainly by beryllium. The neutrons are produced in the reaction as follows:



The neutron yield of these neutron sources is 10^6 – 10^8 neutrons/s.

The radium–beryllium (RaBe) neutron source has undesirably high gamma radiation, and therefore it is no longer used.

Neutrons can be produced by the spontaneous fission of ${}^{252}\text{Cf}$. The yield of the commercial ${}^{252}\text{Cf}$ neutron sources is about 10^7 – 10^9 neutrons/s.

Neutrons can be produced by (γ, n) nuclear reactions (see Section 6.2.2). Gamma photons can initiate nuclear reactions if their energy is higher than the binding energy of the target nucleus. For example, the ^{24}Na isotope has high-energy gamma photons. The gamma photons can initiate nuclear reactions with deuterium, lithium, beryllium, and boron. For example:



Therefore, when a salt containing an ^{24}Na isotope is dissolved in heavy water (D_2O), a mobile neutron source can be produced (as described in Section 6.2.2).

In neutron generators, the isotopes of hydrogen are used in nuclear reactions. Mostly deuterium, tritium nuclei, or the mixture of these nuclei are accelerated in linear accelerators, and the metal hydride target containing deuterium, tritium, or both is bombarded by the accelerated nuclei. The nuclear reactions (described further in Section 6.2.4) are:



The energy of the neutrons produced in neutron generators is about 14 MeV. The yield of the neutron is about $10^8 - 10^9$ neutrons/s.

Neutrons can be produced in cyclotrons by (p, n) nuclear reactions. For this reaction, lithium or beryllium is used as target material.

The neutron production in nuclear reactors will be discussed in detail in Section 6.2.1 and Chapter 7. Thus, it is not detailed here; we will just mention that in the fission reaction, high-energy gamma photons are also produced, which initiate the reaction (5.102). This reaction produces extra neutrons, which affects the neutron balance of the nuclear reactors.

The greatest neutron yields can be obtained by nuclear spallation. Spallation is a nuclear reaction in which photons or particles with high energy (e.g., protons with GeV) hit a nucleus, resulting in the emission of many other particles (such as neutrons or light nuclei) or photons. The target is a heavy element (e.g., mercury, tungsten, or lead). Recently, there are only a few spallation neutron sources all over the world.

The lifetime of free neutrons is short; they transform into protons, beta particles with 0.782 MeV, and antineutrinos.



The half-life of the reaction is 10.25 min.

5.5.3 Interaction of Neutrons with Matter

The most important characteristics of neutrons have been mentioned in previous chapters (Chapter 2); thus, they are summarized only briefly here. The rest mass of a neutron is 1.0086 amu, and it has no net charge. However, it consists of one up quark and two down quarks, so a neutron has magnetic momentum.

The de Broglie wavelength (Eq. (4.93)) of neutrons is about 10^{-10} m, which is in the range of the atoms. Therefore, neutrons can be applied for analytical purposes on a molecular scale.

Neutrons are classified according to their kinetic energy as follows:

- \approx meV: cold neutrons
- <0.1 eV: thermal neutrons
- 0.1–100 eV: slow neutrons
- 100 eV–100 keV: neutrons with intermediate energies and epithermal neutrons
- >100 keV: fast neutrons.

The interaction of a neutron with matter is determined by the properties mentioned previously and the energy of the neutron. The most important interactions are summarized in [Table 5.7](#).

As seen in [Table 5.7](#), the important interactions of neutrons with matter are nuclear reactions and the scattering phenomena, including elastic and inelastic scattering. The tracks of protons thrown by neutrons emitted in a PuBe neutron sources are shown in [Figure 5.31](#).

Having no charge, neutrons can be captured easily by the different atomic nuclei. All elements, except for helium, have isotopes reacting with neutrons. This is used for radionuclide productions (as discussed in Chapter 8). Some nuclei, such as boron, cadmium, and dysprosium, have an extremely high cross section for neutron captures. The nuclear reactions with neutrons will be discussed in detail in Section 6.2.1.

The neutrons play an essential role in the production of nuclear energy: the (n,f) reaction of ^{235}U is the basic reaction (see Chapter 7 for more detail). The inelastic scattering of neutrons causes the neutrons to lose energy, which is an essential

Table 5.7 Interactions of Neutrons with Matter

| Reacting Particles and Fields | Changes | |
|---|--|--|
| | In Radiation | In Matter |
| Orbital electron | | No interaction |
| Magnetic field of unpaired electrons | Elastic scattering, inelastic scattering | Excitation or magnetic relaxation |
| Nuclear field | | No interaction |
| Nucleus | Nuclear reaction, elastic scattering, inelastic scattering | New nucleus, chemical change— excitation or magnetic relaxation |

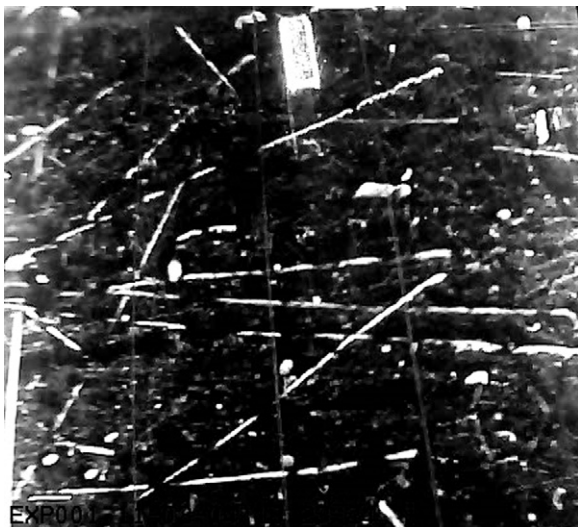


Figure 5.31 Cloud chamber photograph of the tracks of protons (long linear pathways) thrown by neutrons emitted in PuBe neutron source. The short thick lines are the pathways of alpha particles emitted by plutonium in the neutron source. (Thanks to Dr. Péter Raics, Department of Experimental Physics, University of Debrecen, Hungary, for the photograph.)

condition in the operation of nuclear reactors (see Table 7.2). The energy production reaction is regulated by nuclear reactions with a high cross section (as discussed in Section 7.1.1.6).

Neutrons can be applied in the different fields of natural sciences:

- In physics, the statistical physical systems, the magnetic structure, and dynamic of solids can be studied. The elementary particles composing neutrons (quarks, pions, and gluons) have significant effects on many physical properties of nuclei, such as radioactive decay, magnetic momentum, and electric dipole momentum.
- In material science, the substances used in magnetoelectronics (magnetic sensors, hard discs, spin valves, etc.) can be investigated. The imaging procedures, neutron radiography, and tomography are also important (see Section 10.2.2.3).
- In chemistry, each substance containing hydrogen can be studied. The transition between phases on a molecular scale (e.g., liquids and glasses) can be examined. Neutrons can assist in the molecular design and the production of materials with improved performance in the different fields of chemistry (nanocomposites, implants, drugs, catalysts, etc.). Neutrons are especially important in biological, biotechnological, and medical studies because the dynamics of the atoms and molecules and the changes in the structure of the biological molecules can be studied by neutron scattering methods (see Section 10.2.2.4).
- In energy production: the possibilities of the safe storage of hydrogen as an energy carrier (metal hydrides and ionic compounds of the lighter elements) can be studied by neutron scattering (see Section 10.2.2.4). In addition, a large portion of natural gas exists as methane–water clathrates in the shallow earth, which means that there are enormous energy resources. Methane, however, can release from the clathrate, increasing the greenhouse effect. For this reason, it is important to understand the structural and dynamical properties of these substances.
- In geology, the study of the structure and dynamics of minerals and magmas under the Earth's mantle can assist the causes that are responsible for geohazards such as earthquakes and volcanic eruptions.

- In archeology, neutron activation (see Section 10.2.2.1) and neutron scattering/diffraction (see Section 10.2.2.4) provide information on the chemical composition and technological procedures of ancient artifacts.

The analytical applications of the nuclear reaction and scattering of neutrons will be discussed in Section 10.2.2. The activation analytical methods are based on the nuclear reactions with the isotopes of all elements except helium. The scattering methods are based on the interaction of the neutrons with the nuclei and the magnetic field of matter, providing information on both the nuclei and the magnetic field.

Further Reading

- Bothe, W. and Becker, A. (1930). Künstliche Erregung von Kern-Strahlen. *Z. Phys.* 66:289–306.
- Chadwick, J. (1932). The existence of a neutron. *Proc. R. Soc. A* 136:692–708.
- Choppin, G.R. and Rydberg, J. (1980). *Nuclear Chemistry, Theory and Applications*. Pergamon Press, Oxford.
- Curie, I. and Joliot, F. (1932). The emission of high energy photons from hydrogenous substances irradiated with very penetrating alpha rays. *Comptes. Rendus.* 194:273–275.
- Friedlander, G., Kennedy, J.W., Macias, E.S. and Miller, J.M. (1981). *Nuclear and Radiochemistry*. Wiley, New York, NY.
- Haissinsky, M. (1964). *Nuclear Chemistry and its Applications*. Addison-Wesley, Reading, MA.
- Kiss, I. and Vértes, A. (1979). *Magkémia (Nuclear Chemistry)*. Akadémiai Kiadó, Budapest, Hungary.
- Komlósi, A., Kuzmann, E., Homonnay, Z., Nagy, N.M., Kubuki, S. and Kónya, J. (2006). Effect of FeCl₃ and acetone on the structure of Na-montmorillonite studied by Mössbauer and XRD measurements. *Hyperfine Interact.* 166:643–649.
- Lagoutine, F., Ciursol, N. and Legrand, J. (1983). *Table de radionucléides*. Commissariat à l’Energie Atomique, France.
- Lieser, K.H. (1997). *Nuclear and Radiochemistry*. Wiley-VCH, Berlin.
- McKay, H.A.C. (1971). *Principles of Radiochemistry*. Butterworths, London.
- Müller, R.H. (1957). Interaction of beta particles with matter. *Anal. Chem.* 29:969.
- Némethy, A., Kövér, L., Cserny, I., Varga, D. and Barna, P.B. (1996). The KLL and KLM Auger spectra of 3d transition metals, Z=23–26. *J. Electron Spectrosc. Relat. Phenom.* 82:31–40.
- Szilágyi, E., Petrik, P., Lohner, T., Koós, A.A., Fried, M. and Battistig, G. (2008). Oxidation of SiC investigated by ellipsometry and Rutherford backscattering spectrometry. *J. Appl. Phys.* 104:014903.

6 Nuclear Reactions

The inelastic collision of radiation and the nuclei of a substance may result in the formation of new nuclei. Rutherford observed in 1919 that a proton and a new nucleus, ^{17}O , form in the reaction of alpha particles with nitrogen (Figure 6.1). This nuclear reaction can be described by any chemical reaction:



The nuclear reactions have the following nomenclature:



The substance (^{14}N) irradiated in this case with alpha particles is called the “target,” the emitted particle is the proton, and the product nucleus is ^{17}O . A cloud chamber photograph shows the tracks of the alpha particle, the proton, and the recoiled ^{17}O hot nucleus (described in Section 6.4) can be observed (Figure 6.1). The product (^{17}O) is a stable isotope; thus, the first artificial nucleus produced by humans was stable.

The first artificial radioactive nucleus was produced by Joliot and Irene Curie in 1932 by the irradiation of aluminum with alpha particles. The irradiated aluminum was dissolved in sodium hydroxide solution; the product was distilled and collected on the cold wall of a glass tube. (This procedure, which is the separation by thermodiffusion, is similar to the Marsch test for detecting arsenic.) The product emitted β^+ -particles with a half-life of 2.5 min:



The partners of the nuclear reactions are the target nucleus and the irradiating particles. The important properties, the selection of a target nucleus, and charged particles will be discussed in Section 8.5.2, and the production of the irradiating particles was shown in Section 5.5.2 (neutrons). The opportunities for the production of a nuclide with a Z atomic number and an A mass number will be summarized in Section 6.3. Moreover, the production of the important radioactive isotopes will be discussed in detail in Sections 8.5–8.7.

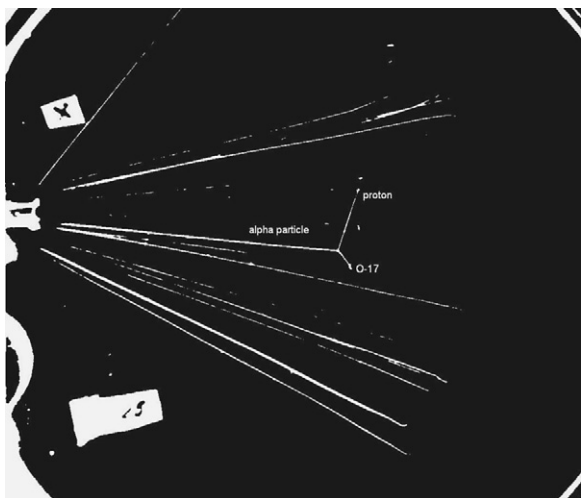


Figure 6.1 Cloud chamber photograph of the first nuclear reaction by Rutherford (see Eq. (6.1)).

As seen from nuclear reactions (6.2) and (6.3), the following rules of conservation apply:

1. The number of nucleons
2. The charges

In addition,

3. spin,
4. parity,
5. momentum,
6. energy, including both the kinetic energy and the energy originating from the change of the masses of the reactants and products, are conserved.

Similar to chemical reactions, the nuclear reaction can be exoergic (exothermic) or endoergic (endothermic). The energy of the nuclear reaction (ΔE) can be calculated from the difference between the mass of the products (product nucleus + emitted particle) and the reactants (target nucleus + irradiating particle) multiplied with the energy equivalent to the atomic mass unit (931 MeV):

$$\Delta E = 931 \text{ MeV}[(m_{\text{product_nucleus}} + m_{\text{emitted_particle}}) - (m_{\text{target_nucleus}} + m_{\text{irradiating_particle}})] \quad (6.4)$$

When the mass of the reactants is greater than that of the products, the nuclear reaction is exoergic; when the mass of the reactants is less than that of the products, the nuclear reaction is endoergic. The activation energy needed for nuclear reactions is provided by the irradiating particles. In case of exoergic nuclear reactions, the released energy will compensate for the activation energy invested. In nuclear reactions with neutrons, the activation energy can be close to zero. In the case of endoergic nuclear reactions, the energy of the irradiating particle must

provide both the activation energy and the energy of the reaction. The energy of the reaction (plus the recoiling energy of the product nucleus) gives the threshold energy, the minimal energy needed for a successful nuclear reaction. In the nuclear reactions where charged particles react (which always means positively charged particles), the Coulomb barrier of the target nucleus has to be overcome:

$$E_C = \frac{2Ze^2}{r_1 + r_2} \quad (6.5)$$

where Z is the atomic number of the target, e is the elementary charge, and r_1 and r_2 are the radii of the target nucleus and the irradiating particle.

6.1 Kinetics of Nuclear Reactions

The general equation of nuclear reactions shows that they always have second-order kinetics:



where A is the target nucleus, x is the irradiating particle, A^* is the transition state, or compound nucleus, B is the product nucleus, and y is the emitted particle. (The activation energy is needed for the formation of the compound nucleus.) The number of the product nuclei (N^*) depends on the quantity of the two reactants: the number of the target nuclei (N) and the flux of the irradiating particles (Φ). The rate constant of the nuclear reaction is called a “cross section” and is signed by $\sigma(E)$, expressing that the cross section depends on the energy of the irradiating particles:

$$\frac{dN^*}{dt} = \sigma(E)\Phi N \quad (6.7)$$

Equation (6.7) is analogous to Eq. (5.2), the absorption equation of the reaction of the radiation with substance.

Equation (6.6) refers to the case when the product nuclide is inactive (e.g., Eq. (6.2)). In nuclear reactions, however, the formation of stable nuclides is rare because it should be too expensive. Usually, the product nuclide of the nuclear reactions is radioactive; therefore, the radioactive decay of the product nuclide has to be included in the kinetic equation:

$$\frac{dN^*}{dt} = \sigma(E)\Phi N - \lambda N^* \quad (6.8)$$

where λ is the decay constant of the product nuclide.

The cross section is frequently given in barn units, $1 \text{ barn} = 10^{-24} \text{ cm}^2 = 10^{-28} \text{ m}^2$. This value is approximately the geometric cross section of the nuclei, meaning that if every particle colliding with a nucleus causes a successful nuclear reaction, the cross section is about 1 barn. Thus, this value should be the upper limit of the cross sections of the nuclear reactions. However, there are reactions with cross sections much higher than this value. For example, the cross section of the (n, γ) nuclear reaction of cadmium is about 10,000 barn. This is explained by the wave-particle duality: the de Broglie wavelength of the neutron is about 10^{-10} m , similar to the radius of the atoms. When the neutrons approach the nuclei within 10^{-10} m , a nuclear reaction can take place. The ratio of the de Broglie wavelength of the neutron to the radius of the nuclei is about 10,000:1, which is in very good agreement with the cross section of the (n, γ) reaction of cadmium.

The solution of Eq. (6.8) is as follows:

$$N^* = \frac{\sigma(E)\Phi N}{\lambda} (1 - e^{-\lambda t_{\text{irradiation}}}) = N_{\infty}^* (1 - e^{-\lambda t_{\text{irradiation}}}) \quad (6.9)$$

where $t_{\text{irradiation}}$ is the time of irradiation. This is not a general solution; it is valid only if $\sigma(E)\Phi \ll \lambda$, which is usually the case. As a result of the nuclear reaction, the number of the target nucleus (N) continuously decreases, but this decrease can be ignored because $\sigma(E)\Phi \ll \lambda$.

The $\sigma(E)\Phi N/\lambda$ in Eq. (6.9) can be expressed by a constant (N_{∞}^*) for a given nuclear reaction (all the cross sections, the flux of the irradiating particles, and the number of the target nuclei are constant). N_{∞}^* expresses the maximal number of the product nuclei, which can be produced when the irradiation time is about 10 times the half-life of the product nucleus. Due to practical and economical considerations, the irradiation time is usually about 3–4 times the half-life of the product nucleus.

When the irradiation is finished, the product nuclei decays according to the rules of the usual kinetics of radioactive decay:

$$N^* = N_{\infty}^* (1 - e^{-\lambda t_{\text{irradiation}}}) e^{-\lambda t_{\text{cooling}}} \quad (6.10)$$

where t_{cooling} is the cooling time, the time of decay after irradiation ends.

The activity of the product nucleus (Figure 6.2) can also be expressed by multiplying the number of the radioactive nuclei with the decay constant:

$$A^* = \lambda N^* = \lambda N_{\infty}^* (1 - e^{-\lambda t_{\text{irradiation}}}) e^{-\lambda t_{\text{cooling}}} = A_{\infty}^* (1 - e^{-\lambda t_{\text{irradiation}}}) e^{-\lambda t_{\text{cooling}}} \quad (6.11)$$

6.2 Classification of Nuclear Reactions

In nuclear reactions, a target nucleus (A) is irradiated with a particle (x) and a compound nucleus (A^*) is formed. A compound nucleus can be formed from different target nuclei and irradiating particles (Figure 6.3). Since the nuclear reactions occur

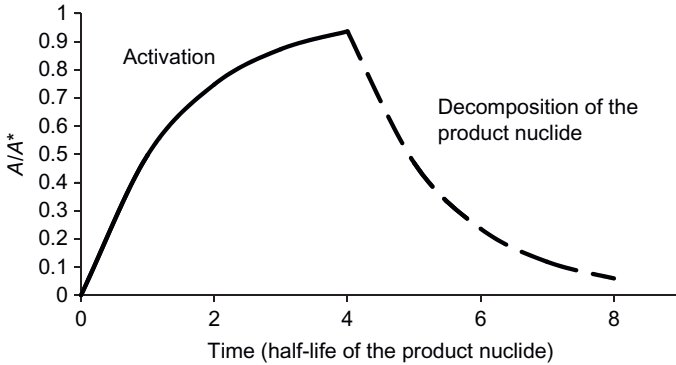


Figure 6.2 The activity versus time function of a radioactive nucleus produced in a nuclear reaction. The time of activation is four times the half-life of the product nuclide (solid line). After finishing the irradiation, the product nuclide decomposes (dotted line).

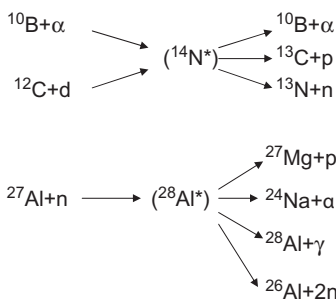


Figure 6.3 Steps of the nuclear reaction. The excited transitional nuclides are in brackets.

through strong interactions, the lifetime of the compound nucleus is short, and it can emit another particle (γ), producing a new nucleus (B) (Eq. (6.6)). The compound nucleus can decompose in different ways.

Nuclear reactions are classified on the basis of the irradiating and the emitted particles. The characteristic types are listed in Table 6.1.

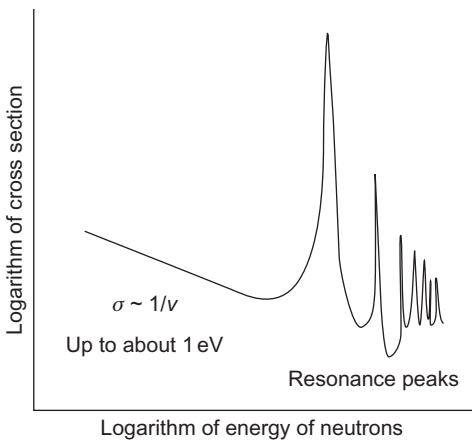
6.2.1 Nuclear Reactions with Neutrons

As discussed in Section 5.5.3, neutrons are classified according to their kinetic energy as cold, thermal, slow, epithermal, and fast neutrons. Since neutrons are neutral, there is no Coulomb repulsion between them and nuclei. As a result, even thermal neutrons can initiate nuclear reactions. When the neutron collides with the nucleus, an excited nucleus forms, which can emit a neutron whose energy is different from the neutron that initiated the process.

The cross section of nuclear reactions with neutrons versus neutron energy is shown in Figure 6.4. The plot has two general features. First, the cross section decreases when the energy and velocity of the neutron increase. This means that at

Table 6.1 Classification of Nuclear Reactions

| | Irradiating Particle | Nuclear Reaction |
|------------------|----------------------|--|
| Neutral particle | Neutron | $n, \gamma; n, p; n, \alpha; n, 2n; n, f$ (fission) |
| | Gamma photon | $\gamma, n; \gamma, p$ |
| Charged particle | Proton | $p, \gamma; p, n; p, \alpha$ |
| | Deuteron | $d, p; d, n; d, 2n; d, \alpha$ |
| | Alpha | $\alpha, n; \alpha, p$ |
| | Other nuclei | See the discussion of the production of transuranium elements in Section 6.2.6 . |

**Figure 6.4** Cross section of nuclear reactions with neutrons versus neutron energy. The cross section is inversely proportional to the velocity (energy) of neutrons up to ~ 1 eV.

lower velocities, the neutron spends more time near the nucleus, so the probability of the nuclear reaction increases.

Second, the cross section is enormously high at certain energy values, so-called resonances can be observed. This is explained by the discrete energy state of the compound nucleus. The resonances are observed at the energies equal to any excitation energy of the compound nucleus. The two effects are observed simultaneously.

The most frequent nuclear reactions with neutrons are the (n, γ) reactions:



In this process, the emitted particle, a gamma photon, is also neutral, so there is no Coulomb barrier for either neutrons or gamma photons. Therefore, the (n, γ) reactions are simple, and they take place for each element except helium. They are exoergic, releasing about 8 MeV of energy. The disadvantage of the (n, γ) reactions is that the target and the product nuclei have the same atomic number—only the mass number increases by 1. This means that carrier-free radioactive isotopes

cannot be produced directly by this nuclear reaction; the product radioactive nuclide is diluted with the stable nuclide of the same element. Since the product number is rich in neutrons, it usually emits negative beta particles. An example of (n, γ) reactions, the production of ^{24}Na isotope is shown:



The (n, γ) reactions are applied in the neutron activation analysis and prompt gamma activation analysis (PGAA discussed in Sections 10.2.2.1 and 10.2.2.2).

The competitive reaction of the (n, γ) reactions is the (n,p) reactions:



Since the emitted particle (proton) is heavier than a gamma photon, the (n,p) reactions should have a greater cross section. The proton, however, is positively charged, so its emission is inhibited by the Coulomb barrier of the product nucleus (similar to the emission of the alpha particles, as discussed in Section 4.4.1). As a result, light elements react in the (n,p) reactions, while heavier nuclides prefer the (n, γ) reactions. Similar to (n, γ) reactions, the (n,p) nuclear reactions are also exoergic. The atomic number of the product nucleus is reduced by 1, and both the target and the product nuclei have the same mass number. The product nucleus is rich in neutrons, so it is a negative beta emitter. Since the target and the product nuclei have different atomic numbers, they are chemically different, so they can be separated by chemical procedures. In this way, carrier-free radioactive isotopes can be prepared. For example:



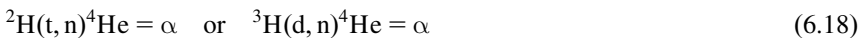
After irradiation with neutrons, the compound nuclide can emit alpha particles too:



The (n, α) nuclear reactions are endoergic. Only light elements can react in this way because of the high Coulomb barrier between the alpha particle and the product nucleus. For example:



If the reaction (6.17) takes place in heavy water (D_2O), the product nucleus, tritium, can react with the nucleus of deuterium as follows:



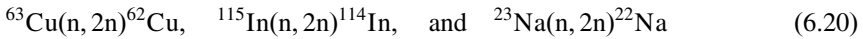
As a result, the neutron is recovered. The irradiating neutrons are thermal neutrons with different energies; the produced neutrons, however, are fast and have a

well-determined energy, ~ 14 MeV. This reaction takes place in the hydrogen bomb too.

The $(n,2n)$ reactions such as



are also endoergic, since the mass of the neutron increases when emitted from the nucleus (as discussed in Section 2.2). Since the number of the neutrons in the produced nucleus decreases, the product nucleus decays with positive beta decay or electron capture. Since the atomic number remains the same, carrier-free radioactive isotopes cannot be obtained directly. Some examples of $(n,2n)$ reactions are:



A very important type of nuclear reaction with neutrons is the fission of heavy nuclei under the effect of thermal neutrons. This is called the “ (n,f) reaction.” From the natural nuclides, only the fission of ${}^{235}\text{U}$ has a high cross section. As a result of this fission, two nuclei with intermediate mass, called “fission products,” and more than one neutron are produced:



The binding energy of the two fission products is less than the binding energy of the target nucleus, meaning that the fission reaction is exoergic, releasing 200 MeV of energy. This energy can be used for energy production in nuclear power plants and has been used in the atomic bombs (see Chapter 7). The fission is usually asymmetric; the ratio of the masses of the fission product is about 2:3. In [Figure 6.5](#), the ratio of the fission products of ${}^{235}\text{U}$ by thermal neutrons and the

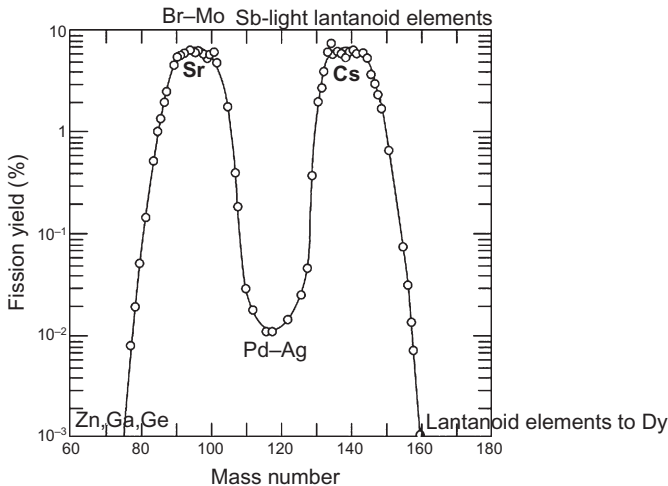


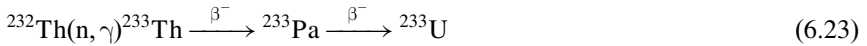
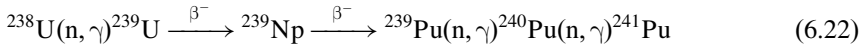
Figure 6.5 Products of the fission of ${}^{235}\text{U}$ by thermal neutrons.

main ranges of elements are illustrated, including the small- and high-fission yields. Strontium and cesium, the most important fission products of the low- and intermediate-level nuclear wastes, are labeled with bold letters.

A significant number of the fission products are radioactive, and some of them have long half-lives. Therefore, the treatment of the radioactive fission products is a very important environmental and safety problem with the production of nuclear energy.

The fission products can be the parent nuclides of decay series. For example, the simplified scheme of the formation of strontium isotopes is shown in [Figure 6.6](#).

In addition to ^{235}U , three artificially produced isotopes, namely, ^{239}Pu , ^{241}Pu , and ^{233}U , also have high fission cross sections. They can be produced from isotopes, which are more abundant naturally than ^{235}U : the plutonium isotopes can be produced from the ^{235}U isotope (the ratio of ^{235}U to ^{238}U is 1:139, as detailed in Section 4.3.1), ^{233}U can be obtained from ^{232}Th . The nuclear reactions of the production of ^{239}Pu , ^{241}Pu , and ^{233}U isotopes are as follows:



The irradiating neutrons are obtained from neutron sources, neutron generators, or nuclear reactors (see Section 5.5.2).

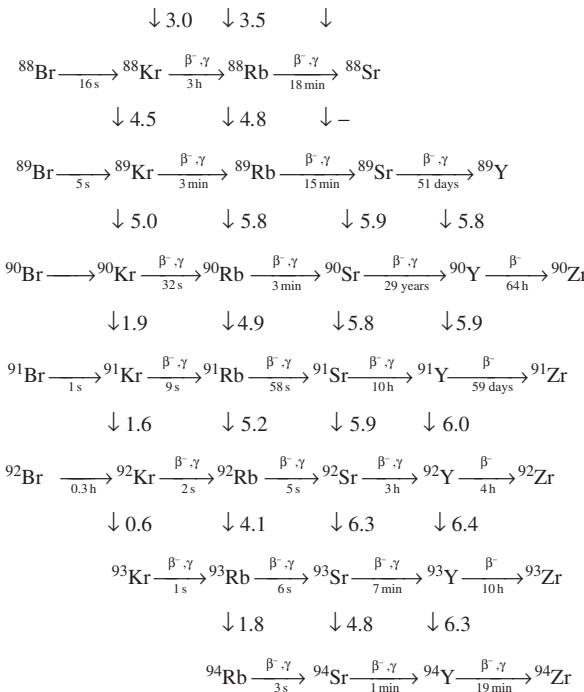


Figure 6.6 A simplified scheme of the formation of strontium isotopes by fission of ^{235}U . The numbers next to the vertical arrows indicate the fission yield of the given isotope; the half-lives are shown below the horizontal arrows. (Thanks to Dr. Nóra Vajda, RadAnal Ltd., Budapest, Hungary, for the scheme.)

Some isotopes of the transuranium elements have great cross sections for neutrons, but their produced quantity is too low to be used as fuel in nuclear reactors. Their only application is neutron bombs, which contain ^{252}Cf (see Section 7.5).

6.2.2 Nuclear Reactions with Gamma Photons

Gamma photons can initiate nuclear reactions if their energies are higher than the binding energy of the target nucleus. Therefore, there are relatively few nuclear reactions with gamma photons. The reaction



was already discussed in Section 5.5.2. This reaction can be initiated by the gamma photons of ^{24}Na isotopes since the energy of the gamma photons is 2.76 MeV, while the binding energy of the deuterium nucleus is 2.2 MeV. So, when a salt containing ^{24}Na isotopes is dissolved in heavy water (D_2O), a mobile neutron source can be produced.

6.2.3 Nuclear Reactions with Charged Particles

The positively charged irradiating particle has to pass through the Coulomb barrier of the target nucleus, so the energy of the irradiating particle has to be higher than the threshold energy, even in the case of exoergic reactions. The Coulomb barrier of light nuclei is always lower, so the nuclear reaction of the charged particles with light elements is more feasible. The maximal energy of the alpha particles is about 9 MeV, which is enough to overcome the Coulomb barrier of the light elements (e.g., (6.1) and (6.2) reactions). For most nuclear reactions with charged particles, however, the energy of the particles has to be amplified, i.e., the charged particles have to be accelerated. This has been done in van de Graaf generators, and more recently, linear accelerators and cyclotrons have been used (see Section 8.5.2).

The characteristic types of nuclear reactions with charged particles were shown in Table 6.1. They are presented here on the basis of irradiating particles.

6.2.3.1 Nuclear Reactions with Protons

Among the reactions involving protons, the (p, γ) and (p,n) reactions are relatively simple because the emitted particle is neutral. The two reactions are competing reactions, however, with the (p,n) reactions (governed by strong interactions) being more frequent. The threshold energy of (p,n) reactions is about 2–4 MeV, and the reactions are endoergic. In the (p,n) reaction, the number of protons increases and the number of neutrons decreases. The product nuclei are rich in protons, so they usually decompose by positive beta decays or electron captures. Carrier-free radioactive isotopes can be produced. For example:

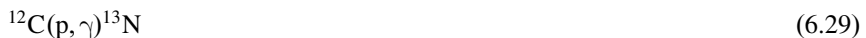




An example of the (p, γ) nuclear reaction is



The energy of the emitted photon is extremely high—about 17 MeV. Another example is the



reaction. The product nucleus has positive beta decay; it has some medical applications.

The (p, α) has little importance. The Coulomb barrier acts both on the irradiating proton and on the emitting alpha particle. The reaction is always endoergic. The ratio of neutrons increases, so the product nuclei decompose by negative beta decay. Carrier-free isotopes can be produced. For example:



6.2.3.2 Nuclear Reactions with Deuterons

The nuclear reactions of deuteron are important in the production of isotopes in cyclotrons. They have the advantage that deuteron can easily be accelerated, and it can enter the target nucleus from the direction of the neutron, decreasing the Coulomb repulsion. When, in addition, the emitted particle is a proton,

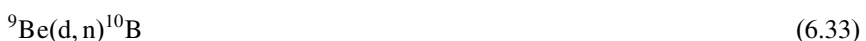


the Coulomb barrier decreases to almost zero, so the cross section of the (d, p) , or Philips–Oppenheimer reaction, is high. The (d, p) reaction takes place with all elements. For example:



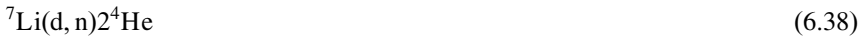
The (d, p) reaction is analogous to the (n, γ) nuclear reaction, and the target and product nuclei are the same. Carrier-free isotopes cannot be produced directly. The product nuclide is rich in neutrons, emitting negative beta particles.

The (d, n) reactions are analogous to (p, γ) reactions: the atomic number of the product nucleus increases by 1, so the product is carrier-free and decomposes with positive beta decays or electron captures. For example:





Some of the (d,n) reactions, such as



are used in neutron sources.

The (d,2n) reactions are strongly endoergic, and they are analogous to (p,n) reactions. This means that there are relatively many protons in the product nucleus and the positive beta decay and electron capture are characteristic. They are used for isotope production as follows:



In the (d, α) nuclear reaction, carrier-free product nuclides with positive beta decays or electron captures can be produced mostly in exoergic reactions. For example:



A special example of the (d, α) nuclear reaction is the



reaction, where the product (^{86}Rb) emits negative beta particles.

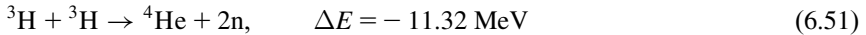
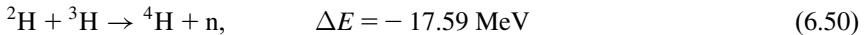
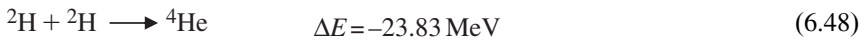
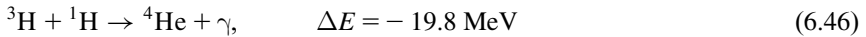
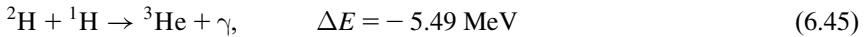
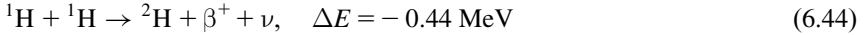
6.2.3.3 Nuclear Reactions with Alpha Particles

Some examples of the nuclear reactions with alpha particles ((α ,n) and (α ,p)) have been shown in previous discussions of the first nuclear reaction (see Eqs. (6.1) and (6.3)) and neutron sources (see Section 5.5.2). The (α ,xn) reactions are important in the production of the transuranium elements (see Section 6.2.6).

6.2.4 Thermonuclear Reactions

As seen in Figure 2.2, the binding energy in each nucleon has an extremum as a function of the mass number. This means that energy can be obtained by the fission of heavy elements and by the fusion of light elements. (Fission is discussed in Section 6.2.1.)

The most important fusion reactions of the isotopes of hydrogen are exoergic:



The activation energy of the fusion processes, however, is very high. The ignition temperature is the lowest for the ${}^2\text{H}$ – ${}^3\text{H}$ reaction (see Eq. (6.50) and Figure 6.7), it is about 10^7 K; the ignition temperature of the ${}^2\text{H}$ – ${}^2\text{H}$ reaction (see Eqs. (6.47)–(6.49)) is in the range of 10^8 K. The H–H reaction requires an even higher temperature, about 10^{10} K. These reactions take place in stars. Natural fusion reactions will be discussed in Section 6.2.5.

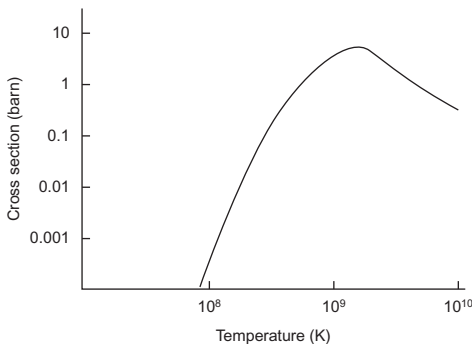


Figure 6.7 The cross section of the D–T reaction as a function of temperature.

All products of the reactions ((6.44)–(6.51)) are inactive, so fusion energy production should be more desirable than fission energy production. However, there are many technical problems that have not been solved yet, as will be outlined in Section 7.4.

The thermonuclear reactions take place in the hydrogen bomb. The nuclear bomb will be discussed in Section 7.5.

6.2.5 Nucleogenesis: The Production of Elements in the Universe

The elements in the universe are formed through nuclear reactions. The history of the universe, in some way, could be considered to be a process consisting of nuclear reactions.

The scientific interpretation of the universe is based on observations and experiences of theoretical and experimental physics, astronomy, and the spectral analysis of the universe. The first observation to be considered is the relative abundance of the elements in the universe, as illustrated in Figure 6.8. As seen in Figure 6.8, about 90% of the atoms in the universe are hydrogen and about 9% are helium. The amount of all the other elements combined is <1%. The relative abundance of helium in the stars (e.g., the Sun) is about twice that in the universe. An important fact is that the amount of the elements usually decreases as the atomic number or mass number increases. The amount of the elements in the iron group, however, is higher than expected on the basis of the atomic number. Some light elements (lithium, beryllium, and boron) are very rare. The amount of the elements with even atomic numbers is higher than the amount of the adjacent elements with odd atomic numbers. As a result, a theory explaining the amount of the elements in the universe should start from hydrogen and explain how the heavier elements can be produced from hydrogen and the mentioned anomalies in the general tendency of the abundances.

As another starting point, astrophysical observations can be mentioned. The age of the Milky Way is about 15 billion years, or 15 eons. The age of the oldest

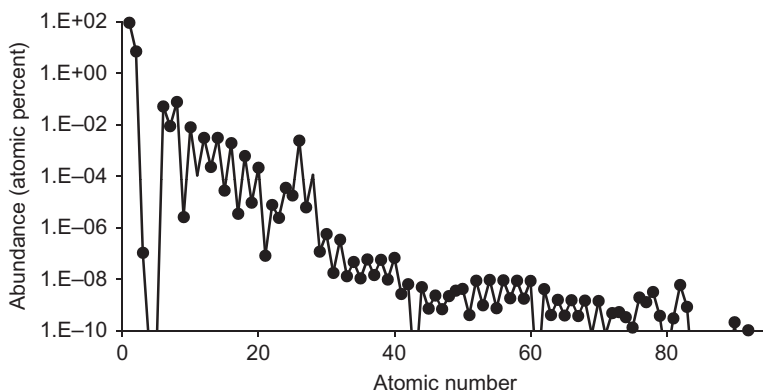


Figure 6.8 The estimated abundances of the chemical elements in the universe.

meteorites and rocks on the Moon is about 4.65 eons. The age of the oldest rocks in the Earth's crust is about 2.6 eons. Some stars of the Milky Way are only about 1 million years old. The different ages of the stars and planets show that they were formed over a long period and they are still in the process of formation/transformation. If the elements are produced in the stars, their formation is continuous.

Information on the universe originates from spectral measurements. These spectral data provide information on the elementary composition, surface temperature, age, density, and movement of the stars. Because of the Doppler effect, the spectra of the stars moving away shift toward higher wavelengths. This is called the "red-shift phenomenon," and it shows the expansion of the universe, i.e., it is thought to have been much smaller during its early stages.

The first theory of the formation of the elements and the stellar revolution has been constructed by G. Gamov and R.A. Alpher, including assumptions by H. Bethe. They proposed that at the moment of the formation of the universe, all matters existed as neutrons in a gigantic nucleus, which exploded. This event is popularly known as "the Big Bang." During this explosion, the neutrons transformed into protons by negative beta decay with ($t_{1/2} = 11$ min). The formation of the elements began with the combination of protons and neutrons. This theory was modified later, postulating that the gigantic nucleus may have contained some other particles heavier than neutrons, and the radiation density (i.e., the number of photons) was much higher than the density of the particles. In the Big Bang, only hydrogen and helium formed; there were no heavier elements. Approximately 25% of the expanding cloud converted to helium; the rest remained as hydrogen. This would explain the relative abundance of hydrogen and helium in the universe.

Assuming that the rate of the expansion of the universe is constant, the Big Bang occurred about 13 billion years ago. Gravity, however, decreases during the expansion, so the age of the universe may be 15–20 billion years.

Later, I.E. Segal found that the red-shift is not linearly proportional, but rather the square of the distance. If so, the most important argument of the Big Bang theory is put into question and that would imply that the universe is eternal.

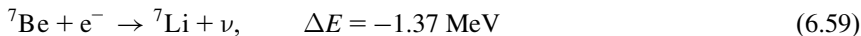
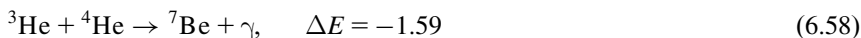
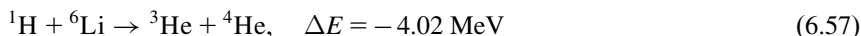
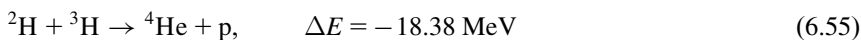
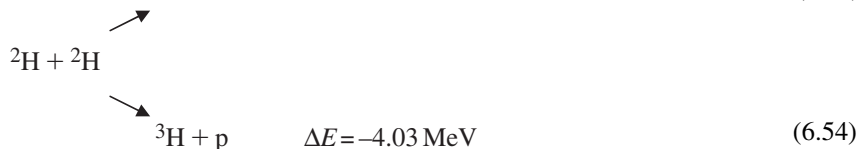
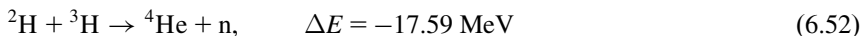
The temperature of the neutron cloud has been hypothesized to be about $2-20 \times 10^9$ K. When such a hot gas cloud is adiabatically expanded, its temperature decreases. From the size of the universe, Alpher, Herman, and Gamov calculated that black body radiation with about 5 K has to be present. Really, black body radiation with 2.7 K can be detected in the whole universe, which proves the Big Bang theory.

The Big Bang theory, however, can only provide an interpretation for the formation of hydrogen and helium. The formation of the other elements can be explained by the processes that occur in stars, assuming that the stars are formed by the condensation of the matter of the interstellar space consisting of hydrogen and helium. In this condensation process, the density of the interstellar matter (atoms/cm³) significantly increases (by about 1000 times). At critical density, hydrogen gas transforms to protons and electrons, plasma is formed, and the pressure significantly decreases. The gravitation accelerates the condensation of the interstellar gas, and the release of the gravitation energy increases the temperature. When the

temperature of the core reaches 5×10^6 K, a thermonuclear reaction, in which hydrogen is converted to helium, can begin. Since the thermonuclear reactions are exoergic, the temperature continues to increase. As a result, a very hot core and a much colder mantle form, as observed in the Sun.

The transformation of hydrogen to helium is not a one-step process because the probability of the collision of four atoms is negligible. Instead, the elementary steps shown in Table 6.2 are assumed to happen. Since the formation of positron occurs through weak interaction, the first elementary step is very slow. One from $\sim 10^{22}$ ${}^1\text{H} + {}^1\text{H}$ collisions results in a successful reaction in the Sun. If this reaction has been going on in the Sun for 4.6 eons, about 6% of the hydrogen has to be already converted to helium.

Beside the main reaction in Table 6.2, other reactions may take place as well, such as:



In the processes (6.52)–(6.55) and (6.57), helium is formed too.

Table 6.2 Elementary Steps of the Formation of ${}^4\text{He}$

| Step | Reaction Energy (MeV) | Mean Reaction Time |
|--|-----------------------|----------------------------|
| ${}^1\text{H} + {}^1\text{H} \rightarrow {}^2\text{H} + \beta^+ + \nu$ | -0.44 | 1.4×10^{10} years |
| ${}^2\text{H} + {}^1\text{H} \rightarrow {}^3\text{He} + \gamma$ | -5.49 | 6 s |
| ${}^3\text{He} + {}^3\text{He} \rightarrow {}^4\text{He} + 2 {}^1\text{H}$ | -12.86 | 9×10^5 years |
| Overall: $4 {}^1\text{H} \rightarrow {}^4\text{He} + 2\beta^+ + 2\nu$ | -24.7 ^a | 1.4×10^{10} years |

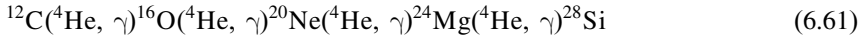
^aSince neutrinos have 0.4 MeV of energy when emitted from the Sun, the net energy release is 24.3 MeV/He.

Since helium is heavier than hydrogen, gravitation acts stronger on helium. Therefore, helium tends to move toward the core of the star, and hydrogen is in the outer mantle. As the quantity of hydrogen in the core decreases, the temperature decreases as well. Gravitation in the core, however, increases, contracting and warming the core. The warming core increases the temperature of hydrogen in the outer mantle, expanding the mantle of the star. In this period, the star emits red light and becomes a red giant.

As discussed previously, the density and gravitation of helium in the core increases, the temperature rises until the thermonuclear reactions (fusions) can start. These fusion processes cause an abrupt increase in temperature, producing the nuclei with the atomic number in the range of 5–8. Two helium nuclei combine to form a nucleus, whose half-life is only 2×10^{-16} s. However, the quantity of ^8Be is enough to react with a third helium nucleus, producing ^{12}C isotope, which is stable:



If ^{12}C is already present, the additional reactions with helium can produce heavier nuclei up to silicon:



As seen in [Figure 6.9](#), the amount of the even nuclides of the light elements is higher than the amount of adjacent odd nuclides. This is in agreement with the reactions in [Eq. \(6.61\)](#).

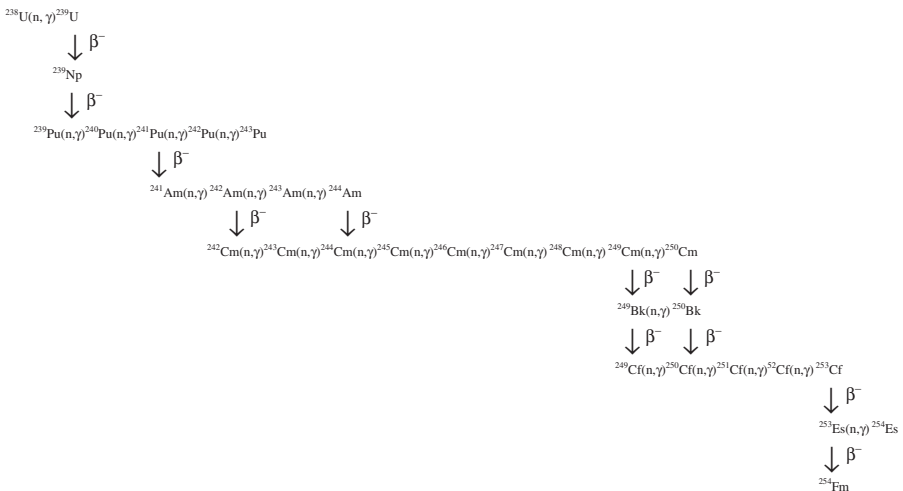


Figure 6.9 Production of transuranium elements by (n,γ) nuclear reactions.

The opportunity of helium burning that leads to the formation of the heavier elements depends on the size of the star. When the mass of the star is less than the half the mass of the Sun, the temperature cannot rise high enough for the helium burning to be initiated. When the mass of the star is <3.5 times the mass of the Sun, the burning of carbon does not take place. These stars become white dwarfs; the gravitation crack, however, can initiate the transformation of the outer hydrogen mantle into helium. This process, called a “nova explosion,” can drive out part of the core matter in the outer mantle.

In the great stars (the masses of which are more than 3.5 times the mass of the Sun), helium burning is an important source of energy. As the temperature rises above 10^9 K, the reactions, some examples of which are listed below, can take place:



The conditions such that these reactions (Eqs. (6.62)–(6.69)) occur are appropriate in stars with a mass of at least 7.5 times that of the Sun. The emission of the gamma photons (see Eqs. (6.65) and (6.69)) assists the emission of nucleons from the nuclides with mass numbers from 12 to 32. As a result, a so-called soup of nuclides, nucleons, alpha particles, and photons forms, in which lighter and heavier nuclides can react further as the temperature rises. These reactions are feasible until the formation of the most stable elements (namely, the elements of the iron group), where the absolute value of the binding energy per nucleon is maximal. The amount of even nuclides and nuclides with closed proton and neutron shells is higher.

The transformation of hydrogen and helium produces neutrons as well. In the formation of heavier elements, the concentration of neutrons significantly increases, so the main procedure of the formation of the elements changes: namely, neutron captures become dominant. The elements from iron and bismuth are formed in so-called slow (s) (n, γ) reactions accompanied by beta decays.

The formation of elements heavier than bismuth cannot be explained by the s-process since these elements have many short-lived isotopes that prohibit additional neutron captures. Their formation is explained as follows: In stars (red giants), where the heavier elements have been accumulated in the core, energy production continues in the outer mantle. The energy release of these stars is very high because of the emission of photons and neutrinos. As a result, the core of the star becomes cooler and contracts, and the gravitation energy decreases, initiating the increase of the pressure and temperature. Under these conditions, the strong photon field causes the photodisintegration of the elements of the iron group, producing helium nuclei and neutrons. Helium burning immediately starts, increasing the temperature of both the core and the mantle. Therefore, fusion reactions start in the mantle too. This process is known as a “supernova explosion.” Because of the high pressure, we can postulate the reaction as follows:



The supernova explosion is a very fast process, but the emission of the neutrons is very intense, producing elements heavier than bismuth in the so-called rapid (r) process.

After the supernova explosion, a very dense (10^{18} kg/m^3) neutron star is formed, starting a new cycle!?

6.2.6 Production of Transuranium Elements

The heaviest natural element is uranium. The next elements, so-called transuranium elements, have been produced artificially by nuclear reactions with neutrons, charged particles, and other nuclei. The production and names of the transuranium elements are summarized in [Table 6.3](#).

As seen in [Table 6.3](#), the production of the transuranium elements started in the United States in 1940, in the period of the development of the atomic bomb. The first transuranium elements (neptunium, plutonium, americium, and curium) were produced by (n,γ) nuclear reactions and the following beta decays, and the new elements (plutonium and americium) were irradiated again with neutrons, which results in additional (n,γ) reactions and beta decay. These transuranium elements are produced in nuclear power plants; some of them (^{239}Pu , ^{241}Pu) are fissile nuclides (as discussed in [Section 6.2.1](#)), and so play a role in the neutron balance of the nuclear reactors. In addition, plutonium isotopes are separated from the burned-out fuels and applied for production of mixed oxide fuels (see [Section 7.1.1.1](#)) or nuclear weapons (see [Section 7.5](#)).

Transuranium elements heavier than curium cannot be produced with (n,γ) reactions because the negative beta decay of curium isotopes is not known. These elements have been produced by nuclear reactions with positively charged particles. The charged particle is an alpha particle to californium. Then, as the atomic number of the transuranium element increases, heavier and heavier charged particles must be used for the irradiation.

Table 6.3 Production of Transuranium Elements

| Atomic Number | Name of Element | Year and Place of Production | Nuclear Reaction |
|---------------|---|--|--|
| 93 | Neptunium | 1940, United States | $^{238}\text{U}(\text{n}, \gamma)^{239}\text{U} \xrightarrow{\beta^-} ^{239}\text{Np}$ $^{238}\text{U}(\text{d}, \text{n})^{239}\text{Np}$ $^{238}\text{U}(\text{n}, 2\text{n})^{237}\text{U} \xrightarrow{\beta^-} ^{237}\text{Np}$ |
| 94 | Plutonium | 1941, United States | $^{238}\text{U}(\text{p}, 2\text{n})^{238}\text{Np} \xrightarrow{\beta^-} ^{238}\text{Pu}$ $^{238}\text{U}(\text{n}, \gamma)^{239}\text{U} \xrightarrow{\beta^-} ^{239}\text{Np} \xrightarrow{\beta^-} ^{239}\text{Pu}(\text{n}, \gamma)^{240}\text{Pu}(\text{n}, \gamma)^{241}\text{Pu}$ |
| 95 | Americium | 1944–1945, United States | $^{238}\text{U}(\alpha, \text{n})^{241}\text{Pu} \xrightarrow{\beta^-} ^{241}\text{Am}$ $^{239}\text{Pu}(\text{n}, \gamma)^{240}\text{Pu} \xrightarrow{\beta^-} ^{240}\text{Am}$ $^{240}\text{Pu}(\text{n}, \gamma)^{241}\text{Pu} \xrightarrow{\beta^-} ^{241}\text{Am}$ |
| 96 | Curium | 1944, United States | $^{239}\text{Pu}(\alpha, \text{n})^{242}\text{Cm}$ $^{241}\text{Am}(\text{n}, \gamma)^{242}\text{Am} \xrightarrow{\beta^-} ^{242}\text{Cm}$ |
| 97 | Berkelium | 1950, United States | $^{241}\text{Am}(\alpha, 2\text{n})^{243}\text{Bk}$ |
| 98 | Californium | 1950, United States | $^{242}\text{Cm}(\alpha, 2\text{n})^{244}\text{Cf}$ |
| 99 | Einsteinium | 1952, United States | $^{238}\text{U}(\text{}^{14}\text{N}, 6\text{n})^{246}\text{Es}$ |
| 100 | Fermium | 1952, United States | $^{238}\text{U}(\text{}^{16}\text{O}, 4\text{n})^{250}\text{Fm}$ $^{238}\text{U}(\text{}^{18}\text{O}, 4\text{n})^{252}\text{Fm}$ |
| 101 | Mendelevium | 1955, United States | $^{252}\text{Es}(\alpha, \text{n})^{256}\text{Md}$ |
| 102 | Nobelium | 1959, United States 1964, Soviet Union | $^{241}\text{Pu}(\text{}^{16}\text{O}, 5\text{n})^{252}\text{No}$ $^{246}\text{Cm}(\text{}^{12}\text{C}, 4\text{n})^{254}\text{No}$ $^{248}\text{Cm}(\text{}^{12}\text{C}, 4\text{n})^{256}\text{No}$ |
| 103 | Lawrencium | 1961, United States 1965, Soviet Union | $^{250,251,252}\text{Cf}(\text{}^{10,11}\text{B}, 2 - 5\text{n})\text{Lr}$ $^{243}\text{Am}(\text{}^{18}\text{O}, 5\text{n})^{256}\text{Lr}$ |
| 104 | Rutherfordium Kurtschatovium Dubnium | 1964, Soviet Union(?) 1969, United States | $^{249}\text{Cf}(\text{}^{12}\text{C}, 4\text{n})^{257}\text{Rf}$ $^{249}\text{Cf}(\text{}^{13}\text{C}, 3\text{n})^{259}\text{Rf}$ $^{242}\text{Pu}(\text{}^{22}\text{Ne}, 4\text{n})^{260}\text{Rf}$ |

| | | | |
|-----|--|---|--|
| 105 | Dubnium Hahnium Joliotium | 1968, Soviet Union 1970, United States | $^{249}\text{Cf} (^{15}\text{N},4\text{n})^{260}\text{Du}$ $^{243}\text{Am} (^{22}\text{Ne},5\text{n})^{260}\text{Du}$ $^{243}\text{Am} (^{22}\text{Ne},4\text{n})^{261}\text{Du}$ |
| 106 | Seaborgium Rutherfordium | 1974, United States and Soviet Union | $^{249}\text{Cf} (^{18}\text{O},4\text{n})^{263}\text{Sg}$ $^{207}\text{Pb} (^{54}\text{Cr},2\text{n})^{259}\text{Sg}$ $^{208}\text{Pb} (^{54}\text{Cr},3\text{n})^{259}\text{Sg}$ |
| 107 | Bohrium Nielsbohrium | 1981, East Germany | $^{209}\text{Bi} (^{54}\text{Cr},\text{n})^{262}\text{Bh}$ |
| 108 | Hassium | 1984, East Germany | $^{208}\text{Pb} (^{58}\text{Fe},\text{n})^{265}\text{Hs}$ |
| 109 | Meitnerium | 1982, East Germany | $^{209}\text{Bi} (^{58}\text{Fe},\text{n})^{266}\text{Mt}$ |
| 110 | Darmstadtium | 1994, Germany 1991–1994, United States 1994, United States/Soviet Union | $^{208}\text{Pb} (^{62}\text{Ni},\text{n})^{269}\text{Ds}$ $^{208}\text{Pb} (^{64}\text{Ni},\text{n})^{271}\text{Ds}$ $^{209}\text{Bi} (^{59}\text{Co},\text{n})^{267}\text{Ds}$ $^{244}\text{Pu} (^{34}\text{S},5\text{n})^{273}\text{Ds}$ |
| 111 | Roentgenium | 1994, Germany | $^{209}\text{Bi} (^{64}\text{Ni},\text{n})^{272}\text{Rg}$ |
| 112 | Copernicium | 1996, Germany | $^{208}\text{Pb} (^{70}\text{Zn},\text{n})^{277}\text{Cn}$ |
| 113 | | 2003, Russia | By alpha decay of the element with $Z = 115$ |
| 114 | | 1998, Russia | $^{244}\text{Pu} (^{48}\text{Ca},4\text{n})^{288}$ $^{244}\text{Pu} (^{48}\text{Ca},3\text{n})^{289}$ |
| 115 | | 2004, United States–Russia | $^{243}\text{Am} (^{48}\text{Ca},4\text{n})^{287}$ $^{243}\text{Am} (^{48}\text{Ca},3\text{n})^{288}$ $^{243}\text{Am} (^{48}\text{Ca},\text{xn})^{291-x}$ |
| 116 | | 2001, Russia | $^{248}\text{Cm} (^{48}\text{Ca},4\text{n})^{292}$ |
| 118 | | 1999, United States(?) | $^{208}\text{Pb} + ^{86}\text{Kr}$ Three atoms have been produced |

From the 1960s, transuranium elements have been produced in the Soviet Union (now Russia) too. At that time, the scientific research became political competition. This is reflected in the names of the transuranium elements: every discoverer gives a name to the new element even if that element already had a name. There have been heated arguments about this issue, for example, the American scientists did not accept the production of kurtchatovium (presently known as rutherfordium) by the Russian scientists since they were said to give an incorrect half-life for the element. For this reason, there are elements in [Table 6.3](#) that have several names. Finally, in 1997, IUPAC accepted the names, and they are official now (shown in bold in the table).

The American and the Soviet scientists had different strategies for the production of the transuranium elements. The American scientists tended to irradiate heavier targets with smaller particles; in these cases, the targets had to be produced in higher quantities. The scheme of this method is shown in [Figure 6.9](#). The Soviet scientists, however, irradiated lighter targets with heavier particles. This procedure required greater and greater cyclotrons.

An important decay mechanism of the transuranium elements is spontaneous fission. The half-life of a transuranium nuclide decreases as the atomic number increases. For example, the half-life of ^{241}Am is 432 years and that of ^{252}Cf isotope is 2 years, but lawrencium isotopes have half-lives measured in seconds. At $Z > 108$, the half-lives are milliseconds or even shorter. For this reason, the production of the element with $Z = 118$ is questionable because only three atoms have been produced, and this result has not been repeated by other institutes.

6.3 General Scheme of Radionuclide Production by Nuclear Reactions and Radioactive Decay

In [Figure 6.10](#), the opportunities of the production of a nuclide with a Z atomic number and an A mass number are summarized. [Figure 6.10](#) includes the formation of the nuclide by radioactive decays too.

6.4 Chemical Effects of Nuclear Reactions

Of course, the production of a nuclide with a different atomic number itself means a chemical change. In this chapter, however, we do not deal with the direct transformation of the nuclei to other ones, but the subsequent chemical effects of the nuclear reactions. These effects are caused by the fact that the energy of the nuclear reactions is several orders of magnitude higher than the energy of the chemical bonds. As mentioned in Section 2.2, the energy of the nuclear processes, including nuclear reactions, is in the range of MeV, while the energy of the primary chemical bonds is in the range of eV. The high energy of the nuclear reactions obviously results in chemical changes in both the target and the product. In this context, the target and product mean not only the target and product nuclide but also their entire chemical environment.

| | | | | | |
|-----|-------------|----------------------------|--------------------|---------------------------|----------|
| | A | A+1 | A+2 | | |
| A-1 | | | | | α |
| Z+1 | | n,p EC, β^+ | n,d γ, p | d, α | |
| Z | | n, γ d,p | A_ZN | γ, n n, 2n | |
| Z-1 | α, p | d, γ α, d | d,n | β^- p,n d, 2n | |
| Z-2 | α, n | | | | |
| | | N-2 | N-1 | N | N+1 |

Figure 6.10 Summary of different options to produce a nuclide with Z atomic number and A mass number. It includes the formation of the nuclide by radioactive decays as well. *Source:* Reprinted from Choppin and Rydberg (1980), with permission from Elsevier.

The energy of the nuclear reaction is not thermal energy; rather, it is the kinetic energy of the nuclide and particles taking in the reaction (Figure 6.7). The kinetic energy, however, can be expressed as temperature. Thus, the energy of the nuclear reactions means a very high temperature, so the atoms formed in the nuclear reactions are frequently called “hot atoms.”

As mentioned in Section 4.4.1, an important process during alpha decay is the recoil. This process also takes place in other radioactive (beta and gamma) decays (as discussed in Section 5.4.7) and in nuclear reactions. The energy of the recoil is higher for the heavier particles. This means that the recoiling energy of the recoiled nucleus decreases as the mass of the emitted particle decreases. However, even the recoiling energy caused by the emission of the lightest-radiation gamma photon can be higher than the energy of the chemical bond. This energy can excite the orbital electrons of the atoms. Depending on the recoiling energy and the atomic number, the inner orbital electrons, as well as the outer orbital electrons, can be excited. The excitation of the inner electrons can result in the phenomena discussed in Sections 4.4.3 and 5.4.4, namely, the emission of characteristic X-ray photons and Auger electrons. The excitation of the outer electrons can result in ionization and breaking of the chemical bonds. This effect, which is the rupture of the chemical bond between an atom and the molecule of which the atom is a part as a result of a nuclear reaction of that atom, is called the “Szilard–Chalmers effect.” The other name of this field is “hot atom chemistry.”

The first reaction studied by Szilard and Chalmers was the (n, γ) reaction of ${}^{127}\text{I}$. Iodine was irradiated as ethyl iodide. The product was an excited, radioactive

^{128}I nuclide, which transformed to an iodide ion that could be extracted by water. As a result of the nuclear reaction, the organic iodine transformed to inorganic iodine, meaning that the target and product nuclides were present as different chemical species. Thus, they could be chemically separated. In spite of the target and product nuclides having the same atomic number, the radioactive ^{128}I could be produced as a carrier-free radioactive isotope. Therefore, a (n,γ) nuclear reaction could be suitable for the production of carrier-free radioactive isotopes if the nuclear reaction were accompanied by a chemical reaction that included a hot atom. Some examples are shown in Sections 8.5.2 and 8.6. In addition to the (n,γ) reaction, (γ,n) , $(n,2n)$, and (d,p) nuclear reactions are used.

From the point of view of radionuclide production, the Szilard–Chalmers effect has two important aspects: the enrichment of the excited, radioactive nuclide in the phase used for the separation of the product, and its retention in the phase containing the target nuclide. Mostly, the target is in an organic phase, and the product is formed as an inorganic ion. Carrier-free chlorine, bromine, iodine, chromium, manganese, phosphorous, and arsenic isotopes are produced in this way.

The reactions of the hot atoms can be applied to the production of labeled compounds. In the reaction $^{14}\text{N}(n,\gamma)^{14}\text{C}$, the ^{14}C hot atom can react with the substances in the environment in different ways, and many different molecules can be formed, such as CO_2 , CO , CH_4 , HCN , CH_3OH , HCOH , and HCOOH . These reactions take place in the nuclear reactors. The neutrons react with the nitrogen of the air, and then the hot ^{14}C atoms with the cooling water produce the molecules listed here.

It is important to note that chemical effects can occur as a result of the radioactive decay processes. For example, during the beta decays, the atomic number changes. If the recoil energy is not strong enough to break the chemical bond, the daughter nuclide remains in the same chemical structure, but it is already unstable. For example, the daughter nuclide of the negative beta decay of ^{14}C is ^{14}N . If ^{14}N is formed and substituted for the carbon atom of the organic molecule, the molecule will dissociate. The products can be radical or ions, which tend to react with any molecules or atoms in the environment, producing labeled substances. For example, the radiolysis of the organic molecules is mentioned here.

Further Reading

- Choppin, G.R. and Rydberg, J. (1980). *Nuclear Chemistry, Theory and Applications*. Pergamon Press, Oxford.
- Friedlander, G., Kennedy, J.W., Macias, E.S. and Miller, J.M. (1981). *Nuclear and Radiochemistry*. Wiley, New York, NY.
- Haissinsky, M. (1964). *Nuclear Chemistry and its Applications*. Addison-Wesley, Reading, MA.
- L'Annunziata, M.F. (2007). *Radioactivity: Introduction and History*. Elsevier, Amsterdam.
- Lieser, K.H. (1997). *Nuclear and Radiochemistry*. Wiley-VCH, Berlin.
- Vajda, N. (1994). Atomreaktorok fűtőelmeinek ellenőrzése új analitikai módszerek segítségével (Analysis of nuclear fuel elements by new methods). Candidate's Thesis. Budapest Technical University, Budapest.

7 Nuclear Energy Production

Radioactive decay is always exoergic since the mass of the parent nuclide is greater than the total mass of the daughter nuclide(s) and the emitted particle(s). The equation expressing the release of energy contains an expression describing the kinetic energy of the particles. When interacting with the environment, the particles slow down and become thermalized, and most of the kinetic energy transforms into thermal energy. The decay of the natural radioactive isotopes plays an important role in the heat balance of the Earth. The decay of 1 mol ^{238}U to ^{206}Pb releases about 4.3×10^{12} J of energy. The half-life of ^{238}U is 4.5×10^9 years, meaning that the release of this energy is a very long process.

Energy can be produced by nuclear reactions as well. This procedure has a very important practical role since energy can be released in a fairly short time in this way. The binding energy per nucleon can be calculated by means of the liquid-drop model of nuclei by Weizsäcker formula (see Eq. (2.17)). As seen in Figure 2.4, energy can be produced by two ways: by fusion of light nuclei (as discussed in Section 6.2.4) or by fission of heavy nuclei (see Eq. (6.21)).

In the fission reaction, two lighter nuclei and some neutrons are formed. The neutrons can initiate additional fission reactions if their energy is relatively low (thermal or slow neutrons). This process can be repeated, producing more and more neutrons. If the quantity of the fissile material reaches critical mass, a continuous fission, chain reaction takes place. The principle of the nuclear chain reaction was formulated and patented by Leo Szilárd in 1934, and it was experimentally proved by Otto Hahn in 1938. For this discovery, Hahn received the Nobel Prize in Chemistry in 1944.

When the number of fissions increases very rapidly and there are enormously high energy releases, the chain reaction becomes unregulated, as in the nuclear bombs (such as the ones used on Hiroshima on August 6, 1945 (U-235), and Nagasaki on August 9, 1945 (Pu-239), discussed in more detail in Section 7.5). The number of fissions, however, can be controlled. Controlled, sustained chain reactions occur in nuclear power plants.

The first nuclear reactor began to operate in the University of Chicago at 3:45 on December 2, 1942. This was the first artificial nuclear chain reaction. The first nuclear reactor constructed directly for energy production was opened in Obninsk, in the Soviet Union, in 1954. According to the International Atomic Energy Agency (IAEA), more than 440 nuclear reactors were operational as of August 2011, and their number increases continuously; more than 60 nuclear reactors are

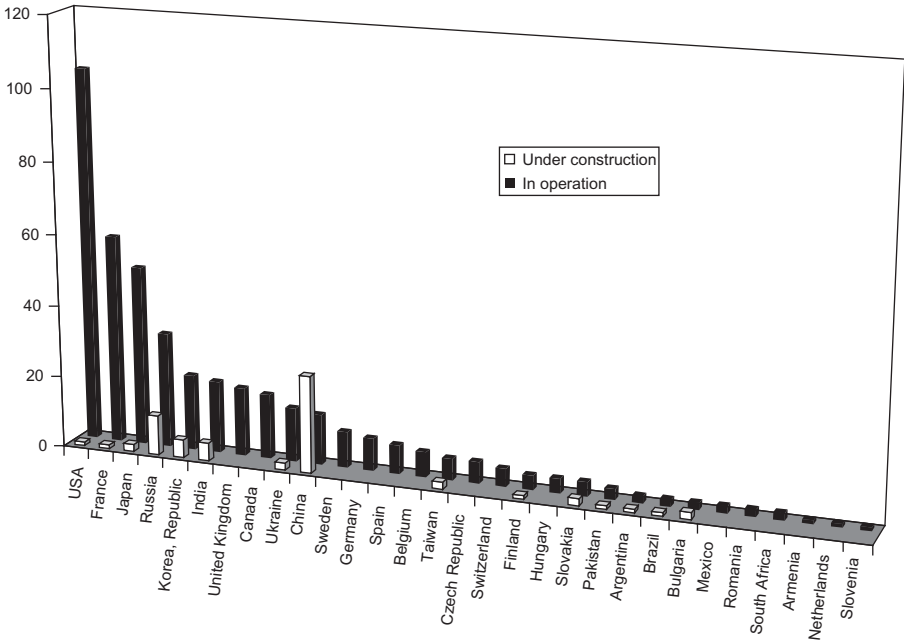


Figure 7.1 Nuclear reactors in operation and under construction worldwide.

under construction (Figure 7.1). The net electric power of the operating nuclear reactors is 365,837 MW and that of the reactors under construction will be 62,832 MW.

7.1 Nuclear Power Plants

The controlled and uncontrolled chain reaction of the fission of ^{235}U is used in nuclear power plants and weapons, respectively. The neutron balance is quantitatively determined using the effective neutron multiplication factor (k), which is the average number of neutrons produced from one fission that cause an additional fission:

$$k = \frac{n_s}{n_p} \quad (7.1)$$

where n_p and n_s are the number of primary and secondary neutrons, respectively.

One of the most important properties of the fission is that two to three neutrons per fission are released (see Eq. (6.21)), which can initiate new fission steps. The

condition of the sustainable chain reaction is that at least one of the released neutrons should initiate an additional fission. If the average number of the neutrons initiating new fission (k) is 1, the released energy becomes constant. In a stationary state, this is the case in nuclear reactors.

When the number of neutrons initiating additional fission is more than 1, the released energy exponentially increases. This is the case, for example, at the startup of nuclear reactors, or when the power produced by nuclear reactors is to be increased. Nuclear weapons are designed to operate in this way.

In fission reactions, the energy of the released neutrons is usually high (1–2 MeV); the additional fission, however, can be initiated only by slow or thermal neutrons (<0.1 eV). For this reason, the velocity or energy of the neutrons has to decrease, which significantly influences the neutron multiplication factor. When the fissile material is assumed to be in an infinite quantity, the multiplication factor (k_{∞}) is given by the so-called four-factor formula as follows:

$$k_{\infty} = \varepsilon p f \eta \quad (7.2)$$

In this equation, ε is the fast fission factor, which takes into consideration that the fast neutron can initiate another fission to a small degree (by 1–3%); p is the resonance escape probability, the fraction of neutrons escaping capture while slowing down. The value of p usually ranges from 0.6 to 0.9 and is increased by all factors assisting the slowing down of the neutrons (e.g., by the improvement of the moderators) by decreasing the size of the fuel and by increasing its distance from the fuel rods. The thermal utilization factor, f , is the ratio of the thermal neutrons initiating additional fission to the number of thermal neutrons captured by another reaction (e.g., by nuclides other than fissile ones). And η is the thermal neutron yield, that is, the number released in the fission process.

If the size of the fuel is finite, the effective multiplication factor (k_{eff} in Eq. (7.1)) is used; $k_{\text{eff}} < k_{\infty}$. At $k_{\text{eff}} < 1$, the chain reaction stops because of the continuous decrease of the neutrons. The reactor is *subcritical*. When $k_{\text{eff}} = 1$, the rate of the chain reaction is constant, and the reactor is critical. When $k_{\text{eff}} > 1$, the number of the neutrons, and, as a consequence, the number of fission reactions, increases and the reactor is supercritical.

A characteristic property of the reactor is the reactivity (ρ):

$$\rho = \frac{k_{\text{eff}} - 1}{k_{\text{eff}}} \quad (7.3)$$

The value of ρ can be negative, zero, or positive, depending on whether the reactor is subcritical, critical, or supercritical, respectively. Since the fissile material is continuously used up by fission, the fission products can also capture neutrons, and a certain excess of reactivity is required for the critical operation.

7.1.1 The Main Parts of Nuclear Reactors

The very simple scheme of a nuclear reactor and the connecting energetic units are shown in [Figure 7.2](#). The arrangement of the fuel and control rods in the reactor vessel is shown in [Figure 7.3](#).

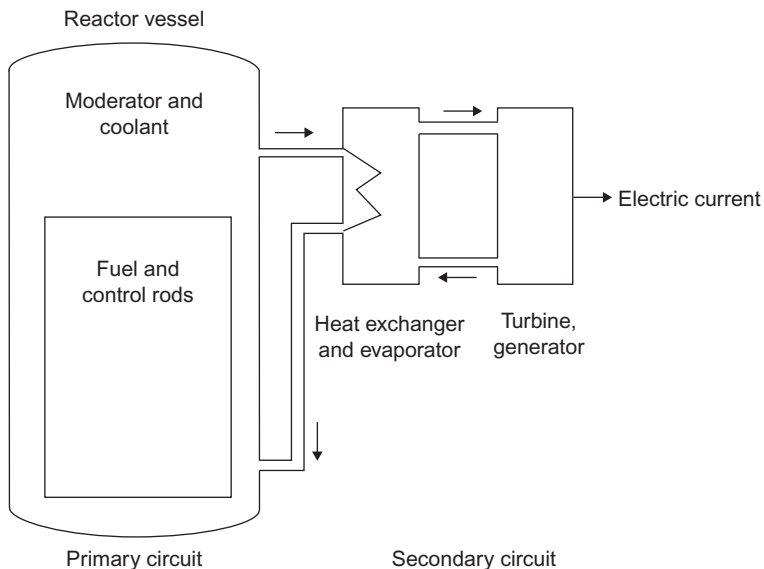


Figure 7.2 A very simple scheme of a nuclear reactor and the connecting energetic units.

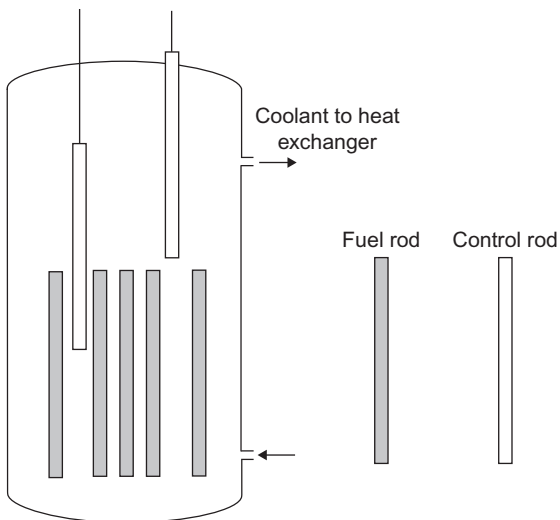


Figure 7.3 The arrangement of the fuel and control rods in the reactor vessel.

The most important parts of the nuclear reactors are the fuel elements, moderator, reflector, cooling system, control rods, and shielding. In the following sections, the material, properties, and operation of these parts will be discussed.

7.1.1.1 Fuels of Nuclear Power Plants

Most nuclear power plants use uranium-235 as fuel. Under geological conditions, the thermodynamically stable species of uranium is the uranyl cation (UO_2^{2+}), which is fairly soluble in water. As a result, uranium is present everywhere in the Earth's crust, its concentration is relatively low, and the average concentration is about 3–5 ppm. Uranium can be extracted economically from rocks that have a concentration of uranium that is at least a couple of thousand parts per million. The most important uranium ore is uranium pitchblende, with mean uranium content about 0.5–0.8%. About 40% of the uranium of the Earth is in Australia.

The uranium is produced from the ore by crashing the ore into smaller pieces, and then concentrated the uranium containing ores by flotation. If uranium is present as U(IV), it is oxidized to U(VI) by air, or sometimes in a microbiological way. Then, the substance is leached by sulfuric acid. The formed uranyl sulfate complex, $[\text{UO}_2(\text{SO}_4)_2]^{2-}$, is separated by ion exchange resins or by extraction using an organic solvent. Since natural uranium contains 99.3% ^{238}U and only 0.7% ^{235}U , and because ^{235}U -enriched uranium compound is needed as fuel for nuclear reactors, the uranyl sulfate must be converted into a species that is appropriate for isotope enrichment. This species of uranium is UF_6 , the gas diffusion of which can be used for isotope enrichment. However, even uranium with a natural isotopic ratio can initiate fission chain reaction.

In addition to uranium, artificial fissile material such as ^{239}Pu , ^{241}Pu , and ^{233}U (see Eqs. (6.22) and (6.23)) can be used as fuels. The fuel has to have a high cross section for thermal neutrons. Since the released energy is huge, the heat resistance of the compound of the fissile isotope is also important. The activation of the other atoms in the compound has to be avoided. These conditions are fulfilled by oxides. Usually, uranium dioxide (UO_2), plutonium dioxide (PuO_2), and thorium dioxide (ThO_2) are used. In some reactors, uranium carbide (UC) has been tested. Mixed oxides, the so-called MOXs, are also produced from plutonium oxide and uranium oxide. For homogeneity, the oxides are co-precipitated from oxalate and then calcinated to oxide. MOX is used in light water reactors (as discussed in Section 2.1.1.2). One advantage of MOX fuel is that it provides a way to dispose of the surplus of weapons-grade plutonium, which otherwise would have to be disposed of as nuclear waste and would remain a nuclear proliferation risk. The characteristic properties of the most important fuels are shown in [Figure 7.4](#).

Uranium dioxide is prepared as pellets and placed into rods made of zircon, zircalloy (zirconium with 1% niobium), or another metal. The rods are hermetically sealed and placed into the active zone of the reactor with the moderator. The seal should ideally be hermetic, but in reality, the fuel rods often have micro- and macro-ruptures through which the gaseous and soluble fission products can escape. A part of the gaseous fission products (Kr-85 , Xe-133 , and Xe-135 isotopes) is

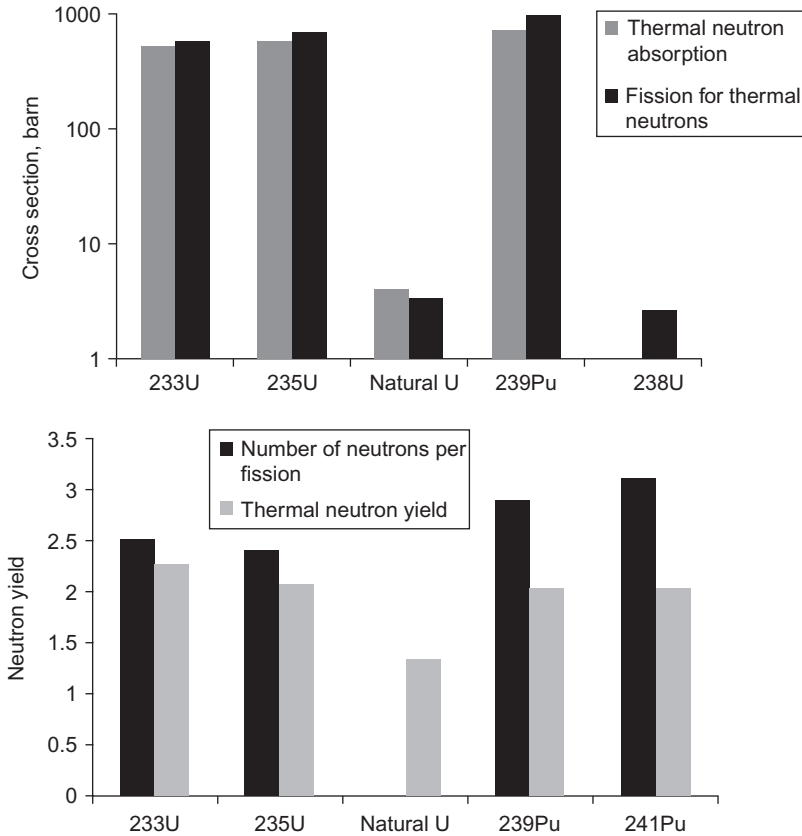


Figure 7.4 The characteristic properties of the most important fuels.

emitted into the atmosphere. The gaseous molecules and compounds of iodine are filtered, usually by coal filters. The relative activities of the iodine isotopes with different half-lives give information on the size of the ruptures. The presence of iodine isotopes with short and long half-lives indicates the existence of macro- or micro-ruptures, respectively. Besides the gaseous fission products, the gaseous compounds of tritium and C-14 (see Section 7.3) are also released into the atmosphere. To decrease the emitted radioactivity, the gas emission is delayed or ignited and the products are condensed.

If the moderator (Section 7.1.1.2) and/or the coolant (Section 7.1.1.5) is water or heavy water, the soluble fission products (e.g., Cs-137, Cs-134, strontium, and iodine ions) can dissolve in them. For this reason, water is continuously purified by ion exchangers.

During the operation of nuclear reactors, the quantity of ^{235}U continuously decreases; the fissile material is burning up. Most of the ^{235}U present in the reactor undergoes fission reaction; however, a small part converts to ^{236}U in an (n,γ) reaction. Similarly, the (n,γ) reaction of ^{238}U produces transuranium elements,

Table 7.1 The Number of Collisions to Thermalize and the Moderation Ratio of Different Substances

| Substance | Number of Collisions to Thermalize | Moderation Ratio |
|------------------|------------------------------------|------------------|
| H ₂ O | 19 | 62 |
| D ₂ O | 35 | 4830 |
| He | 42 | 51 |
| Be | 86 | 126 |
| B | 105 | 0.00086 |
| C | 114 | 216 |

including ²³⁹Pu and ²⁴¹Pu (Eq. (6.23)), which also undergoes fission reaction, increasing the power of the nuclear reactors. There are nuclear reactors specifically made to produce fissile plutonium isotopes, which are called “breeder reactors.”

The operation of the nuclear reactors is influenced by the fission products. Some of them (e.g., ¹³⁵Xe and ¹⁴⁹Sm) strongly absorb neutrons, decreasing the number of the neutrons and the reactivity. These fission products are called “reactor poisons.”

7.1.1.2 The Moderator of Nuclear Power Plants

Another important part of nuclear reactors is the moderator. Its function is to slow down the fast neutrons emitted in the fission reaction by reducing the energy of neutrons to the level of thermal neutrons. Light elements are suitable moderators because they can effectively decrease the energy of the fast neutrons through inelastic collisions with neutrons. According to its atomic mass, hydrogen (¹H) is expected to be the most effective moderator; however, a suitable moderator must also have a small cross section for neutron captures, which hydrogen does not have. Hydrogen can capture neutrons easily, transforming to deuterium. Deuterium is the most effective moderator, but it is rather expensive. The ratio of the moderator effect and the neutron capture can be expressed by the moderation ratio (given in [Table 7.1](#)).

Frequently used moderators are the following:

- Water (H₂O), which is an effective moderator, absorbs part of the neutrons. A water-moderated reactor is shown in [Figure 7.2](#).
- Heavy water (D₂O), which is an effective moderator, absorbs only a few neutrons, but it is expensive.
- Graphite, which is a less-effective moderator than water, absorbs only a few neutrons. Its disadvantage is that it is flammable. In the first nuclear reactor, graphite was applied as the moderator.
- Beryllium and organic solvents are also suitable as moderators.

7.1.1.3 Moderator/Fuel Ratio

The moderator decreases the velocity of the neutrons, as discussed in [Section 7.1.1.2](#). In addition, the moderator acts as a passive controller of the operation of the nuclear reactors.

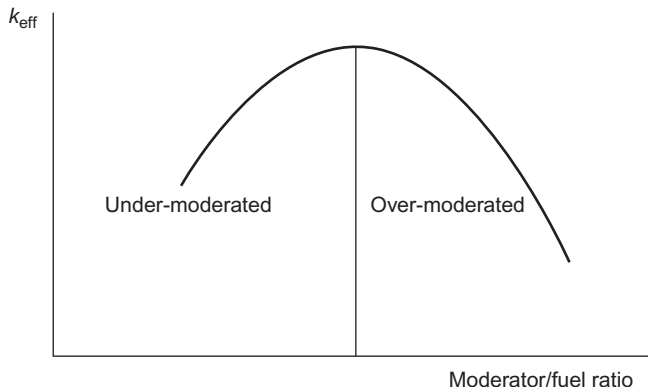


Figure 7.5 The effect of the moderator/fuel ratio on the effective neutron multiplication factor.

All substances, including moderators, more or less absorb neutrons, inhibiting the fission chain reaction. Thus, if the reactor contains too much moderator, the degree of neutron absorption increases. However, if the quantity of the moderator is too low, the velocity of the neutrons does not decrease enough. As a result, the effective neutron multiplication factor versus the moderator/fuel plot function has maximum. Those reactors in which the moderator/fuel ratio is below the maximum are under-moderated, and those in which this ratio is above the maximum are over-moderated (Figure 7.5).

Under- and over-moderation play an important role in the safety operation of the reactors. The under-moderated reactors are safer because the decrease of the quantity of the moderator results in the decrease of the effective neutron multiplication factor, stopping the reactor from entering a subcritical state. In over-moderated reactors, however, the decrease of the quantity of the moderator can increase the effective multiplication factor, and then the reactor can become supercritical (as happened in the Chernobyl accident, discussed in detail in Section 7.2).

7.1.1.4 Reflection of Neutrons

The active zone of the reactors is usually surrounded by a mantle consisting of the moderator (water, graphite, or another substance as previously mentioned). Thus, the number of the escaping neutrons can decrease because this mantle reflects a part of the escaping neutrons. The escaping neutrons influence the effective neutron multiplication factor. The application of the reflector can decrease the size of the reactor, and the fuel can be utilized more economically.

7.1.1.5 Coolants

The greatest part of the energy released in the fission is the kinetic energy of the fission products (Table 7.2). While the fission products are slowing down, the fuel

Table 7.2 Distribution of the Energy Released in the (n,f) Reaction of ^{235}U

| | Energy (MeV) |
|--|--------------|
| Kinetic energy of the fission products | 167 |
| Kinetic energy of neutrons | 5 |
| Prompt gamma radiation | 6 |
| Neutrinos | 12 |
| Beta radiation of fission products | 8 |
| Gamma radiation of fission products | 6 |

rods are heated. In operation, the temperature of the fuel rods may rise above 1000°C , and then they have to be cooled permanently. Therefore, the active zone always contains coolant.

Because of the strong neutron radiation in the active zone, the coolant becomes radioactive. For this reason, the coolant must be circulated in a closed system, which is called a “primary circuit.” The primary coolant is pumped into a heat exchanger full of tubes. Heat is transferred through the walls of these tubes to the lower-pressure secondary coolant located on the sheet side of the heat exchanger, where it evaporates to pressurized steam (a steam generator). In this way, the coolants in the primary and secondary circuits do not touch each other directly, so the secondary coolant remains inactive.

The pressurized steam formed in the steam generator is fed through a steam turbine, which drives the electric generator. In the meantime, the secondary coolant (a mixture of water and steam) is cooled down and condensed in a condenser. Then the condensed steam is pumped back into the steam generator (Figure 7.2).

In reactors moderated by light or heavy water, the moderator acts as a coolant too. In graphite-moderated reactors, the coolant is a gas (CO_2 or He) or water. In some reactors, molten metals (e.g., sodium), salts, organic solvent, He, or steam is applied as the coolant.

In the water reactors, the coolant is continuously purified by ion exchangers to remove the dissolved radioactive ions (e.g., cesium and iodide ions). The colloidal or greater solid particles are filtered.

7.1.1.6 Regulation of Chain Reactions

In the fission process, two or three neutrons are formed (Figure 7.4), 99% of which are emitted within a very short time. These are called “prompt neutrons,” and their mean half-life is about 10^{-4} s. Some fission products also emit neutrons (via neutron decay, as discussed in Section 4.4.4), and these are delayed neutrons. The amount of the delayed neutrons is less than 1% of the total numbers of the neutrons. Delayed neutrons play a role in the neutron balance of the reactor. If all the neutrons were produced as prompt neutrons, the whole fission products would be complete within a very short time and could not be controlled. Therefore, the

nuclear reactors are planned in such a way the controlled chain reaction can be initiated in the same time as the delayed neutrons.

The reactors are controlled by control rods. They are fabricated from very good neutron absorbers, such as boron (as boron carbide) or cadmium. The control rods are inserted among the fuel rods (Figure 7.3). The reactivity is controlled by the movement of the control rods. When the reactor starts, the control rods are raised. The power is measured by neutron detectors. When the power reaches the desired value, the control rods are stopped. So, the power does not continue to increase, the reactor becomes critical.

There are three different types of control rods:

1. Safety rods, whose function is the fast stop of the reactor in an emergency. In normal operation, they are totally raised.
2. Shim rods, which are used for coarse control and/or to change reactivity in relatively large amounts. They equalize the changes of the reactivity resulting in burn-up, poisoning, or breeding. Another tool for the equalization of reactivity is that neutron absorbers (usually boric acid) are dissolved in the coolant, whose concentration can be varied as required. Of course, this method can be applied only in the water reactors.
3. Regulating rods, which are used for fine adjustments and to maintain the desired power or temperature.

7.1.1.7 Shielding

In nuclear reactors, shielding against neutron and gamma radiation is essential. When planning the shielding for neutron radiation, it is important to take into consideration that the cross section for the fast neutron is rather small (see Figure 6.4). So, for shielding material, those substances should be chosen that efficiently slow down the neutrons and then efficiently absorb the thermal neutrons. The same moderators discussed in Section 7.1.1.4 are suitable for this purpose; therefore, the active zone of the reactors is usually surrounded by a mantle consisting of the moderator (water, graphite, etc.).

In nuclear reactors, the gamma radiation is very intense. The intensity of the gamma radiation continuously increases because of the increase of the quantity of the fission products. For protection against the gamma radiation, substances with a high atomic number and density are suitable. The stainless steel reactor vessel itself provides some shielding against gamma radiation. The nuclear reactors are surrounded by a thick concrete wall.

7.1.2 Natural Nuclear Reactors

The analysis of uranium ores shows that the ratio of ^{238}U : ^{235}U isotopes in the natural uranium is constant (139:1), and the concentration of ^{235}U is about 0.7%. There is just one uranium pitchblende, in Oklo (Gabon), in which the ratio of ^{238}U : ^{235}U is higher than the usual value, the concentration of ^{235}U is below 0.5% (^{238}U : $^{235}\text{U} > 200$:1). Studies of this uranium mine have shown that the concentration of the rare earth elements is also higher, and they show similar ratios to the

fission products of ^{235}U . For example, natural neodymium contains 27% ^{142}Nd , while the Oklo ores contain less than 5% ^{142}Nd . The ^{143}Nd content, however, typically is 12%, while its concentration in the Oklo samples is 24%. Neodymium formed in the fission of ^{235}U contains 29% ^{143}Nd and no ^{142}Nd isotope.

These values indicate that the fission of ^{235}U could be taken place a very long time ago; that is, a natural nuclear reactor could have been present long ago. Natural water probably acted as the moderator. Based on the composition of the fission products and the uranium content, the properties of the natural reactors are estimated to be as follows: the neutron flux was $<10^9$ neutron/cm² s in the core of the reactor, and its power was less than 10 kW about 2 billion years ago. It consumed about 6 tons of ^{235}U , and produced about 1 ton of ^{239}Pu .

7.1.3 The First Artificial Nuclear Reactor

The first artificial reactor was built in Chicago in the early 1940s as part of the Manhattan Project. The project supervisor was Enrico Fermi, in collaboration with Leo Szilárd, the discoverer of the chain reaction. The first self-sustaining chain reaction was started on December 2, 1942. The fuel was enriched uranium, and the moderator was graphite. The controls consisted of cadmium-coated rods that absorbed neutrons. The withdrawal of the rods increased neutron activity, leading to a self-sustaining chain reaction ($k_{\text{eff}} = 1$). The reactor had no radiation shielding and no cooling system. Fermi himself described the apparatus as “a crude pile of black bricks and wooden timbers.”

The construction of nuclear reactors for energy production started in the 1950s. As mentioned previously in this chapter, the first nuclear reactor built specifically for energy production opened in Obninsk in 1954.

7.1.4 Types of Nuclear Reactors

Nuclear reactors may be built for many different purposes, such as energy production, breeding of new fissile materials, production of radioactive isotopes, and for research and education. The nuclear reactors are classified based on factors that include the following:

1. Energy of the neutrons: thermal neutrons for energy production or fast neutrons for the breeding of new fissile material;
2. Fuel: natural uranium, enriched uranium, plutonium, or MOX;
3. Moderator: light water, heavy water, graphite, and so on;
4. The distribution of the fuel and moderator: homogeneous, quasi-homogenous, or heterogeneous;
5. Coolant: gas, heavy and light water (boiling or pressurized), molten metals and salt, or organic compounds.

Nuclear power is used in many naval vessels (e.g., submarines and icebreakers), both for military and civil (including scientific) purposes. As an example, the main technical parameters of a frequently used pressurized light-water-moderated

Table 7.3 The Main Technical Parameters of a VVER (PWR)

| | |
|--|--|
| Electric power | 440 MW |
| Heat power | 1375 MW |
| Fuel | |
| Enriched uranium, ^{235}U content | 1.6–2.4–3.6% |
| Quantity of fuel | 42 tons |
| Chemical species | UO_2 |
| Number of fuel rods | 44,000 |
| Number of fuel assemblies | 312 |
| Number of control rod assemblies | 37 |
| Sizes of UO_2 pellets | |
| Diameter | 7.65 mm |
| Height | 30 mm |
| Pellets per rod | ≈ 80 |
| Density of UO_2 | 10.6–10.97 kg/dm ³ |
| Sizes of fuel rods | |
| External diameter | 9.1 mm |
| Length | 2570 mm |
| Thickness of wall | 0.65 mm |
| Filling gas | He |
| Cladding | Zr with 1% Nb |
| Data of fuel assemblies | |
| Number of fuel rods per assembly | 126 |
| Hexagonal size | 144 mm |
| Cladding | Zr with 2.5% Nb |
| Mean burn-up after 3 years | 28,600 MWday/t U |
| Maximal surface contamination | 10^{-9} g $^{235}\text{U}/\text{cm}^2$ |
| Moderator and coolant | Light water |
| Mass of coolant in primary circuit | 1.93×10^5 kg |
| Pressure at the outlet | 12.26 MPa |
| Concentration of boric acid in primary circuit | 0–12 g/kg |
| Concentration of potassium hydroxide | 2–16 mg/kg |
| Concentration of ammonia | 0–5 mg/kg |

and -cooled reactor (PWR) are summarized in [Table 7.3](#). This reactor type was designed in the Soviet Union and referred to as VVER (the Russian translation of “pressurized light-water-moderated and -cooled energy producing reactor”).

7.1.5 Environmental Impacts of Nuclear Reactors

7.1.5.1 Positive Impacts

Nuclear power plants have many positive environmental and economical effects. The specific energy production (energy per mass of fuel) is much higher than that of other types of power plants. For example, the electric energy produced from 10 g uranium dioxide is equivalent to the energy obtained from about 1100 m³ gas,

900 dm³ oil, or 5 tons of coal. Conventional thermal power plants emit many pollutants such as sulfur dioxide, nitrogen oxide, and carbon dioxide, increasing the greenhouse effect and damaging the ozone layer of the Earth's atmosphere. Moreover, the ash produced by coal-based thermal power plants can contain radioactive isotopes; in addition, they emit radon, which is also radioactive, along with its daughter elements. Nuclear power plants, however, do not increase the greenhouse effect and do not damage the ozone layer. In addition, the emission of the radioactive isotopes can be much lower in nuclear power plants than in thermal power plants. For example, a PWR nuclear reactor can emit about 0.01 Bq/s radioactivity, while a coal-based thermal power plant can emit 2700 Bq/s, supposing that coal is rather radioactive.

This is true even if we compare nuclear energy to renewable energy. For example, the production of 2000 MW of electricity by solar energy requires solar elements with 600 km² surface area, supposing sunshine over 24 h/day (a condition not existing in real life). In addition, the production of the solar elements and the accumulators use gallium, arsenic, selenium, and other elements which become heavy pollutants when disposed.

7.1.5.2 Negative Impacts

Under normal operation, nuclear power plants emit few radioactive gases. This emission is regularly checked. In accidents, however, the emission of the radioactive isotopes can increase. Because of the very strict safety regulation, accidents are very rare, and they are always caused by human faults or natural catastrophes, such as earthquakes (see [Section 7.2](#) for more). A very important problem of nuclear energy production is the safety treatment and storage of the nuclear wastes (discussed in [Section 7.3](#)).

7.2 Accidents in Nuclear Power Plants

The safe operation of nuclear power plants is very important. People are very sensitive to all events, both usual and unusual, relating to the nuclear power plants, including their construction, operation and radioactive wastes. The safe operation is controlled by the IAEA. In 1990, an International Nuclear Event Scale was introduced, which evaluates events other than normal operations. The scale is as follows:

Level 1: Anomaly

- Overexposure of a member of the public to radiation in excess of statutory annual limits.
- Minor problems with safety components with significant defense-in-depth remaining.
- Low-activity lost or stolen radioactive source, device, or transport package.

Level 2: Incident

- Exposure of a member of the public to radiation in excess of 10 mSv. (The units of radioactive doses will be discussed in [Section 13.4.1](#).)

- Exposure of a worker to radiation in excess of the statutory annual limits.
- Radiation levels in an operating area of more than 50 mSv/h.
- Significant contamination within the facility into an area not designed for.
- Significant failures in safety provisions but with no actual consequences.
- Found highly radioactive sealed orphan source, device, or transport package with safety provisions intact.
- Inadequate packaging of a highly radioactive sealed source.

Level 3: Serious Incident

- Exposure to radiation in excess of 10 times the statutory annual limit for workers.
- Nonlethal deterministic health effect (e.g., burns) from radiation.
- Exposure rates of more than 1 Sv/h in an operating area.
- Severe contamination in an area not designed to handle it, with a low probability of significant public exposure.
- Near accident at a nuclear power plant with no safety provisions.
- Lost or stolen highly radioactive sealed source.
- Misdelaivered highly radioactive sealed source without adequate procedures in place to handle it.

Level 4: Accident with Local Consequences

- Minor release of radioactive material unlikely to result in implementation of planned countermeasures other than local food controls.
- At least one death from radiation.
- Fuel melt or damage to fuel resulting in more than 0.1% release of core inventory.
- Release of significant quantities of radioactive material within an installation with a high probability of significant public exposure.

Level 5: Accident with Wider Consequences

- Limited release of radioactive material likely to require implementation of some planned countermeasures.
- Several deaths from radiation.
- Severe damage to the reactor core.
- Release of large quantities of radioactive material within an installation, with a high probability of significant public exposure. This could arise from a major accident or fire.

Level 6: Serious Accident

- Significant release of radioactive material likely to require implementation of planned countermeasures.

Level 7: Main Accident

- Major release of radioactive material with widespread health and environmental effects requiring implementation of planned and extended countermeasures.

The most important nuclear accidents and their impacts are briefly presented here.

1957, Windscale (Great Britain): In a plutonium breeding reactor, graphite heated up. As a result, some fuel rods filled with natural uranium were melted and

radioactive isotopes (^{131}I , ^{132}Te , ^{137}Cs , ^{89}Sr , ^{90}Sr , and noble gases) were emitted into the environment. About 700 km^2 was contaminated. The effect on human populations could not be detected. The emitted radioactivity was $4 \times 10^{16}\text{ Bq}$. The average effective dose in the area of the power plant was 0.8 Sv . This incident was categorized as a Level 5 accident on the International Nuclear Event Scale.

1979, Three Mile Island (USA? Pennsylvania): Because of the coincidence of some technical, mechanical problems and human mistakes, the reactor got out of control, and the active zone melted. ^{131}I and radioactive noble gases were emitted into the environment. The polluted coolant was emitted into the Susquehanna River. The effect on human populations could not be detected. The dose evaluation showed that one more instance of cancer was expected for the 2 million inhabitants within 20 years (the usual number of cancer is 350,000). The emitted radioactivity was about 10^{15} Bq . The average effective dose in the area of the power plant is not known. This event was treated as a Level 5 accident on the International Nuclear Event Scale.

1986, Chernobyl (Soviet Union, today Ukraine): This accident took place during a test to determine how long turbines would spin and supply power to the main circulating pumps following a loss of the main electrical power supply. The automatic shutdown mechanisms did not permit some of the operations. For this reason, the operators, who were not well trained in this type of reactor, switched them off, and a sudden power increase boiled up the coolant water. Water vapor is less able to absorb the neutrons than liquid water, so the neutron flux increased. This resulted in an increase of power. By the time the operator attempted to shut down the reactor, the control rods were too high to stop the chain reaction. In addition, the control rods were made of boron carbide with graphite tips. The graphite tips initially displaced coolant before neutron-absorbing material (boron) was inserted and the reaction slowed. As a result, the power continued to increase, and the total volume of coolant boiled up. At the same time, the reactor prompt became critical. The interaction of very hot fuel with the cooling water led to fuel fragmentation, along with rapid steam production and an increase in pressure. The overpressure caused a steam explosion that released fission products into the atmosphere. Seconds later, a second explosion occurred, in which the hydrogen produced from the reaction of the graphite moderator and zirconium cladding with water blew up. In this process, the graphite moderator could react with the oxygen of the air, graphite ignited. Since the reactor was over-moderated (Figure 7.5) and the moderator/fuel ratio decreased, the multiplication factor continued to increase.

In the Chernobyl accident, about 5% of the fuels were emitted into the atmosphere. This contained the fission products (e.g., ^{131}I and other iodine isotopes, ^{134}Cs and ^{137}Cs , Sr isotopes, noble gases), uranium, and transuranium elements. A significant number of the radioactive isotopes were bounded to aerosols. The aerosols and the gaseous isotopes were spread over several thousand miles, at first in a northwest direction, then toward the south. The emitted radioactivity was about $2 \times 10^{18}\text{ Bq}$. The average effective dose in the area of the power plant was 6–16 Sv, in Chernobyl, 0.2–1 Sv, in Kyiv. This incident was categorized as a Level 7 accident on the International Nuclear Event Scale.

2011, Fukushima (Japan): The fourth strongest earthquake in history, followed by a tsunami, occurred in Japan. As a result, the power supply of the nuclear reactors was destroyed. The emergency instruments stopped the reactors; however, the decay of fission products that had already been produced continued and overheated the reactors. About 75% of the fuel melted. The operators tried to cool the melted fuel by adding sea water, which caused hydrogen explosions in four reactors (three operational and one nonoperational). The activity measurements of the radioactive isotopes (iodine-131 and cesium-137) showed the released radioactivity was about 15% of the released radioactivity in the Chernobyl accident. At first, the accident was assigned to Level 4 of the International Nuclear Event Scale, and then raised to Level 5 and then raised again to Level 7.

7.3 Storage and Treatment of Spent Fuel and Other Radioactive Waste

One of the very important aspects of nuclear energy production is the safe treatment and storage of nuclear waste. The sources of nuclear waste are as follows:

- The fission products of the (n,f) nuclear reactions,
- Transuranium elements produced in the (n, γ) reactions of uranium, and
- Radioactive nuclides produced in the (n, γ) reactions of the structural material and the environment.

As seen in Section 6.2.1, the fission reaction of ^{235}U (Eq. (6.21)) produces about 300 fission products, many of which are radioactive because the ratio of neutrons to protons is too high for stability (Figure 6.5). The fission products emit negative beta radiation, which are frequently accompanied by gamma radiation. As seen in the last two rows of Table 7.2, the energy of the beta and gamma radiation of the fission products is about 14 MeV, which is about 7% of the total energy released in the fission reaction. The radioactivity of the fission products as a function of time is shown in Figure 7.6.

As seen in Figure 7.6, the two most important fission products are ^{137}Cs and its daughter nuclide, $^{137\text{m}}\text{Ba}$, as well as ^{90}Sr and its daughter nuclide, ^{90}Y . Their fission yield is relatively high, and they have relatively long half-lives. Twenty years after the irradiation, the radioactivity of the fission products is almost exclusively due to the presence of these isotopes. About 60% originates from the ^{137}Cs – ^{137}Ba pairing, and about 40% originates from ^{90}Sr – ^{90}Y pairing. It should be noted, that cesium and strontium can substitute potassium and calcium in the living organism. Thus, two isotopes are considered to be the most dangerous fission products.

The transuranium elements are formed in the (n, γ) reaction of ^{238}U (Figure 6.22), which composes the main part (>95%) of the fuel elements. Similar reactions produce additional isotopes of the transuranium elements up to ^{246}Pu , ^{244}Am , and some curium isotopes, respectively.

(n, γ) nuclear reactions take place with the structural material and the elements in the environment; for example, with the coolant, the air, and so on. Besides (n, γ),

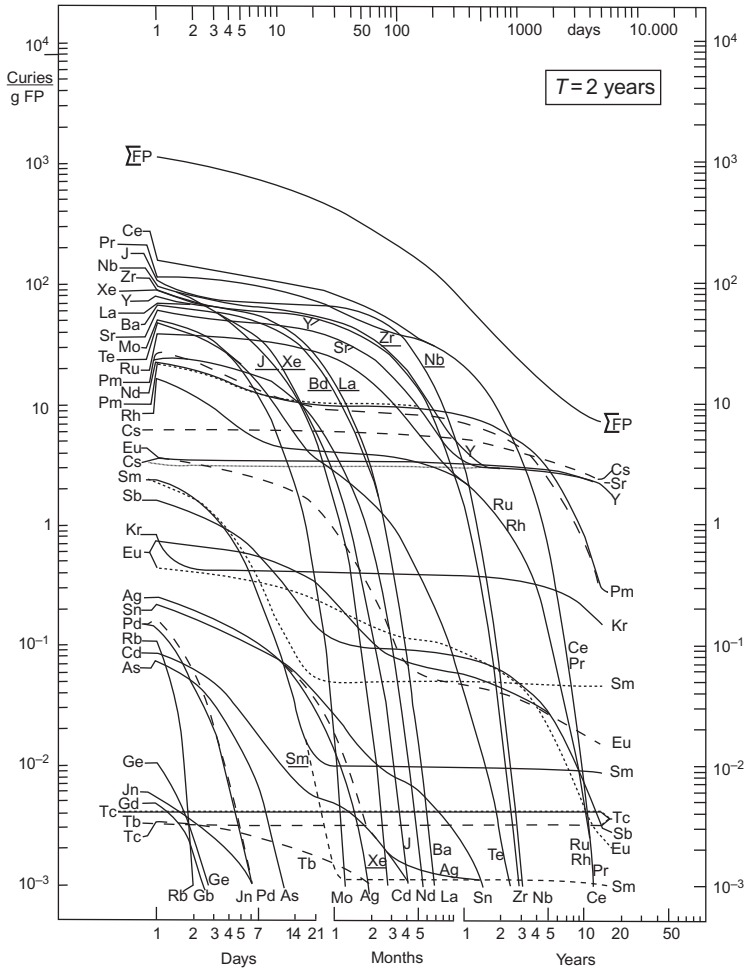


Figure 7.6 Radioactivities of fission products formed in the thermal fission of ^{235}U after an irradiation time of 2 years. The neutron flux is denoted as: ... 10^{12} n/cm² s, 10^{13} n/cm² s, and 10^{14} n/cm² s.

Source: Reprinted from Prawitz and Rydberg (1958), with permission from the Swedish Chemical Society.

other nuclear reactions can also produce radioactive isotopes. For example, C-14 isotope can be formed by the (n,p) reaction of the nitrogen in the air: $^{14}\text{N}(n,p)^{14}\text{C}$. Tritium is also formed from the nitrogen by $^{14}\text{N}(n,3\ ^4\text{He})\text{T}$ and $^{14}\text{N}(n,\text{T})^{12}\text{C}$ reactions. The most important radioactive isotopes produced in these reactions are T, C-14, N-15, N-16, O-19, F-18, Ar-41, Cr-51, Mn-54, Fe-55, Fe-59, Co-58, Co-60, Ni-63, Zn-65, and Ag-110.

Nuclear wastes are formed during the mining and refining of uranium ores, the production and reprocessing (see [Section 7.3.2](#)) of the fuel element, or in the

industrial, medical, or research isotope laboratories and any applications of sealed and unsealed radioactive sources.

The radioactive wastes are classified based on their activities. The classification is different in different countries; the IAEA also has radioactive waste safety standards. The radioactive wastes can be classified as follows:

- Low-level wastes; for example, the wastes of radioactive workplaces, such as contaminated tools, clothes, and laboratory vessels.
- Intermediate-level wastes have higher activity and often require shielding. The ion exchange resins, filters, chemical sludge, and other technological wastes of nuclear power plants belong to this group. Under normal operating conditions, these wastes contain fission products, and the radioactive isotopes produced by the nuclear reactions of the structural material and the nuclides of the environment. The quantity of the transuranium elements is very low. The radioactivity of the isotopes in a container filled with typical intermediate-level waste is shown in [Figure 7.7](#). Low- and intermediate-level wastes are frequently handled together.
- High-level waste, such as the wastes formed in the core of the nuclear reactors; namely, the spent fuel elements. In addition, the reprocessing of the spent fuel elements (see [Section 7.3.2](#)) produces high-level radioactive waste. Their radioactivity and heat emission is high; thus, they require shielding and cooling by air or in basins filled with water. High-level nuclear waste is stored under these conditions up to approximately 50 years.

In the United States, the transuranium nuclear wastes are also differentiated and treated separately, independent of their alpha activity.

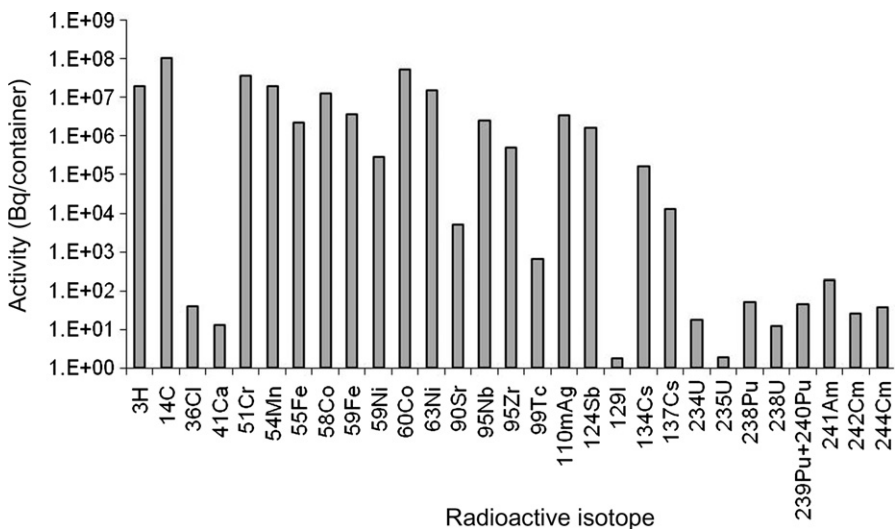


Figure 7.7 Radioactivity of the isotopes in a container filled with typical intermediate-level waste.

7.3.1 Storage of Low- and Intermediate-Level Nuclear Waste

Low- and intermediate-level radioactive wastes are buried in geological repositories. These repositories must isolate the nuclear waste from the biosphere as long as 100,000 years. For the storage of radioactive waste, the geological formations were used where water-soluble compounds have been accumulated for millions of years, such as salt mines, clay rocks, granite, and tuff. In these geological formations, further engineering barriers are constructed. The nuclear waste is placed into stainless steel or reinforced concrete containers and deposited inside the engineering barrier system. Only solid wastes are stored; liquid wastes are solidified by cementation or bitumen. The holes among the containers are filled with cement too.

There are some very important aspects to take into account when selecting a suitable environment for waste disposal. These are, for example, the hydrological properties of the geological environment, the corrosion and erosion of the engineering barrier system, leaching, and migration of the radionuclide in the geological environment. In addition, the microbiological activity and the effects of radiolysis have to be considered.

Low- and intermediate-level radioactive wastes contain the technological wastes of nuclear energy production (clothing, paper, wood, ion exchange resins, plastics, contaminated tools, instruments, etc.). In the corrosion and microbiological degradation of these substances, gaseous compounds are released. The corrosion produces hydrogen, while the microbiological processes transform the organic substances of the nuclear wastes into carbon dioxide or methane, depending on the redox conditions. The formation of carbon dioxide is less important because the anaerobic conditions are dominant in underground disposal. The gases can have unfavorable effects during storage. For example, the increasing pressure can push the radioactive gases and solutions into the environment. As a result of the cementation, the pH of the pore solution is set above 12. This pH inhibits the corrosion of the containers and the microbiological activity, decreasing the rate of gas release.

The radiolysis of water (discussed in Section 13.4.2) also releases gases; however, this reaction can be disregarded for the disposal of low- and intermediate-level nuclear waste.

7.3.2 Treatment and Storage of High-Level Nuclear Waste

As mentioned previously in this chapter, high-level nuclear waste (namely, the spent fuel elements) are stored under shielding and cooling in transitional disposals for about 50 years, and then they are deposited in geological repositories for final storage. The spent fuel elements contain the fission products and the transuranium elements. Before final storage, the spent fuel elements have to be treated in different ways. The aims of these treatments are as follows:

- To utilize the energy of beta and gamma decays,
- To produce additional fuel material (e.g., plutonium),
- To decrease the risk and cost associated with the storage of high-level nuclear waste,

- To decrease the cost of the fuel cycle of nuclear energy production, and
- To gain valuable by-products, e.g., fission products that can be used in other areas.

One possibility of treating the high-level nuclear waste is reprocessing. This is a chemical procedure in which the spent fuel elements are dissolved, and then the fission products, uranium, and transuranium elements are separated. In this way, about 97% of the high-level nuclear waste can be recycled. The steps of reprocessing are as follows:

- The spent fuel elements are cut into pieces and dissolved in 6–11 mol/dm³ HNO₃ solution. If the cladding is zircon or zircalloy, fluoride is also added to the solution. To avoid the chain reaction, neutron absorber (Cd, Gd) is also added.
- The gases released during the dissolution (Kr, Xe, I, T compounds, CO₂, etc.) are treated as they would in the normal operation of the nuclear power plant (see [Section 7.1.1.1](#)).
- By flowing oxygen gas; if there is any uranium in an oxidation state lower than 6, it is oxidized to uranyl cation (UO₂²⁺). As a result of the nitric acidic dissolution, all cations present in the solution are nitrates. The oxidation state of uranium and plutonium is +6 and +4, respectively.
- The uranium and plutonium is extracted by tri-butyl-phosphate dissolved in kerosene. This procedure is called the “PUREX procedure.” The fission products remain dissolved in the aqueous phase.
- The uranium and plutonium are separated by using the reduction of plutonium. For this reason, ferrous(II) sulfamate or U(IV) is added to the kerosene solution. Plutonium is reduced to Pu(III), then extracted by water. The uranium remains in the organic phase (kerosene). If required, this process can be repeated for additional purification.
- The fission products are separated from the aqueous phase using different techniques (precipitation, extraction, ion exchange, etc.). At first, the chemically similar fission products are separated, and then the individual isotopes are separated from the groups of the chemically similar elements. An example will be shown in Sections 8.5.2 (Eq. (8.17)) and 8.7.1.4 (Eq. (8.24)).
- The liquid residue of the procedure is solidified in the form of ceramics by the addition of Al(NO₃)₃ and SiO₂, or vitrified by Al(NO₃)₃, SiO₂, borax, or phosphates.

Besides recycling, isotopes with shorter and longer half-lives may also be separated during the reprocessing. In this way, both the quantity and the radioactivity of the high-level waste can be significantly reduced, and less-disposal capacity is required.

Another possibility for the treatment of high-level nuclear waste may be the transmutation of the fission products of the spent fuel elements to isotopes with shorter half-lives. During this treatment, the fission products are dissolved in melted salts and bombarded with neutrons with high flux. The neutrons are produced by the spallation reaction of an element with a high atomic number (such as Pb, Bi, or Hg) induced by the bombardment of protons with very high energy (>800 MeV). High-energy protons are generated in linear accelerators. The neutrons react with the nuclei of the fission products: fission, neutron capture, and then beta decay take place. Finally, radioactive isotopes with shorter half-lives, or even stable isotopes, can be produced. This process is exoergic; about 20% of the released energy is used for the operation of the linear accelerator, and the rest can

be utilized for other purposes. Thus, the nuclear energy production becomes more economical. The development of transmutation of spent fuel elements is in the experimental phase at the moment; we may have to wait a long time for the implementation of this process.

Independent of the treatment of spent fuel elements, some amount of high-level nuclear waste is always formed; so final disposal of this waste is always required. Today, the only real option for final disposal is storage in geological repositories; however, presently there is no operating geological repository for high-level radioactive waste. Some countries are researching the construction of such waste repositories, and they are expected to be operational by about 2040. In these repositories, high-level wastes are placed in stainless steel containers surrounded by a bentonite layer and natural geological formations.

7.4 New Trends in Nuclear Energy Production

7.4.1 *Improvement of the Fission in Nuclear Power Plants*

On the basis of their history and technical condition, nuclear power plants are classified into four groups. The first-generation (Generation I) nuclear power plants were developed in the 1950s–1960s in the Soviet Union, the United States, Great Britain, and France. Most of them have been dismantled now; only a few of these reactors are still operating. They do not fulfill today's safety, technical, and environmental requirements.

The second-generation (Generation II) nuclear power plants were the improved version of the first-generation plants; they are more safe, economical, and reliable. Most of the power plants in operation today belong to this type. PWRs are the most widespread; they provide about 65% of the total production of nuclear power plants today. The very important difference between first-generation reactors and the PWRs is that in PWR reactors, the total primary circuit (namely, all the contaminated parts of the reactor) is placed in containment, which is a high-volume, pressure-proof, hermetically sealed building. This creates a new safety barrier in case of an accident.

The third-generation (Generation III) nuclear power plants are improvements over the second-generation plants. For this reason, they are called “evolution nuclear power plants.” The number of evolution power plants is relatively low, there are some third-generation nuclear power plants, for example, in Japan, at this time, but they are being planned and constructed all over the world. Their typical features are as follows:

- They will be built using standard plans, so they can be up and running in a relatively short time (a few years); the operation time, however, is longer.
- Their structure is simpler and more robust than the previous reactors.
- They are safer because of the application of passive protection techniques.
- Their environmental impact is very low.
- The fuel is burned up better, so the fuel cycle is more economical and produces less waste.

The fourth-generation nuclear power plants are called “innovative plants” because they apply new technical solutions and have new safety requirements. The most important trends are as follows:

- In addition to ^{235}U , ^{238}U , and ^{232}Th will be utilized for energy production.
- Besides electric energy production, hydrogen will be produced by the electrolysis of water. This in itself should have a significant positive environmental impact because right now, hydrogen is produced from natural gas, which also produces carbon dioxide, increasing the greenhouse effect.
- To decrease the quantity of high-level nuclear waste produced, the facilities for the transmutation of the long-life radioactive isotopes (see [Section 7.3.2](#)) will be included in the nuclear reactor itself.
- The possibility of the production of the nuclear weapons from the spent fuel elements will be significantly reduced.

These aims may be achieved by different reactor types, such as thermal reactors, including the very-high-temperature reactor, the supercritical-water-cooled reactor, and the molten salt reactor; fast reactors, including the gas-cooled fast reactor; and molten metal (sodium, lead, lead–bismuth)-cooled reactors.

7.4.2 Experiments with Fusion Energy Production

As seen in Figure 2.2, the fusion of light elements also can be used for energy production. These thermonuclear processes provide the energy in stars (see Sections 6.2.4 and 6.2.5) and in the hydrogen bomb (see [Section 7.5](#)).

The potential of controlled thermonuclear reactions has been studied for several decades. These processes should provide the energy requirements of the Earth for a million years by the fusion of deuterium in the oceans. In addition, the fusion reactions produce no nuclear waste.

The thermonuclear reactions have two basic requirements. First, the temperature must be about 10^8 K because the ignition temperature of the $^2\text{H}-^2\text{H}$ reaction and the $^2\text{H}-^3\text{H}$ reaction are 3×10^8 and 3×10^7 K, respectively (Section 6.2.4). Second, the $n\tau$ value, the so-called Lawson limit, must be higher than 10^{21} particles s/m^3 for the $^2\text{H}-^2\text{H}$ reaction and 10^{20} particles s/m^3 for the $^2\text{H}-^3\text{H}$ reaction, where n is the particle density and τ is the confinement time. The Lawson limit indicates the ability of the plasma to retain heat. The two conditions depend on each other; that is, a given temperature needs a certain $n\tau$ value.

There are two approaches to achieving a controlled thermonuclear reaction. A part of the reactors is based on the magnetic confinement of the hot ($>10^8$ K) plasma containing the isotopes of hydrogen (deuterium and tritium). The most successful results with this method have been obtained in the Tokamak instrument, in Moscow. In this instrument, the plasma is toroid shaped. The other type of controlled thermonuclear reactor operates in pulsed mode (inertia confinements) when small pellets of solid deuterium and/or tritium are injected into a chamber and irradiated by an intense beam of photons from lasers. Recently, there are experiments with the combination of the magnetic and inertia confinement.

The controlled thermonuclear reactors are in the experimental stage. Some examples of important experimental fusion reactors are JET (Joint European Torus, United Kingdom), DIII-D (USA, San Diego), EAST (Experimental Advanced Superconducting Tokamak, China), TFTR (Tokamak Fusion Test Reactor, USA, Princeton), K-Star (Korea Superconducting Tokamak Advanced Research, South Korea), JT-60 (Japan Torus 60, Japan), TCV (Tokamak à configuration variable, Switzerland), and T-15 (Russian). The International Thermonuclear Experimental Reactor (ITER) in France is under construction. This reactor is scheduled to be operational in 2018. Its objectives are to demonstrate the feasibility of fusion power and to prove that it can work without negative impact. This includes to ignite self-sustaining plasma for at least 8 min, and to produce more than enough energy to ignite the fusion. Commercial reactors may be produced in the second part of the twenty-first century at the earliest. There are still many technical problems to be solved. For example, when heating to a suitably high temperature, the fuel separates from the walls of the vessels (no substances are able to withstand this temperature). In addition, the injection of fuel (deuterium and tritium) and the withdrawal of the product (helium), and the control of the fusion are problematic at this time.

7.5 Nuclear Weapons

The nuclear reactions that are used for energy production are also used for military purposes. Nuclear weapons utilize both the fusion reaction and the combination of the fusion and fission reactions.

In the fission bomb (better known as the atomic bomb), the unregulated fission of ^{235}U (Eq. (6.21)) or another fissile, plutonium, takes place. The fissile is placed in pieces, each containing less fissile than the critical mass. The chain reaction is ignited by a chemical explosion, which causes the addition of the pieces so that the mass will become more than the critical mass. During the unregulated chain reaction, the very high energy of the fission reaction releases in a very short time, causing another explosion. As mentioned in Chapter 1, the first two nuclear bombs were exploded at the end of World War II in Japan. On August 6, 1945, a bomb known as “Little Boy” was exploded in Hiroshima; the fission of ^{235}U took place in the bomb. On August 9, 1945, the “Fat Man” bomb was detonated in Nagasaki; the fissile in this bomb was plutonium.

The combination of the fusion and fission reactions is the thermonuclear or hydrogen bomb. The first hydrogen bomb was developed in 1952. The high temperature needed for the ignition of the fusion reaction of hydrogen isotopes (deuterium and tritium; see Eqs. (6.47) through (6.50)) is provided by a fission reaction; that is, by an atomic bomb. The fusion fuel is tritium, deuterium, or lithium deuteride. As mentioned in Section 6.2.4, the ignition temperature is the lowest for the $^2\text{H}-^3\text{H}$ reaction; so the most favorable fusion reaction is the $^2\text{H}-^3\text{H}$ reaction. The production of tritium, however, is expensive, and in addition, its half-life is 12.4 years. For this reason, lithium deuteride is frequently used. From lithium, tritium is

produced in the reaction (6.17) under the effect of neutrons formed in the fission reaction.

Recently, fission–fusion–fission bombs have been developed. In these bombs, there is an outer mantle, and the fission reaction takes place. In the so-called salted bombs, the nuclear weapon is surrounded by a substance such as cobalt or gold, from which radioactive isotopes are formed via the nuclear reactions initiated by neutrons that are produced in the fission reactions. These bombs can be considered “dirty bombs” because of their high radioactive contamination.

A special type of thermonuclear weapon is the neutron bomb, in which the fissile has low critical mass (e.g., californium). The fusion fuel is the mixture of deuterium and tritium. The bomb is surrounded by a substance that has a very low level of neutron absorption. In this way, the main destructive impact is caused by the escaping neutrons. The mass of the neutron bombs is only a few kilograms, and therefore it can be transported very easily. Because of the small quantity of fissile, the radioactive contamination is relatively low.

Further Reading

- Choppin, G.R. and Rydberg, J. (1980). *Nuclear Chemistry, Theory and Applications*. Pergamon Press, Oxford.
- Friedlander, G., Kennedy, J.W., Macias, E.S. and Miller, J.M. (1981). *Nuclear and Radiochemistry*. Wiley, New York, NY.
- Lieser, K.H. (1997). *Nuclear and Radiochemistry*. Wiley-VCH, Berlin.
- McKay, H.A.C. (1971). *Principles of Radiochemistry*. Butterworths, London.
- Prawitz, J. and Rydberg, J. (1958). Composition of products formed by thermal neutron fission of ^{235}U . *Acta Chim. Scand.* 12:369–377.
- Vajda, N. (1994). Atomreaktorok fűtőelmeinek ellenőrzése új analitikai módszerek segítségével (Analysis of nuclear fuel elements by new methods). Candidate’s Thesis. Budapest Technical University, Budapest.
- European Nuclear Society, 2003. Nuclear power plants, world-wide. < www.euronuclear.org/info/encyclopedia/n/nuclear-power-plant-world-wide.htm (IAEA, August 2011). > (accessed 25.03.12.)

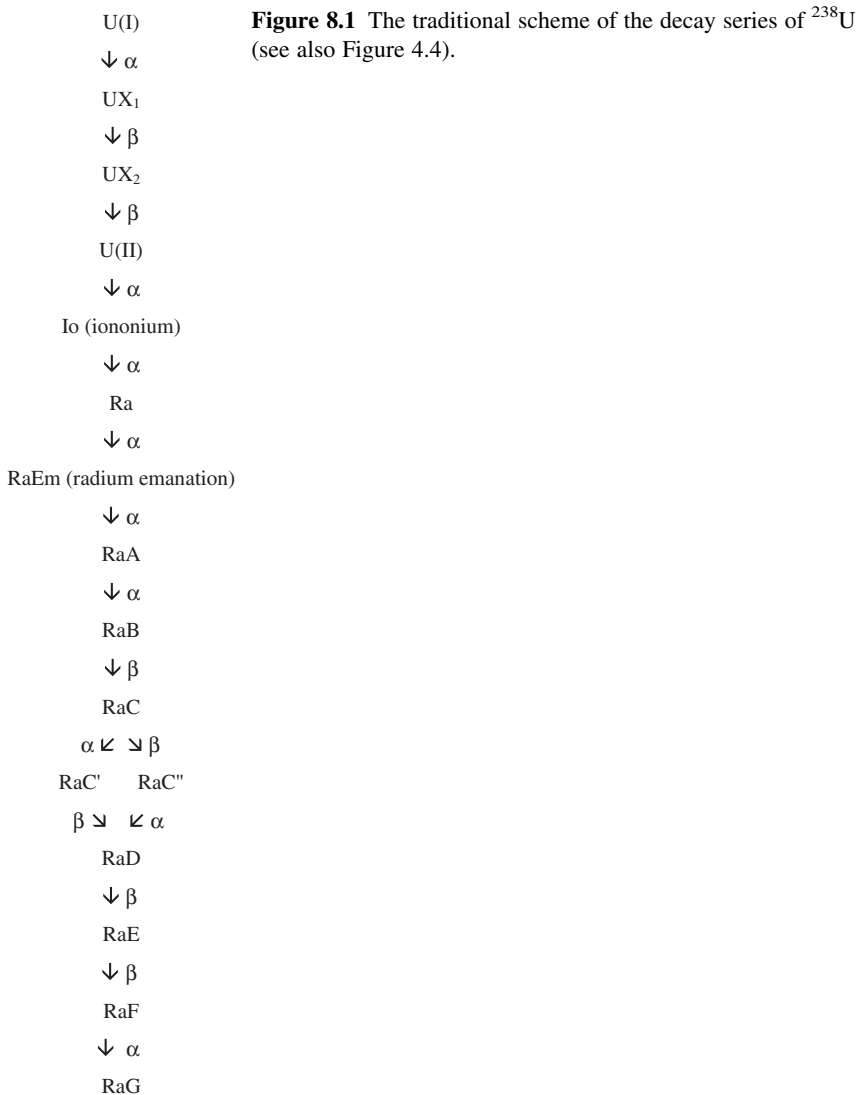
8 Radioactive Tracer Methods

8.1 History of Radioactive Tracer Methods

Radioactive tracing was discovered by George Hevesy in 1911. He was working in Rutherford's laboratory, where radium was prepared from uranium ore by coprecipitation with lead chloride. His goal was to separate RaD from lead chloride. At that time, the term "isotope" had not been defined; the decay series of uranium was described as in [Figure 8.1](#). All radioactive isotopes were considered to be "new radioactive elements," and correspondingly named after the parent element and the place of the given product in the decay series. Thus, RaD indicated the sixth element of the Ra decay series. As comparison, refer to the "modern" decay series of ^{238}U shown in [Figure 4.4](#).

He attempted to separate RaD by many chemical methods but did not succeed. The separation factor was found to be 1 in every method, so Hevesy concluded that RaD could be suitable for labeling lead. Nowadays, we already know that RaD is a radioactive isotope of lead (^{210}Pb); that is, lead and RaD are chemically the same. Using RaD as a radioactive tracer, Hevesy, with F. Paneth, determined the solubility of lead salts (sulfide and chromate) which are very little; the solubility products are about $10^{-33} \text{ mol}^2 \text{ dm}^{-6}$. In 1943, Hevesy received the Nobel Prize in Chemistry for "his work on the use of isotopes as tracers in the study of chemical processes."

Similar to radioactive isotopes, stable isotopes can also be used as tracers. The determination of the stable isotopes, however, requires expensive instrumentation (nuclear magnetic resonance and mass spectrometers), while it is much simpler and cheaper to measure radioactive isotopes. In addition, the radioactive isotopes can be measured easily in very small quantities. Depending on the decay constants, as small quantities as 10^{-16} – 10^{-6} g of the radioactive isotopes can be detected. The application of the radioactive tracers/indicators is independent of the physical and chemical properties (pressure, temperature, chemical species, etc.) because the energy of the nuclear radiation is 6–8 orders of magnitude higher than the energy of the aforementioned physical and chemical effects. Since the radioactive isotopes are chemically the same as the studied inactive isotopes, they do not change the studied system. They can be applied in dry analytical methods. If the radioactive indicator is chemically pure, no contaminants are added to the investigated system.



8.2 Basic Concepts

The isotopes are used as chemical indicators, so they must fulfill the same requirements as the usual chemical indicators. This means that they have to indicate the presence and concentration of a substance in a given place at a given time, but they should not have any effect on the studied process. The radioactive isotopes usually satisfy these criteria, since they are chemically the same as the inactive isotopes of the same elements. For example, when a ^{12}C atom of an organic substance is

replaced by a ^{14}C isotope, the type and strength of the chemical bond and the physical and chemical properties of the compound do not change significantly. Of course, the differences between the masses of the isotopes can result in some differences—in other words, isotope effects (see Chapter 3). These isotope effects, however, can usually be observed only for light elements. For heavier elements, the effects are negligible because the experimental errors are generally higher than the influences of the isotope effects. Therefore, the isotope effects are usually negligible in radioactive indicator methods.

The requirements can be classified into two groups: (1) the usual requirements for all chemical indicators and (2) special requirements only for radioactive indicators. The usual requirements are as follows: the indicator should be sensitive and selective, and can be measured precisely; and the distribution of the indicator should be homogeneous in the system.

The sensitivity of a radioactive indicator depends on its decay rate, and as a consequence, so does the activity of the isotope. The sensitivity can be shown in the next example. Let's take a radioactive indicator with 1000 counts/minute (cpm) radioactive intensity; this intensity can usually be measured easily. The standard deviation of the measurement of 1000 cpm is $\pm 3.3\%$ (see Section 14.7.1). When the measuring efficiency is 10%, this intensity can be obtained if the activity is 10,000 disintegrations/minute (dpm). Assume that the half-life of the radioactive isotope is 60 min (such as for ^{212}Bi). These data can be substituted into Eq. (4.12) as follows:

$$A = -\frac{dN}{dt} = \lambda N = \frac{\ln 2}{t_{1/2}} N \quad (8.1)$$

From Eq. (8.1), $N = 9 \times 10^5$ nuclides are obtained. Expressing this number in mols (dividing by the Avogadro number), you get $9 \times 10^5 / 6 \times 10^{23} = 1.5 \times 10^{-18}$ mol. Therefore, this very small quantity can be measured easily on the basis of its radioactivity. When the decay constant is higher, the sensitivity decreases.

The homogeneous distribution of the radioactive indicator is very important. The radioactive indicator is homogeneously mixed in a system, that is the mixing entropy is maximal (see Section 9.1) if the chemical species of the radioactive indicator and the studied substance is *ab initio* the same or a fast isotope exchange can be possible between the chemical species of the radioactive indicator and the studied substance. The rate of the isotope exchange depends on the strength of the chemical bonds; therefore, it changes in a very wide timescale. For example, the binding energy of iron(II) ion in hemoglobin is high, so the rate of the isotope exchange between iron(II) ions in hemoglobin and in ^{55}Fe ions dissolved in water is practically zero. In such cases, the indicator gives no information on the substance in the other chemical species.

In radioactive tracer experiments, the concentration of the indicator is frequently very small. (As seen in the previous example, even 10^{-18} mol can be measured.) For instance, carrier-free radioactive isotopes could be mentioned. The term

denotes a radioisotope of an element in pure form; i.e., essentially undiluted with a stable isotope. In fact, the term “no-carrier-added” is more correct than “carrier-free.” This means that no carrier is added. However, one can still be present in the system during the experiments, for example, as the result of the interaction with the environment or as the pollutants in the chemicals used.

In other applications, the inactive isotopes (carriers) of the radioactive isotope are added to the system containing the isotope at a low concentration. However, the chemical identity does not need to be the same; chemically similar substances may also behave as carriers. It is known, for example, that potassium or calcium ions are carriers of Cs-137 and Sr-90, respectively, in geological as well as biological systems. It should be mentioned, though, that in such cases, the ratios of the isotopes and the carrier may be different in each phase of the heterogeneous system.

The two cases (carrier-added or no-carrier-added) must be treated differently. In the presence of a carrier, the usual (macroscopic) chemical concentrations are present for the chemical species in question; thus, the usual chemical relations and laws apply.

The chemical properties at these very low concentration ranges (no-carrier-added), however, can be different from the usual properties seen in macroscopic concentrations. In the case of such low concentrations, no chemical system can be considered homogeneous because the number of molecules on the surfaces (the wall of the laboratory vessels, any contaminants in the solution, air bubbles, small particles, great molecules, etc.) is more than, or at least similar to, the number of radioactive nuclides in the solution. The radioactive isotopes can accumulate in bulk on these surfaces and can take part in the subsequent formation of heterogeneous phases (adsorption, colloid formation, precipitation, etc.). Similar accumulation also takes place in the range of macroscopic concentration; however, its effects (the accumulation of 10^{-7} – 10^{-8} mol of the substances) can be neglected. In carrier-free systems, however, the total quantity of the radioactive isotope can be accumulated on the surfaces, resulting in the significant decrease in its concentration and activity of the bulk. The adsorption of thorium isotopes on the walls of laboratory vessels is shown in [Figure 8.2](#).

Besides adsorption on the macroscopic interfaces, the ions in very low concentration can precipitate even when the concentrations do not reach the solubility product (i.e., normally, they would stay in solution) and/or pseudocolloids (or radiocolloids) may form. Even in a solution containing an alkali metal ion, Cs-137 ion in carrier-free concentration, colloid particles are formed under conditions where it would not usually be expected based on thermodynamic parameters.

For the understanding of the formation of heterogeneous phases at extremely low concentrations, two rules called Hahn’s rules (Hahn, 1926a,b, Hahn and Imre, 1929, Wahl and Bonner, 1951) may serve as starting points:

1. The precipitation rule says that an element (isotope) in extremely low concentration coprecipitates with another element in high concentration if it fits into the crystal lattice of this other element.

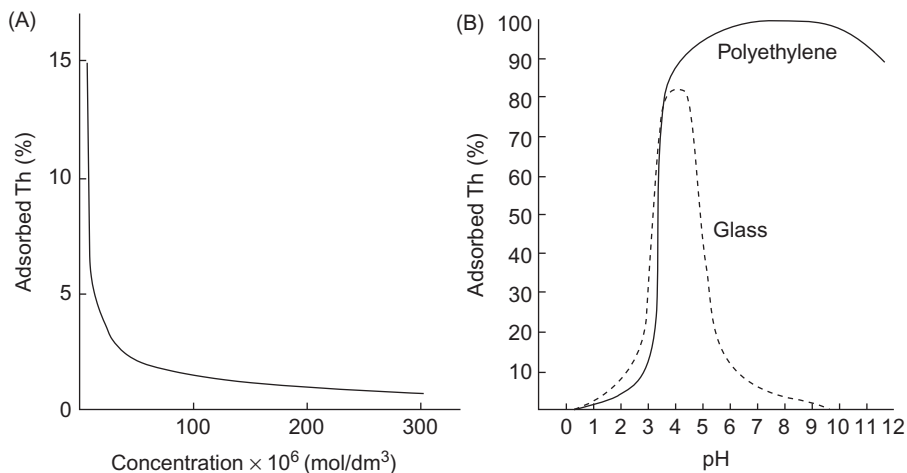


Figure 8.2 (A) Adsorption of thorium from aqueous solution on the wall of a 10 ml pipette versus concentration of thorium salt. (B) Equilibrium adsorption of thorium (thorium concentration is 2×10^{-8} mol/dm³) on the wall of glass and polyethylene vessels as a function of pH.

Source: Reprinted from Choppin and Rydberg (1980), with permission from Elsevier.

- The adsorption rule says that an ion in extremely low concentration adsorbs well on the surface of a solid crystal when the surface charge of solid and ion are opposite and the adsorbed compound is very insoluble. Thus, the ions in very low concentration can be precipitated even when the concentrations do not reach the solubility product (i.e., normally, they would stay in solution), and/or radiocolloids may form.

The formation of radiocolloids can be interpreted by impurities present in the solution (air bubble, dust, cellulose fiber, hydrolytic products, giant molecules, etc.) that act as active sites for heterogeneous nucleation where the radioactive isotopes can adsorb. In the case of the formation of radiocolloids, the radioactive isotope is not evenly distributed in the solution (Figure 8.3), so the formation of radiocolloids must be avoided, for example, by the application of very pure substances, including water, and keeping the isotopes in acidic solutions.

At very low concentrations of the carrier-free radioactive isotopes, the interfaces are not covered totally, and the coverage is smaller than monomolecular. For this reason, the usual thermodynamic requirement, namely that the activity of the surface is one, is not satisfied. As a result, the thermodynamic relations, such as the Nernst equation, have to be applied in their complete form:

$$\varepsilon = \varepsilon_0 - \frac{RT}{zF} \ln \frac{a_{\text{ox}}}{a_{\text{red}}} \quad (8.2)$$

where ε is the redox potential, ε_0 is the standard redox potential, R is the gas constant, T is the temperature, z is the change of charges, F is the Faraday constant, and a_{ox}

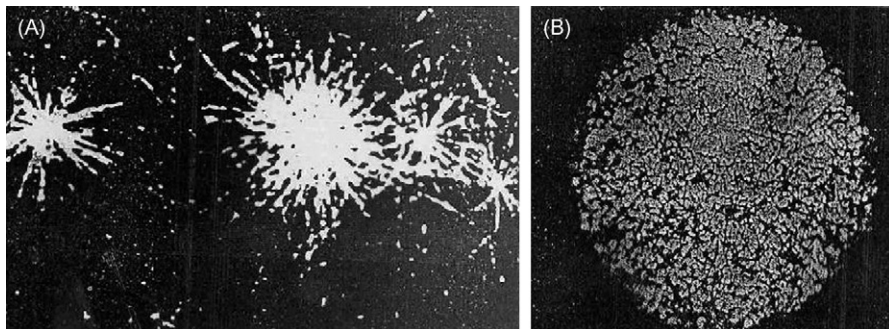


Figure 8.3 (A) Formation of polonium radiocolloid in water. (B) No colloid-formation in acetone. The figure shows positive autoradiograms (discussed in Section 14.5.2), and the white spots show the distribution of the radioactive isotope. The straight lines are the tracks of the alpha particles emitted by polonium.

Source: Adapted from Bouissieres et al. (1947), with permission from Elsevier.

and a_{red} are the activities of the oxidized and reduced species, respectively. In addition, the activity of the solid phase (reduced species of metals) is not known, so the value of the redox potential has to be determined experimentally in each case.

As mentioned in the Hahn's rules, an element (radioactive isotope) in extremely low concentration (microcomponent) coprecipitates with another element in high concentration (macrocomponent) if it fits into the crystal lattice of this other element. The distribution of the micro- and macrocomponents in the coprecipitate can be expressed by different formulas, namely by the Doerner–Hoskins equation:

$$\ln \frac{a}{a-x} = \lambda \ln \frac{b}{b-y} \quad (8.3)$$

or the Henderson–Kracek equation:

$$\frac{y}{x} = D \frac{b-y}{a-x} \quad (8.4)$$

In Eqs. (8.3) and (8.4), D and λ mean the fractionation coefficients, a and b are the quantities of the macro- and microcomponents in the whole system, and x and y are the quantities of the macro- and microcomponents in the crystal phase. When the fractionation coefficient is 1, as in Hevesy's experiments (see Section 8.1), the macro- and microcomponents are chemically the same; they are the isotopes of the same elements. When the fractionation factor is not equal to 1, the micro- and macrocomponents are different (e.g., RaCl_2 and BaCl_2) even if they have similar properties (e.g., isomorphous crystal lattice).

Radioactive indicators have specific properties due to the fact that they are radioactive: (1) the properties originating from the radioactive decay and (2) the properties coming from the different mass numbers.

The radioactive indicator disintegrates, that is, the activity decreases in time. This decrease is determined by the decay constant or half-life. In the tracer studies, it is desirable if the half-life of the radioactive isotopes is comparable to the time needed for the studies. If the half-life is too short, the radioisotope can disintegrate before finishing the investigations. If the half-life is too long, the measurable activity demands a greater quantity of the radioactive nuclides. In addition, as the result of the decay, radioactive wastes form, the treatment of which necessitates particular procedures, and the radiation impact of the environment is also higher. This is especially important in *in vivo* biological and medical applications.

Radiation, especially at high activities, can also initiate chemical and biological processes (radiolytic effects as discussed in Sections 6.4 and 13.4.2). Any operation with radioactive material demands special laboratory conditions, radiation protection, and waste treatment.

As mentioned previously, the sensitivity of the radioactive indication is determined by the properties of the isotope. The same is true for the selectivity. As a result of the radioactive decay, daughter nuclides that are chemically different from the parent nuclides are formed which can contaminate the studied system. A special problem arises when the daughter nuclides are also radioactive. In this case, the measurements of radioactivity can become more complex. The radiations with discrete energy (e.g., alpha and gamma) can be separated by spectrometry. The measurement and separation of the continuous radiation (e.g., beta) may be difficult. As an example, the pure beta emitter parent/daughter nuclide pair, ^{90}Sr — ^{90}Y , is mentioned. Precise activity measurements can be done only in secular equilibrium (see Section 4.1.6). Since the half-life of the daughter nuclide, ^{90}Y , is 64 h, establishing this equilibrium demands a rather long time. However, when the beta energies of the parent and daughter nuclides are different enough, the spectra can be separated by mathematical methods, or the parent—daughter elements can be separated chemically.

Another special property of the radioactive indicators is due to the difference between the mass numbers of the isotopes. This is the isotope effect (discussed in Section 3.1), which is important mainly for light elements. When an inactive carrier is added to the radiotracer, the specific activity decreases because of the isotope dilution. As will be discussed in Section 9.4.1, isotope dilution is the basis of numerous analytical methods. The inactive isotopes of the carrier and the radioactive isotopes participate in an isotope exchange reaction, which was mentioned previously relating to homogeneity.

8.3 Selection of Tracers

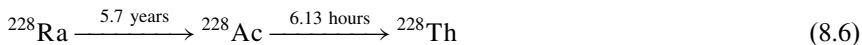
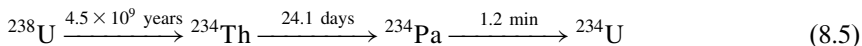
As mentioned in the previous chapter, the half-life of the radioindicator and the duration of the studies have to be comparable. Both too short and too long half-lives have disadvantages. If the half-life is too short, the radioisotope can disintegrate before finishing the investigations. If the half-life is too long, the measurable

activity demands a greater quantity of the radioactive nuclides and the impact of the radiation on the environment is higher than needed. So, the most suitable isotope has to be chosen within these options. The available radioactive isotopes depend on the elements in question. Most light elements have no radioactive isotopes, which could be useful in practical applications; the half-lives are too short. For example, the half-lives of the ${}^6\text{He}$, ${}^8\text{Li}$, and ${}^8\text{B}$ isotopes are less than a second. Tracer studies with these elements can be performed by altering the natural isotope ratio and subsequent activation. Hydrogen is an exception because the half-life of ${}^3\text{H}$, tritium, is fairly long (12.28 years). Tritium emits weak beta radiation.

As the atomic numbers become higher, the choice of radioactive isotopes increases, which can be used well for radioactive indication. If more than one radioactive isotope is available, we can choose the most suitable one for the given study. For example, carbon has two radioactive isotopes: ${}^{11}\text{C}$ with a half-life of 20.48 min and ${}^{14}\text{C}$ with a half-life of 5730 years. ${}^{11}\text{C}$ can be applied for medical applications, while ${}^{14}\text{C}$ is suitable for the synthesis of organic substances or radio-carbon dating (as discussed in Section 4.3.6).

The shortest half-life for tracer studies is about 2–3 min. For example, adsorption studies have been done with the ${}^{208}\text{Tl}$ isotope, whose half-life is 3.1 min. As another example, the application of ${}^{15}\text{O}$ (half-life is 122 s) in medical research is mentioned. Of course, these studies with such short-lived isotopes need careful preliminary training. In addition, the radioactive isotopes have to be produced in very high activities, which require radiation protection and automation. The studies can only be performed in a location where isotope production can take place.

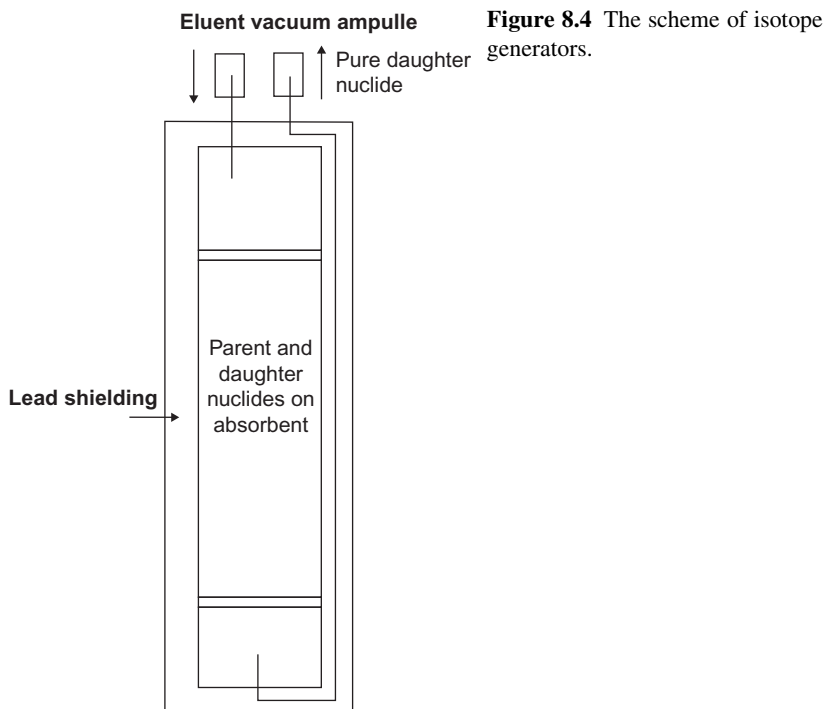
If a radioactive isotope with a short half-life has a parent nuclide with a longer half-life, the daughter element can be separated repeatedly from the parent element. Such a system is called an isotope generator or “cow”; the separation operation is called “milking.” Generators can be produced from the parent–daughter nuclides of decay series, such as:



About 50 parent–daughter pairs can potentially be applied in isotope generators. The most important is the ${}^{99}\text{Mo}$ – ${}^{99\text{m}}\text{Tc}$ generator, which is widely used in medical applications (see Sections 8.7.1.4 and 12.2.6):



The suitable compound of ${}^{99}\text{Mo}$ is adsorbed on a chromatographic column (e.g., aluminum oxide). Since the half-life of ${}^{99}\text{Mo}$ is 66 h, the generator can be



transported and used for several weeks. The short half-life of ^{99m}Tc is desirable for medical applications; this isotope can be eluted (milked) by using physiological sodium chloride solution from the chromatographic column, and after some chemical preparations, it can be used in many ways in medical diagnostics. The scheme of the isotope generators is shown in [Figure 8.4](#).

The radioactive indicators can be used in the most effective way when their specific activity (activity per mass) is fairly high. The specific activity of the carrier-free isotopes is the highest because the radioactive isotope is not diluted with the inactive isotope of the same element (no-carrier-added). Production of the carrier-free isotopes, however, is not always simple, and it is usually more expensive than the production of carrier-added isotopes. As seen in Section 6.2.1, the simplest and cheapest nuclear reactions, namely (n,γ) reactions, do not give carrier-free isotopes because only the number of neutrons changes in the nuclear reaction. The high specific activity is also important in these reactions; however, the production of the isotopes with long half-lives would require a long irradiation time, which is too expensive or even impossible to do. For example, the half-life of ^{36}Cl is about 301,000 years; the irradiation time is obviously much shorter, so most of the target chlorine isotope remains inactive and is present as a carrier. If the presence of the carrier is not allowed (because the specific activity is too low), carrier-free isotopes can be produced through nuclear reactions with charged particles in accelerators. These isotopes are usually more expensive. Nevertheless, the price can differ depending on

the half-lives of the isotopes produced. For example, the ^{24}Na isotope (whose half-life is 24 h) produced in nuclear reactors is much cheaper than the ^{22}Na isotope (whose half-life is 2.6 years). The ^{24}Na isotope can be used for several days, while ^{22}Na can be applied for years. In conclusion, the overall quantities needed for a given period should be considered when deciding which isotope should be purchased.

As usual in chemistry, the radioindicators have to be sufficiently pure. In the case of radioactive isotopes, purity includes different terms: chemical, radioactive, and radiochemical purities can be defined.

Chemical purity is the same as in chemistry: the ratio of the chemical quantities in the number of particles, moles, or masses expressed in the usual concentration units (percent, ppm, etc.). Radioactive purity is measured by the amount of radiation. It represents the fraction of the radioactivity that comes from a given radionuclide. Since the radioactivity depends on the number of radionuclides and the decay constants (Eq. (3.1)), the chemical and radioactive purities are usually different because of the different values of the decay constants. The radioactive purity can be different even for a given isotope mixture if the isotopes emit different particles or electromagnetic radiation. In addition, the probability of the transitions can also be different, which has to be taken into account. This is illustrated by the example of a ^{239}Pu – ^{241}Am isotope mixture shown in Table 8.1.

Radiochemical purity shows what fraction of the radioactive isotope is in the compound defined by a certain chemical formula. For instance, sodium carbonate labeled with the ^{24}Na isotope ($^{24}\text{Na}_2\text{CO}_3$) can contain sodium hydroxide ($^{24}\text{NaOH}$) as an impurity. The radiochemical purity is determined by the ratio of the two compounds. The term of the radiochemical purity is especially important in organic chemistry and in radiopharmaceuticals, where impurities can be formed in the synthesis and by the radiolysis of the product. So, the radiochemical purity is determined mostly by thin-layer chromatography.

The potential use of radioactive indicators is strongly affected by the range of the radiation. Because of their short range, alpha emitters are applicable only for some special cases. An example is the use of the dominantly alpha particles emitting transuranium elements as radioactive indicators. The measurement of alpha activity needs special preparation of the samples, so only static investigations are possible. In addition, alpha emitters are also used for therapy in nuclear medicine.

Table 8.1 Chemical and Radioactive Purities of the ^{239}Pu – ^{241}Am Isotope Mixture. The bold fonts show the purity values

| | ^{239}Pu | ^{241}Am |
|--|----------------------|-----------------------|
| Chemical purity (m/m%) | 99.6 | 0.4 |
| Half-life (years) | 2.11×10^4 | 465 |
| Alpha particle/100 g | 2.3×10^{11} | 4.75×10^{10} |
| Radioactive purity for alpha particles (%) | 80 | 20 |
| Probability of gamma radiation with <i>ca.</i> 60 keV | 0.007 | 36 |
| Radioactive purity for gamma radiation with ≈ 60 keV (%) | 3 | 97 |

Radioactive purity is shown for the alpha particles and the gamma radiation with ≈ 60 keV energy.

In this case, the short range is desirable; the isotope loses its high radiation energy within a short distance (e.g., within a tumor) and does not damage the healthy tissues significantly.

The so-called weak beta emitters (namely, isotopes with low beta energy (e.g., ^3H , ^{14}C , ^{35}S , ^{45}Ca isotopes)) are essential in the biological and medical applications. Because of the self-absorption of the weak beta radiation (see Section 5.3.5), special techniques are needed for the measurements (e.g., liquid scintillation spectrometry, discussed in Section 14.2.1). Similar to alpha radiation, only static investigations can be done in biological systems. In chemical systems, however, dynamic or *in situ* investigations are also possible under special conditions (see Section 9.3.6).

As radioactive indicators, the hard beta emitters (isotopes with high beta energy) and gamma radiators can be used easily. The application of the gamma radiation is especially advantageous because of the discrete energy of the gamma photons. The long range of these isotopes is also required for dynamic and *in situ* studies.

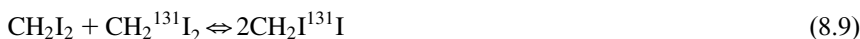
Dual or multiple radioactive indicator methods describe the use of two types of isotopes or isotopes with differing half-lives and/or differing energies of the radiation. When two radioactive isotopes of the same element is used, the isotopes with shorter half-lives results in higher activity, allowing the study of the fast process. The isotope with the longer half-life gives information on the same process on a longer timescale. An additional advantage of the application of the two isotopes of the same element is that less of it is needed; thus, the radiation dose is smaller, which is an important factor in some instances, such as in medical applications.

Exploiting the differences in the energy of the radiation is mostly feasible in the case of the gamma emitters, where the spectra are composed of characteristic peaks with discrete energy, which can be separated. The separation of the beta energies is problematic because of the continuous spectra (see Figure 4.10); thus, the activity measurements frequently have to be complemented by chemical separation.

8.4 Position of the Labeling Atom in a Molecule

In complex molecules (e.g., in organic compounds), it is important to know the position of the labeling atom, and in some cases, such a compound has to be synthesized where the labeling atom is in a desired position. In this latter case, the position of the radioactive atom also has to be determined because the chemical reactions initiated by the radiation (Szilard–Chalmers reactions, discussed in Section 6.4) can influence its position.

When the binding energy of the bond between the labeling atom and the neighboring atom is relatively low, an exchange reaction can take place between the differently labeled species. For example, when labeling diiodine methane with radioactive iodine isotope (e.g., ^{131}I), three types of molecules are formed:



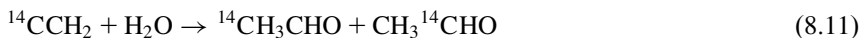
The equilibrium constant of the process is:

$$K = \frac{[\text{CH}_2\text{I}^{131}\text{I}]^2}{[\text{CH}_2\text{I}_2][\text{CH}_2^{131}\text{I}_2]} = 4 \quad (8.10)$$

The equilibrium constant determines the ratio of the differently labeled molecules.

When the binding energy is high, the position of the labeling atom cannot always be changed. For example, in the case of ^{14}C -labeled acetic acid, the carbon atoms of the methyl and carboxyl groups cannot change their positions; therefore, several labeled molecules can be produced. *Specifically labeled* compounds are synthesized when the labeling atom is at a well-defined position of the molecule. In the case of acetic acid, the radioactive isotope (^{14}C) can be in the methyl group ($^{14}\text{CH}_3\text{COOH}$) or the carboxyl group ($\text{CH}_3^{14}\text{COOH}$). When every carbon atom is labeled (in acetic acid, this means two labeling ^{14}C isotopes, $^{14}\text{CH}_3^{14}\text{COOH}$), the molecule is *universally labeled*. A compound is *generally labeled* when the labeling atoms are statistically positioned; every labeled atom has the same specific activity, independent of the position in the molecule. In the case of acetic acid, half of the ^{14}C atoms are in the methyl group, the other half are in the carboxyl group, and the substance is the mixture of $^{14}\text{CH}_3\text{COOH}$ and $\text{CH}_3^{14}\text{COOH}$ in 1:1. The different types of specifically labeled compounds can be produced only when the chemical bonds are strong enough. If not, an exchange can take place between the different labeled molecules, which always results in a generally labeled compound.

The preparation of the different types of the labeled compounds demands suitable labeled reagents and synthetic procedures. Generally labeled organic compounds can be prepared from ^{14}C -labeled carbon dioxide or acetylene. When acetylene contains only one labeled carbon atom ($^{14}\text{CCH}_2$, discussed in [Section 8.6](#)), generally labeled acetaldehyde can be produced by reacting labeled acetylene with water:



From the generally labeled acetaldehyde, specifically labeled acetic acid can be produced in the following reactions. At first, acetaldehyde is transformed into methanol and carbon dioxide:



The carbon dioxide is eliminated, so methanol is obtained in which the ratio of the labeled ($^{14}\text{CH}_3\text{OH}$) and nonlabeled (CH_3OH) molecules is 1:1. By carboxylation of methanol with the Grignard reagent in the presence of inactive carbon dioxide,

specifically labeled acetic acid can be obtained, and only the carbon atoms in the methyl groups are labeled ($^{14}\text{CH}_3\text{COOH}$):

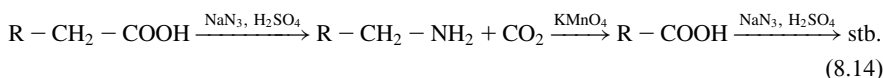


Since half of the methanol molecules are not labeled, half of the acetic acid molecules are also not labeled, and the acetic acid is not carrier-free. The specific activity (radioactivity per mass of carbon) of the acetic acid will be half of the initial, generally labeled acetic acid, since the half of the radioactive carbon atoms was previously lost as $^{14}\text{CO}_2$.

Acetic acid labeled in the carboxyl group can also be prepared. For this, inactive methanol is carboxylated with labeled carbon dioxide ($^{14}\text{CO}_2$) in the same reaction (Eq. (8.13)). Universally labeled acetic acid can be synthesized from universally labeled acetylene ($^{14}\text{C}_2\text{H}_2$).

The position of the labeling atom in the organic molecules can be determined by stepwise decomposition reactions. Some possible ways are as follows:

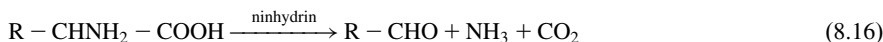
- Schmidt decomposition of carboxylic acids:



- Decarboxylation with copper chromite in boiling kinoline.
- Iodoform reaction, which cuts the bond of the methyl group next CO or CHOH:



- Oxidation of amino acids with ninhydrin:



The position of the labeling atom can be determined by the separation and radioactivity measurements of the products. The side reactions and the isotope exchange in the products, however, may present some difficulties.

The position of the labeling atom also can be determined using biological processes. For instance, the formation of carboxylic acid from carbohydrates (e.g., malonic acid, citric acid, or tartaric acid) can be mentioned. For example, tartaric acid can be dehydrogenized by tartaric acid dehydrogenase enzyme; the product of the reaction, fumarate, is then oxidized by potassium permanganate. Another possibility for determining the position of the labeled atoms in carbohydrates is through their decomposition by acetic acid bacteria, which decompose the carbohydrates to carbon dioxide, acetic acid, and propionic acid. By the separation and activity measurements of the products, the position of the labeled atom can be determined approximately.

Table 8.2 Formulas and Names of Some Labeled Compounds
Recommended by IUPAC

| Formula | Name |
|--|--|
| $^{14}\text{C}\text{H}_4$ | (^{14}C)methane |
| $\text{C}\text{H}_3^2\text{H}$ | ($^2\text{H}_1$)methane |
| $\text{C}\text{H}_2^2\text{H-COOH}$ | (2- $^2\text{H}_1$)acetic acid |
| $^{14}\text{C}\text{H}_3\text{-COOH}$ | (2- ^{14}C)acetic acid |
| $\text{C}\text{H}_3\text{-}^{14}\text{C}\text{OOH}$ | (1- ^{14}C)acetic acid |
| $\text{C}\text{H}_2^2\text{H-CH}^3\text{H-OH}$ | (2- $^2\text{H}_1, 1\text{-}^3\text{H}_1$)ethanol |
| $[^2\text{H}]\text{C}\text{H}_3\text{-CH}_2\text{-OH}$ | [^2H]ethanol, generally labeled |

Some plants and animals can synthesize labeled compounds. *Canna indica* can produce generally labeled carbohydrate from $^{14}\text{C}\text{O}_2$; pigeons produce uric acid from ^{14}C -labeled nutrients.

The number and position of the labeling atoms must be included in the nomenclature of the labeled compounds. The International Union of Pure and Applied Chemistry (IUPAC) has recommendations for the formulas and names of the labeled compounds:

The formula of an isotopically substituted compound is written in the usual way except that appropriate nuclides symbols are used. When different isotopes of the same element are present in the same position, common usage is to write their symbols in order of increasing mass number.

The name of an isotopically substituted compound is formed by inserting in parentheses the nuclide symbol(s), preceded by any necessary locant(s), letters, and/or numerals, before the name or preferably before the denomination of that part of the compound that is isotopically substituted. Immediately after the parentheses there is neither space nor hyphen, except that when the name, or a part of a name, includes a preceding locant, a hyphen is inserted. When polysubstitution is possible, the number of atoms substituted is always specified as a right subscript to the atomic symbol(s), even in case of monosubstitution.

Some examples are listed in [Table 8.2](#).

8.5 General Methods for the Preparation of Radioactive Tracers

Since radioactivity has been discovered as a natural phenomenon, only natural radioactive isotopes were available for the first studies. The basic concepts of radioactivity and radioactive indicators were developed using the natural radioactive isotopes; thus, these isotopes have mainly historical importance. From the late

1940s, artificial radioactive isotopes have been produced in cyclotrons, and later in nuclear reactors. Recently, the artificial radioactive isotopes are dominant in radio-tracer studies. Natural radioactive isotopes are used only in the environmental isotope transport modeling.

8.5.1 Tracers Received from Radioactive Decay Series

Among the members of the decay series of U-238 (see Figure 4.4) and Th-234 (see Figure 4.6), Ra-226, Rn-222, Pb-210, Bi-210, Po-210, and Ra-228, Th-228, Rn-220, Pb-212 isotopes, respectively, have been used in radiotracer studies. Their applications are discussed briefly here.

8.5.1.1 Th-234

As already discussed, the Th-232 isotope is the parent nuclide in a radioactive decay series. Its half-life and decay constant are 14 billion years and $5 \times 10^{-11}/$ years, respectively, so its radioactivity is also very low and can be measured only with difficulty. The half-life of the other thorium isotope, Th-234, is much shorter (24.1 days), so the same number of Th-234 nuclides gives 10^{11} times higher radioactivity than Th-232. Obviously, therefore, Th-234 is used for the labeling of Th-232.

The characteristic oxidation state of thorium is +4, so it has been used as a radioindicator of other elements with +4 oxidation state (e.g., Ce(IV)). These studies have been especially significant in colloid chemistry, where the effect of the tetravalent “ions” on the colloid processes (e.g., adsorption and coagulation) has been investigated.

The Th-234 isotope was separated from U-238 series by extraction with ether by Fajans and Göring.

8.5.1.2 Ra-226

The Ra-226 isotope was discovered and prepared by Marie Curie. This isotope has been applied to the study of the general properties of radioactivity and radiation. Ra-226 has been prepared by coprecipitation with very insoluble lead and barium salts. The coprecipitate has been purified by fractionated crystallization. Metallic radium has been produced by the electrolysis of molten salt in 1910.

The Ra-226 isotope has been used in cancer therapy. Radium is contained in metallic needles, and these needles are implanted next to the tumor. The disadvantage of the application of radium is that it is very toxic; the lethal dose is 1 μ g. Any damage of the needle containing radium could cause death.

8.5.1.3 Rn-222

The Rn-222 isotope can be produced using the Hahn emanation source. The solution of $^{226}\text{Ra(II)}$ ions is mixed with FeCl_2 solution, and then iron hydroxide is precipitated with ammonia solution that contains no carbonate. The precipitate

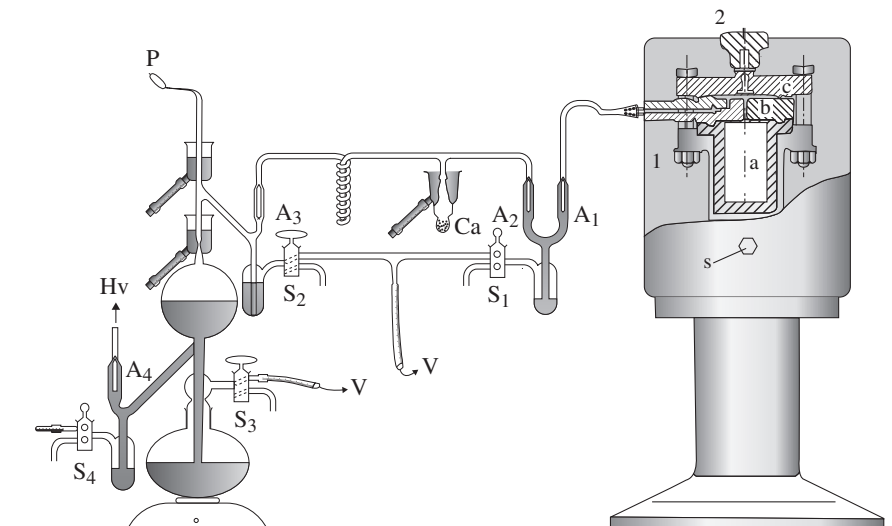


Figure 8.5 Hahn emanation source. Radium is located on the place denoted by a, and Rn-222 can be collected in the ampoule P. b and c are the closing system, A_n and S_n mean valves and tapes, and Hv means high vacuum.

obviously contains radium ions, which disintegrate to radon. At the optimal Ra: Fe = 1:55 ratio, about 95% of radon gas is emanated. As the precipitate ages, the quantity of the emanated radon decreases. When that happens, the precipitate is suspended in water; iron hydroxide is separated by extraction with ether. Radium remains in the aqueous phase, from where it can be precipitated again by iron chloride and ammonia. It is very important that the ammonia solution should not contain carbonate ions; otherwise, radium carbonate is formed, which cannot be separated from iron hydroxide.

A scheme of an emanation source is shown in Figure 8.5. Radon can be collected in the ampoule (P). Radon gas has been used in medical therapy to replace the toxic Ra-226.

8.5.1.4 Pb-210

As mentioned previously in Section 8.1, de Hevesy used the Pb-210 isotope in the first tracer experiments to determine the solubility of lead salts. Pb-210 has been used for self-diffusion studies of metallic lead, and the determination of exchange current density of lead amalgam.

As seen in Figure 4.4, Pb-210 is an intermediate member of the decay series of U-238, and it has a longer half-life (21.6 years) than the previous and the subsequent members of the U-238 decay series. Therefore, it has the tendency to accumulate and is considered as a polluting radioactive isotope in the environment. In some

places (e.g., Mátraderecske, a village in Hungary), the atmospheric concentration of Ra-222, and simultaneously the concentration of Pb-210, is higher as usual. Since Pb-210 is formed as a result of alpha decays (see Figure 4.4) due to the recoil of the nucleus, Pb-210 can introduce into the glass plates of the pictures, photos on the walls of the houses in these places. If the age of the glass plates is known (e.g., photos were taken on special occasions such as a wedding), the change of the radon concentration in the house can be determined from the Pb-210 activity.

Pb-210 emits weak beta particles; recently, it usually has been measured by the liquid scintillation technique (see Section 14.2.1). Before the construction of liquid scintillation spectrometers, the weak beta radiation of Pb-210 was determined by measuring the activity of Bi-210, the daughter nuclide of Pb-210. Before the measurements, Pb-210 and Bi-210 were separated. The sample containing Pb-210 was covered by aluminum foil to absorb the weak beta particles. The daughter nuclide of Pb-210, Bi-210, however, emitted beta particles with higher energy, which can transmit through the aluminum foil. The accumulation of Bi-210 gives information on the activity of Pb-210. After reaching the secular equilibrium between Pb-210 and Bi-210 (which takes approximately 50 days), the activities become the same.

8.5.1.5 Bi-210

Bi-210 has been separated on nickel plate by electrolysis, and then bismuth sulfide has been prepared. This has been used for the radioactive indicator of proteins.

8.5.1.6 Po-210

Po-210 has been used for the preparation of alpha radiation sources.

From the members of the decay series of Th-232 (see Figure 4.6), Ra-228, Th-228, Rn-220, and Pb-212 isotopes have been used as radioactive indicators. Since these are the isotopes of the same elements as the members of the decay series of U-238, the applications are also similar. An emanation source can be produced from Th-228, from which Rn-220, and its daughter nuclide, Pb-212 can be separated electrostatically (see Figure 8.6) and applied as radioactive indicators. The electrostatic separation is based on the recoil of the daughter nucleus when emitting the alpha particle (as discussed in Section 4.4.1). As a result of the recoil, the daughter nuclide is ionized; the positive ions can be collected electrostatically on the negative electrode.

In Table 8.3, the quantities of radioactive isotopes in secular equilibrium in 1 g uranium-238, uranium-235, and thorium-232 isotopes are shown. These are the upper limits of the quantities of isotopes that can be obtained from 1 g of uranium and thorium isotopes. According to the natural isotopic ratio of uranium, 1 ton of uranium contains 993 kg of ^{238}U and 3 kg of ^{235}U . In addition, the uranium and thorium concentration of the rocks is also very small ($<0.1\%$). These data illustrate that the separation of the natural radioactive isotopes is very difficult.

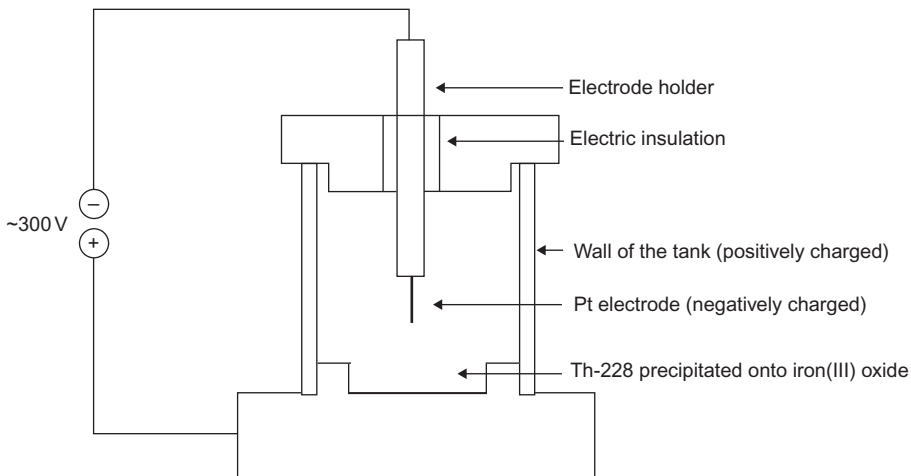


Figure 8.6 Electrostatic separation of daughter elements of Th-228.

Table 8.3 Quantities of Radioactive Isotopes in 1 g Thorium-232, Uranium-235, and Uranium-238 Parent Nuclides, Calculated from the Secular Equilibrium (see Eq. (4.59))

| Parent Nuclide | Decay Constant (1/s) | Daughter Nuclide | Decay Constant (1/s) | Quantity (g) |
|-------------------|----------------------|-------------------|----------------------|--------------|
| ^{232}Th | 1.6–18 | ^{228}Th | 1.1E–08 | 1.3E–10 |
| | | ^{228}Ra | 3.8E–09 | 4.0E–10 |
| | | ^{212}Pb | 1.8E–05 | 7.9E–14 |
| ^{235}U | 3.1E–17 | ^{231}Pa | 6.7E–13 | 4.5E–05 |
| | | ^{227}Ac | 1.0E–09 | 3.0E–08 |
| ^{238}U | 4.9E–18 | ^{234}Th | 3.3E–07 | 1.5E–11 |
| | | ^{234}U | 9.0E–14 | 5.4E–05 |
| | | ^{230}Th | 2.9E–13 | 1.7E–05 |
| | | ^{226}Ra | 1.3E–11 | 3.5E–07 |
| | | ^{222}Rn | 2.1E–06 | 2.2E–12 |
| | | ^{210}Pb | 9.9E–10 | 4.4E–09 |
| | | ^{210}Po | 5.8E–08 | 7.5E–11 |

8.5.2 Artificial Radioactive Tracers

In nuclear reactors, radioactive tracers can be produced by nuclear reactions with neutrons or by the reprocessing of spent fuel elements (fission products and transuranium elements). Fission products can also be obtained by the radiation of uranium as the target. In accelerators (cyclotrons or linear accelerators), the targets are irradiated with positively charged particles. The general characteristics of nuclear

reactions are discussed in Chapter 6. The most important radioactive tracers are shown separately in [Section 8.6](#).

The preparation of radioactive tracers consists of two steps: the preparation of the isotope by nuclear reaction and the preparation of the desired compound by chemical processes. In most irradiation processes, the chemical species of the target and the product are different, that is, the chemical species needed for the application cannot always be produced directly. Two main processes are responsible for this. First, the radiolysis of the target can take place during irradiation, resulting in the change of the chemical species. Second, the other constituents of the target can also be transformed in nuclear reactions, and the product can contain other radioactive isotopes too. In addition, further reactions that may lead to the formation of undesired side products are the nuclear reactions of the other isotopes and chemical impurities of the target, and secondary nuclear reactions with the already produced radioactive isotopes.

The target has to be selected so that the quantity of the polluting product is kept at a minimum. For this reason, the target has to be a very pure substance and, if possible, in elementary form. Oxides and carbonates are also suitable because the nuclear reactions of oxygen and carbon can be ignored, and the products are stable isotopes.

When the other nuclides of the irradiated element enter in nuclear reactions producing undesirable radioactive isotopes, the target has to be enriched after irradiation, that is, the concentration of the isotope has to be increased. For example, natural silver consists of two isotopes: ^{107}Ag and ^{109}Ag . By irradiation of silver with neutrons, ^{108}Ag and ^{110}Ag isotopes are produced in a (n,γ) reaction. When only one of these isotopes is needed, silver isotopes can be separated by mass spectrometry.

Enriched targets are used when the concentration of the target nuclide is very low in the substance with a natural isotopic ratio. For example, ^{18}F isotope is produced from ^{18}O by proton irradiation. In the case of enriched targets, the specific activity of the product nuclide also increases.

In some nuclear reactions, secondary nuclear reactions can also take place. For example, in the production of ^{125}I , the subsequent nuclear reaction of ^{125}I occurs: $^{125}\text{I}(n,\gamma)^{126}\text{I}$. The effect of the secondary nuclear reactions can be limited by controlling the irradiation time or cooling the undesirable isotope if its half-life is shorter than that of the main product.

The desired radioactive isotopes can be separated by radiochemical methods (such as chromatography, ion exchange, distillation, sublimation, precipitation, and thermochromatography). The simpler the method is, the better.

As mentioned previously, the radioactive isotopes have to be manipulated further to obtain the chemical compounds needed for the specific application, which includes the production conditions (pH, redox potential, etc.), chemical reactions, and purification procedures.

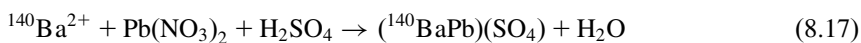
It is important to remember during the production of the radioactive isotope that a carrier-free or just minimally carrier-containing isotope has a high level of specific activity. Carrier-free isotopes can be produced in nuclear reactions in which the atomic number changes or the daughter nuclide of the product is also radioactive, and they can be separated from the parent nuclide produced by the nuclear

reaction. For example, the Szilard–Chalmers reaction can be used to produce certain carrier-free radioactive isotopes. This method is based on the recoiling of the produced radioactive isotope, which leads to breaking its chemical bond. In this way, a new chemical compound is formed, and the target and the product, containing different isotopes of the same elements, can be separated by chemical procedures because the radioactive and the inactive isotopes are in different chemical compounds. For example, in $^{127}\text{I}(n,\gamma)^{128}\text{I}$ nuclear reactions, the iodine in the target can be an organic compound or iodate, and the radioactive iodine is present as iodide ion. Bromine and chlorine isotopes have similar nuclear and Szilard–Chalmers reactions. In addition, the same reactions can be used for the inactive chromium, manganese, phosphorus, and arsenic isotopes in chromate, manganate, phosphate, and arsenate ions. No-carrier-added radioactive isotopes with high specific activity can be produced by nuclear reactions with high cross sections, especially when the half-life of the product is too short to allow irradiation for a suitably long time, that is, the maximum activity of the radioactive product can be approached (see Section 6.1 and Eqs. (6.9) and (6.11)).

As discussed in Section 6.2.1, the nuclear reactions with neutrons can easily be created in nuclear reactors. Radioactive isotopes can be produced by the irradiation of a target substance located on the irradiation channels of the nuclear reactors. The other possibility for the production of radionuclides in nuclear reactors is the reprocessing of spent fuel elements. Fission products and isotopes transuranium elements can be obtained in this way. The two methods can be combined: a target containing ^{235}U isotope can be irradiated in the irradiation channels of the reactor, and then the radioactive isotopes can be separated from the target. This procedure is significant in the production of fission products with short half-lives.

As discussed in Section 7.3.2, the first step of reprocessing of spent fuel elements (or the irradiated ^{235}U) is the separation of transuranium elements, in most cases by extraction with tributyl phosphate, followed by subsequent chemical procedures. The number of fission products is about 300, including the isotopes with longer half-lives. These fission products are the isotopes of many chemical elements; therefore, the chemical procedure is usually complicated. At first, the chemically similar fission products are separated by such methods as extraction, ion exchange, and precipitation, and then the individual isotopes are separated from the groups of the chemically similar elements.

As an example of the separation of fission products, the separation of ^{140}Ba is shown here. Lead nitrate solution is added to the solution of fission products, and then lead sulfate containing $^{140}\text{Ba}(\text{II})$ ions is precipitated with sulfuric acid (coprecipitation):



The precipitate, polluted with ^{90}Sr , is digested with KNaCO_3 and dissolved in nitric acid. Then barium–lead carbonate is precipitated with ammonium carbonate and dissolved in nitric acid again. The precipitation with carbonate and dissolution with nitric acid is repeated until the radioactive purity of the precipitate becomes

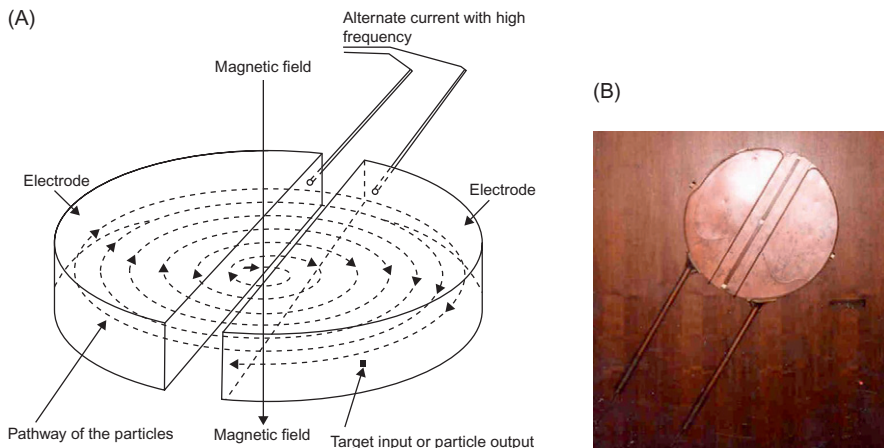


Figure 8.7 (A) The scheme of cyclotron. (B) The first cyclotron in Berkeley (the diameter of the accelerating channel is about 12 cm).

high. When the desired purity is attained, concentrated hydrochloric acid is added to the solution at 0°C . Lead ions are precipitated as lead chloride, and barium ions remain in the solution. The residual lead ions are eliminated by electrolysis. By this method, carrier-free ^{140}Ba isotopes are obtained.

Radioactive isotopes can be produced by irradiation with charged particles (as discussed in Section 6.2.3) in cyclotron (see [Figure 8.7](#)), or in linear accelerators (see [Figure 8.8](#)). This method is older than the nuclear reaction with neutrons in nuclear reactors. As discussed in Section 6.2.6, the heavier transuranium elements have been produced by irradiation with charged particles. During the isotope production in accelerators, the target becomes very hot; therefore, the cooling is very important, and even cryogenics are applied, if required (see [Figure 8.9](#)). The requirements to the target are the same as in the nuclear reactors.

Some radioactive isotopes are produced by spallation reactions too (see Section 7.3.2).

In [Figure 6.7](#), the different possibilities that lead to the production of a nuclide with a Z atomic number and an A mass number are summarized, including the formation of the nuclide by radioactive decays. When selecting a method for isotope production, the general nuclear reactions, the requirements of the isotope in terms of purity and use, and the available techniques are to be taken into account.

8.6 Radioactive Isotopes in Tracer Methods

In this chapter, the radioactive tracers of the individual elements and their production are sketched briefly. In the case of tritium and C-14, the nuclear reactions, as well as the chemical syntheses of labeled organic compounds, are outlined.

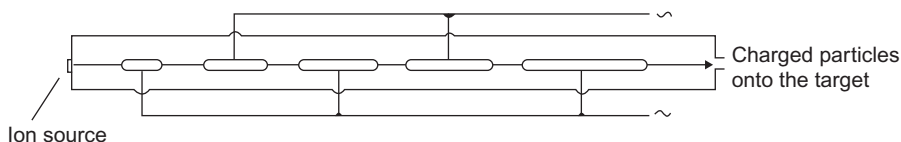


Figure 8.8 The scheme of a linear accelerator. Protons fly through the tubes operated with alternating voltage supply. The length of the tube is adjusted in relation to the frequency of alteration that the protons meet an accelerating voltage whenever they pass from one tube to the next.

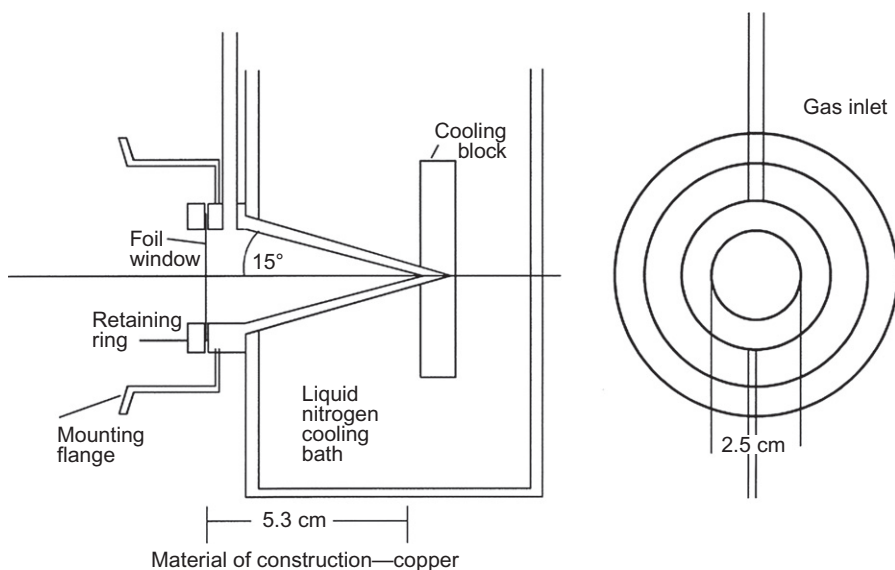


Figure 8.9 The cryogenic target design in a cyclotron.

Source: Reprinted from Firouzbakht et al. (2006), with permission from Elsevier.

8.6.1 Tritium

Tritium (^3H) is the isotope of hydrogen and emits negative beta particles with 18.6 keV maximal energy. Its half-life is 12.3 years. Tritium is produced by the $^6\text{Li}(n,\alpha)^3\text{H}$ nuclear reaction. A foil from an MgLi alloy is used as target; tritium is separated by heating. Tritium is applied as T_2 gas or tritiated water (T_2O) in the syntheses of different organic compounds.

- Alkanes can be produced by isotope exchange reactions of hydrogen in organic compounds:



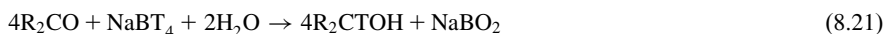
- Alkane (methane) can be prepared in the reaction of tritiated water with aluminum carbide:



- Alkanes are formed in the Grignard reaction:



- Double bonds can be saturated by tritium gas.
- Alcohols can be obtained by the reduction of carbonyl compounds with NaBT_4 or LiAlT_4 :



- By the exchange of the labile hydrogen of malonic acid and decarboxylation, acetic acid is produced. In addition, the labeled malonic acid can be used in many organic syntheses.
- By the reaction of calcium carbide and tritiated water, tritium-labeled acetylene can be prepared, which can be a starting material in many organic syntheses.

8.6.2 Carbon-14

^{14}C emits negative beta particles with 165 keV maximal energy. Its half-life is 5,730 years. It is produced by the $^{14}\text{N}(\text{n,p})^{14}\text{C}$ nuclear reaction. B-, Be-, or Al-nitrides are used as the target, and it is oxidized after irradiation, e.g., by hydrogen peroxide. By this method, $^{14}\text{CO}_2$ can be obtained, and it then can be dissolved in NaOH and precipitated with $\text{Ba}(\text{OH})_2$ as $\text{Ba}^{14}\text{CO}_3$. This is the basic compound, which is mostly used in organic syntheses. The procedure is shown in [Figure 8.10](#).

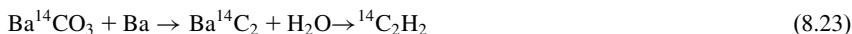
For organic syntheses, $\text{Ba}^{14}\text{CO}_3$ is transformed in several different ways:

- It can be dissolved in hydrochloric acid. In this process, $^{14}\text{CO}_2$ is formed. From $^{14}\text{CO}_2$, the following compounds can be produced:
 - Carboxylic acids (e.g., acetic acid) can be prepared in the Grignard reaction:



The acetic acid is specifically labeled on the carboxylic carbon atom.

- $^{14}\text{CO}_2$ can be reduced with LiAlH_4 to methanol.
 - Methanol can be converted to methyl iodide, formaldehyde, or methyl cyanide.
- By heating $\text{Ba}^{14}\text{CO}_3$, different compounds are obtained, dependent on the conditions and reagents:
 - With metallic potassium in molten NH_4Cl , K^{14}CN is produced.
 - With metallic barium, it gives universally labeled acetylene:



- Acetylene can be used in many syntheses, e.g., universally ^{14}C -labeled benzene. By addition of water, acetaldehyde is obtained. In the reaction of labeled acetylene with formaldehyde, heterocyclic compounds with oxygen as a heteroatom can be produced.

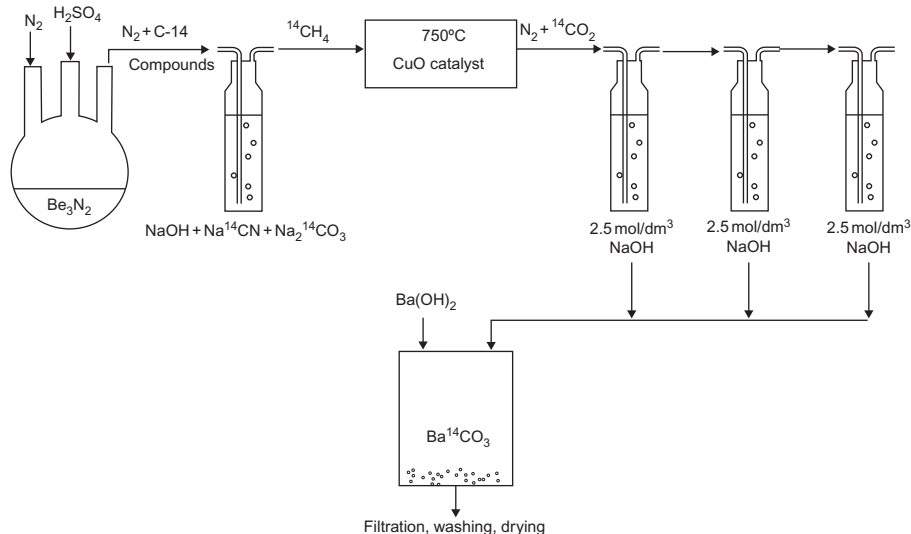


Figure 8.10 The separation of C-14 from Be_3N_2 and preparation of $\text{Ba}^{14}\text{CO}_3$.

- By heating $\text{Ba}^{14}\text{CO}_3$ in dry NH_3 , barium cyanamide is produced, from which urea, thiourea, and guanidine can be synthesized.
- 3. By the reduction of $\text{NaH}^{14}\text{CO}_3$ or $\text{KH}^{14}\text{CO}_3$ by H_2 , formic acid is produced, using Pd as a catalyst.
- 4. A special problem of organic chemistry is the preparation of labeled aromatic compounds. As seen previously, universally ^{14}C -labeled benzene can be produced from $^{14}\text{C}_2\text{H}_2$.

As mentioned in [Section 8.4](#), biological syntheses are also possible:

- *Clostridium aceticum* is produced from CO_2 to acetic acid.
- *Chlorella vulgaris* is produced from CO_2 to amino acid in an L-configuration.
- *Canna indica* is produced from CO_2 to carbohydrate in a D-configuration.
- Pigeon produces from formiate to acetic acid.
- Rat produces from acetate to cholesterol.

8.6.3 Isotopes Used in Medical PET

These radioactive isotopes (preparation reactions, half-lives) are summarized in [Table 8.4](#). They are produced in cyclotrons.

8.6.4 Sodium Isotopes

Na-24 can be prepared by the $^{23}\text{Na}(n,\gamma)^{24}\text{Na}$ reaction in nuclear reactors. The product is not carrier-free. Its half-life is 24 h, and it emits β^- and hard gamma

Table 8.4 Isotopes Used in Medical PET

| Isotope | Nuclear Reaction | Half-Life |
|--------------------------|--|-----------|
| C-11 | $^{14}\text{N}(p,\alpha)^{11}\text{C}$ | 20.3 min |
| N-13 | $^{16}\text{O}(p,\alpha)^{13}\text{N}$ | 10 min |
| O-15 | $^{14}\text{N}(d,n)^{15}\text{O}$ | 122 s |
| F-18 (see Section 8.7.2) | $^{18}\text{O}(p,n)^{18}\text{F}$ | 109 min |

radiation. Carrier-free ^{24}Na isotopes can be produced in the $^{26}\text{Mg}(d,\alpha)^{24}\text{Na}$ nuclear reaction, but this procedure is more expensive.

Na-22 can be prepared by the $^{23}\text{Na}(n,2n)^{22}\text{Na}$ nuclear reaction. The isotope contains an inactive carrier (Na-23). Since the (n,2n) nuclear reaction is endoergic, fast neutrons are needed. Its half-life is about 2 years, and it emits β^+ and gamma radiation. Carrier-free ^{22}Na isotopes can be produced in the $^{24}\text{Mg}(d,\alpha)^{22}\text{Na}$ nuclear reaction.

8.6.5 Magnesium-28

^{28}Mg can be produced in $^{27}\text{Al}(\alpha,3p)^{28}\text{Mg}$ or in $^{26}\text{Mg}(t,p)^{28}\text{Mg}$ nuclear reactions. Its half-life is 20.9 h, and it emits negative beta particles.

8.6.6 Aluminum-28

For the nuclear reactions and in the neutron-activation analysis (see Section 9.2.2.1) the target or the sample is placed into aluminum holders since irradiation of aluminum with neutrons ($^{27}\text{Al}(n,\gamma)^{28}\text{Al}$) produces radioisotope with a short half-life (2.8 min). ^{28}Al emits β^- and gamma radiation. As a by-product, Na-24 is formed in the $^{27}\text{Al}(n,\alpha)^{24}\text{Na}$ nuclear reaction. A negative conclusion of this reaction is the long time gamma radiation of the aluminum sample holders after irradiation in nuclear reactors.

Al-28 can be obtained from $^{28}\text{Mg}/^{28}\text{Al}$ generators too.

8.6.7 Phosphorus-32 (P-32)

P-32 is widely applied in biological and agricultural research. It is produced by irradiation of red phosphorus with neutrons in $^{31}\text{P}(n,\gamma)^{32}\text{P}$ nuclear reaction. The half-life of ^{32}P is 14.3 days, and it emits negative beta particles. By the dissolution of red phosphorus in water, phosphoric acid is formed. Therefore, the oxidation state of phosphorus is +5. When dissolving red phosphorus in hydrochloric acid, chloride and oxychloride are formed, the oxidation state of phosphorus is also +5. A ^{32}P -labeled compound with a +3 oxidation state has not been produced yet. Carrier-free ^{32}P can be produced from sulfur by the $^{32}\text{S}(n,p)^{32}\text{P}$ nuclear reaction. ^{32}P can be gained as a $\text{H}_3^{32}\text{PO}_4$ solution by water vapor, and sulfur remains back

as a solid. Another way to separate ^{32}P is the dissolution of sulfur with an organic solvent (e.g., CS_2), which makes the residue react with chlorine gas. The product is PCl_5 . For additional information, see [Section 8.7.1.2](#).

8.6.8 Sulfur-35 (S-35)

The production of S-35 is similar to the production of carrier-free P-32; it is produced in the $^{35}\text{Cl}(n,p)^{35}\text{S}$ nuclear reaction by irradiating the KCl target. The irradiated KCl is dissolved in water, while sulfur is dissolved as sulfate. Chloride and sulfate are separated by anion exchange. The half-life of ^{35}S isotope is 87.9 days, and it emits weak beta particles, similar to C-14. As a by-product, a weak beta emitter ^{36}Cl isotope is formed by the $^{35}\text{Cl}(n,\gamma)^{36}\text{Cl}$ nuclear reaction, the half-life of which is 301,000 years. In addition, the ^{41}K isotope of KCl is activated in the $^{41}\text{K}(n,\gamma)^{42}\text{K}$ nuclear reaction. The half-life of the beta and gamma emitter ^{42}K , however, is short enough (12.6 hours) so its disintegration can be waited. For additional information, see [Section 8.7.1.2](#).

8.6.9 Chlorine-36

See at the production of S-35.

8.6.10 Potassium Isotopes

K-38: produced in $^{35}\text{Cl}(\alpha,n)^{38}\text{K}$ nuclear reaction, $t_{1/2} = 7.6$ min, emits β^+ particles.

K-42: see at the production of S-35.

8.6.11 Calcium-45

^{45}Ca can be produced in the $^{44}\text{Ca}(n,\gamma)^{45}\text{Ca}$ reaction. Its half-life is 163 days, and it emits β^- particles, similar to C-14 and S-35. ^{45}Ca is mostly applied in biological research.

8.6.12 Chromium-51 (Cr-51)

Cr-51 can be produced in the $^{50}\text{Cr}(n,\gamma)^{51}\text{Cr}$ nuclear reaction, half-life is 27.7 days, and it emits β^- and gamma radiation. ^{51}Cr isotope is applied in biological and medical research in the so-called chromium release assay studies. This method is based on the adsorption of Cr-51 on the cell walls. For additional information, see [Section 8.7.1.1](#).

8.6.13 Manganese-54

Carrier-free ^{54}Mn can be produced from the natural isotopes of the iron ^{56}Fe (d,α) ^{54}Mn and $^{54}\text{Fe}(\text{n},\text{p})^{54}\text{Mn}$ nuclear reactions. In carrier-added form, it can be produced from natural manganese by the $^{55}\text{Mn}(\text{n},2\text{n})^{54}\text{Mn}$ nuclear reaction. Manganese is one of the rare elements that consists of only one isotope—in this case ^{55}Mn . The half-life of ^{54}Mn is 312 days, and it disintegrates by electron capture and gamma radiation.

8.6.14 Iron Isotopes

Fe-52 is produced by the spallation of nickel-58 with protons ($^{58}\text{Ni}(\text{p},\text{spallation})^{52}\text{Fe}$); its half-life is 8.3 h, it is a positron emitter nuclide, but its daughter nuclide, the metastable Mn-52m, has a shorter half-life, so an Fe-52-Mn-52m generator can be prepared.

Fe-55 is produced from iron by the $^{54}\text{Fe}(\text{n},\gamma)^{55}\text{Fe}$ nuclear reaction. Carrier-free Fe-55 isotopes is produced from manganese by the $^{55}\text{Mn}(\text{d},\text{p})^{55}\text{Fe}$ reaction. half-life is 2.7 years, and it decays by electron capture.

Fe-59 forms from the subsequent (n,γ) nuclear reaction of stable iron isotopes, half-life is 44.5 days, and it emits β^- and gamma radiation.

8.6.15 Cobalt-60

It can be produced from the stable isotope of cobalt in the $^{59}\text{Co}(\text{n},\gamma)^{60}\text{Co}$ nuclear reaction, and its half-life is 5.5 years. It has two gamma lines at 1178 and 1333 keV. Co-60 is applied in sterilizing and therapeutic irradiations. For additional information, see [Section 8.8](#).

8.6.16 Nickel-63

Nickel-63 can be produced from the stable isotope of nickel in the $^{62}\text{Ni}(\text{n},\gamma)^{63}\text{Ni}$ nuclear reaction. Its half-life is 100 years, and it emits β^- -radiation. It is used as a radiation source of electron capture detectors in gas chromatographs.

8.6.17 Copper Isotopes

Cu-64 can be obtained from natural copper by the $^{63}\text{Cu}(\text{n},\gamma)^{64}\text{Cu}$ nuclear reaction, half-life is 12.7 h. Copper-64 has branching decay emitting both positive and negative beta particles. The carrier-free Cu-64 isotope can be obtained from zinc in the $^{64}\text{Zn}(\text{n},\text{p})^{64}\text{Cu}$ nuclear reaction. Simultaneously, the $^{64}\text{Zn}(\text{n},\gamma)^{65}\text{Zn}$ reaction also takes place. The two product nuclides, Cu-64 and Zn-65, can be separated by electrolysis.

Cu-66 is produced from copper by the $^{65}\text{Cu}(n,\gamma)^{66}\text{Cu}$ nuclear reaction. The half-life of Cu-66 is 5 min, and it emits negative beta particles.

Natural zinc contains ^{66}Zn isotope, too. By the (n,γ) and (n,p) nuclear reactions of ^{66}Zn , inactive ^{67}Zn and ^{65}Cu , respectively, are formed. However, the half-life of ^{65}Cu is short enough (5 min), so its decomposition can be waited, it does not pollute ^{64}Cu .

8.6.18 Zinc-65

See at copper isotopes. The half-life is 244 days, and decays are electron capture and negative and positive beta decays.

8.6.19 Gallium and Germanium Isotopes

Ga-67 is produced in cyclotrons (Eq. (8.26)).

Ga-68 can be obtained by reprocessing of spent fuel elements since it is a fission product.

Ge-68 is used in Ge-68/Ga-68 generators. The complexes of Ga-68 have medical applications.

8.6.20 Arsenic-76 (As-76)

As-76 is produced by the $^{75}\text{As}(n,\gamma)^{76}\text{As}$ nuclear reaction. When an organic arsenic compound is irradiated, an inorganic radioactive arsenic isotope is obtained as a result of the Szilard–Chalmers reaction. The inorganic arsenic can be separated by chemical procedures, so As-76 is carrier free.

8.6.21 Radioactive Isotopes of Selenium, Bromine, and Rare Earth Elements

These isotopes can be obtained as fission products from reprocessing of the spent fuel elements. They are applied for medical purposes only in special cases because the products of reprocessing contain long-life fission products of the same elements. The isotopes can be separated by mass spectrometry.

Sm-153: the production will be discussed in detail in [Section 8.7.1.1](#).

8.6.22 Bromine Isotopes

Br-80 is produced in the $^{79}\text{Br}(n,\gamma)^{80\text{m}}\text{Br} \rightarrow ^{80}\text{Br}$ nuclear reaction and in the decay of the metastable $^{80\text{m}}\text{Br}$. The half-life of the metastable $^{80\text{m}}\text{Br}$ is 4.4 h, and this disintegrates to the ^{80}Br isotope, the half-life of which is 18 min (isomeric transition). By irradiation of organic bromine compounds, the bond of bromine-80m can break as a result of the Szilard–Chalmers effect, producing inorganic bromine. When the inorganic bromine is separated immediately after the irradiation, it contains the

ions of both radioactive isotopes, namely ^{80m}Br and ^{80}Br . After a few hours, only the product of the isomeric transition (^{80}Br) can break out of the organic molecules, so it can be separated with high purity. The Br-80 isotope disintegrates with electron capture and negative and positive beta decays.

Br-82 is produced in the $^{81}\text{Br}(n,\gamma)^{82}\text{Br}$ nuclear reaction. Its half-life is 35.9 h, and it emits β^- and gamma radiation. For more information, see [Section 8.7.1.1](#).

8.6.23 Krypton-85

Kr-85 is a fission product, which is emitted into the air during the operation of nuclear reactors or reprocessing plants. By measuring the krypton activity in the air, the volume of reprocessing and nuclear weapon production can be estimated. The half-life is 10.7 years.

8.6.24 Rubidium-86

^{86}Rb is produced in the $^{85}\text{Rb}(n,\gamma)^{86}\text{Rb}$ nuclear reaction. Its half-life is 18.7 days, and it emits β^- and gamma radiation. It is used in nuclear medicine for metabolism studies.

8.6.25 Strontium Isotopes

Sr-85 is produced by the spallation of molybdenum (natural Mo(p,spallation) ^{85}Sr). Its half-life is 65 days, and it disintegrates with electron capture and gamma radiation.

Sr-89 is produced in the $^{88}\text{Sr}(n,\gamma)^{89}\text{Sr}$ nuclear reaction. Its half-life is 50 days, β^- -emitter.

Sr-90 is obtained as a fission product. Its half-life is 29 years, β^- -emitter. Its daughter nuclide is the ^{90}Y isotope, which can be obtained from $^{90}\text{Sr}/^{90}\text{Y}$ -generators and used for palliative therapy.

8.6.26 Yttrium-90

Y-90 is the daughter nuclide of Sr-90, so the production has been discussed at strontium isotopes. The industrial production will be shown in [Section 8.7.1.1](#).

8.6.27 Technetium-99m (Tc-99m)

Tc-99m is the most frequently used radioisotope in nuclear medicine. In medical laboratories, Tc-99m is obtained from Mo-99/Tc-99m generators (see Eq. (8.8)). The parent nuclide, Mo-99, is produced as a fission product in the reprocessing of spent fuel elements. For more information, see [Section 8.7.1.4](#).

8.6.28 Rutenium, Rhodium, and Palladium Isotopes

These isotopes are produced in (n,γ) nuclear reactions. They are of little importance.

8.6.29 Silver Isotopes

Ag-110 is produced from silver by the $^{109}\text{Ag}(n,\gamma)^{110\text{m}}\text{Ag} \rightarrow ^{110}\text{Ag}$ nuclear reaction and isomeric transition. The half-life of Ag-110 is 250 days, and it emits β^- and gamma radiation. ^{110}Ag is an important polluting isotope of nuclear reactors since the silver in solders is activated.

Ag-111: a carrier-free ^{111}Ag isotope is obtained by the $^{110}\text{Pd}(n,\gamma)^{111}\text{Pd}$ nuclear reaction and the subsequent β^- -decay. Pd and Ag are separated by the electrolysis of the amine complexes. The half-life of ^{111}Ag is 7.45 days, and it has β^- and gamma radiation.

8.6.30 Cadmium-115m

Since the cross section of cadmium for neutrons is about 10^4 barns, cadmium targets have to be placed in the nuclear reactors very carefully. Cd-115m is produced by the $^{114}\text{Cd}(n,\gamma)^{115\text{m}}\text{Cd}$ nuclear reaction. Its half-life is 44.6 days, and it emits β^- and gamma radiation.

8.6.31 Indium Isotopes

In-111 is produced in cyclotrons. Its half-life is 2.8 days, and it disintegrates with electron capture and gamma radiation.

In-114 is produced by the $^{113}\text{In}(n,\gamma)^{114}$ in nuclear reaction. Its half-life is 72 s, and it disintegrates with electron capture and β^- and gamma radiation. This nuclear reaction is used for the measurement of neutron flux in neutron generators.

In-114m is produced by the $^{113}\text{In}(n,\gamma)^{114\text{m}}\text{In}$ nuclear reaction. Its half-life is 50 days, and it disintegrates with electron capture and β^- and gamma radiation.

8.6.32 Iodine Isotopes

I-123 is produced from Xe-123 in cyclotron (see Eq. (8.28)). Its half-life is 13 h, and it disintegrates with electron capture and gamma radiation. Because of its short half-life, the I-125 isotope is used in nuclear medicine for examinations of pregnant women and children.

I-125 is applied as irradiation source in X-ray fluorescence studies. Its half-life is 60 days, and it disintegrates with electron capture and gamma radiation. For more information, see Section 8.7.1.3.

I-131 is formed by the irradiation of tellurium and by beta decay of the product: $^{130}\text{Te}(n,\gamma)^{131}\text{Te} \rightarrow ^{131}\text{I}$. The half-life of ^{131}I is 8 days, and it has β^- and gamma radiation. During the production of Mo-99 from the spent fuel elements of nuclear

reactors, I-131 is separated by acidic treatment, that is, I-131 is a by-product of Mo-99 production. I-131 obtained in this way has a higher specific activity than I-131 produced by irradiation of tellurium. I-131 has important medical applications. For more information, see [Section 8.7.1.3](#).

8.6.33 Xenon Isotopes

Similar to Kr isotopes, xenon isotopes are fission products and emitted into the air from nuclear reactors and reprocessing plants.

8.6.34 Cesium Isotopes

In the fission of U-235, two cesium isotopes form with a high cross section, Cs-134 and Cs-137. Their ratio of the two isotopes as the result of fission is well determined; however, the decay rate of Cs-134 is higher. Therefore, the ratio of the two fission cesium isotopes gives information on the time of the environmental pollution by radioactive cesium. Cs-134 can be produced in the $^{133}\text{Cs}(n,\gamma)^{134}\text{Cs}$ nuclear reaction; its half-life is 2 years, and it has β^- and gamma radiation. The half-life of Cs-137 is 30 years, and it emits β^- and gamma radiation. Since cesium ion is strongly sorbed on soils, its migration is rather slow. For these reasons, Cs-137 can be applied to study soil formation and erosion. In these studies, the activity of Cs-137 already present in the soil from the nuclear pollutions is measured. For more information see [Section 8.8](#).

8.6.35 Rhenium-186

^{186}Re is produced by the $^{185}\text{Re}(n,\gamma)^{186}\text{Re}$ nuclear reaction. Its half-life is 90.6 h, and it has β^- -radiation. It has medical applications.

8.6.36 Iridium-192

^{192}Ir is produced by the $^{191}\text{Ir}(n,\gamma)^{192}\text{Ir}$ nuclear reaction. Its half-life is 74 days, and it disintegrates by electron capture and β^- and gamma radiation. This nuclide has historical importance, as the isotope was used in the discovery of the Mössbauer effect. For more information, see [Section 8.8](#).

8.6.37 Gold-198

^{198}Au is produced by the $^{197}\text{Au}(n,\gamma)^{198}\text{Au}$ nuclear reaction. The half-life is 2.7 days, and it emits β^- and gamma radiation. ^{198}Au is an ancient radiopharmaceutical; gold colloids have been produced by the reduction of gold salt with ascorbic acid, and they are used in cancer therapy.

8.6.38 Mercury-203

^{203}Hg is produced by the $^{202}\text{Hg}(n,\gamma)^{203}\text{Hg}$ nuclear reaction. Its half-life is 46.6 days, and it emits β^- and gamma radiation. As a widespread industrial tracer, ^{203}Hg is used to determine the volume of mercury in the cells of sodium chloride electrolysis with mercury cathode (see Section 11.2.4).

8.6.39 Isotopes of Elements Heavier than Mercury

The isotopes of the elements that are heavier than mercury are all part of the radioactive decay series except At-211, which is produced in cyclotrons. The half-life of At-211 is 7.21 h, and it has alpha radiation. In addition, Pb-201 is produced from Tl-203 (Eq. (8.27)).

8.6.40 Transuranium Elements

The production of transuranium elements was discussed in Section 6.2.6.

8.7 The Main Steps of the Production of Unsealed Radioactive Preparations (Lajos Baranyai)

Isotope production technologies developed on the principles discussed in Section 8.5.2 consists of the following typical steps: IAEA TECDOC-1341 (2003) and IAEA Technical Reports Series No.63 (1966).

1. selection of the optimal physical and chemical form, as well as the isotope abundance of the target,
2. calculation of the irradiation time and selection of the irradiation parameters,
3. selection of a research reactor or a cyclotron for the irradiation,
4. cooling of the short-lived contamination isotopes,
5. opening and dissolution of the irradiated target,
6. separation of the target radionuclide from the contaminating radionuclides (if necessary),
7. chemical processing of the target, developing the necessary chemical form,
8. purification of the product (if necessary),
9. adjustment of the radioactive concentration of the product,
10. dispensing and sterilization of the product (the latter for radiopharmaceuticals only).

Of course, not all these steps are necessary for each production technology; the actual details of the procedure are determined by the product being sought.

The dissolution of the target generally requires the use of a strong acid or alkaline. However, such an aggressive chemical medium is often not desired in the final formulation; so to eliminate the acid or alkaline, a frequently used method is dry evaporation of the solution. Dry evaporation and the following dissolution of the

dry residue in an arbitrary liquid composition (e.g., buffer or isotonic solution) are simple, and they allow adjustment of the chemical form of the product as required.

8.7.1 *Unsealed Radioactive Preparations Using Reactor Irradiation*

The most frequent sources of nuclear reactions generating artificial radioisotopes are neutrons produced through uranium fission. Based on their kinetic energy, these neutrons can be classified into three groups (as discussed in Section 6.2.1): thermal, epithermal, and fast neutrons, and each of these generate different nuclear reactions. The ratio of the neutrons belonging to the three groups is different at various points of the reactor core, so it is possible to select the neutron energy necessary for the required nuclear reaction either by selecting the appropriate irradiation channel or by shielding the target with cadmium foil.

Neutron flux in research reactors (i.e., in reactors not used for energy production) is typically in the range of 10^{12} – 10^{15} $\text{n cm}^{-2} \text{s}^{-1}$. While in reactors at the lower end of this range, low-activity radioisotopes can be generated, and reactors with higher neutron flux result in products with high specific activity and provide a means of cost-effective radioisotope production. For example, a research reactor with 20 MW power has neutron flux in the range of 1 – 3×10^{15} $\text{n cm}^{-2} \text{s}^{-1}$. Other, low-power reactors (e.g., training reactors) are not suitable for regular, technology-based isotope production, but only for physics measurements and neutron-activation analysis.

Considerations for target selection were discussed in Section 8.5.2, while time-dependence of the neutron activation is found in Section 6.1. Besides, the irradiation time belonging to a given flux has to be calculated based on the activity to be achieved and on the target mass.

8.7.1.1 *Isotope Preparations Generated with Thermal Neutron Irradiation*

Isotope preparations belonging to this group are generated with the (n,γ) nuclear reaction, followed by dissolution and chemical processing of the target. Radiochemical separation is needed only in those cases when other atoms in the compound besides the desired one are highly activated. The products typically contain carriers; for this reason, their specific activity is relatively low.

Among the production methods described in the following section, the first two technologies are very simple because, due to the homogeneous isotope composition and ideal chemical composition of the target, only the target nuclide is generated during irradiation without contaminating radionuclides, and so radiochemical separation is not needed.

The ^{90}Y radionuclide (Table 8.5) with its energy belongs to the group of high-range beta-emitting radionuclides: its penetration in tissues of the living organ is 1–2 cm, so it is suitable for the therapeutic treatment of bone metastases of similar size. The organ-specific behavior of this radionuclide—e.g., penetration of ^{90}Y radionuclide into bone metastases—is ensured by adding ethylene diamine methylene phosphonate (EDTMP) to the radionuclide at the treatment site and the formed

Table 8.5 Preparation of ^{90}Y -Labeled YCl_3

| | |
|---|---|
| Nuclear parameters | Half-life: 64 h. Decay mode and energy: β^- (keV) 2281. |
| Utilization | Used in nuclear medicine for isotope therapy, for treating inflammations and bone metastases. Its high-energy β^- -radiation is absorbed within a distance of couple of centimeters in the body tissues, while the emitted energy has inflammation and pain reduction effect. |
| Target material | Yttrium oxide, $^{90}\text{Y}_2\text{O}_3$, with natural isotope abundance. |
| Target irradiation | In research reactor with thermal neutrons, for some days. |
| Primary nuclear reaction | $^{89}\text{Y}(n,\gamma)^{90}\text{Y}$. |
| Nuclear reactions resulting in contaminating nuclides | None. Note, however, that activation of the chemical impurities present in the target can generate contaminating radionuclides. |
| Target processing | Dissolution in diluted hydrochloric acid with light heating. |
| Chemical processing | For eliminating hydrochloric acid, evaporation to dry. Dissolution of the dry residue in highly diluted hydrochloric acid. pH adjustment to 2–3 with $1 \text{ mol/dm}^3 \text{ HCl}$. |
| Product finishing | Adjustment of radioactive concentration, dispensing to the ordered number of ampoules and steam sterilization in an autoclave. |
| Other ways of production | By extraction of fission products of uranium irradiation with a nuclear reaction of: $\text{U}(n,f) \sim ^{90}\text{Sr} \rightarrow ^{90}\text{Y}$ (yield: 5.9%) |

complex is intravenously injected to the patient. Typical activity of the injection is 17.5–37 MBq. The total activity of the production batches is approximately 370 MBq.

The ^{153}Sm radionuclide (shown in the [Table 8.6](#)) with its energy belongs to the group of low-range beta-emitting radionuclides. Its penetration in tissues of the living organ is 1–2 mm, so it is suitable for the therapeutic treatment of bone metastases of similar size. The organ-specific behavior of this radionuclide—e.g., penetration of ^{153}Sm radionuclide into bone metastases—is ensured by adding EDTMP to the radionuclide on the treatment site, and the formed complex is intravenously injected into the patient. The typical activity of the injection is 150–260 MBq. The total activity of the production batches is approximately 2600 MBq.

Other radionuclides belonging to the group that does not require isotope separation are ^{186}Re , ^{166}Ho , ^{169}Yb , ^{165}Dy , ^{177}Lu , ^{89}Sr , ^{59}Fe , and ^{198}Au (for medical applications), as well as ^{24}Na , ^{42}K , ^{45}Ca , ^{65}Zn , ^{86}Rb , ^{65}Zn , and ^{203}Hg (for industrial applications) (details in [Section 8.6](#)).

Table 8.6 Preparation of ^{153}Sm -Labeled SmCl_3

| | |
|---|---|
| Nuclear parameters | Half-life: 46 h. Decay mode and energy: β^- (keV) 705 and γ (keV) 103 and 635. |
| Utilization | Used in nuclear medicine for isotope therapy, for treating inflammations and bone metastases. Its low-energy β^- -radiation is absorbed within a distance of a few millimeters in the body tissues, while the emitted energy has inflammation and pain reduction effects. |
| Target material | Samarium oxide, $^{152}\text{Sm}_2\text{O}_3$ enriched to 99% abundance. |
| Target irradiation | In a research reactor with thermal neutrons, for some days. |
| Primary nuclear reaction | $^{152}\text{Sm}(n,\gamma)^{153}\text{Sm}$. |
| Nuclear reactions resulting in contaminating nuclides | None. Note, however, that activation of the chemical impurities present in the target can generate contaminating radionuclides. |
| Target processing | Dissolution in diluted hydrochloric acid with light heating. |
| Chemical processing | For eliminating hydrochloric acid, evaporation to dry. Dissolution of the dry residue in highly diluted hydrochloric acid. pH adjustment to 5–6 with 1 mol/dm^3 HCl. |
| Product finishing | Adjustment of radioactive concentration, dispensing to the ordered number of ampoules and steam sterilization in an autoclave. |
| Other ways of production | Not known. |

The following two production procedures (^{51}Cr and ^{82}Br) are examples of having multiple chemical elements present in the target. Consequently, the activation of the target, in addition to the target isotope, results in contaminating radionuclide of significant activity, thus requiring subsequent radiochemical separation.

In medical applications, the typical injected activity of ^{51}Cr administered to patient is 10–18.5 MBq, so typical batch activity of the production is around 370 MBq.

In industry, the ^{51}Cr radioisotope (shown in Table 8.7) is widely used for tracer investigation of metallurgical processes and for studying corrosion processes due to the fact that chromium is an important component of the iron- and steel-based structures.

The ^{82}Br radioisotope (see Table 8.8), as a halogen element, can be used as a tracer isotope for halogenation of various industrial components. It has high-energy gamma radiation; therefore, it can be detected outside industrial equipment or pipelines. Due to its short half-life, it decays rapidly after the investigation.

The most important industrial application of the ^{82}Br radioisotope is the leakage test of oil pipelines. This ^{82}Br -labeled methyl bromide with an activity of

Table 8.7 Preparation of ^{51}Cr -Labeled Na_2CrO_4

| | |
|---|--|
| Nuclear parameters | Half-life: 28 days. Decay mode and energy: EX (100%) and γ (keV) 323. |
| Utilization | Applied in medical diagnosis for labeling intravenously injectable blood plasma preparations. The labeled preparations are used for hematological tests, e.g., blood volume determination. |
| Target material | Enriched (86%) barium chromate, $^{50}\text{BaCrO}_4$. The target is not Cr_2O_3 because it cannot be dissolved easily. Although contaminating radionuclides generated from Ba do not have very high activity, radiochemical separation is necessary. |
| Target irradiation | In the research reactor, with thermal neutrons, for some months. |
| Primary nuclear reaction | $^{50}\text{Cr}(n,\gamma)^{51}\text{Cr}$. |
| Nuclear reactions resulting in contaminating nuclides | $^{59}\text{Co}(n,\gamma)^{60}\text{Co}$, $^{58}\text{Fe}(n,\gamma)^{59}\text{Fe}$, $^{130}\text{Ba}(n,\gamma)^{131}\text{Ba}$, $^{132}\text{Ba}(n,\gamma)^{133}\text{Ba}$, and $^{138}\text{Ba}(n,\gamma)^{139}\text{Ba}$. |
| Target processing | In dilute alkaline, adding hydrogen peroxide under boiling to facilitate dissolution and formation of trivalent Cr^{3+} . |
| Radiochemical separation | Acidification by adding diluted hydrochloric acid. Boiling. Precipitation of Ba ions by adding Na_2SO_4 followed by filtration. |
| Chemical processing | Forming Na chromate by neutralizing the solution with diluted sodium hydroxide. pH adjustment to 6–8. |
| Product finishing | Adjustment of radioactive concentration, dispensing to the ordered number of ampoules and steam sterilization in an autoclave. |
| Other ways of production | <ol style="list-style-type: none"> Neutron irradiation of metallic chromium and chemical processing. Vanadium irradiation with deuteron by the following nuclear reactions: $^{50}\text{V}(d,n)^{51}\text{Cr}$ or $^{51}\text{V}(d,2n)^{51}\text{Cr}$ High specific activity can be reached by applying the Szilard–Chalmers effect on chromium compounds with natural abundance (Section 6.4). It is also produced in the form of a ^{51}Cr–EDTA complex. |

37–74 MBq is injected into the pipeline, and after passing the radioactive cloud, leakage spots are identified using a radiation detector built into a “pig,” together with a distance meter running along the inside of the pipeline. The radiation detector identifies the spots where radioactive tracer oozed outside the pipeline.

In the environment, ^{82}Br is the tracer of choice for tracing surface water and groundwater movements, since the nonadsorbing character of halogens on solid components of soils allows tracking of the movement of flowing waters. The chemical form of Na^{82}Br meets this requirement.

Table 8.8 Preparation of ^{82}Br -Labeled NaBr

| | |
|---|--|
| Nuclear parameters | Half-life: 35 h. Decay mode and energy: β^- (100%) and γ (keV) 55, 619, 698, 777, 828, 1044, 1317, 1475. |
| Utilization | Due to its high gamma energy, this radioisotope is mainly used for investigating industrial and environmental processes. |
| Target material | Potassium bromide (KBr) with natural abundance (49%). Because K is activated in addition to Br, the generated ^{42}K and ^{80}Br radioisotope must be separated from the product. |
| Target irradiation | In a research reactor with thermal neutrons, for some days. |
| Primary nuclear reaction | $^{81}\text{Br}(n,\gamma)^{82}\text{Br}$. |
| Nuclear reactions resulting in contaminating nuclides | $^{41}\text{K}(n,\gamma)^{42}\text{K}$. $^{79}\text{Br}(n,\gamma)^{80}\text{Br}$. |
| Target processing | Dissolution of $^{42}\text{K}^{82}\text{Br}$ in water. |
| Radiochemical separation | Passing the solution through ion-exchange resin in order to exchange K^+ ions to Na^+ ions. Due to its short half-life (17.6 min) ^{80}Br can be cooled from radionuclides. |
| Chemical processing | Dissolution of the eluent of the cation resin in 1 mol/dm ³ NaOH. Adjusting the pH to 6–8 with diluted NaOH. |
| Product finishing | Adjustment of radioactive concentration, dispensing to the ordered number of ampoules. |
| Other ways of production | If $\text{NH}_4^{82}\text{Br}$ is chosen as the irradiated target, no ion exchange is necessary, but this target material is less stable. |

8.7.1.2 Isotope Preparations Generated with Fast Neutron Irradiation

Isotope preparations that are produced through the (n,p) nuclear reaction generated by epithermal or fast neutrons belong to this group. These nuclear reactions change the atomic number of the target element; for this reason, the product must be separated from the target by radiochemical methods. Such products do not contain non-radioactive nucleus (carrier atoms), so their specific activity is high, which is very beneficial for tracer reactions.

Phosphorus is a basic element of some fertilizers, so the ^{32}P radionuclide (see in Table 8.9) plays an important role in agrochemical and related studies. At the same time, it is also frequently used in industrial tracer investigations for studying corrosion inhibitors.

Typical production batch activity for ^{32}P is around 740 GBq. Due to its relatively long half-life, this radionuclide can be dispensed for applications for weeks.

The details of the production of sulfur-35 isotope are given in Table 8.10. The typical production batch is 370 GBq. Due to its relatively long half-life, the product can be dispensed for utilization during periods of months.

Table 8.9 Preparation of ^{32}P -Labeled H_3PO_4

| | |
|---|---|
| Nuclear parameters | Half-life: 14 days. Decay mode and energy: β^- (keV) 1710. |
| Utilization | General radioactive tracer with high β^- energy. Used for labeling, e.g., nucleotides in biochemical research. |
| Target material | Elementary sulfur, ^{32}S with natural abundance (95%). |
| Target irradiation | In a research reactor with fast neutrons, for some months. |
| Primary nuclear reaction | $^{32}\text{S}(n,p)^{32}\text{P}$. |
| Nuclear reactions resulting in contaminating nuclides | $^{34}\text{S}(n,\gamma)^{35}\text{S}$, $^{33}\text{S}(n,p)^{33}\text{P}$. |
| Target processing | Elementary sulfur is irradiated in molten form, followed by dissolution in tetrachloroethylene (TCE) under reflux and heating. |
| Radiochemical separation | Separation of the generated ^{32}P from the irradiated sulfur is made by extraction with water under reflux and heating. |
| Separation of phases | Made in a separation funnel by adding diluted hydrochloric acid to the water phase until reaching a pH of 1–1.5. |
| Purification of the product | Ion exchange on Dowex cation- and anion-exchange resin for the removal of sulfuric acid (generated at the irradiation) and that of metal ions. Elution with diluted hydrochloric acid. Adjusting pH to 3–6. |
| Product finishing | Adjustment of radioactive concentration, dispensing to the ordered number of ampoules. |
| Other ways of production | a. Distillation or coprecipitation made with magnesium hydroxide is also used for separation. b. The nuclear reaction $^{31}\text{P}(n,\gamma)^{32}\text{P}$ provides a lower activity yield. |

Production of the P-33 radionuclide (for medical use) also belongs to this group. It is made from the S-33 target through the (n,p) nuclear reaction (see [Section 8.6](#)).

8.7.1.3 Isotope Preparations Generated with Neutron Irradiation Followed by β^- -Decay

In this group, there are isotope preparations that are made through the (n,p) nuclear reaction, followed by a decay mode causing a change in atomic number, and by the subsequent separation of the product from the irradiated target. Such products do not contain nonradioactive nucleus (carrier atoms), so their specific activity is high.

The I-131 radionuclide (see [Table 8.11](#)) can be listed in this group. Its typical production batch activity is around 740 GBq which—due to its high dose rate constant—needs thick shielding. Air exhausted from the production hot cell passes

Table 8.10 Preparation of ^{35}S -Labeled H_2SO_4

| | |
|---|--|
| Nuclear parameters | Half-life: 87 days. Decay mode and energy: β^- (keV) 167. |
| Utilization | General radioactive tracer with low β^- -energy. Used for labeling, e.g., nucleotides in biochemical research. |
| Target material | Potassium chloride, KCl, with natural abundance of ^{35}Cl (36%). |
| Target irradiation | In a research reactor with fast neutrons, for some months. |
| Primary nuclear reaction | $^{35}\text{Cl}(n,p)^{35}\text{S}$. |
| Nuclear reactions resulting in contaminating nuclides | $^{33}\text{S}(n,p)^{36}\text{P}$, $^{35}\text{Cl}(n,\gamma)^{36}\text{Cl}$, $^{35}\text{Cl}(n,\alpha)^{32}\text{P}$. |
| Target processing | Dissolution in diluted hydrochloric acid. |
| Radiochemical separation | Adsorbing ^{36}P , ^{36}Cl , and ^{32}P contaminating radionuclides on the alumina column. Elution of ^{35}S from the column with diluted ammonium hydroxide. pH adjustment of the eluent with hydrochloric acid to 1.5. |
| Purification of the product | Passing the solution through Dowex cation-exchange resin to bind ammonium, aluminum, potassium, and other metallic ions. The resin is then washed with water. Dry evaporation of the eluent for eliminating HCl generated during ion exchange. Re-dissolution of the dry residue in water. |
| Product finishing | Adjustment of radioactive concentration, dispensing to the ordered number of ampoules. |
| Other ways of production | a. Starting from the ^{35}Cl target, other chemical procedures are also used. b. The $^{34}\text{S}(n,\gamma)^{35}\text{S}$ nuclear reaction with a low-activity yield. |

through a charcoal filter impregnated with iodine absorbent. Both the filter and the absorbent material will be handled later as radioactive waste.

In addition to the ^{131}I radioisotope, there is another iodine radioisotope suitable for *in vitro* investigations; namely, ^{125}I (see Table 8.12) which also has low X-ray and gamma energy. It is produced from Xe gas, and the typical batch size is around 370 GBq. Its low gamma energy does not require high shielding. Air exhausted from the production hot cell passes through a charcoal filter impregnated with iodine absorbent. (The third important iodine radioisotope, ^{123}I , is a cyclotron product.)

8.7.1.4 Isotope Preparations Extracted from Fission Products Generated by Neutron Irradiation of Uranium

Neutron irradiation of the ^{235}U nuclide generates a wide variety of fission products, which are then stabilized through β^- -decays or transformed to radionuclides with

Table 8.11 Preparation of ^{131}I -Labeled NaI

| | |
|---|---|
| Nuclear parameters | Half-life: 8 days. Decay mode and energy: β^- (keV) 608 and γ (keV) 364. |
| Utilization | Its gamma radiation is used for diagnostics, and its β^- radiation is used for therapy of thyroid abnormalities. In addition, several organic molecules (e.g., ^{131}I -MIBG (<i>meta</i> -iodobenzylguanidine), fatty acids, and sodium- <i>o</i> -iodo-hippurate) can be labeled with ^{131}I radionuclide through iodination. |
| Target material | Tellurium dioxide, $^{130}\text{TeO}_2$ with natural isotope abundance (35%). |
| Target irradiation | In a research reactor with thermal neutrons, for some days. |
| Primary nuclear reaction | $^{130}\text{Te}(n,\gamma)^{131}\text{Te}$ and $^{130}\text{Te}(n,\gamma)^{131m}\text{Te} \rightarrow ^{131}\text{Te}$. |
| Decay of the generated radionuclide | $^{131}\text{Te} \xrightarrow{\beta^-} ^{131}\text{I}$ |
| Nuclear reactions resulting in contaminating nuclides | $^{120}\text{Te}(n,\gamma)^{121}\text{Te}$, $^{124}\text{Te}(n,\gamma)^{125}\text{Te}$, $^{126}\text{Te}(n,\gamma)^{127}\text{Te}$, $^{128}\text{Te}(n,\gamma)^{129}\text{Te}$. |
| Target processing | The target material is placed into a ceramic vessel and molten in an electric furnace at a temperature of 850°C. |
| Radiochemical separation | Iodine is separated from the irradiated molten target by dry distillation. Evaporated iodine is collected in diluted NaOH-containing absorbers. As iodine is stable in alkaline solution only; the pH in the absorbers is adjusted to 6–8. |
| Product purification | Distilled iodine is bubbled through sulfuric acid in a scrubber in order to deposit tellurium isotopes, contaminating isotopes generated from chemical contaminants (e.g., Cu, Fe, Ni, Ag, Se, and Pb), as well as to trap chemical contaminants. This purification is a part of the separation procedure (distillation). |
| Product finishing | Adjustment of radioactive concentration, dispensing to the ordered number of ampoules. |
| Other ways of production | a. Technologies of wet distillation, extraction, and chemical separation are also used. b. ^{131}I can be extracted from fission products generated by uranium irradiation. |

longer half-lives, suitable for various applications. The ^{99}Mo , ^{131}I , ^{137}Cs , and ^{85}Kr fission products have practical importance. Among them, ^{99}Mo is very significant because its daughter element, the ^{99m}Tc radionuclide, is appropriate for isotope generation (a “cow,” as discussed in [Section 8.3](#)), is the most important radioisotope of the medical diagnostics IAEA TECDOC-1065 (1999).

Table 8.12 Preparation of ^{125}I -Labeled NaI

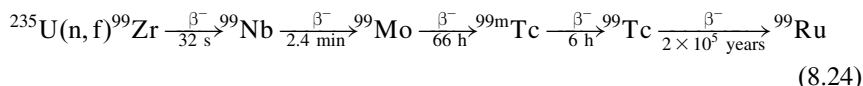
| | |
|---|--|
| Nuclear parameters | Half-life: 60 days. Decay mode and energy: EC (100%), X-ray (keV) 28, and γ (keV) 35. |
| Utilization | General radioactive tracer. Mainly used for labeling RIAs for <i>in vitro</i> investigations, that is, for testing samples extracted from the living body (blood, urine, etc.). |
| Target material | Xenon gas with natural isotope abundance (0.096%) or enriched xenon gas (99.9%) encapsulated in a pressure-proof aluminum capsule. |
| Target irradiation | In a research reactor with thermal neutrons, for some days. |
| Primary nuclear reaction | $^{124}\text{Xe}(n,\gamma)^{125}\text{Xe}$. |
| Decay of the generated radionuclide | $^{125}\text{Te} \xrightarrow{\text{EC}} ^{125}\text{I}$ |
| Nuclear reactions resulting in contaminating nuclides | a. Subsequent activation of the generated ^{125}I isotope through the nuclear reaction $^{125}\text{I}(n,\gamma)^{126}\text{I}$. Reduction of the rate of ^{126}I nuclide below 0.1% by cooling. b. Nuclear reactions resulting in contaminating products: $^{126}\text{Xe}(n,\gamma)^{127}\text{Xe}$, $^{128}\text{Xe}(n,\gamma)^{129}\text{Xe}$, $^{130}\text{Xe}(n,\gamma)^{131}\text{Xe}$, $^{132}\text{Xe}(n,\gamma)^{133}\text{Xe}$, $^{134}\text{Xe}(n,\gamma)^{135}\text{Xe}$, and $^{136}\text{Xe}(n,\gamma)^{137}\text{Xe}$ |
| Radiochemical separation | After decay, the ^{125}I radionuclide is adsorbed on the inside surface of the aluminum capsule. Xe isotopes are eliminated from the opened capsule by blowing them away. The aluminum capsule is then heated in an electric oven for the dry distillation of the iodine. Iodine vapors are absorbed in diluted sodium hydroxide. Because iodine is stable in alkaline solution only, the pH is adjusted to 8–10. |
| Product purification | Distilled iodine is bubbled through a scrubber that first has been filled with concentrated sulfuric acid to remove chemical contaminants. |
| Product finishing | Adjustment of radioactive concentration, dispensing to the ordered number of ampoules. |
| Other ways of production | a. By periodic tapping, the loop built into the reactor zone in which Xe gas is circulated and irradiated. b. In a cyclotron, through nuclear reactions $^{125}\text{Te}(p,n)^{125}\text{I}$, $^{124}\text{Te}(d,n)^{125}\text{I}$, and $^{125}\text{Te}(d,2n)^{125}\text{I}$ with a lower yield. |

The common feature of this group is that individual fission products can be extracted from the mixture with multistep separation methods. They are noncarrier added radionuclides, but they contain many potentially contaminating radionuclides; thus, sophisticated purification is required to obtain sufficiently pure isotopes.

Table 8.13 Preparation of ^{99}Mo -Labeled $\text{Na}_2^{99}\text{MoO}_4$

| | |
|---|--|
| Nuclear parameters | Half-life: 66 h. Decay mode and energy: β^- (keV) 1214 and γ (keV) 740. |
| Utilization | For the preparation of $^{99}\text{Mo}/^{99\text{m}}\text{Tc}$ isotope generator |
| Target material | Enriched uranium containing 45% ^{235}U in aluminum alloy. |
| Target irradiation | In high-flux research reactors, with thermal neutrons, for some days. |
| Primary nuclear reaction | A $^{235}\text{U}(\text{n},\text{f})$ mixture of fission products (^{99}Mo content 6%). |
| Target processing | Dissolution of the target in NaOH with addition of oxidizing agent (e.g., H_2O_2), in order to assist dissolution and to provide an oxidized medium. |
| Extraction from the mixture of fission products | When dissolving the target in alkaline, beside ^{99}Mo , only a few other elements will be found in the solution. These contaminating elements are separated in two ion-exchange columns and in another column filled with a chelating agent. ^{99}Mo is eluted from the third column; the eluent is evaporated to dry and dissolved again in NaOH. To lower the reduction effect of radiolysis, an oxidizing agent (hypochlorite) is added to the solution. |
| Product finishing | In alkaline solution, the chemical species is sodium molybdate ($\text{Na}_2^{99}\text{MoO}_4$). This solution with very high activity is transported in depleted uranium containers that have a much higher attenuation coefficient against radiation than lead containers. |
| Other ways of production | With a nuclear reaction of $^{98}\text{Mo}(\text{n},\gamma)$, ^{99}Mo can also be obtained, but specific activity is much lower. |

The production of the ^{99}Mo radionuclide in fission nuclear reaction is followed by subsequent β^- -decays:



The activity of ^{99}Mo represents only approximately 6% of the fission mixture. Its extraction from the isotope mixture and its production as sodium molybdate is carried out in steps described in [Table 8.13](#).

Considering the fact that the portion of the ^{99}Mo in the mixture of fission products is low (6%), producers supply several users, and users apply several orders of magnitude of TBq ^{99}Mo activity for generator production; the total activity produced is extremely high. Moreover, the ^{99}Mo radionuclide has high gamma energy; thus, the production of ^{99}Mo requires hot cells with very thick (40–50 cm) lead shielding and results in a huge amount of radioactive waste.

Recently, five countries (Canada, France, Belgium, the Netherlands, and South Africa) produced ^{99}Mo in good quantity, which satisfies these high technical requirements and from which users ($^{99}\text{Mo}/^{99\text{m}}\text{Tc}$ generator producers) are supplied.

The extracted ^{99}Mo is used for preparing $^{99}\text{Mo}/^{99\text{m}}\text{Tc}$ radionuclide generators. The principle of isotope generators is described in [Section 8.3](#). Because the half-lives of the parent (^{99}Mo) and daughter ($^{99\text{m}}\text{Tc}$) nuclides are within the same orders of magnitude, transient equilibrium will develop (see [Section 4.1.6](#)). The activity of the system will be directed by the parent nuclide decay. The daughter nuclide is separated from its parent on the place of use. As this separation is made not in the generator production facility but at the user (e.g., in hospitals), it is important that the separation should be simple. From this aspect, chromatographic separation—where the daughter nuclide is eluted from its parent fixed on a chromatographic column—is the most beneficial.

Although many types of isotope generators exist, only some of them have practical importance; e.g., $^{188}\text{W}/^{188}\text{Re}$, $^{90}\text{Sr}/^{90}\text{Y}$, $^{113}\text{Sn}/^{113\text{m}}\text{In}$, $^{82}\text{Sr}/^{82\text{m}}\text{Rb}$, and $^{99}\text{Mo}/^{99\text{m}}\text{Tc}$ for medical use, and $^{137}\text{Cs}/^{137\text{m}}\text{Ba}$ for industrial use. Among them, the $^{99}\text{Mo}/^{99\text{m}}\text{Tc}$ isotope generator has the highest significance because it provides the most important radionuclide ($^{99\text{m}}\text{Tc}$) used for isotope diagnostics in nuclear medicine. As much as 80% of the isotope diagnostic investigations in medicine are made with this radionuclide; for this reason, this system is described in detail next.

The dominant role of the $^{99}\text{Mo}/^{99\text{m}}\text{Tc}$ isotope generator can be attributed not only to the ideal nuclear characteristics of the $^{99\text{m}}\text{Tc}$ daughter nuclide (with gamma energy, which can penetrate through body tissues and with an ideal half-life), but also to its desirable chemical properties. The technetium as transition metal can be bound with several organ-specific complexes, which transfer the labeling isotope to the intended organ. Consequently, the same radionuclide with its beneficial nuclear features is suitable for investigating various organs by varying the linked chemical chelating agent.

In addition to these benefits, the $^{99\text{m}}\text{Tc}$ radionuclide can be easily extracted (eluted) from the $^{99}\text{Mo}/^{99\text{m}}\text{Tc}$ isotope generator on site if this isotope mixture is adsorbed on a chromatographic column. The chromatographic separation is based on the different retention coefficient of the two radionuclides. Molybdate ions form so-called oligomer aggregates in acidic solutions, so they adsorb stronger in the alumina column than single pertechnetate ions. This binding is strengthened further by higher charges of the molybdate ions. The chemical composition of molybdate and pertechnetate ions present in various pH ranges is summarized in [Table 8.14](#).

The best chromatographic separation is achieved when both the ^{99}Mo parent and the $^{99\text{m}}\text{Tc}$ daughter nuclides are maintained in the highest oxidation state. This means that the isotope mixture must be maintained under strongly oxidized conditions during the whole production.

However, the high activity of the isotope mixture and the resulting dose cause permanent radiolysis (chemical decomposition caused by radiation effect) in the water solution, causing chemical reduction. As a result, the radiation of the isotope mixture has a countereffect against maintaining an oxidizing medium and a good separation because oligomers cannot be separated in lower oxidation states.

Table 8.14 The Chemical Composition of Molybdate and Pertechnetate Ions in Various pH Ranges

| pH Range | Chemical Species | Features |
|--------------------------------|--|-----------------------------|
| Mo-99 Parent Nuclide | | |
| pH < 1.5 | $[\text{Mo (VI) O}_2]^{2+}$ | Single molybdate cations |
| 1.5 < pH < 3 | $[\text{Mo}_8 \text{ (VI) O}_{26}]^{4-}$ | Octamolybdate anions |
| 3 < pH < 6 | $[\text{Mo}_7 \text{ (VI) O}_{24}]^{6-}$ | Heptamolybdate anions |
| pH > 6 | $[\text{Mo (VI) O}_4]^{2-}$ | Single molybdate anions |
| Tc-99m Daughter Nuclide | | |
| 1.5 < pH < 3 | $[\text{Tc (VII) O}_4]^-$ | Single pertechnetate anions |

To maintain a permanent oxidized state with suitable redox potential in the solution, an oxidizing agent, such as hydrogen peroxide and bubbled air, must be added to the isotope mixture.

Based on these considerations, the production of the $^{99}\text{Mo}/^{99\text{m}}\text{Tc}$ isotope generator from fission molybdenum ($\text{Na}_2^{99}\text{MoO}_4$) is carried out through steps described in [Table 8.15](#).

The total activity of ^{99}Mo in the generator production plants is in the TBq range at production time. Activities dispensed to individual generators are in the range of 37–370 GBq. Activity to be dispensed to the generator column can be chosen by the user when ordering the generator. As the dose rate constant of the parent nuclide is high, processing the total activity needs hot cells with a lead wall thickness of 15 cm, while shielding of the generators requires a lead pot with a lead wall thickness of 5 cm.

The half-life of the daughter nuclide ($^{99\text{m}}\text{Tc}$) is relatively short (6 h), so it will decompose shortly after the diagnostic investigation. At the same time, the longer half-life (66 h) of the parent nuclide provides comfortable access for the daughter nuclide at least for a week. In practical terms, this means that a hospital laboratory can perform around 100 diagnostic investigations with the daughter nuclide by ordering fresh isotope generator every week and by eluting it once a day.

The principal operation scheme of the $^{99}\text{Mo}/^{99\text{m}}\text{Tc}$ isotope generator is demonstrated in [Figure 8.4](#). The two tubes of the chromatographic column end in injection needles for which the elution agent solution and a vacuumed ampoule are attached by piercing. A vacuum will suck the eluent through the column, which desorbs the generated $^{99\text{m}}\text{Tc}$ daughter nuclide from the column.

The activity versus time functions of the ^{99}Mo parent nuclide decay and of the $^{99\text{m}}\text{Tc}$ daughter nuclide generation are shown in [Figure 8.11](#). The process leads to transient equilibrium. It should be noted that the daughter activity reaches its maximum at 24 h, which coincides with the hospital practice, e.g., the elution of the generator once a day guarantees the daily maximum activity for the elution.

[Figure 8.11](#) shows that daughter activity theoretically exceeds parent activity at transient equilibrium (dotted line). However, due to the branching decay of ^{99}Mo (the value of branching factor = 0.96), the activity of the $^{99\text{m}}\text{Tc}$ daughter nuclide

Table 8.15 The $^{99}\text{Mo}/^{99\text{m}}\text{Tc}$ Isotope Generator

| | |
|---|--|
| Nuclear parameters | Half-life of the parent nuclide: 66 h. Decay mode and energy: β^- (keV) 1214 and γ (keV) 740. Half-life of the daughter nuclide: 6 h. Decay mode and energy: IT and γ (keV) 141. |
| Utilization | The most important radionuclide of the medical diagnostic applications. A multipurpose organ-specific tracer if bound to various chelating agents. |
| Base material | A fission-based ^{99}Mo radionuclide in the chemical form of $\text{Na}_2^{99}\text{MoO}_4$. |
| Preparation of the chromatographic column | Chromatographic column filled with alumina is pretreated by passing through diluted nitric acid to create positive binding places for molybdate ions with negative charges. |
| Chemical processing of the base material | Oxidizing the $\text{Na}_2^{99}\text{MoO}_4$ solution with H_2O_2 to ensure suitable redox potential for depressing the chemical reduction caused by radiolysis. Titrating the solution with HNO_3 up to pH 3 to initiate formation of octamolybdate oligomer anions. |
| Binding isotope mixture on the chromatographic column | Binding ^{99}Mo on an Al_2O_3 chromatographic column by passing the isotope mixture through the column. |
| Elution of the column | Separation of the $^{99\text{m}}\text{Tc}$ daughter from the parent by elution made with 0.9% NaCl solution (so-called physiologic solution). This is necessary to wash down the column, followed by measuring the newly generated $^{99\text{m}}\text{Tc}$ nuclide activity for testing the generator. |
| Product finishing | After assembling with elution tubes, the filled chromatographic columns are put into lead containers for transporting isotope generators to the users. |
| Elution made by the user | The producer of the isotope generator provides ampoules (one for each day filled with 0.9% NaCl solution and one for each day with a vacuum) for making the elutions. Each elution is carried out by piercing the elution ampoule and the vacuum ampoule to injection needles connected to the two ends of the chromatographic column. |
| Other ways of production | Based on the $^{98}\text{Mo}(n,\gamma)^{99}\text{Mo}$ nuclear reaction, produced by “direct” reactor irradiation. For the separation, various techniques have been developed: extraction, sublimation, elution of gel-generators, and so on. |

remains systematically below the parent activity (continuous line). So, approximately 90% of the parent activity can be eluted as $^{99\text{m}}\text{Tc}$ in equilibrium (Figure 8.12).

The activity curve corresponding to the hospital practice—daughter elution once a day—is demonstrated in Figure 8.13. $^{99}\text{Mo}/^{99\text{m}}\text{Tc}$ radionuclide generators can be used economically for a week, with daily activities decreasing according to the parent decay.

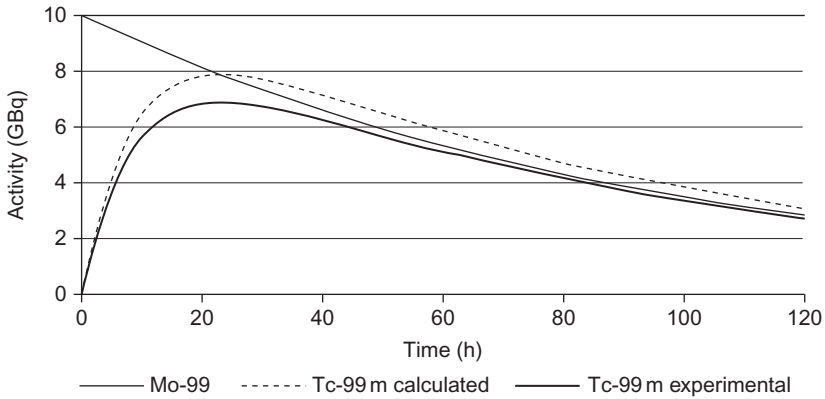


Figure 8.11 Activity versus time curves of ^{99}Mo parent and $^{99\text{m}}\text{Tc}$ daughter nuclides.

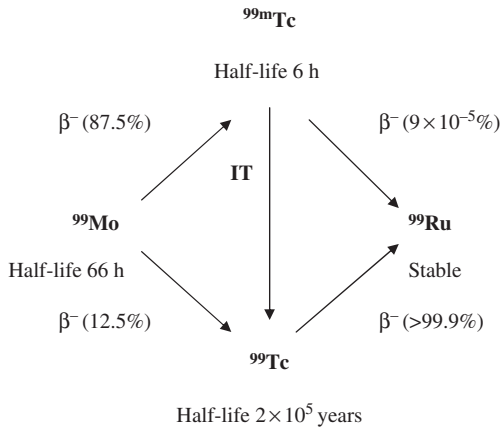
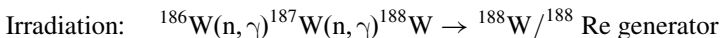


Figure 8.12 The decay scheme of a ^{99}Mo radionuclide.

While $^{99\text{m}}\text{Tc}/^{99}\text{Mo}$ generators are used for diagnostic purposes, another important generator (produced by high-flux reactor irradiation) is the $^{188}\text{W}/^{188}\text{Re}$ generator, which also serves a diagnostic purpose:



8.7.2 Unsealed Radioisotope Preparations Based on Cyclotron Irradiation

Charged particles (e.g., protons and deuterons) generated in cyclotrons may participate in nuclear reactions, resulting in several new radionuclides used mainly for medical purposes. According to proton energy, the following cyclotron types are known:

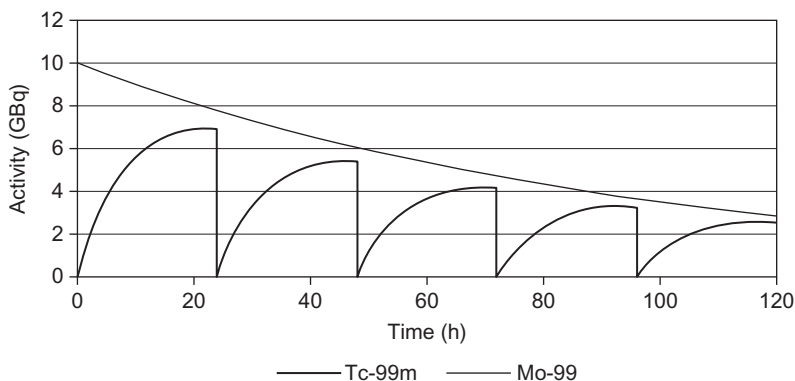


Figure 8.13 The activity curve representing daily elutions.

- Medical or “baby” cyclotrons installed on the site of the application of radionuclide with maximum proton energy of 10–12 MeV, suitable for producing very short-lived ($T_{1/2} < 2$ h) radionuclides (^{18}F , ^{13}N , ^{11}C , ^{15}O ; see Table 8.4). These radionuclides are tracers for PET, and all except ^{18}F are found in living organs as chemical elements. Thus, they have the advantage that no foreign atom is used for labeling the organ-specific molecule and atoms naturally present in living organs can be labeled with their PET radionuclides.
- In industrial cyclotrons with higher proton energy (30–40 MeV), radionuclides of longer half-lives used both as industrial and medical tracers (^{67}Ga , ^{201}Tl , ^{111}In , ^{123}I , and ^{81}Rb) can be produced. The latter is the parent of the isotope generator $^{81}\text{Rb}/^{81}\text{Kr}$, the daughter of which, as noble gas, is used for lung diagnostics.
- The main application of the very-high-energy cyclotrons (70–200 MeV) is tumor therapy. In addition, cyclotrons with a high current density are used for producing radionuclides of a low-proton-absorption cross section (e.g., ^{103}Pd).

For cyclotron irradiation, the yield Y ($\text{Bq}/\mu\text{A} \cdot \text{h}$) of the nuclear reaction can be calculated with the following formula:

$$Y = N\Phi(1 - e^{-\lambda t}) \int_0^E \sigma(E) dX \quad (8.25)$$

where N is the number of target atoms in a given volume, Φ is the flux of the bombarding particle, σ is the cross section of the target element, E is the energy of the bombarding particle, and X is the thickness of the target. (This equation is another form of Eq. (6.9).)

Among cyclotron isotopes, the ^{18}F radionuclide and its labeled compound, ^{18}F -fluorodeoxyglucose (^{18}F FDG), has the most important and the highest utilization.

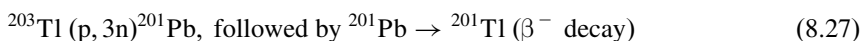
Today, the fluorination reaction following the target irradiation is a fully automated, computer-controlled process using “synthesis panels,” which carry out computed steps of the reaction without human intervention (see Table 8.16).

Among radionuclides with longer half-lives produced in industrial cyclotrons, ^{67}Ga , ^{201}Tl , and ^{123}I have practical importance in medical applications. These

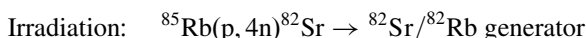
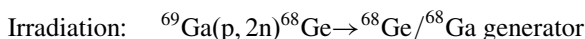
Table 8.16 Preparation of ^{18}F -Labeled FDG

| | |
|---|--|
| Nuclear parameters | Half-life: 1.7 h. Decay mode and energy: β^+ (keV) 650 and γ (keV) 512. |
| Utilization | Deoxyglucose labeled with fluor ^{18}F is suitable for detecting glucose consumption that cells use for energy supply. Tumor cells, for instance, consume glucose at an increased rate, so diagnosis of such cells is possible with FDG. In addition to this, it is also suitable for detecting certain myocardial disorders and inflammations. |
| Target material | Water enriched with ^{18}O . |
| Target irradiation | In cyclotron, at 75 μA . |
| Primary nuclear reaction | $^{18}\text{O}(\text{p},\text{n})^{18}\text{F}$. |
| Nuclear reactions resulting in contaminating nuclides | During chemical synthesis following irradiation, only the target isotope is bound to the molecule to be labeled, so carrier-free product is produced. |
| Steps of the FDG synthesis | Separation of fluor from the irradiated target on ion-exchange resin. Transfer of ^{18}F into the organic phase with crown-ether. Fluorination of the FDG precursor with nucleophilic substitution. Hydrolysis of the protecting groups with acid or alkaline. Separation of ^{18}FDG from the reaction mixture. |
| Product finishing | Dispensing to the ordered number of ampoules. |
| Radiochemical yield | Approximately 70% |
| Obtained activity | Approximately 3.7×10^{11} Bq ^{18}F corresponding to 2.5×10^{11} Bq ^{18}FDG . |
| Radiochemical purity | >99%. |

products—due to their longer half-lives—can be transported over longer distances. Nuclear reactions that serve to generate these radionuclides are:



Some radionuclides produced in high-energy cyclotrons are important radionuclide generators.



As daughter nuclides emit positrons, these generators are used for PET images.

Table 8.17 The Most Frequently Used Quality Control Methods for Open-Vessel Radioactive Preparations

| Tested Parameter | Test Method |
|--|--|
| Activity | Activity meter with ionization chamber |
| Specific activity | Activity/mass (determination by calculation, e.g., with ion-selective electrode) |
| Radioactive concentration | Activity/volume (by calculation) |
| Radionuclide purity | Gamma and beta spectroscopy |
| Radiochemical purity | Thin-layer chromatography |
| pH | pH paper and pH electrode (potentiometric method) |
| Separation yield of the parent and daughter radionuclides (at generators) | Measurement of the parent and daughter activities |
| Parent nuclide concentration (as contamination) in the separated daughter nuclide—called a parent breakthrough | Measurement of the parent and daughter activities |
| Sterility | Innoculation onto a medium; incubation |
| Endotoxin content (pyrogenity) | LAL (limulus ameobocyte lysate) test |

8.7.3 Quality Control of Unsealed Radioactive Preparations

Quality control of the unsealed radioactive preparations includes the determination of the following quality parameters:

- radionuclidic purity (detection and quantity determination of the contaminating radionuclides),
- radiochemical purity (detection and quantity determination of radionuclides found in another chemical form as that of the product),
- control of radioactive concentration,
- control of the pH of the solution,
- checking microbiological purity.

The most frequently applied quality control methods of the unsealed radioactive preparations are summarized in [Table 8.17](#). The quality parameters of the unsealed radioactive preparations are determined on samples taken from the bulk solution. Microbiological control tests are carried out as retrospective tests after decay.

8.8 Production of Encapsulated Radioactive Preparations (Sealed Sources) (Lajos Baranyai)

Sealed radioactive preparations emitting gamma radiation (e.g., ^{192}Ir - and ^{60}Co -sealed sources) are produced by placing reactor-irradiated metal pellets or cylinders into steel capsules, followed by sealing by welding. The overall activity

of the assembled source can be controlled by using the appropriate number of the individual pellets/cylinders of known (measured) activity. The activities of such gamma-emitting sealed sources are extremely high; they are in the range of TBq (terra-Becquerel).

Beta-emitting (e.g., ^{137}Cs) sealed sources are produced by chemical processing of ^{137}Cs extracted from fission mixtures to $^{137}\text{CsCl}$, followed by embedding these particles into glass beads and finally by sealing glass beads into metal capsules. Alpha-emitting (e.g., ^{241}Am) sealed sources are produced by extracting the given radionuclide from fission mixture and deposited onto foils.

Sealed radiation sources are used both for medical and for industrial applications. In medical applications, external radiation therapy and brachytherapy, while in industrial applications radiography (e.g., testing welding seams) and gamma sterilization are generally known.

8.8.1 The Main Steps of the Production of Sealed Radioactive Sources

The production process that consists of neutron irradiation of the target and the subsequent encapsulation of the irradiated pellets is demonstrated through the example of ^{192}Ir -sealed source production (see [Table 8.18](#)).

^{60}Co -sealed sources are produced in the nuclear reaction of $^{60}\text{Co}(n,\gamma)^{60}\text{Co}$ with similar processing as that of ^{192}Ir , but applying much longer irradiation time (i.e., several months).

8.8.2 Quality Control of Sealed Radioactive Sources

At the production of sealed (encapsulated) radioactive sources, quality control includes activity testing, surface contamination testing, and leakage testing (see [Table 8.19](#)).

8.9 Facilities, Equipment, and Tools Serving for Production of Radioactive Substances (Lajos Baranyai)

The facilities and equipment for producing radioactive preparations (generally representing high activities) must fulfill three conditions simultaneously:

- protection against radiation of the radioactive material (e.g., radiation protection for employees),
- protection against radioactive contamination (e.g., protection of the surrounding area from radioactive contamination and prevention of incorporation of radioactive materials in human organs),
- protection against microbiological contamination (e.g., avoiding infection of the product caused by bacteria and fungi); this third type of protection relates to radiopharmaceuticals only.

Table 8.18 Preparation of ^{192}Ir -Sealed Radiation Source

| | |
|---|--|
| Nuclear parameters | Half-life: 74 days. Decay mode and energy: β^- (keV) 675, β^- (keV) 539, with γ (keV) 296, γ (keV) 308, and EX, with γ (keV) 316, γ (keV) 468. |
| Utilization | Industrial radiography, e.g., testing welding seams. |
| Target material | Metal iridium (Ir) pellets. |
| Target irradiation | In a research reactor, with thermal neutrons, for some weeks. |
| Primary nuclear reaction | $^{191}\text{Ir}(n,\gamma)^{192}\text{Ir}$. |
| Nuclear reactions resulting in contaminating nuclides | $^{23}\text{Na}(n,\gamma)^{24}\text{Na}$, $^{35}\text{Cl}(n,\gamma)^{36}\text{Cl}$, $^{35}\text{Cl}(n,p)^{35}\text{S}$, $^{37}\text{Cl}(n,\gamma)$, and ^{38}Cl . |
| Steps of processing | <ol style="list-style-type: none"> 1. Cool the contaminating radionuclides until suitable decay occurs. 2. Measure the activity of pellets in a dose calibrator built into the hot cell. 3. Place irradiated pellets into a capsule, assembling the required activity. 4. Arc weld the capsules under argon protection, within the hot cell. |
| Product finishing | Placing capsules (sealed sources) into a lead container. |
| In-process control | <ol style="list-style-type: none"> 1. Leakage testing on the welded sealed sources. 2. Checking surface contamination of the welded sources. |

Table 8.19 Quality Control of Encapsulated Radioactive Preparations (Sealed Sources)

| Tested Parameter | Testing Method |
|---|---|
| Activity control | With ion-chamber dose calibrator. |
| Checking surface contamination (dry and wet sampling) | A smear test is made on the surface of the sealed radiation source, and activity on the sponge is detected. |
| Leakage test (method I): Leakage test based on seepage in ultrasonic bath | The sealed radiation source is soaked in a solvent in which solubility of the radiation source (pellet) is good but that of the capsule is low. The activity of the solvent is then measured. |
| Leakage test (method II): Leakage test with bubbling | The sealed radiation source is placed into ethylene glycol, the vessel is vacuumed, and the appearance of bubbling is observed. |

Protection against radiation depends on the type of radiation IAEA Safety Series No.1 (1973). As most radioactive products emit gamma radiation, which has the highest range, the highest level of protection is against gamma radiation. The efficient protection against gamma radiation is the application of absorbing shielding walls made of high-density materials (lead, heavy concrete, etc.). However, against

pure beta radiation, which is free of gammas, shielding material is made of elements of low atomic number (e.g., plexi).

In radioactive isotope processing facilities, monitoring systems indicating the level of radiation are installed, and personnel are supplied with personal dosimeters.

So-called hot cells, which are separated from their surroundings by shielded walls and equipped with manipulators provide protection against radioactive contamination of the surrounding area and prevention from incorporation in humans (e.g., introduction of radioactive materials into the human body, mainly by inhalation). From hot cells, the air is continuously exhausted and led to chimneys through filters. Shielding walls serve not only to separate the space from its surrounding but also for radiation protection by absorbing radiation (Figure 8.14). Simultaneously, fresh air is continuously introduced into the surrounding area by ventilators which, together with the exhaustion, provide the necessary pressure differences, forcing the air flow from potentially less-contaminated areas toward potentially contaminated areas (e.g., from dressing rooms toward the working area, and then toward the hot cells and the chimney).

Facilities serving for handling radioactive materials are classified into “A,” “B,” and “C” radiation protection categories depending on the harm and activity of the handled radioactive material. Facilities processing high activities classified in category A are equipped with series of hot cells and are separated from the surrounding areas by dressing rooms.

The third type of protection, namely protecting the product from microbiological contamination, requires the opposite air flow direction than that is applied against radioactive contamination. Because airborne particles are typical carriers for bacteria and mainly responsible for dissemination, a filtered air flow free of bacteria is introduced into the area around the product in the direction of the outside area (such systems are called “clean rooms” in the traditional pharmaceutical manufacture). In addition to controlling air flow conditions, working surfaces need to be regularly disinfected, which in closed hot cells is not easy to do. In addition to



Figure 8.14 A hot cell system equipped with radiation-shielding walls.

these protections, operators executing production are also microbiological contamination sources; for this reason, special protection clothing is necessary.

Consequently, radioactive contamination protection requires manufacturing areas with negative pressure (Figure 8.14), while microbiological protection requires areas with positive pressure (Figure 8.15).

Due to the opposite requirements relating to the air flow and considering requirements for radiation protection, radioactive materials in the pharmaceutical grade are manufactured in facilities that combine the two systems. Such combined systems are radioactive hot cells installed in aseptic clean rooms, where filtered air from the clean room is introduced into the hot cells or alternatively, hot cells with controlled internal air supply—so-called negative pressure isolators—where filtered air with a lower flow rate is introduced into the hot cell, while air with a higher flow rate is extracted from the hot cell. The difference between the air flow rate of the inlet and outlet guarantees that negative pressure is required for radioactive contamination protection within the hot cell. The introduction of filtered air and the maintenance of negative pressure provide simultaneous protection against microbiological and radioactive contamination in the same space.

The protocol to satisfy the requirements of radiation protection, protection against radioactive contamination, and protection against microbiological contamination is not completely developed yet. The harmonization of these opposite requirements is difficult and sometimes involve conflicts and must be based on compromises. IAEA exists to develop solutions and systems that satisfy the requirements of both the nuclear and pharmaceutical authorities.

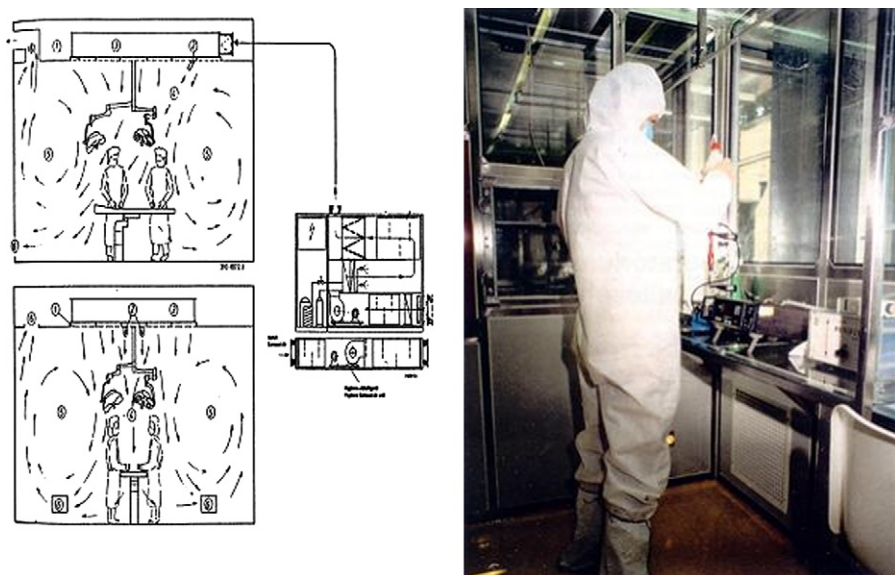


Figure 8.15 A clean room for aseptic handling of pharmaceuticals.

For handling of radioactive products that are not used as pharmaceuticals (so-called radiochemicals) and for sealed radioactive sources, only radiation protection and radioactive contamination protection are necessary.

The main requirements for equipment and tools in hot cells that are used for the execution of manufacturing operations (e.g., rotating knives for cutting targets, distillation equipment, pipettes for dispensing, magnetic stirrers, heating devices, auto-claves, ampoule capping devices) are operability with manipulators and small size. Such equipment and tools have become more and more automated. Automation fosters not only modernization but also radiation protection for humans and quality assurance. Modern isotope manufacturing technologies are already automated and computer controlled, in which the need for human interaction is minimal.

An important environmental aspect is the safe deposition of radioactive material generated as radioactive wastes in the manufacturing process. The usual approach for short-lived radionuclides is storage until decay, while for long-lived ones is deposition. This implies that liquid radioactive wastes are first bound to cement, placed into metal drums, and then, together with other solid radioactive wastes, are transported to authorized radioactive repositories (see Section 7.3) for final disposal.

Further Reading

- Bouissieres, G., Chastel, R. and Vigneron, L. (1947). Etats de dispersion du polonium dans l'eau, l'alcool et l'acetone. *Comptes Rendus* 224:43–45.
- Choppin, G.R. and Rydberg, J. (1980). *Nuclear Chemistry, Theory and Applications*. Pergamon Press, Oxford.
- Elvidge, J.A. and Jones, J.R. (1979). *Isotopes: Essential Chemistry and Applications*. The Chemical Society, Burlington House, London.
- Erbacher, O. (1942). Radium und isotope. In: *Handbuch der Analytischer Chemie* (eds. Fresenius, R., Lander, G.). Springer, Berlin, p. 403.
- Firouzbakht, M.L., Schlyer, D.J. and Fowler, J.S. (2006). Cryogenic target design considerations for the production of [F]fluoride from enriched [O]carbon dioxide. *Nucl. Med. Biol.* 26:749–753.
- Friedlander, G., Kennedy, J.W., Macias, E.S. and Miller, J.M. (1981). *Nuclear and Radiochemistry*. Wiley, New York, NY.
- Hahn, O. 1926a. Gesetzmäßigkeiten bei der Fällung und Adsorption kleiner Substanzmengen und ihre Beziehung zur radioaktiven Fällungsregel. (Nach gemeinsam mit Hrn. O. Erbacher und Frl. N. Feichtinger ausgeführten Versuchen) Ber. Dtsch.chem.Ges. 59:2014–2025. Published Online: Jan 23 2006. DOI:10.1002/cber.19260590855.
- Hahn, O. 1926b. "<http://www.springerlink.com/content/x15543368334611k/?p=2db46d7d6a6f40e0979c7bbf98ef60f9&pi=9>" Über die neuen Fällungs- und Adsorptionssätze und einige ihrer Ergebnisse. *Naturw.* 14:1196–1199.
- Hahn, O. and Imre, L. (1929). Über die Fällung und Adsorption kleiner Substanzmengen. III. Der Adsorptionssatz, Anwendungen, Ergebnisse und Folgerungen. *Z. physikal.Ch. (A)* 144:161–186.
- Haissinsky, M. (1964). *Nuclear Chemistry and its Applications*. Addison-Wesley, Reading, MA.

-
- IAEA TECDOC-1341 (2003) and IAEA Technical Reports Series No.63 (1966)
- IAEA Safety Series No.1 (1973). *Safe Handling of Radionuclides*. International Atomic Energy Agency.
- IAEA Technical Reports Series No.63 (1966). *Manual for Radioisotope Production*. International Atomic Energy Agency.
- IAEA-TECDOC-1065 (1999). Production technologies for molybdenum-99 and technetium-99m, International Atomic Energy Agency.
- IAEA-TECDOC-1340 (2003). Manual for reactor produced radioisotopes, International Atomic Energy Agency.
- Lambrecht, R.M. and Morcos, N. (1982). *Application of Nuclear and Radiochemistry*. Pergamon Press, New York, NY.
- Lieser, K.H. (1997). *Nuclear and Radiochemistry*. Wiley-VCH, Berlin.
- McKay, H.A.C. (1971). *Principles of Radiochemistry*. Butterworths, London.
- Murray III, A. and Williams, D.L. (1958). *Organic Syntheses with Isotopes*. Interscience Publishers, New York, NY.
- Wahl, C.A. and Bonner, N.A. (1951). *Radioactivity applied to Chemistry*. John Wiley and Sons, Inc., New York.

9 Physicochemical Application of Radiotracer Methods

9.1 The Thermodynamic Concept of Classification (Distribution of Radioactive and Stable Isotopes)

For radioactive indications, the most important factor that has to be considered is the distribution of the radioactive tracer (microcomponent) and the inactive carrier (macrocomponent). As mentioned in Section 8.2, the radioactive indicator has to be homogeneously distributed in the studied system. In this chapter, the condition of the homogeneous mixing of the radioactive indicator and the inactive (stable) carrier will be investigated via examining the change of the mixing entropy.

Let us assume two solutions with the same concentration C , each containing the macro- and microcomponent, respectively, as the same chemical species and have the same temperature. When the concentration C is the same, the dilution-free energy does not have to be taken into account; thus, the entropies of the two solutions are expressed as:

$$S_n = n(R \ln T - R \ln C + S_n^0) \quad (9.1)$$

$$S_N = N(R \ln T - R \ln C + S_N^0) \quad (9.2)$$

N and n are the atoms of the macro- and microcomponents, respectively; T is the temperature; R is the gas constant; and S^0 is the absolute entropy. When the solutions are mixed, the entropy changes as follows:

$$S'_n = n \left(R \ln T - R \ln \frac{n}{n+N} C + S_n^0 \right) \quad (9.3)$$

$$S'_N = N \left(R \ln T - R \ln \frac{N}{n+N} C + S_N^0 \right) \quad (9.4)$$

When mixing the solution, it will be diluted for both components. The dilution can qualitatively be expressed by the molar fractions of the micro- and macrocomponents:

$$\frac{n}{n+N} = X_n \quad (9.5)$$

$$\frac{N}{n+N} = X_N \quad (9.6)$$

where X_n and X_N are the molar fractions. The partial molar concentration of the components is:

$$C_n = C \frac{n}{n+N} \quad (9.7)$$

$$C_N = C \frac{N}{n+N} \quad (9.8)$$

The change of the entropy as a result of mixing can be expressed in Eqs. (4.1)–(4.4) as follows:

$$\Delta S_{\text{elegy}} = (S'_n + S'_N) - (S_n + S_N) = -nR \ln X_n - NR \ln X_N \quad (9.9)$$

By dividing both sides of Eq. (9.9) by the value of $(n+N)$, the molar mixing entropy is obtained for mixing:

$$\Delta S_{\text{elegy}}^M = -\frac{n}{n+N} R \ln X_n - \frac{N}{n+N} R \ln X_N \quad (9.10)$$

when the system consists of i components (besides two), the molar mixing entropy for i components is:

$$\Delta S_{\text{elegy}}^M = -R \sum_i X_i \ln X_i \quad (9.11)$$

The end of the mixing process is mathematically reached when the primary differential quotient of the entropy is equal to zero:

$$\delta(\Delta S_{\text{elegy}}^M) = 0 \quad (9.12)$$

This extremum of mixing entropy can be calculated as follows. Let us divide the whole mixture to elementary volumes containing $(\Delta n + \Delta N)$ atoms and choose an arbitrary k th element, in which the molar ratio of the i th component is:

$$(X_i)_k = \frac{(\Delta n_i)_k}{\Delta n + \Delta N} \quad (9.13)$$

From Eqs. (9.11)–(9.13), we obtain the following:

$$\delta \left[R \sum_k \sum_i \frac{(\Delta n_i)_k}{\Delta n + \Delta N} \ln \frac{(\Delta n_i)_k}{\Delta n + \Delta N} \right] = 0 \quad (9.14)$$

$$R \sum_i \sum_k \left[\frac{\delta(\Delta n_i)_k}{\Delta n + \Delta N} \ln \frac{(\Delta n_i)_k}{\Delta n + \Delta N} + \frac{(\Delta n_i)_k}{\Delta n + \Delta N} \frac{\Delta n + \Delta N}{(\Delta n_i)_k} \frac{\delta(\Delta n_i)_k}{\Delta n + \Delta N} \right] = 0 \quad (9.15)$$

Equation (9.15) is divided by $\frac{R}{\Delta n + \Delta N}$:

$$\sum_i \sum_k \left[\ln \frac{(\Delta n_i)_k}{\Delta n + \Delta N} + 1 \right] \delta(\Delta n_i)_k = 0 \quad (9.16)$$

Equation (9.12) can be solved for any i th component, assuming that the total quantity of this component remains the same:

$$\sum_k \delta(n_i)_k = 0 \quad (9.17)$$

From Eq. (9.16), we obtain the following:

$$\sum_k \left[\ln \frac{(\Delta n_i)_k}{\Delta n + \Delta N} + 1 \right] \delta(\Delta n_i)_k = 0 \quad (9.18)$$

Equation (9.18) is solved by using the method of the Lagrange multiplier, i.e., each member of Eq. (9.16) is multiplied by an undetermined constant (α) and added to Eq. (9.18):

$$\sum_k \left[\ln \frac{(\Delta n_i)_k}{\Delta n + \Delta N} + 1 + \alpha \right] \delta(\Delta n_i)_k = 0 \quad (9.19)$$

In Eq. (9.19), the coefficients of $\delta(\Delta n_i)_k$ are equal to zero, i.e.:

$$\ln \frac{(\Delta n_i)_k}{\Delta n + \Delta N} = -(1 + \alpha) \quad (9.20)$$

From here:

$$\frac{(\Delta n_i)_k}{\Delta n + \Delta N} = e^{-(1+\alpha)} = \text{constant} \quad (9.21)$$

Equation (9.21) expresses the well-known fact that when mixing equilibrium, the radioactive indicator is homogeneously distributed in the whole system.

Previously, the system has been divided into elementary volumes containing $(\Delta n + \Delta N)$ atoms. When the total number of the elementary volumes is r , the moles of the i th components (any of these components can be the radioactive indicator) in the whole system are:

$$r(\Delta n_i)_k = n_i \quad (9.22)$$

The total number of atoms of all components in the whole system is:

$$r(\Delta n + \Delta N) = n + N \quad (9.23)$$

Therefore, the molar fractions are as follows:

$$\frac{(\Delta n_i)_k}{\Delta n + \Delta N} = \frac{n_i}{n + N} = X_i \quad (9.24)$$

Equation (9.24) expresses that the ratio of the micro- and macrocomponents is the same in any elementary volume as it is in the whole system. It also means that in this case, the mixing entropy is maximal.

Equation (9.12) and its solution, Eq. (9.24), are valid even if the radioactive indicator is distributed among different chemical species of the macrocomponents. However, the value of α has not been restricted, so the different chemical species may be characterized by different constants. Therefore, X_i can be different for chemical species. As an example, the iron ions and hemoglobin are mentioned (see Section 8.2). Since there are no exchanges between iron ions dissolved in water and the iron(II) ions within the hemoglobin, when a radioactive iron isotope is added, it will be mixed with the iron ions dissolved in water, but it will not exchange with the iron ions of hemoglobin. Therefore, the specific activity of the two species of iron will be different. Depending on the chemical bonds, the distribution of a radioactive isotope can be different within the same molecules. For example, a ^{14}C -labeled side-chain can be bonded to a ^{14}C -labeled benzene; the specific activities of the two carbon atoms may be different, depending on the specific activities of the reactants. In these cases, mixing entropy has local maxima for the different species and bonds. When the radioactive indicator is homogeneously distributed among the different chemical species and bonds (e.g., isotope exchange can take place), the mixing entropy has reached its absolute maximum. In this case, the subsequent effects cannot change the homogeneous distribution, as shown by Hevesy's experiments for the separation of ^{210}Pb (RaD) from lead chloride (PbCl_2) (discussed in Section 8.1).

The molar fraction, X_i , can decrease because of the decay of the radioactive isotope; this effect, however, can be taken into consideration easily using decay kinetics.

9.2 Classification of Tracer Methods

Equation (9.24), expressing the ratio of the radioactive and inactive atoms at the maximum mixing entropy, has another meaning. When the nominator of Equation

(9.24) is multiplied by the decay constant of the radioactive isotope (λ), the denominator is divided by Avogadro number (N_A) and multiplied by the molar mass (M), the equation is obtained as follows:

$$\frac{n_i}{n + N} \left(\frac{\lambda}{\frac{M}{N_A}} \right) = \frac{A}{m} = a \quad (9.25)$$

where A is the radioactivity of the tracer, m is the mass of the i th component, including the tracer and the inactive carrier, and the A/m ratio is the specific activity.

On the basis of the specific activity, the tracer studies are classified into two groups:

1. The specific activity is constant, which means that the mixing entropy of the system is maximal during the whole period of the studies. In this case, the activity is measured at different places of the system and at different times, the ratio of the activities quantitatively gives the distribution of the substance. This method is applied, for example, for the determination of the solubility of very insoluble salts (such as in Hevesy's first tracer experiments, described in Section 8.1) or for the study of the efficiency of electrolysis.
2. The specific activity changes because the radioactive isotope is diluted with the stable isotope of the same element. In these studies, the specific activity has to be determined before and after the dilution. The change in specific activity gives information on the quantity of the diluting substance. This principle is applied to isotope dilution methods, including some important medical applications (such as RIA, described in Section 12.3).

The principle of the isotope dilution methods is discussed here. Let us suppose a radioactive substance with activity A :

$$A = \lambda n \quad (9.26)$$

where n is the number of radioactive nuclides and λ is the decay constant. The initial specific activity before dilution (a_0) is:

$$a_0 = \frac{\lambda n}{n + N} \left(\frac{1}{\frac{M}{N_A}} \right) \quad (9.27)$$

where N is the number of the inactive nuclides (carrier), M is the molar mass, and N_A is Avogadro number (see also Eq. (9.25)). If N' inactive carrier nuclides are added to this system (dilution), the total activity (A) remains the same (a closed system); the specific activity (a'), however, decreases:

$$a' = \frac{\lambda n}{n + N + N'} \left(\frac{1}{\frac{M}{N_A}} \right) \quad (9.28)$$

Since the activity (A) is the same, from Eqs. (9.27) and (9.28), we obtain:

$$A = \lambda n = a_0(n + N) = a'(n + N + N') \quad (9.29)$$

From here,

$$N' = (n + N) \left(\frac{a_0}{a'} - 1 \right) \quad (9.30)$$

Since $n \ll N$, the number of the radioactive nuclides can be disregarded. The quantity of the diluting substance can be calculated when we know N , and the specific activities before (a_0) and after (a') the dilution.

According to the classification by the specific activity, group 1 (constant specific activity, the mixing entropy is maximal) contains, for example, the determination of solubility, a part of diffusion studies (self-diffusion is not included), radiometric analysis, and autoradiography. Group 2 (specific activity changes, the mixing entropy increases) contains, for example, the determination of specific surface area, the different types of isotopic dilution methods, substoichiometric analysis, RIA, the study of isotope exchange reactions, self-diffusion, and the determination of exchange current.

The radiotracer methods can also be classified based on the field of applications, such as physicochemical, analytical, biological, medical, and industrial applications. Physicochemical applications include, for example, the determination of solubility, the study of diffusion, the distribution of substance between phases, and the study of reaction mechanisms. It is important to note that radiotracer methods are widely used in the study of interfacial processes because of the high sensitivity of radioindicators. Analytical applications include the radiometric analysis, isotopic dilution methods (including RIA), autoradiography, neutron activation analysis, and all analytical methods based on the interaction of radiation with matter (see the discussion of this in Chapter 10).

Isotope labeling can also be done by stable isotopes, in which case the natural abundance of a given element is altered. In other words, a stable isotope is enriched. The concentration of the stable isotopes can be determined in two ways:

- The samples are activated after the studies and the number of isotopes is determined on the basis of the produced radioactive nuclides.
- The number of isotopes can be determined by mass spectrometry, infra spectrometry, and so on.

These methods, however, are much more complicated than simple radioactivity measurement methods.

Of course, the basic concepts of labeling by stable isotopes are just the same as those of radioactive isotopes, only the detection methods are different. Therefore, all of the principles and relation mentioned above for radioactive isotopes apply to stable isotopes.

9.3 Physicochemical Applications of Tracer Methods

Because of the easy detection of their radiation, radioactive isotopes provide a useful approach to determine the local, time, and concentration distribution of substances. Consequently, the radioisotopic tracer method can be used for reaction kinetic, mechanism, and equilibrium studies. In this chapter, some radiotracer methods will be shown. In these studies, the radiotracer is most often in solution, so the most important properties of highly diluted solutions (solutions of carrier-free radioactive isotopes) and the basic rules of working with them will be discussed.

When an isotope has a relatively short half-life, the number of the radioactive nuclides is very few. For example, when the half-life of an isotope is 100 years, 1 kBq activity is emitted by about 7.5×10^{-12} mol radioactive nuclides. So, the preparation of a solution in so small concentration range demands very careful procedures. The stock solution is usually kept in a 10^{-1} or 10^{-2} mol/dm³ concentrated acidic solution (e.g., in nitric or perchloric acid to avoid the formation of complexes with the radioactive isotopes), and this acidic stock solution is diluted step by step. In each dilution process, the solution has to be left to mix for at least 12 h before the next solution, since the carrier-free isotopes are mixed via the self-diffusion of the solvent and stirring does not increase considerably the rate of this process. To avoid the formation of radiocolloids, the pH of the solution may be increased gradually. The radioactivity of the solution must be checked regularly. Only very pure solvents (bidistilled or tridistilled water) are applied because even these pure solutions can contain more contaminants than the total quantity of the radioindicator.

The solutions containing carriers in macroconcentrations can be handled more easily; however, carrier-free radioisotopes have to be added to the solution of the carrier according to the rules mentioned previously.

9.3.1 Solubility Measurements

The solubility of very insoluble salts was first determined by Hevesy (as discussed in Section 8.1). The method was based on the specific activity of the salt, which was identical in both the solid and solution phases, $a/m = \text{constant}$. At first, a precipitate of known specific activity (e.g., lead sulfide) was produced:



The specific activity of the precipitate is measured. Then the precipitate is dissolved, and the activity of the solution is measured. From the activity of the solution and the specific activity, the concentration of the solution can be calculated. The solubility product of lead sulfide, for example, is $L_{\text{PbS}} = 10^{-33}$ mol² dm⁻⁶. At this small value of solubility product, the solubility determination needs a very sensitive analytical method.

9.3.2 Measurements of the Rate of Migration, Diffusion, and Self-Diffusion

As mentioned previously, radioactive tracers can be used to determine the local, time, and concentration distribution of the substances, so they are appropriate to use for studying transport processes, including migration, diffusion, and self-diffusion. As discussed in Section 3.2, diffusion is a suitable means of separating isotopes, especially for the isotopes of the light elements. Even heavy isotopes, such as ^{235}U and ^{238}U , were successfully separated for military purposes by diffusion in the United States between 1945 and 1948.

In this chapter, the application of radioactive tracers will be discussed in some arbitrarily chosen solid/gas, solid/liquid, and solid/solid systems. In addition, self-diffusion will be investigated. In the diffusion studies, the application of radioactive isotopes is only one of the available methods, though it is one of the cheapest and most elegant. In the self-diffusion studies, however, the radiotracer method is the only simple possibility. In the diffusion studies, the mixing entropy is maximal; the process is directed by the concentration gradient. The specific activity is constant, meaning that the activity is proportional to the concentration. In the self-diffusion studies, the specific activity changes, and the process is directed by the increase in the mixing entropy.

9.3.2.1 Diffusion in a Solid/Gas System

In this section, some examples of the diffusion of gases in solid media will be shown.

Diffusion of ^{222}Rn in Soil

In porous media, the free volume can well be characterized by the diffusion of a gas that does not adsorb on the interfaces of the pores. For example, the diffusion of ^{222}Rn gas is mentioned. Radon is a noble gas, and it has no interactions with the surrounding medium. Carrier-free ones can easily be produced (see Section 8.5.1) and their activity can be measured through the gamma radiation of its daughter nuclides. The diffusion of ^{222}Rn has been studied in soil components, sand and clay, as porous media. The diffusion is described by the Fick's laws; in this case, Fick's second law, applied to linear diffusion, is used:

$$\frac{\partial C}{\partial t} = D \frac{\partial^2 C}{\partial x^2} \quad (9.32)$$

where D is the diffusion coefficient (surface area/time), C is the concentration of the diffusing substance, and t is the time. When the concentration of the diffusing substance is measured by a radiotracer, the radioactive intensity (I) depends on the concentration, i.e.:

$$I = f(C) \quad (9.33)$$

Equation (9.32) does not have a general solution—only some solutions for special initial and boundary conditions. For linear diffusion at a constant temperature, a partial solution of Eq. (9.32) can be expressed by Eq. (9.34) when at $t = 0$, the total quantity of the diffusing substance is at a place $x = 0$ as a point source:

$$I = \frac{I_0}{\sqrt{4D\pi t}} \exp\left(-\frac{x^2}{4Dt}\right) \quad (9.34)$$

The diffusion coefficients can be determined in two ways. I values are measured as a function of time (t) at a given place ($x = \text{constant}$), or as a function of the distance (x) at a given time ($t = \text{constant}$). This solution is frequently called “the parabolic law of diffusion.” Depending on the method employed, the diffusion coefficients can be determined approximately from the slope of the $\ln I$ versus x^2 or $\ln I$ versus $1/t$, respectively. This gives a first-order relation; thus, it is a simple method for the determination of the diffusion coefficient. When, however, $x = \text{constant}$ and t changes, a systematic error develops because the time is present in the intercept as well. Nowadays, computer programs are used for the estimation of diffusion coefficient from the original form of Eq. (9.34); in this way, this error can be ignored.

Simple laboratory equipment for the measurement of diffusion is shown in Figure 9.1, and the experimental results are plotted in Figure 9.2.

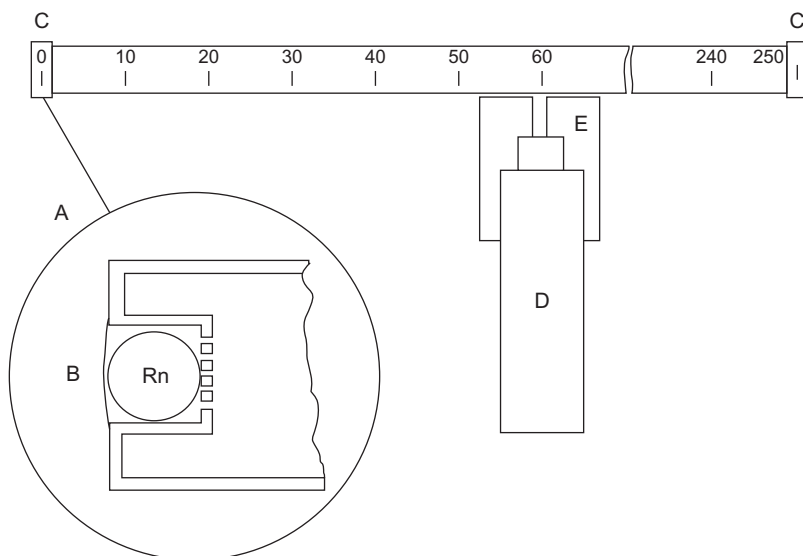


Figure 9.1 Study of linear diffusion of radon gas in soil. (A) breaking tool, (B) elastic membrane, (C) cap, (D) detector (NaI(Tl) scintillation detector with photomultiplier), and (E) lead shielding. The time of breaking the sphere is the initial time ($t = 0$) of the diffusion of radon.

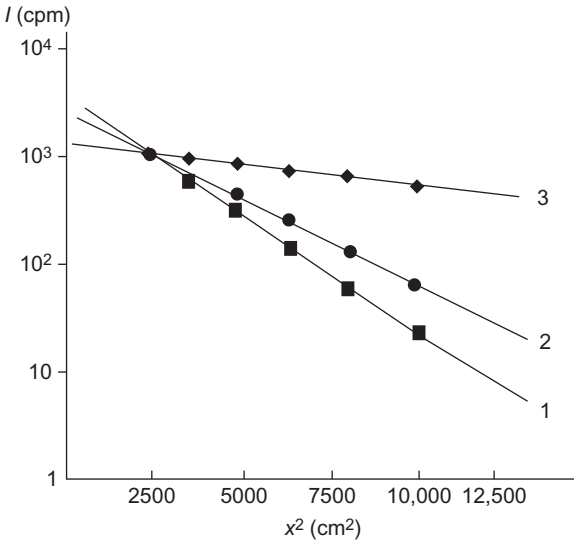


Figure 9.2 Linear diffusion of ^{222}Rn gas in sand with different humidities. Humidity increases in the order: $1 > 2 > 3$.

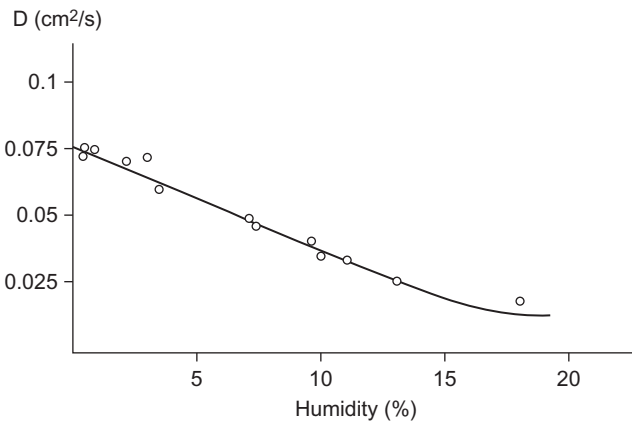


Figure 9.3 The virtual diffusion coefficient of Rn-222 in sand versus humidity.

As seen in [Figure 9.2](#), the volume of the free pores decreases when the humidity of sand increases, resulting in the decrease of migration rate of radon ([Figure 9.3](#)). Since the migration rate depends on the pore size, the determined diffusion coefficient is a virtual diffusion coefficient.

Diffusion or migration measurements can be done *in situ*, under natural conditions. In this case, the solution of [Eq. \(9.32\)](#) applied to spatial diffusion has to be used. Under similar initial and boundary conditions as described in [Eq. \(9.34\)](#), the solution for spatial diffusion in an isotropic medium is:

$$I = \frac{I_0}{\sqrt{4D\pi t}} \exp\left(-\frac{r^2}{4Dt}\right) \quad (9.35)$$

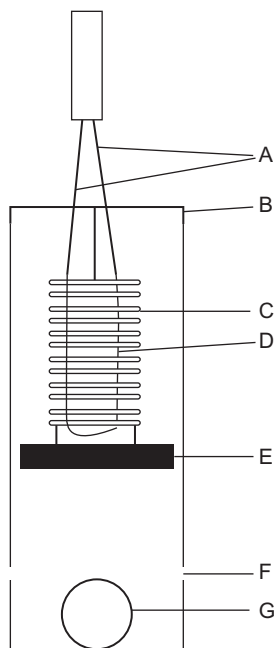


Figure 9.4 Equipment for breaking a glass sphere containing ^{222}Rn gas. (A) electric cable, (B) cap, (C) pushed spring, (D) thin wire, (E) breaking iron disc, (F) gas outlet, and (G) glass sphere containing radon.

where r is the distance from the point source (considered as the origin of a sphere). In the studies of spatial diffusion, the diffusing gas (^{222}Rn) is located as shown in Figure 9.4.

The spatial diffusion studies give similar results as linear diffusion studies, namely the virtual diffusion coefficient depends on the humidity—i.e., on the free volume of pores. Also, similar results are obtained in clay; however, clay contains less free volume pore space, and the virtual diffusion coefficients are about an order of magnitude smaller.

Diffusion of ^{203}Hg Vapor in Plastic

The diffusion of mercury vapor in plastics can be studied by a radiotracer method using the ^{203}Hg isotope. ^{203}Hg has a half-life of 46.9 days and emits beta particles of 208 keV and gamma radiation of 279 keV. The gamma activity of ^{203}Hg can be measured easily by a NaI(Tl) scintillation detector.

The diffusion studies are as follows. Discs are cut from the plastic samples and they are placed onto the plane top of glass vessels containing a drop of mercury labeled with ^{203}Hg . The diameters of the plastic discs and the top of the glass vessels have to be the same and they have to be fitted tightly to avoid the escape of mercury from the vessel. Mercury evaporates in the glass vessel and introduces into the plastic disc. After a given experimental time, the plastic disc is sliced by a microtome into layers that are about 10 micrometers thick. The gamma activities of the plastic slices are plotted as a function of the square of the distance measured

from the surface connecting to the mercury vapor. The virtual diffusion coefficient can be determined using Eq. (9.34).

In Figure 9.5, the logarithm of gamma activities ($\ln I$) is plotted as a function of the square of the distance measured from the surface connecting to the mercury vapor ($t = \text{constant}$). From the slope of the straight line, the virtual diffusion coefficient is determined if the time of diffusion is known. The virtual diffusion coefficients of different plastic samples are very similar, around $10^{-10} \text{ cm}^2 \text{ s}^{-1}$.

During the migration of mercury in plastic samples containing sulfur, a chemical reaction takes place between mercury and sulfur, influencing the profile of the $\ln I$ versus x^2 plot. As a result of this chemical reaction between mercury and sulfur, a maximum is observed at a given distance (Figure 9.6). The place of the maximum

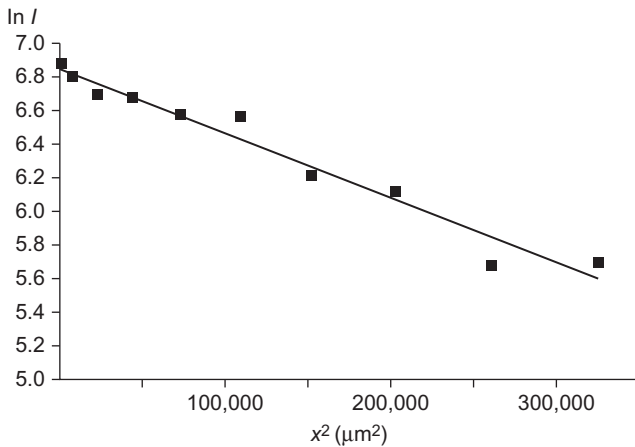


Figure 9.5 $\ln I$ versus x^2 plot for the diffusion of ^{203}Hg in plastic.

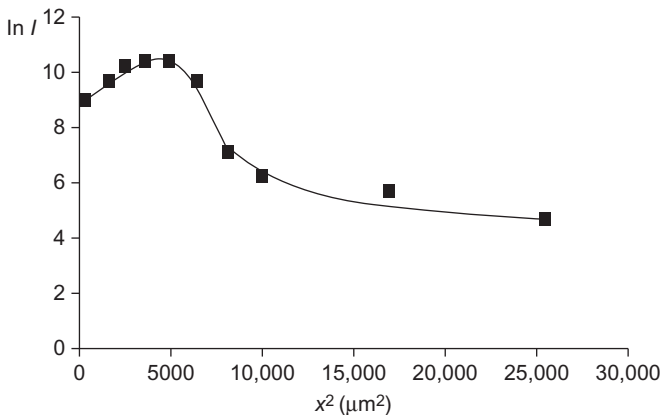


Figure 9.6 $\ln I$ versus x^2 plot for the diffusion of ^{203}Hg in plastic containing sulfur.

depends on the sulfur concentration in the plastic and the time of migration. This phenomenon is analogous to the principle of chromatography.

9.3.2.2 Diffusion in Solid/Solution Systems: Transport of Radioactive Isotopes in Porous Systems

Each substance in the environment, including radioactive isotopes, interacts with groundwater and geological formations (soils and rocks). Transport in the pores of rocks and soils occurs via the migration of water-soluble materials. The migration in porous solid media is influenced both by hydrological processes and by the interaction between the soluble substances and the geological formations. The migration of a substance in a porous solid medium is influenced by the flowing medium (typically groundwater in geological formations), the chemical species of the migration substance, and its sorption properties. Thus, the migration is affected by the following factors:

- Advection: the migration of soluble components with flowing medium.
- The mixing of solutions in macropores of the solid medium, which is due to the different flowing rates of solutions in the pores with different sizes.
- Diffusion of dissolved components in the liquid phase.

In addition, the interactions of solid matrices and dissolved substances are the following:

- Adsorption and ion exchange
- Precipitation
- Structural modification and destruction of materials.

In the case of the migration of nonsorbing substances, the transport of the dissolved substances is determined by the first three processes, namely advection, mixing, and diffusion. This means that the dissolved components move with water (e.g., chloride ions in geological formations). The flux of flow is described by different migration equations. A frequently used migration equation is:

$$J_0 = -[\Theta D_h + \Theta D_{\text{eff}}] \frac{\delta c}{\delta x} + \nu \Theta c = -\Theta D \frac{\delta c}{\delta x} + qc \quad (9.36)$$

where J_0 is the flowing rate of water (flux), Θ is the humidity of medium, D_h is the hydrodynamic dispersion coefficient, D_{eff} is the effective diffusion coefficient, c is the concentration of flowing material at place x , $\nu \Theta = q$ is the volume flowing in a unit time, and ν is the linear flowing rate.

If the solid medium reacts with the dissolved components (e.g., by adsorption or ion exchange), their flowing rate decreases:

$$\frac{\delta(\Theta c)}{\delta t} = \frac{\delta}{\delta x} \left[D \frac{\delta c}{\delta x} \right] - \frac{\delta qc}{\delta x} - \frac{\delta \rho a}{\delta t} \quad (9.37)$$

where ρ is the density of the matrix and a is the sorbed amount.

When the dissolved components are adsorbed on the solid matrix or they take place in ion exchange reactions, or precipitate, their migration rates can decrease significantly. The degree of decrease is determined by the chemical species of the given substance under chemical conditions characteristic of the solutions in geological formations (groundwater).

As discussed in Section 9.3.2.1.1, the migration equations (including Eqs. (9.36) and (9.37)) cannot be solved generally; only partial solutions can be obtained in certain initial and boundary conditions. In addition, the sorption has to be included, e.g., by a sorption isotherm equation that describes the relation between the concentration of the dissolved components in the solid and solution phases. As an example, the Langmuir adsorption isotherm is mentioned:

$$\frac{m y}{w x} = \frac{m}{w} \frac{1}{k} = \frac{C_e}{a} = \frac{1}{z} (C_e + K) \quad (9.38)$$

where m is the mass of the adsorbent (g), w is the pore volume saturated with water (dm^3), y is the ratio of the substance dissolved in the pore water, x is the ratio of the substance sorbed on the solid phase, k is the distribution coefficient ($k = x/y$), C_e is the equilibrium concentration of the solution, a is the adsorbed quantity, z is the number of the active sites of sorption, and K is the parameter that is characteristic of the sorption energy.

Neglecting the advection, Eq. (9.37) is simplified as follows:

$$\frac{\delta(\Theta c)}{\delta t} = \frac{\delta}{\delta x} \left[D \frac{\delta c}{\delta x} \right] - \frac{\delta \rho a}{\delta t} \quad (9.39)$$

By substituting the adsorbed quantity (a) from Eq. (9.38), we obtain:

$$\frac{\partial C}{\partial t} + \frac{w}{m} k \frac{\partial C}{\partial t} = D \frac{\partial^2 C}{\partial x^2} \quad (9.40)$$

and from here,

$$\frac{\partial C}{\partial t} = \left[\frac{D}{1 + \frac{w}{m} k} \right] \times \frac{\partial^2 C}{\partial x^2} \quad (9.41)$$

The quantity of the value in brackets can be interpreted as migration coefficient (D_m):

$$\frac{\partial C}{\partial t} = D_m \frac{\partial^2 C}{\partial x^2} \quad (9.42)$$

Equation (9.42) is equivalent to Fick's second law (Eq. (9.32)), but the interpretation of D_m is slightly different. A similar mathematical procedure can be applied for ion exchange too.

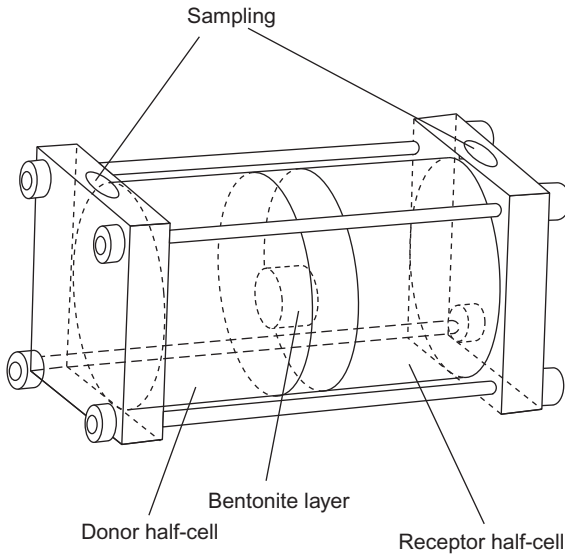


Figure 9.7 Migration cell for the study of radionuclide transport. *Source:* Reprinted from Nagy and Kónya (2005), with permission from Elsevier.

The denominator of Eq. (9.41) is called the “retardation factor,” which is the ratio of the migration coefficients of a nonsorbing substance (e.g., chloride or the migrating medium, water, itself) and a sorbing substance.

As discussed in Section 7.3, geological repositories play an important role in the safe storage of nuclear waste. The migration rate of the radioactive isotopes, both in the engineering barrier system and in the surrounding geological formation, is a significant factor that must be considered. The migration rate of the radionuclides studied in laboratory model experiments using a migration cell is shown in Figure 9.7.

In the migration cell, the sample (a bentonite clay layer in Figure 9.7) is located in the middle of the donor and receptor half-cells. The solution of the studied radioactive isotopes is filled into the donor half-cell and is permitted to migrate through the sample in the middle. As discussed in Section 9.3.2.1.1, there are two possibilities to determine the diffusion coefficient: the first is that solution samples are taken at different times from the receptor cell and the concentration of the migrating substances is determined as a function of time (in this case, $x = \text{constant}$). The other possibility is that the rock sample is cut into thin layers after a given time ($t = \text{constant}$), and the concentration of the migrating substances is determined as a function of distance.

The solution of Fick’s second law for this migration cell is as follows, assuming the boundary condition ($C = C_0$, $x = 0$, $t > 0$) and the initial condition ($C = 0$, $x > 0$, $t = 0$):

$$C_{(x,t)} = C_0 \operatorname{erfc} \frac{x}{2\sqrt{(D_m t)}} \quad (9.43)$$

where $\operatorname{erfc}(z) = 1 - \operatorname{erf}(z)$, where z is the fraction behind the erfc function in Eq. (9.43).

The two possibilities to determine the diffusion coefficient are shown in [Figures 9.8 and 9.9](#).

These figures show the migration studies of chloride ions labeled by the ^{36}Cl isotope and carrier-free $^{137}\text{Cs}^+$ ions in bentonite clay. The diffusion coefficient of a chloride ion provides the maximum migration rate in the bentonite clay because the chloride ion is not sorbed in the clay. However, cesium ions are fairly easily sorbed by cation exchange in bentonite clay. As a result, the diffusion coefficient in this case is about two orders of magnitude lower than in the case of chloride ion. This illustrates that the sorption process in clay plays an important role in the isolation of radioactive ions from the environment.

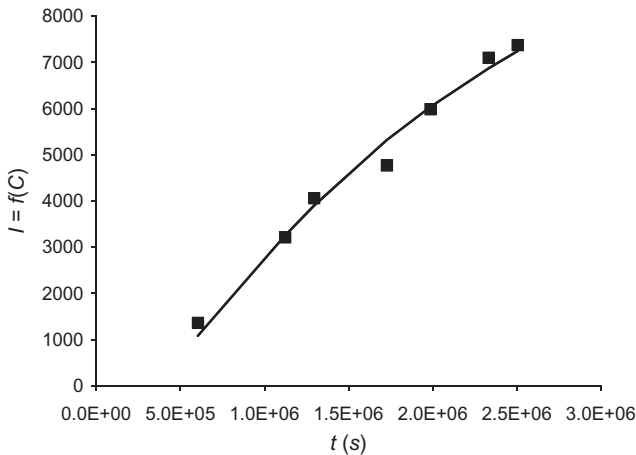


Figure 9.8 Migration of $^{36}\text{Cl}^-$ ions bentonite clay: intensity proportional to the concentration versus time. Diffusion coefficient calculated by Eq. (9.43) is $7.76 \times 10^{-12} \text{ m}^2/\text{s}$.

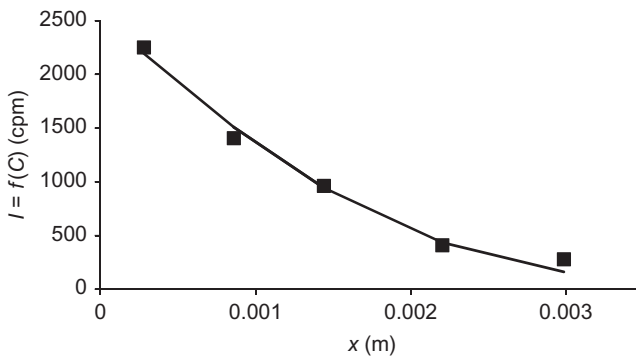


Figure 9.9 Migration of $^{137}\text{Cs}^+$ ions in bentonite clay: intensity proportional to the concentration versus distance. The diffusion coefficient calculated by Eq. (9.43) is $7.71 \times 10^{-14} \text{ m}^2/\text{s}$.

9.3.2.3 Study of the Formation of Surface-Oxidized Layers Using Diffusion

Under the effect of oxidative agents, oxidized layers form on the metal surfaces. The mechanism of the formation of the oxidized layer can be studied easily by labeling one of the reaction partners (e.g., the oxidative agent) with its radioactive isotope. The distribution of the radioactive isotopes resulting in the different oxide formation mechanisms is schematically shown in Figure 9.10. The study of the activity profile, such as by autoradiography as described in Section 14.5.2, gives information on the mechanism and rate-determining step of oxidation reactions.

9.3.2.4 Self-Diffusion Studies

In pure substances, the movement of the own particles, the so-called self-diffusion, can easily be studied by a labeled species of the substance. As mentioned in Section 8.1, both stable and radioactive isotopes can be used for labeling. In the case of stable labeling isotopes, mass spectrometry or subsequent activation is used to measure self-diffusion. Other techniques that can differentiate the isotopes with different mass numbers, such as nuclear magnetic resonance, are also used for the study of self-diffusion.

In this chapter, the application of radioactive isotopes in self-diffusion studies is discussed. As an example, the self-diffusion of metals is studied so that the bottom of

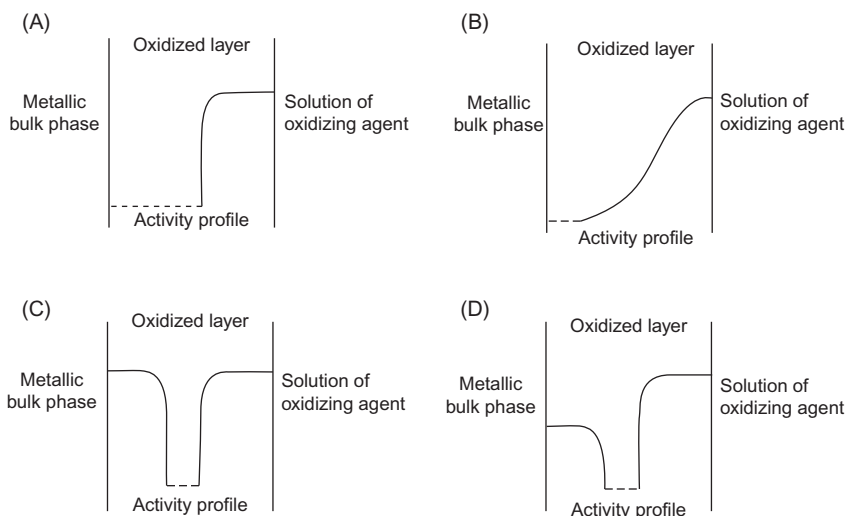


Figure 9.10 The distribution of the radioactive isotopes resulting in the different oxidized layer formation mechanisms. The oxidizing agent is labeled by the radioactive isotope. (A) The oxidation process is determined by the diffusion of metal toward the solution. (B) Both the metal and the oxidizing agent diffuse toward each other. (C) The oxidizing agent moves faster than metal atoms. (D) The oxidizing agent moves faster than metal atoms; the difference of the transport rate, however, is smaller than in C.

Table 9.1 Self-Diffusion Coefficients (D) and Activation Energies (E) of Self-Diffusion

| Element | Melting Point (°C) | Measuring Temperature (°C) | D (cm ² /s) | D_0 (cm ² /s) | E (kJ/mol) |
|----------------|--------------------|----------------------------|--------------------------|----------------------------|--------------|
| Na | 97.8 | 39.6 | 1.31×10^{-8} | 0.242 | 43.8 |
| Mg c -axis | 650 | 551 | 3.6×10^{-9} | 1 | 135 |
| Mg⊥ c -axis | 650 | | | 1.5 | 136 |
| Zn c -axis | 420 | | | 0.13 | 91 |
| Zn c -axis | 420 | | | 0.13 | 92 |
| Zn⊥ c -axis | 420 | | | 0.58 | 102 |
| Zn⊥ c -axis | 420 | | | 0.18 | 96 |
| In | 456 | 150 | 6.6×10^{-10} | 1.02 | 75 |
| Cd c -axis | 320.9 | | | 0.05 | 76 |
| Cd c -axis | 320.9 | | | 0.12 | 78 |
| Cd⊥ c -axis | 320.9 | | | 0.10 | 80 |
| Cd⊥ c -axis | 320.9 | | | 0.18 | 82 |
| Liquids | | | | | |
| Na | 97.8 | 134.3 | 5.39×10^{-5} | 1.1×10^{-3} | 10.18 |
| Hg | -38.9 | 23 | 1.79×10^{-5} | 1.26×10^{-4} | 4.86 |
| In | 156 | 250 | 4.62×10^{-5} | 1.76×10^{-5} | 5.66 |

D is the experimental value determined at the given temperature, D_0 is the value extrapolated to infinite temperature ($D = D_0 \exp(-E/RT)$).

Source: Haissinsky (1964) and Philibert (1991).

the metal piece is evenly covered (e.g., electrolysis) by a layer of the carrier-free radioactive isotope of the metal, and then the local distribution of the isotope is measured after a given length of time. In the meantime, the temperature is kept constant. Under these conditions, the self-diffusion can be described by Eq. (9.34); thus, the self-diffusion coefficient is determined from the slope of the $\ln I$ versus x^2 function. The transport of the radioactive tracer increases the mixing entropy. The change of enthalpy can be disregarded because of the very low concentration of the radiotracer. The first self-diffusion studies were done by George Hevesy and Gyula Gróh.

In Table 9.1, the self-diffusion coefficients of different metals are listed. As seen, the diffusion coefficients give information on the crystal lattice, and consequently on the properties of metals. In noncubic lattices, the diffusion coefficients depend on the direction, the diffusion is anisotropic. In Table 9.1, || and ⊥ denote the directions parallel and perpendicular to the c -axis of the crystal lattice, respectively. As seen, different authors sometimes give different values, but within the same order of magnitude. This shows the uncertainty of self-diffusion measurements.

In solid crystalline substances, diffusion has two mechanisms:

- Diffusion in a crystal grain or volume diffusion. This takes place inside a crystal grain or in a single crystal.
- Grain boundary diffusion, which is characteristic in polycrystals. An example of this is shown in Figure 9.11.

The self-diffusion coefficients are suitable to study the structural changes of substances under different physical effects. An example is shown in Figure 9.12, where

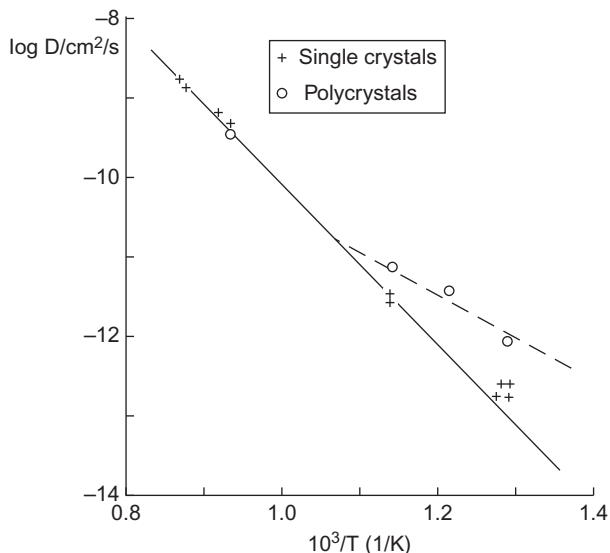


Figure 9.11 Self-diffusion of silver. In a single crystal, only the volume diffusion is observed. In polycrystal silver, the grain boundary diffusion with lower activation energy is dominant at low temperature.

Source: Reprinted from R.E. Hoffman and D. Turnbull (1951), with permission from the American Institute of Physics.

the effect of heat treatment and deformation by compression is seen. Primary recrystallization takes place as a result of compression, while secondary recrystallization occurs by 1 h anneal at an elevated temperature.

Table 9.1 also shows the self-diffusion coefficients for some liquids. As seen, the self-diffusion coefficients of liquids are several orders of magnitude higher than those of solid substances. In addition, the activation energy of self-diffusion in liquids is less by about an order of magnitude.

9.3.2.5 Self-Diffusion in Solutions

The self-diffusion of water was studied using D, T, and ¹⁸O isotopes as tracers. The results of these experiments showed that the identity of the tracer hardly influences the self-diffusion coefficient, which is about 2×10^{-5} cm²/s. The activation energy of the self-diffusion of water is 18 kJ/mol. In electrolytes, the self-diffusion coefficient of water slightly depends on the electrolyte concentration. The carrier-free isotopes diffuse via the self-diffusion of water molecules (see Section 9.3).

9.3.3 Isotope Exchange Reactions

The chemical reactions in which the reactants and products are chemically identical but have different isotopic composition are called “isotope exchange reactions” (see Section 3.1.5). This also means that there are no chemical changes and the

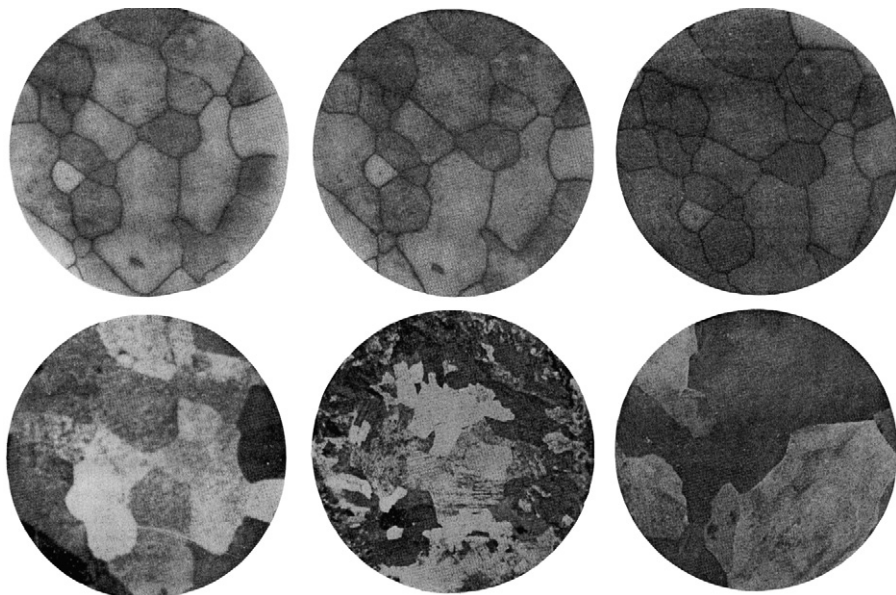


Figure 9.12 Autoradiograph and photomicrograph of a tin ingot. (A) After an 166 h diffusion of Sn-123 at 176°C in a depth of 40 μm from the original surface ($\times 4$). (B) After a 20% deformation by compression ($\times 4$). (C) After an 1 h anneal at 190°C ($\times 4$). Lattice diffusion still can be seen in some of the grains because of the anisotropy of the diffusion in the tetragonal tin lattice. (Thanks to Prof. László Bartha, Research Institute for Technical and Materials Science, Budapest, Hungary.)

Source: Reprinted from Bartha (1967), with permission from Elsevier.

enthalpy of the reaction is zero, and therefore the reaction is directed by the change of entropy (ΔS) ($\Delta G = -T\Delta S$). The isotope exchange studies are classified on the basis of the phases present as homogeneous and heterogeneous isotope exchange studies.

9.3.3.1 Isotope Exchange in Homogeneous Systems

In a homogeneous system containing isotope molecules of the different substances, an isotope exchange may occur. The rate of the isotope exchange depends on the binding energies. Through kinetic studies of the isotope exchange, the binding energy of the isotope in a given substance can be determined. The reaction is directed by the increase of the entropy and reaches equilibrium when the distribution of the isotopes becomes homogeneous (maximum mixing entropy). This means that in equilibrium, the specific activities will be the same for each substance.

The McKay equation can be used for the kinetic description of the isotope exchange reaction. As an example, the isotope exchange reaction of ethyl iodide and sodium iodide labeled with ^{131}I is mentioned. AX and BX mean the ethyl

iodide and the sodium iodide, respectively. The labeled forms of these compounds are indicated by '. The exchange reaction is defined as:



At a given time (t), the specific activity of the two compounds can be defined by the following:

$$a_A = \frac{[A']}{[A]} \quad \text{and} \quad a_B = \frac{[B']}{[B]} \quad (9.46)$$

where $[A']$ is the activity of the labeled AX' and $[A]$ is the quantity of AX . Similarly, $[B']$ is the activity of the labeled BX' and $[B]$ is the quantity of BX . For the isotope exchange reaction of ethyl iodide and sodium iodide, $[A']$ and $[B']$ are the activities of ^{131}I in the ethyl iodide and sodium iodide, respectively. As postulated by the definition of the specific activity, the mass of the iodine has to be taken into account. (NB: Similar equations can be written when the molar activities of the two compounds are expressed where the moles of AX and BX are substituted into Eq. (9.46).)

The total activity of the system is constant at any time (a closed system):

$$[A'] + [B'] = [A'_\infty] + [B'_\infty] \quad (9.47)$$

where $[A'_\infty]$ and $[B'_\infty]$ are the equilibrium activities of AX' and BX' , respectively. In equilibrium, the mixing entropy has maximum value, and the distribution of ^{131}I is directed by the ratio of the quantity of AX and BX :

$$\frac{[A'_\infty]}{[B'_\infty]} = \frac{[A]}{[B]} \quad (9.48)$$

that is, both the ratio of the activities and the ratio of quantities are the same.

To be able to solve the kinetic equation of the exchange reaction (see Eq. (9.51)), only one parameter should be variable. This means that the change of the activity of only one of the reactants is to be taken into account. To eliminate the activity of the other reactant, some equivalent mathematical transformations are necessary. At first, $[B'_\infty]$ is expressed from Eq. (9.48):

$$[B'_\infty] = \frac{[A'_\infty][B]}{[A]} \quad (9.49)$$

Let us substitute $[B'_\infty]$ into Eq. (9.47) and then express $[B']$:

$$[B'] = [A'_\infty] + \frac{[A'_\infty][B']}{[A]} - [A'] \quad (9.50)$$

Since the system is closed, the change of the activity of AX' ($[A']$) as a function of time is as follows:

$$\frac{d[A']}{dt} = Ra_B(1 - a_A) - Ra_A(1 - a_B) \quad (9.51)$$

where R is the rate constant of the isotope exchange. Equation (9.51) expresses both the transmission of the labeling atom from BX' to AX and the reversed process. After an equivalent mathematical transformation, we obtain:

$$\frac{d[A']}{dt} = R(a_B - a_A) \quad (9.52)$$

By substituting the specific activities (Eq. (9.46)), after some transformation:

$$\frac{d[A']}{dt} = R \left[\frac{[B']}{[B]} - \frac{[A']}{[A]} \right] = \frac{R}{[A][B]} ([A][B'] - [B][A']) \quad (9.53)$$

By substituting $[B']$ from Eq. (9.50), we obtain:

$$\frac{d[A']}{dt} = ([A][A'_\infty] + [A'_\infty][B] - [A][A'] - [B][A']) = \frac{R}{[A][B]} ([A'_\infty] - [A'])([A] + [B]) \quad (9.54)$$

By the separation of the variates, the equation is given as follows:

$$\frac{d[A']}{[A'_\infty] - [A']} = R \frac{[A] + [B]}{[A][B]} dt \quad (9.55)$$

The solution of Eq. (9.55) is:

$$\ln([A'_\infty] - [A']) = -R \frac{[A] + [B]}{[A][B]} t + C \quad (9.56)$$

The integration constant (C) can be determined by assuming that at $t = 0$, $[A'] = [A'_0]$. Thus,

$$C = \ln([A'_\infty] - [A'_0]) \quad (9.57)$$

The solution is:

$$\ln \frac{[A'_\infty] - [A']}{[A'_\infty] - [A'_0]} = -R \frac{[A] + [B]}{[A][B]} t = -R't \quad (9.58)$$

when $t = 0$, $[A'_0] = 0$, there are no labeling atoms in AX (only sodium iodide is labeled with the ^{131}I isotope), the solution is as follows:

$$\left(1 - \frac{[A']}{[A'_\infty]}\right) = (1 - F) = -e^{R't} \quad (9.59)$$

The ratio of the activities at any time and in equilibrium is frequently denoted as:

$$\frac{[A']}{[A'_\infty]} = F \quad (9.60)$$

This means that the ratio of exchanged activity to equilibrium activity is to be measured. This is a widely used technique in radiotracer experiments because the relative activity measurements are often much easier.

Equation (9.59) is similar to the kinetic equation of first-order chemical reactions; however, R' depends on the quantities of the two compounds, AX and BX. The half-time of the reaction depends on the quantities of AX and BX. Thus, the reaction is only formally a first-order reaction; instead, it is a pseudo first-order reaction.

When $[A]$ and $[B]$ are constant, the activation-free energy (i.e., the binding energy of the labeling atom) can be calculated from the R s determined at different temperatures using the Arrhenius equation.

An isotope exchange reaction can have three different kinetic profiles:

- The isotope exchange starts at $t = 0$ and it reaches equilibrium (Figure 9.13).
- The isotope exchange has an initial period before starting. After that, the kinetic is similar to that in Figure 9.13 (Figure 9.14).
- The isotope exchange is complicated and strongly depends on the initial conditions (e.g., the concentrations of the reactants).

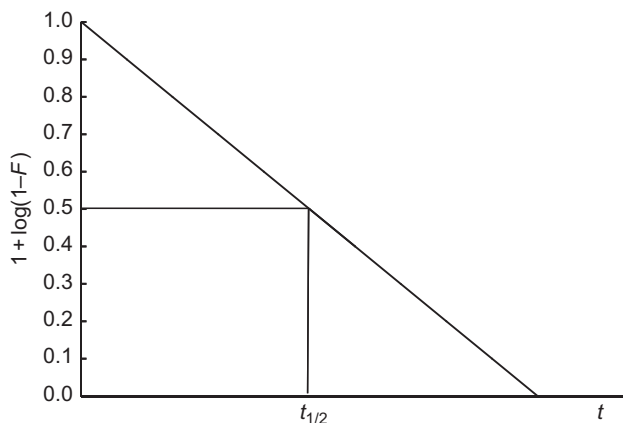


Figure 9.13 Isotope exchange starts at $t = 0$.

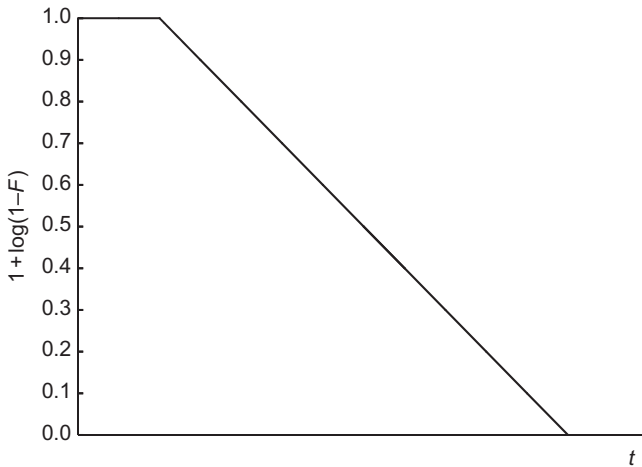


Figure 9.14 Isotope exchange with initial period.

9.3.3.2 Isotope Exchange in Heterogeneous Systems

As usual for heterogeneous reactions, the heterogeneous isotope exchange processes consist of several consecutive steps. The most important steps are the transport of the substances from the bulk to the interface, the exchange reaction, and then the reaction products leave the location of the exchange process and transfer into any phase. This latter process can imply dissolution, intraparticle, interparticle, surface diffusion, recrystallization, and so on. The overall kinetics of the isotope exchange process is determined by the slowest step(s); under steady-state condition, this is the rate-determining process.

Exchange-Controlled Heterogeneous Isotope Exchanges

In this section, the kinetics of a heterogeneous isotope exchange reaction will be shown, the rate-determining step of which is the isotope exchange. As an example, the isotope exchange of potassium ions between blood plasma and red blood cells will be mentioned.

Let us assume that the mass of the potassium ions is m_1 and m_2 in plasma and red blood cells, respectively. Potassium ions are exchanged continuously between the two phases, plasma and red blood cells, reaching steady state. In order to determine the rate of the exchange in steady state, radioactive potassium ions are added to the plasma in such a small quantity that the steady-state exchange is not disturbed. The reaction is directed by the increase of the entropy (see Section 9.3.3.1).

The activity of the radioactive potassium ions is I and can be expressed as:

$$I = m_1 a_{01} \quad (9.61)$$

where a_{01} is the initial ($t = 0$) specific activity of potassium ions in the plasma. After the addition of radioactive potassium ions to plasma, the radioactive potassium ions enter red blood cells as a result of the potassium exchange. After an arbitrary t amount of time, the radioactivity of the plasma will be I_1 , and the specific activity of the potassium ions will be a_1 :

$$I_1 = m_1 a_1 \quad (9.62)$$

Similarly, for the radioactivity (I_2) and the specific activity (a_2) of the red blood cells:

$$I_2 = m_2 a_2 \quad (9.63)$$

Since the system is closed for potassium ions (no potassium ions, including radioactive and inactive, are added later):

$$I = I_1 + I_2 \quad (9.64)$$

In the time period dt , $dm_{2 \leftarrow 1}$ of potassium ions goes from the plasma to the red blood cells, and simultaneously, $dm_{1 \leftarrow 2}$ of potassium ions goes from the red blood cells to the plasma. As a result, the change of the potassium ions in the red blood cells is:

$$dm_2 = dm_{2 \leftarrow 1} - dm_{1 \leftarrow 2} \quad (9.65)$$

and conversely, the change of the potassium ions in the plasma is:

$$dm_1 = dm_{1 \leftarrow 2} - dm_{2 \leftarrow 1} \quad (9.66)$$

Mathematically, the change of the radioactivity both in the red blood cells and in the plasma can be expressed by the total differential quotient of the radioactivity:

$$dI_2 = m_2 da_2 + a_2 dm_2 \quad (9.67)$$

$$dI_1 = m_1 da_1 + a_1 dm_1 \quad (9.68)$$

Also, the change of the radioactivity can be expressed by the transport (Eqs. (9.65) and (9.66)) and the specific activities of potassium ions:

$$dI_2 = a_1 dm_{2 \leftarrow 1} - a_2 dm_{1 \leftarrow 2} \quad (9.69)$$

$$dI_1 = a_2 dm_{1 \leftarrow 2} - a_1 dm_{2 \leftarrow 1} \quad (9.70)$$

By comparing Eqs. (9.67) and (9.69) with Eqs. (9.68) and (9.70), we arrive at the following two equations:

$$a_1 dm_{2\leftarrow 1} - a_2 dm_{1\leftarrow 2} = m_2 da_2 + a_2 dm_2 \quad (9.71)$$

$$a_2 dm_{1\leftarrow 2} - a_1 dm_{2\leftarrow 1} = m_1 da_1 + a_1 dm_1 \quad (9.72)$$

By equivalent mathematical transformations, we obtain:

$$m_2 da_2 = a_1 dm_{2\leftarrow 1} - a_2(dm_{1\leftarrow 2} + dm_2) \quad (9.73)$$

$$m_1 da_1 = a_2 dm_{1\leftarrow 2} - a_1(dm_{2\leftarrow 1} + dm_1) \quad (9.74)$$

Taking into consideration Eqs. (9.65) and (9.66), we get:

$$m_2 da_2 = a_1 dm_{2\leftarrow 1} - a_2 dm_{2\leftarrow 1} \quad (9.75)$$

$$m_1 da_1 = a_2 dm_{1\leftarrow 2} - a_1 dm_{1\leftarrow 2} \quad (9.76)$$

From here:

$$m_2 da_2 = (a_1 - a_2)dm_{2\leftarrow 1} \quad (9.77)$$

$$m_1 da_1 = (a_2 - a_1)dm_{1\leftarrow 2} \quad (9.78)$$

Now, let us study the change of the mass of the potassium ions in a period of time, dt , in the red blood cells:

$$\frac{dm_{2\leftarrow 1}}{dt} = \frac{m_2}{a_1 - a_2} \times \frac{da_2}{dt} \quad (9.79)$$

and in the plasma:

$$\frac{dm_{1\leftarrow 2}}{dt} = \frac{m_1}{a_2 - a_1} \times \frac{da_1}{dt} \quad (9.80)$$

As mentioned previously, the system is under steady-state conditions, i.e., the transport rate of the (inactive) potassium ions is the same in both directions, from the plasma to the red blood cells and vice versa. Let us denote this transport rate with C :

$$\frac{dm_{2\leftarrow 1}}{dt} = \frac{dm_{1\leftarrow 2}}{dt} = C \quad (9.81)$$

Using Eqs. (9.79) and (9.80), we obtain:

$$\frac{da_2}{dt} = \frac{C}{m_2}(a_1 - a_2) \quad (9.82)$$

$$\frac{da_1}{dt} = \frac{C}{m_1}(a_2 - a_1) \quad (9.83)$$

Since the system is closed for potassium ions (see Eqs. (9.62)–(9.64)), the total radioactivity at any time t is the sum of the radioactivities of the plasma and red blood cells:

$$I = m_1a_1 + m_2a_2 \quad (9.84)$$

Equation (9.84) can also be expressed to mean specific activity (\bar{a}):

$$I = m_1\bar{a} + m_2\bar{a} \quad (9.85)$$

From Eqs. (9.84) and (9.85), we get:

$$m_1a_1 + m_2a_2 = m_1\bar{a} + m_2\bar{a} \quad (9.86)$$

In Eqs. (9.82) and (9.83), there are two variables, a_2 and a_1 , which depend on each other. For the solution of these equations, one of the variables must be eliminated. In order to do this, from Eq. (9.86), the specific activities, a_2 and a_1 , and their differences, $a_1 - a_2$ and $a_2 - a_1$, are expressed:

$$a_2 = \frac{m_1\bar{a} + m_2\bar{a} - m_1a_1}{m_2} \quad (9.87)$$

$$a_1 = \frac{m_1\bar{a} + m_2\bar{a} - m_2a_2}{m_1} \quad (9.88)$$

$$a_1 - a_2 = \frac{(m_1 + m_2)(\bar{a} - a_2)}{m_1} \quad (9.89)$$

$$a_2 - a_1 = \frac{(m_1 + m_2)(\bar{a} - a_1)}{m_2} \quad (9.90)$$

Then, Eqs. (9.89) and (9.90) are substituted into Eqs. (9.82) and (9.83), thus:

$$\frac{da_2}{\bar{a} - a_2} = \frac{C}{m_2} \frac{m_1 + m_2}{m_1} dt \quad (9.91)$$

$$\frac{da_1}{\bar{a} - a_1} = \frac{C}{m_1} \frac{m_1 + m_2}{m_2} dt \quad (9.92)$$

The solution of Eqs. (9.91) and (9.92) is:

$$-\ln(\bar{a} - a_2) = \left(\frac{C}{m_2} \frac{m_1 + m_2}{m_1} \right) t + K \quad (9.93)$$

$$-\ln(\bar{a} - a_1) = \left(\frac{C}{m_1} \frac{m_1 + m_2}{m_2} \right) t + K' \quad (9.94)$$

where K and K' are integration constants.

For the calculation of the integration constants K and K' , we assume that at $t = 0$, $a_2 = a_{20}$, and $a_1 = a_{10}$:

$$K = -\ln(\bar{a} - a_{20}) \quad (9.95)$$

$$K' = -\ln(\bar{a} - a_{10}) \quad (9.96)$$

By substituting Eqs. (9.95) and (9.96) into Eqs. (9.93) and (9.94):

$$\ln \frac{\bar{a} - a_2}{\bar{a} - a_{20}} = -\frac{C}{m_2} \frac{m_1 + m_2}{m_1} t \quad (9.97)$$

$$\ln \frac{\bar{a} - a_1}{\bar{a} - a_{10}} = -\frac{C}{m_1} \frac{m_1 + m_2}{m_2} t \quad (9.98)$$

The Kinetics of the Change of the Radioactivity in Red Blood Cells (a_2) Since at $t = 0$ and $a_{20} = 0$ (radioactive potassium ions were added to the plasma), from Eq. (9.97), we obtain:

$$\ln \frac{\bar{a} - a_2}{\bar{a}} = -\frac{C}{m_2} \frac{m_1 + m_2}{m_1} t \quad (9.99)$$

After equivalent mathematical transformations:

$$\bar{a} - a_2 = \bar{a} \exp\left(-\frac{C}{m_2} \frac{m_1 + m_2}{m_1} t\right) \quad (9.100)$$

$$a_2 = \bar{a} - \bar{a} \exp\left(-\frac{C}{m_2} \frac{m_1 + m_2}{m_1} t\right) \quad (9.101)$$

Since at $t = 0$, $a_{20} = 0$, and $a_1 = a_0$, from Eq. (9.86):

$$a_0 m_1 = \bar{a} m_1 + \bar{a} m_2 \quad (9.102)$$

From here:

$$\bar{a} = \frac{m_1 a_0}{m_1 + m_2} \quad (9.103)$$

Substituting Eq. (9.103) into Eq. (9.101), after mathematical transformation, we obtain:

$$\frac{a_2}{a_0} = \frac{m_1}{m_1 + m_2} \left(1 - \exp\left(-\frac{C}{m_2} \frac{m_1 + m_2}{m_1} t\right) \right) \quad (9.104)$$

The Kinetics of the Change of Radioactivity in Plasma (a_1) As mentioned previously, at $t=0$, radioactive potassium ions were added only to the plasma; thus, $a_{10} = a_0$. Substituting this into Eq. (9.98), we get:

$$\ln \frac{\bar{a} - a_1}{\bar{a} - a_0} = -\frac{C}{m_1} \frac{m_1 + m_2}{m_2} t \quad (9.105)$$

Similar to the transformations done previously for red blood cells, the change of radioactivity in the plasma can be expressed as follows:

$$\ln \frac{(m_1/m_1 + m_2)a_0 - a_1}{(m_1/m_1 + m_2)a_0 - a_0} = \ln \frac{(m_1/m_1 + m_2) - (a_1/a_0)}{(m_1/m_1 + m_2) - 1} = -\frac{C}{m_1} \frac{m_1 + m_2}{m_2} t \quad (9.106)$$

$$\frac{(m_1/m_1 + m_2) - (a_1/a_0)}{(m_1/m_1 + m_2) - 1} = \exp\left(-\frac{C}{m_1} \frac{m_1 + m_2}{m_2} t\right) \quad (9.107)$$

$$\frac{m_1}{m_1 + m_2} - \frac{a_1}{a_0} = \left(\frac{m_1}{m_1 + m_2} - 1\right) \exp\left(-\frac{C}{m_1} \frac{m_1 + m_2}{m_2} t\right) \quad (9.108)$$

$$\frac{a_1}{a_0} = \frac{m_1}{m_1 + m_2} - \left(\frac{m_1}{m_1 + m_2} - 1\right) \exp\left(-\frac{C}{m_1} \frac{m_1 + m_2}{m_2} t\right) \quad (9.109)$$

when reaching equilibrium ($t \rightarrow \infty$), from Eqs. (9.104) and (9.109), we obtain:

$$a_1 = a_2 = \frac{m_1}{m_1 + m_2} a_0 \quad (9.110)$$

This means that the specific activity is the same in the whole system; that is, the mixing entropy reached the absolute maximum.

Of course, this discussion can also be applied to other cases of heterogenous isotope exchange systems on the condition that the system has a component that can exchange freely between the phases.

Thus, we conclude that the heterogeneous isotope exchange allows us to study transport processes between phases under equilibrium conditions. Similar to the McKay equation (see Section 9.3.3.1) describing homogeneous isotope exchange, Eqs. (9.104) and (9.109) also show pseudo first-order kinetics, depending on the quantities in the two phases (m_1 and m_2). The rate of the transport (C) can be measured when the isotope exchange is the rate-determining process and the quantities in the two phases (m_1 and m_2) are known. Moreover, it is enough to know only one of the two quantities (m_1 and m_2) because there are two kinetic equations, one for each phase. Thus, the quantity in the unknown phase also can be calculated. To provide an example of this latter application, we can mention the determination of the quantity of the exchangeable phosphate ions in soils. By the usual analytical methods, the total phosphate quantity present in the soil can be measured; however, only a portion of this phosphate can be dissolved in the soil solution. When the phosphate quantity of the soil solution is measured (it can be considered as m_1), and the heterogeneous phosphate exchange between the soil solution and the soil is studied by adding radioactive phosphate to the soil solution, based on the kinetic studies, the quantity of the exchangeable phosphate of soil (m_2) and the rate of isotope exchange (C) can be determined from Eqs. (9.104) and (9.109). The value of m_2 can be calculated from the equilibrium-specific activities too (see Eq. (9.110)).

The heterogeneous isotope exchange clearly illustrates the most important aspects and advantage of the radiotracer methods: systems in thermodynamic equilibrium can be studied without disturbing equilibrium. The rate of processes in equilibrium can be given quantitatively. To do this, the isotope tracer method is the only option.

The rate of the isotope exchange reaction can also be determined at different temperatures. From the obtained values, the binding energy between the atoms participating in the isotope exchange can be calculated using the Arrhenius equation.

Nowadays, isotope exchange reactions are frequently used to study the rate of biological metabolisms and to determine the binding energy in heterogeneous catalytic reactions. In addition, the study of isotope exchange reactions provides useful information in geology (see Section 3.4).

Transport-Controlled Heterogeneous Isotope Exchange

The rate-determining step of the heterogenous isotope exchange is very frequently the transport of the substances from the bulk to the interface. The transport means the convection, the mixing, and the diffusion of the dissolved substance from the solution phase to the interface, i.e., the reaction zone. The transport in the solution phase has two steps: the movement of the dissolved substances in the bulk solution and through a so-called adhesion layer. The convection and mixing influences only the transport in the bulk phases; in the adhesion layer, only diffusion (called “film diffusion” in this case) is possible, governed by the concentration gradient through the adhesion layer. Mixing decreases the thickness of the adhesion layer.

Since the concentration of the radioactive nuclide in radiotracer experiments is frequently very low, the diffusion plays an important role. In the adhesion layer,

the diffusion can be described by Fick's first law, assuming that the concentration gradient is constant through the adhesion layer:

$$\frac{dc}{dt} = D \frac{dc}{dx} \quad (9.111)$$

In this case, the net kinetics of the isotope exchange is of the first order.

9.3.3.3 The Empirical Equation of the Heterogeneous Isotope Exchange

The heterogeneous isotope exchange in solid/liquid systems cannot be described by the usual, theoretically correct kinetic equation. For the interfacial reaction of very insoluble salts, an empirical equation was derived by Imre in 1933:

$$x_{\infty} - x_t = A_1 e^{-k_1 t} + A_2 e^{-k_2 t} + A_3 e^{-k_3 t} \quad (9.112)$$

where x_t and x_{∞} are the relative amount of the radioactive isotope on the solid surface at time t and in equilibrium, respectively; k_1 , k_2 , k_3 are rate constants; and A_1 , A_2 , and A_3 are empirical coefficients. The members in Eq. (9.112) refer to simultaneous first-order reactions. However, the equation is formal; thus, it gives no information on the mechanism of the net reaction. In the literature, there are many frequently speculative interpretations for the rate constants and the empirical coefficients. These interpretations include speculation about the rate-determining step. Similar equations are used for the kinetic description of the interfacial processes of the crystalline powder/solution or the metal/solution. The experimental data are interpreted by including additional members to the kinetic equation.

Many heterogeneous isotope exchange processes between metal and the ions of the same element were studied to determine the exchange rate in equilibrium. The Ag/Ag^+ system was intensively studied. The kinetics of the exchange process was interpreted as follows:

$$x_t = x_{\infty} \left(1 - \exp\left(-\frac{t}{\tau}\right) \right) \quad (9.113)$$

and

$$\tau = x_{\infty} \frac{v_0 v_j + v_d v_j + v_0 v_d}{v_0 v_j v_d} \quad (9.114)$$

where v_0 is the rate of surface diffusion, v_j is the rate of the electron exchange, and v_d means the rate of diffusion in the solution. Equations (9.113) and (9.114) take into consideration the steps and mechanism of the heterogeneous isotope exchange on the interface of the metal/electrolyte solution. The τ versus concentration function gives information on the rate-determining step and the mechanism of the isotope exchange.

The kinetics of the heterogeneous isotope exchange was described by empirical equations that take into account the heterogeneity of the surface. For example:

$$x_t = bt^n \quad (9.115a)$$

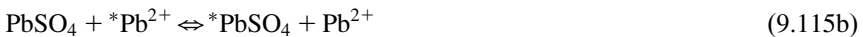
where b and n are empirical values. These values are interpreted by the energy distribution of the exchange sites of the surface.

The main conclusions of the heterogeneous isotope exchange studies on metal surfaces are as follows:

- In equilibrium between the metal and the solution phase, continuous isotope exchange takes place.
- The rate of the electron exchange (exchange current) can be measured only in special cases; namely, when the rate-determining step of the surface reaction is the electron exchange, such as in the Fe/Fe^{2+} system.

9.3.3.4 Paneth's Method of Surface Determination

The Paneth surface determination postulates that the heterogeneous isotope exchange is much faster on the surface of the bulk solid phase than inside it. Thus, the specific surface area of a solid substance can be determined from the ratio of the radioactivities of the solid and its saturated solution. For example, the specific surface area of lead sulfate can be determined using radioactive lead ions (e.g., $^{212}\text{Pb}^{2+}$). The isotope exchange takes place between the lead ions in the solution and on the surface of the solid lead sulfate:



Since there are no chemical reactions, the process is directed by the change of the mixing entropy. When the exchange takes place only on the surface, the ratio of the activities of the solution and solid is determined by the ratio of the atoms/ions in the solution and on the surface of the solid, as follows:

$$\frac{\text{Activity of solution}}{\text{Activity of solid}} = \frac{cV}{X} \quad (9.116)$$

where X is the number of the atoms/ions on the surface, c is the concentration of saturated solution (solubility), and V is the volume of the solution. After multiplying X by the cross section of the surface atoms/ions, the specific surface area is expressed in area units.

The radioactive atoms/ions can be buried into the bulk by isotherm transcrystallization. This effect is corrected by the kinetics of the isotope exchange; the radioactivity is measured as a function of time (Figure 9.15). The kinetic curve has two sections: a sharp and a slight increase; and the fast surface exchange is followed by a slow exchange (transcrystallization) with the bulk phase. Extrapolating the slight

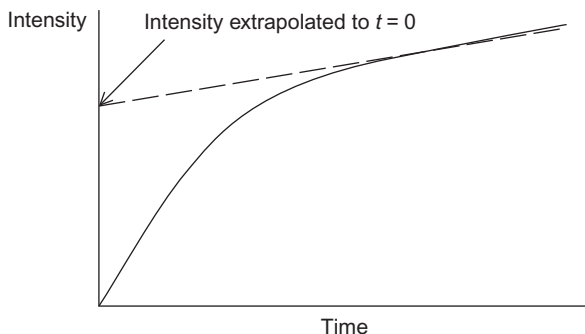


Figure 9.15 The determination of the surface exchange from the radioactivity versus time function by a heterogeneous isotope exchange.

increase to the initial time ($t = 0$), it cut the vertical axis at the radioactivity belonging to the pure surface exchange.

For crystalline substances, only a portion of the surface sites, the so-called active surface, exchanges with the radioactive atoms/ions in the solution. The active surface depends on the temperature. According to Imre, the relation of the total surface (X) and the active surface (X^*) is as follows:

$$X^* = X \exp\left(-\frac{E}{RT}\right) \quad (9.117)$$

where E is the activation energy of the isotope exchange and T is the temperature. The total surface area can be determined from the active surface areas measured at different temperatures.

9.3.4 Study of Interfacial Reactions

Because of their fairly high sensitivity, radiotracer methods are widely applied in all fields where the interface plays an important role in the reactions (interfacial chemistry, colloid chemistry, heterogeneous catalysis, etc.). The surface quantity of the substances is about 10^{-9} – 10^{-8} mol/cm²; thus, the study of the interfacial reactions requires analytical methods that are able to detect and precisely measure the change of these small quantities. The radioactive isotopes fulfill this requirement. In addition, radiotracer studies are applicable in a very broad concentration range of the solution or gas interacting with the interface: from carrier-free to saturation concentrations or to critical pressure. The high concentrations are reached using inactive carriers (isotopic effects can usually be disregarded).

Another advantage is the possibility of multiple indications if the radioactive isotopes can be separated using their radiochemical properties (type and/or energy of radiation and half-life, as discussed in Section 8.3). By multiple indications, interfacial processes can be studied from the direction of both bulk phases. For example, in ion exchange processes, both ions can be labeled. In this way, the equivalency of the process can be checked or the effect of other interfacial processes (e.g., adsorption) or the influence of the exchange of additional ions (e.g., hydrogen and hydroxide ions of the water) can be studied. These experiments

give significant information on the interfacial processes of ion exchangers, including natural ion exchangers such as clay minerals, rocks, and soils.

The study of the cation exchange of calcium montmorillonite clay mineral and manganese(II) ions illustrates the difficulties of multiple radioactive indication. Calcium ions can be labeled as weak beta emitter ^{45}Ca isotopes. For labeling manganese(II) ions, the ^{54}Mn isotope can be used, which disintegrates via electron capture and emits X-ray and gamma radiation. The gamma radiation of the ^{54}Mn isotope can be measured by scintillation (see Section 14.2) as well as semiconductor (see Section 14.3) detectors, and the beta radiation of the calcium isotope does not disturb the measurement of gamma radiation. However, the radiation of the ^{54}Mn isotope disturbs the measurement of beta emitter isotopes. The weak beta particles of ^{45}Ca can be measured by the liquid scintillation technique (discussed in Section 14.2). The liquid scintillation beta spectrum of ^{45}Ca is shown in Figure 9.16. The spectrum of ^{54}Mn obtained by a liquid scintillation spectrometer can be seen in Figure 9.17. The sharp peak originates from the electrons emitted after the electron capture from the K orbital. The energy of these electrons is 4.7 keV. When both isotopes, ^{45}Ca and ^{54}Mn , are present simultaneously, the shape of the spectrum is determined by their ratio (Figures 9.18 and 9.19). In Figures 9.16–9.19, the horizontal axis is the channel number proportional to the logarithm of the energy; the vertical axis shows the intensity.

As seen in Figures 9.18 and 9.19, the sharp peak of ^{54}Mn can be eliminated when its activity is relatively large. Thus, the activity of ^{45}Ca can be determined. When the radioactivity of ^{54}Mn is small, however, the peaks corresponding to ^{45}Ca and ^{54}Mn cannot be separated, and the activity of ^{45}Ca cannot be measured. This is a rare and interesting case in chemical analysis when the interfering effect of the “impurity” (^{54}Mn) is higher if it is present in small quantities than if it is present in large quantities. The degree of interference has been experimentally determined as follows: the gamma and “beta” activities of solutions containing ^{54}Mn isotopes

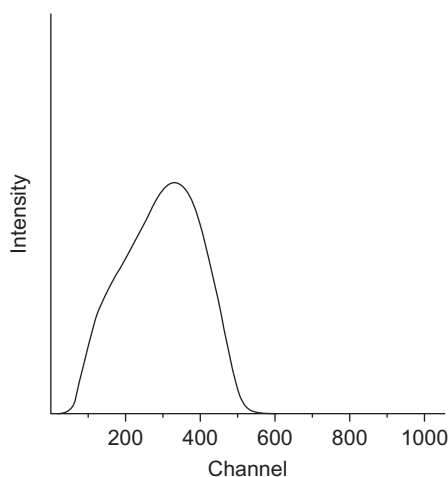


Figure 9.16 Liquid scintillation beta spectrum of the ^{45}Ca isotope.

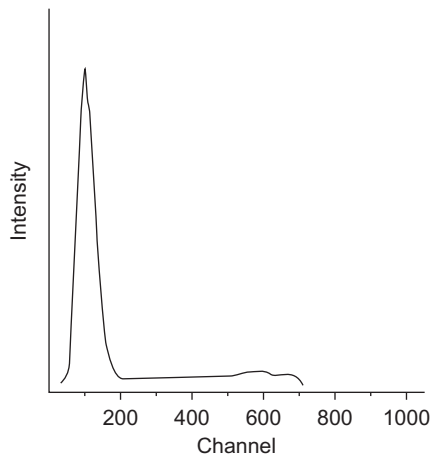


Figure 9.17 Liquid scintillation beta spectrum of the ^{54}Mn isotope. The sharp peak originates from the electrons emitting after the electron capture from K orbital.

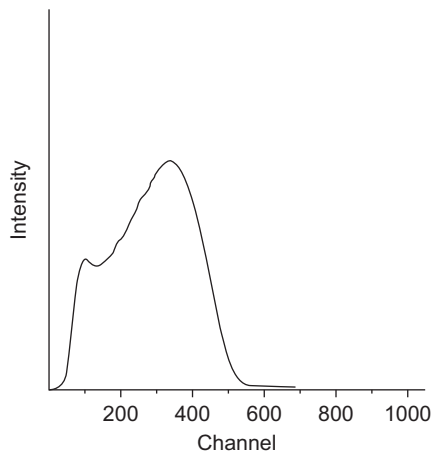


Figure 9.18 Liquid scintillation spectrum of ^{45}Ca and ^{54}Mn in small quantities.

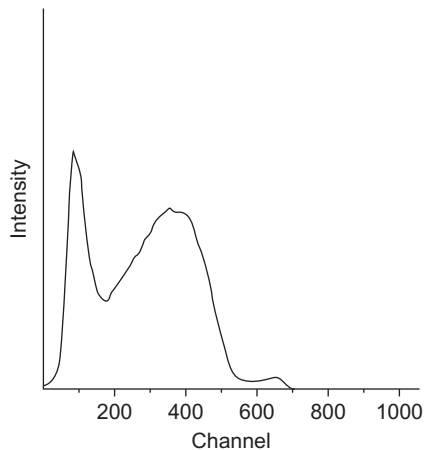


Figure 9.19 Liquid scintillation spectrum of ^{45}Ca and ^{54}Mn in large quantities.

with different activities are determined; the beta activity is plotted as a function of gamma activity. When the solutions contain both ^{45}Ca and ^{54}Mn isotopes, the beta activity of the ^{54}Mn isotope is calculated on the basis of gamma activity using a predetermined plot, and then this value is subtracted from the total beta activity. The difference is treated as the beta activity of ^{45}Ca isotope.

9.3.5 Coprecipitation

As mentioned in Section 8.2, the radioactive indicator applied in carrier-free or very low concentrations can coprecipitate with any macrocomponent of the system if they can form isomorphous crystals. As an example, barium chloride (macrocomponent) and radium chloride (microcomponent) have been mentioned.

In the initial step of coprecipitation, the macro- and microcomponents are mixed in solution. When mixing entropy becomes maximal, the solution will be homogeneous. Then, there are two ways to achieve coprecipitation:

- By fast cooling of the solution. In this case, fine grains are produced. For example, $(\text{RaBa})\text{Cl}_2$ is precipitated by the addition of concentrated hydrochloric acid under cooling. The composition of the crystalline phase is the same in any small volume. This can be expressed by the Henderson–Kracek equation:

$$\frac{y}{x} = D \frac{b-y}{a-x} \quad (9.118)$$

where x and y are the quantities of the macro- and microcomponents in the crystalline phase, respectively; a and b are the quantities of the macro- and microcomponents in the whole system; and D is the fractionation coefficient. Fractionation by coprecipitation is possible when $D \neq 1$.

- The crystals are grown slowly; e.g., by the slow evaporation of the solvent. In this way, the composition of the solution continuously changes, and therefore the composition of the phases also change continuously. As a result, the composition of the crystal varies with the depth of the grains, as expressed by the Doerner–Hoskins equation:

$$\ln \frac{a}{a-x} = \lambda \ln \frac{b}{b-y} \quad (9.119)$$

where λ is the fractionation coefficient and the other signs have the same meaning as in Eq. (9.118).

Equations (9.118) and (9.119) can be related, assuming a thermodynamical equilibrium for any infinitely short time of the crystal growing:

$$\frac{dx}{dy} = \lambda \frac{a-x}{b-y} \quad (9.120)$$

Separating the variables:

$$\frac{dx}{a-x} = \lambda \frac{dy}{b-y} \quad (9.121)$$

Equation (9.121) can be solved for the whole period of crystal growth, assuming that the crystal growth is determined by the surface equilibria at any time:

$$\int \frac{dx}{a-x} = \lambda \int \frac{dy}{b-y} \quad (9.122)$$

The solution is:

$$\ln(a-x) = \lambda \ln(b-y) + C \quad (9.123)$$

In order to determine the integration constant (C), we assume that at the initial time of the crystal growth, ($t = 0$), $x = 0$ and $y = 0$ (no crystal yet):

$$\ln a = \lambda \ln b + C \quad (9.124)$$

From here:

$$C = \ln a - \lambda \ln b \quad (9.125)$$

Substituting C into Eq. (9.123), the Doerner–Hoskins equation is obtained:

$$\ln(a-x) = \lambda \ln(b-y) + \ln a - \lambda \ln b \quad (9.126)$$

Experiments have shown that crystals that have a composition characterized by the Doerner–Hoskins equation can transform to crystals with uniform composition characterized by the Henderson–Kracek equation by isothermic transcrystallization.

9.3.6 Tracer Techniques in Electrochemistry

The combination of electrochemical studies with radiotracer methods can help solve many electrochemical and corrosion problems, such as the corrosion of the structural material of nuclear power plants and the contamination and decontamination of the corrosion products.

Important factors of contamination and decontamination are the sorption processes which, as discussed previously, can be well studied by radiotracer methods. In such studies, the radioactivity of the solution and/or the solid phase, including the electrodes in the electrochemical studies, can be measured. The radioactivity of the surface is proportional to the surface excess concentration of the sorbed species. The measurements frequently can be obtained by stopping the process and

measuring the activities after sampling. In addition, the processes can also be studied *in situ*. The *in situ* methods are based on the thin-layer principle. This means that the self-absorption of beta particles with low and medium energy, as well as gamma- or X-ray radiation below 20 keV energy, is so high that the detectors can observe the radiation of only a thin liquid layer. If the solution phase is eliminated from the surface of the solid (electrode), the radioactivity of the sorbed species can be determined. It can be achieved in three ways:

1. In the foil method, the detector and the solution of the labeled adsorbate is separated by the adsorbent deposited on a thin foil (or the adsorbent itself is the foil).
2. In the thin-layer method, the solution is continuously circulated in a thin layer (about 0.5 mm) between the detector and the electrode.
3. In the so-called electrode sinking method, which is the combination of the two previous methods, radioactivity is measured alternatively in the two positions of the electrode. Sinking to the bottom where the background is very low, the surface excess concentration is measured, while in a position higher than the range of the beta radiation, the radioactivity of the solution is measured.

Further Reading

- Atkins, P.W. (1998). *Physical Chemistry*. 6th edition. Oxford University Press, Oxford.
- Bartha, L. (1967). Observation of recrystallization of tin by autoradiography. *J. Appl. Radiat. Isot.* 18:789–790.
- Crank, J. (1979). *The Mathematics of Diffusion*. Clarendon Press, Oxford.
- Elektrochemie, Z. Berichte der Bunsengesellschaft für physikalische Chemie. 56:380–386. <http://onlinelibrary.wiley.com/doi/dx.doi.org/10.1002/bbpc.19520560427/abstract>. May 3, 2010.
- Gerischer, H. Vielstich, W. (1952). Untersuchungen mit radioaktiven Indikatoren über Austausch- und Diffusionsvorgänge an Silberelektroden.
- Haissinsky, M. (1964). *Nuclear Chemistry and its Applications*. Addison-Wesley, Reading, MA.
- Hoffman, R.E. and Turnbull, D. (1951). Lattice and grain boundary self-diffusion in silver. *J. Appl. Phys.* 22:634–639.
- Imre, L. (1933). Grenzflächengleichgewichte und innere Gleichgewichte in heterogenen Systemen. Teil I. *Z. Phys. Chem. Abt. A* 164:343–363.
- Imre, L. (1933). Zur Kinetik der Oberflächenvorgänge an Kristallgittern. II. Die Elementarprozesse bei der Ausbildung einer aus mehreren Komponenten bestehenden Grenzschicht. *Z. Phys. Chem. Abt. A* 164:327–342.
- Imre, L. (1942). Über die Anwendbarkeit der radioaktiven Indikatormethode zur Bestimmung Der Oberfläche fester Körper I. *Kolloid Z.* 99:147–157.
- Imre, L. (1944). Über die Anwendbarkeit der radioaktiven Indikatormethode zur Bestimmung der Oberfläche fester Körper II. *Kolloid Z.* 106:39–46.
- Kazarinov, V.E. and Andreev, V.N. (1984). Tracer methods in electrochemical studies. In: *Comprehensive Treatise of Electrochemistry* (eds. Yeager, E., Bockris, J.O'M., Conway, B.E., Sarangapani, S.). Plenum Press, New York, NY, London, pp. 393–443.
- Kónya, J. (1977). Study of surface reactions of the Fe/Fe heterogeneous isotope-exchange system with a radioactive indicator (^{59}Fe), part I. Determination of iron exchange current. *J. Electroanal. Chem.* 84:83–91.

- Kónya, J. and Bába, Á. (1980). Study of surface reactions of the Fe/Fe heterogeneous isotope-exchange system with a radioactive indicator (^{59}Fe), part II. Rates of anodic and cathodic part-processes at corrosion potential. *J. Electroanal. Chem.* 109:125–139.
- Nagy, N.M. and Kónya, J. (2005). The relations between the origin and some basic physical and chemical properties of bentonite rocks illustrating on the example of Sarmatian bentonite site at Sajóbáony (HU). *Appl. Clay Sci.* 28:257–267.
- Nagy, N.M. and Kónya, J. (2009). *Interfacial chemistry of rocks and soils*. Taylor & Francis, Boca Raton, FL.
- Philibert, J. (1991). *Atom Movements. Diffusion and Mass Transport in Solids*. Les Editions de Physique, Paris.
- Sheppard, C.W. (1948). The theory of the study of transfers within a multi-compartment system using isotopic tracers. *J. Appl. Phys.* 19:70–76.
- Solomon, A.K. (1949). Equations for tracer experiments. *J. Clin. Invest.* 28:1297–1307. < <http://www.ncbi.nlm.nih.gov/pmc/articles/PMC439688/pdf/jcinvest00400-0051.pdf> > (accessed 25.03.12.)
- Varga, K., Hirschberg, G., Baradlai, P. and Nagy, M. (2001). Combined application of radiochemical and electrochemical methods for the investigation of solid/liquid interfaces. In: *Surface and Colloid Science* (ed. Matijevic, E.), vol. 16. Plenum Press, New York, NY, pp. 341–393.
- Varga, K. (2004). The role of interfacial phenomena in the contamination and decontamination of nuclear reactors. In: *Radiotracer Studies of Interfaces, Interface Science and Technology* (ed. Horányi, G.), vol. 3. Elsevier B.V., Amsterdam, pp. 313–358.

10 Radio- and Nuclear Analysis

Radioactive isotopes and their radiation have many uses in analytical chemistry. The procedures involving them can be divided into two groups. The procedures in the first group are based on the principle that radioactive isotopes have the same chemical properties as the stable isotopes of the same element (here, the isotope effects are ignored). These analytical methods employ radioactive isotopes called tracers (see [Section 10.1](#)).

The second group of the analytical applications of radioactivity includes the methods in which the samples are irradiated by particles or electromagnetic radiation, and the impacts of these radiations on the matter or the change in the properties of the irradiating particles or photons are studied. This means that analytical and structural information are obtained via studying the interactions of radiation with matter (see [Section 10.2](#)).

10.1 Radioactive Isotopes as Tracers

10.1.1 *The Measurement of Concentration Using Natural Radioactive Isotopes*

The quantity of an element present in the same sample can be determined if the relative abundance of its isotopes is constant, and among these isotopes, there is at least one natural radioactive isotope with a long half-life. Such elements are potassium, rubidium, samarium, lutetium, rhenium, and uranium. In these concentration measurements, the activity of the radioactive isotopes is measured. When we know the relative abundance of the radioactive isotopes, the quantity of the element that is present can be calculated from Eq. (4.12), taking into account the relative abundance of the radioactive isotopes.

As an example, the data required for the quantitative measurement of lutetium is illustrated in [Table 10.1](#). The ^{176}Lu isotope, which is in the natural lutetium in 2.59%, is used for the measurements. As calculated from the data in [Table 10.1](#), 10^{-4} mol of lutetium provide about 100 dpm of activity. This activity can be measured easily by a 4π -counter (as described in [Section 14.6](#)). If other types of nuclear detectors are used, the measuring efficiency has to be included in the correction. Unfortunately, the half-lives of these very long-lived radioactive isotopes are frequently determined with a relatively high number of errors; thus, the quantitative measurements may have a high level of uncertainty.

Table 10.1 The Data Required for the Quantitative Measurement of Lutetium Using the ^{176}Lu Isotope

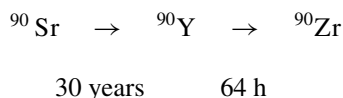
| Mass Number | Relative Abundance (%) | Half-life (min) | Decay Constant (1/min) |
|-------------|------------------------|------------------------|------------------------|
| 175 | 94.71 | Stable | |
| 176 | 2.59 | $2.02 \times 10^{+16}$ | 3.42×10^{-17} |

10.1.2 Determination Yield of Separation Reactions by Radioactive Tracers

A very common task in analytical chemistry is the separation of the different components to be analyzed. The components are typically separated by distribution reactions using phase separation. For example, the precipitation, extraction, ion exchange, electrolysis, and different chromatographic methods are mentioned.

In order to have accurate analytical results, the distribution ratio (in other words, the yield of the separation procedure) must be determined. Radioactive tracers can assist in determining the yield. The application of the radioactive tracers is especially useful in multicomponent systems if the radioactive isotopes of components have distinguishable radiation properties, such as different gamma energies.

The following two examples demonstrate how this method can be used to determine distribution ratios. First, the separation of the ^{90}Sr – ^{90}Y parent–daughter pair is mentioned. These are fission products of ^{235}U in nuclear reactors (see Figure 6.5 and Section 7.3). Since their fission yield is relatively high, and ^{90}Sr has a relatively long half-life, it is important to be able to determine precisely the activity concentration of ^{90}Sr in different samples. However, as a result of the negative beta decay of ^{90}Sr , ^{90}Y is formed:



Both isotopes have pure negative beta radiation, and the maximum beta energies are 546 and 2284 keV for ^{90}Sr and ^{90}Y , respectively. As a result, the activity of the parent nuclide, ^{90}Sr , can be measured directly only in secular equilibrium (as discussed in Section 4.1.6). The time needed to reach the secular equilibrium is determined by the half-life of the daughter nuclide, ^{90}Y . This is 64 h, so the secular equilibrium is reached after about a month, which is too long to obtain the analytical result. To avoid this problem, ^{90}Sr and ^{90}Y isotopes are separated chemically using several different procedures. Each separation procedure requires the determination of the yield of separation. This can be done easily using the ^{85}Sr isotope as a tracer that has beta and gamma radiation. Since neither ^{90}Sr nor ^{90}Y has gamma radiation, the gamma radiation of ^{85}Sr (514 keV) is used for the analysis. ^{85}Sr with

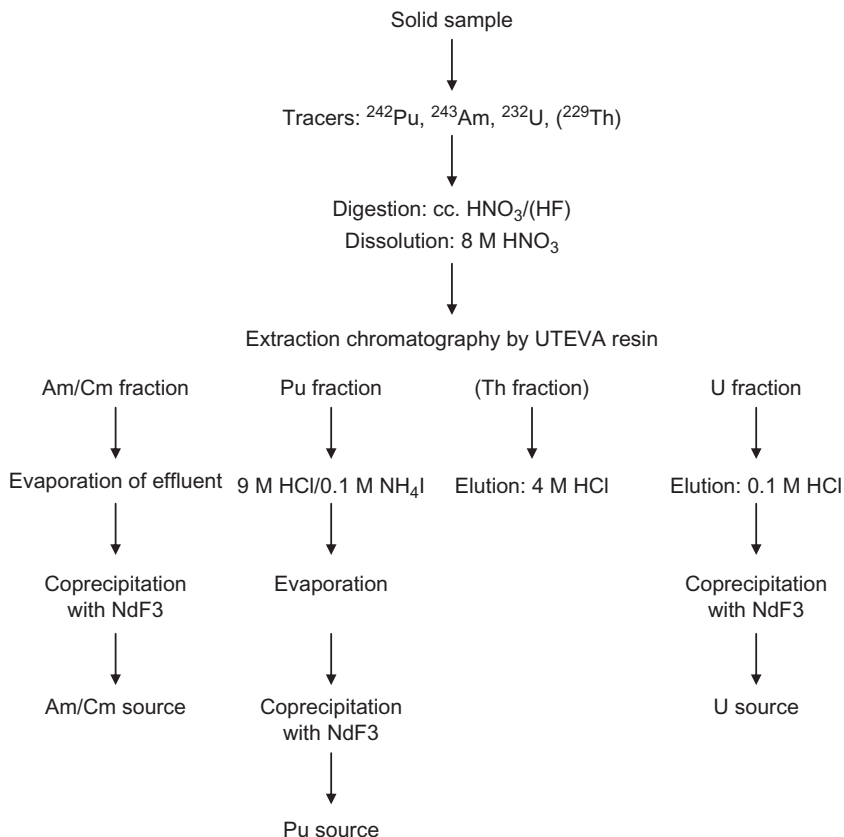


Figure 10.1 The scheme of the separation and sample preparation from a mixture of uranium (thorium) and transuranium elements. The separation yield is determined by addition of radioactive tracers. (Thanks to Dr. Anikó Kerkápoly, Budapest Technical and Economical University, Hungary, for the scheme.)

known activity/intensity is added to the mixture of ^{90}Sr – ^{90}Y before the separation. The yield is calculated on the activity/intensity measurement of the pure strontium fraction after the separation.

The other example illustrating the use of radioactive isotopes to determine separation yields is the analysis of the uranium (sometimes thorium) and transuranium elements. As discussed in Section 6.2.1 (Eqs. (6.22) and (6.23)), these isotopes are produced from ^{238}U in nuclear reactors. For their quantitative analysis, precipitation, extraction, and ion exchange separations are used. The separation yields are determined by radioactive tracers that are not present in the samples, i.e., nonfission products, such as ^{242}Pu , ^{243}Am , ^{232}U , and ^{229}Th . An example for the separation and sample preparation is shown in Figure 10.1.

In these two examples, the radioactive tracers are applied in radioactive samples. Obviously, similar procedures can be applied for nonradioactive samples. The separation yield of different processes (precipitation, gravimetry, extraction, ion exchange, chromatography, etc.) can be determined using radioactive tracers, both in the analytical and in the preparative scale. The traditional analytical methods coupled with radioactive tracers include radiogravimetry, radiochromatography, and so on.

10.1.3 Solubility Measurements

As mentioned in Section 8.1, the first radiotracer studies by G. Hevesy and F. Paneth included the determination of the solubility of lead salts (sulfide and chromate) using RaD (^{210}Pb) as a radioactive tracer.

The solubility measurements are based on the specific activity of a substance, which is the same in any physical state, such as in solids and in solutions. Thus, if we measure the specific activity (a_{solid}) of a very insoluble salt, as Hevesy did for lead salt, this will be the same in the saturated solution of the same salt (the mixing entropy reaches absolute maximum for the total system). Thus, from the activity of an aliquot of the saturated solution (A), the mass of the dissolved substance (m) in the measured volume can be calculated, since $m = A/a_{\text{solid}}$. This method can be used to determine such small quantities as the concentration of lead and sulfide ions in the saturated solution of lead sulfide, the solubility product of which is $L_{\text{PbS}} = 10^{-33} \text{ mol}^2 \text{ dm}^{-6}$. This means that the concentration measurement is in the range of about $3 \times 10^{-16} \text{ mol dm}^{-3}$.

The solubility can be measured in the presence of indifferent electrolyte solution at different concentrations. The results obtained at different ionic strengths give information on the activity coefficients of the ions.

10.1.4 Radiochromatography

As mentioned in Section 10.1.2, traditional analytical methods can be coupled with radioactive tracer techniques, or qualitative and quantitative analysis of the labeled compounds can be performed by any traditional analytical technique. One such method is radiochromatography, which is frequently used for purification and quality control of radiochemicals and radiopharmaceuticals (radiochemical purity control, as discussed in Section 8.3). Any types of chromatography, namely, HPLC, thin-layer chromatography, and ion exchange chromatography, can be used for this purpose. The detection is done by measuring the radioactivity of the fractions. Radiochromatogram scanners are commercially available.

10.1.5 Radiometric Titration

Radiometric titration is a two-phase titration method when the equivalence point (i.e., end point) is indicated by the disappearance of a radioactive isotope from one phase. It can be used if the unknown substance and the titrant form very insoluble

precipitates or an easily extractable compound, and if one of the reagents has a suitable radioactive isotope. During the titration process, different volumes of the titrant are added to the unknown compound, the phases formed are separated by filtration and extraction, and the activity/intensity of any phases is measured. The main advantage of the radiometric titration is that the titration curve usually consists of linear portions; thus, few points are enough for drawing the titration curve. In addition, the linear character provides opportunities for automation.

Both the unknown compound and the titrant can be labeled. When precipitate is produced during the titration, the titration curves will be as follows:

- The titrant is labeled by a radioactive isotope; the activity of the solution shows the background activity until the equivalence point. After the equivalence point, the activity of the solution containing the excess of the titrant increases (Figure 10.2, plot A).
- The unknown compound is labeled: the activity of the solution decreases until the equivalence point, and then it shows the activity determined by the solubility of the precipitate (Figure 10.2, plot B).
- Both the unknown compound and the titrant are labeled: the activity has a minimum at the equivalence point (Figure 10.3).

Two or more unknown compounds can be analyzed simultaneously by precipitation radiometric titration if the solubility of the precipitates is fairly different. For example, copper and zinc ions can be determined by titration with $\text{Fe}(\text{CN})_6^{4-}$. Zinc ions are labeled with a radioactive ^{65}Zn isotope. The solubility of $\text{Cu}_2[\text{Fe}(\text{CN})_6]$ is much less than that of $\text{Zn}_2[\text{Fe}(\text{CN})_6]$. By adding the solution of $\text{Fe}(\text{CN})_6^{4-}$ to the solution of copper and zinc ions, at first, $\text{Cu}_2[\text{Fe}(\text{CN})_6]$ precipitates, and then the activity of the solution remains constant. After the equivalence point of the precipitation of the copper ion, $\text{Zn}_2[\text{Fe}(\text{CN})_6]$ starts to precipitate and the activity of the solution decreases. After the precipitation of the total quantity of the zinc ions, the activity of the solution becomes constant again, determined by the solubility of $\text{Zn}_2[\text{Fe}(\text{CN})_6]$ (Figure 10.4).

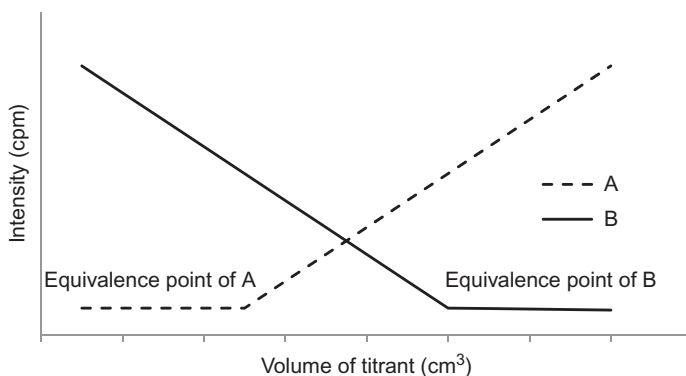


Figure 10.2 Radiometric titration curves when the titrant is labeled (A) and the unknown compound is labeled (B). The activity of the solution is measured.

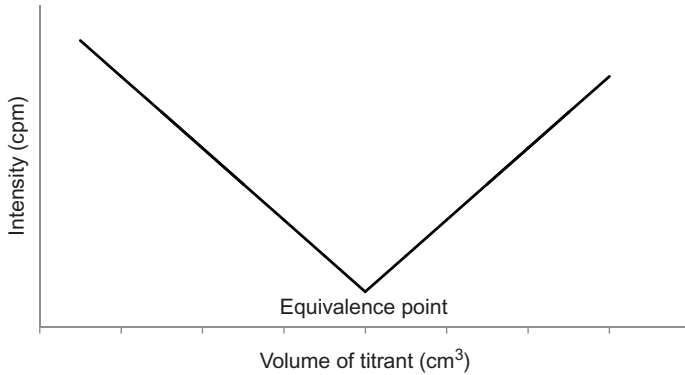


Figure 10.3 Radiometric titration curves when both the titrant and the unknown compound are labeled. The activity of the solution is measured.

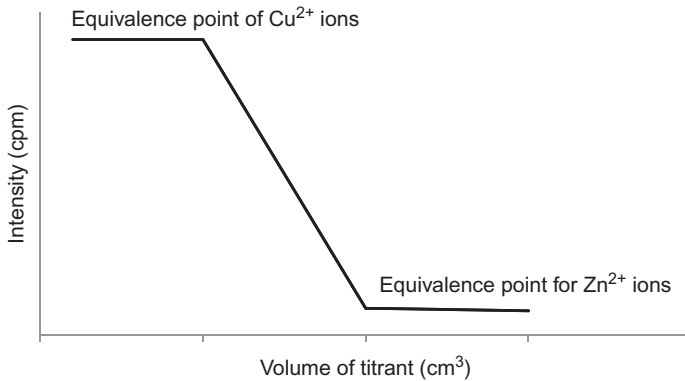


Figure 10.4 A radiometric titration curve of Cu²⁺ and Zn²⁺ ions with [Fe(CN)₆]⁴⁻ ions. The zinc ion is labeled with a ⁶⁵Zn isotope. The activity of the solution is measured.

Dual labeling gives additional analytical opportunities. For example, the quantity of sulfate and iodide ions in the same solution can be measured. Both sulfate and iodide ions are labeled by radioactive sulfur (³⁵S) and iodine (¹³¹I) isotopes, respectively. The solution is titrated with barium chloride and barium sulfate precipitates. Then the activity of the solution decreases until the equivalence point of sulfate is reached. When barium chloride is added in excess, the activity becomes constant. Then, titration is continued using silver nitrate and precipitating silver iodide. Silver iodide is separated, and the activity of the solution decreases again until the equivalence point of iodide ions is reached, and then it becomes constant again (Figure 10.5).

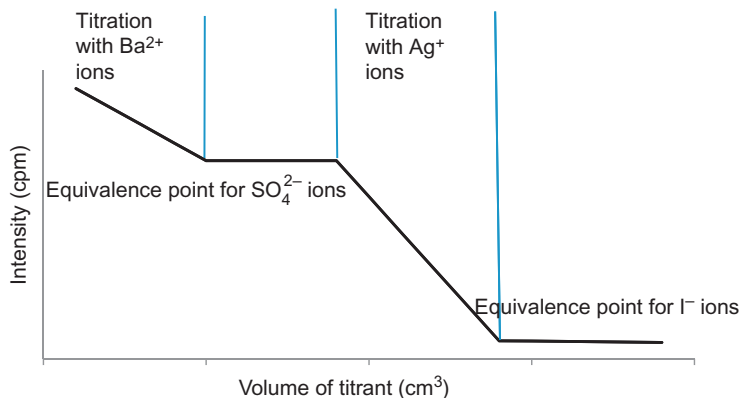


Figure 10.5 A radiometric titration curve of sulfate and iodide ions with barium and silver ions, respectively. Sulfate and iodide ions are labeled by the ^{35}S and ^{131}I isotopes. The activity of the solution is measured.

Radiometric titration can also be made by extraction. For example, the unknown metal ion is titrated with a complex forming agent. The complex compound is extracted with an organic solvent. The concentration of zinc ions can be determined by titrating dithizone dissolved in chloroform. The zinc dithizone complex dissolves in the chloroform. When zinc ions are labeled (e.g., by the ^{65}Zn isotope), the activity of the aqueous phase decreases until the equivalence point is reached, and then it remains constant.

10.1.6 Isotope Dilution Methods

In isotope dilution methods, radioactive isotopes are used as tracers. When diluting with a stable isotope, the specific activity decreases and the mixing entropy increases. Thus, the specific activity is measured before and after dilution; the quantity of the diluting substance is determined by the change of the specific activity, as discussed in Section 9.2. Equations (9.26)–(9.30) are the basic formulas of the isotope dilution methods. In this section, the different isotope dilution methods and their applications will be discussed.

As seen in Eq. (9.30), specific activities provide the required analytical information, so the quantitative isolation of the studied substance is unnecessary. However, the isolated substance has to be pure (selective isolation) and must have a well-defined stoichiometry. In Eq. (9.30), mass or volume can replace the number of moles, so it is possible to determine these quantities as well. The absolute activity is frequently substituted by radioactive intensity (as discussed in Section 4.1.2). Of course, when we use intensities, we must ensure that the conditions of the measurements stay the same.

Isotope dilution methods are frequently applied to the measurement of the concentration of substances which otherwise are difficult to analyze, such as the concentration of a particular lanthanoid element in the mixtures of rare earth elements or the concentration of a particular hydrocarbon in mixtures of hydrocarbons. The isotope dilution is suitable to measure the volume of substances in large tanks, such as molten metal in furnaces or mercury in electrolytic cells (see Section 11.2.4), in addition to the volume or flow rate of flowing liquids (blood, river, pipelines, etc.). A very important application of isotope dilution methods is the RIA in nuclear medicine (see Sections 12.2.1 and 12.3.1). The main types of isotope dilution methods will be discussed next.

10.1.6.1 The Simple Isotope Dilution Method

In the simple isotope dilution method, the quantity of an inactive substance (m) is determined by the addition of a radioactive indicator. The labeled species (standard) of the substance to be analyzed is added to the unknown samples. The quantity ($m_0 + m^x$) and the specific activity (a_0) of the standard are exactly known. The system is homogenized, and the substance in question is selectively isolated as a well-defined compound; then it is purified to the required high level. As mentioned previously, the yield of isolation is unimportant. The specific activity of the compound obtained after the dilution (a) is determined.

If the quantity of the radioactive indicator can be disregarded ($m^x \ll m_0$), the quantity of the unknown substance from Eq. (9.30) is:

$$m = m_0 \left(\frac{a_0}{a} - 1 \right) \quad (10.1)$$

or is expressed by radioactive intensities:

$$m = m_0 \left(\frac{i_0}{i} - 1 \right) \quad (10.2)$$

Thus, the specific activity or intensity of the labeled substance has to be measured before and after the isotope dilution. The degree of the dilution is determined by the ratio of m to m_0 . The precision is usually suitable in the range of $m = 0.01 \times m_0$ to $m_0 = 0.01 \times m$. The simple dilution method is a fairly good option in all cases when the substance to be analyzed cannot be separated quantitatively.

10.1.6.2 The Reverse Isotope Dilution Method

The reverse isotope dilution method is used for the quantitative analysis of radioactive substances, especially in mixtures of radioactive substances. The quantity of the radioactive substance ($m_0 + m^x$) is determined by adding inactive substance (m) (standard). The steps of the procedure are the same as in the simple isotope dilution

method. It is usually true that $m^x \ll m_0$ and $(m^x + m_0) \approx m_0$. From Eq. (10.1) or (10.2), the quantity is:

$$m_0 = \frac{m}{\frac{a_0}{a} - 1} \quad (10.3)$$

or is expressed by intensities:

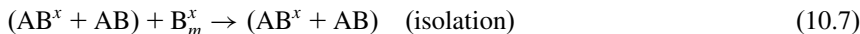
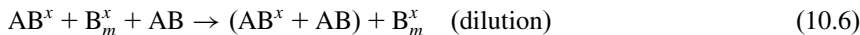
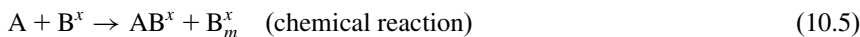
$$m_0 = \frac{m}{\frac{i_0}{i} - 1} \quad (10.4)$$

Similar to the simple isotope dilution method, the specific activity or intensity has to be measured before and after the isotope dilution. Since the quantity m is known, m_0 can be calculated. The sensitivity is determined by the minimum quantity that is needed to measure a_0 .

Reverse isotope dilution is used in microanalyses (e.g., for the analysis of purity), and the yield of nuclear reactions is used in the activation analysis (see Section 10.2.2.1).

10.1.6.3 The Derivate Isotope Dilution Method

If the radioactive species of the substance to be analyzed is not available, the isotope dilution method cannot be applied directly. In this case, the substance to be analyzed is reacted with a radioactive reagent. This radioactive product can be then subjected to the reverse isotope dilution method (described in Section 10.1.6.2). The method, therefore, combines the preparation of a radioactive compound and the reverse isotope dilution method. The steps following the preparation of the radioactive compound are the same as for reverse isotope dilution. For example, the substance to be analyzed is A, the radioactive reagent is B^x , the excess of the reagent is B_m^x , and the derivate isotope dilution consists of the following steps:



Similar to the other types of isotope dilution, the specific activities have to be determined before and after dilution, and the quantity of AB has to be known.

10.1.6.4 The Double Isotope Dilution Method

Double isotope dilution gives an opportunity to determine the quantity of a radioactive substance (m_0) if it is present in such small quantities that the specific activity

before the dilution (a_0) cannot be determined. In this case, two aliquot samples are taken from the substance to be analyzed, and they are diluted with inactive isotopes in different quantities (m_1 and m_2 , $m_1 \neq m_2$). After homogenization, the pure substances of the two diluted samples are isolated and the specific activities (a_1 , a_2) are measured. For the two dilutions, the following equation applies:

$$a_0 m_0 = a_1 (m_0 + m_1) \quad (10.8)$$

and

$$a_0 m_0 = a_2 (m_0 + m_2) \quad (10.9)$$

From Eqs. (10.8) and (10.9), we obtain:

$$a_0 = \frac{a_1 a_2 (m_2 - m_1)}{a_2 m_2 - a_1 m_1} \quad (10.10)$$

$$m_0 = \frac{a_1 m_1 - a_2 m_2}{a_2 - a_1} \quad (10.11)$$

Thus, m_0 can be calculated from the quantities m_1 and m_2 as well as the specific activities after the dilutions, a_1 and a_2 .

The double isotope dilution method is applied in nuclear chemistry, organic, and biochemistry; however, it is the least accurate of the isotope dilution methods. This is because to determine the specific activities, a relatively large quantity of diluting substance has to be added. If m_0 will become negligible compared to m_1 and m_2 , the method cannot be applied.

10.1.6.5 Substoichiometric Analysis

Similar to double isotope dilution, substoichiometric analysis is applied to the quantitative analysis of a radioactive substance (m_0) if it is present in such a small quantity that the specific activity before the dilution (a_0) cannot be determined. The radioactivity of the standard and the unknown sample should be the same. A reagent is added to both the standard and the unknown solution in unequivalent quantities. This is why the method is called "substoichiometric analysis." The product of the reaction (e.g., a complex compound) is separated (e.g., by extraction), and the activity of an aliquot is measured. As a result of the addition of the reagent in an unequivalent quantity, the activity of the product is inversely proportional to the concentration of the solution.

When several standard solutions with the same activity are used, a calibration curve is plotted (Figure 10.6). The concentration of the unknown sample is determined using this calibration curve. This method is applied in RIA studies (as discussed in Section 12.3.1).

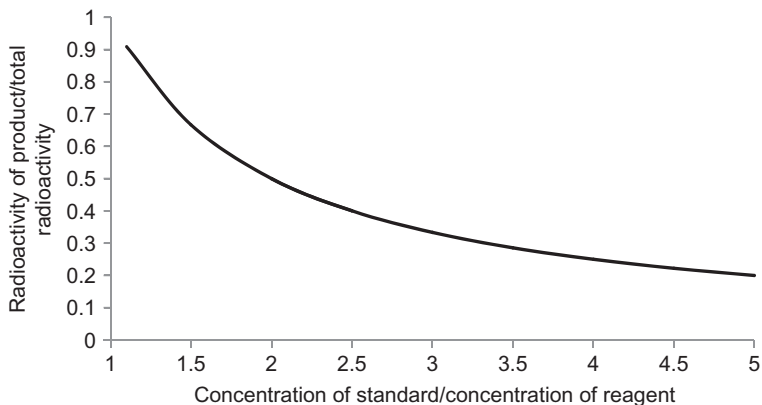


Figure 10.6 A calibration curve obtained in substoichiometric analysis.

10.1.6.6 The Dynamic Isotope Dilution Method

The isotope dilution method can be applied in open-flowing systems (see Section 11.2.6). Let us assume a tank with volume V and flow rate w of a liquid passing through the tank. At $t = 0$, a radioactive indicator with a_0 specific activity (or intensity) is added to the liquid. Assuming the mixing to be ideal, at t time, the specific activity (intensity), a , of the liquid leaving the tank is:

$$a = a_0 e^{-\frac{wt}{V}} \quad (10.12)$$

For a series of tanks, the specific activity (intensity) of the liquid leaving the i th tank is:

$$a_i = a_0 \frac{\left(\frac{w}{V}\right)^{i-1}}{i-1} e^{-\frac{wt}{V}} \quad (10.13)$$

10.2 Radioanalytical Methods Using the Interaction of Radiation with Matter

10.2.1 Basic Concepts

As discussed in detail in Chapters 5 and 6, radioactive (and other) radiations may have different impacts on the substances. The radiation can be absorbed or scattered, and, as a result of the interactions with the radiation, the irradiated substances themselves can emit different radiations, including particles or electromagnetic photons. All these phenomena provide analytical information on the different

structural levels of matter. The changes of intensity of the entering radiation, as well as the type, energy, or energy distribution, and the activity or intensity of the emitted radiation can be used in qualitative, quantitative, structural, and species analysis of the bulk phases, interfaces, and species bound to the surfaces of the substances.

Different types of radiations (namely, photons in the whole range of the electromagnetic spectrum, electrons and beta particles, neutrons, and positively charged particles) are used for the irradiation. The emitted radiations can also be photons and particles (electrons and positively charged particles). The emission is the result of the interactions between the entering radiation and the nuclei, nuclear field, and orbital electrons.

As seen from the list of the entering and emitted radiations, there are many analytical methods using the interaction of radiation with matter. They can be classified on the basis of the entering and the emitted particles, as summarized in [Table 10.2](#). As usual, the interactions are significantly influenced by the mass and charge of the particles (as discussed in Section 5.1). The classification is made on the basis of the mass of the particles.

For the sake of completeness, [Table 10.2](#) includes the analytical method in which the substance is irradiated with photons with lower energy than the nuclear radiation (e.g., nuclear magnetic resonance, electron spin resonance, infrared, near-infrared, visible, ultraviolet spectroscopy, or dynamic light scattering). Of course, these methods traditionally belong to other disciplines of chemistry, so they are not discussed in detail here. It is important to note, however, that they also utilize the interactions of radiation with matter. In addition, nuclear magnetic resonance can be considered to be a nuclear analytical method in which the magnetic field of special nuclei is excited by electromagnetic radiation with low energy. At the same time, the highest-energy electromagnetic radiation (gamma photons) also excites the nuclei: the two terminal ranges of the electromagnetic spectrum have an impact on the same part—namely, the nucleus of the atoms.

In each row of [Table 10.2](#), the emitted particles are the same; only their energy is different. The photons or particles within the same energy range are detected with the same methods, independent of the irradiation. As an example, the emission of X-ray photons of X-ray fluorescence analysis (XRF), electron microprobe, and ion (including proton)-induced XRF is mentioned. As will be discussed later in this chapter ([Section 10.2.3.1](#)), the X-ray photons (shown in row 4 of [Table 10.2](#)) are emitted as a consequence of the electron emission from the K or L electron orbital of the samples to be analyzed (the photoelectric effect, discussed in Section 5.4.4). High-energy gamma photons (shown in row 4 of [Table 10.2](#)) are emitted when irradiation with neutrons or charged particles induces nuclear reactions (such as NAA, PGAA (see [Sections 10.2.2.1](#) and [10.2.2.2](#)), and charged particle activation analysis (CPAA; [Section 10.2.5.2](#))).

As seen in row 5 of [Table 10.2](#), electrons can be emitted after irradiation of the matter with photons, electrons, or ions. When Auger electron emission (see Sections 5.3 and 5.4.4) results from electron emission from the K or L electron orbital of the samples to be analyzed, they are detected and measured by the same techniques,

Table 10.2 Analytical Methods Using the Interaction of the Radiation with Matter

| Induced Process | Irradiation | | | |
|----------------------------|---|--------------------------|--|--|
| | Photon | Electron | Neutron | Ion |
| Transmission or absorption | Spectroscopic method, depending on the wavelength: NMR, ESR, IR, NIR, visible, UV, Mössbauer spectroscopy | | Neutron absorption | |
| Scattering | Dynamic light scattering XRD | EELS LEED RHEED | Neutron scattering SANS Inelastic neutron scattering | RIBS ISS |
| Photon emission | XANES or NEXAFS EXAFS XRF | EMP | NAA PGAA | IMXA IEX PIXE CPINRA CPAA INS |
| Electron emission | AES XPS (ESCA) UPS | AES SAM SEM TEM | | |
| Ion emission | LAMMA | EIID | Nuclear reactions (e.g., (n,p), (n, α)) | SIMS IMMA CPINRA |

α , alpha particle; AES, Auger electron spectroscopy; CPINRA, charged particle-induced nuclear reaction analysis; CPAA, charged particle activation analysis; EIID, electron-induced ion desorption; EELS, electron-energy-loss spectroscopy; EMP, electron microprobe; ESCA, electron spectroscopy for chemical analysis; ESR, electron spin resonance; EXAFS, extended X-ray absorption fine structure; IEX, ion-excited X-ray fluorescence spectroscopy; IMMA, ion microprobe mass analyzer; IMXA, ion microprobe X-ray analysis; INS, ion neutralization spectroscopy; IR, infrared spectroscopy; ISS, ion scattering spectrometry; LEED, low-energy electron diffraction; LAMMA, laser microprobe mass analysis; n, neutron; NAA, neutron activation analysis; NEXAFS, near-edge X-ray absorption fine structure; NIR, near-infrared spectroscopy; NMR, nuclear magnetic resonance; p, proton; PGAA, prompt gamma activation analysis; PIXE, particle-induced X-ray emission; RHEED, reflection high-energy electron diffraction; RIBS, Rutherford backscattering spectroscopy; SAM, scanning Auger microanalysis; SANS, small-angle neutron scattering; SEM, scanning electron microscopy; SIMS, secondary ion mass spectroscopy; UPS, ultraviolet photoelectron spectroscopy; UV, ultraviolet spectroscopy; XPS, X-ray photoelectron spectroscopy; XRD, X-ray diffraction analysis; XRF, X-ray fluorescence analysis; XANES, X-ray absorption near-edge structure.

Source: Adapted from Nagy and Kónya, with permission from Taylor & Francis.

independent of the irradiation method. On the basis of the emitted radiation, gamma, X-ray, electron, and charge particle spectroscopic methods are classified.

In classical radioanalysis, those methods are used when the emitted radiation originates from the nucleus or the internal electron orbitals. Accordingly, classical analytical methods are the activation analytical methods, especially NAA and XRF. In fact, XRF does not require nuclear processes: the irradiating X-ray photons can be produced by an X-ray tube using the electron transition between the internal electron orbitals of the cathode of the X-ray tubes. Furthermore, the emitted X-ray

photons also originate from electron transition between electron orbitals. As discussed previously in this chapter, the emission of the same particles with similar energy requires similar detection and measuring techniques, independent of the irradiation method. For this reason, the methods providing X-ray photons and electrons (e.g., electron microprobe, AES, and X-ray photoelectron spectroscopy (XPS)) are also considered to be nuclear analytical methods. At the same time, the photoelectric effect may or may not be accompanied by a nuclear process. Thus, the term “radioanalysis” is used in a very broad sense: all methods may be considered to be radioanalysis in which emitted particles and photons are analyzed.

To summarize, nuclear analysis refers to all types of detection and measurement techniques of the emitted radiation. As mentioned several times previously, radiation can be emitted both from the nucleus and from the orbital electrons. The radiation that originates from the nucleus can be the consequence of nuclear reactions or excitation of the nucleus. The radiation that originates from the electron orbitals relates to the excitation and de-excitation of the electrons or ionization. Common characteristics of these methods are that they are selective, sensitive, and frequently indestructible.

The methods listed in [Table 10.2](#) differ in the depth of the introduction of the radiation, the interacting part of the substance, and the number of the interactions of the radiation with matter; and these characteristics determine which properties of the substance can be investigated using a particular method. The depth of the introduction of the radiation determines how thick the studied layer is, i.e., whether the properties of bulk phases, the interface, or the species adsorbed on the surfaces may be studied. The mass, charge, and energy of the radiation influences the thickness of the studied layer. The layer of absorption of the radiation is usually deeper in the case of light and neutral radiations. The energy of the radiation, however, strongly modifies this general tendency. For example, high-energy X-rays or electrons are introduced deeply, so the properties of the bulk can be studied. At small X-ray or electron energies, the structure of the surface layer can be studied.

In [Table 10.3](#), the thickness of the studied layer, the primary information, the typical sensitivity, and the detectable elements and species of the methods included in [Table 10.2](#) are summarized.

10.2.2 Analytical Methods Using Irradiations with Neutrons

As discussed in Section 5.5.3, the interactions of a neutron with matter are defined by its neutrality, the magnetic momentum, and the de Broglie wavelength (about 10^{-10} m). The most characteristic interactions are the nuclear reactions and the scattering phenomena. The analytical methods involving neutrons utilize the following characteristics of neutrons:

- Having no charge, neutrons can be captured easily by the different atomic nuclei. Except for helium, all atoms can capture neutrons, a fact that makes them ideal for analytical purposes.
- Neutrons interact with the nuclei, and light and heavy elements can be analyzed at the same time.

Table 10.3 Some Characteristic Properties of Analytical Methods

| Irradiation | Method | Thickness of the Studied Layer | Typical Sensitivity | Primary Information | Detectable Elements and Species |
|--------------------|--|---------------------------------------|--|--|---|
| Photon | NMR | Bulk | — | Chemical state of bulk and adsorbed molecules | Magnetically active nuclei (with $\frac{1}{2}$ spin isotopes, ~ 80) |
| | ESR | Bulk | — | Electron structure | Paramagnetic species |
| | IR, NIR | 0.5–2.5 μm | 0.1–0.5% | Bonding geometry and strength of bulk and adsorbed molecules | Functional groups |
| | Visible, UV spectroscopy | 0.1 μm | 0.001–1000 ppm | Elementary and molecular analysis | Li–U |
| | UPS, XPS (ESCA) | 3 nm | 0.1% | Species, surface elemental composition, valency, chemical bond | Li–U |
| | LAMMA | — | 0.5% inorganic; 0.1–10 ppm organic | Microelement and molecular analysis | Na–U |
| | AES | 1 nm | 0.1% | Elemental composition, adsorbate analysis | Li–U |
| | EXAFS, XANES, NEXAFS | 50 nm | 500 ppm | Oxidation state, species, coordination number, some structure | Li–U |
| | XRF | 10^4 nm | 1–10 ppm | Chemical composition of bulk and near surface region | Na–U |
| | XRD | 10^4 nm | — | Structure of bulk and surface, mineral composition | |
| Mössbauer | Bulk | 1–1000 ppm | Site locations, structure, bonding, chemical environment | Isotopes with Mössbauer transitions | |
| Electron | Electron diffraction, including LEED and RHEED | 1 nm | — | Identification of microcrystalline phases | Li–U |

(Continued)

Table 10.3 (Continued)

| Irradiation | Method | Thickness of the Studied Layer | Typical Sensitivity | Primary Information | Detectable Elements and Species |
|--------------------|--------------------|---------------------------------------|----------------------------|--|--|
| | AES | 1 nm | 0.1% | Elemental composition, adsorbate analysis | Li–U |
| | SAM | 1 nm | 0.1% | Elemental composition, adsorbate analysis | Li–U |
| | EMP | 10 ³ nm | 0.1% | Chemical composition of bulk and near surface region | Na–U |
| | EELS | 100 nm | <0.1% | Elemental composition, species like IR, bonds, structure | Li–U |
| | SEM | 5 nm | | Surface and bulk morphology | |
| | TEM | | | Surface and bulk morphology | |
| Ion | ISS | 1–100 μm | 100 ppm | Elemental composition, location of adsorbed species | Li–U |
| | SIMS | 3–10 nm | 0.1–10 ppm | Elemental, isotopic, and molecular composition | H–U |
| | IMMA | 3–10 nm | 0.1–10 ppm | Elemental, isotopic, and molecular composition | H–U |
| | CPINRA | 10 ⁴ nm | 0.1–10 ppm | Elementary composition | |
| | IEX, PIXE | 10 ⁴ nm | 0.1–10 ppm | Elemental composition, location of adsorbed species | Na–U |
| | IMXA | 10 ⁴ nm | 0.1–10 ppm | Elementary composition | |
| | RIBS | 10 ³ nm | 0.01–1% | Elemental composition, location of adsorbed species | Li–U |
| Neutron | NAA | Bulk | 0.001–0.1 ppm | Elemental analysis of bulk | Li–U |
| | PGAA | Bulk | 0.001–0.1 ppm | Elemental analysis of bulk | H–U |
| | Neutron scattering | Bulk | | Structure and morphology | |
| | SANS | Bulk | | Structure and morphology | |
| | Nuclear reactions | Bulk | 0.001–0.1 ppm | Elemental analysis of bulk | Li–U |

Source: Adapted from Nagy and Kónya, with permission from Taylor & Francis.

- Neutrons have magnetic moments. The scattering methods based on the interaction of the neutrons with the nuclei and the magnetic field of matter provide information on both the nuclei and the magnetic field.
- The information obtained is on a molecular scale because of the very short de Broglie wavelength of neutrons.
- The energy of the neutrons can vary widely and can be compared to the energy of atomic and molecular motions.
- The range of neutrons is fairly large; thus, microscopic properties of bulk phases can be studied, even in industrial sizes.
- Neutrons are indestructible: biological, archeological, criminal, and other kinds of samples can be analyzed without destruction.

The application of neutrons in the natural sciences was discussed in Section 5.5.3. The different types of NAA and neutron scattering will be discussed next.

10.2.2.1 Neutron Activation Analysis

NAA, discovered by G. Hevesy and H. Levi in 1936, is an activation analytical method (see Section 10.2.1).

In NAA, the sample is irradiated with neutrons, initiating nuclear reactions. Having no charge, neutrons can be captured easily by the different atomic nuclei. All elements, except for helium, have isotope(s) reacting with neutrons (as detailed in Section 6.2.1) in an (n,γ) nuclear reaction. As a result of the nuclear reaction, radioactive isotopes are produced. This process is called “activation.” These isotopes have one more neutron than the inactive target, so they will typically decompose by emitting negative beta particles. Because of the continuous spectra, beta particles are measured with difficulty, especially when the sample contains many components. The beta decay, however, is frequently followed by the emission of gamma photons with discrete energies. The energy of these gamma photons is characteristic of the target elements and suitable for qualitative analysis. The activity/intensity of gamma photons provides quantitative analytical information. The gamma photons are the result of radioactive decay, and they are present after the irradiation.

Besides neutrons, the samples can be activated by charged particles too. Table 10.2 describes this method as CPAA. The basic concepts (the detection of the emitted photons) are similar to NAA.

As discussed in Section 5.5.2, neutrons are produced in neutron sources, generators, nuclear reactors, or spallation neutron sources. Since there are only a few spallation neutron sources all over the world, the irradiation is generally achieved in nuclear reactors (or sometimes neutron generators).

The way of neutron production determines the flux (neutron sources < neutron generators < nuclear reactors) and energy of the neutrons. In neutron generators, fast neutrons with 14 MeV energy are formed, which induce (n,γ) , (n,p) , (n,α) , $(n,2n)$ nuclear reactions. As seen in Figure 6.4, the general tendency is that the cross section of nuclear reactions with neutrons is inversely proportional to the

neutron energy. For this reason, thermal neutrons produced in nuclear reactors are the most important in the (n,γ) nuclear reactions of NAA. In addition, the flux of the neutrons is highest in the nuclear reactors. As a result, neutron activation studies are usually performed in the research nuclear reactors.

The high range of gamma radiation provides the possibility of nondestructive NAA. In this method, the samples are analyzed directly by an instrumental technique called instrumental neutron activation analysis (INAA). Of course, the instrumental measurements can be supplemented by radiochemical separation, if required. This method is called radiochemical neutron activation analysis (RNAA).

During activation, the inactive nuclei transform to radioactive ones via nuclear reactions. This means that the specific activity of the sample increases, usually from zero to a certain value. The sensitivity of the method is determined by the number of the radioactive nuclei formed. The number of the radioactive nuclei is determined by the kinetic law of activation, as discussed in Section 6.1. Equation (6.11) gives the number of radioactive nuclei formed from any stable nuclide at a certain nuclear reaction characterized by cross section, flux of the irradiating particles, irradiation, and cooling time. If all these factors are known, and the activity can be measured with high accuracy, absolute measurements can also be done.

These absolute measurements, however, are usually limited by the lack of accurate knowledge of the cross sections, the flux at the position of the sample, and activity after irradiation and cooling. In practice, mostly relative measurements are made; the samples are compared to a standard with known concentration of the elements expected in the sample. The standard is simultaneously irradiated with the sample under the same conditions (flux, time, and irradiation position). The gamma radiation of the sample and the standard are measured under the same conditions as well. Standard samples may be homemade or purchased: commercial multielement Standard Reference Materials (SRMs) are available.

The advantages of NAA are that small sample sizes (1–200 mg) are suitable for the simultaneous analysis of many elements with low detection limits. The detection limits of the elements are shown in [Table 10.4](#). The accuracy of NAA is about 5%, and the relative precision may be better than 0.1%. INAA does not destroy the samples; thus, it can be useful when the sample has to remain intact (archeological, artistic, criminal, and other samples).

Because of the very small size of the sample, the sampling and preparation of the sample is critical. The sample must characterize the average composition of the object to be analyzed. Any contamination must be avoided.

The method's major limitation is that, although almost all elements have isotopes that can participate in nuclear reactions with neutrons, the produced radioactive isotopes of some light elements have very short half-lives, so they cannot be analyzed in neutron activation. Similarly, some elements have small neutron capture cross sections, which cause difficulties in the analysis, and there are other analytical methods, which often provide better sensitivities.

The nuclear reactions of the different nuclides can interfere with each other, for example, because the nuclear reactions produce the same radioactive nuclide. The

Table 10.4 Detection Limits of INAA. Irradiation Flux of Thermal Neutrons:
 1×10^{13} neutron $\text{cm}^{-2} \text{s}^{-1}$

| Atomic Number | Element Symbol | $\mu\text{g/g}$ | Atomic Number | Element Symbol | $\mu\text{g/g}$ | Not Analyzed by NAA | |
|---------------|----------------|--------------------|---------------|----------------|--------------------|---------------------|----------------|
| | | | | | | Atomic Number | Element Symbol |
| 63 | Eu | 2×10^{-6} | 72 | Hf | 1×10^{-3} | 1 | H |
| 66 | Dy | 2×10^{-6} | 76 | Os | 1×10^{-3} | 2 | He |
| 49 | In | 5×10^{-6} | 17 | Cl | 2×10^{-3} | 3 | Li |
| 71 | Lu | 2×10^{-5} | 28 | Ni | 2×10^{-3} | 4 | Be |
| 77 | Ir | 2×10^{-5} | 37 | Rb | 2×10^{-3} | 5 | Be |
| 67 | Ho | 2×10^{-5} | 55 | Cs | 2×10^{-3} | 6 | C |
| 75 | Re | 2×10^{-5} | 30 | Zn | 2×10^{-3} | 7 | N |
| 25 | Mn | 3×10^{-5} | 32 | Ge | 2×10^{-3} | 8 | O |
| 13 | Al | 5×10^{-5} | 34 | Se | 2×10^{-3} | 9 | F |
| 23 | V | 5×10^{-5} | 48 | Cd | 2×10^{-3} | 10 | Ne |
| 21 | Sc | 1×10^{-4} | 56 | Ba | 3×10^{-3} | 18 | Ar |
| 33 | As | 1×10^{-4} | 19 | K | 4×10^{-3} | 22 | Ti |
| 53 | I | 1×10^{-4} | 42 | Mo | 5×10^{-3} | 36 | Kr |
| 57 | La | 1×10^{-4} | 44 | Ru | 5×10^{-3} | 43 | Tc |
| 59 | Pr | 1×10^{-4} | 52 | Te | 5×10^{-3} | 45 | Rh |
| 69 | Tm | 1×10^{-4} | 58 | Ce | 5×10^{-3} | 54 | Xe |
| 70 | Yb | 1×10^{-4} | 60 | Nd | 5×10^{-3} | 61 | Pm |
| 35 | Br | 2×10^{-4} | 78 | Pt | 5×10^{-3} | 84 | Po |
| 74 | W | 2×10^{-4} | 47 | Ag | 6×10^{-3} | 85 | At |
| 79 | Au | 2×10^{-4} | 80 | Hg | 7×10^{-3} | 86 | Rn |
| 51 | Sb | 2×10^{-4} | 24 | Cr | 1×10^{-2} | 87 | Fr |
| 65 | Tb | 2×10^{-4} | 50 | Sn | 1×10^{-2} | 88 | Ra |
| 46 | Pd | 3×10^{-4} | 82 | Pb | 1×10^{-2} | 89 | Ac |
| 62 | Sm | 3×10^{-4} | 40 | Zr | 2×10^{-2} | 90 | Th |
| 11 | Na | 4×10^{-4} | 83 | Bi | 2×10^{-2} | 91 | Pa |
| 29 | Cu | 4×10^{-4} | 12 | Mg | 3×10^{-2} | | |
| 31 | Ga | 4×10^{-4} | 38 | Sr | 3×10^{-2} | | |
| 73 | Ta | 4×10^{-4} | 81 | Tl | 3×10^{-2} | | |
| 39 | Y | 5×10^{-4} | 14 | Si | 5×10^{-2} | | |
| 92 | U | 5×10^{-4} | 20 | Ca | 1×10^{-1} | | |
| 15 | P | 1×10^{-3} | 16 | S | 2×10^{-1} | | |
| 27 | Co | 1×10^{-3} | 26 | Fe | 5×10^{-1} | | |
| 64 | Gd | 1×10^{-3} | 41 | Nb | 5×10^{-1} | | |
| 68 | Er | 1×10^{-3} | | | | | |

activation of bronze or brass results in the following nuclear reactions: $^{64}\text{Zn}(n,\gamma)^{65}\text{Zn}$, $^{64}\text{Zn}(n,p)^{64}\text{Cu}$, and $^{63}\text{Cu}(n,\gamma)^{64}\text{Cu}$. As seen, ^{64}Cu is produced from both zinc and copper. These interferences, namely, all possible nuclear reactions in the sample, always must be taken into consideration.

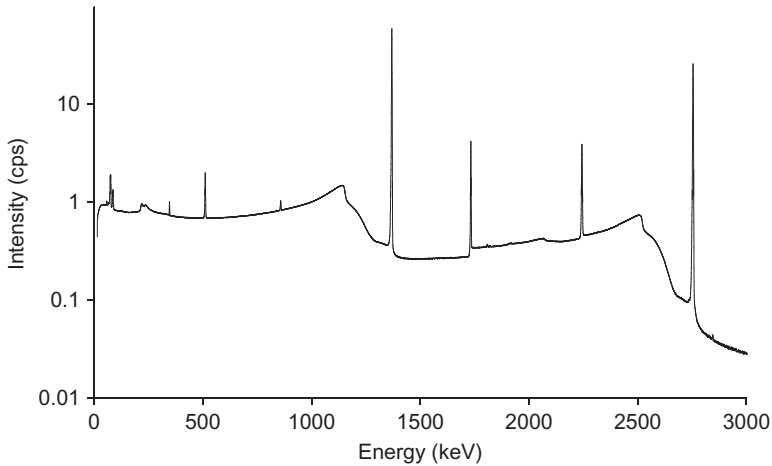
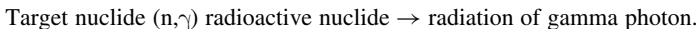


Figure 10.7 A neutron activation spectrum of sodium showing the gamma lines characteristic of ^{24}Na . The spectrum was taken by an HPGe (see Section 14.3) with 25% relative efficiency. (Thanks to Dr. Zsolt Révay, Department of Nuclear Research, Institute of Isotopes, Budapest, Hungary, for the spectrum.)

The neutron activation spectrum of sodium is shown in [Figure 10.7](#). As a result of the irradiation, a $^{23}\text{Na}(n,\gamma)^{24}\text{Na}$ nuclear reaction takes place, and the spectrum shows gamma lines characteristic of ^{24}Na .

10.2.2.2 Prompt Gamma Activation Analysis

As mentioned previously, during the activation by neutrons, a (n,γ) reaction takes place. This reaction produces radionuclides that can also emit gamma photons. This means that two gamma photons are formed as expressed by the following scheme:



NAA (see [Section 10.2.2.1](#)) provides analytical information using the gamma photons irradiated by the radioactive nuclide. The gamma photons formed in the nuclear reaction itself are called “prompt gamma photons” because they are formed within 10^{-14} s after neutron capture. PGAA detects these gamma photons and provides analytical information independent of whether the product nuclide is stable or radioactive. Similar to NAA, the energy of gamma photons gives qualitative information, while the activity or intensity provides quantitative information. The kinetics of activation is also the same.

The prompt gamma photons can be detected only during irradiation, i.e., the excited nucleus formed by neutron capture, called a “compound nucleus” (see [Section 6.1](#)) emits gamma photons. The excitation energy is in the range of

the binding energy of neutrons (7–8 MeV). The de-excitation (i.e., the emission of gamma photons) can happen in one step or in several steps, emitting one gamma photon with high energy or a cascade of gamma photons with low energies. For this reason, the prompt gamma spectra are rather complicated.

PGAA has the same advantageous properties as NAA. In addition, PGAA can detect all elements because prompt gamma photons as emitted photons are produced in every (n, γ) reaction. (In NAA, only radioactive product nuclides with suitable half-lives can be measured after irradiation.) Thus, PGAA is especially important in the analysis of light elements (such as H, B, and N; see Table 10.4). Because of its high sensitivity, it is a very useful method to use in the analysis of elements in tracer quantities (Cd, Hg, etc.). The disadvantage of this method, however, is that the gamma photons have to be measured directly in the neutron beam. This results in high background radiation. In addition, to detect the prompt gamma photons, the neutron beam has to exit the nuclear reactor, which significantly decreases the neutron flux. Since gamma photons can be produced as cascades of photons with low energy, the gamma spectra are usually very complicated and require special evaluation procedures. At the same time, PGAA is an expensive method, which restricts its widespread application.

As seen in Figure 6.4, the cross section of the nuclear reaction with neutrons is inversely proportional to the neutron energy. Thus, by decreasing the energy of the neutrons (i.e., using cold neutrons (see Section 5.5.3)), the cross section can increase by as much as two orders of magnitude. This increases the number of nuclear reactions, improving the sensitivity of PGAA. The application of the cold neutrons in PGAA is the most important supplement to the traditional NAA. When irradiating with cold neutrons, the background intensity is significantly smaller, providing a possibility for *in vivo* applications.

The detection limit of this method is in the range of 10^{-5} – 10^{-9} g, depending on the cross section of the (n, γ) reaction of the isotopes of the elements. It is applied in the analysis of the following:

- Light elements (H, B) for which NAA cannot be used.
- Main (Si, Al, H, C), trace- (Cu, Cd, Hg, Pb) and indicator (B, Rb, Sm, Gd) elements in geological formations.
- Toxic elements (Cd, Hg)—macro- (H, C, O, Ca) and microelements (Cu, Zn, Fe) in biological, medical samples.

In Figure 10.8, a prompt gamma activation spectrum of a standard cement sample taken using a high-purity germanium detector (HPGE) with Compton suppression is shown.

10.2.2.3 Neutron Radiography and Tomography

Neutron radiography and tomography are imaging procedures that are based on the different absorption properties of the substances. An object is irradiated by a neutron beam; the intensity of the neutrons is measured on the other side of the object

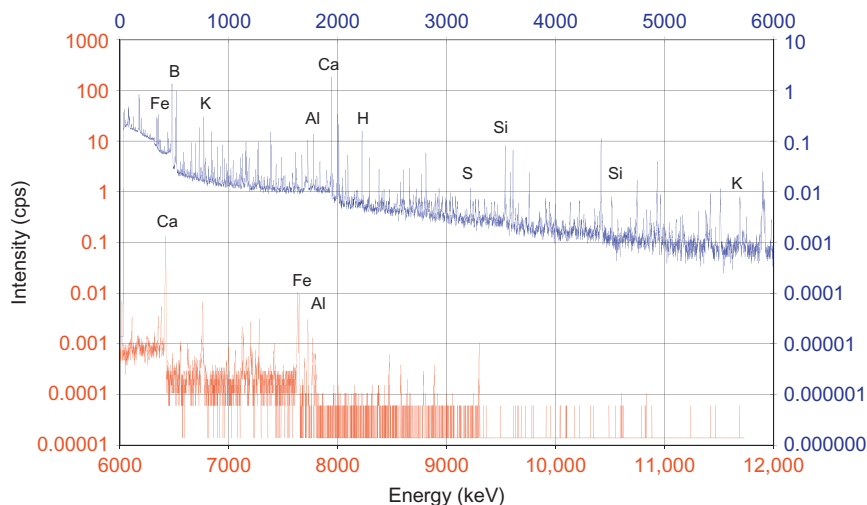


Figure 10.8 A prompt gamma activation spectrum of a standard cement sample using an HPGE detector with Compton suppression. (Thanks to Dr. Zsolt Révay, Department of Nuclear Research, Institute of Isotopes, Budapest, Hungary, for the spectrum.)

(Figure 10.9). The neutrons are detected using a LiF + ZnS detector (as discussed in Section 14.5.5). The measuring time is between a few seconds to even a day, depending on the resolution and the neutron flux. When the neutron beam is parallel, the size of the object and the image is the same; the resolution is 100–300 μm . If the beam is divergent, a magnified image is obtained; the resolution is about 10 μm .

Neutron radiography and tomography can be combined with PGAA (see Section 10.2.2.2). In this way, the chemical composition of the objects can also be analyzed (Figure 10.10).

10.2.2.4 Neutron Scattering/Diffraction

Scattering methods are based on the interaction of neutrons with nuclei to study the microscopic structure, kinetic processes, and magnetic field (see Section 5.5.3). Most applications, which are interesting for chemists, were made in the first two fields and commenced in the 1970s, when the first high-flux research reactors were built.

The diffraction is quantitatively described by the well-known Bragg formula (Figure 10.11):

$$\Delta s = (n)\lambda = 2d \sin \Theta \quad (10.14)$$

where d is distance in a chemical system determined by the structure, λ is the wavelength, Θ is the angle of incidence at which the intensity maximum occur,

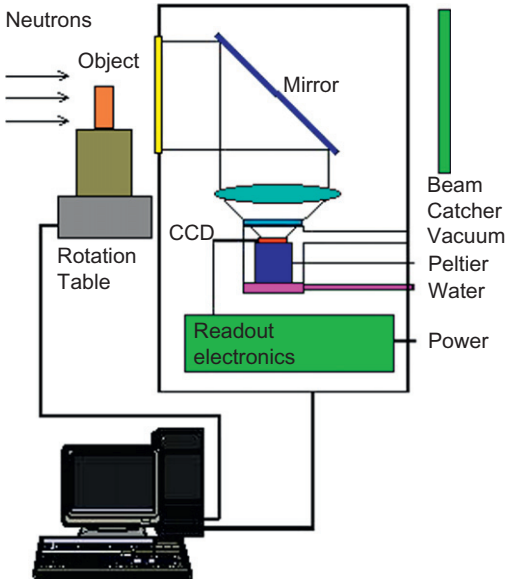


Figure 10.9 A scheme of neutron radiographic/tomographic system. (Thanks to Dr. Zsolt Révay, Department of Nuclear Research, Institute of Isotopes, Budapest, Hungary, for the spectrum.)

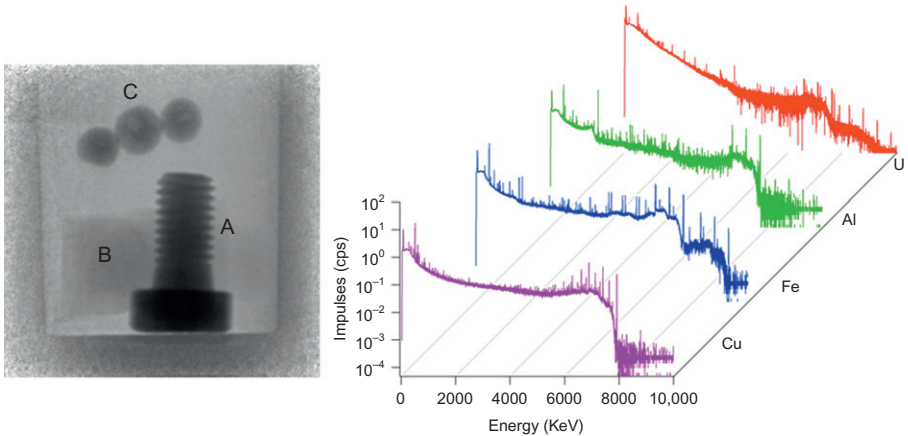


Figure 10.10 Left: A neutron radiogram of objects within a lead container (wall thickness: 7 mm). A: M6 iron bolt; B: U_3O_8 powder, C: three copper balls. Right: Prompt gamma spectra of the object in the lead container. There is an aluminum rod in the container which cannot be seen well on the radiogram, but its spectrum is well-seen. (Thanks to Dr. László Szentmiklósi and Dr. Zsolt Révay, Department of Nuclear Research, Institute of Isotopes, Budapest, Hungary, for the radiogram and the spectrum.)

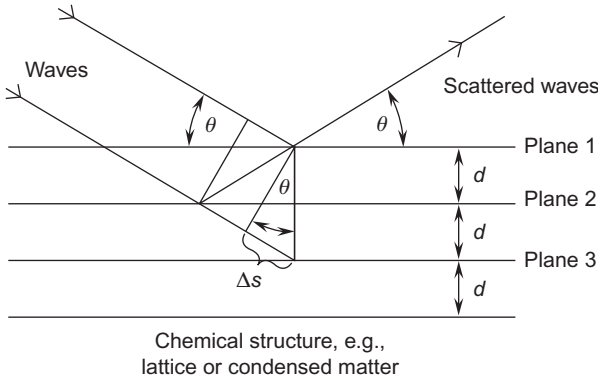


Figure 10.11 Diffraction of a wavelength on chemical substances.

and n is a small integer (at the first interference, n is 1), Δs is the difference of the path of the interfering waves.

On the basis of the Bragg formula (Eq. (10.14)), when we know the wavelength and the intensities at different angles, it is possible to calculate the distance characteristic of the different chemical structures. This is true for any electromagnetic or particle radiation; e.g., X-ray diffraction and electron diffraction are used for structural analysis.

In structural research, the application of the probe particle (neutron, electron, or photon) is provided by its (energy-dependent) wavelength: it should be comparable to the characteristic size of the microstructure to be investigated. The neutron velocities produced in a nuclear reactor follow the Maxwell distribution determined by the temperature of the nuclear reactor zone, passing the neutrons through a cooled moderator; thereafter a velocity selector (between rotating slits), $\sim 5 \times 10^{-11} - 10^{-9}$ m wavelength, usually can be obtained, which is calculated using Eq. (4.93). Assuming a thermal neutron with 0.01 eV energy:

$$\lambda = \frac{h}{mv} = \frac{6.6256 \times 10^{-34} \text{ J/s}}{1.67 \times 10^{-27} \text{ kg} \times v} \quad (10.15)$$

and about 10^{-10} m is given for the de Broglie wavelength.

The incident neutron is represented by a transversal plane wave:

$$\psi(\vec{k}) = \psi_0 \exp(i \vec{k} \cdot \vec{r}) \quad (10.16)$$

where ψ_0 is a constant amplitude, $\vec{k} = 2\pi \vec{n} / \lambda$, and \vec{n} is the unit vector in the direction of propagation. The upper arrows mean vectors. The moving front of the wave interacts with nucleus j at point \vec{r}_j of the sample with probability defined by the scattering cross section (σ_j) and may generate around the nucleus a spherical wave $b_j \exp[-i \vec{k} \cdot \vec{r}] / r$ with amplitude b_j specific of the nucleus. The wavelengths

Table 10.5 Scattering Length Density (Q) of Several Isotopes/Elements

| Isotope/Element | Q (10^{-14} m) |
|-----------------|---------------------|
| H | -0.3742 |
| D | 0.6671 |
| C | 0.6651 |
| N | 0.940 |
| O | 0.5804 |
| P | 0.517 |
| S | 0.2847 |

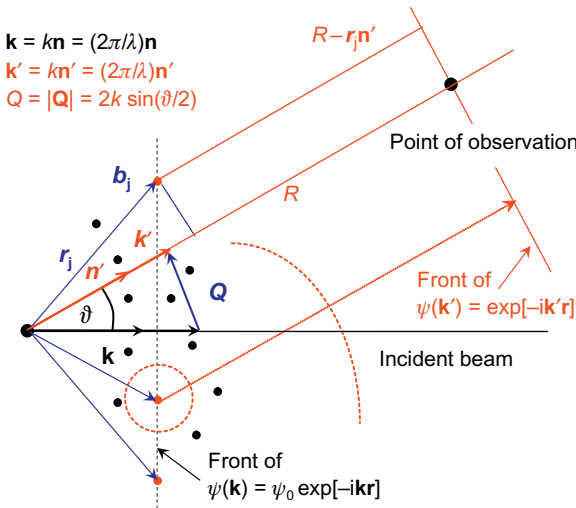


Figure 10.12 Principles of neutron diffraction (bold letters designate vectors).

of the incident and scattered waves are equal; thus, the scattering process is elastic. Because of its length dimension, b_j is called “scattering length” and

$$\sigma_j = 4\pi b_j^2 \tag{10.17}$$

At the applied neutron energies, the phase of the scattered waves is $\approx bk$ for the individual nuclei.

The scattering length of some isotopes/elements is listed in [Table 10.5](#).

Far from the j th nucleus, the front of the spherical waves can be expressed by plane waves ([Figure 10.12](#)):

$$\psi_j(\vec{k}') = b_j \exp(-i \vec{k}'[\vec{R} - \vec{r}_j]) \tag{10.18}$$

The scattered wave from a system of N nuclei (in vacuum) is equal to:

$$\psi(\vec{k}') = \exp(-i \vec{k}' \cdot \vec{R}) \sum_j b_j \exp(i \vec{k}' \cdot \vec{r}_j) \quad (10.19)$$

and the scattering intensity is the thermodynamic average of the squared scattered waves:

$$\begin{aligned} \langle \psi^*(\vec{k}') \psi(\vec{k}') \rangle &= \left\langle \exp(-i \vec{k}' \cdot \vec{R}) \exp(-i \vec{k}' \cdot \vec{R}) \sum_j b_j \exp(i \vec{k}' \cdot \vec{r}_j) \sum_k b_k \exp(i \vec{k}' \cdot \vec{r}_k) \right\rangle \\ &= \left\langle \sum_j \sum_k b_j b_k \exp(-i \vec{k}' \cdot [\vec{r}_j - \vec{r}_k]) \right\rangle \end{aligned} \quad (10.20)$$

where the complex conjugate is denoted by $*$ and the summation is made for $j, k = 1, \dots, N$.

Considering that $\vec{k}' = \vec{k} + \vec{Q}$, the intensity will be divided into two terms:

$$\begin{aligned} I(\vec{k}') &= I(\vec{k}) + I(\vec{Q}) = \left\langle \sum_j \sum_k b_j b_k \exp(-i \vec{k}' \cdot [\vec{r}_j - \vec{r}_k]) \right\rangle \\ &\quad + \left\langle \sum_j \sum_k b_j b_k \exp(-i \vec{Q} \cdot [\vec{r}_j - \vec{r}_k]) \right\rangle \end{aligned} \quad (10.21)$$

where $I(\vec{k})$ is a contribution to the direct beam, and the $I(\vec{Q})$ is the actual scattered intensity, where \vec{Q} is the scattering vector (Figure 10.12). The magnitude of the scattering vector is:

$$Q = \frac{4\pi}{\lambda} \sin \frac{\vartheta}{2} \quad (10.22)$$

where ϑ is the scattering angle (Figure 10.12).

Considering that the b s are independent of one another and the coordinates, we obtain:

$$I(Q) = N \langle b^2 \rangle + \langle b \rangle^2 \left\langle \sum_{j \neq k} \exp(-i \vec{Q} \cdot [\vec{r}_j - \vec{r}_k]) \right\rangle \quad (10.23)$$

For a condensed phase in thermal equilibrium:

$$\begin{aligned} &\left\langle \sum_{j \neq k} \exp(-i \vec{Q} \cdot [\vec{r}_j - \vec{r}_k]) \right\rangle \\ &= \frac{1}{V^N} \int_V \dots \int_V \sum_{j \neq k} \exp(-i \vec{Q} \cdot [\vec{r}_j - \vec{r}_k]) \Phi_N(\vec{r}_1 \dots \vec{r}_N) d\vec{r}_1 \dots d\vec{r}_N \end{aligned} \quad (10.24)$$

where $(1/N^N) \Phi_N$ is the N -particle spatial correlation function.

Because the scattered intensity depends on the difference of two-particle coordinates, in isotropic systems, the averaging is reduced to the Fourier transform of the pair-correlation function:

$$\frac{N(N-1)}{V} \int_V g(r) \exp(-i \vec{Q} \cdot \vec{r}) d\vec{r} = S(Q) - 1 \quad (10.25)$$

From here,

$$I(Q) = N\{\langle b^2 \rangle - \langle b \rangle^2 + \langle b \rangle^2 S(Q)\} \quad (10.26)$$

In this equation, $S(Q)$ is called the “structure factor”; it provides information on the interference caused by the spatial distribution of the scattering nuclei. $\langle b^2 \rangle - \langle b \rangle^2$ is the incoherent part of the scattered intensity, and $\langle b \rangle^2 S(Q)$ is the coherent part of the scattered intensity and is determined by the nuclear spin.

The practical applications of this result are promoted by introducing the concept of scattering length density (ρ), defined as b/v , where b is the sum of scattering lengths in a sufficiently small volume (v). For example, the volume of a water molecule (v_w) is:

$$v_w = V_w/N_A \quad (10.27)$$

where V_w and N_A are the molar volume of water and Avogadro’s number, respectively. The scattering length of a water molecule is calculated from the scattering length of the atoms:

$$b = 2b_H + b_O \quad (10.28)$$

The scattering length density of water is:

$$\rho_w = b_w/v_w \quad (10.29)$$

A dissolved molecule with a certain scattering length (b_s) and volume (v_s) in aqueous solution is seen by the neutrons only if the excess scattering length

$$\Delta b_s = b_s - v_s \rho_w \quad (10.30)$$

or the scattering contrast

$$\Delta b_s/v_s = \Delta \rho_s = \rho_s - \rho_w \quad (10.31)$$

is not equal to zero.

It can be shown that the scattered intensity from mesoscopic inhomogeneities caused by molecular systems (association colloids, macromolecules, polymers, and biological structures) in the solution is described by the same expression as before,

if the bs are replaced by the Fourier transform of the spatial distribution of the scattering contrast:

$$B(Q) = \int_V \Delta\rho_s(\vec{r}) \exp(-i\vec{Q}\cdot\vec{r}) d\vec{r} \quad (10.32)$$

By dividing $I(Q)$ by the sample volume (V), we obtain the macroscopic scattering cross section ($d\Sigma/d\Omega$, given in cm^{-1} units):

$$d\Sigma/d\Omega = \frac{N}{V} \{ \langle B \times (Q) B(Q) \rangle - \langle B \times (Q) \rangle \langle B(Q) \rangle + \langle B \times (Q) \rangle \langle B(Q) \rangle S(Q) \} \quad (10.33)$$

On the basis of the neutrons discussed here, neutron scattering is applied for the structural studies in condensed phases. Since the neutrons are scattered by the nuclei, substances containing light elements are also studied. As seen in Table 10.5, the scattering length can be different for the isotopes of the same elements. This is especially important for the isotopes of hydrogen, ^1H and ^2H . The great difference in the scattering lengths of hydrogen and deuterium provides the possibility of studying hydrogen compounds, such as biological or other organic molecules, in which the exchangeable hydrogen atoms can be investigated.

During the application of neutron scattering, the intensity of the scattered neutrons (in other words, the macroscopic scattering cross section ($d\Sigma/d\Omega$)) is plotted as a function of the scattering vector (Q). Models elaborated for $B(Q)$ and $S(Q)$ are fitted to the experimental scattering patterns, and the reliability of the fitting parameters is judged by the quality of the fit. In Figure 10.13, the neutron-scattering patterns from micellar solutions of sodium alkyl sulfates are plotted, together with the best-fit curves and the squared deviations of the experiment and theory. The systematic study with different alkyl chain length results in reliable structural data and in a direct proof of the electrostatic potential acting among the ionic micelles.

One of the most important technical features of neutron scattering is contrast variation. By varying the hydrogen isotope composition (hydrogen/deuterium ratio) of water (Table 10.5), ρ_w can have a varied range, which is wide enough to cover the scattering contrast of most components of organic molecules. Therefore, certain parts of the molecules can be excluded from the observed scattering patterns (Figure 10.14). The method is unique and is used mainly in biological systems.

In condensed phases, many important kinetic processes are random and occur over a relatively long time scale. Rotational jumps of a molecule and the diffusion of a particle in liquid are two examples of the types of motion that contribute to the quasi-elastic component of the inelastic spectrum, where the sum of the changes in the energy of the neutrons scattered in a particular direction (ΔE) equals zero.

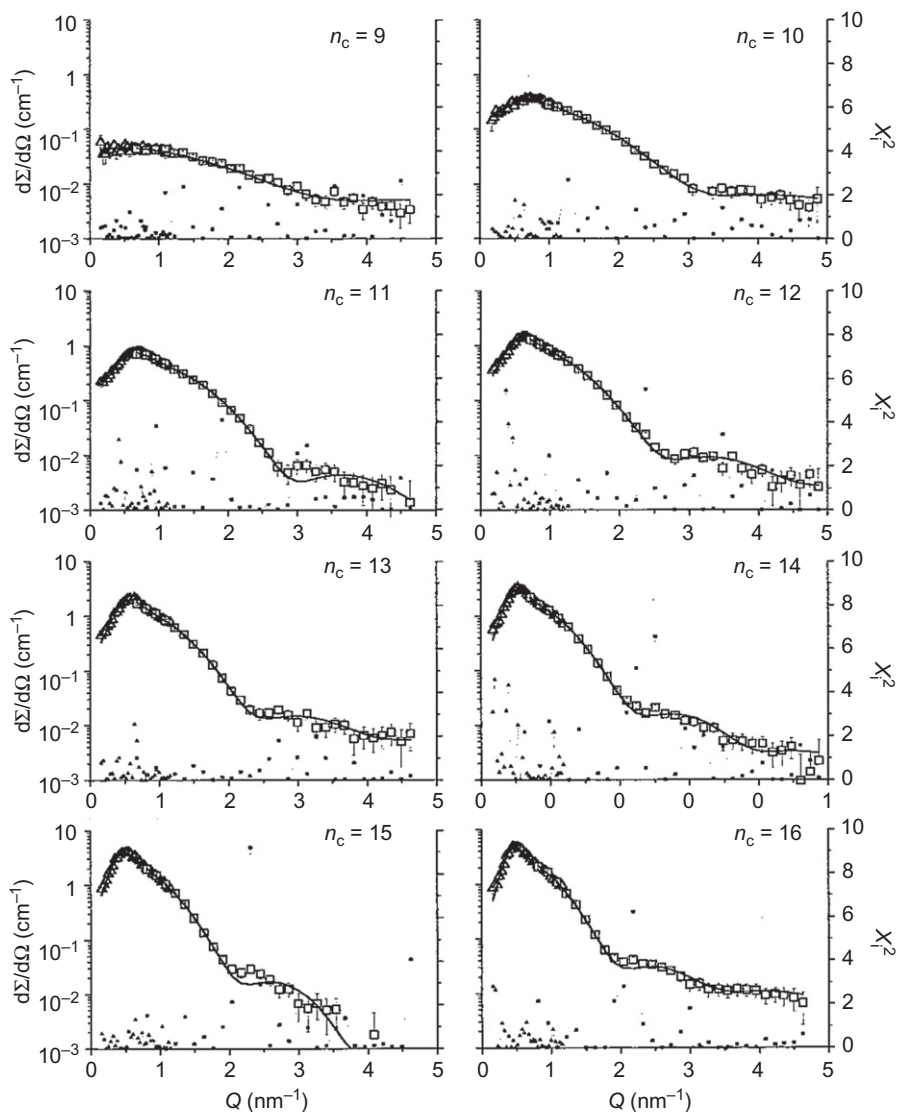


Figure 10.13 SANS patterns from 0.0729 mol/dm^3 solutions of sodium alkyl sulfates of different chain lengths (open symbols) with best-fit curves (solid lines). Residual squares are plotted with solid symbols connected with dotted lines.

Source: Adapted from Vass et al. (2000), with permission from American Chemical Society.

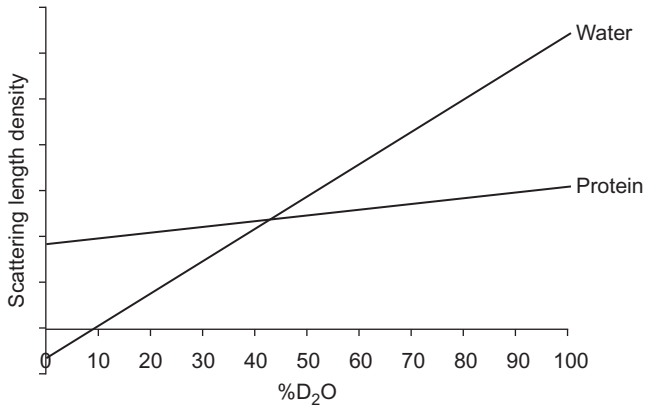


Figure 10.14 Scattering length density of water and proteins at different H:D ratios obtained by small-angle neutron scattering.

The intensity $I(Q, \Delta E)$ scattered in the angle defined by Q , stemming from diffusing molecules in a liquid, is described as follows:

$$I(Q, \Delta E) = A \frac{\frac{h}{2\pi} D Q^2}{\pi [(\Delta E)^2] + \left(\frac{h}{2\pi} D Q^2\right)^2} \quad (10.34)$$

where A is the amplitude defined by the scattering amplitude b and apparatus constants, h is the Planck constant, ΔE is the energy change of the neutron (inelastic component), and D is the self-diffusion coefficient of the molecule. Quasi-elastic neutron scattering provides a precise tool for determining the self-diffusion coefficient in the bulk phase of liquids. Figure 10.15 shows the decomposition of a quasi-elastic neutron-scattering spectrum of a micellar solution. The solvent molecules were found in two kinetic states: along with the major ($\sim 94\%$) component moving with the bulk-phase self-diffusion coefficient, a slower water component ($\sim 6\%$) could also be observed. The slow component was assumed to form the hydrate sphere of the micelles.

10.2.3 Irradiation with X-Ray and Gamma Photons

As discussed in Section 5.4, electromagnetic radiation with high energy (X-ray and gamma radiation) interacts with the orbital electron, the nuclear field, and the nuclei. The interactions with the orbital electrons and the nuclei are used for analytical purposes.

During interactions with the orbital electrons, the intensity of X-ray or gamma radiation decreases due to the photoelectric effect and elastic and inelastic

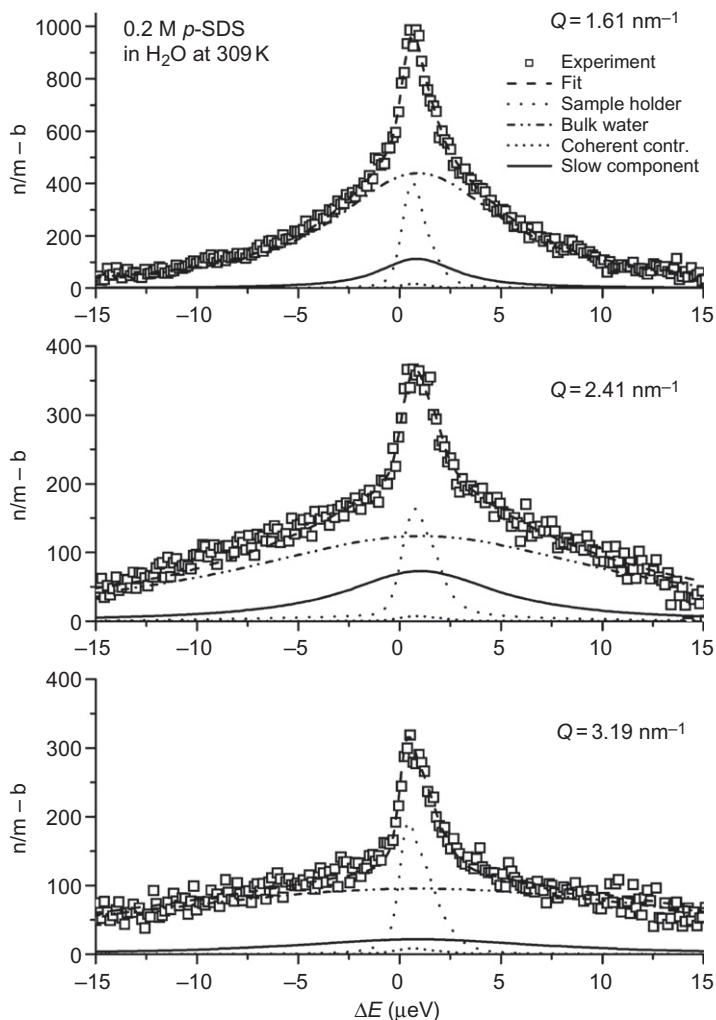


Figure 10.15 Background-corrected backscattering intensities from a 0.2 M H₂O solution of sodium dodecyl sulfate at 309 K in detector positions at Q 1.61, 2.42, and 3.19 nm⁻¹. *Source:* Reprinted from Vass et al. (2005), with permission from American Chemical Society.

scattering (see Figure 5.25) as determined by the general formula of radiation absorption (see Eqs. (5.3) and (5.93)).

As discussed in Section 5.4.4, the photoelectric effect produces electrons, including photoelectrons and Auger electrons, and characteristic X-ray photons. The ratio of the Auger electron emission to the characteristic X-ray photon emission depends on the atomic number. For light elements, Auger electron emission

has a high probability, while for heavier elements, X-ray photons are produced (see Figure 4.12).

The measurements of the energy and intensity of electron and X-ray radiation are used in different analytical techniques. The measurement of the photoelectrons gives analytical information on the chemical environment of the atoms in a substance [high-resolution beta spectroscopy and XPS]. AES (see Figure 5.24) can be used for the analysis of surface layers (Table 10.2). The characteristic X-ray photons provide information on the quality and quantity of the elements of a substance (X-ray fluorescence spectroscopy, as discussed in Section 10.2.3.1).

The elastic scattering process or X-ray diffraction (discussed in Section 10.2.3.2) is used to determine chemical structures.

The excitation of the nuclei is applied for species analysis of the compounds of the elements with isotopes that have recoil-less nuclear resonance absorption (Mössbauer spectroscopy, described in Section 10.2.2.3).

10.2.3.1 X-Ray Fluorescence Analysis

During XRF, an electron is ejected from the K or L electron orbital of the elements to be analyzed. The vacancy is filled with an electron from an outer orbital. The energy difference between the two orbitals is emitted as a characteristic X-ray photon. The energy of the X-ray photons relates to the elements, thus providing qualitative analysis. The intensity of the X-ray photons provides quantitative analytical information.

The X-ray photons can be produced by the excitation with charged particles (electron microprobe, discussed in Section 10.2.4.2, and proton-induced X-ray emission, discussed in Section 10.2.5.1) or by electromagnetic radiation. Electromagnetic radiation is produced in an X-ray tube, or it may be the gamma radiation emitted by a radioactive isotope. In an X-ray tube, the photocathode emits X-ray radiation. During isotopic excitation, ^{55}Fe (5.9 keV), ^{109}Cd (22–25 keV), ^{125}I (27–31 keV), and ^{241}Am (60 keV gamma energy) are used as exciting sources.

The initial process of excitation with electromagnetic radiation is the photoelectric effect. The excitation takes place if the energy of the exciting particle exceeds the binding energy of the electron. The exciting photons transfer their energy to the orbital electron. The energy equal to the binding energy ejects the electron, and the residual part of the energy becomes the kinetic energy of the ejected electron:

$$E_k = h\nu_0 - E_b \quad (10.35)$$

where E_k is the kinetic energy of the emitted electron, E_b is the binding energy of the electron, and $h\nu_0$ is the energy of the exciting photon before the photoelectric effect. This process occurs if the energy of the exciting photon is close to the binding energy of the electron. This means that the electrons are ejected from the K and L orbitals.

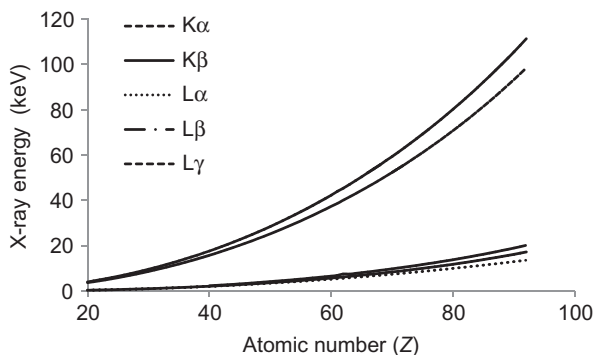


Figure 10.16 The energy of characteristic X-ray photons emitted by the different elements versus atomic numbers.

As discussed previously, the excited state can be relaxed by the emission of characteristic X-ray photons. The wave number of the X-ray photons is expressed by Moseley's law (Eq. (5.88)). The wave number (i.e., the energy of the characteristic X-ray photons) increases along with the increase of the atomic number, providing information for qualitative analysis. As seen in Figure 4.12, the light elements practically do not emit characteristic X-ray photons, XRF is useful for the elements $Z > 20$. For the elements $10 < Z < 19$, the X-ray photons are absorbed in air and thus can only be measured in a vacuum.

In Figure 10.16, the energy of characteristic X-ray photons emitted by the different elements is shown as a function of the atomic number. K and L mean the orbitals where the vacancies are formed under the excitation, and α , β , and γ mean the outer orbitals from which the vacancy is filled. For instance, K_{α} means that a vacancy on the K orbital is filled with an electron from the next orbital, L.

The sensitivity of X-ray fluorescence spectrometry is influenced by two factors, both of which relate to excitation: the energy of the exciting photons should be higher than the binding energy but not by too much. The excitation is optimal if the energies exciting and the emitted photons are close, but not identical, so they can be separated spectroscopically in the given measuring system. For this reason, the excitation source and the element to be analyzed should be correlated. Practically, the "light" ($Z > 20$) elements are excited by low energy, and the K lines are measured. The heavy elements are analyzed using the L lines.

The X-ray fluorescence spectrum of a mixture of Fe_2O_3 , ZnO , KBr , $\text{Sr}(\text{NO}_3)_2$, MoO_3 , AgNO_3 , CsNO_3 , and Nd_2O_3 is shown in Figure 10.17. The exciting source was the gamma radiation of the ^{241}Am isotope, and the detector is SiLi semiconductor detector (as discussed in Section 14.3). The concentrations of the elements in the mixture are Fe: 0.012523 mol/g; Zn: 0.01229 mol/g; K and Br: 0.008403 mol/g; Sr: 0.004725 mol/g; Mo: 0.006947 mol/g; Ag: 0.005887 mol/g; Cs: 0.005131 mol/g; and Nd: 0.005944 mol/g. Since the exciting energy is about 60 keV, the K lines of all elements are detected. As seen, the light elements (nitrogen and oxygen) do not have lines in the spectrum.

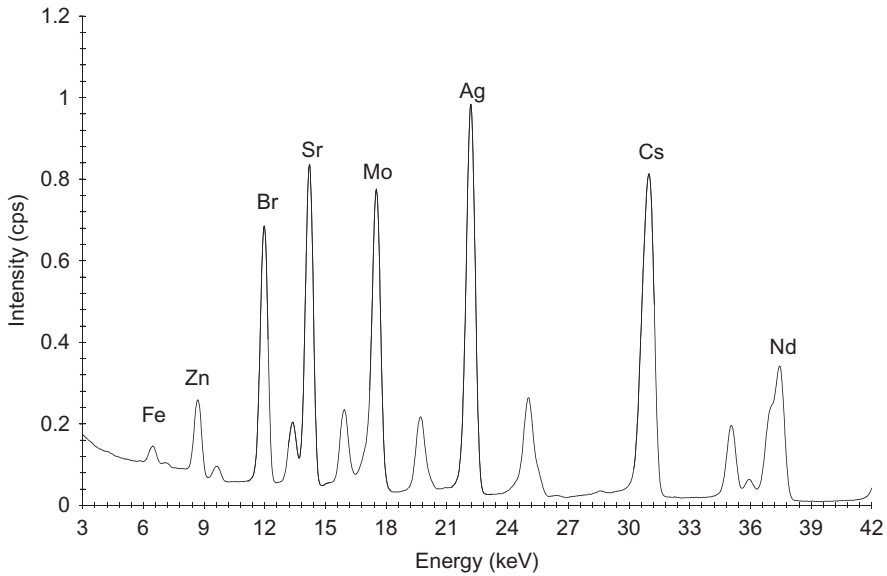


Figure 10.17 An X-ray fluorescence spectrum of a mixture of Fe_2O_3 , ZnO , KBr , $\text{Sr}(\text{NO}_3)_2$, MoO_3 , AgNO_3 , CsNO_3 , and Nd_2O_3 . The exciting source is the gamma radiation of the ^{241}Am isotope, and the detector is a SiLi semiconductor detector. (Thanks to Zoltán Nemes, Isotope Laboratory, Department of Colloid and Environmental Chemistry, University of Debrecen, Hungary, for the spectrum.)

As in most spectroscopic methods, the intensity of the emitted X-ray photons provides quantitative analytical information. This intensity is expressed by the following formula:

$$I_i = S_i C_i \frac{1 - e^{-d \left(\frac{\mu_{S,E_0}}{\sin \Psi_{1\text{eff}}} + \frac{\mu_{S,i}}{\sin \Psi_{2\text{eff}}} \right)}}{\frac{\mu_{S,E_0}}{\sin \Psi_{1\text{eff}}} + \frac{\mu_{S,i}}{\sin \Psi_{2\text{eff}}}} \quad (10.36)$$

where S_i is the sensitivity for the i th element expressed in the mass unit of the pure element; C_i is the concentration of the i th element; d is the surface density of the sample (g/cm^2); μ_{S,E_0} and $\mu_{S,i}$ are the mass absorption coefficient of the sample for the exciting radiation and the characteristic X-ray photons of the i th element (cm^2/g), respectively; and $\Psi_{1\text{eff}}$ and $\Psi_{2\text{eff}}$ are the angles of irradiation and detection related to the surface of the sample.

Equation (10.36) shows that the intensity versus concentration function should be linear. In most cases, the intensity of the characteristic X-ray and the concentration are not in linear relation because the sample contains other elements (such as a

matrix) which are also excited. This effect is called the “matrix effect.” The matrix effect can influence the intensity–concentration relation in two ways:

1. The intensity is smaller than expected from linear intensity–concentration plot. This is the case if the mass absorption coefficient of the matrix is greater than the mass absorption coefficient of the element to be analyzed. The mean atomic number (Eq. (5.74)) of the matrix exceeds the atomic number of the element.
2. The intensity is higher than expected from the linear intensity–concentration plot. This is the case if the mass absorption coefficient of the matrix is smaller than the mass absorption coefficient of the element to be analyzed. The mean atomic number (Eq. (5.74)) of the matrix is less than the atomic number of the element.

Besides the matrix effect, the intensity–concentration plot is influenced by the so-called internal excitation effect. This means that the studied element is excited not only by the exciting radiation but also by the characteristic X-ray photons of elements with higher atomic numbers. As a result, the intensity increases.

In conclusion, we can say that the matrix effect is significant in XRF. This effect is corrected in different experimental and theoretical ways, as summarized in Table 10.6.

In Figure 10.18, the calibration curves for the X-ray fluorescence spectrum of iron is shown when the mean atomic number of the matrix is smaller (boric acid matrix) or larger (barium nitrate matrix), respectively, than the atomic number of the element in question (iron).

The X-ray fluorescence method is used for the direct analysis of samples without any chemical pretreatment, or after chemical preparations (e.g., separation and enrichment). As mentioned previously in this chapter, all elements from calcium to uranium can be analyzed, or, using a vacuum, even the elements that are heavier than sodium can be measured. The concentration range is from about 1 ppm to 100%.

The arrangement of an XRF is shown in Figure 10.19. The excitation source is a gamma emitter radioactive isotope. The characteristic X-ray photons induced in the sample are detected by a SiLi semiconductor detector (as described in Section 14.3).

Table 10.6 Ways to Correct the Matrix Effect in X-Ray Fluorescence Analysis

| | | | | |
|----------------------|----------------------|------------------------------|--------------------|-------------------------------|
| Experimental methods | Compensation methods | External standard method | | |
| | | Internal standard method | | |
| | | Standard addition | | |
| | | Dilution method | | |
| | | Double dilution method | | |
| | | Thin-layer method | | |
| | | Scattering method | | |
| | | Emission–transmission method | | |
| | | Mathematical methods | Absorption methods | Elementary sensitivity method |
| | | | | Method of basic parameters |
| Numerical methods | | | | |
| Monte Carlo method | | | | |

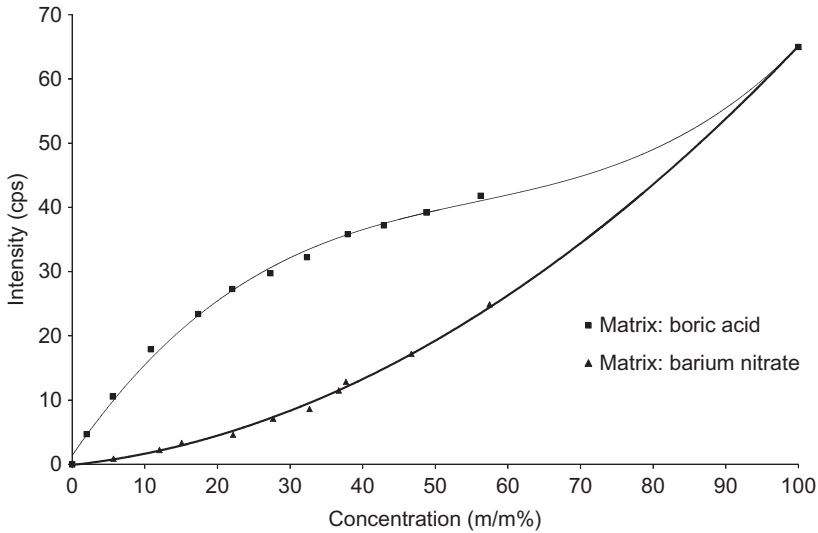


Figure 10.18 Calibration curves for an X-ray fluorescence spectrum of iron in matrices in which the mean atomic number of the matrix is smaller (boric acid matrix) or greater (barium nitrate matrix), respectively, than the atomic number of iron. The exciting source is the gamma radiation of the ^{125}I isotope, and the detector is a SiLi semiconductor detector. (Thanks to Zoltán Nemes, Isotope Laboratory, Department of Colloid and Environmental Chemistry, University of Debrecen, Hungary, for the figure.)

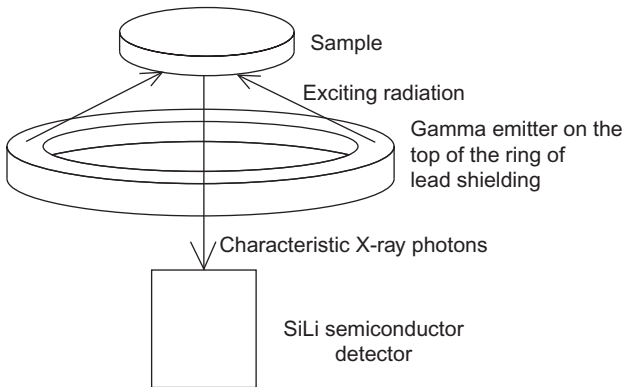


Figure 10.19 Arrangement of an XRF.

10.2.3.2 X-Ray Diffraction

In Section 10.2.2.4, the principle of the diffraction of waves was discussed in detail. It is not repeated here; only the main differences of the X-ray and neutron diffraction studies are summarized in Table 10.7.

Table 10.7 Differences Between the Characteristic Features of X-Ray and Neutron Diffraction

| | X-Ray Diffraction | Neutron Diffraction |
|----------------------------|---|--|
| Interacting part of matter | Electron orbitals | Nuclei and magnetic field |
| Depth of introduction | 10^4 nm | Bulk |
| Cross section | Increases as the atomic number increases: the light elements can be analyzed only with difficulty or not at all | Independent of the atomic number: the light elements are seen well |
| Analytical possibilities | Structure of bulk and surface, mineral composition | Structure and morphology, magnetic interactions |

The X-ray diffraction is applied to the structural analysis of crystalline substances. Correct structural analysis can be obtained on monocrystals from small inorganic compounds to complex macromolecules. The study of polycrystals and crystalline powders is frequently used to study the qualitative and semiquantitative analysis of crystalline substances when diffractograms of the unknown samples can be compared to those of standards. A very important application is the study of the mineral composition of rocks. An example is shown in [Figure 10.20](#).

10.2.3.3 Mössbauer Spectroscopy

The principle of the recoil-less nuclear resonance absorption, or Mössbauer spectroscopy, was discussed in detail in Section 5.4.7. Here, the emphasis is on its chemical applications: Mössbauer spectroscopy allows the analysis of chemical compounds that contain elements which have a Mössbauer nuclide. From a practical point of view, the most important is iron, the Mössbauer nuclide of which is ^{57}Fe . Its abundance in natural iron is about 2.2%. The gamma radiation source is ^{57}Co , and its gamma radiation of 0.0144 MeV can excite the nucleus of the ^{57}Fe isotope. The chemical state (valency) and the chemical environment modify the energy of the nuclear levels, which can be measured, thus allowing the study of the chemical species.

10.2.4 Irradiation with Electron and Beta Radiation

As mentioned in Section 4.4.2, electrons are emitted from the nuclei as a result of radioactive decay and from the electron orbitals. The electrons emitted from nuclei are called “beta particles.” Electrons emitted from the extranuclear shell are called electrons and are designated by e^- . The two terms “beta particle” and “electron” differentiate the location of the emission. The main important difference is that

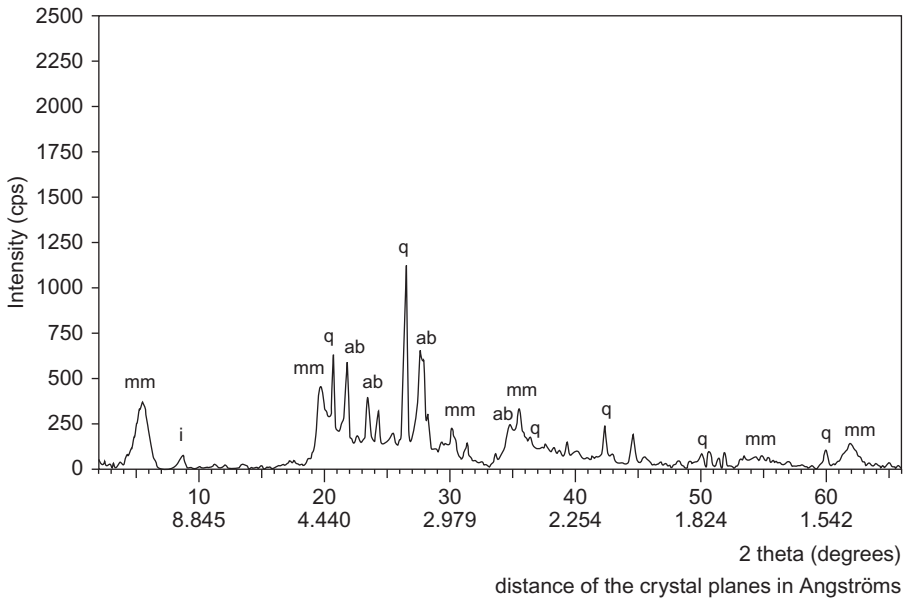


Figure 10.20 An X-ray diffractogram of bentonite clay. mm = montmorillonite (47%), ab = albite (13%), q = quartz (15%), i = illite (10%), other minerals 15% (chlorite, kalifeldspar, crystalalbite, amorphous). (Thanks to Dr. Péter Kovács-Pálffy, Geological Institute of Hungary, Budapest, for the diffractogram.)

beta particles have continuous spectra, while the electrons originating from the orbitals have discrete energy. Independent of their origin, the electrons and beta particles interact with the electrons and nuclear field of other atoms. The characteristic interactions are ionization, scattering (elastic and inelastic), and absorption.

The analytical applications of beta particles were described in Sections 5.3.4 and 5.3.6. Furthermore, the industrial applications using the scattering/reflection and absorption of beta radiation will be discussed in Section 11.3. In this section, the application of electron beams with discrete energy will be illustrated. The discrete energy means that these electrons are ejected from the electron orbitals. The energy of these electrons can be increased in accelerators.

The most important application of the electron radiation is the electron microscope. There are two types of electron microscope: transmission electron microscope (TEM) and scanning electron microscope (SEM). The image taken by each type of microscope originates from the electrons that were elastic scattered. Besides, electrons can transfer energy to the orbital electrons of the matter (inelastic scattering) and eject electrons from the K and L shells. The processes following electron ejection are the same as in the case of the photoelectric effect: Auger electrons can be emitted, or the vacancy can be filled with an electron from the outer shell. As a result, similar to XRF, characteristic X-ray photons are formed, which

can be used for qualitative and quantitative analysis. This process is used in electron microprobes.

10.2.4.1 Transmission Electron Microscopy

In TEM, the sample is bombarded by an electron beam. The resolution is determined by the wavelength of the electron and the numerical aperture of the electron optical lens. Similar to the wavelength of neutrons, the wavelength of the electrons is calculated by Eq. (4.93). The energy of the electrons in TEM microscopes is typically 100–300 keV. At 100 keV electron energy, and taking into consideration the mass of the electron, the wavelength of the electron is about 4×10^{-12} m. The resolution (d) is quantitatively expressed as follows:

$$d = \frac{\lambda}{2n \sin \alpha} = \frac{\lambda}{2NA} \quad (10.37)$$

where λ is the wavelength of the electron, n is the refractive index of the medium of the lens, α is the half-angle of the maximum cone of radiation that can enter or exit the lens, and NA is the numerical aperture. This means that theoretically the maximum resolution of the electron microscope is about 2 pm. Practically, the best resolution is in the order of tenths of a nanometer.

Since the electron is a charged particle with a relatively short range, the sample must be thin to transmit the electrons. Therefore, the method requires special preparation of the samples. The thin samples are placed on gold sample holders, as illustrated in Figure 10.21.

As mentioned previously, the imaging is possible using the elastically scattered electrons. Inelastic electron scattering has a positive and a negative effect. Although it disturbs the imaging because the change of the wavelength changes the focal length (chromatic error), it allows chemical analysis via the emission of the characteristic photons (electron microprobe).

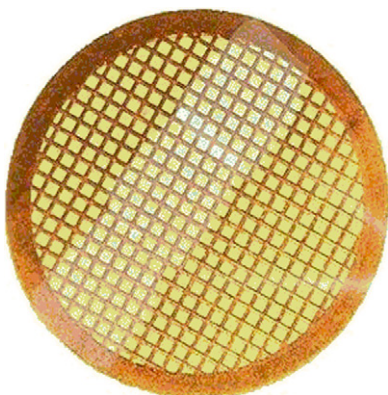


Figure 10.21 A gold sample holder for TEM. The diameter is about 3 mm.

The irradiating electrons are scattered on the electrons of the irradiated atoms. Thus, the light elements have a smaller degree of scattering than the heavier ones. For this reason, the compounds consisting of light elements, such as organic substances, are covered by contrast material with a high atomic number (e.g., osmium, lead, gold, silver, etc.). These metals are evaporated or adsorbed onto the surface of the sample.

10.2.4.2 SEM and Microprobe Analysis

SEMs image the sample to be analyzed using the electrons elastically scattering from the surface. Thus, the surface of thick layers can be studied. The surface of the sample has to be covered by a conductive layer, such as metal or graphite. The surface is scanned by an electron beam. The diameter of this electron beam ($<1 \mu\text{m}$) determines the horizontal resolution of the SEM.

A portion of the electrons scatters inelastically, ejecting electrons from the K or L electron orbitals. Similar to XRF, the following characteristic X-ray emission provides qualitative and quantitative analytical possibilities. These instruments are called “electron microprobes.”

In electron microprobes, the characteristic X-ray photons are detected in two ways: in an energy-dispersive or a wavelength-dispersive manner. Similar to X-ray fluorescence spectrometers, energy-dispersive systems are equipped with semiconductor detectors, the resolution of which is about 130 eV. In wavelength-dispersive systems, the detector is a single crystal at a precise angle. The structure, including the characteristic spacing between the planes of the crystal lattice, is known. The wavelength of the X-ray photons is measured using the Bragg formula (Eq. (10.14)). The resolution of the wavelength-dispersive detectors is about (10 eV). All elements, except hydrogen, helium, and lithium, can be measured.

Electron microprobes have 0.01% relative and 10^{-14} g absolute detection limits with 3% relative accuracy.

In [Figure 10.22](#), the SEM picture of montmorillonite clay treated with lead ions is shown. The left picture shows the image (morphology) obtained by the elastically scattered electrons. The right picture is the lead map obtained by the energy-dispersive spectrum of the characteristic X-ray photons.

In [Figure 10.23](#), the wavelength-dispersive X-ray spectrum obtained at a certain area of a clay sample treated by manganese ions is shown.

The scanning of a sample surface provides the possibility of analyzing the elementary composition along a straight line. The concentration profiles of different elements of montmorillonite clay treated with lead ions are shown in [Figure 10.24](#).

10.2.5 Irradiation with Charged Particles

The irradiation with charged particles always means irradiation with positively charged particles ranging from protons to heavier nuclei. The most important interactions of the positively charged particles are similar to the interactions of the alpha particles with matter (see [Table 5.2](#)). For analytical purposes, protons are

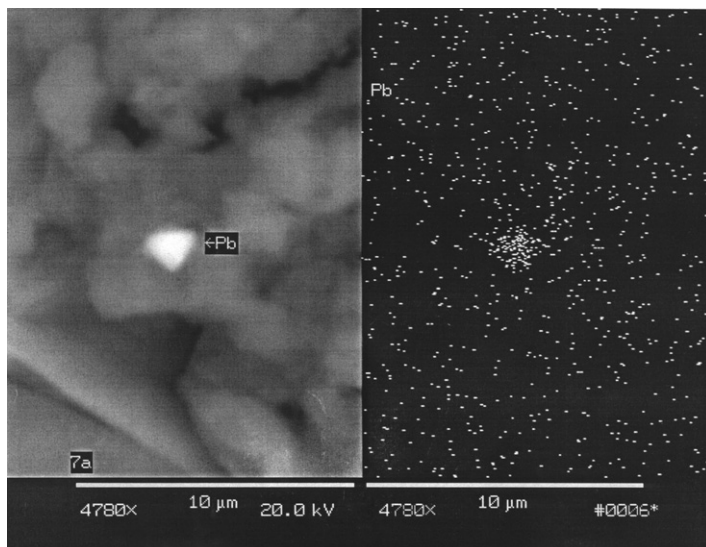


Figure 10.22 An SEM picture of montmorillonite clay treated with lead ions. Left: morphology of the sample based on electron scattering. Right: lead map made by characteristic X-ray photons.

Source: Reprinted from Nagy et al. (2003), with permission from Elsevier.

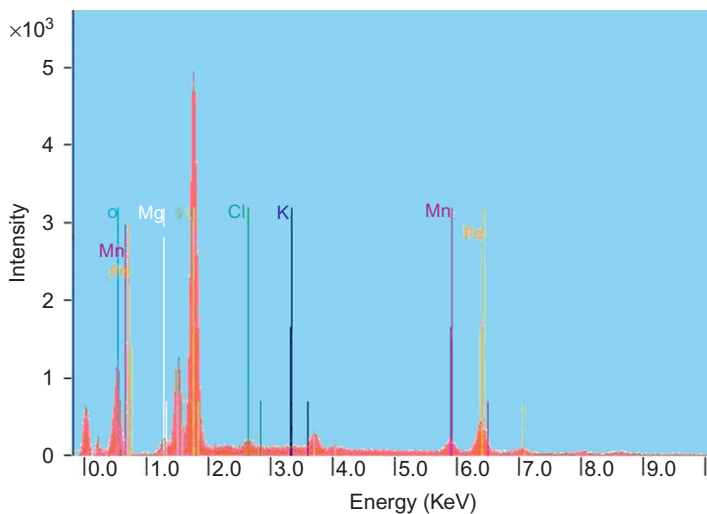


Figure 10.23 A wavelength-dispersive X-ray spectrum of a certain area of a clay sample treated by manganese ions. (Thanks to Dr. Katalin Papp, Chemical Research Center, Budapest, Hungary for the spectrum.)

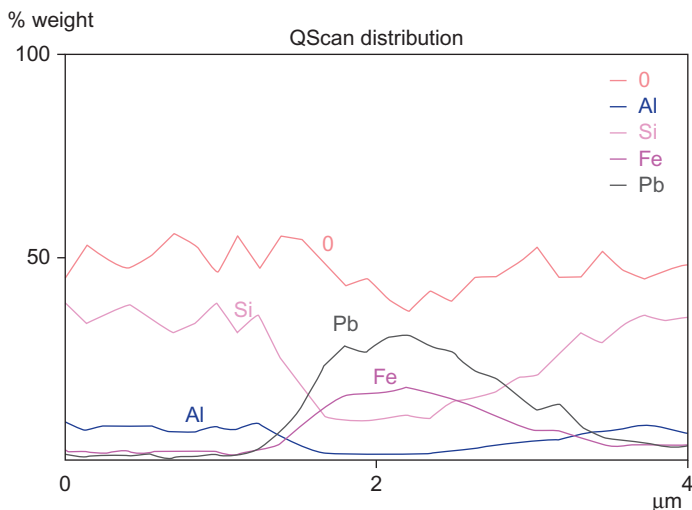


Figure 10.24 The concentration profiles of different elements of montmorillonite clay treated with lead ions.

Source: Reprinted from Nagy et al. (2003), with permission from Elsevier.

used most frequently. In some cases, alpha particles are also applied. For example, in Rutherford spectroscopy, an example of which was presented in Section 5.2.2, the scattering of alpha particles from the nuclear field is used to obtain information on the sample.

Besides the interaction with the nuclear field, the interaction with the orbital electrons and the nucleus can be used in the analysis. The positively charged particles, similar to X-ray and gamma photons, or electrons, can eject electrons from the K or L orbitals, providing qualitative and quantitative analytical tools. This analytical method is particle-induced X-ray emission (PIXE; see Section 10.2.5.1).

The nuclear reactions of charged particles can be used for analytical purposes in the same way as NAA. The method is called "CPAA" or "charged particle-induced nuclear reaction analysis (CPINRA)." In addition, the prompt gamma photons of the nuclear reactions with charge particles can be measured in particle-induced gamma emission (PIGE; see Section 10.2.5.2).

10.2.5.1 Particle-Induced X-Ray Emission

For PIXE, typically protons are produced in small energy accelerators. Quadrupole magnets focus the protons, and the sample to be analyzed is hit by this proton beam. The protons eject electrons from the K or L orbital of the atoms in the sample. From here, the processes are the same as in XRF: the characteristic X-ray photons emitted by the sample are detected by semiconductor detectors (e.g., SiLi).

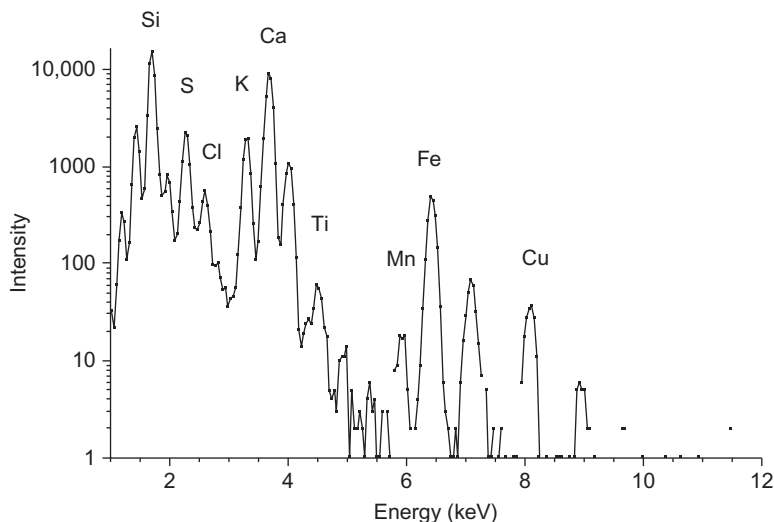


Figure 10.25 A PIXE spectrum of an aerosol using a traditional SiLi PIXE detector. (Thanks to Dr. Zsófia Kertész, Laboratory of Ion Beam Applications, Institute of Nuclear Research, Debrecen, Hungary, for the spectrum.)

Using traditional SiLi PIXE detectors, the concentration of the elements that have an atomic number greater than 13 can be measured. The sensitivity of the K and L lines is the highest in the range of atomic number $20 < Z < 35$ and $75 < Z < 85$, respectively. The most important trace elements of the biological and geological systems are mostly in just these ranges. This gives the significance of PIXE studies. There are special SiLi detectors with an ultrathin window, which are applied for the measurement of elements from carbon to iron. In [Figures 10.25 and 10.26](#), the spectrum of an aerosol is shown using two detectors: a traditional SiLi PIXE detector and a SiLi detector with an ultrathin window.

The method has 10^{-6} – 10^{-7} g/g relative, and 10^{-9} – 10^{-12} g absolute detection limits with 5–10% error. The sensitivity can be increased using a very thin proton beam (with a diameter measured in micrometers). The method is called micro-PIXE, and its absolute detection limit is 10^{-15} – 10^{-16} g. This very high sensitivity is the main advantage of PIXE compared to XRF.

The main field of PIXE applications is the study of atmospheric aerosols. Filtering through different pore-sized membranes, fractions of air with different particle sizes are collected. The quantity of each fraction is small; thus, the analysis requires very sensitive techniques. Using PIXE, the elementary composition of the different fractions is measured directly, positioning the membrane filter to the window in front of the proton beam ([Figure 10.27](#)). The sample remains unchanged after the PIXE analysis, so it can be subjected to another analytical technique (gravimetry, microscopy, particle distribution analysis, or other spectroscopic

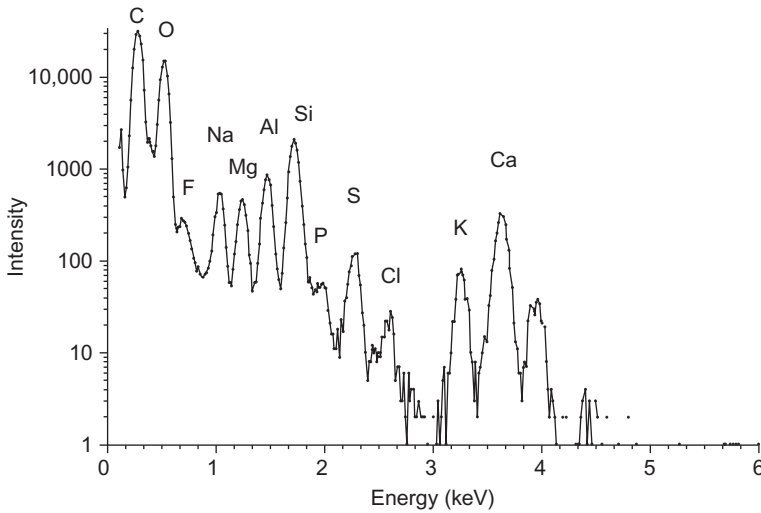


Figure 10.26 A PIXE spectrum of an aerosol using a SiLi detector with an ultrathin window. (Thanks to Dr. Zsófia Kertész, Laboratory of Ion Beam Applications, Institute of Nuclear Research, Debrecen, Hungary, for the spectrum.)

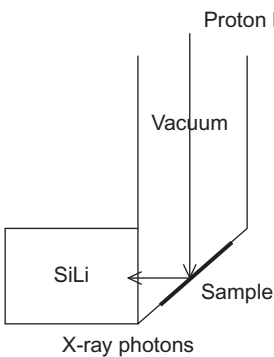


Figure 10.27 A sketch of an arrangement of a PIXE spectrometer.

techniques), which is essential since main light elements (H, C, N, O) composing aerosol particles (soil, humus, etc.) cannot be analyzed by PIXE. Therefore, PIXE and chemical analysis of the light elements (e.g., PGAA and electron microprobe) can be combined.

10.2.5.2 Particle-Induced Gamma Emission

Nuclear reactions with charged particles are induced by irradiation, e.g., by protons with high energy (in the range of MeV; see Sections 6.2.3 and 6.2.3.1). The (p,γ) reactions are relatively simple because the emitted particle is neutral. The prompt

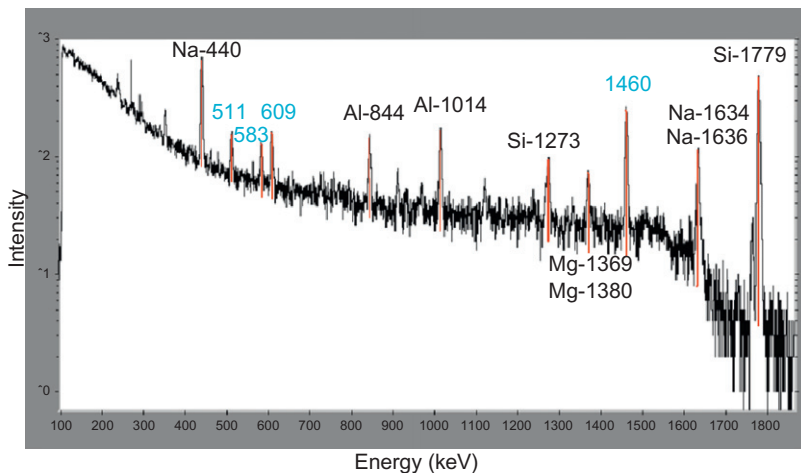


Figure 10.28 A PIGE spectrum of glass. (Thanks to Dr. Zsófia Kertész, Laboratory of Ion Beam Applications, Institute of Nuclear Research, Debrecen, Hungary, for the spectrum.)

gamma photons are detected. Since the Coulomb repulsion is smaller for light elements, the proton-induced gamma emission is especially suitable for the analysis of light elements (e.g., Li, Be, B, F, Na, and Al). The analysis of light elements is the main advantage of PIGE. A PIGE spectrum of glass is shown in [Figure 10.28](#).

Further Reading

- De Soete, D., Gijbels, R. and Hoste, J. (1972). *Neutron Activation Analysis*. Wiley, New York, NY.
- European Spallation Centre, 2011. EES Fields of Research. <<http://ess-scandinavia.eu/ess-fields-of-research>> (accessed 28.03.12.)
- Glascok, M.D., 1996–2011. Overview of Neutron Activation Analysis. <http://archaeometry.missouri.edu/naa_overview.html> (assessed 26.12.11.)
- Kertész, Zs., Szikszai, Z., Szoboszlai, Z., Simon, A., Huszánk, R. and Uzonyi, I. (2009). Study of individual atmospheric aerosol particles at the Debrecen ion microprobe. *Nucl. Instrum. Methods B* 267:2236–2240.
- Molnár, G.L. (ed.) (2004). *Handbook of Prompt Gamma Activation Analysis with Neutron Beams*. Kluwer Academic Publishers, Dordrecht/Boston, MA/London.
- Molnár, Zs., 2003–2009. Neutron Activation Analysis. <http://www.reak.bme.hu/Wigner-Course/WignerManuals/Budapest/NEUTRON_ACTIVATION_ANALYSIS.htm> (accessed 15.11.11.)
- Nagy, N.M. and Kónya, J. (2009). *Interfacial Chemistry of Rocks and Soils*. Taylor & Francis, Boca Raton, FL.
- Nagy, N.M., Kónya, J., Beszedá, M., Beszedá, I., Kálmán, E., Keresztes, Zs., et al. (2003). Physical and chemical formations of lead contaminants in clay and sediment. *J. Colloid Interface Sci.* 263:13–22.

- Révay, Zs. (2009). Determining elemental composition using prompt gamma activation analysis. *Anal. Chem.* 81:6851.
- Simon, A., Matiskainen, H., Uzonyi, I., Csedreki, L., Szikszai, Z., Kertész, Zs., et al. (2011). PIXE analysis of Middle European 18th and 19th century glass seals. *X-Ray Spectrom.* 40:224–228.
- Szentmiklósi, L., Kis, Z., Belgya, T., Kasztovszky, Zs., Kudejova, P., Materna, T., et al., and the Ancient Charm Collaboration. (2008). *A new PGAI-NT setup and elemental imaging experiments at the Budapest Research Reactor*, NRC7—Seventh International Conference on Nuclear and Radiochemistry, Budapest, Hungary, 24–29 August 2008.
- Tölgyesi, J. (1962). *Jadrove ziarenie v chemickej analyse (Nuclear Radiation in Chemical Analysis)*. SVTL, Bratislava.
- Vass, Sz., Gilányi, T. and Borbély, S. (2000). SANS study of the structure of sodium alkyl sulfate micellar solutions in terms of the one-component macrofluid model. *J. Phys. Chem. B* 104:2073–2081.
- Vass, Sz., Grimm, H., Bányai, I., Meier, G. and Gilányi, T. (2005). Slow water diffusion in micellar solutions. *J. Phys. Chem. Lett.* 109:11870–11874.

11 Industrial Application of Radioisotopes

Lajos Baranyai

Isotope Institute Co. Ltd., Konkoly Thege Miklós út 29-33,
Budapest, Hungary

11.1 Introduction

Industrial equipment is typically large, and for this reason, processes taking place in them need testing methods with high sensitivity. This requirement is well satisfied by radioactive isotopes (radionuclides) because of their extremely high detection sensitivity.

Another feature of industrial processes is that they often take place in closed systems, so taking the direct approach to materials is difficult or impossible. For this reason, testing methods that allow investigation of the processes without opening the equipment, disrupting the technological systems, disturbing the processes, and providing qualitative and quantitative information on processes taking place in the “black box” are required.

An important requirement for testing methods applied in industry is rapidity because industrial processes cannot be stopped for long periods. This is partly because it is not allowed technologically and partly because it would cause considerable economic loss. At continuous technologies, for instance, a startup needs considerable preparations (e.g., heating up the systems). Additional startup can be avoided if the system is tested without stopping the process. However, the removal of the materials for measuring its mass or volume is also impossible due to the large quantities or other hindering effects (e.g., dangerous or toxic materials). The radiotracer technique provides the opportunity to measure large quantities. Besides this, testing methods applying radionuclides often offer noninvasive testing opportunities on the production line itself (“online” testing).

11.2 Tracer Investigations with Open Radioisotopes

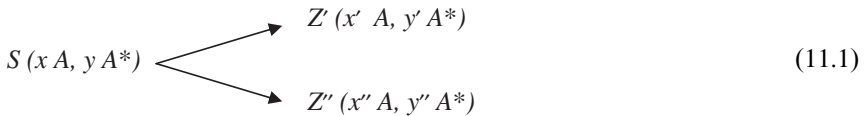
For tracer studies carried out with open radioisotopes, the material or materials to be tested are labeled with a radioactive isotope prior to the investigation. During

the test, radiation of the isotope is detected outside the equipment, which identifies disposition of the labeled material or its rate of distribution among several branches of pipes or equipment. At the same time, intensity of the radioactive tracer is proportional to the quantity of the material or its concentration. With suitable calibration, the intensity can be corresponded with the quantitative mass or volume of the material.

11.2.1 *The Principle, Types, and Sensitivity of the Radiotracer Technique*

Radioisotopes used for radiotracer labeling are present in micromasses (as low as 1×10^{-16} g), but they have strong radiation that can be sensitively and rapidly detected. They behave identically with the labeled material during investigation without modifying its characteristics. Radiation is detected outside the equipment or pipes, so sampling or installing instruments into the material flow can be avoided.

The basic requirement for labeling with a radiotracer is that the radiotracer always has to follow the tested material proportionally during its flow; in other words, the mass rate of the tracer has to be identical to the mass rate of the tested material in each phase of the flow.



$$x'/x = y'/y \quad (11.2)$$

$$x''/x = y''/y \quad (11.3)$$

where x, x', x'' are the number of atoms of the tested material in an S, Z', Z'' system, y, y', y'' are the number of radioactive tracer atoms in an S, Z', Z'' system, A is the type of atoms of the tested material (nonradioactive), and A^* is the type of atoms of the tracer (radioactive).

While an ideal tracer for every material would be its radioactive isotope, not every element has radioactive isotopes with favorable measuring characteristics. For this reason, a generally accepted and applied method is the incorporation of the radioactive atom into the tracer molecule. However, such chemical *labeling* is necessary only if tested material goes through chemical reaction or phase modification. When studying physical behavior (e.g., flow investigations), the so-called physical *labeling* is acceptable where the behavior of the material is affected not by chemical but by physical characteristics.

However, a tracer must follow the tested material even in the case of physical labeling (e.g., a salt as tracer dissolved in water to be followed). An extreme case for physical labeling is when a radioactive colloid is bound on the surface of

grained materials. In such cases, attention must be paid to the fact that radioactive concentration of fractions will be dependent on the grain size (this is called “surface labeling”). Only fractions with the same grain size can be labeled homogeneously.

The relationship between activity of the labeling isotope and the measurable count rate is expressed as follows:

$$I_{\text{rel}} = 2.22 \times 10^6 A \sigma \eta \quad (\text{count/min}) \quad (11.4)$$

where I_{rel} is the measured count rate, A is the activity of the labeling radioisotope (μCi), σ is the number of gamma counts per decay, and η is the total measuring efficiency ($\eta = f\varepsilon G$), in which f is the self-absorption efficiency, ε is the counting efficiency, and G is the space angle factor.

For tracer studies, when calculating the minimal required activity of the labeling radioisotope, dilution rate in the industrial equipment and measuring accuracy also must be taken into consideration. While the former is expressed by a simple multiplication factor, the latter can be deducted from the expected value and standard deviation of the Poisson distribution, which is applied to radioactive decay. Based on these, 1% measuring accuracy needs 10,000 counts, 0.3% accuracy needs 100,000 counts, and 0.1% accuracy needs 1,000,000 counts to be detected (see Section 14.7.1).

11.2.2 Unsealed Radionuclides Used for Labeling in Industrial Tracer Studies

Considering the characteristics of nuclear data, the time needed for the investigations (several days) should match the half-life of the radionuclides. For measurements outside the equipment wall, gamma-emitting radionuclides with relatively high energy (>300 keV) are suitable. Radionuclides emitting a high number of gamma quanta per decay are advantageous; because of their higher count rate, lower activity is necessary for the investigations (see the role of the σ factor in Eq. (11.3)). Certainly an important consideration when selecting the radionuclide is simplicity of its preparation, which should take place in the research reactor through the (n,γ) nuclear reaction, favorably with a high activity yield (as discussed in Section 8.5.2).

In addition to nuclear data, physical and chemical features will determine which radionuclides can be selected for a given tracer study. Radionuclides most frequently used for industrial tracer studies are summarized in Table 11.1.

In the preparatory phase of the tracer study, at the preparation of the radionuclide, and during the investigation, rules governing the handling of radioisotopes must be complied with. The fate of the radioactive isotopes used for industrial tracer studies is important to define in advance and solve in an authorized manner.

The simplest way is to store the material labeled with relatively short-lived radionuclides in a well-separated place until its radioactivity decays below the

Table 11.1 Radionuclides Used for Industrial Tracer Studies

| Radioisotope | Half-Life | Gamma Photon Energy (keV) | Application Field |
|--------------|-----------|---------------------------|---|
| Na-24 | 15 h | 1370 | For labeling solid grains |
| K-42 | 12 h | 1520 | For labeling solid grains |
| Sc-46 | 84 days | 890 | For labeling solid grains, e.g., in silicate industry |
| Cr-51 | 28 days | 323 | For labeling metals and alloys |
| Mn-56 | 2.6 h | 1360 | For labeling metals and alloys |
| Fe-59 | 45 days | 1100 | For labeling ferrous metals |
| Cu-64 | 13 h | 510 | For labeling metals and alloys |
| Zn-65 | 245 days | 1110 | For labeling metals and alloys |
| Br-82 | 36 h | 780 | For labeling stream waters |
| I-131 | 8 days | 360 | For halogenation |
| Rb-86 | 19 days | 1080 | For labeling solid grains |
| Ag-110m | 253 days | 660 | For labeling metals and alloys |
| La-140 | 40 h | 1600 | For labeling solid grains, e.g., in silicate industry |
| Au-198 | 2.7 days | 412 | For labeling solid grains as colloid |
| Hg-203 | 47 days | 279 | For mercury electrolysis as metal |
| Kr-85 | 10 years | 510 | For labeling gases |

exempted activity level. Storing time can be considerably reduced if the labeled material is diluted during the technological processes or is artificially diluted after the study. In such cases, the exempted radioactive concentration will be the precondition of the release. For instance, the dilution rate of a radioactive-labeled component that is introduced into a huge storing container with a great volume of nonradioactive material can even grant an exemption from separated storage.

11.2.3 Exploration of Leaks

Utilizing sensitivity of the radioactive tracers, it is possible to detect leakages in technological equipment or pipes far earlier than appearance of the leaked materials would be observed in the contaminated component or would endanger product quality or cause any technical risk. For instance, if there is a leakage in a heat exchanger, where migration of the cooling agent into the cooled material (e.g., product) causes obvious deterioration in the product quality, this contamination is detected using traditionally applied analytical methods only if the rate of leakage exceeds detection limits of the given method. With radioactive tracers, however, leakages even in the very early phase can be detected and eliminated readily (Figure 11.1).

Among the radiotracer leakage test methods, leak detection and leak localization on oil pipelines have the utmost importance. Pipelines generally run underground.

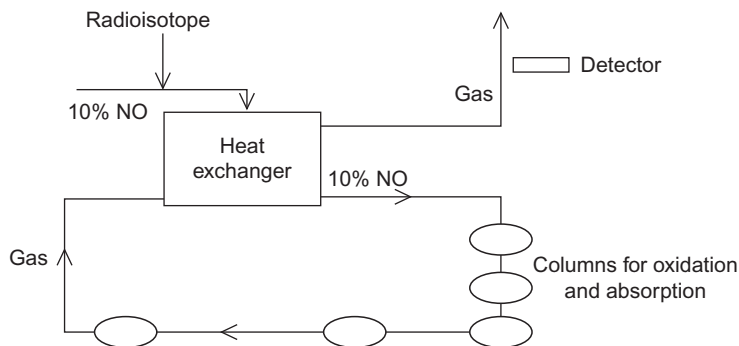


Figure 11.1 Detection of leakage loss in a heat exchanger.

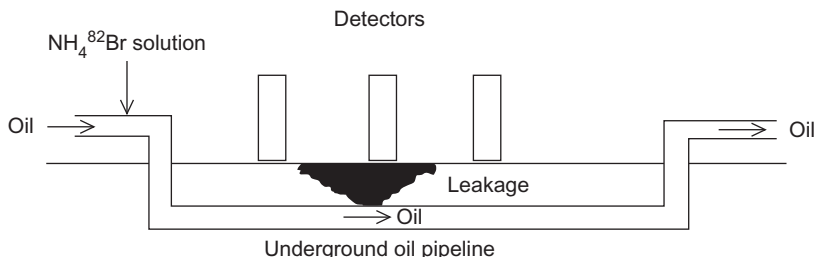


Figure 11.2 A leak test on an oil pipeline.

For a radiotracer test, $\text{NH}_4^{82}\text{Br}$ solution is injected into the streaming oil at a pressure upgrading station. This radioactive tracer is miscible with the oil, so the streaming oil will incorporate and transport the radioactive tracer along the pipeline. At those spots where the pipeline leaks, oil seeps out to the surrounding soil layers. When the radioactive cloud reaches these spots, together with the oil, a small amount of radioactive tracer will also get into the soil. The $\text{NH}_4^{82}\text{Br}$ tracer is well adsorbed in the soil. The nonradioactive natural oil stream fills up the pipeline gradually, washing the radioactive cloud into a huge storage tank. But the small radioactive contamination remains in the soil at the location of the leak. With suitable detectors, its location and intensity can be determined.

In the past, the location of the radioactive spot was identified with hand detectors by walking along the pipeline on the surface. For this technique, high radio-tracer activities (10–100 GBq) were necessary because soil layers covering the pipeline absorbed a considerable portion of the radiation (Figure 11.2). Today, new detectors have been developed that are built into so-called pigs passing together with the oil stream inside the pipeline, and they both detect radioactivity and measure the distance. Based on this modern detection technique, count versus distance plots provide information on the location of leakage, and the detected counts give

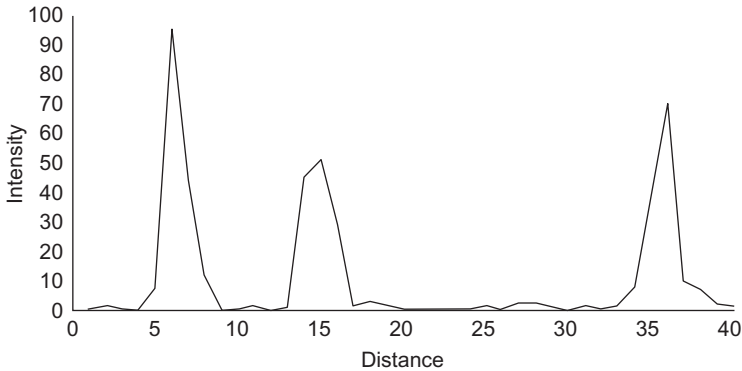


Figure 11.3 A count versus distance plot for leakage spots on a crude oil pipeline.

the rate of leakage. For this detection technique, 1–10 GBq of radiotracer is sufficient for a leakage test (Figure 11.3).

Further examples of leakage tests that were carried out using the radioisotope tracer technique include the following:

- Localization of leaking spots on high-voltage electric cables under gas pressure.
- Localization of leaks in gas-filled telecommunication cables.
- Localization of damaged spots on bitumen-lined concrete tanks.

11.2.4 Determination of Flow Rates

Determination of the flow rate of streaming substances is one of the most important measurements in the chemical industry. In addition to direct flow rate determination, movements based on mechanical principles (e.g., the rotation speed of a propeller built into the stream) need accurate calibration. Both can be performed by the radiotracer technique.

A great advantage of the flow rate measurements executed with the tracer technique is that these measurements provide direct flow rate values in volume per time unit. This is in contrast to other methods that measure linear flow velocity, which also need to determine the flow cross section. In chemical technology, the cross section is not always well defined, e.g., there are pipes with changing cross sections where internal deposits can cause the change, or liquid flow with bubbles where the liquid volume is not defined, or open channels with changing cross sections.

In addition to this, in the case of several phases flowing together, the flow rate of the individual phases can be determined separately with the tracer technique. For instance, in the case of pneumatic powder transport, it is possible to label the transported air and powder separately, or in the case of suspensions transported with water, the water and the solid granules can be labeled separately. These examples demonstrate the unique character of the radiotracer technique. When labeling

the phases individually and determining flow rates for the phases separately, the slip between the transporting (e.g., air and water) and the transported phases can also be determined.

Determination of the flow rates with the tracer method is based on measuring the dilution rate of the injected tracer in the pipe. The injected total activity is expressed as the volume and radioactive concentration of the radioactive tracer:

$$A = Va \quad (11.5)$$

The dilution process of the tracer is described as integral to the radioactive concentration by cross section and length as follows:

$$Va = \iint a_t(K, L) dK dL \quad (11.6)$$

Introducing linear velocity of the flow:

$$v = dL/dt \quad (\text{and from this, } dL = v dt) \quad (11.7)$$

Substituting dL into Eq. (11.4), we obtain:

$$Va = \iint a_t(K, L) dK v dt \quad (11.8)$$

Separating the double integral to members of cross section and time:

$$Va = \int v dK \int a_t dt \quad (11.9)$$

One member of Eq. (11.9) corresponds to the desired flow rate:

$$\int v dK = Q \quad (11.10)$$

So

$$Va = Q \int a_t dt \quad (11.11)$$

$$Q = Va / \int a_t dt \quad (11.12)$$

Technically, the measurement consists of a tracer injection at a given point of the pipe (Figure 11.4) and of a detector installed at another point over the mixing distance plotting the intensity function in time. Spreading the radioactive “cloud” is

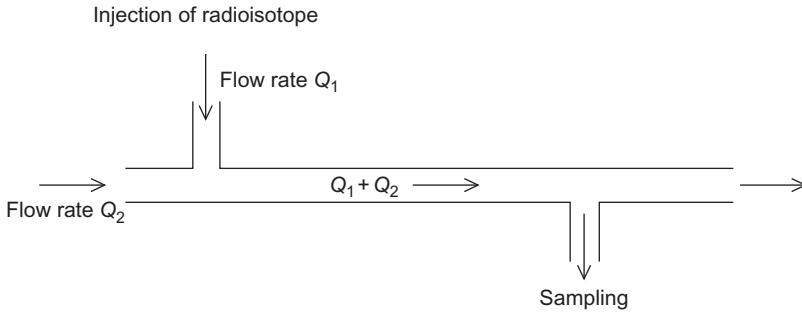


Figure 11.4 Injection of a radioactive tracer into the tested pipeline.

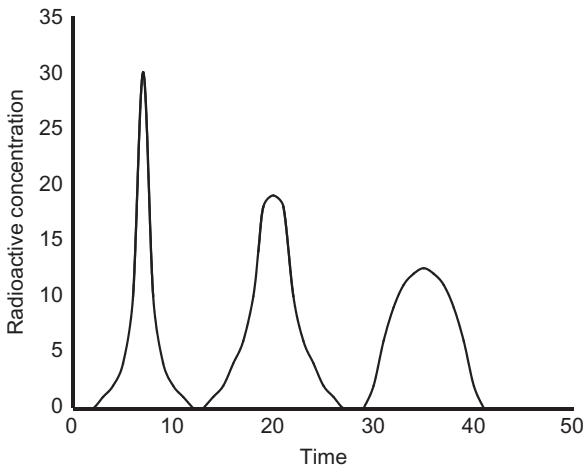


Figure 11.5 Spreading the radioactive “cloud” in time.

demonstrated in [Figure 11.5](#). Mixing distance is $100 \times D$, where D is the diameter of the pipe. For quantitative measurements, prior to the tracer injection, both the activity and volume of the radioactive tracer and its activity versus count rate are determined.

In addition to direct flow rate measurements, if the flow cross section is well-defined, linear velocity measurements with radiotracer technique are also possible. Such so-called peak-to-peak methods have practical importance in the calibration of rotameters.

In this method, the tracer is injected instantaneously and the passing of the tracer peak is sensed by two detectors installed onto the pipe at two points ([Figure 11.6](#)). The linear velocity of the flowing substance (v) can be calculated from the distance of detectors ($L_2 - L_1$) and from the time difference of intensity peaks ($t_2 - t_1$):

$$v = \frac{L_2 - L_1}{t_2 - t_1} \quad (11.13)$$

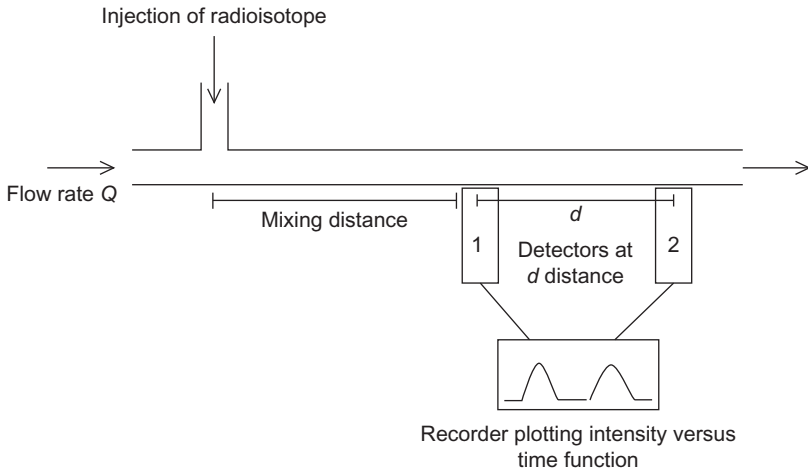


Figure 11.6 Linear velocity measurement by the peak-to-peak method with two detectors.

Practical examples for flow rate determinations with the radioisotope tracer technique (1—direct flow rate measurement; 2—linear velocity measurement):

- Testing for flow rate ventilation systems (1).
- Cooling water consumption determination in an oil refinery (1).
- Cooling water consumption determination in heat power stations (1).
- Determination of wastewater flow rates in various factories (1).
- Capacity measurement of pneumatic powder transport pipes in a cement factory (1).
- Flow rate measurement of moving solid grains in a drum furnace of a cement factory (2).
- The flow rate in natural streams, rivers, karst waters, surface waters, and irrigation systems (1).

The peak-to-peak method (2) suitable for linear velocity measurement is used primarily for calibrating flow meters.

11.2.5 Measuring Volume and/or Mass of Large Quantities of Substances in Closed Equipment

From both the technology management and economic points of view, knowing the quantity of substances processed in large and closed industrial equipment is essential. In the same time, in most cases, removal of large quantities of substances for volume or mass measurement outside the equipment is not feasible, or else it would cause considerable contamination and substance loss.

For substances that are or can be stirred to a homogeneous mixture, the radio-tracer technique offers a simple method for determining their quantity. The known dosage (activity and volume) of a radiotracer should be added to the substance of unknown quantity, and after thorough mixing, a sample should be taken for

determining the radioactive concentration of the homogeneous mixture. The decrease in radioactivity compared to that of the tracer reflects the dilution rate of the tracer in the total quantity of the substance. Thus, the simple isotope dilution principle (discussed in Section 10.1.6.1) can be applied to the measurement:

$$Va_0 + V_j a_j = (V + V_j) a_h \quad (11.14)$$

where V is the volume of the substance to be determined, V_j is the volume of the tracer, a_0 is the radioactive concentration of the substance to be determined, a_j is the radioactive concentration of the tracer, and a_h is the radioactive concentration of the mixture developed after homogeneous stirring.

Arranged to the volume of the substance to be measured:

$$V = V_j \frac{a_j - a_h}{a_h - a_0} \quad (11.15)$$

As $a_0 = 0$ and $a_j \gg a_h$:

$$V = V_j \frac{a_j}{a_h} \quad (11.16)$$

Consequently, the volume (V) of the substance in the equipment can be determined by measuring the volume (V_j) and radioactive concentration (a_j) of the tracer as well as the radioactive concentration of the pool (a_h) after dilution. Equations (11.11)–(11.13) are valid not only for volumes but also for masses; therefore, substance masses can also be determined based on the same principle.

A well-known example of the substance quantity (mass or volume) determination with the radiotracer technique is the regular measurement of metal mercury mass (used as a cathode metal) circulating in chloro-alkali-electrolysis cells. For this measurement, the Hg-203 radioisotope is used in metal mercury form with activity of 37 MBq per electrolysis cell. In one cell, approximately 1–4 tons of mercury is circulated, and generally, 40 electrolysis cells are operated in one plant.

Some additional examples of substance quantity measurement with radiotracer technique are mentioned here:

- Determining the slag quantity in metallurgical shaft and cupola furnaces.
- Determining the metal melt quantity in electric furnaces.
- Determining the raw meal residue in fluidization homogenizers in a cement factory.

11.2.6 Investigation of Homogeneity of Mixtures

Batch mixing of solid granular substances or materials of other consistencies is one of the most frequently applied technological operations in this industry. Although a homogenization process depends on several parameters (physical features of the substance, type of mixer, and operation mode), the most frequent question is how

long a mixture in the applied mixer must be mixed to achieve the required homogeneity.

To answer this question, one component of the mixture is labeled with a radioactive tracer prior to the study. The labeled component is placed in the mixing equipment in accordance with the normal technological process and the mixing process is launched. Depending on the required information (e.g., if homogeneity is needed to describe with a quantitative metric number or only information on the sufficient homogenization time is needed to achieve the best homogeneity which cannot be improved with longer mixing), sampling or an outer detection technique is applied.

For sampling, the mixing process is suspended in certain time intervals and a statistically sufficient number of samples are taken from the mixture, followed by measuring the count rates of the samples and the statistical processing of the count rates. The mixture homogeneity is determined by calculating the relative standard deviation of the sample counts:

$$\text{rsd} = \sqrt{\frac{\sum (a_n - \bar{a})^2}{\bar{a}^2(n-1)}} \quad (11.17)$$

where a is the count rate of a sample, \bar{a} is the average of the counts, and n is the serial number of the sample.

By plotting the obtained relative standard deviation values as a function of time, the optimal homogenization time (where homogeneity does not change further) can be determined (as shown in [Figure 11.7](#)).

When applying the outer detection technique ([Figure 11.8](#)), the detector(s) are installed outside the mixing equipment wall, which will follow movement of the radioactive tracer and concentration equalization of the mixture. The time change of the detector signal does not provide quantitative information on the homogeneity of the mixture; it only shows how much time is needed for the equalization (for ending the signal fluctuation). The outer detector technique requires

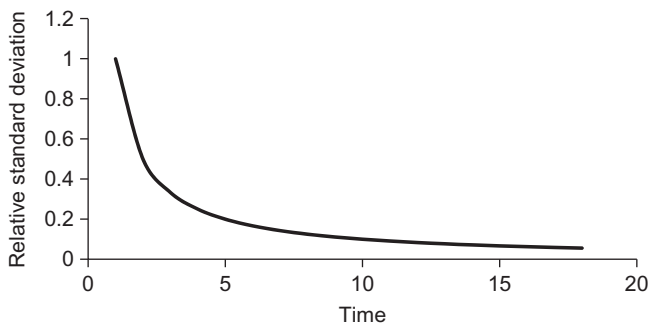


Figure 11.7 Investigation of the homogeneity with sampling technique.

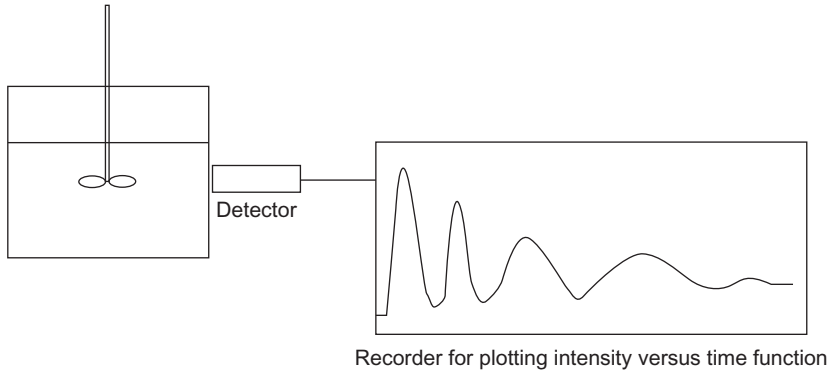


Figure 11.8 A homogenization study with outer detectors.

approximately 10 times more activity than the sampling technique, but it is much faster and it is a noninvasive method.

Most of the homogenization studies have been performed in Hungary in the field of porcelain manufacturing and cement production using fluidization raw meal mixers.

Examples for homogenization studies carried out with radiotracer technique include:

- Homogenization of components (Co and W metal powder) of hard metal production.
- Homogenization of components of porcelain mixture with labeling a powder fraction.
- Homogenization of a wet porcelain mixture with labeling the wetting agent.
- Study of the raw meal fluidization type homogenization in cement factories (with Au-198 colloid tracer).

11.2.7 Characterization of Material Flow and Determination of Chemical Engineering Parameters

Flow parameters of substances processed in continuously operated chemical industrial systems are very important factors that influence chemical yield and product quality because the residence time of the substance in the system determines the contact time for reaction partners (namely, it defines the time of a chemical reaction).

If the residence time of a substance in an equipment is shorter than required, the chemical reaction will not be fully complete, but if it is unnecessarily long, the equipment efficiency will decrease. In addition to the length of time, there is the question of whether the full substance volume is involved in the entire reaction or only a part of it. This latter option may be due to dead spaces that have been formed with stagnating substances in the equipment, which also helps determine the efficiency.

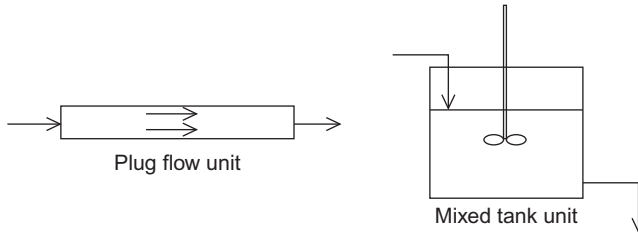


Figure 11.9 Plug type and fully mixed tank type flow models.

A possible way to determine the important parameters of the chemical engineering behavior of equipment and substances is to investigate and evaluate the material flow characteristics in an equipment or system. Material flows can be well studied by means of the radioisotope tracer technique using outer detectors. For such studies, a radioactive tracer is instantaneously injected into the inlet stream, and detector(s) are installed outside the system at the outlet stream. Detectors continuously measure radioactive concentration of the tracer as count/time and plot the count rate versus time function. For obtaining chemical engineering parameters, these plots are evaluated.

Basic models of flow types are shown in [Figure 11.9](#).

By quantitative evaluation of plots obtained from a radiotracer test, the following chemical engineering parameters can be determined:

- Average residence time of the substance.
- Extension of dead spaces.

In addition to quantitative parameters, the shape of plots provides important information on the character and deformation of flows.

The theoretical (designed) and actual (measured) residence time of a substance are determined on the basis of the following formulas:

$$\bar{t}_{\text{elm}} = \frac{V \text{ ml}}{Q \text{ ml/s}} \quad (11.18)$$

$$\bar{t}_{\text{kis}} = \frac{\int_0^{\infty} t_i c(t) dt}{\int_0^{\infty} c(t) dt} \quad (11.19)$$

where $c(t)$ is the radioactive concentration. ml/s (milliliter/second) is the measuring unit.

The residence time of the substance in a chemical reactor corresponds to the reaction time for the chemical reaction. Optimally, the residence time is identical to the chemical reaction time. When designing continuously operated chemical reactors, the volume of the vessel and the flow rate of the substance passing

through the vessel are matched to the optimal residence time. The radioactive tracer test reveals if the experimentally measured residence time corresponds to the theoretically designed residence time or not.

The theoretical residence time refers to the total volume of a vessel, while the experimental residence time obtained from the radiotracer test gives the active volume of the vessel in which the material flow really takes place. The remaining space (difference of the theoretical and experimental) is the dead space where the material is stagnating, meaning that this material does not participate in the chemical reaction.

$$V_{\text{holttér}} = V_{\text{elm}} - V_{\text{eff}} \quad (11.20)$$

$$V_{\text{holttér}} = V_{\text{elm}} - \bar{t}_{\text{kís}} Q \quad (11.21)$$

If there are dead space(s) in a vessel, average residence time becomes shorter and reaction volume and reaction efficiency will decrease.

Count rate versus time plots obtained from different measurements that used different tracer activities can be compared to each other by converting them to standard plots independent of the applied activity. This is performed by dividing each point (count rate) of the plot by the integrated count rate, i.e., the area under the curve on the plot.

This so-called density function ($DE(t)$) gives the relative frequency of the substance portion, leaving the chemical reactor between t and the $t + dt$ time interval. If values of the density function are integrated between 0 and t time-point, the so-called distribution function ($DI(t)$) is obtained, which represents the relative frequency of the occurrence of portions belonging to less than t time intervals. By combining the values of the density function and the distribution function, the so-called intensity function ($I(t)$) is obtained, which highlights flow irregularities (Figure 11.10). If an intensity function descends monotonously or has a maximum, these reflect a stagnating substance. In the case of ideal mixing or plug type flow, the intensity function is monotonously ascending.

From the shape of density, distribution, and intensity functions, the type of flow and flow irregularities can be concluded. On one hand, it can be determined if the flow pattern corresponds to the designed one or not (e.g., the tested flow is of plug or mixing type); on the other hand, it can be determined if deviation from the ideal flow pattern is significant or not and whether there are significant irregularities in the flow pattern or not (Figure 11.11).

The plug flow characterizes chemical reactors where mixing of the substance portions representing different residence times is not needed. A simple physical example of this type of flow is the motion of heated water in a boiler passing through a drum without mixing with the entering cold water. However, there are several chemical reactors that operate on the principle of plug flow where reaction partners are introduced continuously into the reactor and only components representing the same residence time are required to contact, and mixing with those portions entering or leaving the reactor earlier or later is not needed.

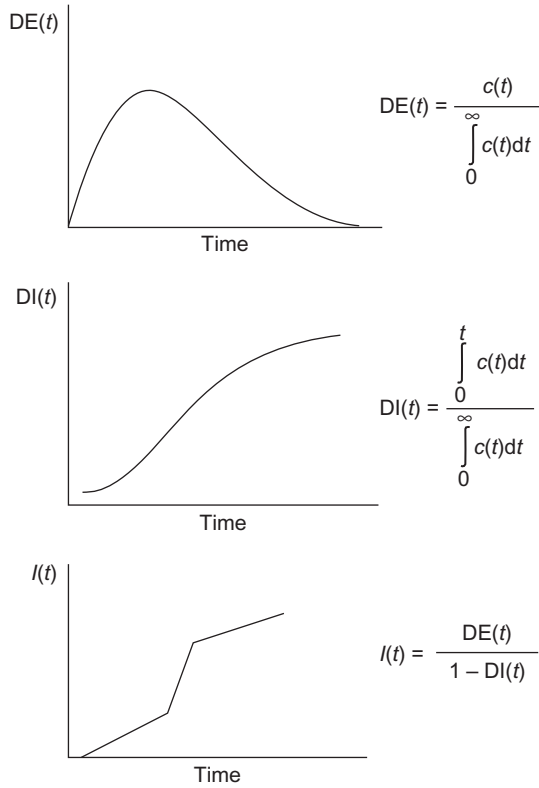


Figure 11.10 Standardized time functions of different flow types: density ($DE(t)$), distribution ($DI(t)$), and intensity ($I(t)$) functions.

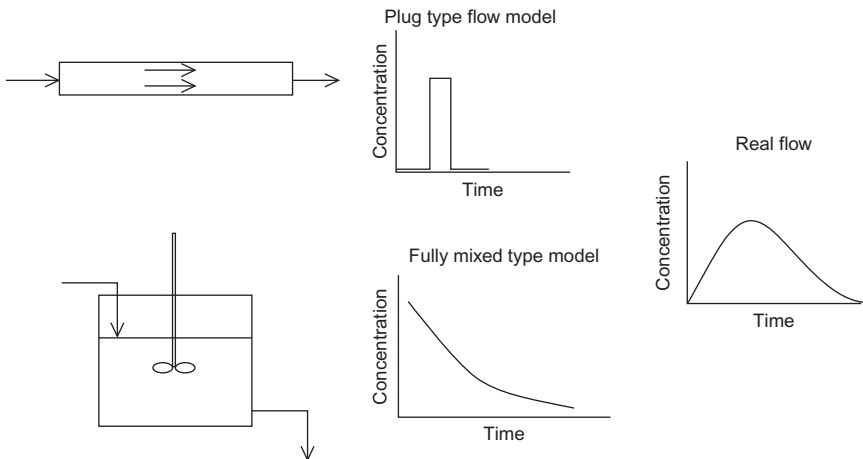


Figure 11.11 Ideal flows (plug flow and mixed flow) and a practical case.

Contrary to this flow pattern, mixing-type chemical reactors ensure intensive mixing among substances of various residence times, e.g., entering and leaving the reactor in various timepoints. A typical example of this is the so-called equalization basin, which collects wastewater from various chemical plants with the aim of equalizing concentration peaks and fluctuations of various wastewaters by mixing and dilution.

None of these ideal flow types exists in pure form in practice. The actual flow pattern is always a combination of plug flow and mixing-type flow. It is important to know which type of theoretical flow pattern resembles the measured quantity and to what extent. To determine this, flow models are developed that provide quantitative parameters for expressing the extent of adequacy to one or the other basic flow type. In such models, compartments of ideal type flow are combined until an adequate description of the actual flow pattern is found.

The cascade model is built from n number of mixed tanks with identical volumes, connected to each other in series. In chemical engineering, by connecting an infinite number of mixed tanks in series, a plug flow pattern is obtained. When fitting a cascade model to the actual plot obtained for the measured system, the question is how many mixed tanks are necessary to connect in series to obtain a density function that fits well with the actual measured plot.

Figure 11.12 demonstrates density functions corresponding to cases when connecting mixed tanks of $n = 1, n = 2, n = 3, n = 4, n = 5, n = 6, n = 7$ numbers. It is seen that as the number of mixed tanks connected in series increases, the density function gets closer and closer to the density function describing a plug type flow. NB: residence time of the moving substance is identical for each case.

The cascade model is based on mixed type flow compartments and quantitatively gives the extent of deviation from the ideally mixed flow pattern with an increasing number of cascades (e.g., the number of mixed tanks). The higher the n number of tanks, the greater the deviation of the actual flow from the ideally mixed flow pattern. The cascade model is applied for equipment designed for mixed type flow (Figure 11.12).

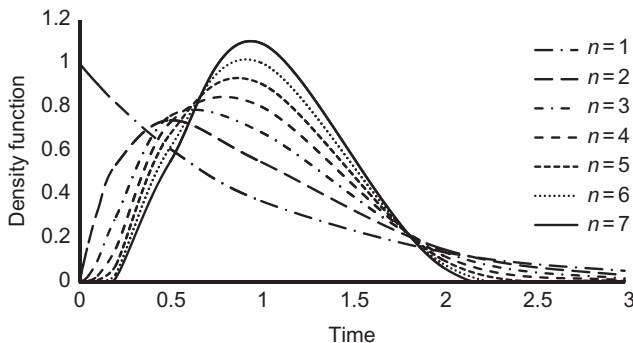


Figure 11.12 Cascade model and density functions deduced for various cascade numbers.

The density function of the cascade model is found as follows:

$$DE(t) = \frac{n^n t^{n-1} e^{-nt}}{(n-1)!} \quad (11.22)$$

where n is number of the members of the cascade.

The dispersion model (Figure 11.13) is exactly the opposite of the cascade model; it is based on the plug type flow, and deviation from such flow pattern is characterized with a dispersion coefficient. The higher the dispersion coefficient is, the greater the deviation from ideal plug flow is. The dispersion model is applied for equipment designed for plug type flow (Figure 11.13).

The density function of the dispersion model is calculated as follows:

$$DE(t) = \frac{1}{2\sqrt{\pi D/\mu L}} \exp\left\{-\frac{(1-t)^2}{4(D/\mu L)}\right\} \quad (11.23)$$

where D is the dispersion coefficient and $D/\mu L$ is the inverse of the Peclet number.

Mixed models combine the number, size, and connection way of plug flow and mixed tank units. As an example, one plug flow unit is connected to one mixed tank unit in a series in Figure 11.14. More complicated models can also be constructed where the number, size, and method of connection (in series or parallel) of the units are varied until the density function of the theoretical model fits best to the plot measured with the radiotracer technique.

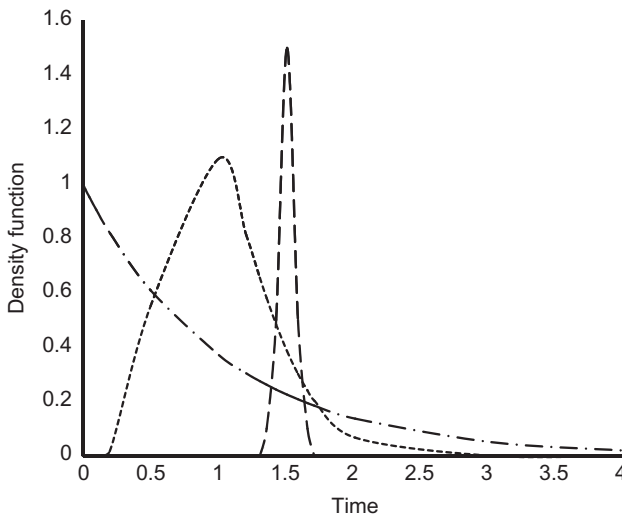


Figure 11.13 The dispersion model and density functions deducted for various dispersion coefficients.

Deviation from ideal flow models can predict the types and effectiveness of the processes as well as expected quality of the material produced in the equipment.

In the case of serious deviations, the shape of the plots gained from the radio-tracer test itself refers to flow disturbances. Such serious flow disturbances are shown in [Figure 11.15](#), demonstrating (a) plug type flow as designed with higher residence time than expected, (b) three channels formed within one flow, and (c) two channels within one flow.

Radiotracer investigations of such flow tests are justified partly by their simple technical implementation, partly because they do not require previous calibrations,

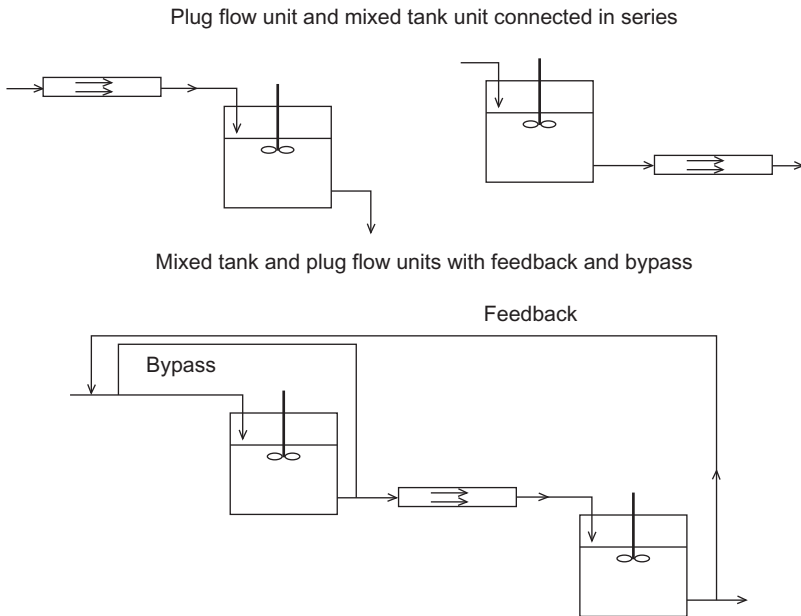


Figure 11.14 Mixed flow models.

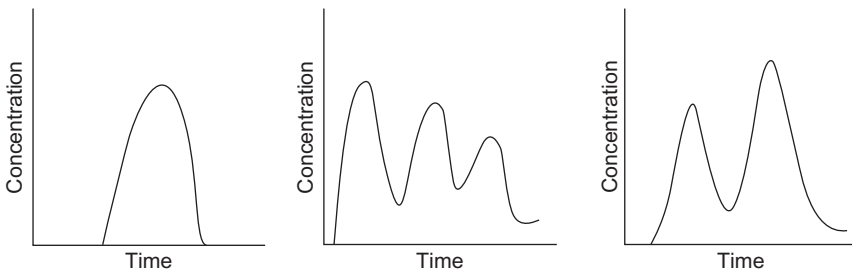


Figure 11.15 Plots indicating flow disturbances.

and partly because of significant information can be obtained about the efficiency of chemical reactors and expected product quality.

To cite a practical example, a chemical factory operates a mixed tank type basin for equalizing wastewater effluents originating from several plants. Flow tests carried out with the radiotracer technique resulted a much shorter residence time than calculated and test plots indicated a multichannel type flow. This test revealed that due to gradual sludge deposition, wastewater flows through several channels without the intended intensive mixing and dilution. A consequence of the radiotracer test was dredging and repeating the test.

Further industrial examples for the qualification of material flows include:

- Flow testing of the slurry in autoclaves digesting bauxite in an alumina factory.
- Measuring whitening reaction (residence) time of cellulose fibers in the pulp industry.
- Mixing of the benzene and gasoline fractions during flow in an oil pipeline.
- Mixing of the cold and warm water in electric boilers during flow.
- Testing the flow of melt in a bath furnace of a plate glass factory.

11.2.8 Wear Studies

If the equation relating to isotope dilution (11.15) is deduced not to material volume (V), but to tracer volume (V_j), the reverse isotope dilution equation is obtained:

$$V_j = V \frac{a_h - a_{j0}}{a_j - a_h} \quad (11.24)$$

This equation is valid not only for volumes but also for the mass of materials.

When applying the reverse isotope dilution method (discussed in Section 10.1.6.2), the volume of the tracer is intended to determine. This requires knowledge of the total volume in which the radioactive tracer of known activity is mixed.

Such investigation is, for example, a wear study carried out with the radiotracer technique (Figure 11.16). The plug of a motor vehicle is a part that is particularly exposed to wear. For the study, a plug in its full mass is neutron-irradiated in the research reactor or locally irradiated with charged particles in a cyclotron, and then the radioactive part is inserted into the motor. Fine particles from the plug of the running motor get into the lubrication oil as the result of wearing. The oil volume/mass and activity on the plug are measured prior to the test. This is followed by measuring the radioactive concentration/specific activity of the oil contaminated with worn particles. Then, using the equation related to reversed isotope dilution, either volume or mass of the radioactive tracer (worn particles in the oil) can be calculated.

In addition to wear studies, other corrosion processes can be tested by the reverse isotope dilution method. Such tests are wear of enamels, removal of surface degreasers at galvanization, and chromium loss at welding technologies.

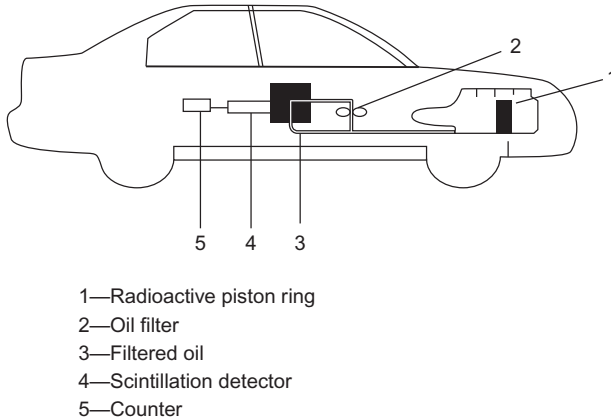


Figure 11.16 A wear study of a radioactive plug built into the motor of a vehicle.

11.2.9 Groundwater Flow Studies

The linear velocity of groundwater can be determined by determining the dilution of a tracer as a function of time. Concentration decreases over time t at a groundwater flow with a Q flow rate according to the following equation:

$$\frac{dc}{dt} = -\frac{Qc}{V} \quad (11.25)$$

where V is the volume of the labeled water column, and c is the radioactive concentration of the tracer at a time t .

Introducing an internal cross section of the well (A), the groundwater velocity v can be determined by integrating Eq. (11.25) as follows:

$$V = \frac{Q}{A} = \frac{v}{At} \left(-\ln \frac{c_t}{c_0} \right) \quad (11.26)$$

Consequently, for determining the flow velocity of groundwater, a continuous decrease of radioactive concentration of the tracer injected instantaneously into the well is measured (Figure 11.17).

A measuring probe automatically detects the residual concentration of the radioactive tracer diluted continuously with groundwater, while a connected meter records the concentration versus time plot (Figure 11.18).

To determine the direction of the groundwater flow, the intensity plot of the radioactive tracer escaping from the well is recorded for every direction. This can be done by rotating a probe sunken into the well which is collimated (opened) in one direction. The plot of a rotating probe is shown in Figure 11.19. The flow direction of the groundwater corresponds to the direction of the longest drawn tracer spot on the plot.

Groundwater flow velocity and flow direction studies serve typically to determine local conditions, while large field flow conditions are better determined by measuring

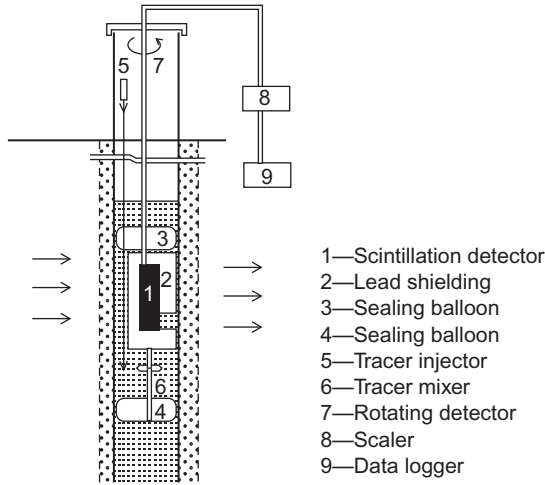


Figure 11.17 The arrangement of a measuring probe sunken into a well after radioactive tracer injection.

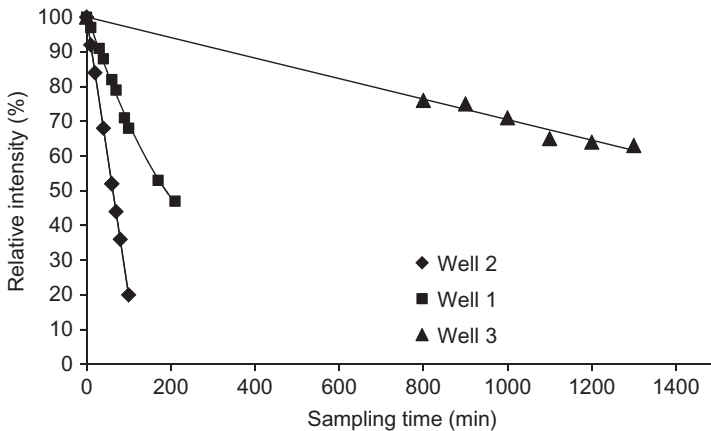


Figure 11.18 A radioactive concentration change measured with a probe in wells.

water level changes in several drilled wells. Mapping groundwater local flow conditions were executed in practice in the surrounding of industrial waste repositories.

11.3 Absorption and Scattering Measurements with Sealed Radioactive Sources

11.3.1 Principle of the Measurements

Investigations executed with sealed radioactive sources are based on absorption or scattering of the radiation. Gamma radiation of a sealed radiation source installed

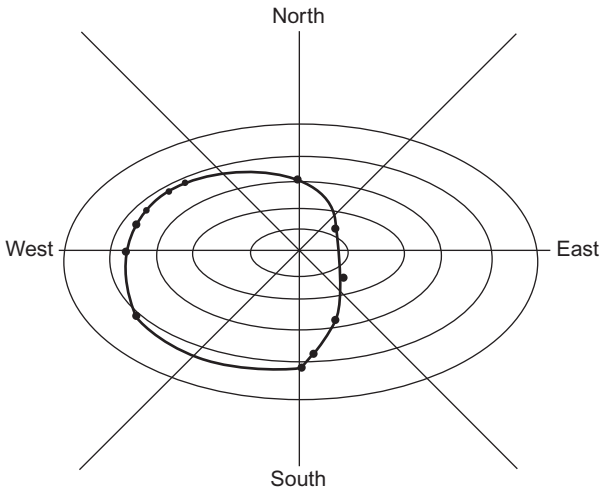


Figure 11.19 An activity distribution plot obtained by rotating the probe.

on one side of a piece of equipment penetrates into the equipment/contained material and generates signals in a detector placed on the opposite side of the equipment. This signal indicates the presence or lack of the material, while its intensity is proportional with the rate of absorption which depends on the physical features of the material in the equipment. In this way, some physical features (density, thickness) of the material inside the equipment can be determined from the intensity measured.

11.3.2 Sealed Radioactive Sources Used for Measurement

The radioisotopes that are used most frequently for radiation absorption and scattering type measurements are listed in [Table 11.2](#).

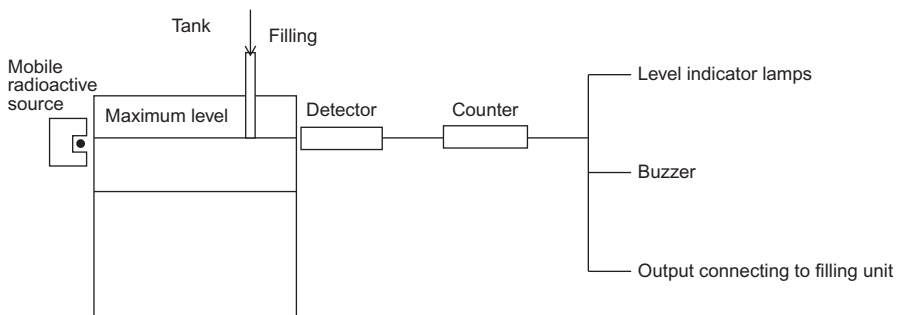
11.3.3 Level Indication of Materials in Tanks

For detecting the level of materials in industrial equipment, nuclear level indicators and level measuring instruments can be used ([Figure 11.20](#)). Level indicators are suitable for detecting and transmitting given level limits (min, max), while level measuring instruments are used for continuous detection, recording, and transmitting the material level.

The level of materials in industrial equipment can be continuously determined either by absorption measurement of the radiation or by installing a level indicator on the servo-motor driven mechanism following the material level. [Figure 11.21](#) shows the principle of absorption type measurement. Measurement based on radiation absorption utilizes the change in the relative absorption caused by the material level. Similar equipment can utilize reflection of the radiation. Radiation sources

Table 11.2 Radioisotopes Used for Radiation Absorption and Scattering Type Measurement

| Radioisotope | Half-Life | Type of Radiation | Application Field |
|--------------|------------|---------------------|---------------------------------------|
| Co-60 | 5.3 years | γ (1170 keV) | For materials with high thickness |
| Cs-137 | 30 years | γ (661 keV) | For materials with low thickness |
| Ir-192 | 74 days | γ (316 keV) | For welding seams |
| Tm-170 | 134 days | γ (84 keV) | For plastic and rubber layers |
| Am-241 | 458 years | γ (67 keV) | For plastic and rubber layers |
| Kr-85 | 10.7 years | β (700 keV) | For paper, plastic, and rubber layers |
| Sr-90 | 28 years | β (546 keV) | For paper, plastic, and rubber layers |
| Pm-147 | 2.6 years | β (224 keV) | For paper, plastic, and rubber layers |
| Tl-204 | 3.8 years | β (766 keV) | For paper, plastic, and rubber layers |
| Ra-206/Be | 1602 years | Neutron source | For moisture content determination |
| Po-210/Be | 138 days | Neutron source | For moisture content determination |
| Am-241/Be | 48 years | Neutron source | For moisture content determination |

**Figure 11.20** The principle of level indication with the radioisotope technique.

used for such measurements (depending on the wall thickness of the equipment) are 37 MBq to 3.7 GBq Co-60, and Cs-137 sealed sources. Applied detectors are the Geiger–Müller counter and the scintillation detector.

Examples of industrial level indication and level measuring solutions include:

- Maintaining the level of the mixture between limit values in a blast furnace.
- Automation of a miner's tram filling.
- Piece counting on tile production lines.

11.3.4 Material Thickness Determination

Measurement based on the principle of radiation absorption is mainly used to determine the thickness of rolled metals. The intensity of the radiation penetrating a

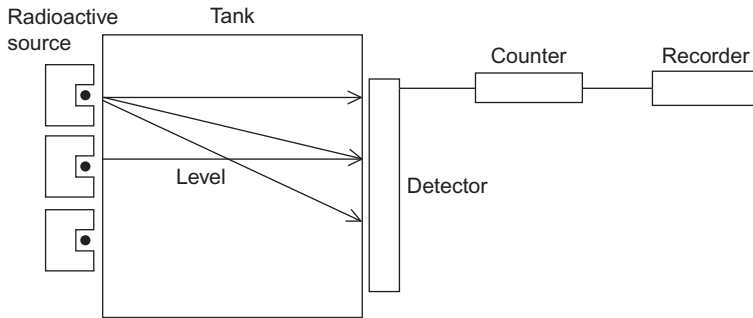


Figure 11.21 Continuous level indication with point radiation sources and a linear detector.

material depends on the elemental composition, thickness, and density of the material placed in the path of the radiation. For thickness measurements, the material must have a permanent chemical composition and density.

The intensity change caused by a material layer is described by the following formula (see also Eq. (5.46)):

$$\frac{I}{I_0} = \exp(-\mu(E)l) \quad (11.27)$$

where I_0 is the intensity of radiation entering, I is the intensity of radiation leaving the material, $\mu(E)$ is the linear absorption coefficient, and l is the thickness of the material layer.

The upper part of [Figure 11.22](#) shows a measuring arrangement based on radiation absorption, while the bottom part shows a measuring arrangement based on radiation reflection. The measuring technique based on reflection is mostly applied when access to both sides of the equipment is impossible due to the mechanical arrangement of the equipment.

Radiation sources used for thickness measurements include gamma- and beta-emitter nuclides. The radiation energy is selected to match the material density. As detectors, ionization chambers and proportional counters are applied.

To obtain the best sensitivity for the thickness measurements by absorption, optimal measuring conditions are applied by selecting the best radiation source (with given $\mu(E)$). The conditions of the optimization measurements can be deduced from Eq. (5.48) as follows:

$$\frac{I}{I_0} = \exp(-\mu\rho l) = \exp(-\mu d) \quad (11.28)$$

where I_0 is the intensity of radiation entering, I is the intensity of radiation leaving the substance, μ is the mass-absorption coefficient, ρ is the density, l is the thickness, and d is the surface density of the paper layer.

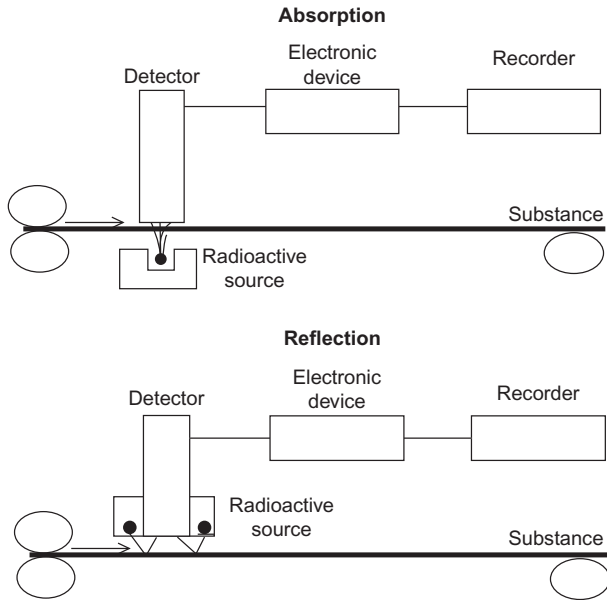


Figure 11.22 Measuring principles based on radiation absorption and reflexion.

The optimal value of μ is obtained using the relative measuring sensitivity (Q), which is defined as:

$$Q = \left| \frac{\frac{\Delta I}{I_0}}{\frac{\Delta d}{d}} \right| \quad (11.29)$$

For simplification, ΔI is expressed by the difference quotient of Eq. (11.28):

$$\Delta I = I^1 \Delta d \quad (11.30)$$

and

$$\Delta I = -\mu I_0 \exp(-\mu d) \Delta d \quad (11.31)$$

By substituting Eq. (11.31) into Eq. (11.29), we obtain:

$$Q = \frac{\mu I_0 \exp(-\mu d) \Delta d}{\frac{I_0}{\frac{\Delta d}{d}}} = \mu d \exp(-\mu d) \quad (11.32)$$

The differential quotient of the relative measuring sensitivity Q , according to the mass-absorption coefficient μ , is:

$$Q^1 = \frac{dQ}{d\mu} = d \exp(-\mu\rho l) - \mu d^2 \exp(-\mu d) \quad (11.33)$$

The function (Eq. (11.33)) has a maximum if $Q' = 0$. From here,

$$d \exp(-\mu\rho l) = \mu d^2 \exp(-\mu d) \quad (11.34)$$

From Eq. (11.34), we obtain:

$$\mu = \frac{1}{d} \quad (11.35)$$

In conclusion, the sensitivity of the thickness measurement is the best if Eq. (11.35) is fulfilled.

For the thickness measurement by backscattering, a similar equation to Eq. (11.35) can be derived from Eq. (5.69).

Examples of applying industrial thickness-measuring systems include the following:

- Continuous thickness measurement on paper-manufacturing machines with beta-emitting radionuclides.
- Continuous thickness measurement of metal sheets on cold rolling machines.
- Thickness measurement of hot rolled steel sheets.
- Thickness measurement of surface layers deposited on thick basic sheets (coatings).
- Thickness measurement gauges on plate glass production lines.
- Thickness measurement of concrete at construction of containers.

11.3.5 Material Density Determination

In the case of permanent material thickness, the density of a material is determined on the basis of the principle of radiation absorption (Figure 11.23). For this, the so-called mass-absorption coefficient (μ) should be introduced (see Eq. (5.48)), with which:

$$\frac{I}{I_0} = \exp(-\mu\rho l) \quad (11.28)$$

The material density measured by radiation absorption can be determined by solving Eq. (11.28) for (ρ) density. Other members of the equation are identical to the parameters found in Eq. (11.27).

Typical application fields of both thickness and density measurements are paper industry, metal sheet rolling, and plastic foil production as well as measuring and

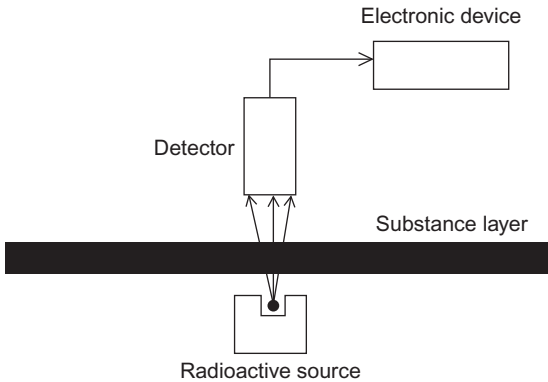


Figure 11.23 Material density determination based on radiation absorption.

continuous monitoring of the thickness of textiles, glass sheets, and laminated wooden sheets.

Industrial examples for the application of density measuring systems are:

- Density measurement of a streaming medium (such as crude oil, benzine, or petrol) in oil pipelines.
- Monitoring of chemical technology processes by measuring material density.
- Monitoring of efficiency in grinding machines by measuring the density of powder.
- Continuous monitoring of the density of materials transported on conveyors.

11.3.6 Moisture Content Determination

The best-known application of measuring methods based on neutron scattering and attenuation is moisture content determination, which relies on the special character of hydrogen as a neutron-scattering medium. When high-energy neutrons collide with hydrogen atoms, the former lose their energy and slow down. The rate of slowing down is great since the masses of the neutron and the hydrogen nucleus are similar.

If an Am-241/Be radiation source with activity of some GBq emitting fast neutrons and a detector sensitive only to slow neutrons are placed into the medium to be tested, the intensity of low-energy neutrons detected by the sensor will be proportional to the hydrogen content of the material tested (Figure 11.24).

The fact that hydrogen, but not water content, is determined must be taken into consideration because this method also measures, for example, chemically bound hydrogen in organic compounds or crystal water. The measurement is also disturbed by the presence of other neutron-absorbing elements (B, Cd) and modification of the composition with elements that have low atomic numbers (Cl, O, S).

For reliable measurement, a permanent consistency must be maintained. If the consistency of the material is changing, the density must be measured separately. Today, moisture-measuring instruments with two separate radiation sources (one is gamma, and the other is a neutron emitter) and two detectors, already performing density compensation, are available (Figure 11.25).

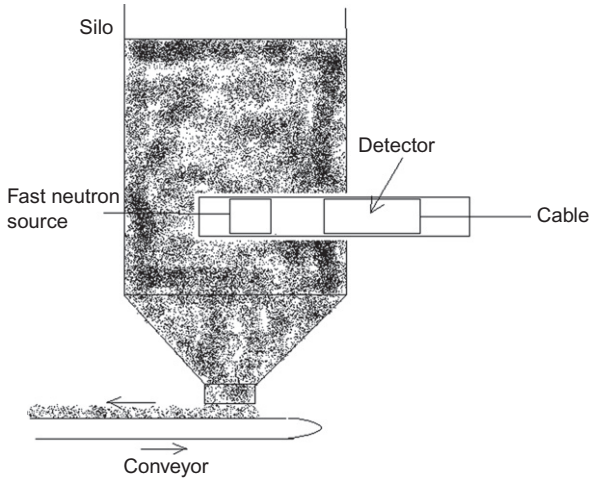


Figure 11.24 Moisture content measurement with a fast neutron source.

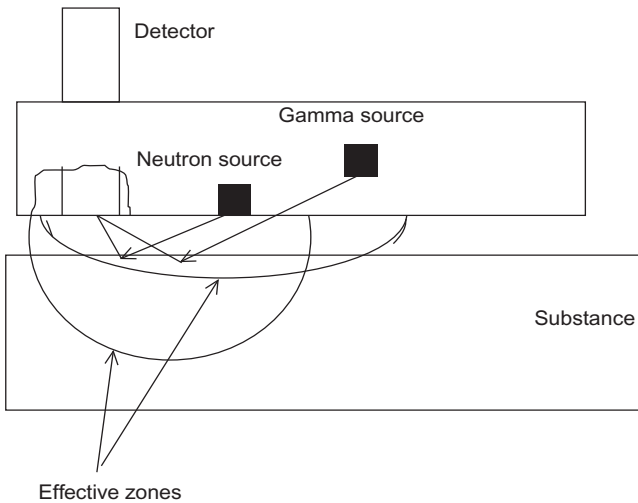


Figure 11.25 Moisture measurement with density compensation.

Nuclear moisture-measuring instruments operated with a neutron source are mostly used in foundries and in producing materials in industry for the sampling-free, quick, and accurate measurement of the moisture content of various mixtures and the consistency of additives.

Examples of industrial applications include the following:

- Water addition is determined in concrete panel factories by the continuous measurement of the moisture content of river sand (this is the component that has the highest moisture content, as compared to dry components).

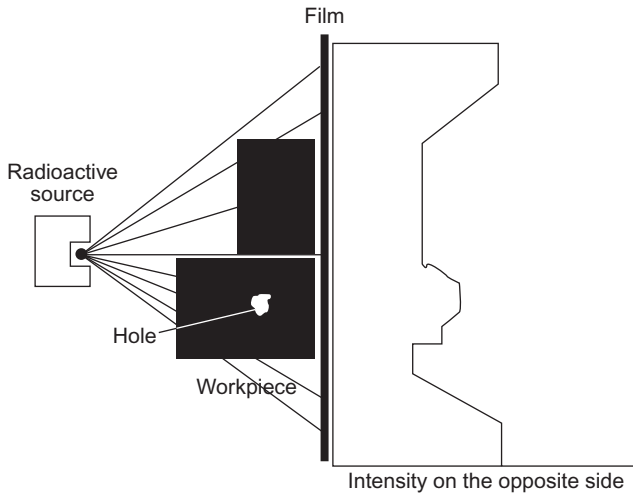


Figure 11.26 The intensity change of gamma radiation when penetrating a material containing inclusion.

- For determining the moisture content of soils, portable soil moisture-measuring instruments have been developed.
- Moisture content measurement is very important in road, railway, and basement construction.

11.3.7 Industrial Radiography

Radiography (discussed in Section 14.5.2) is a nondestructive material testing method using X-ray or gamma radiation to image internal parts, structural defects, or internal structures of nontransparent materials, parts, or equipment. The main application is testing defects of welding seams by means of a radiography record (radiogram).

To make a radiogram, ionizing radiation leaving the source through a collimator penetrates the workpiece placed in front of the beam and replicates the internal structure of the material on a film placed on the opposite side (Figure 11.26).

A container with a source-controlling device is called a “defectoscope,” which is a structure on wheels. Its control unit is suitable for transporting the shielding container within the pipe to the spot of the welding seam, and it has a pneumatic device to pull the source out of the container for the length of the exposition. Prior to the exposition, the welding seam is covered outside the pipe with high-resolution photo film (Figure 11.27). To test steel structures for wall thickness between 15 and 65 mm, Ir-192 is used; between 20 and 90 mm, Cs-137 is used; and between 40 and 150 mm, Co-60 is used.

By means of radiograms, gas intrusions, slag intrusions, metallic intrusions, binding defects, welding defects, cracks, and surface deficiencies can be visualized.

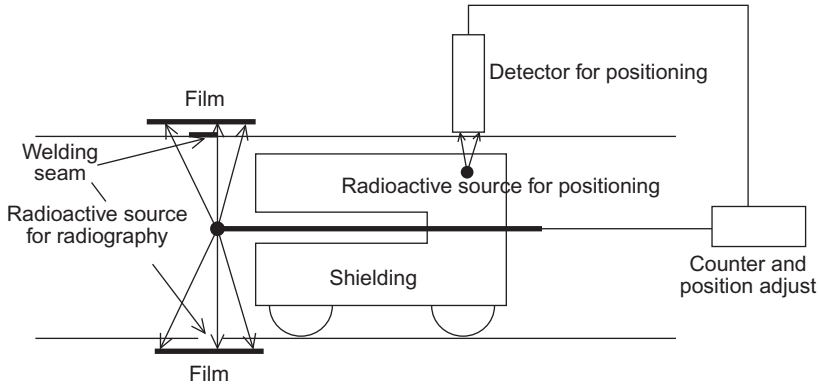


Figure 11.27 A self-propelled isotope container (defectoscope).

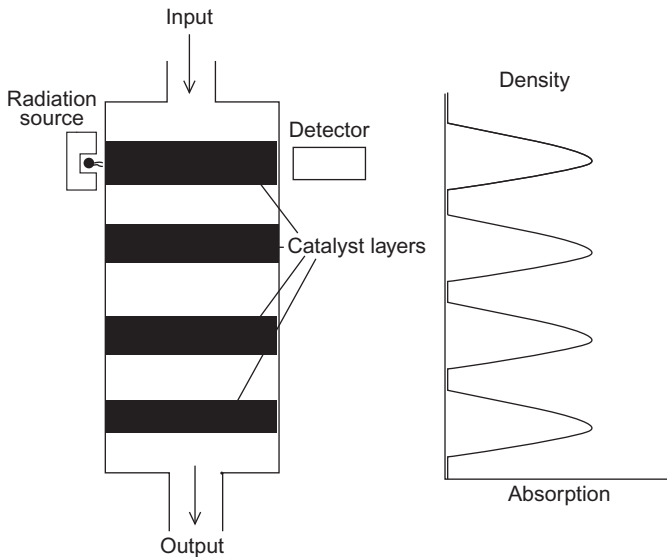


Figure 11.28 A visualized catalyzer bed tested with a gamma-transmission technique.

A modern variant of industrial radiography does not search for material defects; rather, its objective is to visualize volumes, arrangements, and phases of materials to monitor the operation of equipment.

Radiation absorption executed with parallel movement of the detector and a gamma radiation source requires simpler techniques (Figure 11.28). In more complicated cases, a high number of detectors is installed, surrounding the entire equipment.

The measuring technique based on transmitting the entire volume of equipment was used, e.g., for testing the cross-sectional density distribution of distillation

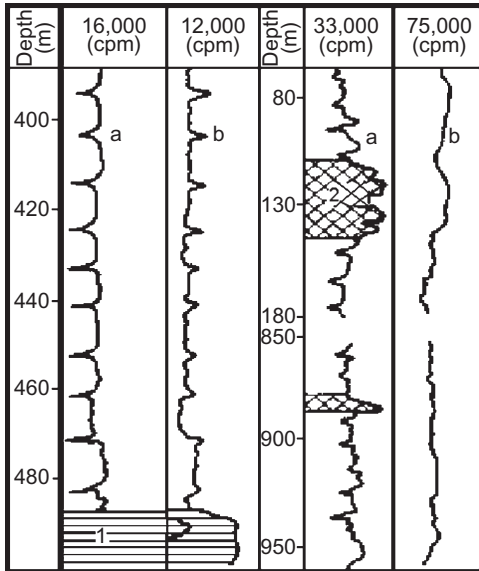


Figure 11.29 Natural gamma borehole logging.

columns where, in addition to the substance distribution on trays, the disposition of the steam and liquid phase and their relative volume rate were determined. In another case, a transmission study of a catalyzer bed was performed (Figure 11.28).

11.3.8 Geological Borehole Logging with Nuclear Methods

Nuclear methods for logging geological boreholes are used in the hydrocarbon and coal industries, in ore mining, and in water resource exploitation. The well-fitting detector is introduced into the borehole by means of a wellhead installed on a vehicle. The detected signals are transferred to the measuring instrument located on the surface of cables (Figure 11.29).

Three types of nuclear borehole measurements exist:

- Measuring the natural radiation in each layer.
- Tracking radiation excited with sealed radiation sources.
- Methods using radiotracers introduced into boreholes.

An excitation radiation source can be a sealed gamma source, sealed neutron source, or neutron generator. According to the type of the measured radiation, natural gamma logging, gamma-excited gamma-density logging, neutron detection, and NAA are distinguished. Methods applying open radioisotopes belong to tracer techniques.

Figure 11.29 shows depth distribution of the natural gamma radiation in an exploration of coal mine prospecting. Coal spots located among sandstone and marl layers represent higher gamma intensities.

A great benefit of nuclear borehole techniques is that they also serve data on the chemical composition of penetrated stones and then can be executed in natural

conditions where other methods are not successful. At the same time, their drawback is that they are more labor-intensive and require complicated measuring instruments and other equipment.

Further Reading

- Földiák, G. (1986). *Industrial Application of Radioisotopes*. Akadémiai Kiadó, Budapest.
- Charlton, J.S. (1986). *Radioisotope Techniques for Problem-Solving in Industrial Process Plants*. Leonard Hill, Glasgow and London.
- Rózsa, S. (1979). *Nukleáris mérések az iparban*. Műszaki Könyvkiadó, Budapest.
- Baranyai, L., and Ivicsics, F. (1990). *A talajvíz áramlási sebességének meghatározása. (Determination of flowing rate of groundwater.)*. *Vízügyi Közlemények* 32 (4): 399–400. Lapkiadó Vállalat, Budapest.

12 An Introduction to Nuclear Medicine

József Varga

Department of Nuclear Medicine Institute, University of Debrecen,
Debrecen, Hungary

Nuclear medicine applies *unsealed radioactive preparations* for medical purposes. A preparation is called “unsealed” if it can mix with its environment and may participate in both chemical reactions and biological processes.

Note that radioactive materials are applied in medicine as external and sealed radiation sources as well (Figure 12.1). The *cobalt gun* has been used extensively as an external source for radiation therapy of tumors (teletherapy). *Brachytherapy* involves treating a disease by exposure to a radioactive substance. Doctors place a small radioactive source (pellet or seed) in or a short distance from a malignant (e.g., cervical) tumor. Thus, high doses of radiation can be used while reducing the risk of damage to nearby healthy tissue and increasing the likelihood that the tumor is destroyed. The sealed source is then removed so that no radioactive substance is left in the patient’s body. Both teletherapy and brachytherapy belong to *radiation therapy* rather than nuclear medicine.

The basis of nuclear medicine is the *radiotracer* technique developed by György Hevesy (1885–1966) in 1924; he was awarded the Nobel Prize for chemistry for this achievement in 1943. The principle is that changing an atom in a molecule for its radioisotope will not significantly change its chemical and biological behavior, while the movement, distribution, and concentration of the molecule (and its derivatives) can be followed by measuring its radiation—even processes in a live human or animal can be studied using external radiation detectors. Modern devices allow the detection of such small amounts of the tracer that the function of the organ that we want to study is not affected (in contrast to some X-ray contrast materials). However, biological processes are so complicated that human applications require special considerations; see further details in Sections 12.4 and 12.6.

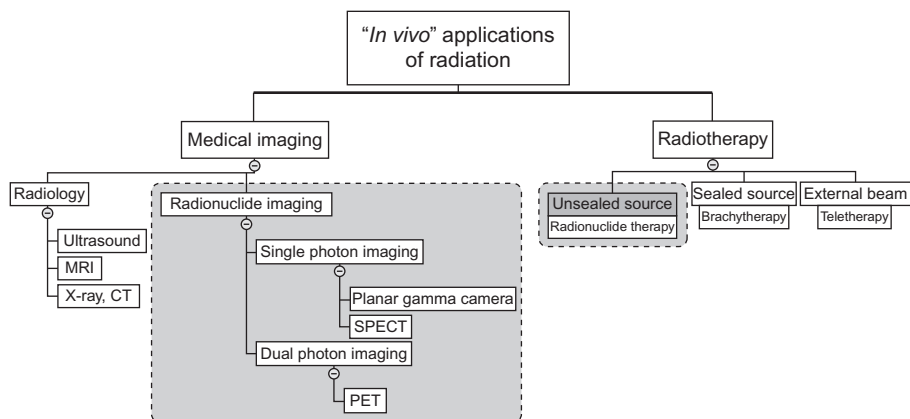


Figure 12.1 Medical applications of radiation. Gray areas indicate the fields of nuclear medicine.

12.1 Fields of Nuclear Medicine

There are three main fields of nuclear medicine.

12.1.1 In Vitro Diagnostics

The meaning of *in vitro* is “measurement in a vial.” In this case, the patient does not make direct contact with the radioactive material, but the sample (blood, urine, etc.) is taken and analyzed using a radioactive component; in most cases, the concentration of a constituent will be measured. The first such procedures were developed by Yalow and Berson (1959) to measure insulin and by Ekins (1960) to measure thyroxin concentrations in blood. *Rosalyn Yalow* was awarded the Nobel Prize for medicine in 1977 for developing several peptide hormone RIAs. For further details, see [Section 12.3](#).

12.1.2 In Vivo Diagnostics

The term *in vivo* refers to measuring or imaging the distribution of a radiopharmaceutical in a living organism. Such procedures have been known for a long time, but the most commonly used imaging device, the so-called *gamma camera* (see [Section 12.4.1](#)), was developed by *Hal Anger* in Berkeley in 1957. While the gamma camera detects single photons, the pair of photons emitted when a positron meets an electron (annihilation radiation, as discussed in [Section 5.3.3](#)) can also be imaged using a so-called PET (discussed further in [Section 12.6](#)).

12.1.3 Therapy with Unsealed Radioactive Preparations

If it is possible to deposit beta- or alpha-emitting radiopharmaceuticals into or close to the organ or tissue to be deactivated or destroyed, then this short-range radiation will affect only a few layers of cells, or, when evenly distributed in an organ, it will irradiate the targeted organ selectively. This procedure requires radiopharmaceuticals accumulating specifically in the target organ, and preferably nowhere else in the body.

12.2 The Role and Aspects of Applying Radiotracers in Medicine

Before we go into further details, we must first answer this question: what justifies the application of radioactive substances in medicine at all? Quite frequently, very low concentrations of substances have to be measured either in the body or in biological samples, or we have to follow the physiological or pathological metabolic, secretory, or excretory processes, making otherwise invisible phenomena observable by applying suitable tracers.

12.2.1 Comparison of Methods for In Vitro Measurement of Concentrations

Although more and more accurate laboratory (photometric, fluorometric, and enzymatic) methods had been developed for the measurement of concentrations in biological fluids, about two decades ago, there was still no method apart from RIA and immunoradiometric assay (IRMA; for more details about this, see [Section 12.3](#)), which were simple and cheap enough for routine measurements of concentrations in the nmol/L range.

Note that recently various “alternative” (nonradiotracer) methods have been introduced that have similar sensitivity to that of IRMA. However, *in vitro* nuclear diagnostic methods are still indispensable parts of laboratory medicine (and probably will be for a long time), primarily due to their low cost. (From an environmental point of view, the waste produced by the alternative assays is no less hazardous than the radiotracer.)

12.2.2 Measurement of Tracers and Contrast Materials Inside the Organism by External Detectors

A crucial point of imaging methods is the amount of the contrast material or tracer necessary for obtaining a reasonable image quality (see [Table 12.4](#)). For example, if a contrast agent is used to enhance X-ray imaging, the amount needed may have physiological effects, and it may activate defense mechanisms (induce an immune reaction) or saturate a secretion channel. In contrast, we need such a small number

of molecules of a radiotracer that it will not change or influence the studied function.

The radiotracers used for the *in vivo* diagnostic and therapeutic procedures of nuclear medicine are called *radiopharmaceuticals* (i.e., medicines that emit radiation). In fact, these are not medicines in the traditional sense since they do not have any effect on the patient as chemicals due to their extremely low concentrations. However, similar to normal pharmaceuticals, strict rules apply for tests to be carried out before they are allowed to be administered to humans. Moreover, their radiation may have biological effects—that is what we use for radioisotope therapy.

In general, we use molecules that either are present in the body anyway in their unlabeled form or behave similarly to those present. In this way, we can image and/or study the undisturbed function.

12.2.3 Production of Artificial Radionuclides

For medical applications (explained in later chapters), we usually need rather short-lived radionuclides that have to be artificially produced because we cannot separate them economically from natural sources. We can produce radioactive materials in the following ways (also see Chapter 8):

- In *nuclear reactors*, where irradiation channels are formed through the nuclear reactor shield to put the target in the way of high neutron flux. The neutrons induce nuclear transformations.
- The other possibility is to use accelerators, especially *cyclotrons*, invented by Ernest Lawrence (1901–1958) at Berkeley, who was awarded the Nobel Prize in physics in 1939. In 2005, there were about 130 cyclotrons in the European Union, 80% of which were dedicated to routine medical radioisotope production.
- The daughter element of a radionuclide may also be radioactive; this fact is utilized in *radioisotope generators* (see later in this chapter and Section 8.7.1.4).

From a practical point of view, the most important difference is that radioisotopes produced in nuclear reactors are usually cheaper than cyclotron products. We shall list some other aspects next.

12.2.4 How Do You Choose Radiotracers for Medical Applications?

The range (path length) of various types of radiation in body tissues primarily determines the areas of possible application. Body tissues are practically water equivalent at the gamma energies used for imaging (see [Tables 12.1 and 12.2](#)).

12.2.4.1 Selection of Radionuclides for Imaging

- Only electromagnetic radiation (gamma- or X-rays) can be detected from outside the patient's body, as beta radiation (and alpha even more) is adsorbed in a few millimeters of body tissue at most ([Table 12.1](#)).

Table 12.1 Maximal Range of Particles

| Particle | In Air | In Water or Body Tissue |
|--------------------|--------|-------------------------|
| Alpha | ~ cm | <0.1 mm |
| Beta | ~ m | 1–10 mm |
| 10–20 MeV electron | ~ 10 m | ~ cm |

Table 12.2 Half-Value Layer for Different Gamma-Ray Energies (in cm)

| Medium | 100 keV | 200 keV | 500 keV |
|--------|---------|---------|---------|
| Air | 3555 | 4359 | 6189 |
| Water | 4.15 | 5.1 | 7.15 |
| Lead | 0.012 | 0.068 | 0.42 |

- Besides, gamma energy should be in the range of 60–500 keV. The majority of lower-energy photons will be attenuated inside the patient's body, while higher-energy photons most likely fly through the detector without any interaction; the counting efficiency is low in both cases.
- An important aspect is the half-life of the radionuclide: several hours (or a few days in some cases) are preferred, so that radioactive material will disappear from the patient's body shortly after the imaging is completed, thus limiting the radiation dose. If a shorter-lived radionuclide was used, a large proportion of the radioisotope would decay during the procedure of labeling the selected molecule, thus increasing the cost of production.
- If the radionuclide also emits alpha or beta radiation, they unnecessarily increase the patient's radiation dose while not contributing to image formation.

12.2.4.2 Are There Radionuclides Emitting Exclusively Electromagnetic Radiation?

As a matter of fact, gamma emission always results from some other form of nuclear transformation (as described in Section 4.4.6). However, there are two cases when the emission of photons is separated from the preceding nuclear transformation either in time or in space, so the patient's radiation exposure is limited to that of photons:

- The atomic kernel may get into a *metastable* (excited in contrast to ground) state after beta decay, from which it can later decay to the ground state by emitting gamma photon (s). We need to separate the metastable element from the parent radionuclide with a suitable solvent and administer it to the patient after binding it to a selected molecule.
- *Electron capture* is a special case of positive beta decay, in which (instead of emitting a positron) the kernel captures an electron from the K shell, thus reducing the atomic number (the number of protons; see Section 4.4.3). This can be accompanied by emitting gamma photon(s) as well, but more importantly, an electron from a higher-energy state

will always “drop” into the hole left in the K shell, emitting the energy difference between the two shells in the form of characteristic X-rays. In the case of heavier atoms, the photon energy may be high enough to allow imaging by a gamma camera (see Section 12.2.5).

12.2.4.3 Chemical Limitations

Besides the physical requirements listed previously, we can utilize a radionuclide only if a suitable molecule can be labeled with it. There are very important classes of molecules in the body that are so small that we cannot label them with any gamma-emitting radioisotope without altering their structure, i.e., they do not contain any atom with a suitable gamma-emitting radioisotope, so we could label them only by attaching a group of atoms that would significantly change their biological behavior.

Fortunately, there is another possibility for labeling many biologically important molecules: applying positron emitters (see Section 4.4.2). There are positron-emitting radioisotopes of the most important constituents of organic molecules: carbon, oxygen, nitrogen, and fluorine (see Table 12.6).

12.2.4.4 The Use of Positron Emitters for Imaging

When a positron leaves the atomic nucleus, after traveling along a short path (a few millimeters at most, along which it can ionize or excite other molecules or atoms), it will inevitably collide with an electron, resulting in the annihilation of both. Their combined energy will be transferred to two gamma photons (each having approximately 511 keV of energy) that will fly in almost opposite directions (as described in Section 5.3.3). In this way, positron decay results in gamma radiation that can be detected easily; moreover, we can utilize the coincidence detection of the pair of photons traveling in opposite directions to identify the line of their source and thus to enable the imaging of the tracer’s distribution.

12.2.4.5 How Do You Select Radionuclides for In Vitro Applications?

The demands of *in vitro* isotope diagnostic procedures are different from those of imaging as follows:

- A longer half-life is desirable, so labeled products can be stored for a longer time.
- A wider range of radiation energy is acceptable. A lower gamma energy is even preferable so that the staff dose can be decreased. The reason is that we can ensure the same measurement geometry of the radioactive specimen (see Chapter 14), i.e., both the standards and the samples are in the same type of (plastic) vial, volume, and medium. Therefore, the attenuated fraction of the radiation is the same, and the accuracy of the measurement is not reduced. Iodine-125 is the radionuclide most frequently used for *in vitro* diagnostic procedures.
- For concentration measurements, beta emitters can also be used, but for this procedure, a special measuring technique, the so-called *liquid scintillation counting*, is required, as beta radiation is absorbed in the sample and its vial, so we cannot use an external radiation detector to measure it (see also Sections 5.3.4, 5.3.5, and 14.2.1).

12.2.4.6 Liquid Scintillation Counting

The sample is mixed with a liquid scintillator that converts beta radiation into light, which can be detected using photomultiplier tubes (PMTs). Unfortunately, there are various factors that may interfere with the conversion of decay energy emitted from the sample into light photons reaching the PMTs, which usually reduces counting efficiency. This process is called *quenching* and should be corrected. We usually encounter three major types of quenching:

- *Photon quenching* occurs with the incomplete transfer of beta particle energy to solvent molecules.
- *Chemical* (sometimes called “impurity”) quenching causes energy losses in the transfer from solvent to solute.
- *Optical or color quenching* causes the attenuation of photons produced in the solute. For example, plasma samples contain many different substances in variable amounts, so each sample may absorb light to a different extent.

We can estimate the quenching effect by applying external or internal standards or by using multiple energy channels.

12.2.5 Types of Electromagnetic Radiation

Gamma radiation belongs to the family of electromagnetic waves. We utilize electromagnetic waves of different energies (i.e., frequencies) every day, as shown in Figure 12.2.

The quantum of any kind of electromagnetic radiation is called a “photon.” Photons have both wave and particle properties (“wave–particle duality”). Photons

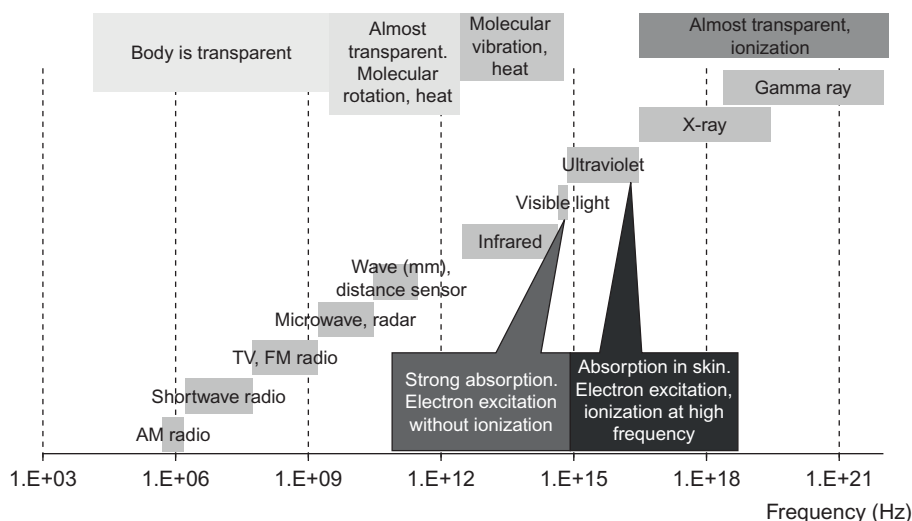


Figure 12.2 The electromagnetic spectrum and interactions with body tissue.

show wave-like phenomena, such as refraction by a lens, and destructive interference when reflected waves cancel each other out. On the other hand, it is regarded as a particle with zero rest mass and charge, unit spin, and energy equal to the product of the frequency of the radiation and the Planck constant.

12.2.5.1 What Is the Difference Between Gamma- and X-Rays?

If we encounter a photon with, for example, 80 keV energy, there is no way to tell whether it is an X-ray or a gamma photon because the names refer to the origin of the photon: X-rays always come from the electron shells, while gamma rays originate from the nucleus.

Since there is a wide energy range (up to ~ 100 keV) where both gamma- and characteristic X-rays can occur, the devices for detecting gamma rays are also capable of measuring X-rays of the same energy. So the gamma camera might also be called “electromagnetic camera”; for instance, when using thallium-201 for imaging, which decays with electron capture, actually we mainly detect its characteristic X-rays between 68 and 85 keV.

Note that the number of photons detected by a gamma camera and an X-ray device is different by several orders of magnitude. So a gamma camera would be blinded by a regular X-ray generator, while the radiation of a patient injected with 600 MBq of a Tc-99m-labeled radiopharmaceutical would be under the detection limit of a standard medical X-ray detector.

12.2.6 Most Common Radionuclides in Nuclear Medicine

From the radionuclides used for medical applications (shown in [Table 12.3](#)), the (metastable) technetium-99m (Tc-99m) is the most commonly used with a share of

Table 12.3 Radionuclides Used Frequently for Medical Purposes

| Nuclide | Decay Mode | Photon Energy (keV) | Half-Life | Applications | Production |
|---------|------------|---|-----------|----------------------------------|------------|
| Tc-99 m | IT | 141 | 6 h | Many | Generator |
| Tl-201 | EC | 167 (γ -rays) 65–82 (X-rays) | 73 h | Myocardial perfusion | Cyclotron |
| I-131 | β | 364 | 8 days | Thyroid (+ therapy) | Reactor |
| I-123 | EC | 159 | 13 h | Thyroid; proteins | Cyclotron |
| Ga-67 | EC | 93, 185, 300 | 78 h | Tumor; inflammation | Cyclotron |
| In-111 | EC | 172 | 67 h | Tumor; immunoscintigraphy | Cyclotron |
| F-18 | β^+ | a.r. | 109 min | Glucose metabolism <i>PET</i> | Cyclotron |
| I-125 | EC | 27–35 | 60 days | <i>In vitro</i> (in kits) | Reactor |

EC, electron capture; IT, isomeric transition; a.r., annihilation radiation.

about 80% since it optimally meets the previously mentioned requirements, having a gamma energy of 141 keV and a half-life of 6 h. Last but not least, it is a generator product.

12.2.6.1 Radioisotope Generators

We have to face two contradicting requirements: we should administer short-lived radionuclides to patients (as discussed in [Section 12.2.4](#)), while radioisotopes are generally produced either in a nuclear reactor or by an accelerator, in most cases far from the location of the application. The best solution is the use of radioisotope generators, in which case its longer-lived radioactive parent element is transported. For example, to produce Tc-99m, its parent element, molybdenum-99, is used. A key point of a generator is a suitable solvent that selectively dissolves the daughter element from a porous column, but not the parent element. Fortunately in the Mo-99→Tc-99m generators, physiological saline (NaCl) can be used as a solvent, so that the eluate is suitable for intravenous injection. (In other cases, we are not so lucky. For instance, before gamma cameras came into general use, indium-113m generators applied hydrochloric acid as an eluent that had to be neutralized before being administered to a human.)

12.2.6.2 Other Radionuclides

- Besides Tc-99m, Tl-201 as thallium chloride and Ga-67 in the form of gallium citrate are commonly used for gamma camera imaging.
- From among the radioisotopes of iodine, I-131 was first applied for imaging (see [Table 12.3](#)), but it has serious drawbacks: its gamma energy (with the highest peak at 364 keV) is too high, and its half-life (8 days) is longer than is generally desirable for imaging. Moreover, it is a beta emitter as well, increasing its radiation dose; that is why it is mainly used today for therapeutic purposes (and to measure iodine uptake before the therapy of hyperthyreosis). Iodide injected into the circulation primarily accumulates in the thyroid, which explains its application in measuring and imaging thyroid function already from the first half of the twentieth century (see more in [Section 12.5.1](#)). Sodium iodide labeled with I-131 was the first and is still the most common radioactive substance used for therapy, utilizing its beta radiation. Hyperthyreosis and thyroid cancer are the main indications.
- Another common radioisotope of iodine is I-123, as its 159 keV gamma energy and 13-h half-life make it a close runner-up after Tc-99m for use in gamma imaging. However, it is a cyclotron product, like Tl-201 and Ga-67, which makes it rather expensive.
- Radioisotopes of iodine, built into tyrosine, are suitable for labeling various protein molecules. For *in vitro* concentration measurements, I-125 is most commonly used. Its characteristic X-rays around 27 keV and gamma peak at 35 keV lead to a relatively low personnel dose, while its 60-day half-life allows a longer time for usage. In practice, it can only be used for about 6 weeks after labeling since radiolysis (chemical decomposition caused by radiation) degrades the radiochemical purity of the preparation (the percentage of the radionuclide in the desired chemical form).

12.3 *In Vitro* Diagnostics with Radioisotopes

Most isotope diagnostic methods for concentration measurement belong to the family of “*protein binding assays*.” Generally, they have the following main components:

- The specimen from which the concentration of a constituent (L, “ligand,” “analyte,” or “antigen”) is to be measured.
- A substance (e.g., antibody, Ab) specifically binding the ligand (L).
- A tracer, which can be either:
 - The labeled version of the ligand (L*, in case of competitive assays) or
 - A second, labeled antibody (Ab*, in excess amount) against the ligand to be measured.
- A method to separate the bound and free tracers.

In *immunoassays*, the specific binding material is a monoclonal or polyclonal antibody. Labeling may use a radioisotope, enzyme, chemiluminescent, or fluorescent tracer.

Immune binding reactions are greatly influenced by a number of conditions (temperature, reaction times, pH, etc.); therefore, standards with known concentrations of the analyte are included in each series of measurements. A *calibration curve* based on these standards is used to calculate the concentration from the signal measured from an unknown sample.

In practice, various combinations of tracers, labeled components, competitive or sequential reactions, limited or excess amounts of components, and separation methods are used. The basic principles of the two most widespread methods are summarized next.

12.3.1 *Basic Reaction of Immunoassays*

This method is also known as saturation or displacement analysis:

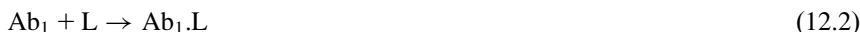


The analyte to be measured (L) and its labeled version (L*) compete for occupying a limited number of binding sites (Ab). The labeled component may be added some time later. The more (unlabeled) analyte is present in the reaction mixture, the less labeled ligand will be bound. The last step is the separation of bound from free ligand. If a radioactive tracer is used, the method is called *radioimmunoassay* (RIA). RIAs were first introduced in the 1960s by *Yalow* and *Berson* for insulin and by *Ekins* for thyroxin. The precise measurement of minute amounts of such a hormone was considered a breakthrough in endocrinology; *Rosalyn Yalow*, a biophysicist, received the Nobel Prize in medicine for the development of RIAs of peptide hormones in 1977.

The accuracy of a RIA is limited by both the competitive nature of the reaction and the efficiency of the separation method applied.

12.3.2 Immunometric (“Sandwich”) Assay

This is a sequential, double-antibody technique:



The first, *catcher* antibody (Ab_1) is usually fixed to some solid phase (the wall of the vial, spheres, pearls, etc.). After reaction (12.2), unbound ligand is washed off, and then a second, *tracer* antibody (Ab_2^*) is added that binds to the ligand molecules present and already fixed. The amount of the bound fraction of Ab_2^* increases with the ligand (L) concentration. Free Ab_2^* is washed off as well.

Sandwich methods usually apply excess amounts of the reagents as they are based on the occupation of, rather than competition for, the binding sites. Such methods allow fast, sensitive, and specific measurements. When applying radioactive labeling, the method is called *immunoradiometric assay* (IRMA). The accuracy of IRMA methods is superior to that of RIA and similar to the “alternative” methods that do not apply radioactive tracers.

12.4 Radionuclide Imaging

The main field of nuclear medicine today is imaging with gamma cameras. What can justify the *in vivo* use of radioactive preparations delivering radiation dose to humans? Other generally applied modalities of medical imaging, including ultrasound, X-ray, and X-ray computed tomography (CT), and most routine procedures of magnetic resonance imaging (MRI) are *structural* imaging methods. A pathological process is visible in these images only when it has already caused structural changes. For instance:

- The borders between tissues of different acoustic impedance (determined by the elasticity and density) can be seen in ultrasound images. An abnormal process will be visible only when it has already altered the structure of the tissue.
- X-ray (including CT) images will distinguish tissues with different radiation attenuation, i.e., density. The easiest is to differentiate solid bones from soft tissues.

On the contrary, by applying radioactive tracers, we can follow the accumulation, secretion, metabolism, and excretion process of various molecules, so that a pathological process can be identified even in an early stage, when the structure of the investigated organ is not yet significantly different from its normal state. That is why the imaging methods of nuclear medicine are considered *functional* rather than anatomical.

Moreover, much smaller molar concentrations of radiotracers can be detected than the usual concentrations of contrast materials used for structural imaging

Table 12.4 Concentration of Contrast and Tracer Materials Used for Medical Imaging

| Imaging Modality | Concentration (mol/kg body mass) |
|--|----------------------------------|
| Ultrasound | 10^{-3} |
| CT | 10^{-3} |
| Gamma camera (planar and SPECT) | 10^{-9} – 10^{-12} |
| PET | 10^{-9} – 10^{-12} |
| MRI | 10^{-5} |

Table 12.5 Distribution of Gamma Camera Imaging Procedures in the United States (2006)

| | |
|----------------------|-----|
| Myocardial perfusion | 56% |
| Other cardiac | 4% |
| Bone | 17% |
| Liver, hepatobiliary | 7% |
| Lung | 4% |
| Thyroid, parathyroid | 3% |
| Kidney | 3% |
| Infection, abscess | 2% |
| Tumor imaging | 2% |
| Other | 2% |

(see [Table 12.4](#)); thus, the application of a radiotracer does not interfere with or change the function of the organ investigated.

PET studies contribute about 6% to nuclear medical imaging, and the distribution of gamma camera studies depends on both health-care protocols and the reimbursement policy of a country (see [Table 12.5](#) and [Figure 12.3](#)).

12.4.1 Parts of a Gamma Camera

In this section, we describe the main components of a “traditional” Anger camera: a gamma camera with analog signal processing ([Figure 12.4](#)).

1. The *collimator* is a sheet or disc made of lead, containing (mostly parallel) holes. Radiation arriving from the patient’s body can get across it only along the holes (i.e., in a perpendicular direction); otherwise, the septa of the holes will absorb it. As a result, the “image” of a point source will be a small spot on the crystal. The spatial resolution of the camera is primarily determined by the collimator.
2. The *special scintillation detector* is generally a thallium-activated sodium iodide [NaI(Tl)] monocrystal, which is rectangular or circular in most cases. For imaging the 141 keV gamma radiation of Tc-99m, the crystal thickness is around 9 mm. Gamma photons hitting the crystal will produce light in a process called “scintillation.”

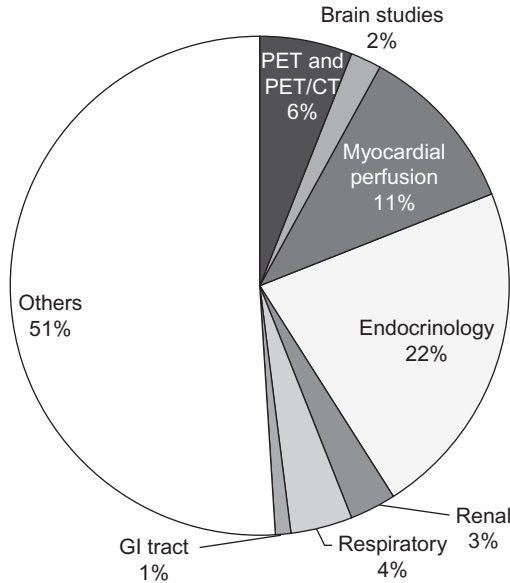


Figure 12.3 The distribution of nuclear medical imaging procedures in Europe. Source: *Status of Nuclear Medicine in Europe—2009*. EANM, Vienna, 2010.

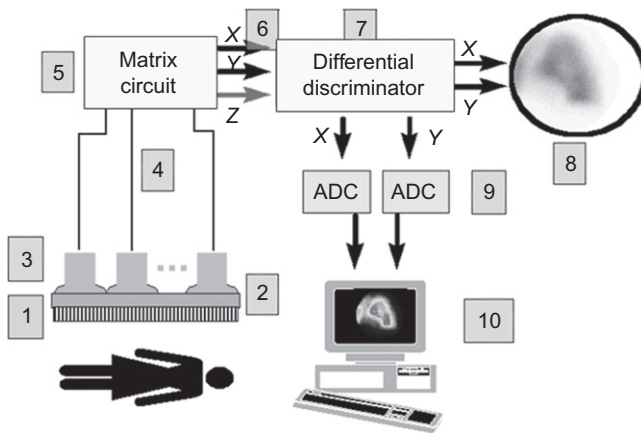


Figure 12.4 Components of an analog gamma camera. (See explanation of numbered parts in the text.)

3. There are many (19–100) *photomultiplier tubes* (PMTs) attached to the crystal. Each of them responds to the light, and those closer to its source produce larger electric signals than the distant ones.
4. The output signals of all PMTs are forwarded to the *matrix (or Anger) circuit*.

5. It calculates the X and Y coordinates, and a Z signal proportional to the energy of the original gamma particle.
6. The three signals (X , Y , and Z) are interfaced to a *differential discriminator*.
7. The discriminator selects only the signals in a specified narrow (15–20%) energy window; in this way, Compton-scattered radiation can be partly removed from the image.
8. In older cameras, a *persistent scope* helps to position the patient.
9. *Analog–digital converters* (ADCs) will form numbers from the X and Y signals.
10. A computer will form a *digital image* from the signals. Each picture element (pixel) contains the number of photons detected in the corresponding small (square) area of the detector. We then display, process, and store these digital images.

12.4.2 Digital Gamma Cameras

Digital image processing plays a more and more important role in the development of gamma cameras.

- Modern gamma cameras apply real-time, position-dependent digital corrections to compensate for various degrading factors, such as differences in signal amplification (*energy correction*), geometric distortions (*linearity correction*), and the remaining differences in sensitivity (*uniformity correction*).
- So-called *full digital cameras* digitize the output of each PMT directly, and then all the rest of the processing, including the calculation of coordinates and corrections, is done by the computer.

12.4.3 Methods for Emission Imaging

To distinguish from the medical imaging modalities that measure the attenuation of radiation originating from an external source, called *transmission imaging* (e.g., conventional X-ray radiography and CT), the imaging of radiation emitted by radiopharmaceuticals inside a patient's body is generally referred to as *emission imaging*.

- *Static scintigraphy*: images from one or several views are acquired after the distribution of the radiopharmaceutical reaches equilibrium.
Static imaging was possible even before the gamma camera was invented, using a radiation detector that scanned the target organ, having a print head yoked to it.
- For *dynamic imaging*, a series of images from the same view is taken, following the process of accumulation, secretion, or excretion of the radiopharmaceutical. Besides obtaining the distribution at different points in time, we can investigate how the radioactivity concentration of any region changes with time.
- *Whole-body imaging* means linking several static images by the computer to show an area bigger than the field of view. A large-field-of-view gamma camera generally covers the width of a patient's body, and we need three to five steps to scan its length. See details of this process later in this chapter.
- The last and most powerful way of imaging is *tomography*, when the distribution of the radiopharmaceutical in various sections of the body is calculated from measurements of many projections. Consecutive slices together represent a three-dimensional distribution:
 - *SPECT* (single photon emission computed tomography) applies gamma emitters, while
 - PET utilizes positron emitters (see [Section 12.6](#)).

12.4.4 Computer-Aided Processing of Nuclear Medical Images

We generally process the data representing the distribution of radiopharmaceuticals with the help of computers. Computers are applied to achieve the following:

12.4.4.1 Enhancing Image Quality

When images are recorded directly to film, depending on the brightness setting of the oscilloscope, they may be over- or underexposed and that cannot be corrected afterward. On the contrary, digitized images allow the best possible contrast in any subarea to be selected by using different color or grayscale palettes.

Image filtering may be applied to suppress the noise and thus enhance the signal-to-noise ratio.

12.4.4.2 Obtaining Quantitative Results

For instance, quantitative comparison of the activity uptake of left and right organs or lobes is possible. [Figure 12.5](#) demonstrates how we measure relative kidney function.

12.4.4.3 Information Extraction

A dynamic image series may contain a huge amount of information. During a hepato-biliary study, for example, 110–120 images are typically taken, each represented by a 128×128 matrix—a matter of nearly 2 million numbers that is impossible to analyze entirely by the human eyes. We need computers to extract useful information from the raw data that can be related to the function of the investigated organ. [Figure 12.6](#) demonstrates the possible solutions:

- By drawing the contours of the organs (ROI = “region of interest”), time–activity curves from the counts inside these regions are generated, and some parameters are calculated from them.
- Alternatively, we may calculate a parameter from the time–activity curve of each pixel, reinsert its value to the respective element of a matrix, and display the resulting “parametric image” as a pseudocolor image.

The two methods can also be combined: parametric images may help with outlining the appropriate regions.

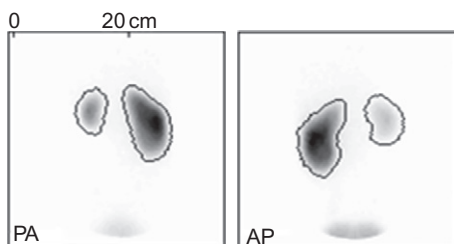


Figure 12.5 Split renal function calculated from the geometric mean of the posterior (PA) and anterior (AP) images (left: 14%, right: 86%).

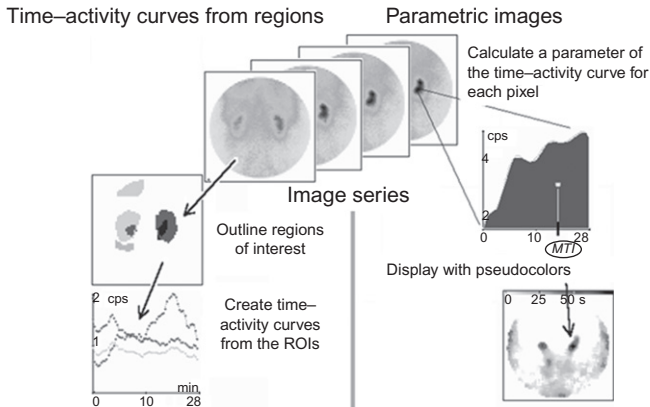


Figure 12.6 Methods for processing a dynamic image series. (Images of the kidneys are shown.)

12.4.4.4 Archiving

Traditionally, X-ray films were used to display and archive medical images; however, this method is rather expensive. Nowadays, it is cheaper by two orders of magnitude to archive the image series of nuclear medicine on CD or DVD.

12.4.4.5 Composing Whole-Body Images

As mentioned earlier, we may put together separate images to form a single whole-body view, without borderlines. However, this method works only for cameras with a rectangular field of view.

There is another way to construct whole-body images: by moving the table continuously, synchronized with the slab of the image matrix to where the acquired counts are added. (If the field of view is not rectangular, we have to correct for the differences in the effective acquisition time of each pixel.)

12.4.4.6 Reconstruction of Spatial (3D) Distribution

We already mentioned “*tomography*” (which means “slice imaging”) in [Section 12.4.3](#). The mathematical procedure that calculates the distribution of cross sections from raw projections is called *reconstruction*.

In SPECT, the gamma camera detector(s) is moved on a 180° or 360° arc around the patient’s body and acquires 30–128 projection images of the distribution of the radiopharmaceutical (see [Figure 12.7](#)). The movement (either continuous or “step and shoot”) is computer controlled.

There are advantages and disadvantages when comparing SPECT to X-ray transmission tomography (CT).

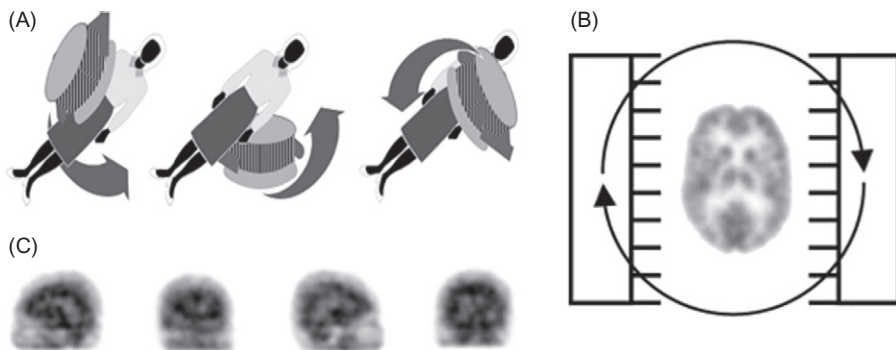


Figure 12.7 The principle of SPECT data acquisition. (A) The detector(s) rotate around the patient. (B) With a dual-head camera, each detector covers 180° . (C) Many projection images are acquired. (Four of the brain projections are shown.)

12.4.4.7 Advantages of SPECT over CT

- Like all gamma camera methods, SPECT allows functional rather than structural imaging.
- We obtain images of a wide zone at once (the field of view is typically 30–40 cm along the body), so many slices can be reconstructed at once—and then slices in any slanting direction as well.

12.4.4.8 Limitations of SPECT

- As with gamma camera imaging in general, spatial resolution is relatively bad.
- Images are noisy because of the statistical nature of radioactive decay.
- Radiation attenuation occurs inside the patient's body, and its extent depends on the depth of the organ as well as the structure of its environment.
- Radiation originating from an organ may scatter in the surrounding tissues, and the scattered photons may also be detected, further degrading spatial resolution.

12.5 Some Examples of Gamma Camera Imaging Procedures

Now we shall present some examples when gamma imaging has particular importance (see [Table 12.5](#)).

12.5.1 Thyroid Scintigraphy

A significant part (normally 15–25%) of iodine will be trapped in thyroid cells from the circulation, and stay there for a long time (in healthy persons it will drop to half in about four months). It will be built into tyrosine, which is converted to the thyroid hormones thyroxin (T_4) and triiodo-L-thyronine (T_3). Per technetate (obtained directly from a technetium generator) gets trapped in the thyroid the

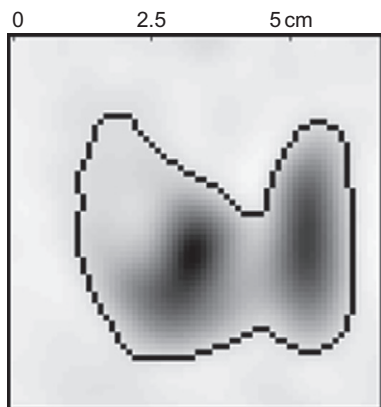


Figure 12.8 A “cold” thyroid nodule at the upper pole of the right lobe.

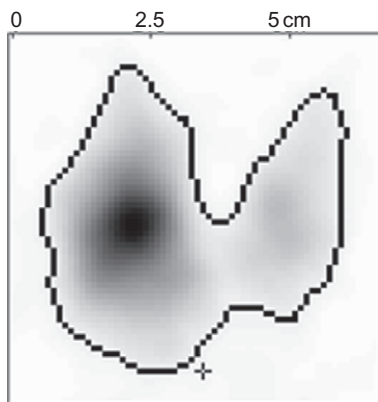


Figure 12.9 A “hot” thyroid nodule in the right lobe (anterior view).

same way, but—as it cannot be built into organic molecules—it will be washed out faster. Both can be used for thyroid scintigraphy, most frequently in order to clarify the functional status of nodules that were palpated or visualized by ultrasound. While some benign and malignant tumors accumulate less radiopharmaceutical than the normal thyroid tissue (“cold” nodules; see [Figure 12.8](#)), in the so-called autonomous adenomas there will be high accumulation, escaping the regular feedback mechanism ([Figure 12.9](#)).

12.5.2 Tumor Imaging

It is a common misunderstanding that nuclear medicine is mainly about tumor imaging. In fact, we search for tumors in about half of all investigations. Unfortunately, we do not have a single optimal method for tumor imaging; however, the methods of nuclear medicine are particularly powerful for many tumor types and able to answer many questions. Today, the PET/CT study of glucose



Figure 12.10 A whole-body bone scintigram with metastases in the vertebrae, skull, and hip (posterior and anterior views).

metabolism is considered the most effective for a wide range of tumors (see [Section 12.6](#)).

For many decades, the most common imaging method in the field of nuclear medicine worldwide has been *bone scintigraphy*. Radiolabeled diphosphonates accumulate in the bones proportionally to bone formation (osteoblast activity). As a consequence, bone metastases of various tumors show an increased uptake of Tc-99m-labeled diphosphonates (see [Figure 12.10](#)). Detecting bone metastases is very important since many of the most common tumors (e.g., lung, breast, and prostate) often have their metastases in the bones, and their early detection may influence the method and prognosis of the therapy applied substantially. Bone scintigraphy may visualize metastases in an earlier phase, months before X-ray images, as the latter detect only an abnormality that has already caused significant changes in the structure and calcification of the bones.

Note that gamma camera images from the anterior and posterior views are different (see [Figure 12.10](#)), resulting from the attenuation of radiation inside the body. (For example, the half-value layer of the 141 keV gamma radiation of Tc-99m is 4.6 cm in body tissue.) In bone scintigrams, the bones closer to the back surface of the body (e.g., the spine and back ribs) are better seen (brighter) from the posterior, while those closer to the frontal surface (e.g., the sternum and the frontal edge of the hip bone) are more prominent from the anterior view.

12.5.3 Myocardial Perfusion Scintigraphy

The most common method of emission tomography in the world is myocardial perfusion SPECT. The reason is that cardiovascular diseases are the leading causes of death (ahead of tumors), especially in highly industrialized countries (WHO, 2004). It is crucial to identify the cases in which the plaques in coronary arteries cause such a serious stenosis that revascularization (either by angioplasty or by bypass graft surgery) is necessary.

The principle is that stenosed coronary arteries cannot dilate on demand (e.g., when the patient performs physical exercise or takes vasodilator medicine) as healthy coronary arteries do. During exercise, the relative perfusion of myocardial regions may be different from when at rest. If the myocardium evenly perfused in a resting state shows a relatively hypoperfused area after stress, it indicates ischemia (a relative shortage of the blood supply) (see [Figure 12.11](#)). The patients suffering from active ischemia are those whose cardiac pumping function will probably improve after revascularization, and who are at risk of further cardiac events if left untreated. For myocardial perfusion SPECT, we most frequently use Tc-99m-labeled methoxy isobutyl isonitrile (MIBI) or tetrofosmin, and less frequently thallium chloride labeled by the potassium-analog Tl-201.

12.5.4 SPECT Imaging of Epilepsy

The second most frequent type of SPECT study is brain perfusion imaging, for similar reasons as those described at the beginning of the previous section. Although brain SPECT is used to assess several types of abnormalities of cerebral circulation, an especially difficult task is to investigate epilepsy. The problem is that the patient usually cannot remain still during seizure, so it is hard to take images of any kind. However, the radiopharmaceutical HMPAO (^{99m}Tc -D, L-hexamethylene-propylamine oxime) reaches an equilibrium distribution in the brain in only 1–2 min after injection, and then the distribution does not change for several hours. So if we succeed in administering HMPAO during seizure, we may take images 1–2 h following the seizure, when the patient is able to lie still for 20–30 min. An epileptic focus is hyperperfused during seizure, while it is hypoperfused in an interictal state.

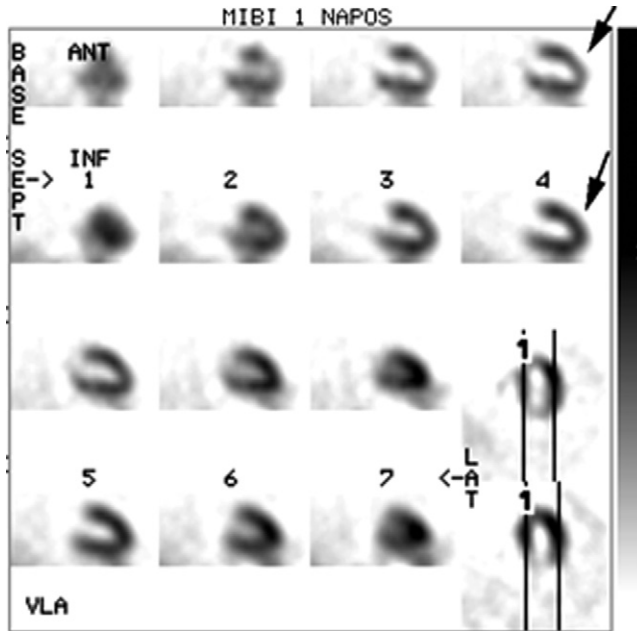


Figure 12.11 Myocardial perfusion imaging with Tc-99m MIBI; vertical slices parallel with the axis of the left ventricle are shown. Rows 1 and 3: stress images, rows 2 and 4: rest images. Arrows label a perfusion defect in the stress slices that normalizes in rest.

12.6 Positron Emission Tomography

12.6.1 The PET Camera

In a PET camera, there are rings of detectors around the patient. The two photons resulting from annihilation fly in opposite directions and will be detected by two detectors at almost the same time. The line of event can be determined by connecting the two detectors (Figure 12.12). So, in contrast to gamma cameras, we do not need a collimator for PET imaging, and consequently both the sensitivity and spatial resolution of PET are better than those of a regular gamma camera for human imaging. Moreover, since the pairs of photons hitting a particular pair of detectors always travel the same path length inside the patient's body (independent of the position where the annihilation occurred along the line), the correction for attenuation is more straightforward.

The rings can simultaneously detect radiation emitted in all directions, so PET is capable of acquiring dynamic tomographic studies as well. Utilizing this, in the beginning, PET was mostly used for research purposes, primarily for pharmacodynamic and receptor kinetic brain studies. Today, most of the PET studies are clinical: they are used to search for tumors and metastases.

PET scanners are rather expensive, and we need positron-emitting radionuclides produced in cyclotrons, both limiting the number of studies. The price of a PET study is typically higher by an order of magnitude than that of a gamma camera procedure.

12.6.2 ^{18}F -FDG PET Studies with PET/CT

At present, most PET studies apply 2- (^{18}F) -FDG (Fluoro-2-Deoxy-D-Glucose). F-18 is preferred for clinical studies because of its favorable half-life (see Table 12.6). Since many kinds of tumor cells have increased glucose metabolism, the most common indication is searching for tumors, especially to explore whether lymph node and distant metastases are present and to identify remnants or recurrent tumors after therapy. After surgery or radiation therapy, the environment of a former tumor will be distorted anyway, so it is hard to distinguish harmless scars from tumor lesions using structural imaging methods like CT and MRI.

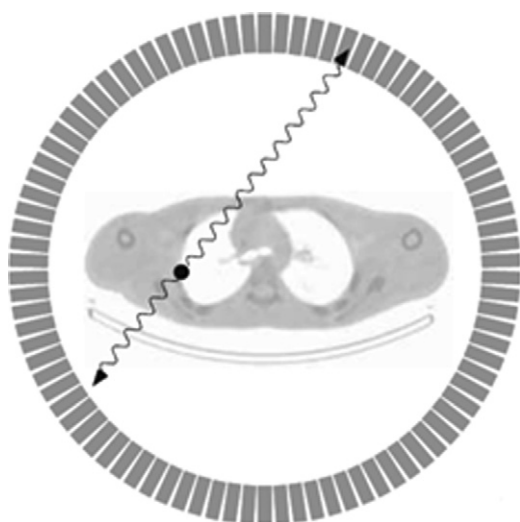


Figure 12.12 The detectors of PET, packed in rings around the patient, detect annihilation radiation in coincidence mode.

Table 12.6 The Most Common Positron Emitters for Medical Applications

| Nuclide | Half-Life | Mean Beta Energy (keV) | Average Range (mm) | P (%) |
|---------|-----------|------------------------|--------------------|---------|
| C-11 | 20.3 min | 386 | 1.1 | 100 |
| N-13 | 10 min | 492 | 1.5 | 100 |
| O-15 | 124 s | 735 | 2.5 | 100 |
| F-18 | 109 min | 250 | 0.6 | 97 |



Figure 12.13 A PET/CT study of a patient with suspected testicular cancer. Arrows show abnormally increased FDG uptake.

Most recently produced PET devices are combined with a CT. In this way, studies with both modalities can be completed sequentially, keeping the same position of the patient on the table. Attenuation correction of the PET images is much faster and less noisy when using CT rather than a separate set of transmission images obtained with an external radioisotope source. Moreover, the more detailed CT image helps determine a better localization of the abnormalities, thus reducing the fraction of false positive reports compared to PET alone. On the other hand, hybrid PET/CT has a much higher sensitivity for the detection of tumors than CT alone (Figure 12.13).

12.6.3 Research Studies Using PET

PET studies for research purposes, especially pharmacokinetic and receptor kinetic investigations, are very important. Several hundreds of different molecules labeled with positron emitters have been administered to animals and humans. The greatest advantage of PET is that any organic molecule can be labeled with positron emitters (see Table 12.6). It is possible to obtain images of such a small number of molecules in a living organism (e.g., bound to receptors) that otherwise can only be detected in sections (by autoradiography) or *in vitro*.

12.6.4 Imaging Myocardial Metabolism

If a myocardial perfusion SPECT study performed after infarction (as described in [Section 12.5.3](#)) shows perfusion defects in both stress and rest images, the study of glucose metabolism is the best known method of distinguishing between two states: long-term diminished blood supply may have resulted in dead (unviable) myocardium, or the cells may still be viable but hibernated, meaning that although they do not presently contract because of the long-lasting oxygen deficiency, the pump function of the heart may improve after restoring the blood supply. Unfortunately, the glucose molecule cannot be labeled with gamma emitter radionuclides since the molecule is too small and its atoms do not have gamma-emitting radioisotopes. However, FDG (mentioned in [Section 12.6.2](#)) allows the imaging of glucose metabolism. While a healthy myocardium gets energy from burning glucose after eating and from fatty acids in fasting state, a hibernated myocardium can consume only glucose, and a scar does not utilize significant amounts of either glucose or fatty acids. So, for instance, in fasting state, only a hibernated myocardium accumulates FDG. A hibernated myocardium can be revived by angioplasty or coronary artery bypass graft surgery, while scars cannot be improved by either therapeutic approach.

Further Reading

- Nobelprize.org. (2012). George de Hevesy - Biography. Retrieved March 23, 2012, from http://www.nobelprize.org/nobel_prizes/chemistry/laureates/1943/hevesy-bio.html [Online].
- Nobelprize.org. (2012). Rosalyn Yalow - Autobiography. Retrieved March 23, 2012, from http://www.nobelprize.org/nobel_prizes/medicine/laureates/1977/yalow.html [Online].
- Wagner, Henry N. (2003). Hal Anger: Nuclear Medicine's Quiet Genius. *J Nucl Med*, 44, 26N, 28N, 34N.
- NuclearPathways Project. (2011). Ernest O. Lawrence. Retrieved March 23, 2012, from <http://www.atomicarchive.com/Bios/Lawrence.shtml> [Online].
- European Association of Nuclear Medicine (2010). *Status of Nuclear Medicine in Europe – 2009*. EANM, Vienna.
- World Health Organisation. (2004). The top 10 causes of death. Retrieved March 23, 2012, from <http://www.who.int/mediacentre/factsheets/fs310/en/index.html> [Online].
- Magill, J. and Galy, J. (2005). *Radioactivity Radionuclides Radiation*. Springer, Berlin.
- Powsner, R.A. and Powsner, E.R. (2006). *Essential Nuclear Medicine Physics*. 2nd ed. Blackwell, Malden.

13 Environmental Radioactivity

As mentioned in Chapter 3, there is a much higher number of radioactive isotopes than stable isotopes. Radioactive isotopes, including natural and artificial ones, are present in the environment, causing part of the background radiation. Radiation of the natural radioactive isotopes has affected living organisms during their evolution. Obviously, living organisms could adapt to natural background radiation. The increase in radiation that results from the anthropogenic-generated radioactive isotope effects must always be compared to natural radioactivity when its effects on living organisms are discussed.

13.1 Natural Radioactive Isotopes

Natural radioactive isotopes have been present since the formation of the Earth and are produced continuously by nuclear reactions of cosmic rays with atoms in the atmosphere.

As seen in Section 6.2.5, the elements in the universe are produced by nuclear reactions. Of course, these nuclear reactions produce both stable and radioactive isotopes. The half-lives of some radioactive isotopes are several billion years, comparable to the age of the Earth and the universe. These radioactive isotopes cannot be formed under natural conditions characteristic to the Earth; thus, as a result of the radioactive decay, their quantity and radioactivity have been decreasing continuously since the Earth was formed. However, because of these long half-lives, their radioactivity have been significant until now. These radioactive isotopes are called “nucleogenesis” or “primordial” isotopes and can be classified into two groups. The first group contains of the isotopes in the natural radioactive decay series (^{235}U , ^{238}U , and ^{232}Th ; see Figures 4.4–4.6). The most important members of these decay series are the parent nuclides (^{235}U , ^{238}U , and ^{232}Th) and the daughter nuclides with relatively long half-lives and the daughter elements of these daughter nuclides, for example, ^{226}Ra , ^{210}Pb , ^{210}Bi , and ^{210}Po . Gaseous radon isotopes (^{222}Rn , ^{220}Rn) are especially important because they enter the lungs through breathing, and their solid daughter elements (the lead, bismuth, and polonium isotopes produced from the radon isotopes in the ^{238}U and ^{232}Th series) are incorporated in the lung tissues, causing internal irradiation. Many of these isotopes emit alpha particles with a short range. The alpha particles transfer their high-energy radiation within a short range inside the lungs. Since the radioactive isotopes of the decay series are always present in the building material, radon gas accumulates in closed

spaces (such as houses and caves). Therefore, the activity of radon is an important part of the background irradiation affecting living organisms.

In the second group of the primordial isotopes, there are the long-life nuclei produced during nucleogenesis, which transform into stable daughter nuclides in one step. For example, ^{40}K , ^{50}V , ^{87}Rb , ^{113}Cd , ^{115}In , ^{123}Te , ^{138}La , ^{144}Nd , $^{147,148}\text{Sm}$, ^{152}Gd , ^{156}Dy , ^{174}Hf , ^{176}Lu , ^{186}Os , ^{187}Re , and ^{190}Pt isotopes can be mentioned in this context. The most important radionuclide in this group is the radioactive isotope of potassium, ^{40}K . The potassium ion is an essential ion in living organisms; its quantity is significant and plays an important biological role. Of course, the abundance of ^{40}K in living organisms is the same as in every other potassium compound. This means that the radioactivity of ^{40}K that is present in the body of adult people is about 3500–4000 Bq, depending on the mass of the body. The ^{40}K isotope emits gamma radiation with high energy (1.46 MeV) and the range of these gamma photons is long. Thus, gamma photons leave the human body, and so the living organisms irradiate each other.

Many natural radioactive isotopes are produced continuously via nuclear reactions of the nuclei of atmosphere (nitrogen, oxygen, and argon) with cosmic radiation. As seen in Section 4.3.6, the basic isotope of the radiocarbon dating, ^{14}C , is produced from the ^{14}N in the air in an (n,p) nuclear reaction (see Section 6.2.1). Beside radiocarbon, many radioactive isotopes are produced in this way, e.g., ^3H , $^{7,10}\text{Be}$, ^{22}Na , ^{26}Al , $^{32,33}\text{P}$, ^{35}S , ^{36}Cl , and ^{39}Ar . These nuclides form from the ^{40}Ar isotope of air under the effect of the cosmic radiation by spallation (see Section 5.5.2).

13.2 Radioactive Isotopes of Anthropogenic Origin

Besides natural radioactive isotopes, artificial radioactive isotopes are present in the environment. They originate from different anthropogenic activities:

1. Radioactive wastes of isotope laboratories, including the research, medical, and industrial laboratories.
2. Radioactive wastes of nuclear energy production and reprocessing technologies (see Section 7.3). From nuclear plants, radioactive isotopes can be introduced into the environment in accidents (Section 7.2) and by regular emissions (Section 7.1.1.1), of which the emission of gaseous radioactive isotopes (T, ^{14}C , ^{85}Kr , ^{133}Xe , ^{135}Xe , and I isotopes) is the most important. A nuclear reactor with 440 MW electric power produces 2.7×10^{19} Bq/year radioactivity. Some important fission products are shown in Figure 13.1. The fission products are present in nuclear waste, as discussed in Section 7.3 and shown in Figures 7.6 and 7.7.

In addition, there are some isotopes which emit beta particles with low energy (^{79}Se , ^{95}Zr , ^{109}Pd , and ^{135}Cs). Their radioactivity is not very high; however, they have long half-lives, so they will be present in nuclear waste disposal and may remain in the environment for a long time.

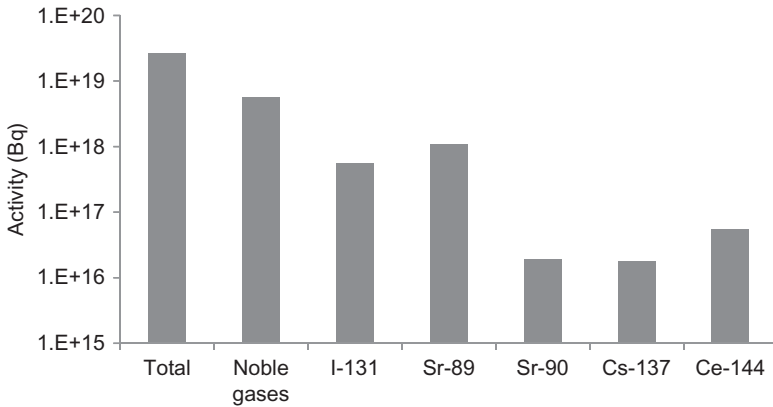


Figure 13.1 The radioactivity of several isotopes produced in a year in a nuclear reaction with 440 MW electric power.

Source: After Szabó (1993), with permission from Akadémiai Kiadó.

3. The radioactive isotopes of nuclear bombs and the experimental nuclear explosions. As discussed in Section 7.5, the first nuclear explosions that affected the atmosphere were two US explosions in Japan (Hiroshima and Nagasaki in August 1945), a Soviet explosion (1949), a British explosion (1952), and a Chinese explosion (1964). When exploding a nuclear bomb equivalent to a 1000 ton traditional trinitro-toluol (TNT) bomb, 48.5 g of fission products is emitted into the atmosphere. This mass seems to be low; however, the radioactivity is extremely high (3.7×10^{21} Bq). A significant portion of the fission products has a short half-life, so the radioactivity decreases rapidly. After 24 h, it is 5.9×10^{16} Bq. This is still a very high level of radioactivity. The radioactive isotopes of the nuclear explosions have the following half-lives (see Figure 7.7): $t_{1/2} < 1$ day for 131 isotopes; $1 < t_{1/2} < 10$ days for 117 isotopes; $10 < t_{1/2} < 30$ days for 9 isotopes; $30 \text{ days} < t_{1/2} < 1$ year for 12 isotopes; $1 \text{ year} < t_{1/2} < 10$ years for 7 isotopes; $10 \text{ years} < t_{1/2} < 100$ years for 3 isotopes; $t_{1/2} > 100$ years for 10 isotopes.

The longtime pollution obviously originates from the isotopes with long half-lives. The most important polluting radioactive isotopes are ^{14}C , ^{90}Sr , ^{137}Cs , ^{95}Nb , ^{106}Ru , ^{106}Rh , ^{140}Ba , ^{140}La , ^{144}Ce , ^{144}Pr , and Pu. Before 1963, 1.2×10^{16} Bq (about 400 kg) of ^{239}Pu were emitted into the atmosphere.

The nuclear wastes of isotope laboratories and nuclear energy production are treated and stored under very strictly checked conditions (as discussed in Sections 7.3 and 8.9). The radioactive products of the nuclear explosions, however, freely got into the environment. In 1963, the United States, the Soviet Union, and the United Kingdom signed the Limited Test Ban Treaty, pledging to refrain from testing nuclear weapons in the atmosphere, underwater, or in outer space. The treaty permitted underground tests. Many other nonnuclear nations have acceded to the Treaty; however, some countries, which possess nuclear weapons, have not. As a result of the Limited Test Ban Treaty, the radioactivity of the atmosphere

originating from the nuclear explosions has decreased, and that from nuclear energy production has increased. The radioactive pollution reached its maximum between 1961 and 1965. Additional significant radioactive pollution entered the environment during the Chernobyl and Fukushima accidents (described in Section 7.2).

13.3 Occurrence of Radioactive Isotopes in the Environment

Both natural and artificial radioactive isotopes are present in the environment (Table 13.1) in the atmosphere, hydrosphere, lithosphere, and living organisms, including the plant–animal–human food chain. The radioactive isotopes in the environment give the external radiation dose to human organisms, while the isotopes incorporated by breathing, feeding, and so on are the source of the internal radiation dose (see Sections 13.4.1 and 13.4.3).

Radioactive isotopes, similar to stable isotopes, continuously circulate among the different parts of the environment, as illustrated in Figure 13.2. The radioactive isotopes in compartments are in direct exchange; in other words, they may pass through to other compartments. The distribution of radioactive isotopes in different compartments is mainly determined by their chemical properties. In nature, radioactive isotopes may react with different components of air (oxygen, nitrogen, carbon dioxide, and aerosols), may dissolve in water, or may be sorbed on the solid phases of the spheres, especially the lithosphere. The chemical reactions of radioactive isotopes produce chemical species, which then distribute in the different compartments in order to approach the thermodynamic equilibria. In nature, of course,

Table 13.1 The Most Important Radioactive Isotopes, Including Natural and Artificial Ones, in the Environment

| Origin | Radioactive Isotope |
|---|--|
| Natural decay series | Parent nuclides of the natural decay series: ^{235}U , ^{238}U , and ^{232}Th Long-life daughter nuclides of the natural decay series and their daughter nuclides: ^{226}Ra , ^{210}Pb , ^{210}Bi and ^{210}Po , ^{222}Rn , ^{220}Rn |
| Natural primordial isotopes | ^{40}K , ^{50}V , ^{87}Rb |
| Natural radioactive isotopes continuously produced under the effect of cosmic ray | ^3H , ^7Be , ^{14}C |
| Artificial: nuclear energy production—regular emission | T, ^{14}C , ^{85}Kr , ^{133}Xe , ^{135}Xe , and I isotopes |
| Artificial: nuclear explosions and accidents | ^{14}C , ^{90}Sr , ^{137}Cs , ^{95}Nb , ^{106}Ru , ^{106}Rh , ^{140}Ba , ^{140}La , ^{144}Ce , ^{144}Pr , and Pu isotopes |

the thermodynamic equilibria are never reached; therefore, only the tendencies of the chemical reactions and the tendency of the distribution of the radioactive isotopes can be discussed.

The occurrence of radioactive isotopes in the different spheres is discussed on the basis of [Figure 13.2](#).

13.3.1 Radioactivity in the Atmosphere

In the atmosphere, the radioactive isotopes, including natural and artificial ones, are present as gases or bounded to aerosols. As mentioned previously, the artificial radioactivity originating from nuclear explosions is decreasing, while that from nuclear energy production is increasing. The net effect of these tendencies is the decrease of radioactivity in the atmosphere because the change of natural radioactivity can be disregarded.

Of the natural radioactive isotopes, radon, ^3H , and ^{14}C are important. The different isotopes of radon are the members of the natural decay series. ^3H , and ^{14}C continuously form from nitrogen under the effects of cosmic radiation. Both elements form many volatile and gaseous compounds, which are present in the atmosphere.

The cloud chamber photograph (see Section 14.5.1) of radon gas (^{222}Rn) is shown in [Figure 13.3](#). The tracks of the alpha particles can be seen well. A solid-state detector picture (see Section 14.5.3) of radon gas is shown in [Figure 13.4](#). The tracks of alpha particles are shown.

Among the artificial radioactive isotopes, the gaseous fission products (iodine and noble gases) and the compounds of ^3H and ^{14}C are the important radioactive isotopes of the air.

All other radioactive isotopes in the air are bounded to aerosols. Practically, all natural and artificial radioisotopes can be bounded to aerosols. The long-life fission products and natural radioactive isotopes, thus, can have an impact on the environment.

The radioactive isotopes of the atmosphere are falling onto the surface of the Earth. Depending on the amount of water that accompanies this fallout, the processes are called “dry out,” “rain out,” and “wash out.” The half-life of the fallout of radioactive isotopes from the stratosphere after a nuclear explosion is 7 years.

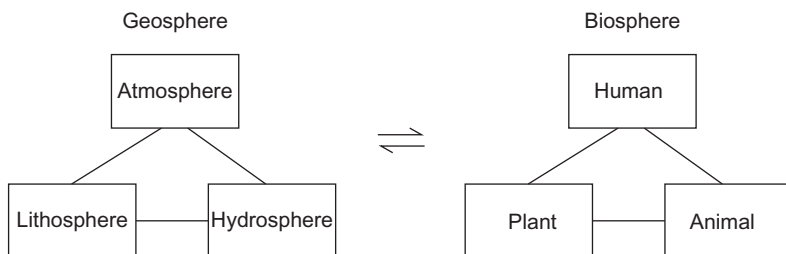


Figure 13.2 Continuous circulation of the radioactive isotopes between and within the geosphere and biosphere.



Figure 13.3 A cloud chamber photograph of radon gas (^{222}Rn). (Thanks to Dr. Péter Raics, Department of Experimental Physics, University of Debrecen, Hungary, for the photograph.)

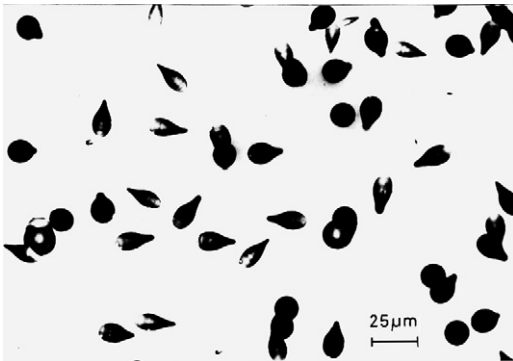


Figure 13.4 A solid-state detector picture of radon gas. (Thanks to Dr. István Csige, Department of Environmental Physics, Institute of Nuclear Research, University of Debrecen, Hungary, for the photograph.)

The radioactivity of the atmosphere has seasonal changes because of the changes in the weather. The mean atmospheric radioactivity in the Northern Hemisphere in January and in June is about 10 and 2 Bq/m^3 , respectively.

13.3.2 Radioactivity in the Hydrosphere

The radioactivity in the hydrosphere also has natural and artificial sources. The most important natural radioactive isotope in the hydrosphere is ^{40}K , which, in the form of a potassium ion, is mostly found dissolved in water. Because of the lower salt concentration, the radioactivity of rivers is much less than that of seawater. For example, the mean radioactivity of the Danube River is 70–90 mBq/dm^3 , and the activity of seawater is about 10–15 Bq/dm^3 . Among the artificial radioactive pollutants, ^{90}Sr , ^{137}Cs , ^{129}I , and ^{131}I dissolve well in water, so the natural water mainly contains these artificial isotopes.

Of course, the radioactive isotope of hydrogen, tritium, is also present in natural waters as tritiated water. As mentioned in Section 7.3, tritium is formed in nuclear

Table 13.2 Natural Radioactivity of Hungarian Soil Samples

| | Radionuclide | Activity (mBq/g) |
|--|-------------------|------------------|
| Daughter nuclides of ^{238}U | ^{40}K | 602 ± 146 |
| | ^{234}Th | 85 ± 36 |
| | ^{226}Ra | 111 ± 64 |
| | ^{214}Bi | 45 ± 29 |
| Daughter nuclides of ^{232}Th | ^{214}Po | 49 ± 32 |
| | ^{228}Ac | 40 ± 12 |
| | ^{212}Bi | 39 ± 16 |
| | ^{212}Pb | 39 ± 11 |
| | ^{208}Tl | 40 ± 9 |

Source: Adapted from Szabó (1993), with permission from Akadémiai Kiadó.

power plants in $^{14}\text{N}(n,3\ ^4\text{He})\text{T}$ and $^{14}\text{N}(n,\text{T})^{12}\text{C}$ reactions. The emission of the nuclear power plants raised the tritium concentration by 1–2 orders of magnitude above the natural level. The tritium activity is generally expressed in tritium units (TUs). One tritium unit means that the ratio of the hydrogen (^1H) and tritium (^3H) atoms in 10^{18} :1. The radioactivity of 1 TU is $0.1184\ \text{Bq}/\text{dm}^3$.

The vegetation in water accumulates dissolved radioactive isotopes. The accumulation depends on the composition of water and the species present. The humus formed from the decomposition of the vegetation also uptakes the radioactive isotopes, which in this way transfers to the lithosphere.

13.3.3 Radioactivity in the Lithosphere

Similar to that of the atmosphere and hydrosphere, the radioactivity of the lithosphere originates from both natural and artificial sources. The main sources of natural radioactivity are rocks; their radioactivity determines the radioactivity of the soils formed on the rocks. The radioactivity of rocks depends on their mineral and chemical composition and can be quite different. As a result, the radioactivity also depends on the geographic position. The mean radioactivity is higher in the Northern Hemisphere than the Southern one, and it is also higher in American continent than in Europe.

The most important natural radionuclides in rocks and soils are ^{40}K and the members of the radioactive decay series. Thorium is accumulated in monazite because it has similar chemical properties as the lanthanoid elements, which are present in significant quantities in monazite. The mean radioactivities of several isotopes present in rocks are listed in Table 13.2. The standard deviations are rather high due to the wide variety of rocks, which were used to measure the activities, and the varying activities of which lead to high uncertainty in the mean values.

As seen in Table 13.2, the radioactivities of ^{214}Bi and ^{214}Po , as well as ^{212}Bi , ^{212}Pb , and ^{208}Tl , are approximately the same, showing that they are in radioactive

equilibrium. ^{214}Bi and ^{214}Po are the daughter nuclides of ^{222}Rn , which is the daughter nuclide of ^{226}Ra (see Figure 4.4). However, the radioactivity of ^{226}Ra is much higher, proving the emission of the intermediate member, ^{222}Rn , into the atmosphere. The activities of the daughter nuclides of ^{232}Th are approximately the same. In this case, a radioactive equilibrium exists because the half-life of ^{220}Rn (55 s) is too short to escape from the soil.

It is important to note that besides the radioactive isotopes listed in Table 13.2, ^{210}Pb and ^{210}Po , the members of the ^{238}U series, are also important because of the long half-life of ^{210}Pb (21.6 years).

As seen in Section 9.3.2.2, the migration of the radioactive isotopes in the geological formations (as porous solids), including the isotopes present in nuclear waste, is determined by hydrological processes. The migration rate of water provides the upper limit for the migration rate of the water-soluble radioactive nuclide. This actual rate may be significantly lower when the radioactive isotopes can be sorbed on the surfaces of rocks and soils. The sorption is mostly influenced by the chemical species (mainly the charge) of the radioactive isotopes. On the basis of the chemical forms characteristic in geological systems, the radioactive isotopes can be classified as follows:

1. Cations (e.g., $^{134,137}\text{Cs}^+$, $^{41}\text{Ca}^{2+}$, $^{90}\text{Sr}^{2+}$, $^{54}\text{Mn}^{2+}$, $^{55}\text{Fe}^{3+}$, $^{58,60}\text{Co}^{2+}$, and $^{59,63}\text{Ni}^{2+}$).
2. Uranium and transuranium elements (U, Np, Pu, and Am isotopes), basically (complex) cations or anions (e.g., $^{99\text{m}}\text{Tc}$ isotopes as pertechnetate TcO_4^- , ^{14}C isotope as carbonate CO_3^{2-} , $^{36}\text{Cl}^-$, and $^{129}\text{I}^-$).
3. Neutral species (e.g., ^3H isotope as water H_2O , metallic $^{110\text{m}}\text{Ag}$).

Migration takes place in the following geological formations: clay rocks (especially bentonite), granitic rocks, soils, oxides, and other minerals (carbonates, sulfates, etc.). Since the surface charge of the rocks and soil is usually negative under usual geological conditions (pH, redox conditions), cations usually adsorb on the geological formations, while anions do not. Cesium, then, can occupy a space in the crystal lattices; thus, the sorption becomes irreversible. Other cations adsorb reversibly. In the case of cations of transition metals and transuranium elements, the adsorption is affected by their hydrolytic products. Transuranium elements can form colloids. Cations, except for cesium, readily form stable complexes that increase migration rate. In addition, precipitation, redox processes, and microbial activity can also influence the sorption and, as a result, the migration rate.

Of course, the different migration rate of cations and anions cannot result in the unbalancing of the electric charges. The faster migration of anion is followed by the migration of inactive cations dissolved from the geological formations.

The neutral species are very different behavior. Two extreme cases are tritiated water migrating with natural water (the isotope effect, described in Chapter 3, can be ignored) and Ag-110m reduced to metallic silver, the migration rate of which is practically zero.

Under equilibrium conditions, the sorption of the radioactive isotopes can be characterized by the distribution coefficient. This is the ratio of the sorbed quantity (mol/g) and the equilibrium concentration of the solution (mol/dm³). In Table 13.3,

Table 13.3 Distribution Coefficients of Radioactive Ions on Rocks or Minerals (g/dm³)

| Rock/mineral | ¹³⁷ Cs | ⁴⁵ Ca | ⁸⁵ Sr | ²²⁶ Ra | ⁶⁰ Co | ¹⁴ C | ^{99m} Tc | ¹³¹ I |
|--------------------------------|-------------------|------------------|------------------|-------------------|------------------|-----------------|-------------------|------------------|
| Montmorillonite | 18 | | | | | | | |
| Montmorillonite + cristobalite | 7.3 | | | | | | | |
| Montmorillonite + cristobalite | 6 | | | | | | | |
| Montmorillonite + quartz | 9.6 | | | | | | | |
| Montmorillonite + cristobalite | 2 | | | | | | | |
| Montmorillonite | 5.9 | | | | | | | |
| Dolomite rock | | | 0.015 | 0.754 | | 0.003 | <10 ⁻⁵ | 0.0007 |
| Vermiculitic rock | 3.9 | | | | | | | |
| Granite | 6.92 | | | | | | | |
| Carbonate rock | 0.59 | 0.05 | 0.044 | | 3.72 | | | 0.0006 |
| Red clay | | | 0.096 | 4.555 | | 0.001 | <10 ⁻⁵ | 0.0006 |
| Restite | 3.93 | | | | | | | |
| Calcite | 6.16 | | | | | | | |
| Chlorite + carbonate | 2.66 | | | | | | | |
| Clay rock | 2.43 | 0.04 | 0.103 | | 7.1 | | | 0.0008 |
| Ankerite + quartz | 5.71 | | | | | | | |
| Chlorite | 1.99 | 0.05 | 0.042 | | 5.22 | | | 0.0004 |
| Granite | 0.18 | 0.02 | 0.021 | | 2.09 | | | 0.0006 |
| Smectite | 5.77 | | | | | | | |
| Dolomite | 3.23 | | | | | | | |
| Paligorscite | 5.56 | | | | | | | |

the distribution coefficients of radioactive ions on different rocks are listed. The higher values of the distribution coefficients mean the stronger sorption of the isotope on the given rock. The data in Table 13.3 illustrate well the differences in the sorption of cationic and anionic radioactive isotopes.

13.3.4 Radioactive Isotopes in Living Organisms

As a result of their metabolism, living organisms can uptake natural and artificial radioactive isotopes from the environment. The degree of uptake depends both on the radioactive isotope/ion and on the living organisms, and it is characterized by so-called discrimination factors (DFs) or observed ratios (ORs). The use of these factors is based on the similar biological properties of potassium and ¹³⁷Cs ions, or calcium and ⁹⁰Sr ions, respectively, and indicates how different living organisms or soil can accumulate the radioactive isotopes. For example, the discrimination of Sr-90 can be expressed as $\frac{N_{\text{Sr-90}}}{N_{\text{Ca}}}$, where $N_{\text{Sr-90}}$ is the activity of ⁹⁰Sr (for example) in a 1 g sample and N_{Ca} is the quantity of calcium ion in a 1 g sample.

The uptake of these radioactive isotopes (¹³⁷Cs and ⁹⁰Sr) is expressed by the transfer factors (TFs), which form the ratio of the DFs. For example, the TFs for

the ^{90}Sr ion can be expressed for the plant/soil, and animal/plant transfers can be expressed as follows:

$$\text{TF} = \frac{\left(\frac{N_{\text{Sr-90}}}{N_{\text{Ca}}}\right)_{\text{plant}}}{\left(\frac{N_{\text{Sr-90}}}{N_{\text{Ca}}}\right)_{\text{soil}}} \quad (13.1)$$

$$\text{TF} = \frac{\left(\frac{N_{\text{Sr-90}}}{N_{\text{Ca}}}\right)_{\text{animal}}}{\left(\frac{N_{\text{Sr-90}}}{N_{\text{Ca}}}\right)_{\text{plant}}} \quad (13.2)$$

where $\left(\frac{N_{\text{Sr-90}}}{N_{\text{Ca}}}\right)$ is the ratio of Sr-90 and Ca in soil, plants, and animals.

The activity of radioactive isotopes in living organisms decreases in two ways: by radioactive decay and biological secretion. The radioactive decay and secretion are characterized by the physical half-life of the radioactive isotope ($t_{1/2\text{fiz}}$) and the biological half-life of the isotope in the living organism ($t_{1/2\text{biol}}$). The net effect of the radioactive decay and secretion is expressed by the effective half-life ($t_{1/2\text{eff}}$):

$$\frac{1}{t_{1/2\text{eff}}} = \frac{1}{t_{1/2\text{fiz}}} + \frac{1}{t_{1/2\text{biol}}} \quad (13.3)$$

The physical, biological, and effective half-lives of several radioactive isotopes are shown in [Table 13.4](#).

As seen in [Table 13.4](#), the physical and biological half-lives range from a couple of days to thousands of years. The effective half-life is determined by the shorter of these half-lives. For example, the physical half-life of ^{137}Cs is rather long (30 years), but the biological half-life is only 17 days; thus, the effective half-life is 17 days.

Table 13.4 Physical, Biological, and Effective half-lives of Several Radioactive Isotopes in the Human Body

| | $t_{1/2\text{fiz}}$ | $t_{1/2\text{biol}}$ | $t_{1/2\text{eff}}$ |
|--------|---------------------|----------------------|---------------------|
| H-3 | 12.3 years | 19 days | 19 days |
| C-14 | 5730 years | 35 days | 35 days |
| Sr-90 | 28.6 years | 10 years | 7.4 years |
| Cs-137 | 30 years | 17 days | 17 days |
| I-131 | 8 days | 120 days | 7.5 days |

13.4 Biological Effects of Radiation

13.4.1 Dose Units

Previously in this book, the radioactive radiation has been characterized by the half-life, the type, the energy or energy distribution of the emitted particles or electromagnetic radiation, and the activity. These properties are not sufficient to characterize the biological effects of radiation because the effects are due to the absorbed energy and the subsequent material changes induced. These effects are characterized by different terms, the radioactive doses.

The most common radiation effect is ionization. The different types of the radioactive radiation ionize the substances directly or via the electrons formed in the scattering processes. Thus, as a first approximation, the biological (or other radiological) effects are characterized by the number of the ions produced in the air under the effect of the radiation. The number of the ions related to the irradiation dose (or ion dose) and expressed as coulomb per kilogram (C/kg) in dry air. It should be pointed out that ionization produces electrons and positive ions in equal quantity, so the total number of the charged particles (ions + electrons) is double the ion dose. The previous unit of irradiation dose was 1 röntgen (R), which expresses the number of ions in 1 cm^3 of air. The relation between the two is the following: $1 \text{ R} = 2.58 \times 10^{-4} \text{ C/kg}$.

The biological effects are due to the absorbed radiation energy. This is defined as an absorbed dose in 1 kg of material and expressed in joules per kilogram (J/kg). This unit has its own name, namely gray (Gy). This means that $1 \text{ J/kg} = 1 \text{ Gy}$ (gray). The previous unit of absorbed dose was rad: $1 \text{ Gy} = 100 \text{ rad}$.

The irradiation and absorption doses can be related by taking into consideration that the formation of one ion and one electron demands $53.9 \times 10^{-19} \text{ J}$, assuming the average composition of the air. Since the charge of an electron is $1.6 \times 10^{-19} \text{ C}$, the formation of 1 C requires 33.7 J of energy. Therefore, a 1 C/kg irradiation dose is equivalent to a 33.7 Gy absorbed dose in air, assuming total absorption.

As discussed in Chapter 5, different radioactive radiations have different interactions with matter. This also applies to the biological effects. The biological effects of the different radiation types are taken into account by the radiation weighting factors, such that the absorbed dose is multiplied by the radiation weighting factors. In this way, the so-called equivalent dose is obtained. The unit of the equivalent dose is the sievert (Sv): $\text{Sv} = \text{radiation weighting factor} \times \text{Gy}$. The value of the factors is very different for each type of radiation. The radiation weighting factor for X-ray and gamma radiation has been chosen to be 1. However, the radiation weighting factor is 5–20 for neutrons, depending on the neutron energy, 5 for protons, and 20 for alpha particles and fission products. The previous unit of equivalent dose was rem: $1 \text{ Sv} = 100 \text{ rem}$.

The effect of the radiation depends not only on the type and energy of the radiation but also the sensitivity of the organs and tissues to the radiation. This different sensitivity to stochastic radiation damage (see [Section 13.4.4](#)) is considered in the Publication 60 published by the International Commission of Radiological

Protection (CRP), in the Euratom basic standards for radiation protection dated May 1996 by the tissue weighting factor: 0.20 for gonads; 0.12 for colon, bone marrow (red), lung, and stomach; 0.05 for bladder, chest, liver, thyroid gland, and esophagus; 0.01 for skin, bone surface, and others. The sum of the tissue weighting factors is 1 for the whole body. The dose of a whole human body is the effective dose. To calculate the effective dose, the individual organ dose values are multiplied by the respective tissue weighting factor and the products added. The unit of the effective dose is sieverts.

If the radiation is present for a long time, the dose rate is used, which is defined as the ratio of the dose and the time of irradiation. The background radiation, for example, is expressed in mSv/year (see [Table 13.5](#)).

13.4.2 Mechanism of Biological Effects

The most significant characteristic of the biological effect of radiation is that a small amount of absorbed energy may have an extremely great effect. A case of

Table 13.5 The Mean Effective Dose Rates of Humans All Over the World

| Source | mSv/years | | |
|---|-------------|-------------|-------------|
| | External | Internal | Total |
| Cosmic ray | | | |
| Charged particles | 0.28 | | 0.38 |
| Neutrons | 0.10 | | |
| Cosmogenic radionuclides, e.g., ^{14}C | | 0.015 | 0.015 |
| Primordial radionuclides | | | |
| ^{40}K | 0.12 | 0.18 | 0.30 |
| ^{87}Rb | | 0.06 | 0.06 |
| ^{238}U and daughter nuclides | 0.1 | 0.12 | |
| ^{232}Th and daughter nuclides | 0.14 | | 0.14 |
| ^{222}Rn and daughter nuclides | | 1.1 | 1.1 |
| ^{220}Rn and daughter nuclides | | 0.1 | 0.1 |
| Natural background dose | 0.74 | 1.58 | 2.36 |
| Natural, but due to anthropogenic activity | | | |
| Coal power plants | | | 1.8 |
| Flights | | | |
| Natural gas (^{222}Rn) | | | |
| Building material (^{222}Rn) | | | |
| Artificial | | | |
| Diagnostic medical irradiation | | | 0.45 |
| Fallout | | | 0.04 |

acute radiation (e.g., a 1000 sievert dose, meaning $1000 \text{ J/kg} = 1 \text{ kJ/kg}$ absorbed energy) causes death immediately. For a man who weighs 70 kg, the total absorbed energy is 70 kJ. This energy is much smaller than the energy produced when a 1 mol substance (e.g., fuel) is oxidized (a few hundred kilojoules). The question arises: why does this small amount of energy have such a dramatic effect? This can be explained by the fact that the small amount of energy is absorbed as great impulses: the energy of each particle is about six orders of magnitude higher than the energy of the chemical bonds (see Section 2.1.2). Another important characteristic is that because of the high energy of each particle, the radioactive radiation ionizes the substances independent of their chemical species. Since any electron of the substances can be ejected, the cross section of the ionization is determined by the number of electrons. This means that the cross section of the ionization of the heavier elements and substances in large quantities is dominant.

The biological effect of the radiation occurs through consecutive physical, chemical, and biological steps. Since the water content of biological systems is the largest (the human body consists of about 70% water), the basic process of the biological effects of radiation is the radiolysis of water. The first step of the radiolysis of water is the ionization of water, a physical process, producing a positively charged water molecule ion. Since this molecule ion contains an unpaired electron, it is a radical:



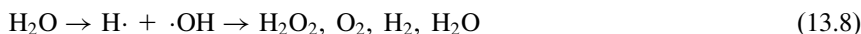
The products of the ionization (Eq. (13.4)), the water molecule ion/radical and the free electron, initiate different reactions, such as:



The products of the reactions in Eqs. (13.5) and (13.6), the hydrogen and hydroxide ions, can neutralize each other:



The net process is the formation of atomic hydrogen and hydroxide radicals. These radicals can combine to water again or can produce other highly reactive species as described in Eq. (13.8):



In the presence of oxygen, which is essential in living organisms, additional radicals can be produced. Some examples are listed in Eqs. (13.9)–(13.12):





The radicals in Eqs. (13.5)–(13.12) and the free electrons can react with each other and any molecules of the biological systems, producing additional radicals. As seen in the reactions in Eqs. (13.6)–(13.12), both oxidizing and reducing compounds form, causing redox reactions of the biological molecules. All these chemical reactions (including the reactions with radicals, electrons, and the redox agents) change the structure of biological molecules; thus, they cannot fulfill their biological functions (biological reactions). The damage to DNA under the effect of radiation has to be emphasized. The chains of DNA can break, leading to somatic effects of radiation, e.g., cancer and inheritable DNA defects.

The living organisms have different ways of protecting against the radiation effect. They contain natural radical scavengers. If they are present in excess of the radiolysis product, they can protect the biological molecules, including DNA. The preventing capacity depends on the age and physical conditions of the given organism. In addition, the cells have various repair mechanisms for restoring the damages of the biological molecules. This mechanism is called “immune activity.” If, however, this repair mechanism fails, the undesirable effects of radiation will appear.

The protection against radiation can be assisted by chemicals, namely by compounds that can scavenge the radicals, e.g., by compounds containing conjugated double bonds (Vitamins A and E) or compounds that are oxidized easily (Vitamin C). Sulfur compounds can also scavenge radicals. Because of the triple bond, a cyanide ion should scavenge the radicals well; however, it cannot be used for radiation protection of living organisms because of its strong toxicity.

13.4.3 *The Natural Background of Radiation*

Before discussing the biological effects of radiation, the dose of the natural background radiation is revealed. This is the radiation dose that has been present during the evolution of living organisms; they obviously somehow adapted to this radiation dose. Every other effect of radiation has to be compared to this effect of background radiation.

Both natural and artificial radioactive isotopes were presented in [Sections 13.1 and 13.2](#); their abundance in the different spheres of Earth was discussed in [Section 13.3](#). These radioactive isotopes and the cosmic ray irradiate living organisms as external radiation sources. The cloud chamber photograph (see [Section 14.5.1](#)) of the background radiation is shown in [Figure 13.5](#). The tracks of the alpha (thick tracks) and beta (thin tracks) are shown well. A solid-state detector picture ([Section 14.5.3](#)) of the cosmic ray exposed on the Cosmos 2044 satellite is shown in [Figure 13.6](#).

In addition, living organisms can incorporate radioisotopes, which cause internal radiation exposure. The types and distribution of the radiation doses, as well as the mean effective doses, are quantitatively given in [Table 13.5](#).

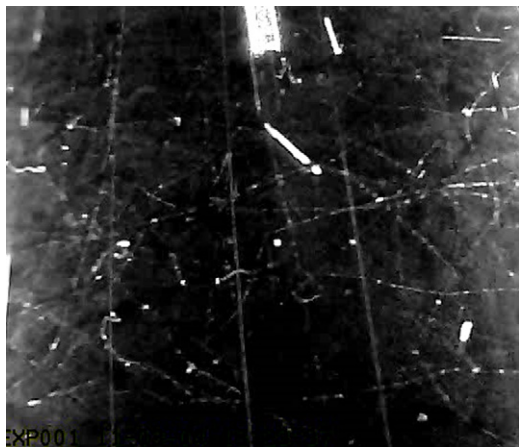


Figure 13.5 A cloud chamber photograph of background radiation. (Thanks to Dr. Péter Raics, Department of Experimental Physics, University of Debrecen, Hungary, for the photograph.)



Figure 13.6 A solid-state detector picture of the cosmic ray exposed on the Cosmos 2044 satellite. The thick track is probably the track of a heavy oxygen ion. (Thanks to Dr. István Csige, Department of Environmental Physics, Institute of Nuclear Research, University of Debrecen, Hungary, for the photograph.)

Table 13.5 shows the part of natural background radiation that lacks any anthropogenic activity, which has been present during the whole history of the Earth. Since the nucleogenesis or primordial isotopes (see [Section 13.1](#)) cannot be formed under natural conditions on the Earth, their quantity continuously decreases. The decrease is obviously very slow because of the very long half-lives. Nowadays, nucleogenesis, cosmogenic isotopes, and the cosmic ray mean an effective dose rate of about 2–2.5 mSv/years, depending on the geographical location.

In addition, there is natural radiation that is present as a result of anthropogenic activity. These are also listed in [Table 13.5](#). For example, the radioactivity of rocks in the deep layer of the Earth's crust does not irradiate the living organisms if they are in their original place. When they are brought to the surface of the Earth (e.g., by mining of coal, phosphates, and natural gas), however, radioactive isotopes get onto the surface, increasing the natural radioactivity and the effective dose. Similarly, the ^{222}Rn isotope is a natural radioactive isotope. It has a high atomic number, so it accumulates in closed places such as in caves. The building materials

always contain uranium and, of course, its daughter nuclides, including ^{222}Rn . As a result, living in houses increases the effective dose rate. As seen in the decay series of ^{238}U (see Figure 4.4), the daughter nuclides of ^{222}Rn are solid, so they accumulate in lungs, increasing the internal radiation dose rate. When flying by aircraft, the cosmic ray increases the external radiation dose rate. The total effective dose rate of these types of radiation (which is natural, but a consequence of anthropogenic activity) is about 2 mSv/years.

The effective dose rate of artificial radioactivity is less than 0.05 mSv/years. This consists of the fallout of nuclear explosions and the emission of nuclear reactors. This accounts for about 1% of natural background radiation, and it continuously decreases. Medical irradiation represents about 0.5 mSv/years, but this value strongly depends on the level of medical intervention. This value can also decrease with the technical improvement of the instruments used in nuclear medicine but can increase by a larger segment of the population taking part in preventive medical examinations.

13.4.4 *Effects of Radiation on Living Organisms*

As mentioned in Section 13.4.1, the organs have different sensitivities to radiation. The sensitivity of an organ to radiation is determined by the proliferation and differentiation of its cells and tissues. This means that cells with faster proliferation are more sensitive to radiation. Moreover, living organisms, in which the biological functions of the cells and tissues are strongly differentiated, are also more sensitive to radiation. These facts have important consequences, both in medical applications and in radiation protection. For example, the cells of tumors can be damaged by irradiation because their proliferation is faster than that of healthy cells and tissues. At the same time, children and pregnant women have to be protected against radiation very carefully.

The radiation exposure can be acute or present for a long period of time (i.e., chronic). Acute radiation exposure refers to the delivery of (usually high) doses of radiation in a short period of time (within days). Acute radiation exposure of human beings can occur through accidents, wars, criminal activity, or medical impacts. Some radiation exposures can be present constantly in the environment, such as background radiation and the continuous elevated doses of radiation in radioactive workplaces.

Radioactive irradiation can cause somatic and genetic effects. The somatic effects manifest themselves in the individual, while the genetic effects (mutations) are observed in their descendants. The most serious genetic effect is when the individual's reproductive capacity is affected, and there are consequently no descendants.

The low and high doses have different biological impacts, which are called "stochastic" and "deterministic" effects, respectively. The term "stochastic" means a random effect that is only the probability of damage (e.g., the induction of cancer and genetic defects) that can be caused by a certain radiation exposure. Stochastic effects are usually related to exposures to low levels of radiation exposure over a long period of time. Stochastic effects have no threshold level of radiation exposure below which we can say with certainty that cancer or genetic effects will not occur.

Deterministic effects are related to much higher levels of radiation exposure, usually over a much shorter period of time than is the case for stochastic effects. The deterministic effects have a threshold radiation dose, below which the deterministic effects are not observed. However, above the threshold dose, the severity of the deterministic effect is proportional to the radiation dose.

The effect of high doses is illustrated in Figure 13.7. Some curves of Figure 13.7 have been obtained in animal tests. The curve for humans has been constructed from the data collected after accidents. As seen, the tumor frequency and absorbed dose are in well-determined correlations. Moreover, there are threshold doses below which no excess cancer cases have been reported.

In Table 13.6, the biological impacts of high radiation doses are listed in the case of acute and chronic radiation exposures. The data are based on the radiation effects observed in human populations following the nuclear explosions in Hiroshima and Nagasaki in 1945.

As seen in Table 13.6, both acute and chronic radiation exposures can cause radiation sickness. This sickness has a variety of symptoms, including the following:

- General symptoms: fainting, fatigue, weakness, nausea and vomiting, diarrhea, dehydration, and hair loss.
- Cutaneous symptoms: inflammation of exposed areas (redness, tenderness, swelling, bleeding), bruising, skin burns (redness, blistering), open sores on the skin, and sloughing of skin.
- Mucosal symptoms: mouth ulcers, ulcers in the esophagus, stomach, or intestines, bleeding from the nose, mouth, gums, and rectum, vomiting blood, and bloody stool.

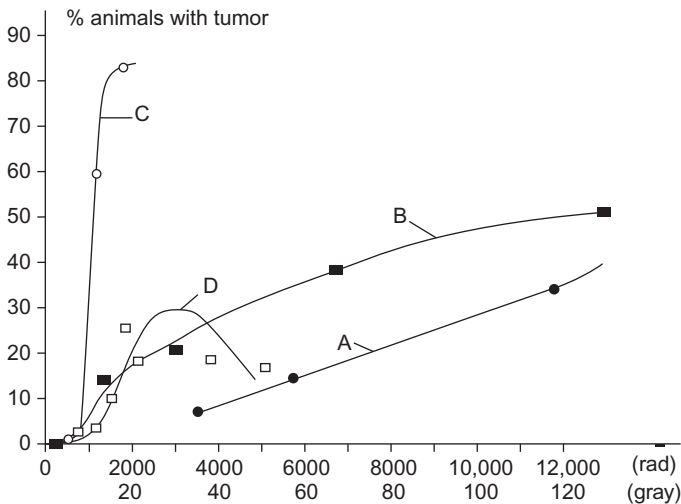


Figure 13.7 Tumor frequency as a function of absorbed dose. (A) Sr-90 induced osteosarcomas in female CBA mice. (B) Bone tumors in men from incorporated Ra-226. (C) Kidney tumors in rats by X-rays. (D) Skin tumors in rats by electrons.

Source: Reprinted from Choppin and Rydberg (1980), with permission from Elsevier.

Low radiation exposure has stochastic effects. This means that only the probability of effects can be provided. The effect–dose functions may show linear, sub-linear (with threshold dose), and supralinear curves (with effects increasing with the increase in the radiation dose). In addition, there are views that very small doses stimulate the repair activity of DNA, so the radiation may have a desirable impact. This process is called “hormesis,” and there are many disputes whether this effect even exists at all. In conclusion, we do not have exact information on the radiation effects, which, in fact, is the most important in life for most of us.

As mentioned in [Section 13.4.2](#), the impact of the radiation is due to radical formation. The effects of low doses can hardly be estimated because there are many other factors that also produce radicals in living organisms. This means that the effects of low-level radiation cannot be separated from the effects of other environmental risks such as stress, carcinogens (tobacco smoke, nonradioactive species, etc.), aging, and individual physical conditions. As mentioned previously, living organisms have different ways to protect against radicals by natural radical scavengers, and they have various repair mechanisms for restoring the damages to the biological molecules. If, however, this repair mechanism fails, different diseases appear. Since any radiation exposure has some risk of producing radicals, it should be avoided if possible. For this reason, the limits of radiation are determined by the “linear-no-threshold” hypothesis. This hypothesis is questioned from time to time; however, it provides a pragmatic means of estimating radiation risks and is consistent with the (limited) data that are available.

The standards of radiation protection control the receipt, possession, use, transfer, and disposal of radioactive material in such a manner that the total dose to an individual (including doses resulting from licensed and unlicensed radioactive material and from radiation sources other than background radiation) does not exceed the standards for protection against radiation prescribed in the regulations. However, nothing shall be construed as limiting actions that may be necessary to protect health and safety. The standards have three basic aspects:

1. It must be proved that the application of radioactive material results in more improvements for the community than the risk to health.
2. The risk has to be decreased as low as reasonably achievable (ALARA).

Table 13.6 The Biological Impact of High Radiation Doses

Acute Radiation Exposure

| | |
|---------|--|
| 1000 Sv | Death immediately |
| 100 Sv | Damage of the central nervous system; death within hours |
| 10 Sv | Damage of blood-forming tissues; death within days |
| 1 Sv | Radiation thickness |

Chronic Radiation Exposure

| | |
|--------------|---|
| 0.01 Sv/nap | Weakness after 3–6 months; death after 3–6 years |
| 0.001 Sv/nap | Radiation sickness, symptoms are observed after several years |

3. There are dose limits that are strictly prohibited under any conditions. There are dose limits for individual members of the public and occupational dose limits.

The standards for individual members of the public say that the total effective dose equivalent to individual members of the public from the licensed operation does not exceed 1 mSv/year, exclusive of the dose contributions from background radiation, medical investigations, and occupational doses. The annual limit of the effective occupational dose is 100 mSv/5 years, but the 50 mSv/year is permitted only in a 5-year period. Therefore, the mean occupation dose limit is 20 mSv/year. Other dose limits are defined for any tissues including occupational and public dose limits. For example, the occupational dose limit for the lens of the eye is 150 mSv/year; for skin, hands, and feet, it is 500 mSv/year. These limits for the members of the public are the tenth part of the occupational dose limits; namely, 15 mSv/year for the lens of the eye, and 50 mSv/year for skin, hands, and feet. The occupational dose limits have been determined such that they should be similar to the risk of other occupational limits (e.g., the risk of death of bus drivers).

Medical applications of radiation have no dose limits. The basic principles of protection for medical exposures can be summarized as follows: medical exposures should be justified by weighing the diagnostic or therapeutic benefits they procure against the radiation detriment they might cause, taking into account the benefits and risks of available alternative techniques that do not involve radiation exposure. The doses from medical exposure should be the minimum necessary to achieve the

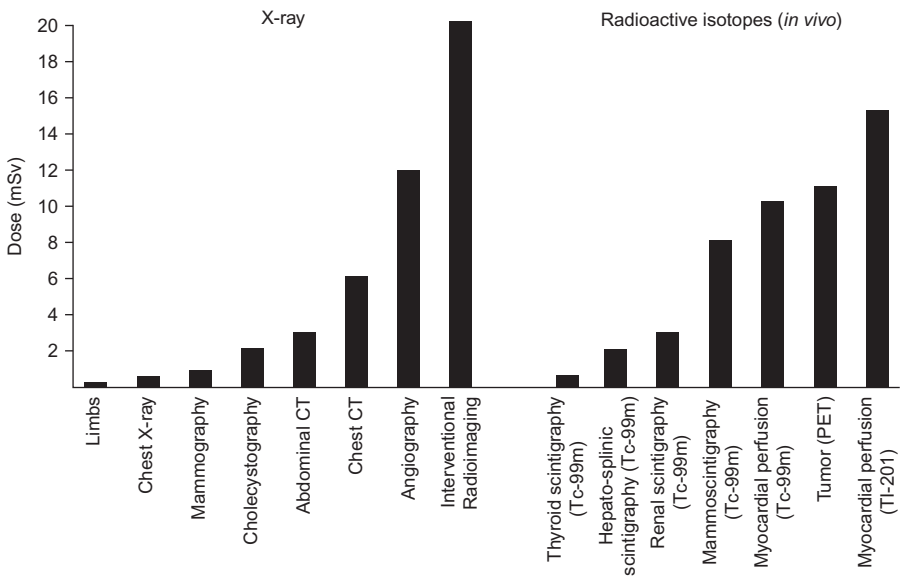


Figure 13.8 The mean effective dose of the patients is shown in several nuclear medical diagnostic methods.

Source: Reprinted from Fehér and Deme (2010), with permission of the copyright owner (Prof. Béla Kanyár).

required diagnostic objective or the minimum required to the normal tissue for the required therapeutic objective. This principle is in accordance with the ALARA principle. In [Figure 13.8](#), the mean effective dose of the patients is shown in several nuclear medical diagnostic methods.

In conclusion, we can say that background radiation has always been present during the history of humanity. Protection from excess radiation exposure is legally controlled. The standards are very strict for protecting the members of the public. The occupational dose limits, of course, must be higher, so that people working with radioactive material and radiation face a higher level of risk. However, safety regulations are to be followed strictly in order to minimize this risk.

Further Reading

- Fehér, I. and Deme, S. (2010). *Sugárvédelem (Radiation Protection)*. ELTE Eötvös Kiadó, Somos Környezetvédelmi Kft, Budapest.
- United States Nuclear Regulatory Comissions, 2007. < <http://www.nrc.gov/reading-rm/doc-collections/cfr/part020/> > (accessed 28.03.12.)
- Szabó, S.A. (1993). *Radioecology and Environmental Protection*. Akadémiai Kiadó/Ellis Horwood, Budapest/New York, NY.
- Valentin, J. (2006). *The Scope of the Radiological Protection Regulation*. Elsevier, Amsterdam, http://www.icrp.org/docs/Scope_of_rad_prot_draft_02_258_05v06.pdf (accessed 28.03.12.)

14 Detection and Measurement of Radioactivity

Radiation is observed via the changes in matter interacting with radiation (Chapter 5). During the detection of radiation, ionization is the most important process. The ionization of matter causes changes in the electric properties. Some of the main detector types (gas-filled and semiconductor detectors) utilize the ionization triggered by radiation. Scintillation of certain substances on the effect of radiation is another characteristic that is frequently used to detect radiation (scintillation detectors).

The chemical changes initiated by ionization provide another possibility to detect and measure radiation (autoradiography, chemical dosimeters, etc.). The thermal effects of the radiation, as well as nuclear reactions (e.g., detection of neutrons), also can be used to detect radiation.

The instruments of radiation detection usually consist of two main parts: the detector and the signal-processing unit. In this textbook, detectors are discussed in detail; the signal-processing units are mentioned as needed in order to understand the operation of the detector and the mechanism of signal formation.

When we talk about detection and measurement of radiation, it includes determining the type, the energy, or the energy distribution of the emitted particle or electromagnetic radiation, as well as the different decay rates (activity or intensity). The type of the particle or electromagnetic radiation and the energy gives information on the radioactive isotope that emitted the radiation (qualitative analysis). The activity or intensity (see Section 4.1.2) gives the number of radioactive nuclides (quantitative analysis). The detectors are characterized based on the following properties:

- The type (or the energy) of the particles, which can be detected by the detector.
- Dead time: the time needed to detect a novel particle after detecting the previous one. Shorter dead time is better. When the dead time is long, the measured activities or intensities have to be corrected; the correction, however, is the source of uncertainty. The dead time determines the maximum activity or intensity, which can be measured by a detector.
- The signal-to-noise ratio should be optimal. The increase of the sensitivity usually increases the noise too.
- The amplitude of the signals in the detector may be proportional to the energy of the particles or electromagnetic radiation or not. This factor determines whether the

energy of the particles can be measured, i.e., qualitative analysis can be done or not. The amplitude of the signal is proportional to the energy only in the case of some detector types. Other types of detectors produce signals independent of the energy of the radiation. This, however, can be advantageous for situations such as dose measurement.

- The signals should be easily treatable by the signal-processing unit. In the case of the most important detector types (gas-filled tubes, scintillation counters, and semiconductor detectors), this is usually not a problem because in all these detectors, electric impulses are formed under the effect of the radiation, which can be amplified and discriminated easily. The signals with different amplitudes belong to well-determined energies and can be discriminated by using the so-called channels. The number of channels defines how many different groups can be divided from the signals with different amplitudes. When all signals are equal or the total activity has to be measured (no qualitative analysis is needed), the signals are not discriminated and a one-channel analyzer is applied. In the case of the particles or electromagnetic radiations with energy that is not uniform, the detector produces signals with different amplitudes, where the number of channels can be up to several thousand. The increase in the channel numbers obviously makes the instruments more complicated and expensive. Thus, the detectors and the signal-processing units must be constructed in accordance.
- When the detector is able to produce signals with different amplitudes, the resolution is an important property of the detector. The resolution indicates the distance of two signals (energy of radiation), which can be separated from each other. Of course, the high resolution of a detector is useful only when the number of the channels in the signal-processing unit is high enough.
- The resolution is significantly affected by the half-width of the signals (Figure 14.1). The half-width is composed from the natural width of the spectrum lines (Eq. (5.98)) and the interactions of radiation with the matter in the detector.
- The efficiency of the detector indicates the ratio of the particles or photons that are detected.

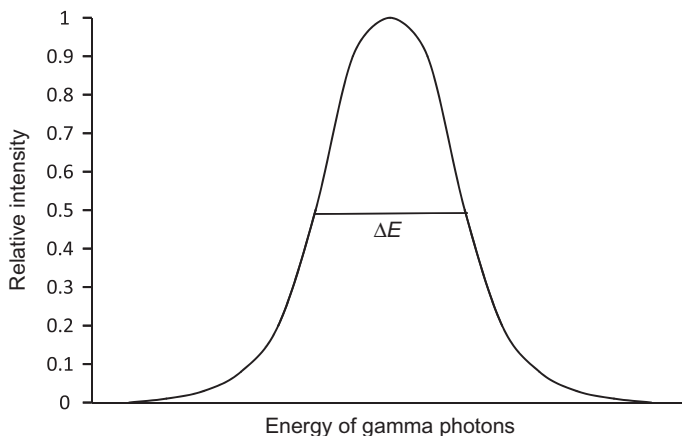


Figure 14.1 The half-width of signals in the case of gamma radiation.

Since detectors score differently in each of the above categories, the detector has to be chosen carefully and adapted to the given task. In the next sections, the most important types of radiation detectors will be discussed.

14.1 Gas-Filled Tubes

A common type of radiation detectors are the gas-filled tubes. These are cylindrical gas-filled capacitors where one electrode is the cylinder itself and the other electrode is a wire that is electrically insulated from the cylinder. Under the effect of ionizing radiation, the atoms or molecules of the gas are ionized, producing positive ions and electrons. When direct potential is applied across the tube, the positive ions will migrate toward the negative electrode (anode), while the electrons toward the positive electrode (cathode) induce an electric current. Thus, the migration of ions to the electrodes results in an electric impulse that can be measured, for example, by a simple electric circuit (see [Section 14.4](#)). The time needed for the ionization and migration to the electrodes determines the dead time, which is about 10^{-4} s. The formation and shape of the electric impulses and the regeneration of the detector are illustrated in [Figure 14.2](#).

The ionization detectors can measure alpha and beta radiation. Since gamma radiation does not form ions directly, only the secondary electrons emitted in the scattering processes and in the photoelectric effect lead to ionization ([Section 5.4](#)), and the efficiency of the measurement of gamma radiation is low.

In [Figure 14.3](#), the quantity of the ions that reaches the electrodes of the gas-filled tube is shown as a function of direct voltage. The function has characteristic ranges, of which some can be used for radiation detection. Range I is the range of

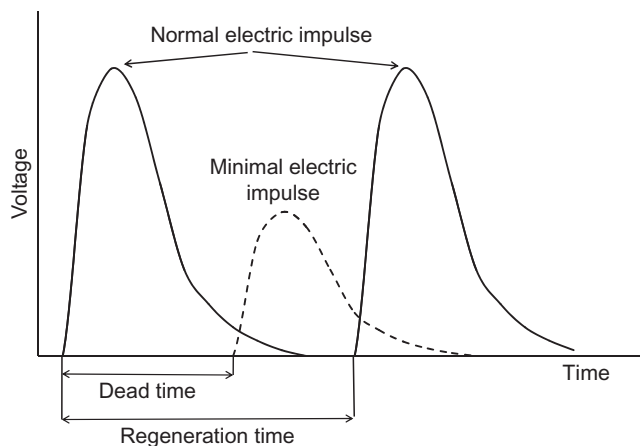


Figure 14.2 Formation and regeneration of electric impulses in gas-filled tubes under the effect of radiation.

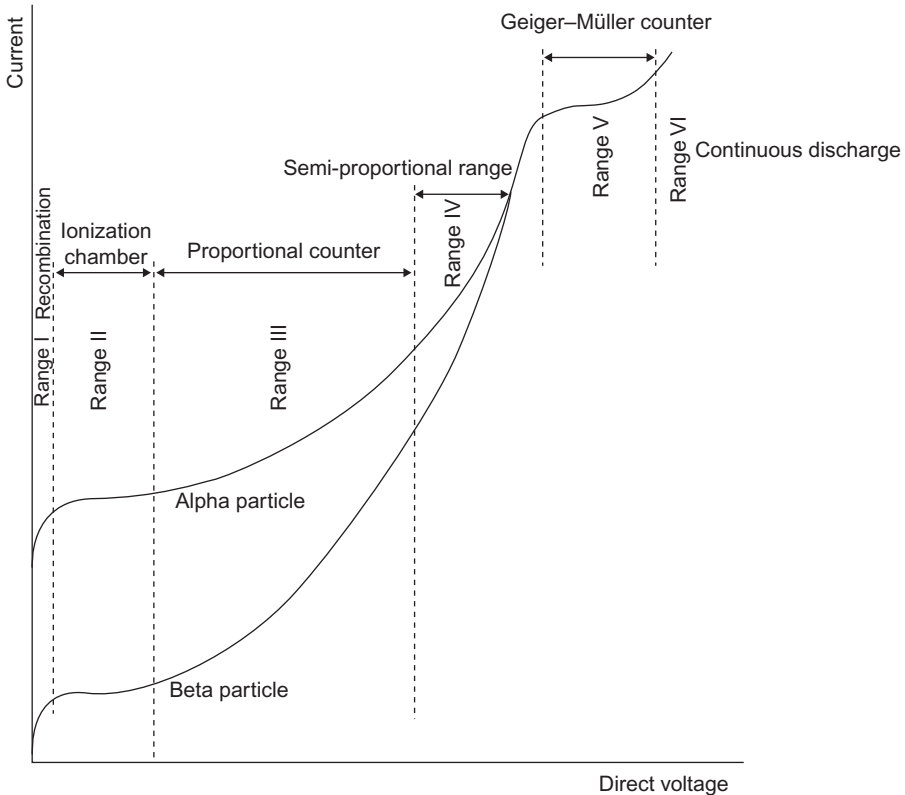


Figure 14.3 The number of ions collected on the electrodes of gas-filled detectors versus voltage.

recombination. In this range, the voltage is too low to collect all the ions and electrons initiated by the radiation. Thus, this range is not used for the detection and measurement of radiation.

Voltage then increases to a threshold value where all ions and electrons can reach the electrodes. By continuing to increase the voltage, a plateau is reached where no additional ions and electrons are formed (Range II). This is the voltage range, where ionization chambers work. As seen in Figure 14.3, there is a big difference in the numbers of ions produced by alpha and beta radiations. Thus, the ionization chambers can differentiate between alpha and beta particles. In the voltage range of the ionization chambers, the number of the primary ions is proportional to the energy of the radiation; therefore, the energy of the radiation can be determined. However, the number of the primary ions is usually low, so the application of the ionization chambers is limited. Therefore, ionization chambers are used to determine the total activity; for example, in dosimeters and signals where different amplitudes are not discriminated, all impulses are counted together. In other words, the measurements are made in an integrated way.

By further continuing to increase the voltage in these detectors, the primary ions ionize additional gas atoms or molecules when flying toward the electrodes, which results in the formation of secondary ions. As a result, the number of the collected ions increases and the current increases by several orders of magnitude. This range (Range III) is the so-called proportional range. The detectors working in this range are called “proportional counters.” Since the number of the secondary ions is proportional to the number of the primary ions, and consequently to the energy of radiation, the proportional counters give some information on the energy of the radiation. By increasing the voltage, the proportionality becomes less clear. Similarly, the number of ions produced by the alpha and beta particles gets closer. This range is the semi-proportional range (Range IV) and is not appropriate for radiation detection.

Beyond the semi-proportional range, a new plateau is formed (Range V). This is the so-called Geiger–Müller range, the range of Geiger–Müller counters or tubes. As seen in [Figure 14.3](#), the electric impulses are independent of both the type and the energy of the radiation. Therefore, the Geiger–Müller counters can measure the total activity or intensity of the alpha and beta radiation. Since the range of the alpha particles is short (as discussed in Section 5.2), the measurement of alpha particles needs very thin windows ($<1.5 \text{ mg/cm}^2$). If the window of the detector is thicker, only the beta particles are detected.

By an additional increase of voltage, continuous discharge is formed (Range VI), which can damage the detector.

14.2 Scintillation Detectors

Some substances emit scintillations under the effect of radiation. These substances can be used as scintillation detectors. Rutherford was the first to use a scintillation detector to measure alpha radiation. However, scintillation detectors became really important when Zoltán Bay constructed photomultipliers which transform scintillations into electric impulses. As a result of the improvement of scintillator and photomultipliers, scintillation detectors became one of the most important and widely applied tools in radiation measurement.

The advantages of using scintillation methods are as follows:

- The scintillator material is solid or liquid; its density is higher by about three orders of magnitude than the density of the gas in gas-filled detectors. Thus, a significant portion of radiation is converted into light photons. The free path of the light photons can be in the range of 1 m, while the free path of the ions in the gas-filled detectors is only a few centimeters.
- The time of the formation, collection of the light photons, electron conversion and multiplication, and signal processing is much shorter in scintillation detectors than in gas-filled detectors, so the dead time of scintillation detectors can be as low as about 10^{-8} s.
- Some scintillator material can be produced as a single crystal. In this case, the intensity of the scintillation is proportional to the energy of the radiation within a wide energy range, so the scintillation detectors are suitable to measure the energy of the radiation.

- The shape of the signals in the scintillation detectors depends on the type of radiation. Thus, it is possible to differentiate between the different types of radiation.
- The scintillation detectors can detect and measure alpha, beta, and gamma radiations. The detectors and the measuring techniques, however, are different for each types of radiation. This will be discussed later.

The scintillation system consists of the following parts:

- The scintillator material converts the radiation into light photons.
- The photomultiplier transforms the light photons into electric impulses.
- The electric processing units amplify, discriminate, process, count, record, the electric impulses.

14.2.1 Scintillator Materials

The scintillator materials are classified into two groups: inorganic and organic. The classification is done on the basis of the mechanism of the scintillation process. In the case of inorganic scintillators, the crystal lattice, including its defects, plays an important role, while in the case of organic scintillators, the physical–chemical processes within the molecules of the solid or liquid scintillator material result in light photon emission.

In inorganic scintillators, the radiation or the electrons produced as the result of interactions between the radiation and the scintillator material excite the electrons on the outer shells of the inorganic crystal. During the return of the excited electrons to the ground state, photons are emitted. As postulated in the theory of solids, instead of having discrete energies as in the case of free atoms, the available energy states form bands. In the ground state, the electrons are in the valence band. The criterion of the electric conduction process is whether there are electrons in the conduction band or not. In insulators, as the inorganic scintillator materials, the electrons in the valence band are separated from the conduction band by a large gap. Under the effect of radiation, the electrons can pass from the valence band to the conduction band and then return to the valence band, emitting photons whose energy is in the ultraviolet range. These photons, however, are absorbed by the scintillator material. The photons can be detected outside the scintillation material only when the crystal defects are such that they result in the formation of luminescence centers in the gap between the valence and the conduction bands. After excitation, the electrons return to the valence band through these luminescence centers, emitting blue light. This blue light then provokes the emission of electrons from the cathode of the photomultiplier. In some inorganic scintillators, the crystal defects are created by adding a small percentage of doping material.

The most important inorganic scintillation materials are as follows:

- Zinc sulfide (ZnS): for scintillation purposes, ZnS crystals are doped with silver or sometimes with copper. ZnS has historical importance (see, for example, the discussion of Rutherford's scattering experiments in Section 2.1.1). A relatively high portion (about 25%) of the radiation is converted into light photons. The wavelength of the emitted photons is within the sensitive range of the photomultipliers. However, the time of the

light emission is relatively long (2×10^{-7} s), resulting in a longer dead time than other scintillation materials. Another disadvantage of ZnS is that it is produced in a polycrystalline form consisting of small particles. Both the gamma photons and the emitted light photons are diffracted on the surfaces of the crystal particles, inhibiting the measurements of the radiation energy. For this reason, the ZnS scintillator is usually applied in thin layers for the detection of radiations in a low range (such as alpha particles, protons, deuterons, and fission products).

- Sodium iodide doped with thallium [NaI(Tl)]: the luminescence centers formed from the thallium doping. The conversion of radiation to light photons is relatively good (about 8%), and the wavelength of the photons is within the sensitive range of the photocathodes. The main advantage of NaI(Tl) detectors is that large single crystals can be produced that will allow the linear movement of the gamma and light photons without diffraction. Thus, the energy of the radiation can be measured.

Sodium iodide is widely used for spectroscopic purposes. Each of its three main interactions with gamma radiation (the photoelectric effect, Compton scattering, and pair formation, as discussed in Section 5.4) result in the emission of electrons. These electrons are the source of the scintillation that is measured in the detector (Figure 14.4). In the case of the photoelectric effect, the number of emitted electrons is proportional to the energy of the gamma radiation, i.e., the intensity of the

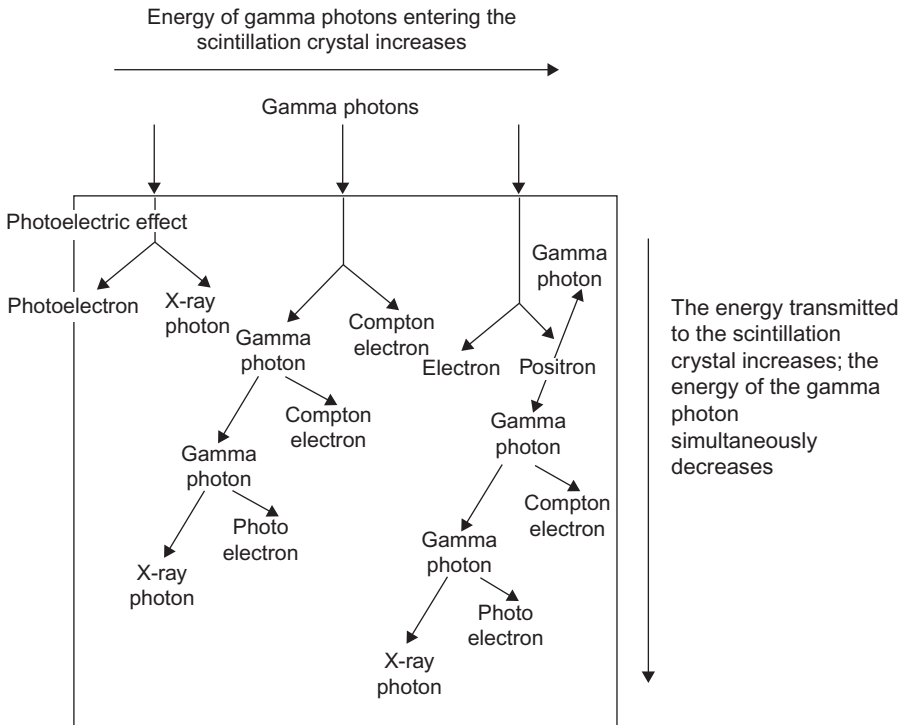


Figure 14.4 Interactions of gamma radiation with scintillator material.

light is also proportional to the energy of the gamma radiation, providing a way to measure gamma energy. The energy of the electrons emitted in the Compton scattering depends on the angle of scattering producing a continuous range in the gamma spectrum. In the case of the pair formation, besides the peak associated with the total energy of the gamma photon, other peaks may also be observed. These peaks have 511 keV and 1.02 MeV less energy than the energy of the gamma photon. The 511 keV relates the rest mass of the electron and positron produced in the annihilation process. The occurrence of these peaks with lower energy depends on whether the annihilation photons (one or both) leave the detector or absorb in it.

As seen in Section 5.4, the interactions of the gamma photons with matter, including the interactions with the scintillation material, strongly depend on the energy of gamma photons. At small energies, the photoelectric effect is dominant. When gamma energy increases, so does the cross section of Compton scattering. This scattering leads to a decrease of the energy of the primary gamma photons, and the produced secondary gamma photons that have smaller energy can cause the photoelectric effect. When the energy of gamma photons exceeds 1.02 MeV, pair formation also takes place, again producing secondary gamma photons with smaller energy. As a result, the gamma photons lose their energy in several consecutive processes. Well-defined peaks with characteristic gamma photon energy are obtained by cascade interaction within a short time if there are no scattering and diffraction.

In Figure 14.5, the scintillation gamma spectrum is shown. The peak associated with the gamma energy, as well as the continuous Compton edge, can be observed. A peak associated with the scattering of gamma photons appears at a lower energy.

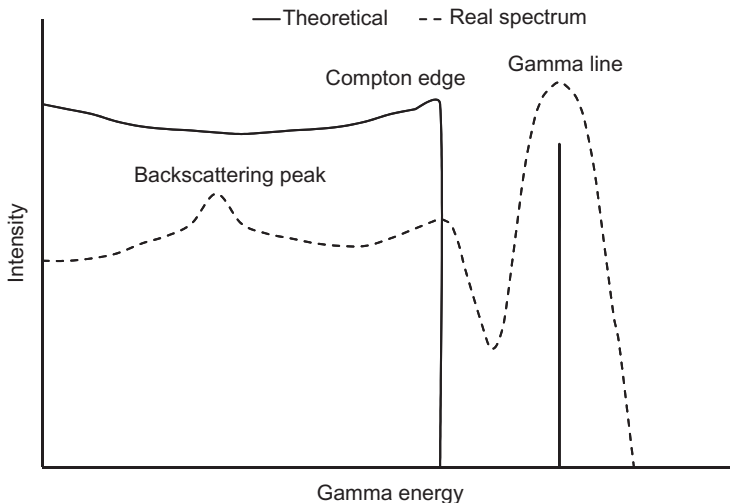


Figure 14.5 The scintillation gamma spectrum of a gamma emitter. The noisy range of the low energies in a real-life spectrum is not shown.

This peak is produced by the gamma photons scattered from substances around the radioactive nuclide and the detector.

Frequently, the gamma spectra contain other peaks with low energies, such as the X-ray lines resulting from the photoelectric effects of the surrounding material, e.g., the X-ray line of the iodine of the NaI(Tl) scintillation crystal or the lead of the shielding. In addition, the X-ray emission of the daughter nuclide may also be present. For example, in the spectrum of the Ba-137 m isotope (the daughter nuclide of Cs-137), the X-ray emission of the stable daughter nuclide, Ba-137, can be seen. This emission is produced when the gamma photons transfer their energy to an electron on the K orbital of the daughter nuclide, ^{137}Ba , and this K electron is emitted. This results in the excited state of the electrons of ^{137}Ba . This excited state returns to the ground state through an electron transfer from an outer (L) orbital to the K orbital emitting the excess energy between the orbitals as a characteristic X-ray photon (see Section 5.4.4).

The energy resolution of spectroscopic scintillators is about 7–10%.

For the measurement of charged particles, NaI scintillators are not used because they are hygroscopic, so they have to be kept sealed and the charged particles with short ranges cannot transfer through the wall of the container.

Besides sodium iodide, other alkali halogenide crystals are applied in scintillation spectroscopy. The most important is cesium iodide, which is not hygroscopic so it can be applied without packaging.

Nowadays, cerium-doped lanthanum bromide [$\text{LaBr}_3(\text{Ce})$] scintillation detectors are used. These detectors have some advantages compared to NaI(Tl) scintillation detectors. For example, the energy resolution of [$\text{LaBr}_3(\text{Ce})$] scintillation detectors is about 3% for the gamma line of $^{137\text{m}}\text{Ba}$ (662 keV). Furthermore, they have a higher photoelectron yield; the photon emission is nearly flat.

Other types of the inorganic scintillators are the Li-glass scintillators. Their application in neutron detection will be shown in [Section 14.5.5](#).

The most important organic scintillators are aromatic compounds containing more than one aromatic ring in different combinations. The scintillations are resulted in the easy excitation of the conjugated double bond systems. The mechanism of scintillation is associated with the individual scintillator molecules and consists of two steps: (1) the particle transfers its energy to the scintillator molecules exciting the electrons and (2) the scintillator molecules go back to the ground state, emitting light photons. The intensity of the light photons is proportional to the excitation energy, i.e., to the energy of the radiation particles. The wavelength of the light depends on the identity of the scintillator.

The organic scintillators are divided into three groups: (1) crystals, (2) liquid solutions, and (3) solid solutions (plastics). From the solid organic scintillators, anthracene and stilbene are used. In principle, they can measure all types of radiation (alpha, beta, and gamma); however, they are used only in some cases because other scintillators are more suitable for the measurement of each radiation.

The liquid scintillators are mainly used in the so-called liquid scintillation technique for the effective measurement of beta radiation with low energy. In this technique, both the sample (beta emitter) and the scintillator are dissolved in an organic solvent. In this way, the sample and the scintillator are in direct connection

within the molecular dimensions; thus, the absorption can be ignored. This is especially important when measuring weak beta emitters used in medical and biological studies (^3H , ^{14}C , ^{35}S , and ^{45}Ca).

The liquid scintillation cocktails is composed of the following substances:

1. Solvent: alkyl-benzenes, aromatic ethers (toluene, xylene, anizole, dioxane).
2. Primary scintillator: diphenyl-oxazols, *p*-terphenyl, PPO (2,5-diphenyl-oxazol).
3. Secondary scintillator: POPOP (1,4-di-(2,5-phenyl-enyl-oxazolyl)-benzene) and dimethyl-POPOP (1,4-bis-2-(4-methyl-5-phenyloxazolyl)benzene) are the most important.

If the sample is water soluble, alcohol is added to the cocktail or dioxane is applied as a solvent. A suspension, an emulsion, or a gel of the sample can also be prepared and used for measurement. Liquid scintillation cocktails are commercially available.

In multicomponent scintillator systems (solvent, primary, and secondary scintillators), the energy flow is not known exactly. In these cocktails, the concentration of the scintillator molecules is as low as 10^{-3} g/dm^3 . According to the most accepted theory, the radiation (whose energy is $h\nu$) excites the molecules of the solvent (S):



The star means the excited state of the molecule. Then these excited molecules (S^*) return to the ground state by exciting the molecules of the primary scintillator (Ps), initiating the scintillation process:



The secondary scintillators (Ss), the concentration of which is about 10^{-4} g/dm^3 , shift the spectrum of the emitted light toward the higher wavelength:



The excited secondary scintillator emits light photons:



The photons with higher wavelength coincide with the sensitive range of the photocathode of the photomultipliers. As a result, the quantity of the electrons emitted by the photocathode (discussed in [Section 14.2.2](#)) increases. By the application of the secondary scintillator, the efficiency of the beta measurement can be improved. When the sensitivity of the photocathode coincides with the energy of the light photon emitted by the primary scintillator, no secondary scintillator is required.

The liquid scintillators are very sensitive to the chemical impurities present in the sample because of the quenching effects. The intensity of the emitted light dramatically decreases if the sample contains substances with a high quenching

effect (organic substances, sulfur, and halogen compounds). Even the compound containing the beta emitter radioactive isotope itself can have a significant quenching effect. If so, the quenching effects have to be corrected by suitable measuring techniques (such as standardization).

Plastic scintillators contain POPOP or terphenyl dissolved in polystyrene. They can measure alpha, beta, and gamma radiations, as well as fast neutrons. They can be applied in any desired geometry, including samples with large sizes.

14.2.2 Photomultipliers

The light emitted by the scintillator molecules is transferred as electric impulses by a photomultiplier. The main parts of the photomultiplier are the photocathode and the multiplying system (dynodes). In the scintillation detector, the scintillation crystal and the photomultiplier are coupled together (Figure 14.6). Very good optical connection is required between the scintillator and the photocathode, which is provided by silicon oil with high viscosity.

The operation of the photomultiplier is as follows. The light emitted by the scintillator produces electrons (photo electrons) in the photocathode. The photocathode is usually located onto the inner wall of the input window. It is semipermeable for the input light. Most frequently, antimony or its compounds are used as photocathodes. The antimony is evaporated and deposited onto the inner wall. Then it is treated with alkali metals or little oxygen. The photocathode SbCsO is an example, with the highest sensitivity at a 440 nm wavelength. This is close to the wavelength of the light emitted by most scintillators (about 400 nm). As mentioned previously, the addition of a secondary scintillator can modify the wavelength of the light if required.

The electrons emitted by the photocathode are transmitted to the dynodes of the multiplying system. The dynodes have an increasingly higher voltage, and the difference between the adjacent dynodes is about 80–150 V; thus, the quantity of the electrons is multiplied from one dynode to another. At the end of the dynode system, the quantity of the electrons (i.e., the current) is high enough to be detected directly by the usual electronic devices. The sensitivity of the photomultipliers (namely, the signal-to-noise ratio) is very good.

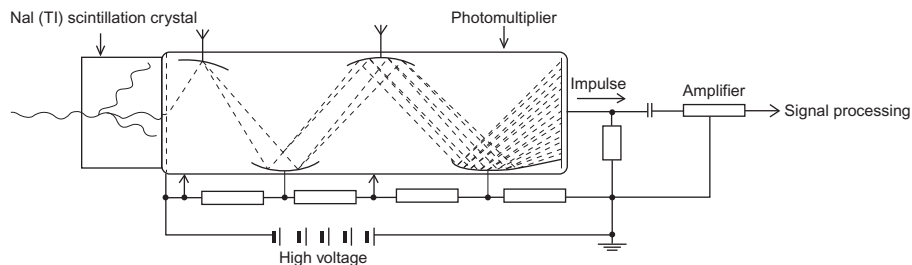


Figure 14.6 The transformation of radiation to electric impulses by scintillation crystals and photomultipliers.

The quantity of the electrons can be multiplied even by a factor of 10^8 . The multiplication factor of the electrons depends on the number, the geometry, and the voltage of the dynodes. Usually, 8–15 dynodes are applied. The multiplication factor is limited by the dark current of the photocathode, which is caused by the spontaneous electron emission of the photocathode. Cooling the photocathode decreases the dark current.

The electric impulse outputs from the photomultiplier are attenuated, discriminated, and registered.

14.3 Semiconductor Detectors

Semiconductor detectors operate similarly to ionization chambers (discussed in Section 13.1). This means that the charged particles produce negative and positive charge carriers, depending on the type of the semiconductor material, which move toward the oppositely charged electrodes. As a result, an electric impulse is formed. The main advantage of the semiconductor detector is that the energy producing the charge carriers (about 3.6 eV) is much less than that in the gas-filled tubes (≈ 30 eV) of detectors or scintillation detectors (2–300 eV). Thus, the same radiation particles are able to produce more electric charges in the semiconductor detectors (by several orders of magnitude) than either in gas-filled tubes or in scintillation detectors.

The basic material of the semiconductor detectors is germanium or silicon. Their operation is usually explained by the theory of solids. This theory postulates that instead of having discrete energies as in the case of free atoms, the available energy states form bands. In the ground state, the electrons are in the valence band. Under the effect of radiation, the electrons can move from the valence band to the conduction band, increasing the conductivity. When an electron moves from the valence band into the conduction band, the produced vacancy, “the hole,” also takes part in the electric conduction because filling the hole with an electron of the adjacent atom requires a small amount of energy. The electrons and the holes move in opposite directions; the hole can be considered to be a positive charge.

When the basic material of the semiconductor (Si or Ge) is doped with an electron donor (such as P, As, and Sb), or electron acceptor (e.g., Al, B, Ga, and In), an excess quantity of the electrons or holes, respectively, are produced. These types of semiconductors are called “n-type” (negative) or “p-type” (positive) semiconductors, respectively. In these semiconductors, the excitation energy is even lower than in the pure germanium and silicon semiconductors.

Ge, Ge(Li), and Si(Li) semiconductor detectors are used for the measurement of gamma and X-ray radiations, respectively. The energy resolution of the Ge(Li) detectors widely applied in gamma spectroscopy is much better than that of scintillation detectors. For example, the half-width of the photoelectric peak of the $^{137\text{m}}\text{Ba}$ isotope (the daughter nuclide of Cs-137) (662 keV) is 2–3 keV (<0.5%) when measured with a semiconductor detector, while this value is 7–10% when measured with a scintillation detector. However, the efficiency of the semiconductor

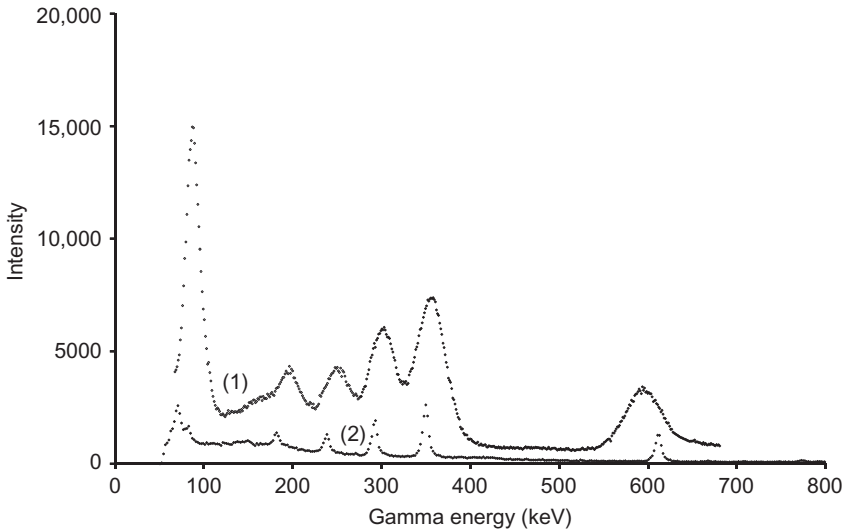


Figure 14.7 The photoelectric peaks of Ra-226 and its daughter nuclides measured by scintillation (1) and semiconductor (2) detectors.

detectors is about one order of magnitude worse than that of the scintillation detectors. In addition, the semiconductor detector requires high-quality signal-processing units (e.g., charge and spectroscopic amplifiers). GeLi and SiLi semiconductor detectors have to be kept continuously at the temperature of liquid nitrogen because the thermal energy is enough to transfer the electrons from the valence band to the conduction band, increasing the noise. Recently, high-purity germanium (HPGe) detectors also have been used, which can be allowed to warm up to room temperature when not in use.

The photoelectric peaks of the Ra-226 and its daughter nuclides measured by semiconductor and scintillation detectors are shown in [Figure 14.7](#). This figure illustrates the differences in the gamma spectra obtained by scintillation and semiconductor detectors. As seen, semiconductor detectors have a higher resolution but a lower efficiency than the scintillation detectors.

14.4 Electric Circuits Connected to Detectors

As discussed previously in this chapter, the most important detectors (gas-filled tubes, the photomultipliers of the scintillation, and the semiconductor detectors) produce electric impulses. The electric impulses formed in the gas-filled tubes can be measured, e.g., by a simple electric circuit, as illustrated in [Figure 14.8](#).

In [Figure 14.8](#), the detector is considered to be a resistance that tends to be infinity (the resistance of the detector is much higher than the resistance of R ,

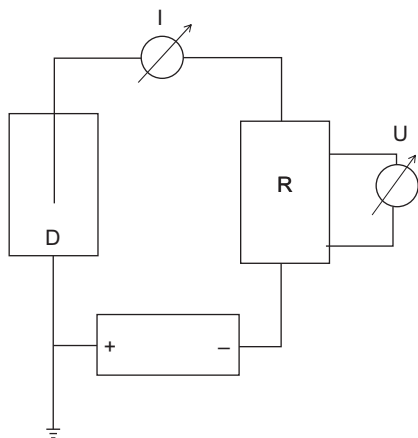


Figure 14.8 A simple electric circuit for the measurement of electric impulses in an ionization detector (D—detector, R—resistance, I—current meter, U—voltage meter).

which is about $G\Omega$) when there are no ions produced in the gas-filled tube (i.e., no radiation). In this case, the current tends to be zero; thus, the voltage measured by the U voltage meter also tends to be zero, as expected by Ohm's law ($U = R \times I$). Under the ionizing effect of radiation, electrons and ions are induced, decreasing the resistance (the resistance of the detector becomes less than the resistance of R). As a result, the current, as well as the voltage on the U voltage meter, increases, and an electric impulse is formed. The voltage is proportional to the amplitude of the electric impulse.

When using scintillation detectors, an anodic resistance and a condenser (RC circle) are used. In the case of semiconductor detectors, a charge-sensitive preamplifier is required.

The obtained electric impulses can also be amplified or attenuated linearly depending on the voltage required by the signal-processing units. Impulses with different amplitudes can be separated by discriminators in one-channel analyzers or multichannel amplitude analyzers.

In one-channel analyzers, the electric impulses with different amplitudes are separated by differential discriminators. These are filters that permit the signals in the range of $V_D \pm \Delta V_D$ to pass. The level V_D and the width ΔV_D can be varied. By varying V_D , the total gamma spectrum can be scanned step by step. The total gamma spectrum is obtained if the V_D is incremented by ΔV_D in each step.

In multichannel analyzers, the total spectrum is recorded in one measurement. It is very comfortable and saves time, which is especially important when the radio-nuclide has a short half-life or low activity.

The signals produced in the amplifier of the detector transfer to an analog/digital converter (ADC). The condenser in the ADC is charged up, as determined by the amplitude of the electric impulse. Then the condenser partially discharges, and in the meantime, an oscillator emits impulses at a constant speed. The number of the impulses emitted during the discharge of the condenser is proportional to the amplitude of the signal input into the ADC, i.e., to the energy of the radiation. The number of the impulses coming out of the oscillator determines the position of the

input signals in the memory. Each position of the memory corresponds to an input signal with a particular energy, and its value always increases by 1 when a signal with the same energy is input into the analog/digital converter.

Previously, the data stored in the memory was recorded by two digital–analog converters (DACs) and an oscilloscope. One of the DACs treated the positions in the memory that define the position of the electron beam along the x -axis of the oscilloscope. The other DAC shows the deviation of the electron beam from the x -axis. As a result, the spectrum is continuously presented on the monitor of the oscilloscope. Nowadays, computers equipped with analyzer cards are used for signal processing. Their operation is not discussed here.

14.5 Track and Other Detectors

Track detectors (cloud chambers, bubble chambers, autoradiography, and solid-state detectors) can visualize the track of the radiation particles. They are mainly used in nuclear physical studies.

14.5.1 *Cloud Chambers and Bubble Chambers*

The Wilson's cloud chamber is filled with supersaturated vapor (e.g., very pure alcohol vapor) in which liquid drops are formed under the effect of radiation. In this way, the trace of the radiation can be seen. The photos taken in cloud chambers have been shown previously in this book (e.g., Figures 4.11, 5.7, 5.14, 5.31, 6.1, 13.3, and 13.5).

Bubble chambers operate similarly, but the phases are opposite. Bubbles are formed in a superheated transparent liquid under the effect of radiation and visualize the track of the radiation particles.

14.5.2 *Autoradiography*

Autoradiography can be used to study the local distribution of the radioactive isotopes. The distribution of the isotopes in the different objects and organs is studied by stripping films or X-ray films. Similar to the photo emulsions used in black-and-white photography, they contain silver bromide particles in a gelatin emulsion. When irradiating, Ag(I) ions are reduced to metallic silver. This reduction takes place only in those spots where the radiation touched AgBr. The silver particles are then magnified by a chemical procedure called “development.” The formation of metallic silver causes the blackening of the film, and a negative image is obtained. The intensity of the blackening is proportional to the intensity of radiation. Similar to traditional photography, a positive image can be produced from the negative image. On the positive image, the places exposed to high radioactive intensity become white.

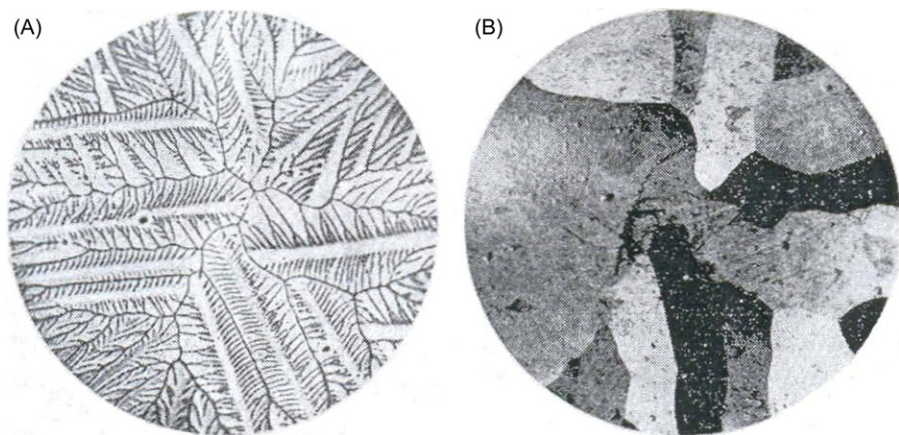


Figure 14.9 An autoradiogram (A) and a microscopic picture (B) of an etched tin alloy containing 10^{-7} m/m% ^{111}Ag ($3\times$ magnification). (Thanks to Prof. László Bartha, Research Institute for Technical and Materials Science, Budapest, Hungary.)

Source: Reprinted from Bartha (1963), with permission from Carl Hanser Verlag.

As mentioned previously in this section, stripping films are frequently applied to autoradiography. These films may be in close contact with the sample, improving the quality of the autoradiographs.

In Figure 8.3, a negative autoradiogram of the radiocolloid formation is illustrated. Moreover, in Figure 14.9, an autoradiogram (left) and a microscopic picture (right) of etched tin alloy containing $10^{-7}\%$ ^{111}Ag are shown. As seen, the introduction of the radioactive silver takes place on the boundaries of the particle in the polycrystal.

An application of autoradiography in medical science is shown in Figure 14.10.

14.5.3 Solid-State Detectors

When passing through some substances, heavy ionizing particles break the chemical bonds and produce damaged channels. The diameter of these channels is about 5 nm; however, their diameter can be augmented to as large as $10\ \mu\text{m}$ using chemical development. In amorphous substances, the tracks are round, assuming that the ionizing particles enter the substance perpendicularly. In crystalline substances, the shape of the tracks fit the crystal lattice. The density of the tracks is proportional to the intensity of the radiation. Solid-state detectors can be used to measure the energy of the particles because the diameter of the tracks is proportional to the energy of the particles, providing that the procedures are done strictly under the same conditions.

In Figure 14.11, the tracks of the alpha particles emitted by ^{252}Cf (6.1 MeV) are shown. Moreover, tracks of the heavy particles are shown in Figures 13.4 and 13.6.

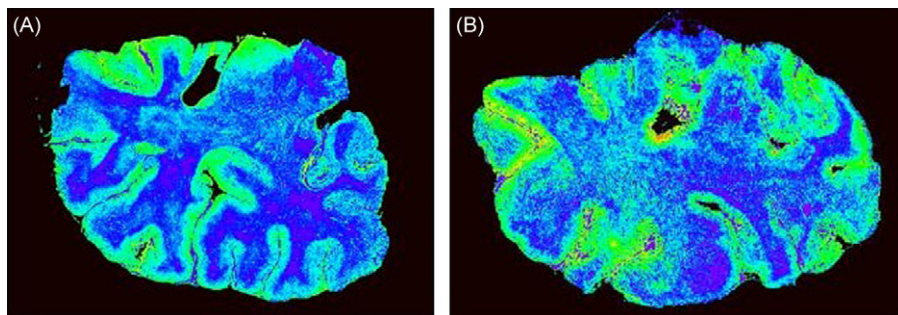


Figure 14.10 An autoradiogram of coronal whole hemisphere slices. The receptors of the brain react with the ^3H -labeled *N*-(2-phenoxy-5-fluorophenyl)-*N*-(2,5-dimethoxybenzyl) acetamide. This compound is used for monitoring the progress of neurodegenerative diseases. (A) Control brain; (B) Alzheimer's disease patient's brain. The tritium activity increases from cold to hot colors. (Thanks to Katalin Nagy and Boglárka Makai, Department of Neurology, University of Debrecen, Hungary, for the autoradiogram.)



Figure 14.11 Tracks of the alpha particles emitted by ^{252}Cf (6.1 MeV). (Thanks to Dr. István Csige, Department of Environmental Physics, University of Debrecen—Institute of Nuclear Research, Hungary, for the photograph.)

The basic characteristics of the most important solid-state detectors are summarized in [Table 14.1](#). The plastic detectors are developed by 6 mol/dm^3 of NaOH or KOH. Glass and silicate (such as mica) detectors are developed by hydrogen fluoride.

An application of solid-state detectors was presented in [Section 4.3.3](#). The minerals also record nuclear processes that occur spontaneously in nature.

14.5.4 Chemical Dosimeters

Chemical dosimeters utilize the chemical effects of radiation. In fact, autoradiography (see [Section 14.5.2](#)) also works in this way. In addition, thermoluminescence

Table 14.1 Solid-State Detectors

| Substances | Chemical Composition |
|---|---|
| Cellulose nitrate | $[\text{C}_6\text{H}_7(\text{NO}_2)_3\text{O}_5]_n$ |
| Cellulose triacetate | $[\text{C}_6\text{H}_7(\text{CH}_2\text{COO})_3\text{O}_5]_n$ |
| Polycarbonate plastics (Lexan and Makrofol) | $[-\text{Ar}-\text{C}(\text{CH}_3)_2-\text{Ar}-\text{O}-\text{CO}-\text{O}-]_n$ |
| Polyethylene terephthalate polymers (Mylar) | $[-\text{CO}-\text{Ar}-\text{CO}-\text{O}-(\text{CH}_2)_2-\text{O}]_n$ |
| Glass | $\text{Na}_2\text{SiO}_3, \text{CaSiO}_3$ |
| Muscovite mica | $\text{KH}_2\text{Al}_3\text{Si}_3\text{O}_{12}$ |

detectors are mentioned: they absorb and store the energy of the radiation at room temperature, and then, after heating to 200–300°C, they emit the energy as luminescent (light) photons. The thermoluminescence detectors are made of calcium sulfate and lithium fluoride doped with dysprosium.

14.5.5 Detection of Neutrons by Nuclear Reactions

The radiation detectors mentioned previously detect radiation by physical and chemical interaction with the substance of the detector. Neutrons, however, have only scattering interactions and initiate nuclear reactions with the nuclei; thus, the detection of the neutrons is problematic and have only a small amount of efficiency.

The nuclear reactions can be used for the detection and measurement of neutrons. Two nuclear reactions are mentioned: $^{10}\text{B}(n,\alpha)^7\text{Li}$ and $^6\text{Li}(n,\alpha)^3\text{H}$. Boron and lithium are present in the form of boron trifluoride or lithium glass, respectively. In both cases, the emitted alpha particles are detected. The intensity of the alpha radiation is proportional to the number of absorbed neutrons. BF_3 gas is placed into a proportional counter, i.e., a gas-filled tube is used to detect the alpha particles. In the case of Li-glass, its scintillation property is used up in the detection.

The neutrons are detected by an $\text{LiF} + \text{ZnS}$ combined detector. In the $^6\text{Li}(n,\alpha)^3\text{H}$ nuclear reactions, two charged particles (the alpha particle and the tritium nucleus) are formed, inducing scintillation of zinc sulfide.

14.6 Absolute Measurement of Decomposition

As mentioned in Section 4.1.2, radioactivity is usually measured not by identifying the radioactive nuclei, but by counting the emitted particles. The absolute measurement of radioactivity means the measurement of the total activity, i.e., all radiating particles have to be counted in 4π spatial angles.

The detectors measuring the total activity are usually gas-filled detectors (as described in Section 14.1) and measured at a direct voltage where the alpha and

beta particles can be differentiated (Figure 14.3). During the measurements, it is assumed that every radioactive decay emits one particle, which is true for most decays.

The very thin layer of the radioactive sample is placed onto a very thin plastic sample holder (at most, $10 \mu\text{g}/\text{cm}^2$), and this sample is located in the middle of two half-sphere detectors. The produced sphere is purged continuously by the mixture of argon and methane gases. These types of detectors are called “ 4π -counters.” The signals produced in the two half-sphere detectors are added together after preamplifying.

The other method for the measurement of the total activity is the coincidence method. This method can be used for measuring two decay types. The first one is when an alpha particle and a gamma photon, or a beta particle and a gamma photon, are emitted at the same time (within 10^{-7} s). In the other case, two gamma photons are emitted together (also within 10^{-7} s). The alpha/beta particle + gamma photon, or the two gamma photons, are measured by two detectors, which are connected in coincidence. This means that signals (I_{1+2}) are obtained only when signals are produced on the outputs of both detectors at the same time. In addition, the alpha/beta particles (I_1) and gamma photons (I_2) are counted separately. Similarly, when two gamma photons are detected, two independent gamma intensities are measured.

The total activity can be calculated as follows. The radioactive intensity (I) can be expressed by the product of the activities (A) and efficiencies (k). For the separately measured alpha/beta particles:

$$I_1 = k_1 A \quad (14.5)$$

For the gamma photon:

$$I_2 = k_2 A \quad (14.6)$$

For the coincidence signals:

$$I_{1+2} = k_1 k_2 A \quad (14.7)$$

By expressing the total activity:

$$A = \frac{I_1 I_2}{I_{1+2}} \quad (14.8)$$

The measurement of the total activity by the coincidence method seems to be very simple. In practice, however, efficiency corrections are required even for isotopes with the simplest decay schemes.

The total activity of radioactive sources with high activities can also be measured using calorimetry. The accuracy of the activity measurements can be improved by the application of differential calorimeters.

14.7 Statistics of Radioactive Decay

14.7.1 Statistical Error of Radioactivity Measurement

The activity of radioactive substances is usually measured indirectly. This means that the number of the particles or photons counted in the detector is proportional to the radioactivity, the number of decompositions in a unit of time (see Section 4.1.2). As mentioned in Section 4.1.1, radioactive decay is a statistical process, so repeated measurements give a statistical distribution around a mean value. On the basis of the statistical laws, the statistical error of the measurements can be determined accurately.

The statistical laws postulate that as the measured counts (N) increase, the absolute error (ΔN) also increases. The relative error ($\Delta N/N$), however, decreases. When N tends to be infinity, the relative error tends to be zero.

$$\lim_{N \rightarrow \infty} \frac{\Delta N}{N} \rightarrow 0 \quad (14.9)$$

The real value of N is determined by the time, which can be chosen for the measurements. Thus, the relative error can be decreased under a certain value at most.

Let's measure the intensity of a radioactive sample k times under the same conditions. The counts are $N_1, N_2, \dots, N_i, \dots, N_k$, and their mean value is \bar{N} . In principle, the distribution of the values (P_N) can be given by Poisson's discrete probability distribution:

$$P_{N_i} = \frac{(\bar{N})^{N_i}}{N_i!} \cdot e^{-\bar{N}} \quad (14.10)$$

For sufficiently large values, the probability distribution obtained for the measured values and Poisson's probability distribution function is the same (Figure 14.12). For smaller values, the regular process of radioactive decay was disturbed by an external factor (e.g., the instability of the measuring tool, the aging of the detector, the change in the position of the sample). On the basis of Poisson's distribution, the standard deviation expected for N counted impulses (s.d.) is:

$$\text{s.d.} = \sqrt{N e^{-\lambda t}} \quad (14.11)$$

At $\lambda t \ll 1$ (i.e., when the activity of the radioactive sample remains the same during the measuring time):

$$\text{s.d.} = \sqrt{N} \quad (14.12)$$

As seen in Eq. (14.8), the standard deviation can be calculated for one measurement when the counts are high enough.

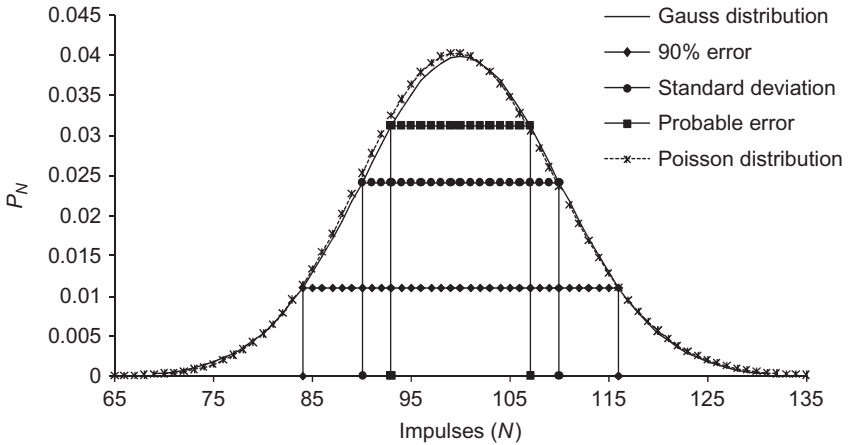


Figure 14.12 The Poisson and the Gauss distributions when the mean value of the counted impulses is 100.

In the case of the many counted impulses ($N > 100$), the Poisson distribution becomes identical to the Gauss distribution, which is simpler and accurate enough:

$$P_N = \frac{1}{\sqrt{2\pi N}} \cdot \exp\left(-\frac{(N_i - \bar{N})^2}{2N}\right) \tag{14.13}$$

The value and the distribution of the differences between the individual measured values and the mean value

$$\Delta_i = N_i - \bar{N} \tag{14.14}$$

usually fulfill the Gauss distribution (Figure 14.12).

The degree of accuracy is the degree of closeness of the measurements to the actual value. When 50% of the measurements are within this given value, it is called “probable deviation.” The mean error or the standard deviation is the error obtained for 68.27% of the measurements.

If the Gauss probability distribution function is integrated from $\bar{N} - \sqrt{\bar{N}}$ to $\bar{N} + \sqrt{\bar{N}}$, 0.6827 is obtained. If the Gauss probability distribution is valid, 68.27% of the measurements fall into the interval $\bar{N} \pm \sqrt{\bar{N}}$. Accordingly, the standard deviation is $\pm \sqrt{\bar{N}}$, the square root of the mean value. This value is equal to the value obtained in Poisson’s probability distribution.

When the Gauss distribution function is integrated from $\bar{N} - c\sqrt{\bar{N}}$ to $\bar{N} + c\sqrt{\bar{N}}$, a certain portion of the measurement falls into the interval $\bar{N} \pm c\sqrt{\bar{N}}$. Table 14.2 shows these probabilities.

Table 14.2 The Portion of the Measurements in the Interval $\bar{N} \pm c \sqrt{\bar{N}}$ at Different Values of c

| c | Percentage of the Measurements in the Interval $\bar{N} \pm c \sqrt{\bar{N}}$ | Name of the Error |
|--------|---|---|
| 0.6745 | 50.00 | Probable error |
| 1.0000 | 68.27 | Standard deviation |
| 1.6449 | 90.00 | 9/10 error (90% error) |
| 2.0000 | 95.45 | Double mean statistical error (95.5% error) |
| 2.5758 | 99.00 | 99/100 error |
| 3.0000 | 99.73 | Triple mean statistical error |
| 3.2905 | 99.90 | 999/1000 error |

In most cases, the standard deviation is used. This value can be calculated as follows:

$$sd = \sqrt{\frac{\sum_{i=1}^k (N_i - \bar{N})^2}{k - 1}} \quad (14.15)$$

As discussed previously, 68.27% of the measurements fall into the interval $N \pm \sqrt{\bar{N}}$.

The standard deviation of the mean value (SD) is less than the standard deviation of the individual measurements (sd) because the mean value is obtained from k independent measurements. The time of the measurements is t , and the number of the counted impulses is N_i . The standard deviation of the mean value is expressed as:

$$SD = \sqrt{\frac{\sum_{i=1}^k (N_i - \bar{N})^2}{k(k - 1)}} = \frac{sd}{\sqrt{k}} = \sqrt{\frac{\bar{N}}{k}} \quad (14.16)$$

The standard deviation of the mean value per time (in other words, the standard deviation of the activity or intensity) is:

$$\frac{SD}{t} = \frac{\sqrt{\bar{N}/k}}{t} \quad (14.17)$$

As seen in Eq. (14.17), the standard deviation can be decreased by increasing the measuring time and the number of the measurements.

14.7.2 Correction of Background Radioactivity

If the results of the intensity measurements with errors are used in subsequent calculations, including even the correction with the background, the spread-error rules must be used. In the case of addition ($A + B$) or subtraction ($A - B$) of two quantities, the standard deviation is:

$$\text{sd} \approx \sqrt{\text{sd}_A^2 + \text{sd}_B^2} \quad (14.18)$$

For other addition and subtraction, additional members have to be included in Eq. (14.18). For multiplication: $C = A \times B$:

$$\text{sd}_C = \sqrt{A^2 \text{s.d.}_A^2 + B^2 \text{s.d.}_B^2} = AB \sqrt{\frac{\text{sd}_A^2}{A^2} + \frac{\text{sd}_B^2}{B^2}} \quad (14.19)$$

For division: $C = A/B$:

$$\text{sd}_C = \frac{A}{B} \sqrt{\frac{\text{sd}_A^2}{A^2} + \frac{\text{sd}_B^2}{B^2}} \quad (14.20)$$

For exponentiation: $C = A^k$:

$$\text{sd}_C = kA^k \frac{\text{sd}_A}{A} \quad (14.21)$$

For logarithm: $C = \ln A$:

$$\text{sd}_A = \frac{\text{sd}_A}{A} \quad (14.22)$$

When measuring radioactive intensities, we always have to correct for the intensity of the background. When it is possible to consider the background intensity constant, the standard deviation of the background measurements (sd_b) has to be negligible compared to the standard deviation of the measurements (sd_m). For the reliable measurement of the intensity of the radioactive sources, the number of impulses to be measured is at least

$$N_{\min} = N - N_b \geq 3\sqrt{N_b} \quad (14.23)$$

where N is the total counted impulses and N_b is the counted background intensity. The measuring times (i.e., the number of readings) must be the same for both. The standard deviation of the intensity corrected with the background is calculated using Eq. (14.18).

Further Reading

- Choppin, G.R. and Rydberg, J. (1980). *Nuclear Chemistry, Theory and Applications*. Pergamon Press, Oxford.
- Friedlander, G., Kennedy, J.W., Macias, E.S. and Miller, J.M. (1981). *Nuclear and Radiochemistry*. Wiley, New York.
- Hendee, W.R. (1973). *Radioactive Isotopes in Biological Research*. Wiley, New York.
- Lieser, K.H. (1997). *Nuclear and Radiochemistry*. Wiley-VCH, Berlin.
- Mann, W.B., Ayres, R.L. and Garfinkel, S.B. (1980). *Radioactivity and its Measurement*. 2nd edition. Pergamon Press, Oxford.
- McKay, H.A.C. (1971). *Principles of Radiochemistry*. Butterworths, London.
- Millner, T., Bartha and Prohászka, J. (1963). Untersuchungen über die Wanderung kleiner Silbermengen in reinem Zinn bei Verwendung von radioaktiven Silber. *Z. Metallkunde* 54:17–19.